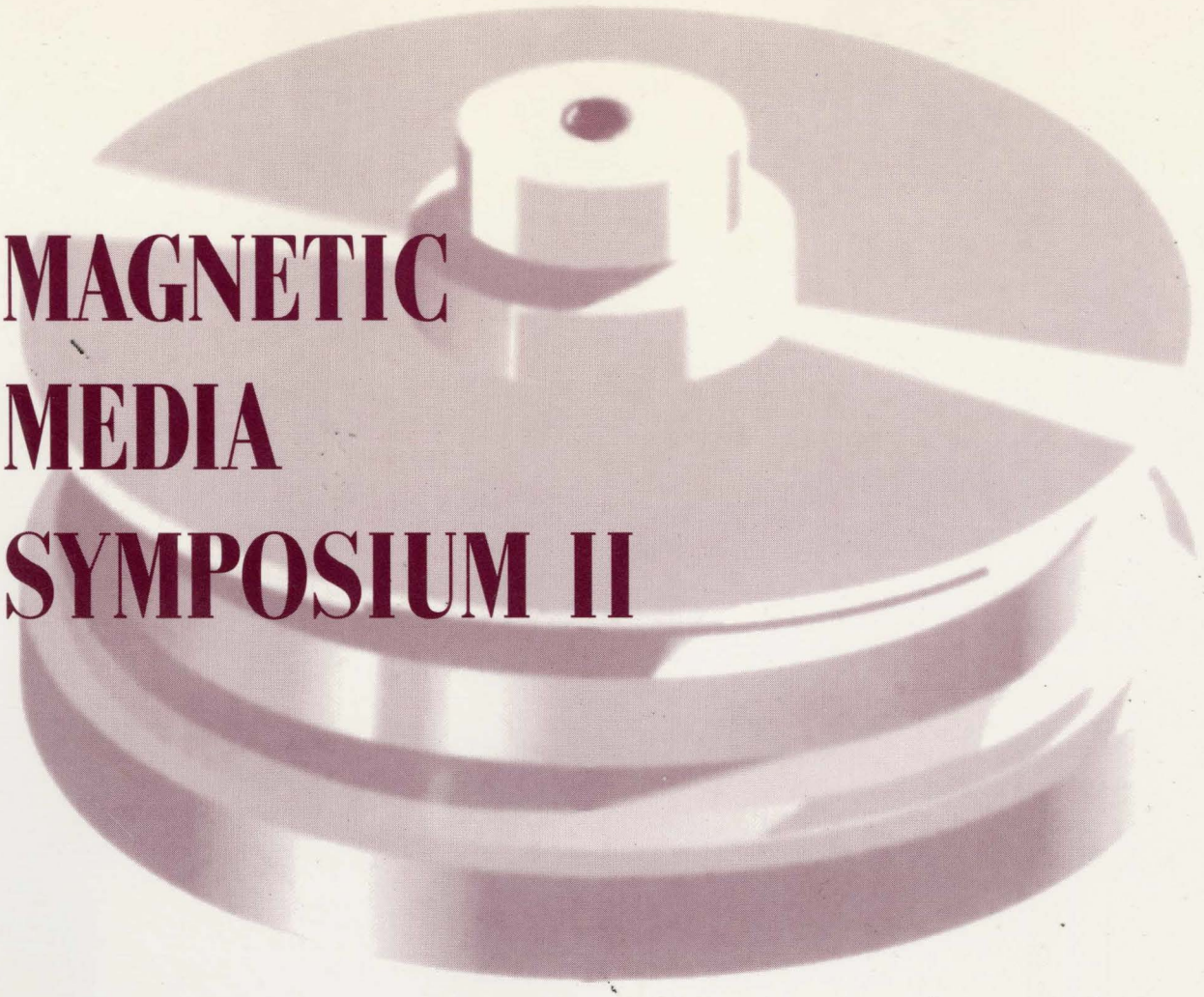

MAGNETIC MEDIA SYMPOSIUM II

December 15-16, 1997

Presented by

IIST

Santa Clara University
Institute for Information Storage Technology

IIST • School of Engineering • Santa Clara University • Santa Clara, California 95053

MAGNETIC RECORDING CHANNELS
an IIST Course

Magnetic Recording Channel Front-Ends

Klaas B. Klaassen, Ph.D.
IBM - Almaden

and

Digital Read/Write Channels for Magnetic Recording

Nersi Nazari, Ph.D.
GEC Plessey

May 28, 1996
Santa Clara University

Magnetic Recording Channel Front-Ends

Considerations and Design

Klaas B. Klaassen

IBM Almaden Research
San Jose, CA

KbeeK96

Contents

INFORMATION THEORETICAL CONCEPTS

Recording Channel ⇒ Information Channel

★ CHANNEL: Physical means for transmitting or storing information.

INFORMATION needs a PHYSICAL CARRIER

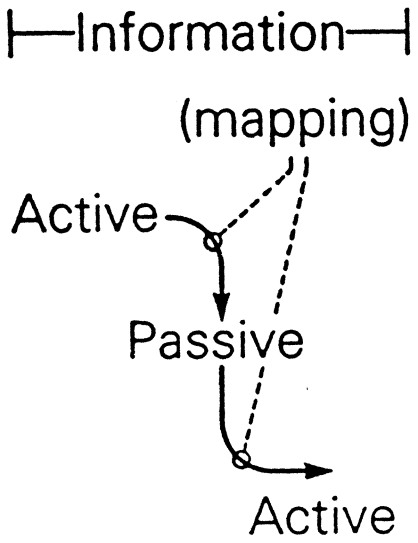

- Active Information:

  Grafted onto energetic carrier (power)

- Passive Information:

  Non-energetic carrier (ordered state of matter)

ACTIVE INFORMATION ≡ SIGNAL

PASSIVE INFORMATION ≡ PATTERN

UTILIZATION

Active Information

- Easily transmitted
  (as electromagnetic power)
- Dissipates away
  (eventually drowns in thermal noise)
- Ideal for communication between systems

Passive Information

- Not readily transmitted
  (shipping of matter)
- Little long-term decay
- Ideal for information storage

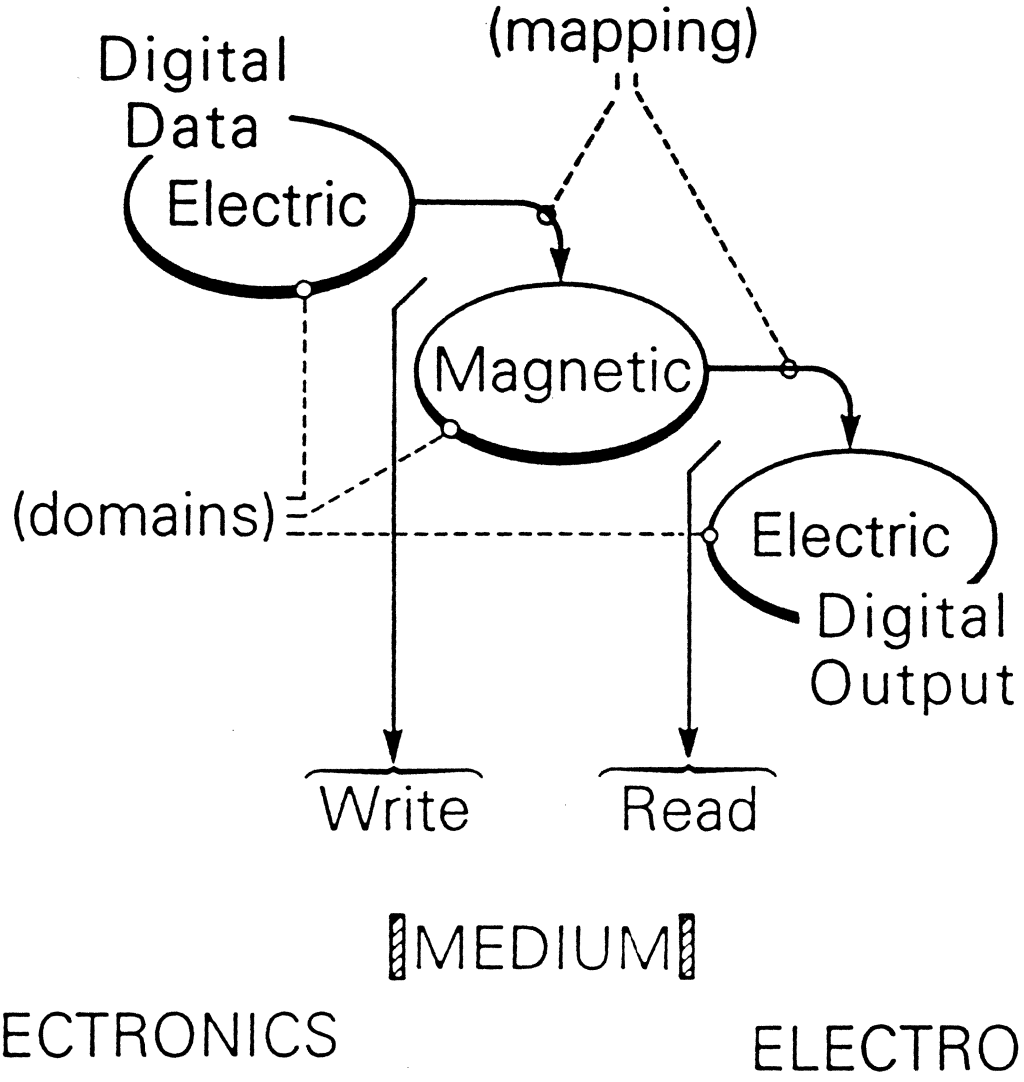
(mapping)
Digital
Data
Electric
Magnetic
(domains)
Electric
Digital
Output
Write
Read
MEDIUM
ELECTRONICS
ELECTRONICS

Physical Channel

Active Information is contained in:

- **Signals**
  - Energetic physical carriers of desired information
  - Waveforms we want to see

These are always accompanied by:

- ***Noise*** (Internal, fundamental)
  - Unpredictable, random perturbations
  - Generated in channel hardware
  - Theoretically inescapable
  - Thermal noise, shot noise, etc.
- ***Interference***
  - Undesirable garbage signals
  - Avoidable
  - Environment generated
  - Electromagnetic interference, cross-talk, etc.
- ***Distortion***
  - (trace) average of difference between waveforms we get and those we want
  - Linear distortion: channel frequency response not adequate
  - Non-linear distortion: channel dynamic range not adequate

Basic Contributors

Magnetic Medium

- Transition, DC-erase, Track edge — *Noise*
- Overwrite, Adjacent track, Texture — *Interference*
- Intersymbol — *Distortion*

Head

- Coil/sensor resistance, Eddy current damping, Barkhausen — *Noise*
- Tribo-electric, Thermal asperity, Conductive contact — *Interference*
- MR head asymmetry — *Distortion*

Electronics

- Thermal, Shot — *Noise*
- Electro-magnetic — *Interference*
- TA dynamics — *Distortion*

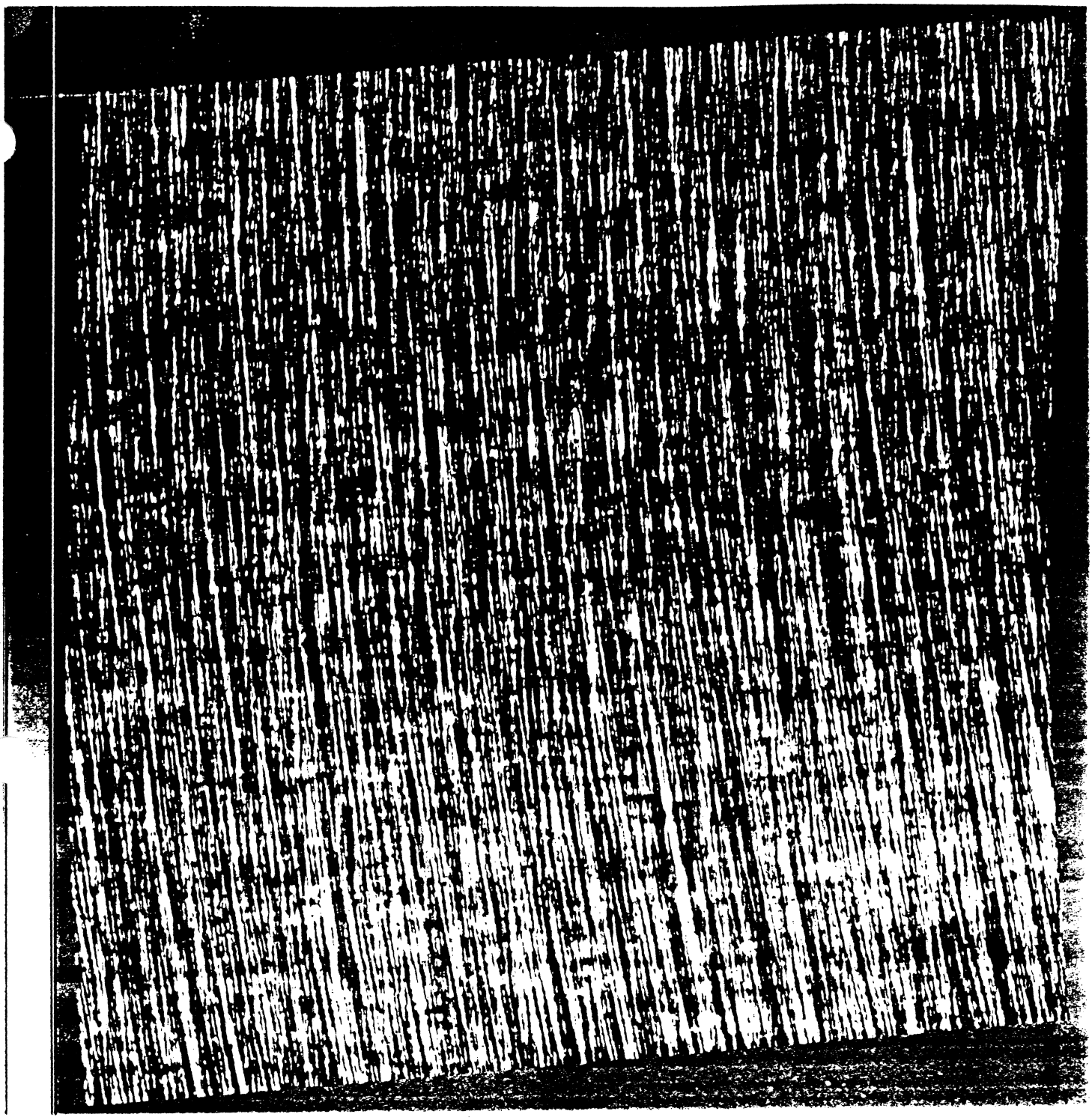

MR signal resolved texture map

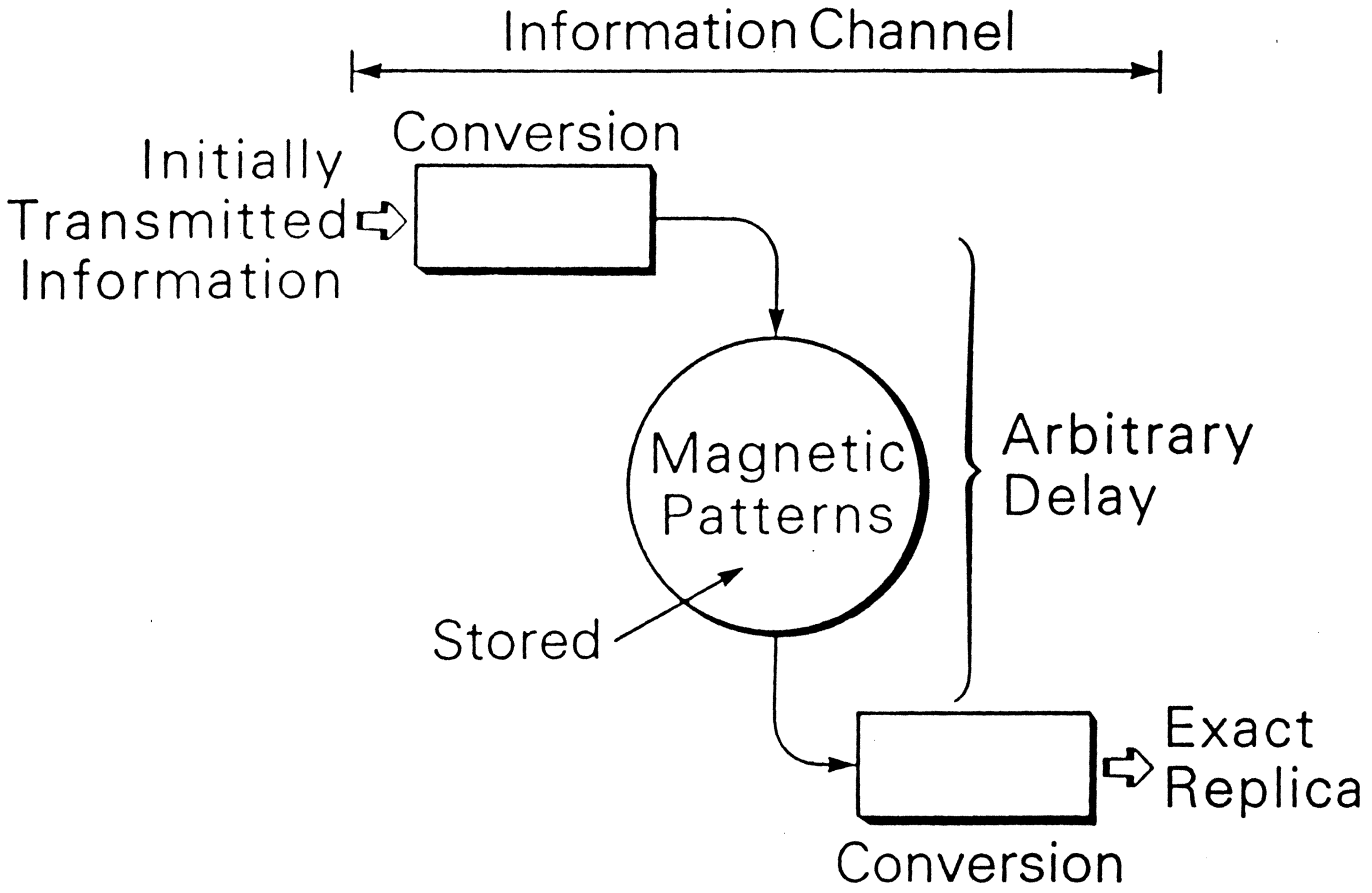
Information Channel
Conversion
Initially
Transmitted
Information
Magnetic
Patterns
Arbitrary
Delay
Stored
Exact
Replica
Conversion

WHY ENCODING-PROCESSING ?

At write-read process (mapping) we lose some information

This is due to:

Noise Contamination

Interference Injection

Signal Distortion 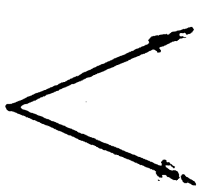 linear, non-linear

This can be counteracted by:

- Encoding
- Signal Processing

Channel Front-End

Definition

The components ahead of the channel data module form the ***channel front-end***

Front-End Components

- Read/Write transducer
- Transducer-electronics interconnect
- Flex cable (input)
- Electronics module
- Flex cable (output)
- Disk enclosure connector
- Traces on drive electronics card

Two Signal Paths

The front-end comprises two data signal paths:

- ★ Read path
- ★ Write path

Front-End is a System

- The components of a front-end form a ***system***
- The mutual matching of these components becomes important for ***high data rates***
- This system approach is needed because the physical dimensions and the signal frequency content in the front-end necessitates the design of a component in the context of its ***environment***
- A good understanding of ***Recording Physics*** is important to arrive at the design specifications of the front-end components

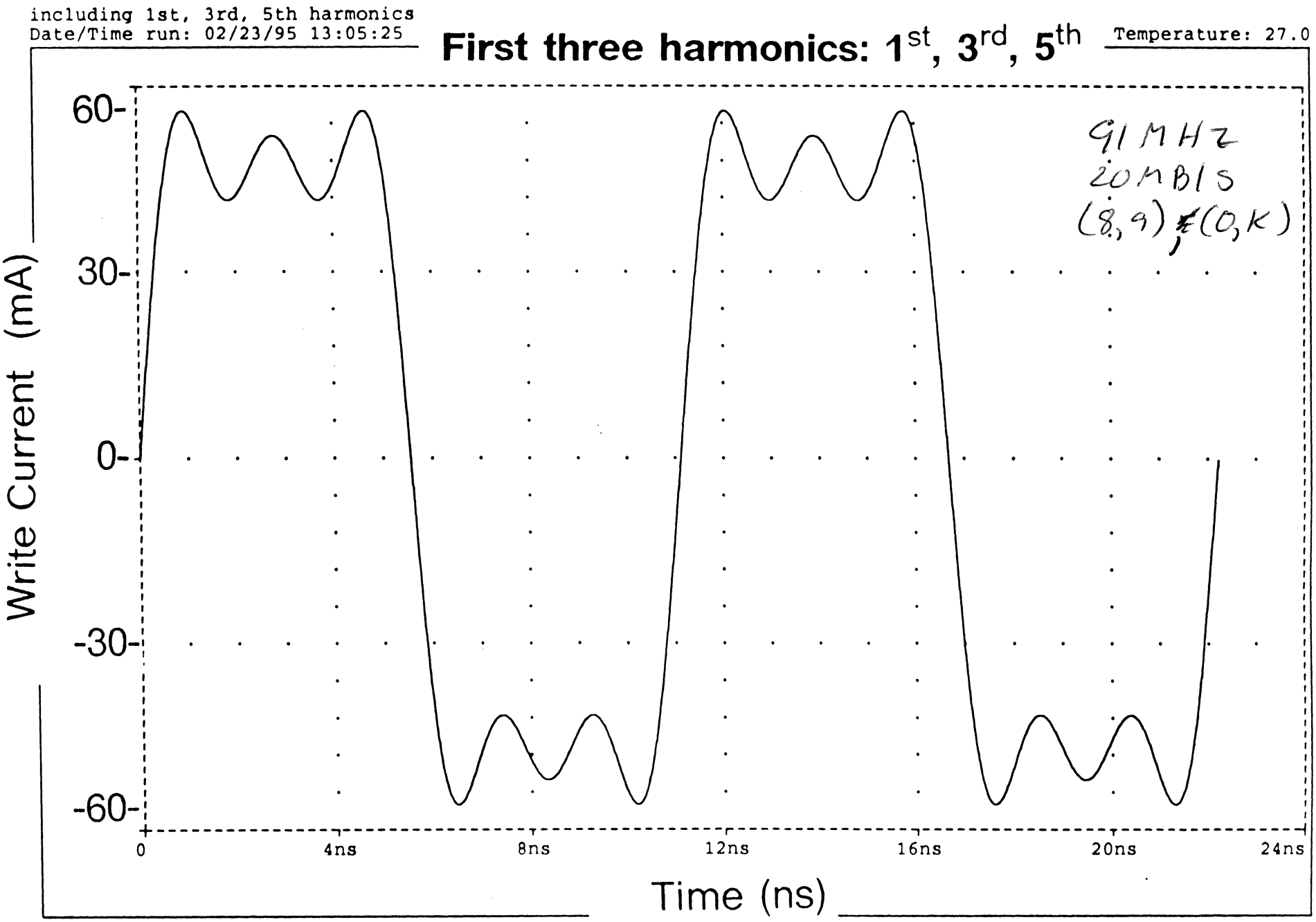
including 1st, 3rd, 5th harmonics
Date/Time run: 02/23/95 13:05:25
First three harmonics: 1st, 3rd, 5th
Temperature: 27.0
91 MHz
20 MBIS
(8,9) (0,K)
60-
30-
0-
-30-
-60-
Write Current (mA)
0
4ns
8ns
12ns
16ns
20ns
24ns
Time (ns)

30 deg phase shift in 5th harmonic
Date/Time run: 02/23/95 13:09:13

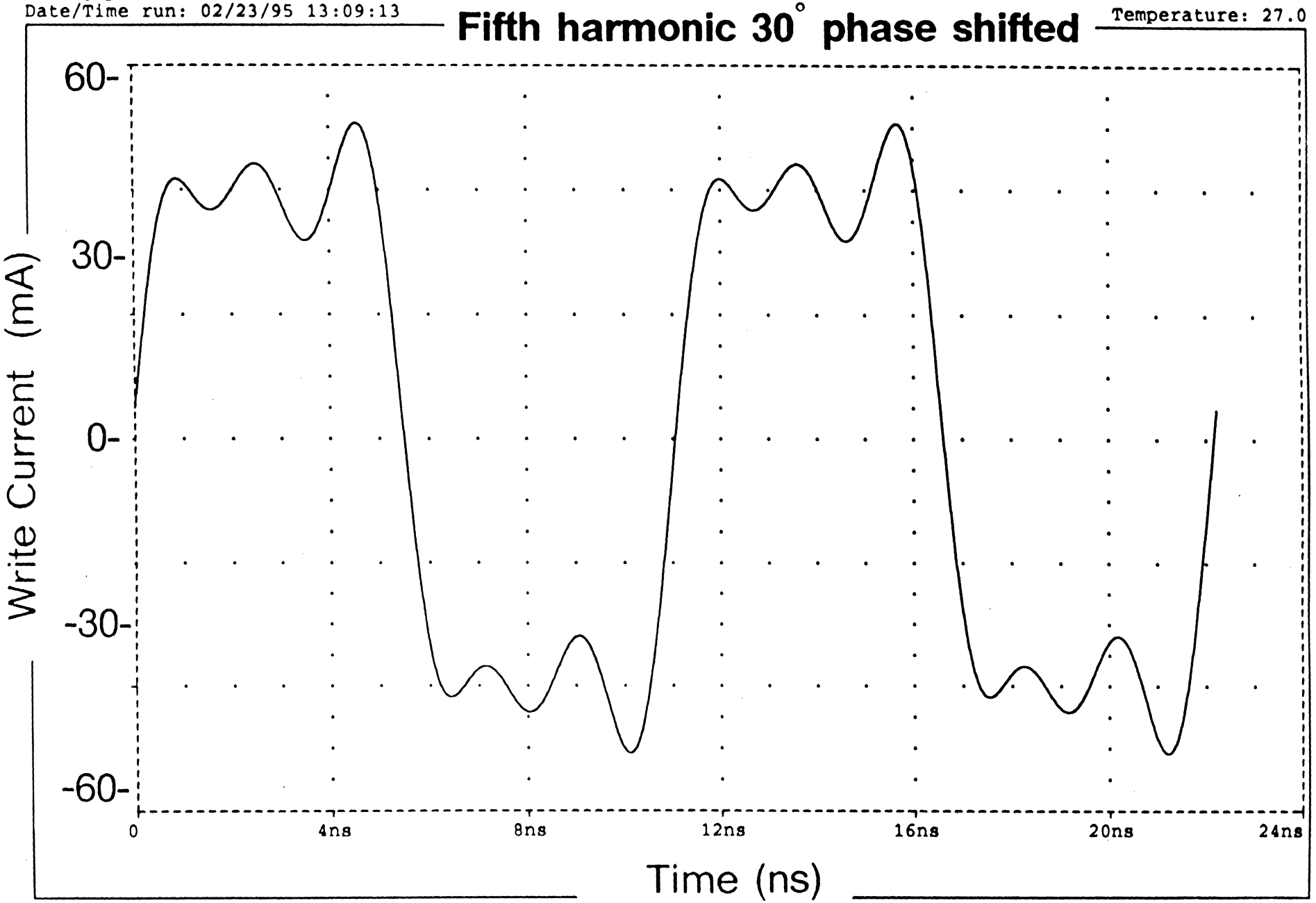

=> write needs much more BW than read channel.

Electronics Role in Information Conversion

- Signal Conditioning (Gain, filtering, TA suppression...)
- Transducer-Electronics Interface (Impedance, biasing...)
- Interference Rejection (CMRR, PSRR...)

Interference Rejection

□ *Input Interference Pick-up*

- Capacitively coupled into head
- Couples equally into both head leads
- "Common-mode" type of interference voltage V_{cm}
- Head signal is "differential-mode" type signal voltage V_h

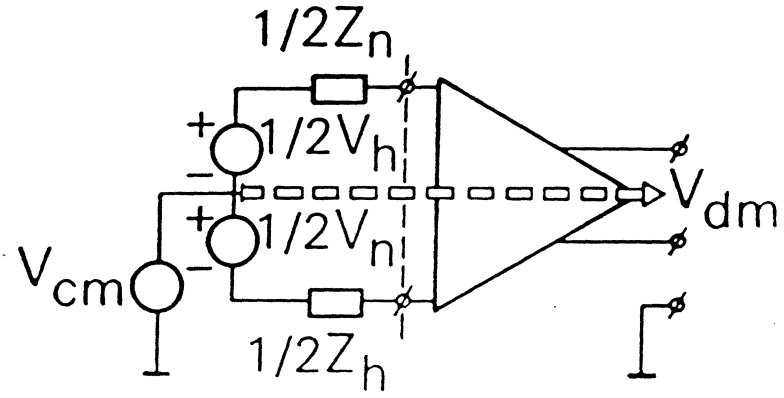

Single-Ended Input Amplifier

(No CM interference rejection)

Differential Input Amplifier

(Rejects CM interference)

Measure of amount of rejection:

Common-Mode Rejection Ratio $\left.\frac{V_{cm}}{V_h}\right|_{same\ V_{dm}}$

$$CMRR = \frac{A_{dm}}{A_{cm}}$$

$$A_{dm} = \frac{V_{dm}}{V_h}$$

$$A_{cm} = \frac{V_{dm}}{V_{cm}}$$

Interference Rejection

- Cause: Any left/right input impedance imbalance causes CMRR to be finite (> 60 dB) ~1k rejection
- Parasitic capacitances cause high-frequency CMRR roll-off of 6 dB/oct Goes to pot @ high freq's.

□ *Power Supply Interference*

- Feedthrough of power supply interference to signal output
- Decouple power supply lines at side of module

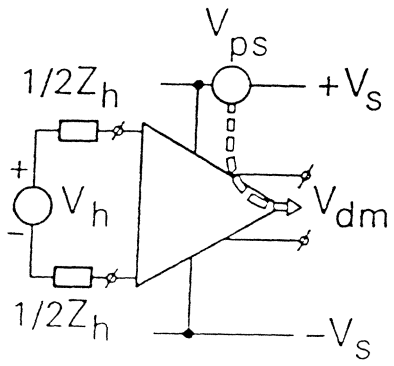

Measure of amount of rejection:

$$\textit{Power Supply Suppression } \frac{V_{ps}}{V_{dm}} = \frac{1}{A_{ps}}$$

Most often "referred to input" (similar to CMRR)

$$\textit{Power Supply Rejection Ratio } \frac{V_{ps}}{V_h}\Big|_{same\ V_{dm}}$$

$$PSRR = \frac{A_{dm}}{A_{ps}}$$

$$A_{dm} = \frac{V_{dm}}{V_h}$$

$$A_{ps} = \frac{V_{dm}}{V_{ps}}$$

Interference Rejection

- Cause: Finite impedance of (vertical) amplifier branches connected between the two supply lines. Supply voltage affects branch current and feeds through into signal output. — single ended
- PSRR is usually worse in SE amplifiers
- High frequency roll-off 6dB/oct

Front-End Electronics

Nomenclature:

- Pre-amplifier
- Head electronics
- Arm electronics

Port-Dedicated ***Port-Common***

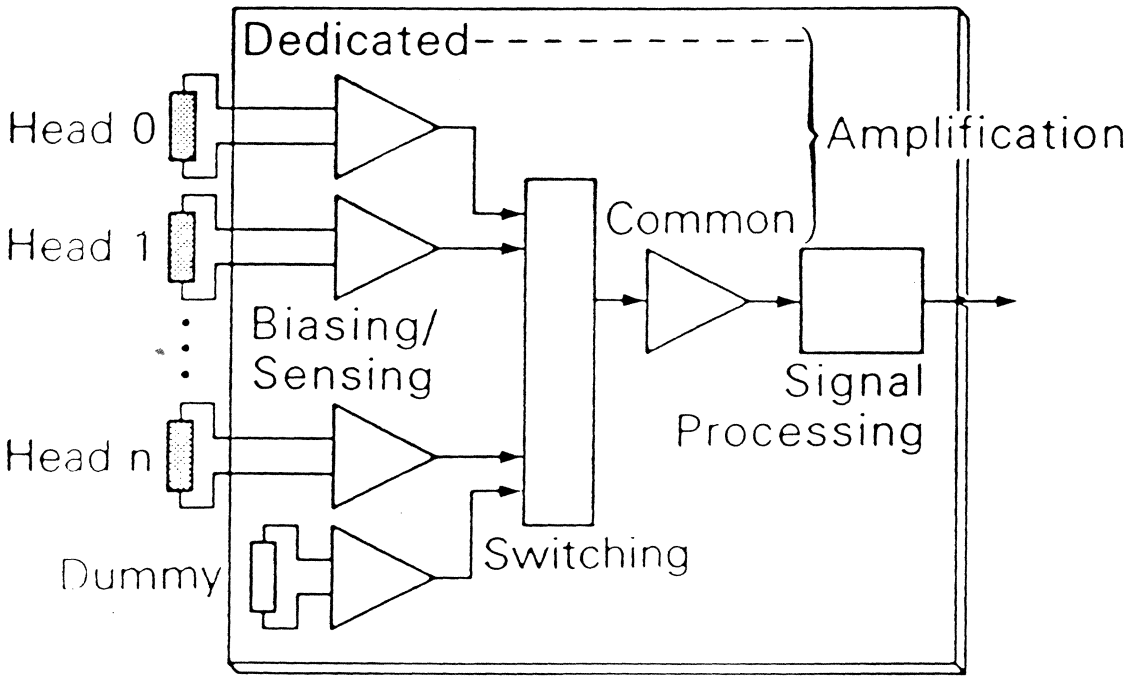

Arm Electronics Module

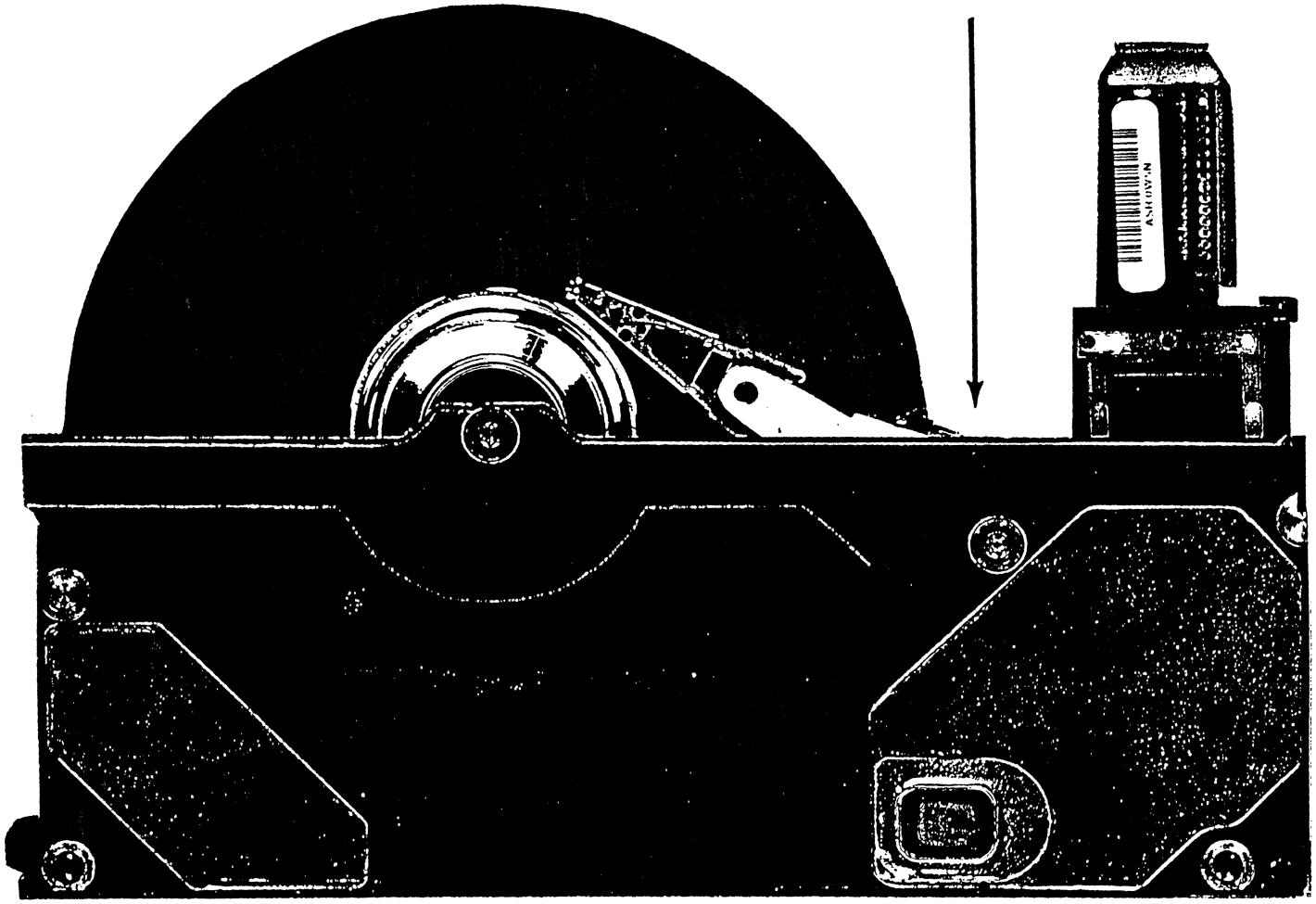

Hard Disk Drive Assembly

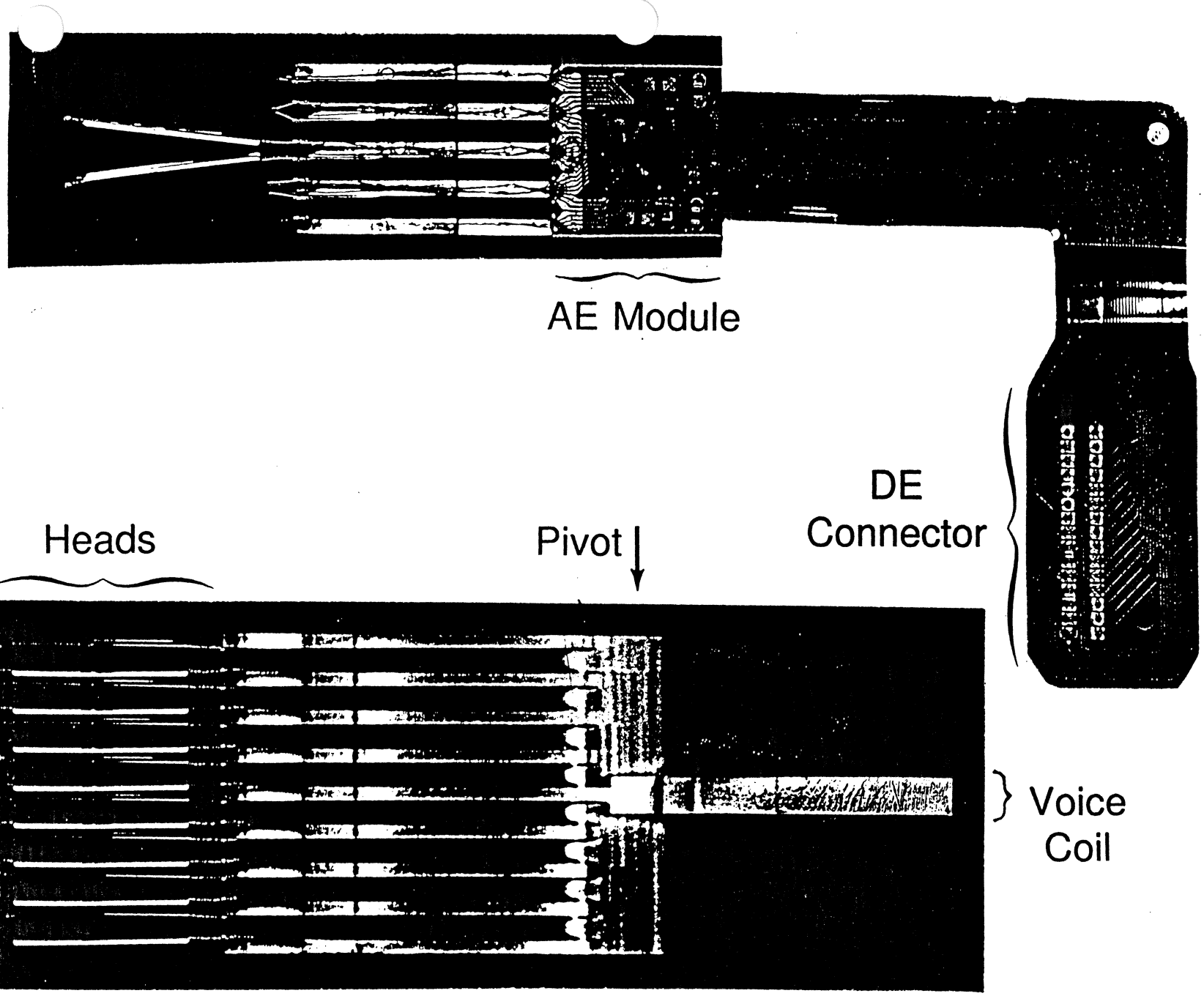

2 elec. modules for high stack.

Magnetic Head Design

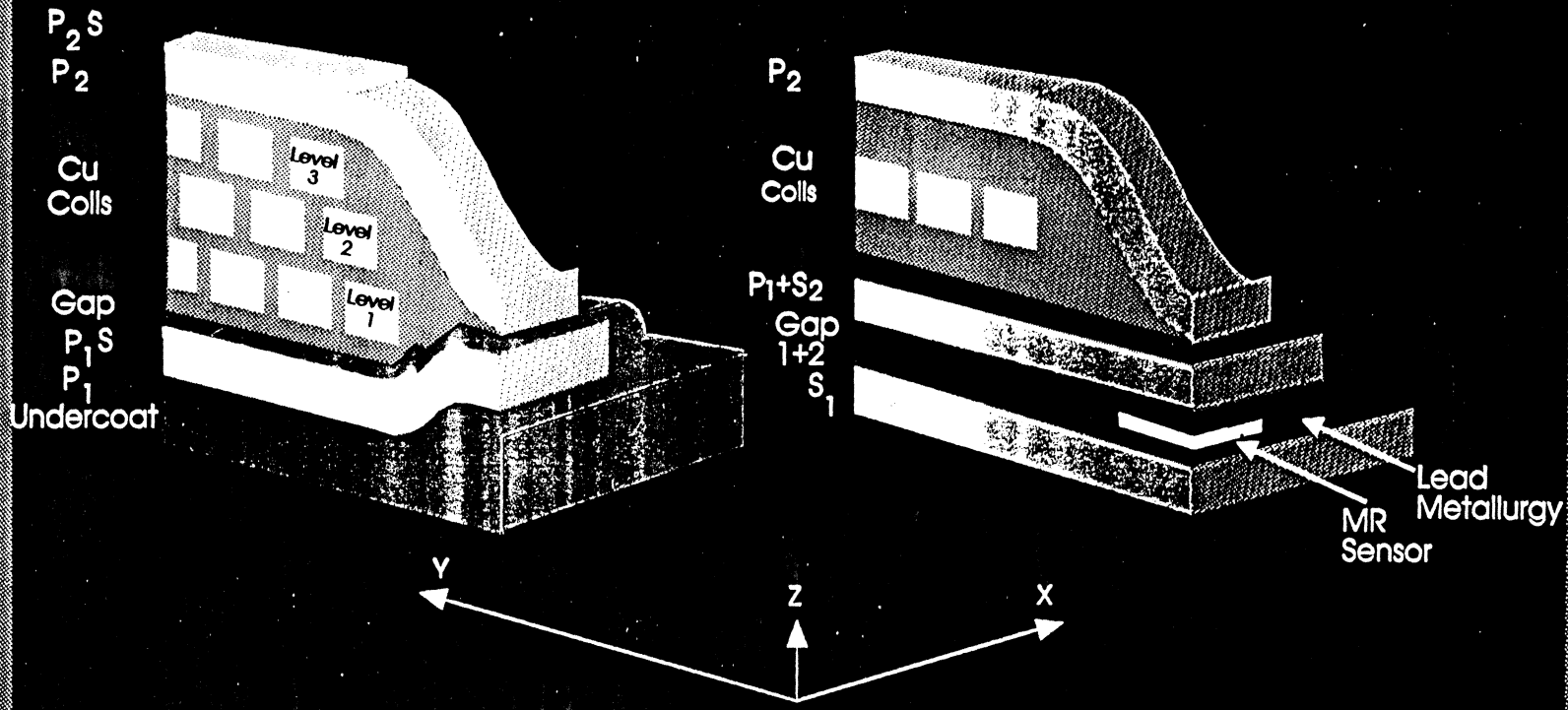

Thin Film Inductive Head Design

Merged MR Head Design

IBM

Ed Grochowski

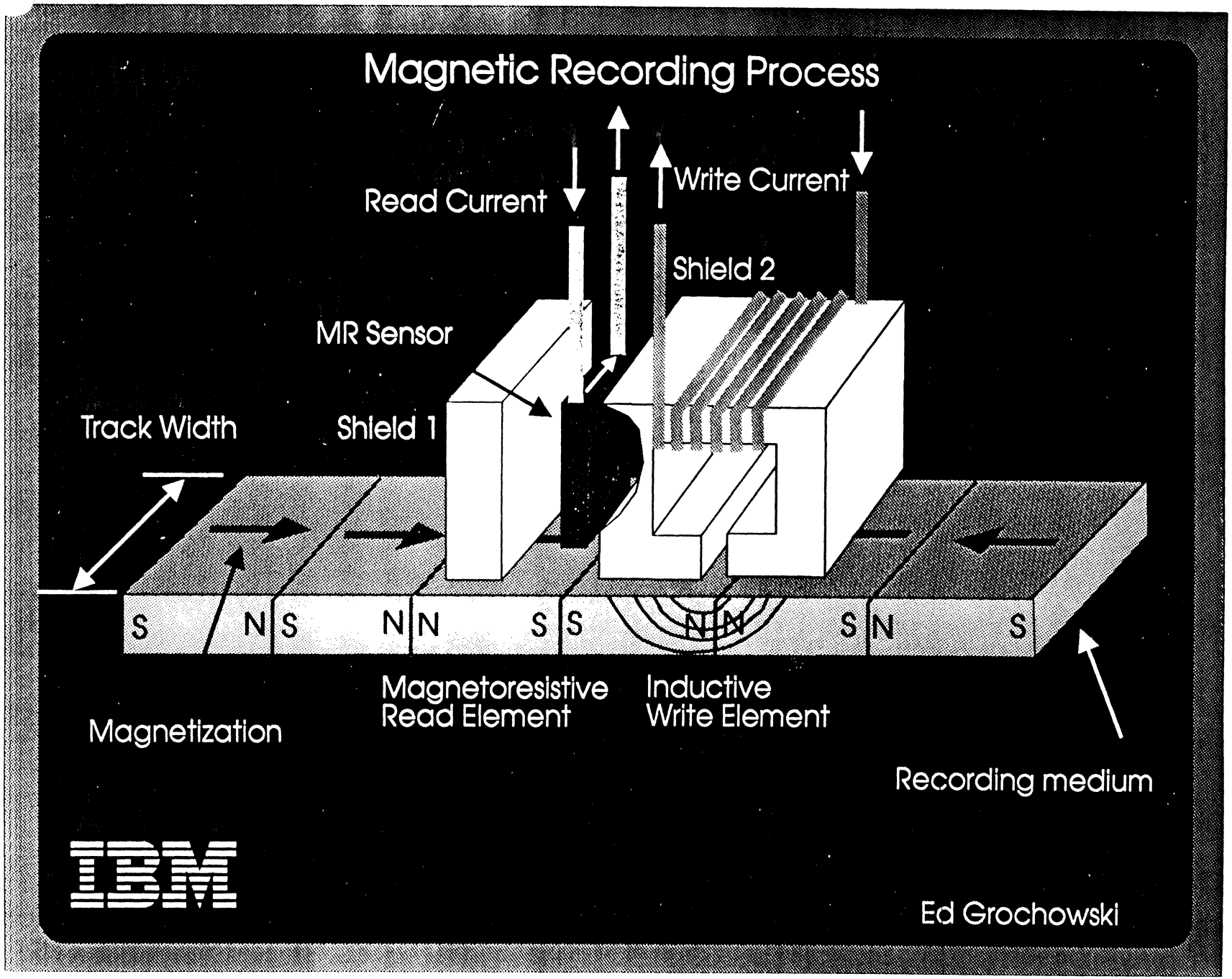
Magnetic Recording Process
Read Current
Write Current
Shield 2
MR Sensor
Track Width
Shield 1
S
N
S
N
N
S
S
N
N
S
N
S
Magnetoresistive
Read Element
Inductive
Write Element
Magnetization
Recording medium
IBM
Ed Grochowski

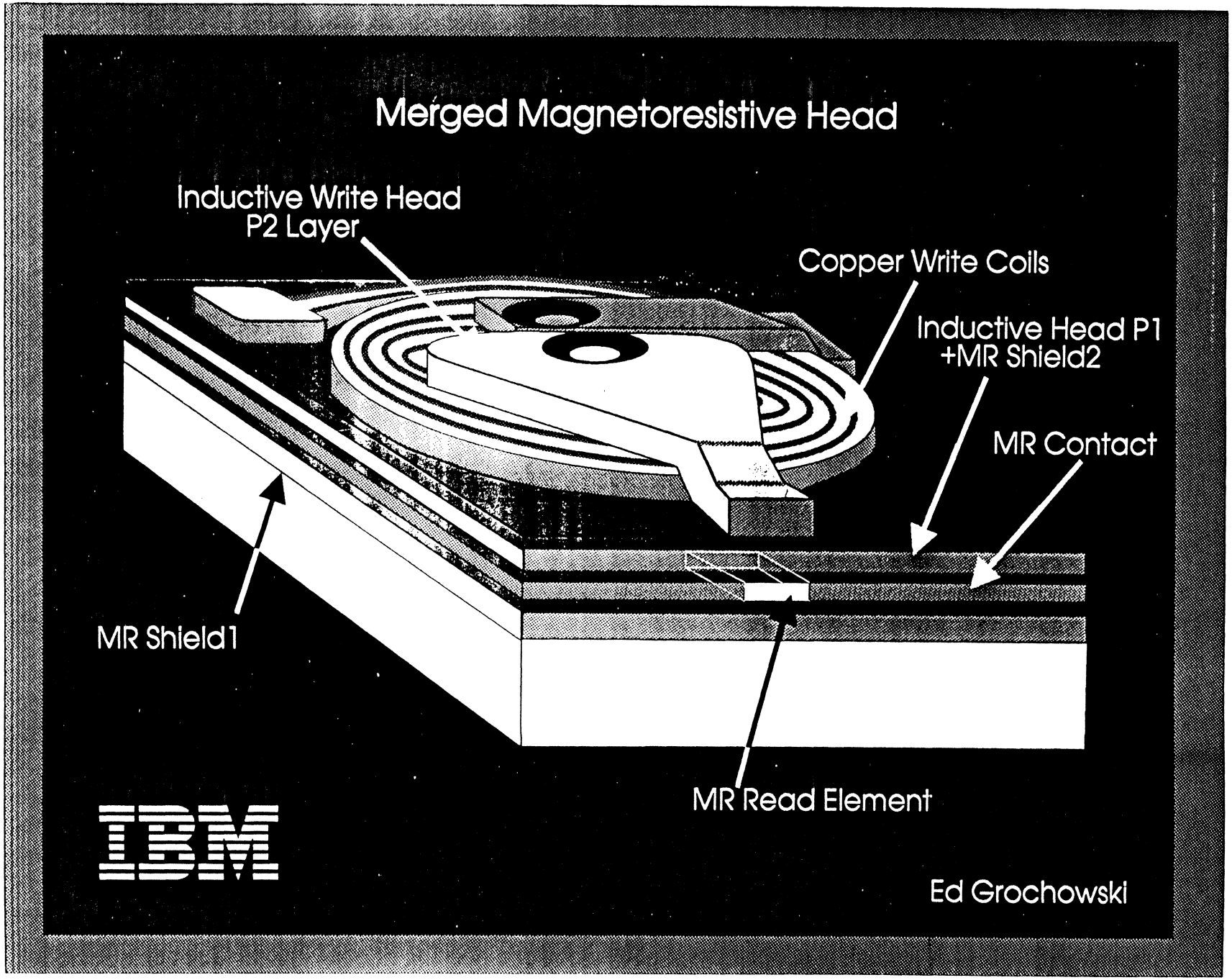
Merged Magnetoresistive Head
Inductive Write Head
P2 Layer
Copper Write Coils
Inductive Head P1
+MR Shield2
MR Contact
MR Shield1
MR Read Element
IBM
Ed Grochowski

AC coupled amp.

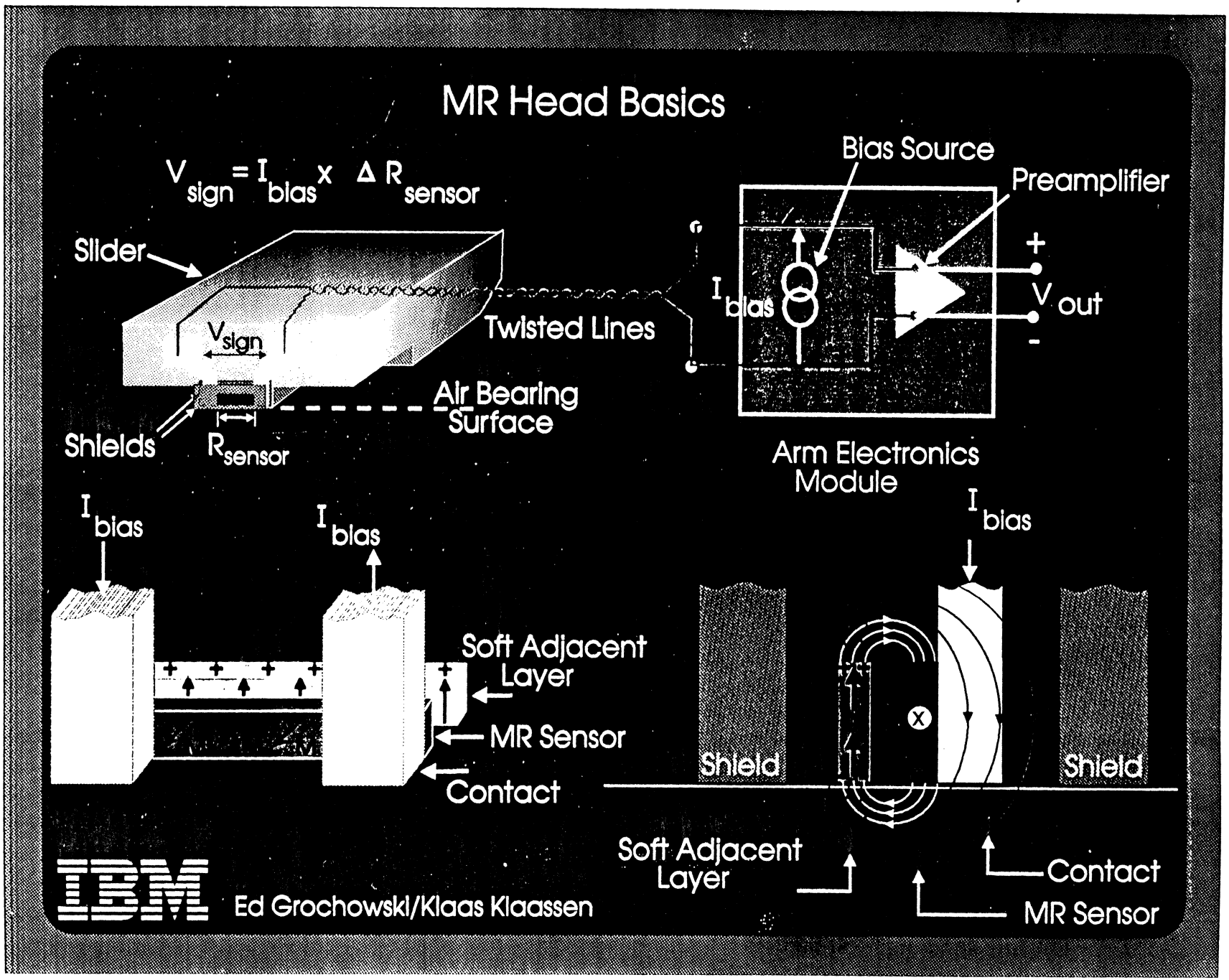

SAL biased so like hard magnet $\mu_r = 1$

Noise/Bandwidth Comparison

Comparing an

- Inductive read head
- MR read head

read-out by the same voltage sensing (high input impedance) pre-amplifier, shows that the

- ***Number of turns n***
- ***(Inverse of) the sensor height h***

have equivalent roles in the

Inductor is limit of useful BW.

- Signal amplitude
- Bandwidth
- Signal-to-noise ratio

Noise and Bandwidth

Comparison (Inductive Read Head / MR Read Head)

Read out by same voltage sensing preamp.

- Input referred noise voltage V_{an}
- Input capacitance C_t

★ Scale inductive head: turns ratio η

$$R_h = \eta R_o\,,\quad L_h = \eta^2 L_o\,,\quad V_h = \eta V_o$$

★ Scale MR head: inverse sensor height ratio η'

$$R_{mr} = \eta' R'_o\,,\quad V_{mr} = \eta' V'_o$$

07/94 (K.B. Klaassen, J.C.L. van Peppen)

Noise, Bandwidth Cont.

- Inductive Head

  Input circuit bandwidth of *critically damped* head:

$$f_{-3dB} = \frac{1}{2\pi\sqrt{\eta^2 L_o C_t}} = \frac{1}{2\pi\eta\sqrt{L_o C_t}}$$

  (Spot) Signal-to-Noise Ratio ($\Delta f = 1$ Hz)

$$SNR = \frac{V_h^2}{4kTR_h + V_{an}^2}$$

  thermal amp

$$SNR = \frac{\eta^2 V_0^2}{4kT\eta R_0 + V_{an}^2}$$

Noise, Bandwidth Cont.

- MR Head

  Input circuit bandwidth:

$$f_{-3dB} = \frac{1}{2\pi R_{mr} C_t} = \frac{1}{2\pi \eta' R'_o C_t}$$

$R_{mr} C_t = \tau$

Spot SNR: $\Delta f = 1\,Hz$ window

$$SNR = \frac{V_{mr}^2}{4kTR_{mr} + V_{an}^2}$$

V_{an}^2 ← all extraneous noise sources e.g. leads.

$$SNR = \frac{\eta'^2 V'^2_o}{4kT\eta' R'_o + V_{an}^2}$$

Noise, Bandwidth Cont.

Hence, the inductive and the MR head have the same scaling factor dependence

Signal: $V = \eta V_o$

Bandwidth: $f_{-3dB} = \dfrac{1}{2\pi\eta\tau_o}$

S/N Ratio $SNR = \dfrac{\eta^2 V_o^2}{4kT\eta R_o + V_{an}^2}$

The role of number of turns n in an inductive head is equivalent to the role of (the inverse of) the sensor height h in an MR head

Some Recording Physics

□ *Single-Element Inductive Read/Write Heads*

- ***Advantages***
  - Self-generating (need no bias)
  - Simple servoing (single element)
    (symmetrical track profile)
  - Linear reader
  - Robust (in view of ESD and corrosion)
  - No thermal asperities (when flying low)

- ***Disadvantages***
  - High velocities only (Faraday, $d\Phi/dt$ sensitive)
  - Large N (narrow trackwidths)
  - High inductance (high speed writing requires large electronics supply voltage, dissipation)
  - Limited bandwidth (coil-electronics resonance)

- ***Probably not extendable beyond***
  (12.5 MB/s, 5 μm tracks)

Inductive Heads

Single-element read/write transducer

- *Scale head turns N*

  $V_h = NV_o$

  $R_h = NR_o$ Leads: $L = L_l$

  $L_h = N^2L_o$

  $C_h = NC_o$ Extra, parallel port:

  $I_W = MMF/N$ $C = C_e$

- Critically damped head band-end:

$$\omega_o = \frac{1}{\sqrt{LC}} = \frac{1}{\sqrt{N^3 L_o C_o}}$$

- Degrades quickly for increasing N
  (needed for decreasing trackwidths)
- Extra burdened by parallel port (C_e)

For higher data rates/narrower tracks an MR head is unavoidable

Some Recording Physics (Cont)

□ *MR Read/Inductive Write Heads*

Positioning of the two elements:

Side-by-side, piggy back, ***merged***, integrated

- ***Advantages***
  - — Large signal/unit trackwidth
  - — Velocity independent (flux-sensing)
  - — Very large bandwidths possible
  - — Separately optimized read and write heads
    - Low *N* write head
    - Write-wide, read-narrow
  - — Isolated pulse shape with no undershoot
- ***Disadvantages***
  - — Active read element exposed at ABS
    - Thermal asperities
    - Electro-erosion
    - Corrosion
    - Smearing

Smears & pop corn type noise.

Some Recording Physics (Cont)

- ESD sensitive (/ electron streams moves atoms in sensor (current density & temp driven))
- Electromigration (sensor temp., current density)
- Interdiffusion (sensor temp.)
- Non-linear read sensor (amplitude asymmetry)
- Needs shields for high resolution
- Asymmetrical track profile
- Write-to-read offset (skewed slider, micro jog)
- Complexity (e.g. lapping)

ESD Discharge

Charge Build-Up

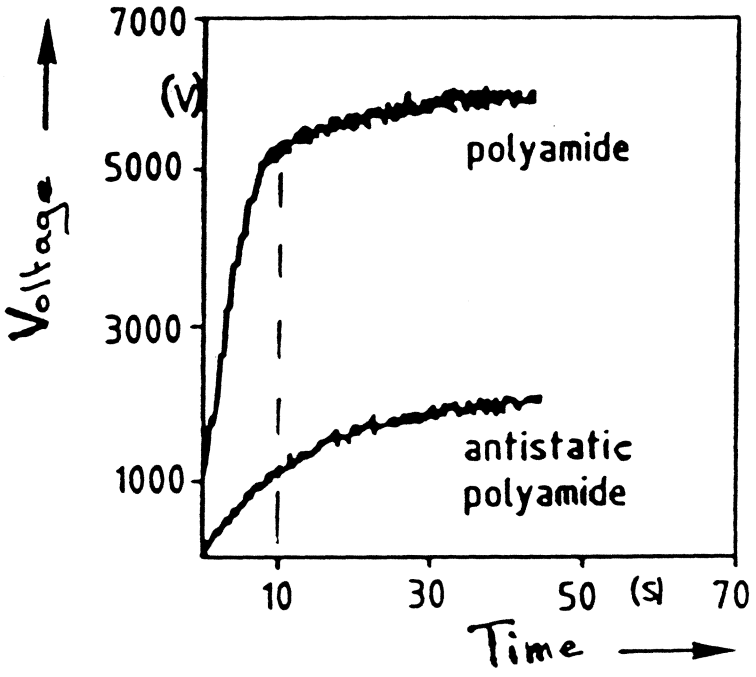

e.g. carpet

Shoe Sole Capacitance

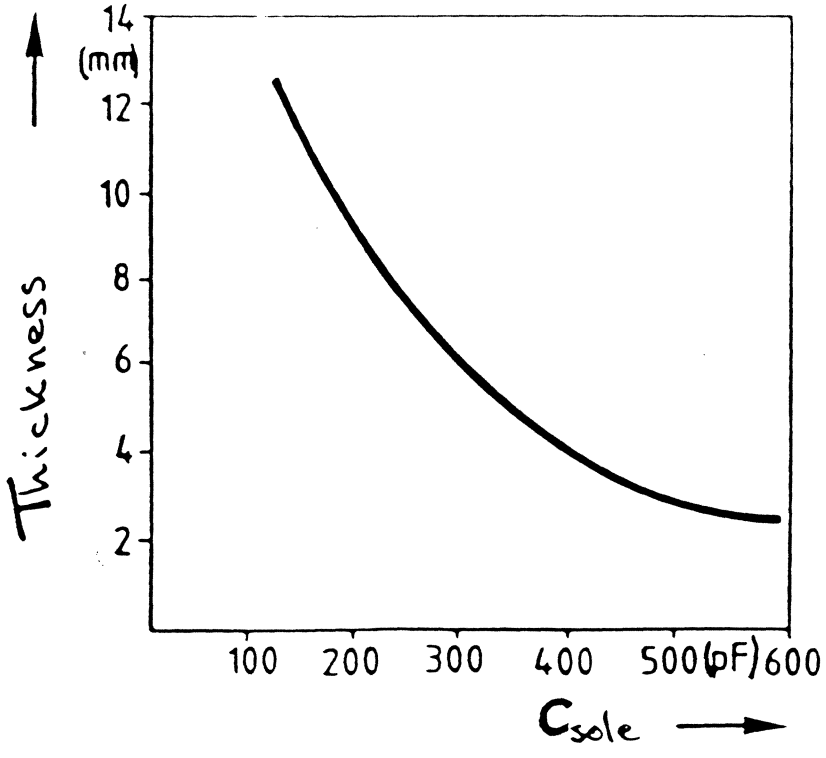

Electro-Static Discharge (ESD)

- MR sensor failure due to ***electical overstress*** caused by accidental electrostatic discharge (tools, people)
- Simulated by ***Human Body Model***

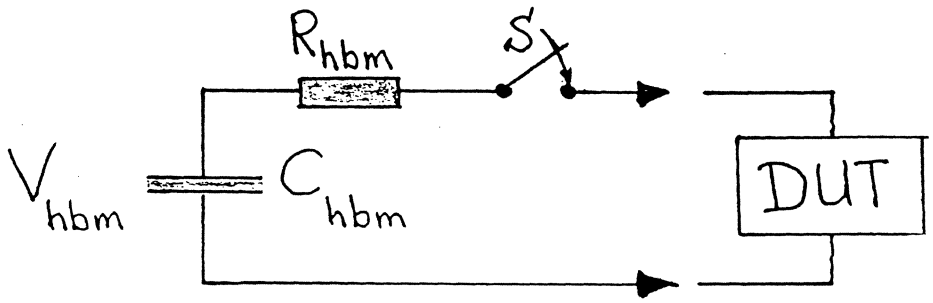

loose metallic object greatly reduces series R & very high currents

$C_{hbm} = 100pF$, $R_{hbm} = 1.5k\Omega$ $(\tau_{hbm} = 150\ ns)$

- ***Energy release*** into MR head

$$E_{MR} = R_{MR} I_o^2 \frac{\tau_{hbm}}{2} \qquad (R_{MR} \ll R_{hbm})$$

$$I_o = V_{hbm}/R_{hbm}$$

$$E_{MR} = \frac{R_{MR}}{R_{hbm}} E_{hbm}, \qquad E_{hbm} = \frac{1}{2} C_{hbm} V_{hbm}^2$$

ESD Discharge

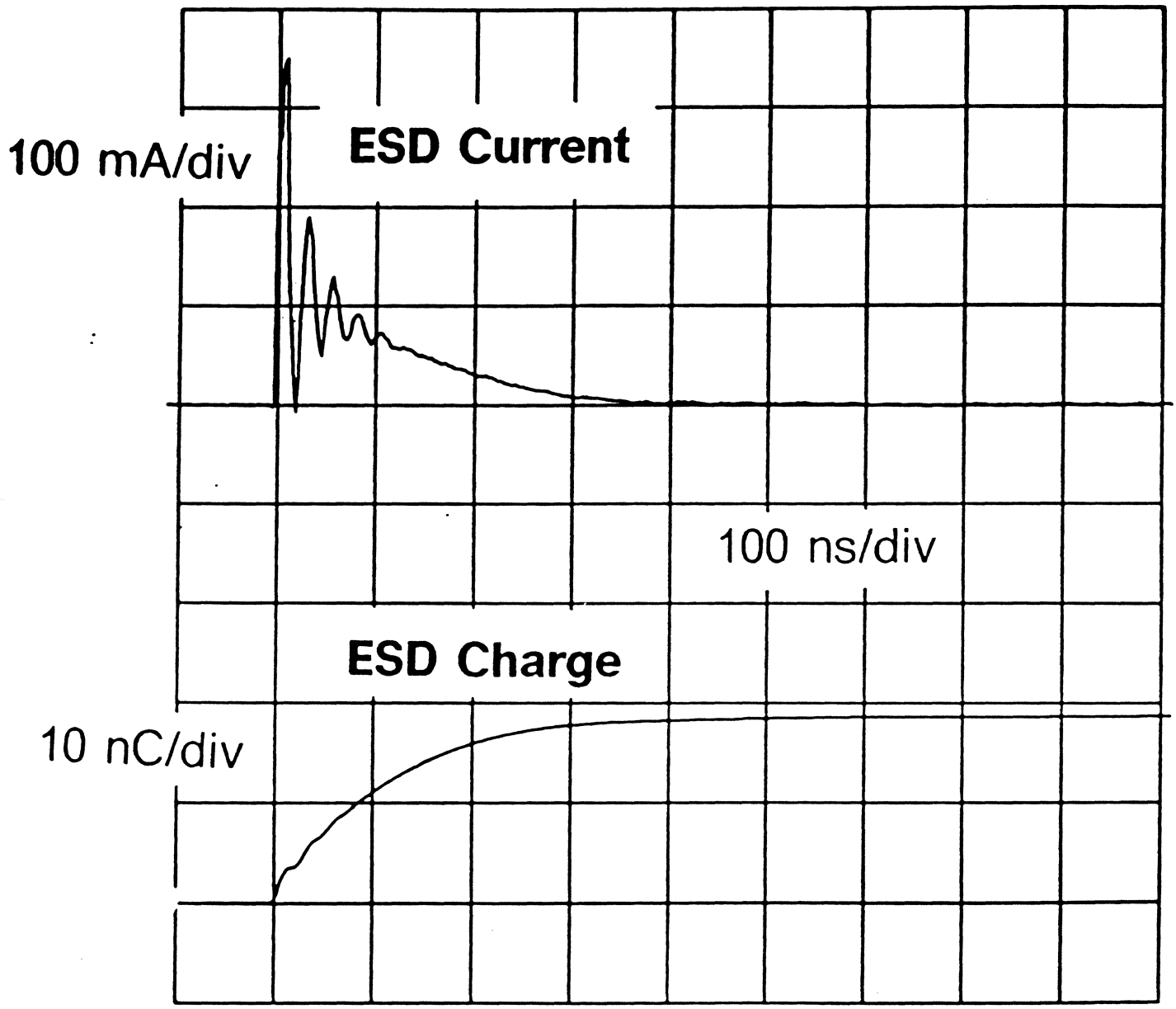

Vertical Desc Avg (Intg (High Prec	Horizontal Desc Main 500MS/sec	Acquire Desc Avg#=172 Backweight	Graticules	Page to All Wfms Status	Rem Wfm 2 Avg (Main
Input Parameters	FFT Control Volts Hanning	Act on Delta None	Main Size 100n s/div	Pan/ Zoom Off	Main Position -110n s

ESD Discharge

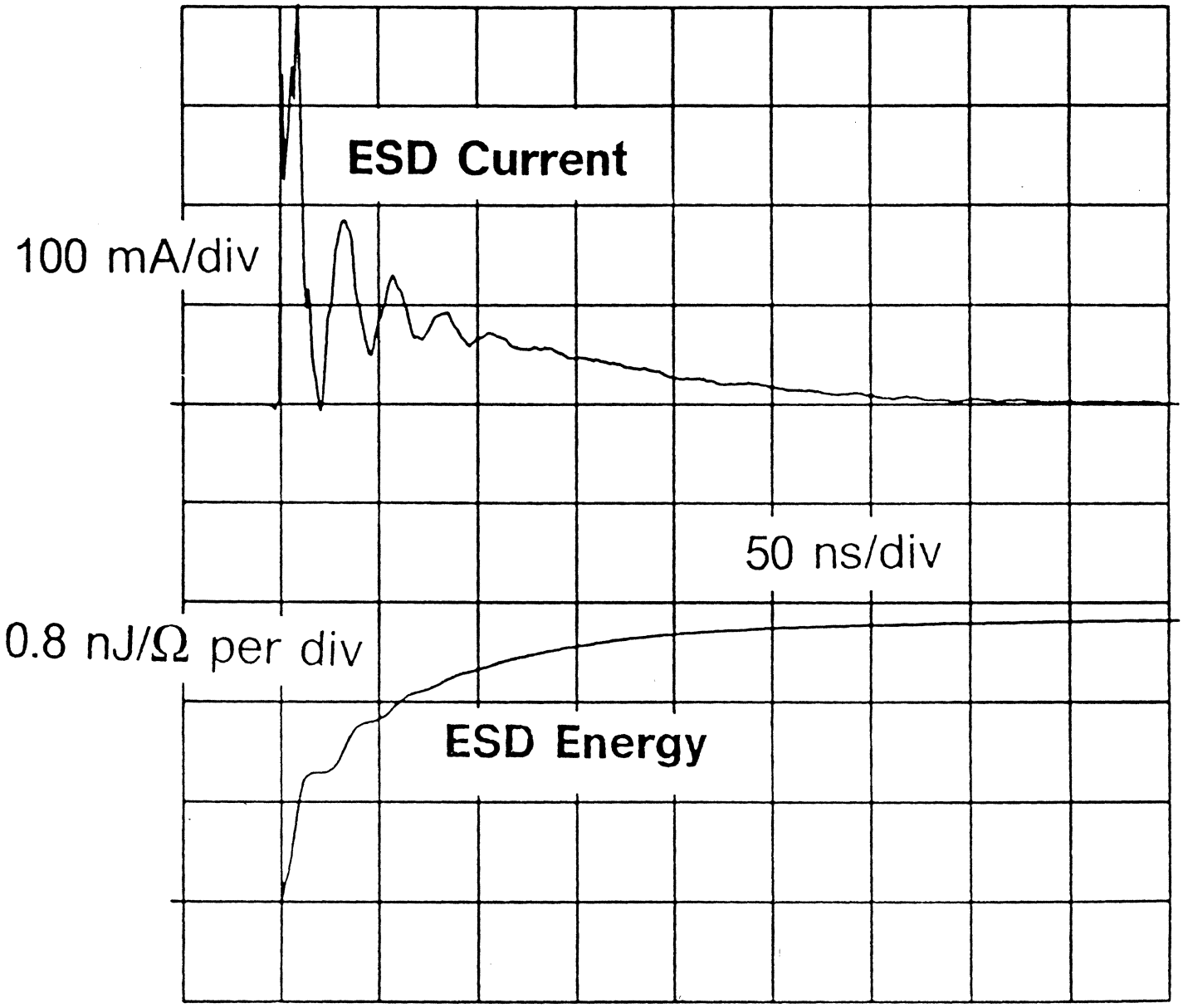

Vertical Desc Avg (Intg (High Prec	Horizontal Desc Main 1GS/sec	Acquire Desc Avg#=228 Backweight	Graticules	Page to All Wfms Status	Rem Wfm 2 Avg (Main
Input Parameters	FFT Control Volts Hanning	Act on Delta None	Main Size 50n s/div	Pan/ Zoom Off	Main Position -55n s

- almost adiabatic damage

Electro-Static Discharge (ESD)

- ***Lethal sensor MR peak voltage***
  Heat flow study:

  $V_{p,MR} = K_1 R_{MR} + K_2 TW$

  $K_1 \simeq 33mA, \qquad K_2 \simeq 1.7 \times 10^5\ V/m$

- ***Typical values***
  For $R_{MR} = 30\ \Omega$ head, track width $TW = 7.5\ \mu$m, we expect:

  $V_{p,MR} = 2.28\ V \qquad V_{hbm} = 114\ V$

  $I_{p,MR} = 74.5\ mA \qquad Q_{MR} = 11\ nC$

  $E_{MR} = 13\ nJ \qquad E_{hbm} = 650\ nJ$

- ***Counter Measures***
  ESD protection devices across electronics port similar to those in place to protect the module from ESD damage

  CMOS circuits - compatible requirements

Electromigration

- ***Mean Time To Failure:***

$$MTTF = cJ^{-n} e^{E_a/kT}$$

c constant (cross sectional sensor area)
J sensor current density
n experimentally determined exponent
E_a activation energy
k Boltzmann's constant
T absolute temperature

- ***Self-accelerating void/crack formation***

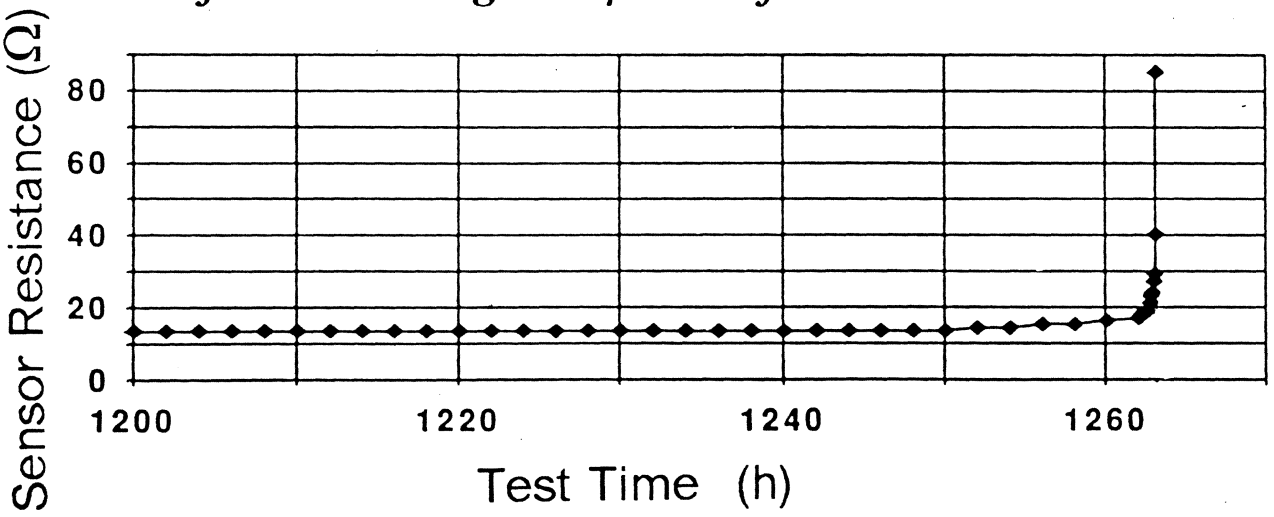

- ***Keep MR bias low enough (T and J), turn off when not needed***

Lapping Issues

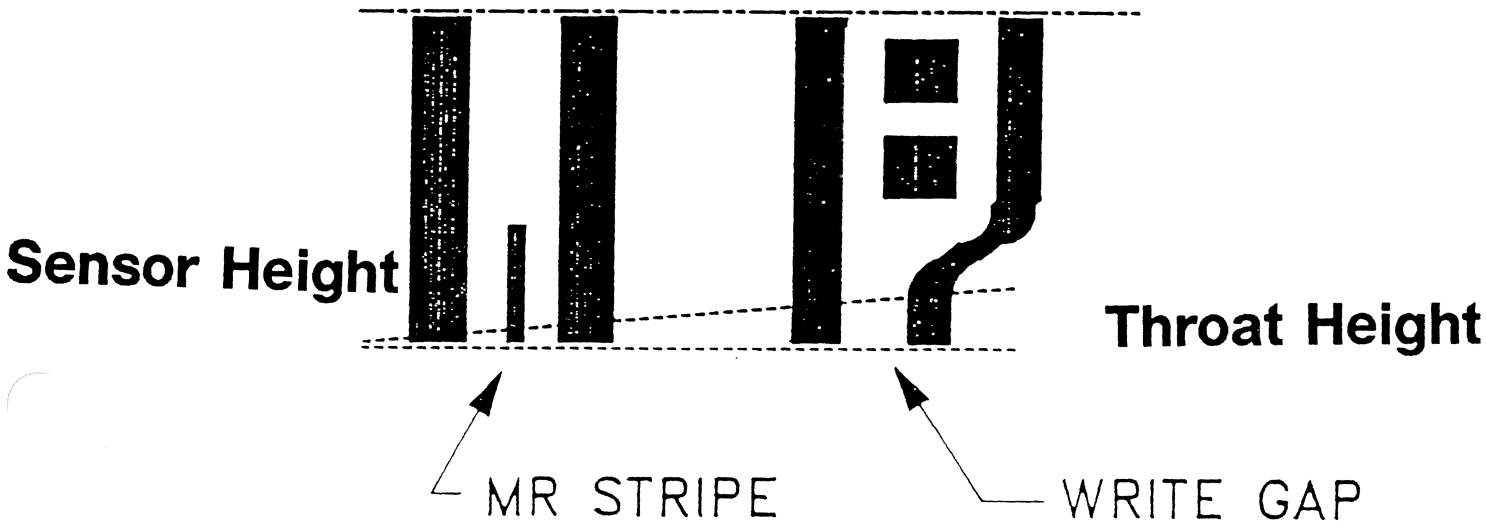

Base Line Disturbances

Base line disturbances (ABS exposed MR heads):

- ***Thermal Events***
  - Additive to data signal

  A. Classical "Thermal Asperity" (TA)
  - o Fast rising (electronics BW limited)
  - o Compound, fixed exponential decay
  - o Mono-polar (positive)
  - o Heating, hard asperity frictional contact

  B. Proximity "Thermal Interference"
  - o Mono-polar
  - o Cooling by lube and proximity of disk "summits"
  - o "Wandering base line" type of disturbance

- ***Conductive Events (CE)***
  - Mono-polar (negative for SE inputs)
  - Short lasting (contact time)
  - Fast rise/fall times (electronics BW limited)
  - Amplitude can be large
  - No data during event

Base Line Disturbances

- ***Smearing Events***
  - Conductive smears across read gap
  - Intermittent contacts
  - Fast rise/fall time (electronics BW limited)
  - Random signal, "Telegraph Noise" (TN)

N.B: High-pass nature of MR front-end electronics affects observed waveshapes

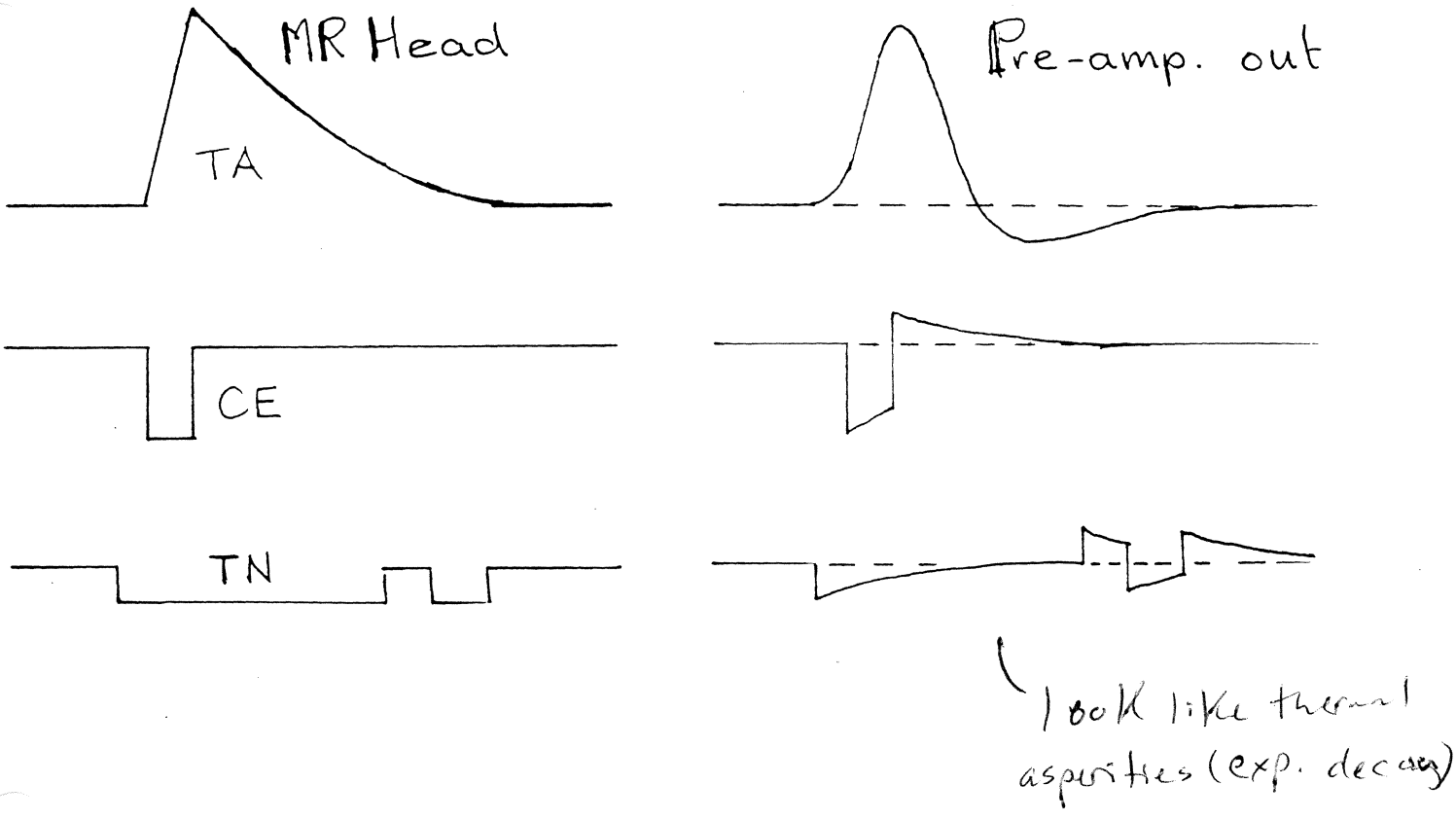

Base Line Disturbances

- ***Counter Measures***

  - *Thermal Events*
    Flag and remove TAs
    Restore base line variations

  - *Conductive Events*
    Turn MR bias off (landing/resting/taking off)
    Minimize voltage difference (sensor-disk)
    Limit ground return current (compare: Ground fault interruptor)

  - *Smearing Events*
    Remove conduction path
    Ground shields, apply potential to MR sensor (flying heads only)

"Classical" Thermal Asperity

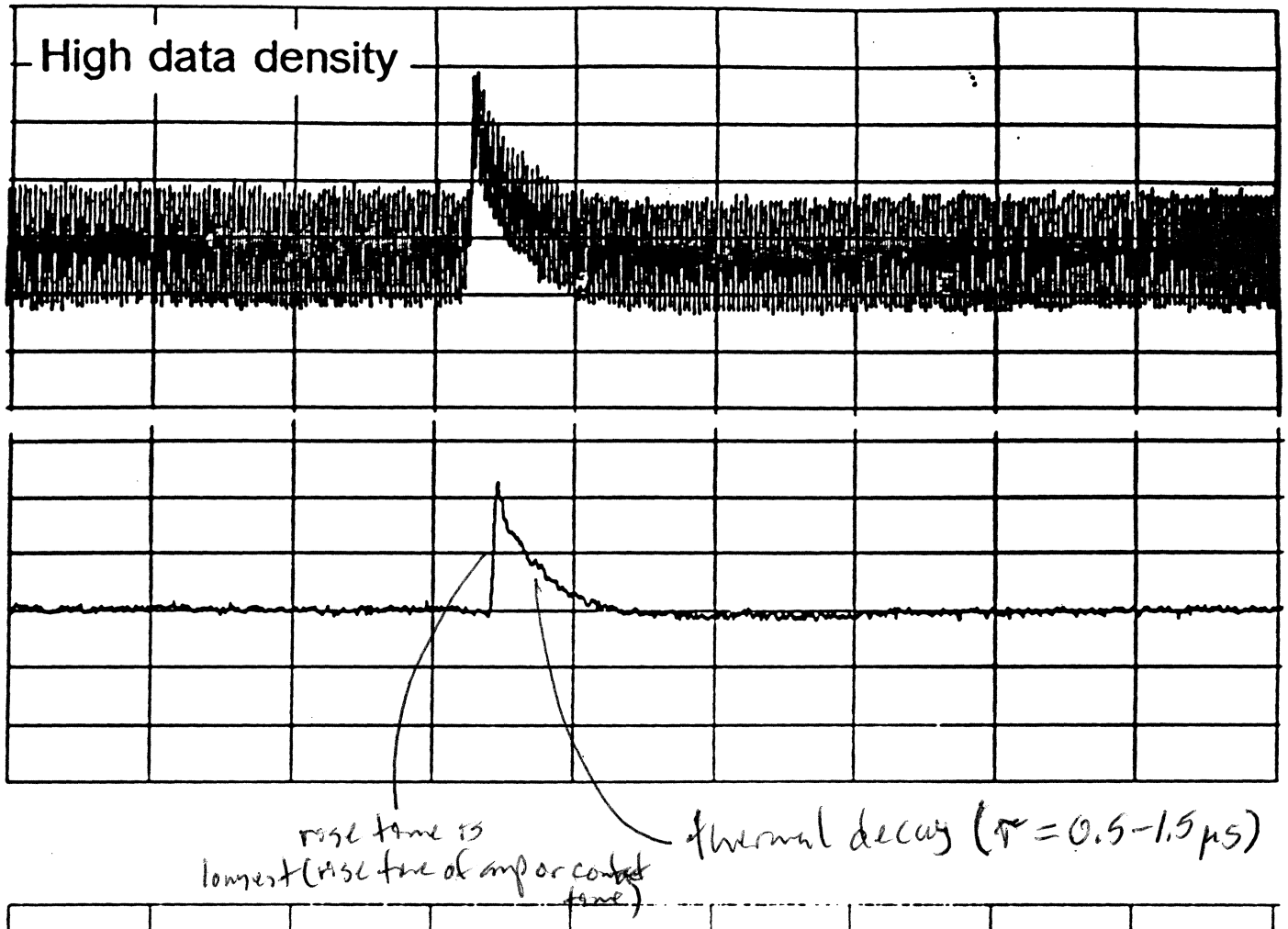

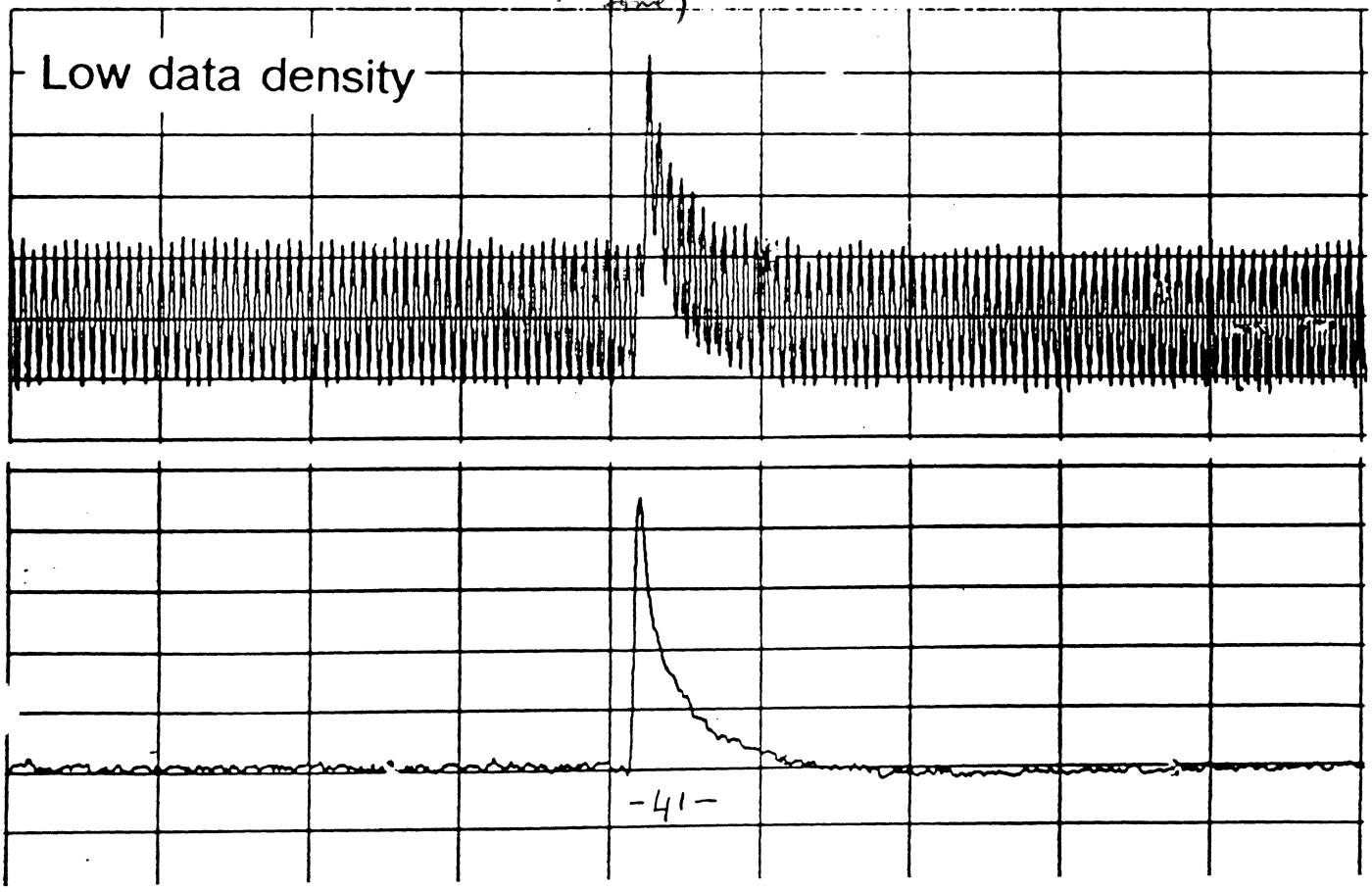

Different Size TAs

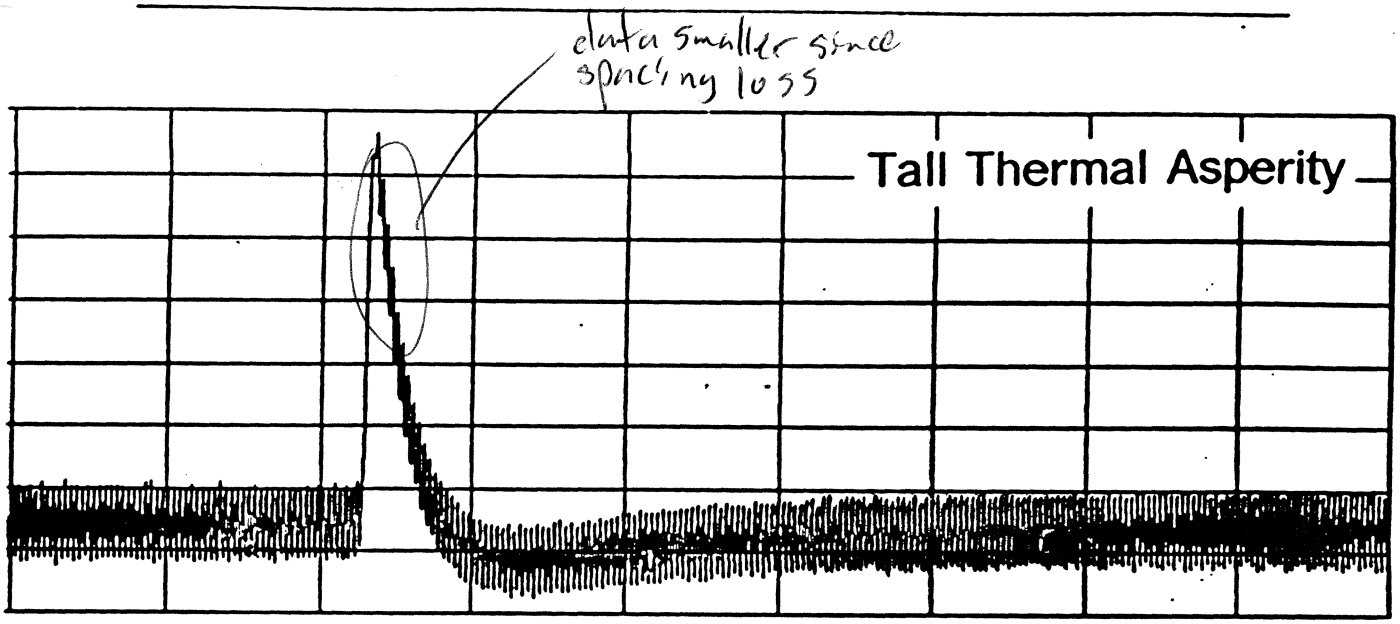

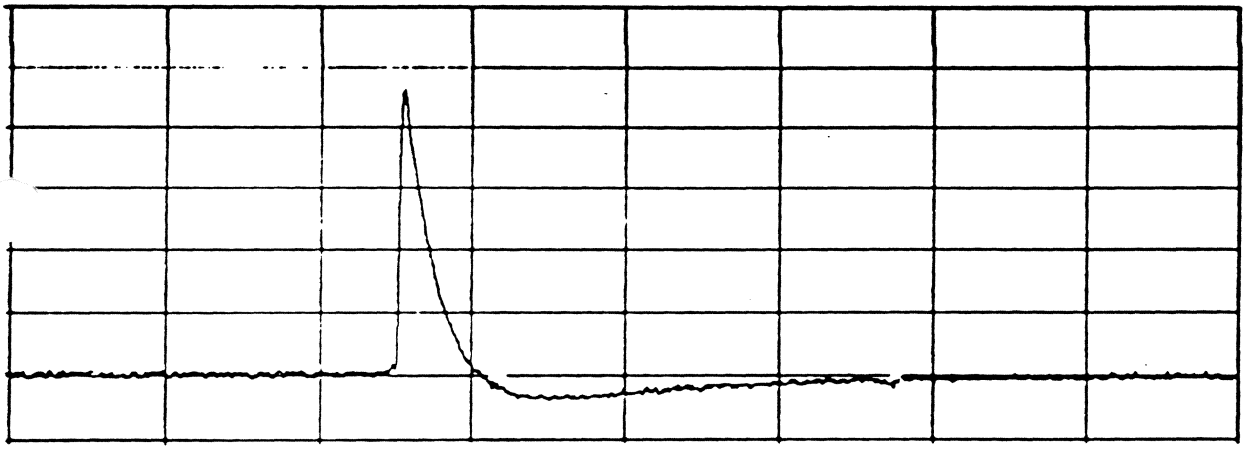

Small Thermal Asperity

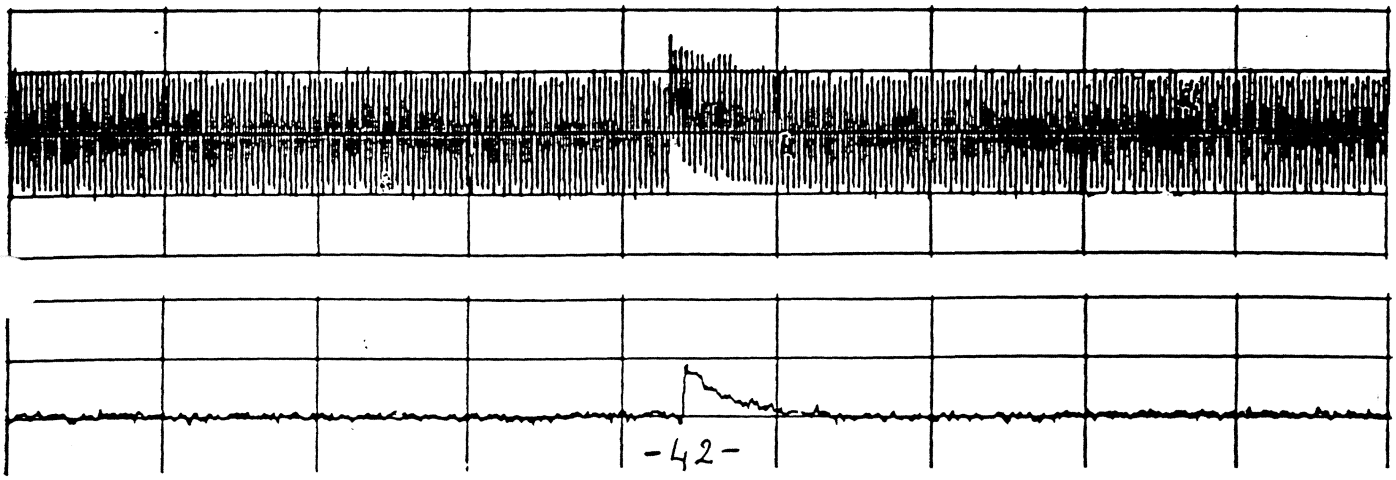

Dual Stripe MR Head

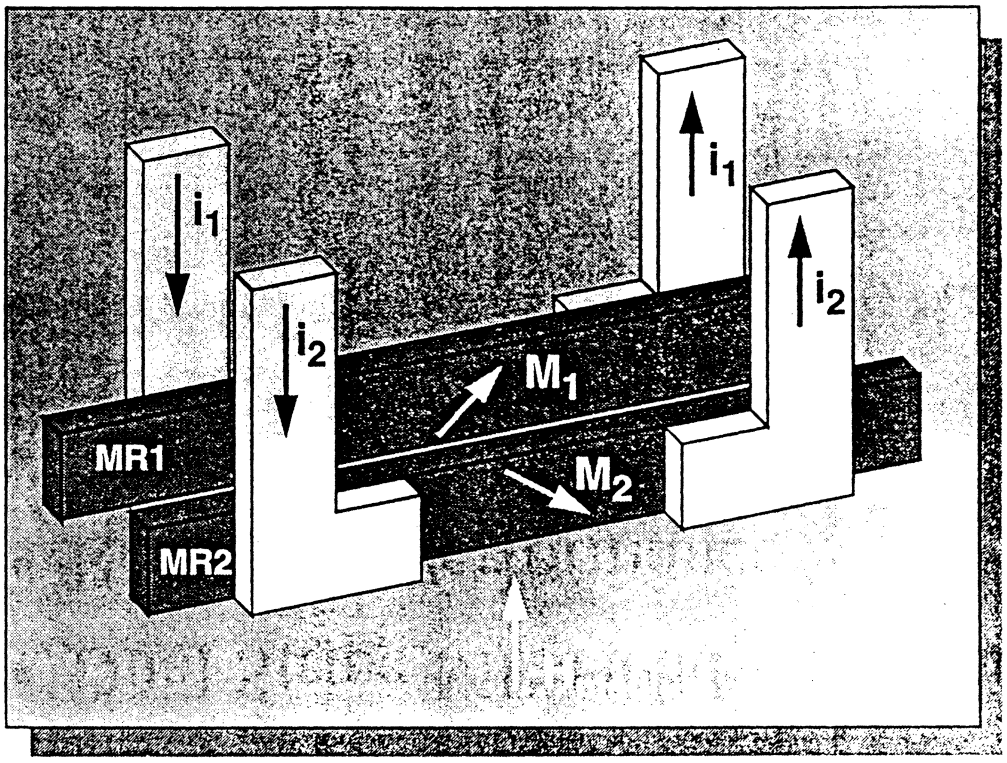

Why Dual Stripe Design?

- Double the signal
  (for same bias current I_B)
- Cancelling of even harmonics
  (on track) — not off-track
- Thermal asperity suppression
  (10% tolerance → 20 dB)
  resistance.
- Symmetrical track profile
  (servo advantage)
- Interference rejection
  (10% tolerance → CMRR = 20 dB)
  resistance

Issues Dual Stripe Design

- Interstripe shorting
- Alignment tolerances
- Needs matched MR sensors
- Needs 3 MR leads
- Temperature rise limited biasing
  → $\frac{1}{2}I_B$ per stripe → same signal

  — only cools to external sinks
- Disk flux shared between sensors
  → smaller signal

Asperity Reduction Circuit (ARC)

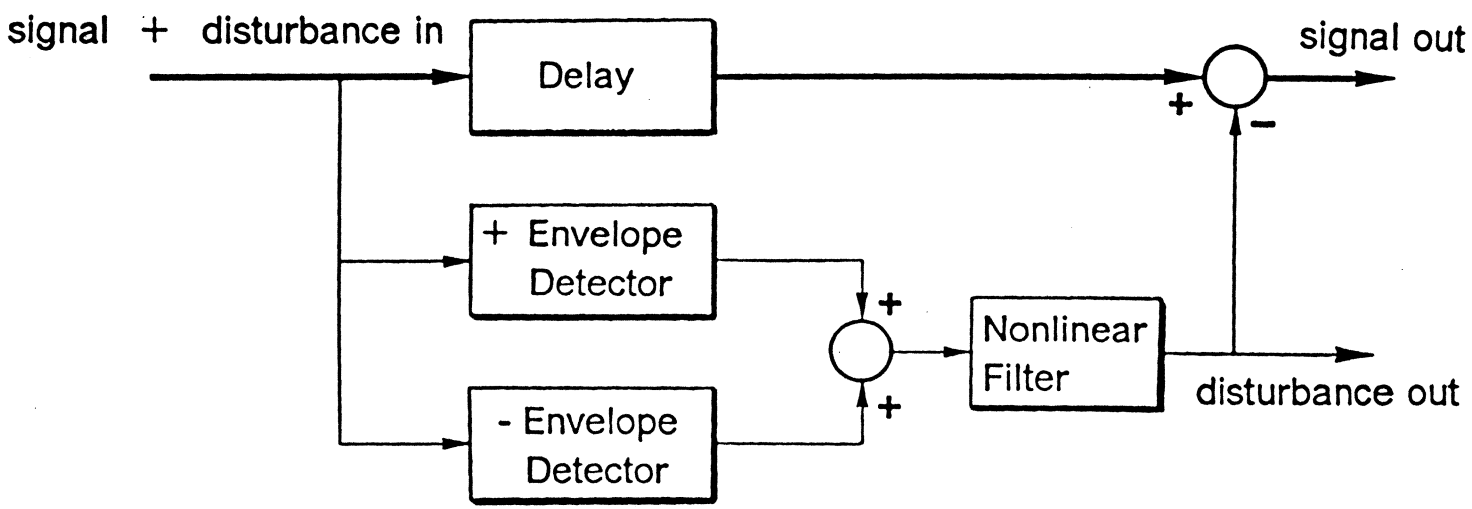

In practice drop delay so do correction after asperity begun.

United States Patent [19]

Jove et al.

[11] Patent Number: 4,914,398

[45] Date of Patent: Apr. 3, 1990

[54] METHOD AND CIRCUITRY TO SUPPRESS ADDITIVE DISTURBANCES IN DATA CHANNELS CONTAINING MR SENSORS

[75] Inventors: Stephen A. Jove, Watsonville; Klaas B. Klaassen; Jacobus C. L. van Peppen, both of San Jose, all of Calif.

[73] Assignee: International Business Machines Corporation, Armonk, N.Y.

[21] Appl. No.: 226,634

[22] Filed: Aug. 1, 1988

[51] Int. Cl.[4] H03K 5/00; H04B 1/10

[52] U.S. Cl. 328/167; 328/162; 307/520; 307/555; 307/350; 455/296; 455/303; 333/14

[58] Field of Search 307/350, 358, 359, 555, 307/520; 328/165, 167, 169, 151, 162; 455/296, 303, 304, 305-308, 222, 225; 333/14; 330/109, 149, 151

[56] References Cited

U.S. PATENT DOCUMENTS

3,473,131	10/1969	Perkins	328/163
3,566,281	2/1971	Baumann	328/171
3,588,705	6/1971	Paine	328/165
3,903,485	9/1975	Dolby	328/169
4,141,494	2/1979	Fisher	307/351
4,163,909	8/1979	Harr	307/351
4,356,389	10/1982	Quirey	235/455
4,433,256	2/1984	Dolikian	328/169
4,698,597	10/1987	Merli et al.	328/165
4,739,518	4/1988	Bickley et al.	455/303
4,780,623	10/1988	Yagi	328/165

Primary Examiner—Stanley D. Miller
Assistant Examiner—Timothy P. Callahan
Attorney, Agent, or Firm—Henry E. Otto, Jr.

[57] ABSTRACT

A method and circuitry are disclosed for suppressing additive transient disturbances in a data channel; e.g., due to thermal transients caused by an MR transducer contacting moving a storage surface. Positive and negative envelope detectors each have their inputs connected to the channel, and provide respective outputs which are summed and contain an envelope component and a residue component. A buffer interconnects the detectors to allow both detectors to follow rapid positive excursions of the data channel signal. A nonlinear signal-adaptive filter is connected to the summed output to further reduce the residue component. The data channel signal (or preferably the output from a delay means connected to the channel) is summed with the output from the filter. The relative amplitudes of these two outputs is set such that the resulting summed output signal is free of additive disturbances.

11 Claims, 4 Drawing Sheets

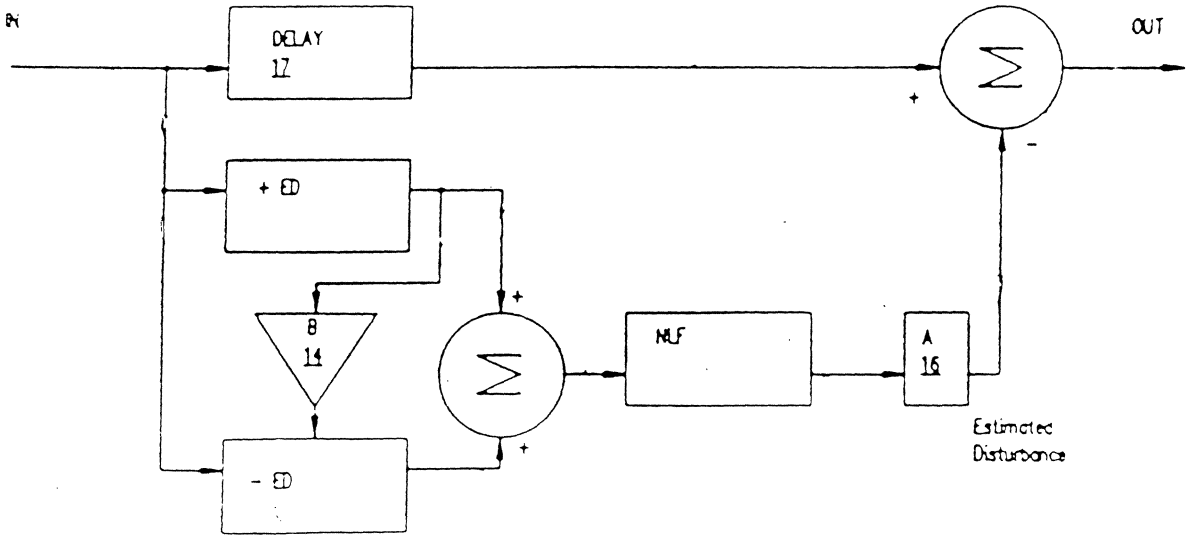

TA Base Line Restoration

Detect base line variation, subtract from signal

Asperity Reduction Circuit (ARC)

Subtractive restoration also provides restored TA

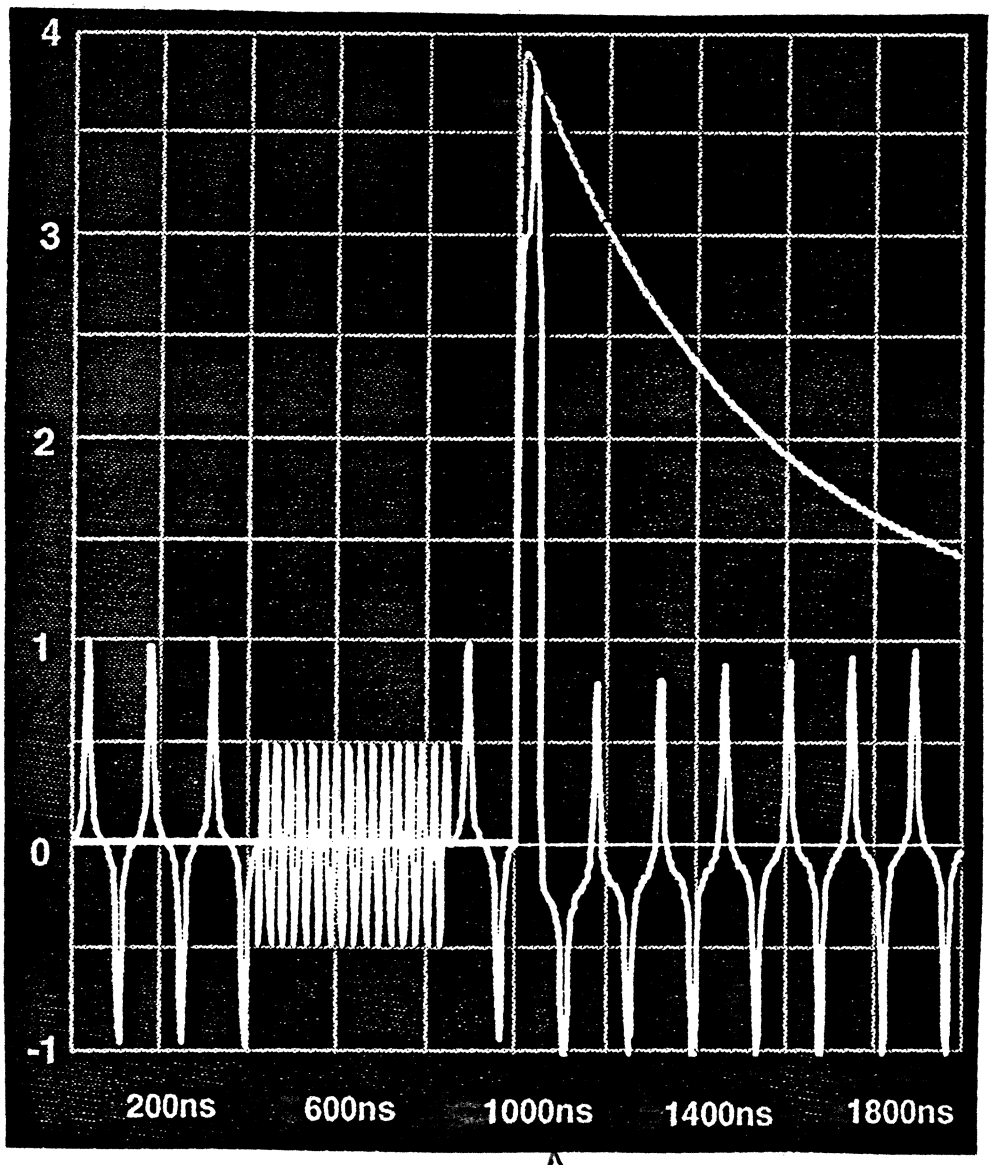

Asperity Reduction Circuit (ARC)

Electronic Thermal Asperity Removal:

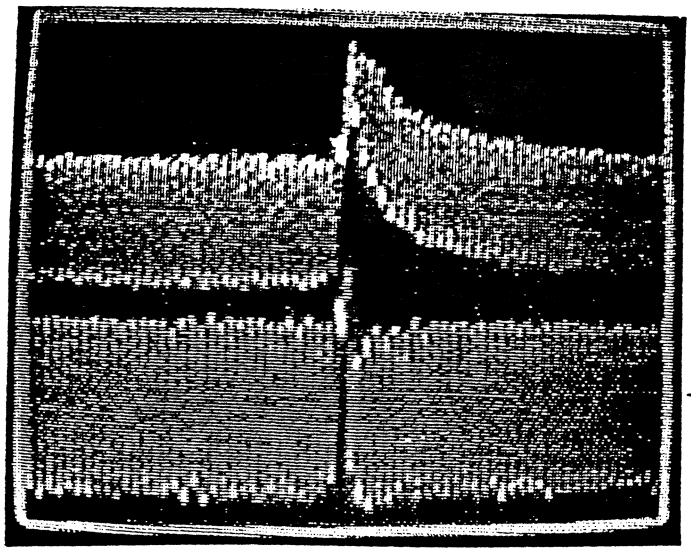

Electronically corrected.
Magnitude 2 times

↑ amplitude loss not corrected (ECC takes care of this)

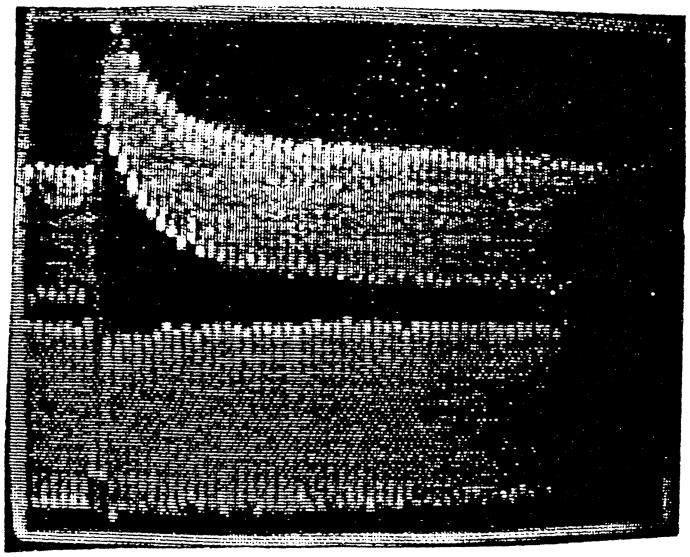

MR Sensor Edge Erosion

Observed phenomenon

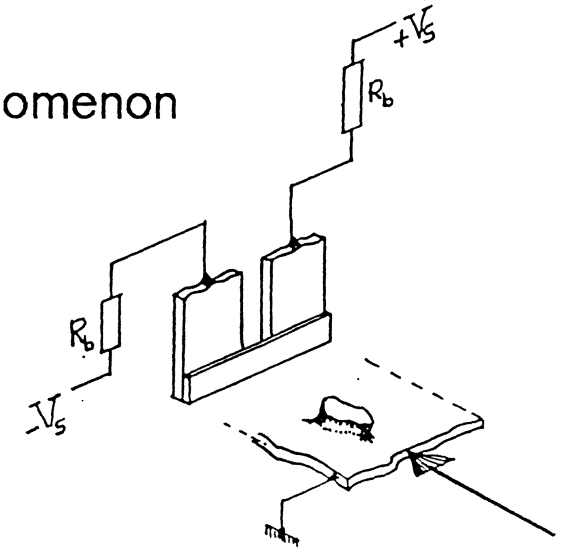

edges of sensor biased different than disk.

Electro-erosion creates recessed sensor
Loss of sensitivity

Counter measures:

- **Keep disk at potential of sensor**
  (floating, biased Disk Enclosure)
- **Keep MR sensor at ground potential**
  (requires dual power supply)
- **Keep one sensor lead at ground potential**
  (single supply, single-ended amplifier input)
  ↳ no CMR
- **Limit ground return currents to safe values**
  (ground fault interruptor analogy)

Sensor Erosion Protection

- Module detects relative resistance variation $\Delta R/R$ (Less sensitivity scatter due to tolerances)
- Maintains **center of MR sensor** at ground potential
- Limits peak ground return current to less than 100 μA for short-lasting conductive events

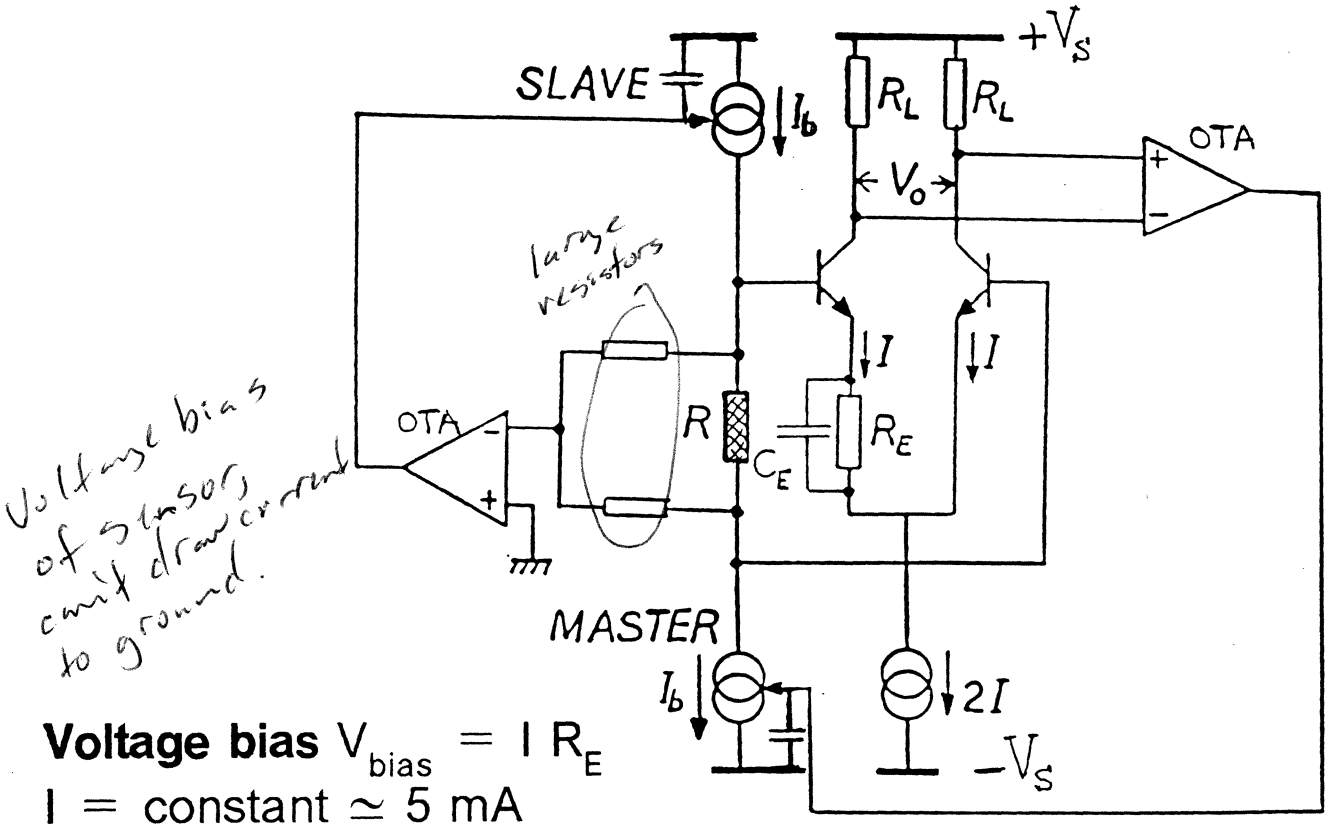

Voltage bias $V_{bias} = I\,R_E$

I = constant $\simeq$ 5 mA

Bias current $I_b = V_{bias}/R$

Output $V_o = A\,V_{bias}\,\Delta R/R$, gain $A = R_L/r_e$

Conductive Asperity Current

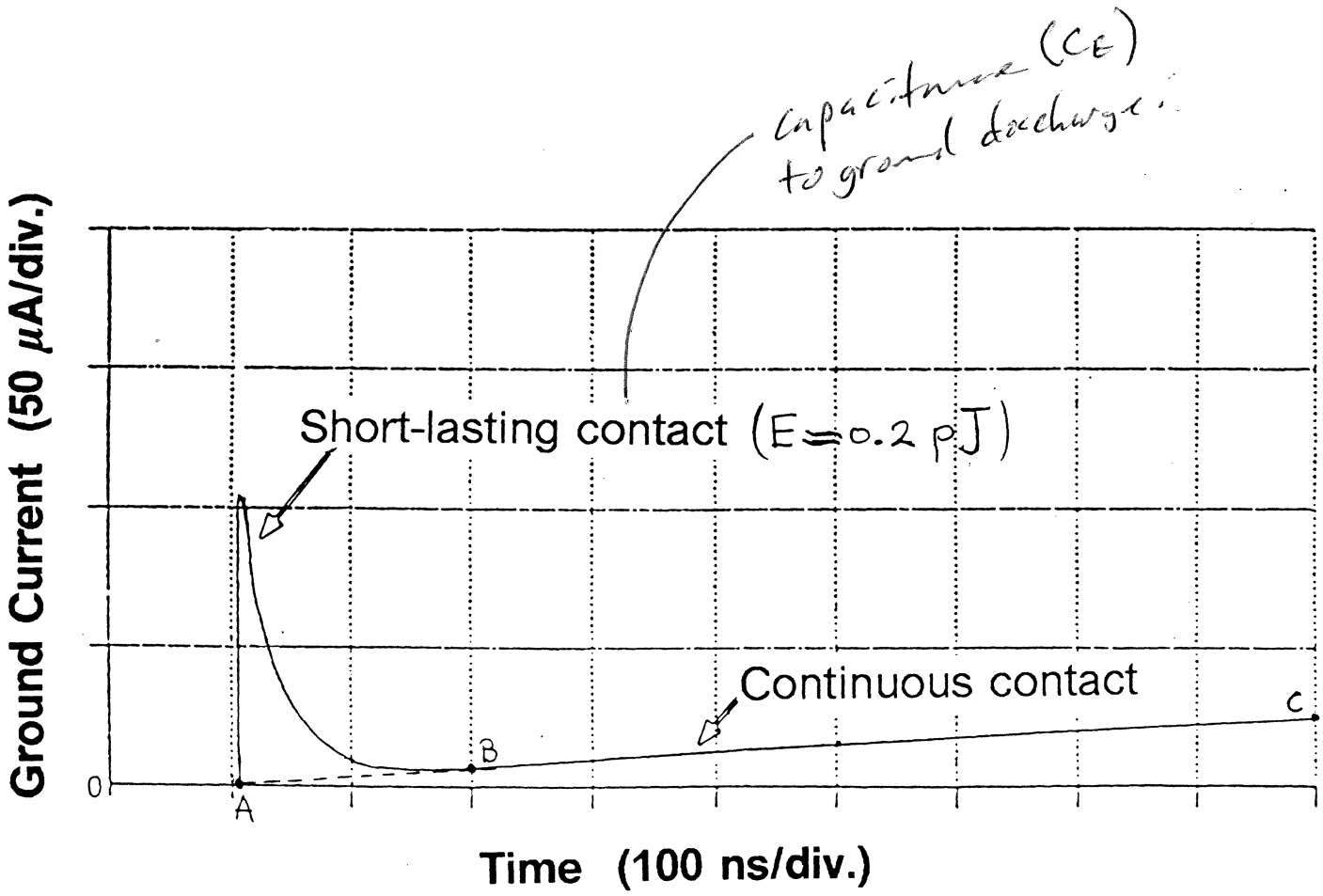

Inductive Front End

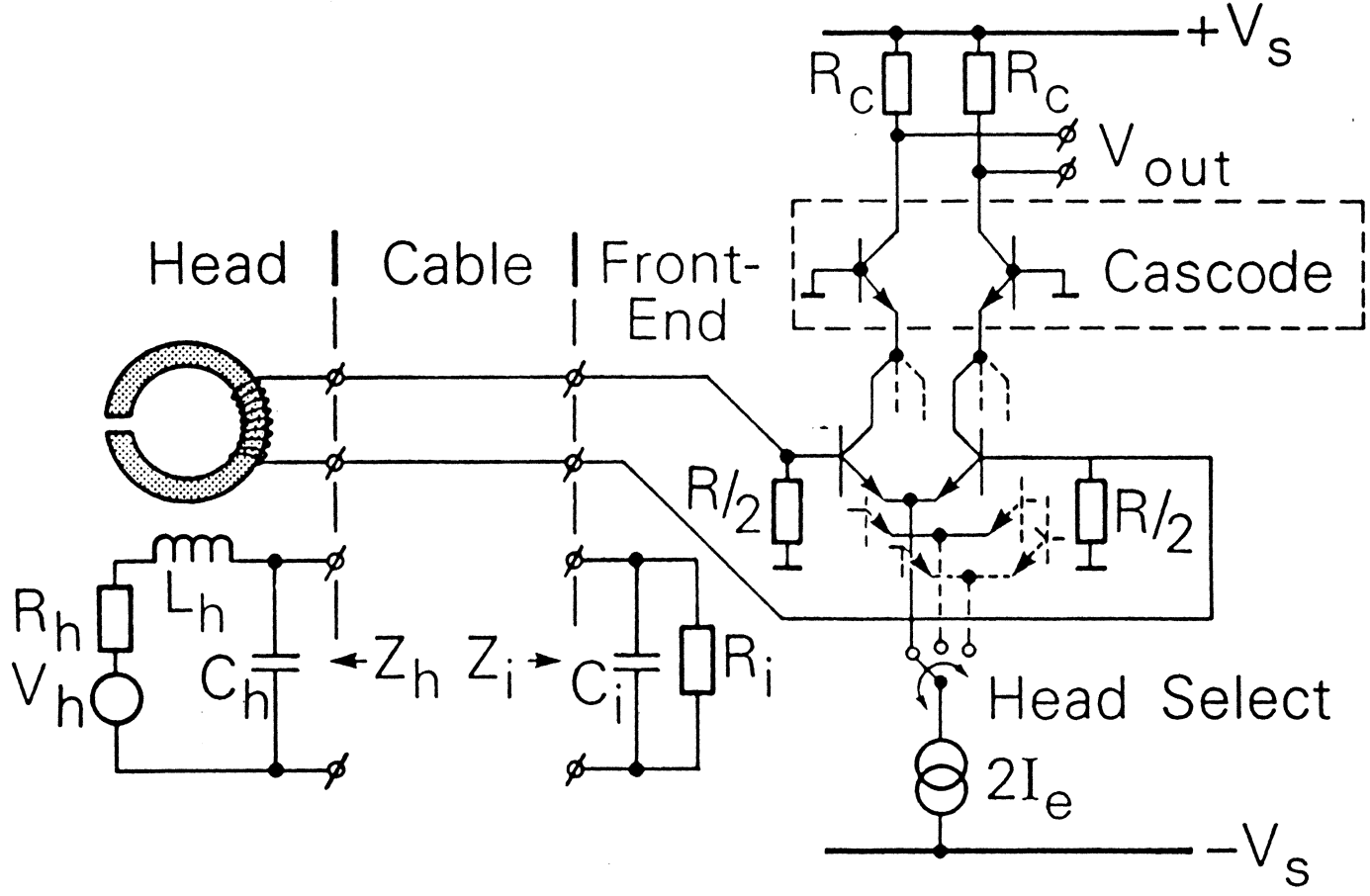

extrinsic gain/attenuation
before reach electronics

- capacitive loading by amp input

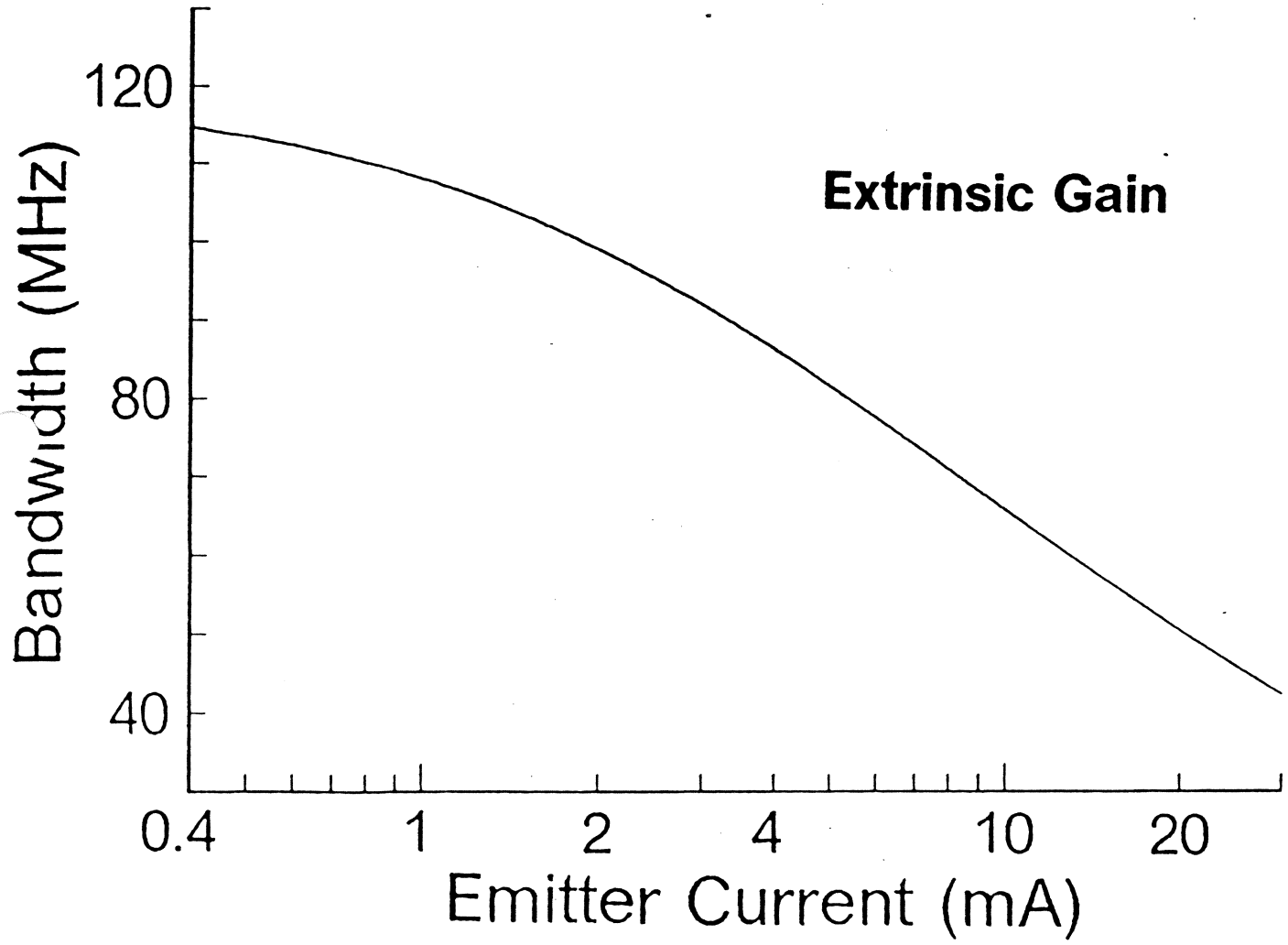

06/91 (K.B. Klaassen)

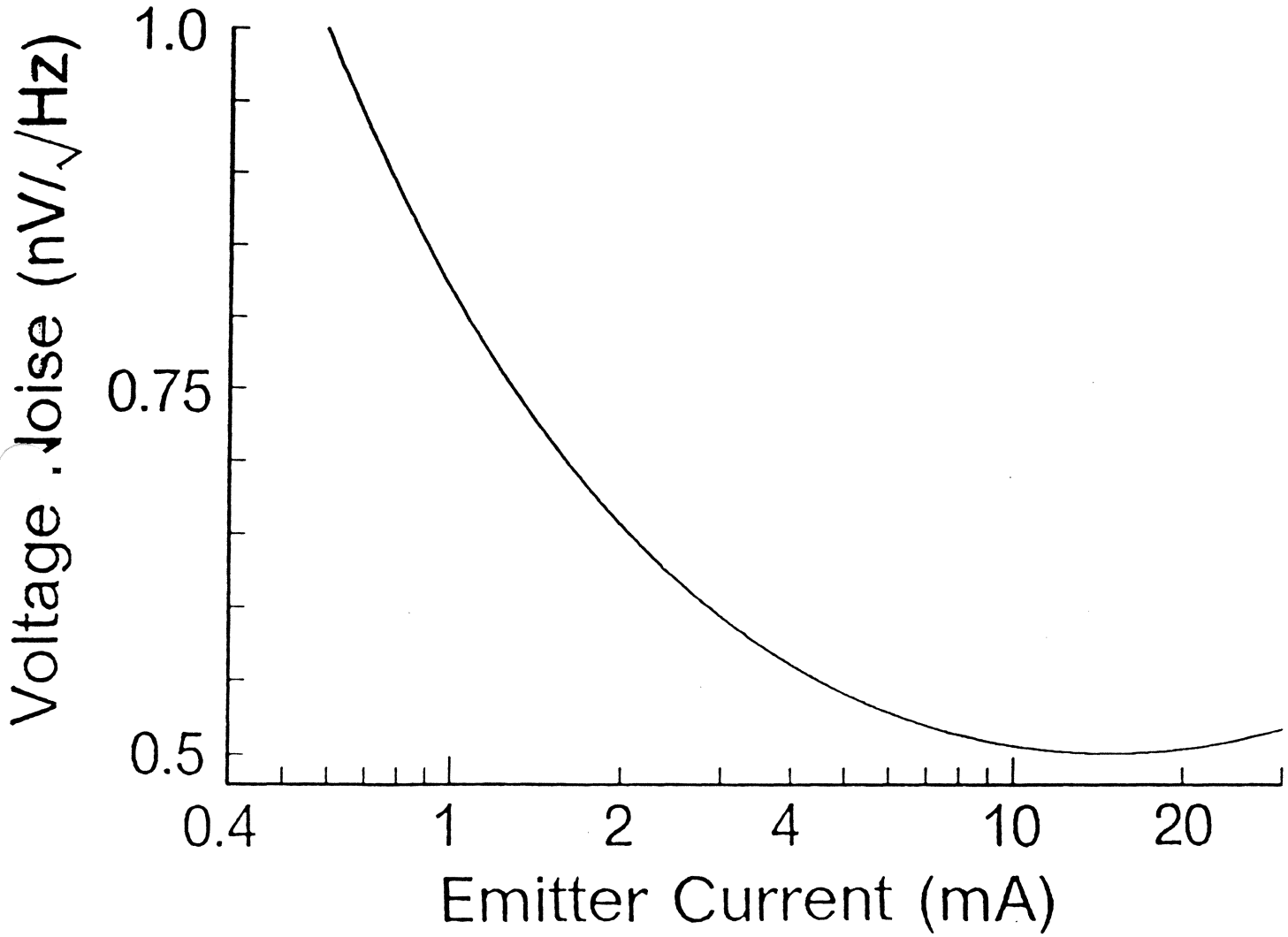

opposes attenuation

Noise Modelling Results

- Noise versus bandwidth dilemma
- Forces compromise value for the input transistor bias current
- For high bandwidth and low noise:

parameter	Current	Performance
high f_t	(5 GHz)	
high β	(80)	For n = 36
low $r_{bb'}$	(2.5 Ω)	BW = 100 MHz
$\lvert Z_h \rvert << 2R_{damping}$	(2 kΩ)	v_{en} = 0.5 nV/√Hz
low K_l — ind./√turn	(1.25 nH)	at bias current
low K_r — res.: single turn	(1 Ω)	2.5 - 5 mA

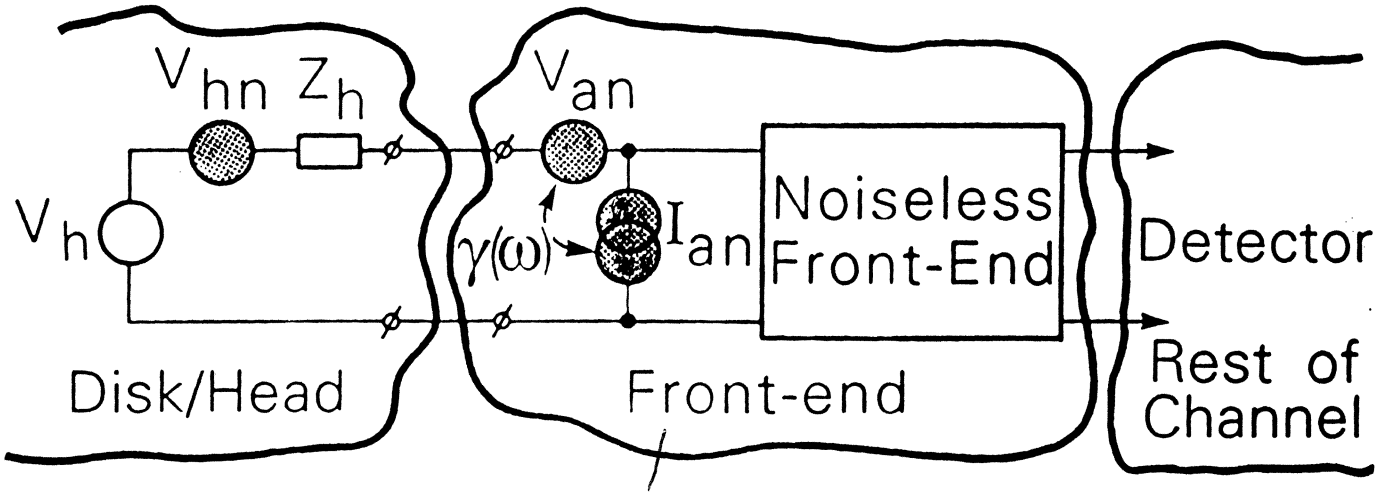

noise source
- can be correlated towards band ends

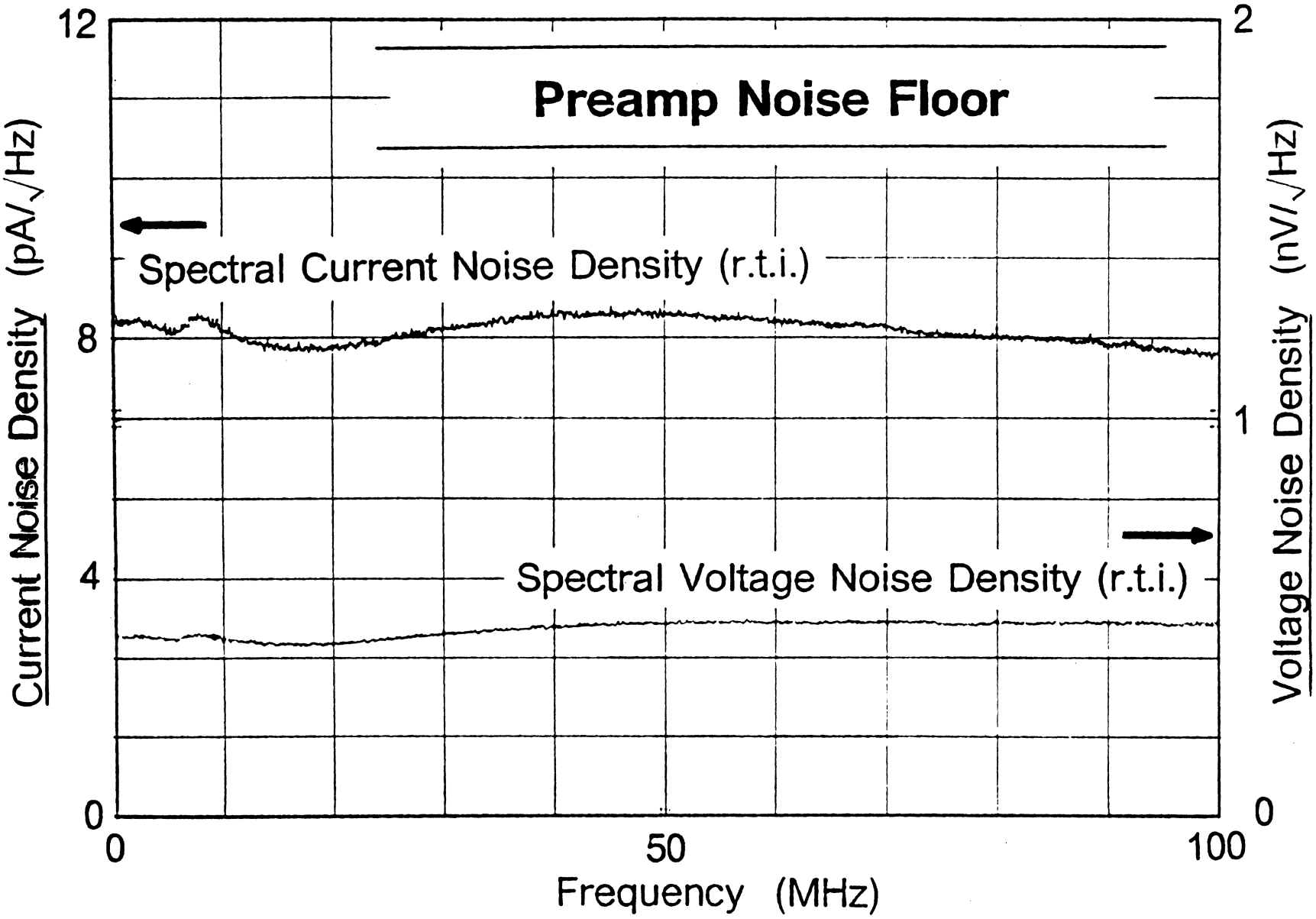

I an through hand impedance gives noise voltage

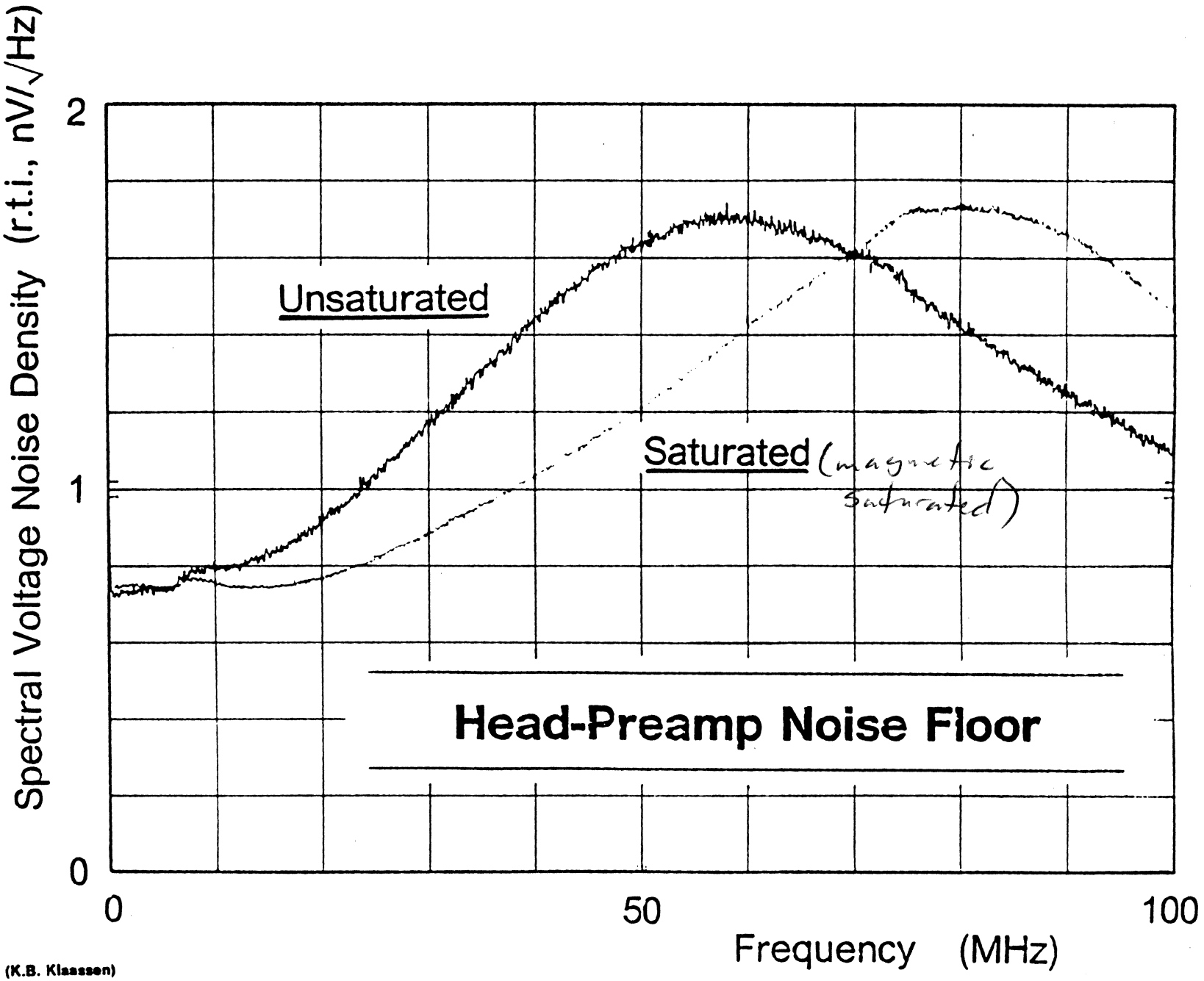

9/91 (K.B. Klaassen)

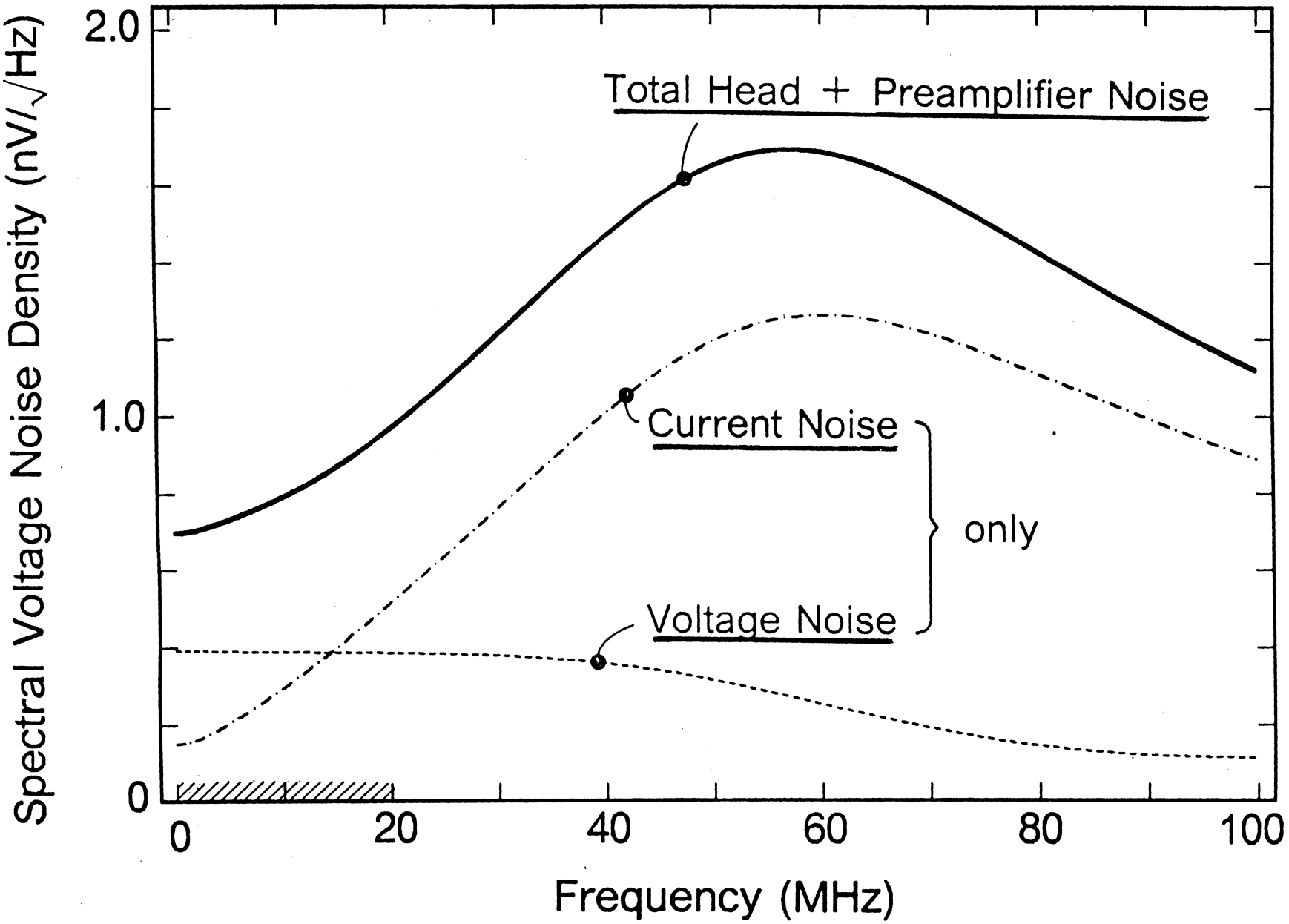

—Where go against resonance current noise dominates

Head Noise

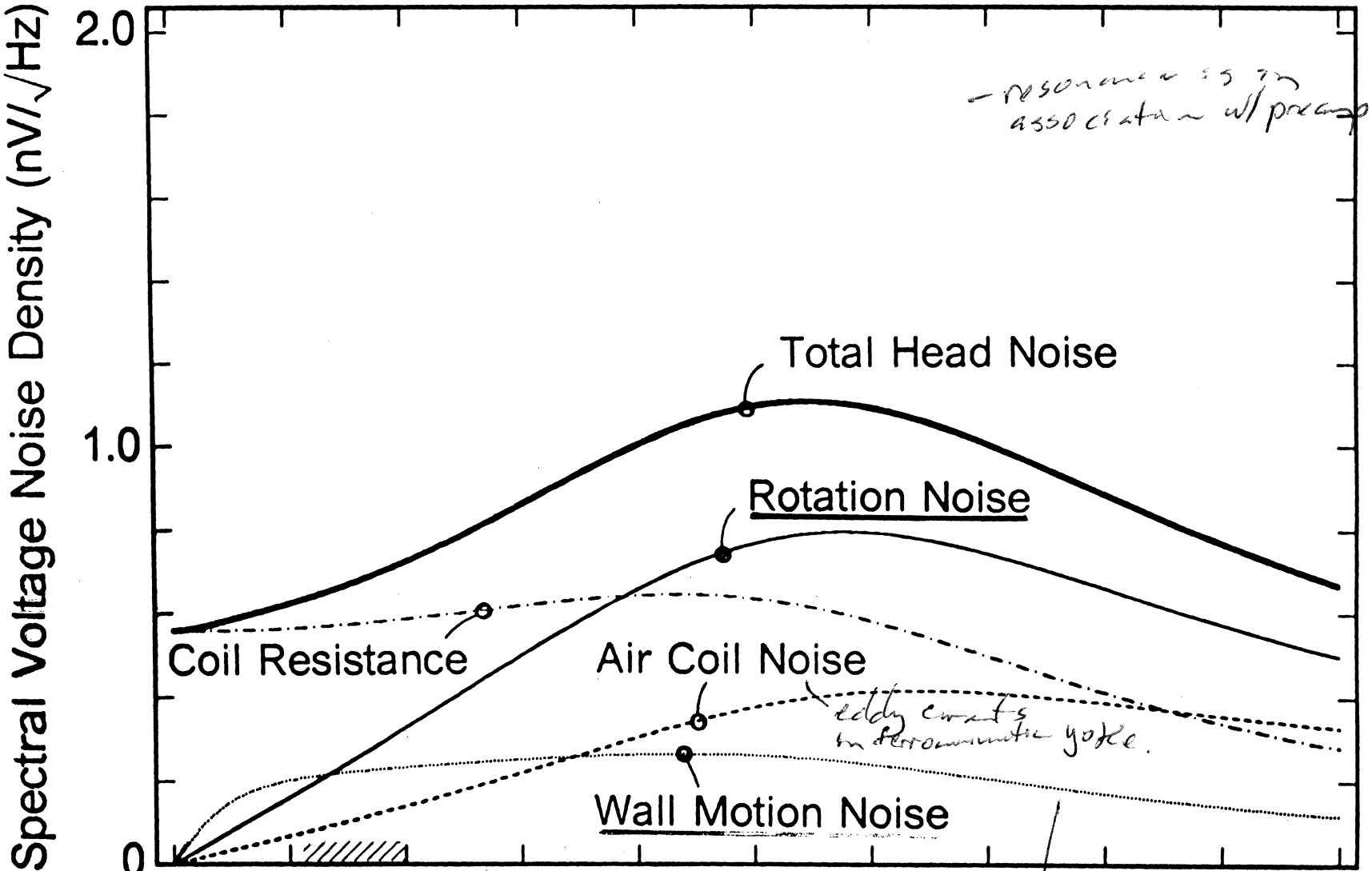
Spectral Voltage Noise Density (nV/√Hz)
2.0
1.0
0
0
20
40
60
80
100
Frequency (MHz)
Total Head Noise
Rotation Noise
Coil Resistance
Air Coil Noise
eddy currents in ferromagnetic yoke.
Wall Motion Noise
- resonance is a function of preamp
Losses => Heat => Noise
Due to lossy process of moving domains

Noise Matching

Often mistaken for ***"Impedance Matching"***

(Transmission lines, reflection free: $Z_i = Z_{TL}$)
(Maximum power transfer: $Z_i = Z_s^{\star}$)
(conjugate load impedance)

Define ***"optimal source resistance"***

$$R_{opt} = \frac{V_{an}}{I_{an}}$$

(Just a ratio, non-physical resistance)

- ***Low Electronics Noise Design***
  - Make V_{an} and I_{an} as small as economically feasible (large area, low-noise input devices)
  - Put most effort into reducing largest contributor: V_{an}, $I_{an}|Z_h|$
    (scale Z_h by changing turns N, scaling limited by write fuction of the head)
  - If $|Z_h| \neq R_{opt}$ further reduction of electronics noise is possible by ***"Noise Matching"***

Noise Matching

- Insert reactive components (no noise contribution) for noise matching:
  - Transformer $N = \sqrt{R_{opt}/|Z_h|}$
  - Series/parallel reactances (finite band)

- but may get interference

Example: IBM 3380 channel front-end obtains 6 dB Signal-to-Electronics-Noise improvement by noise matching

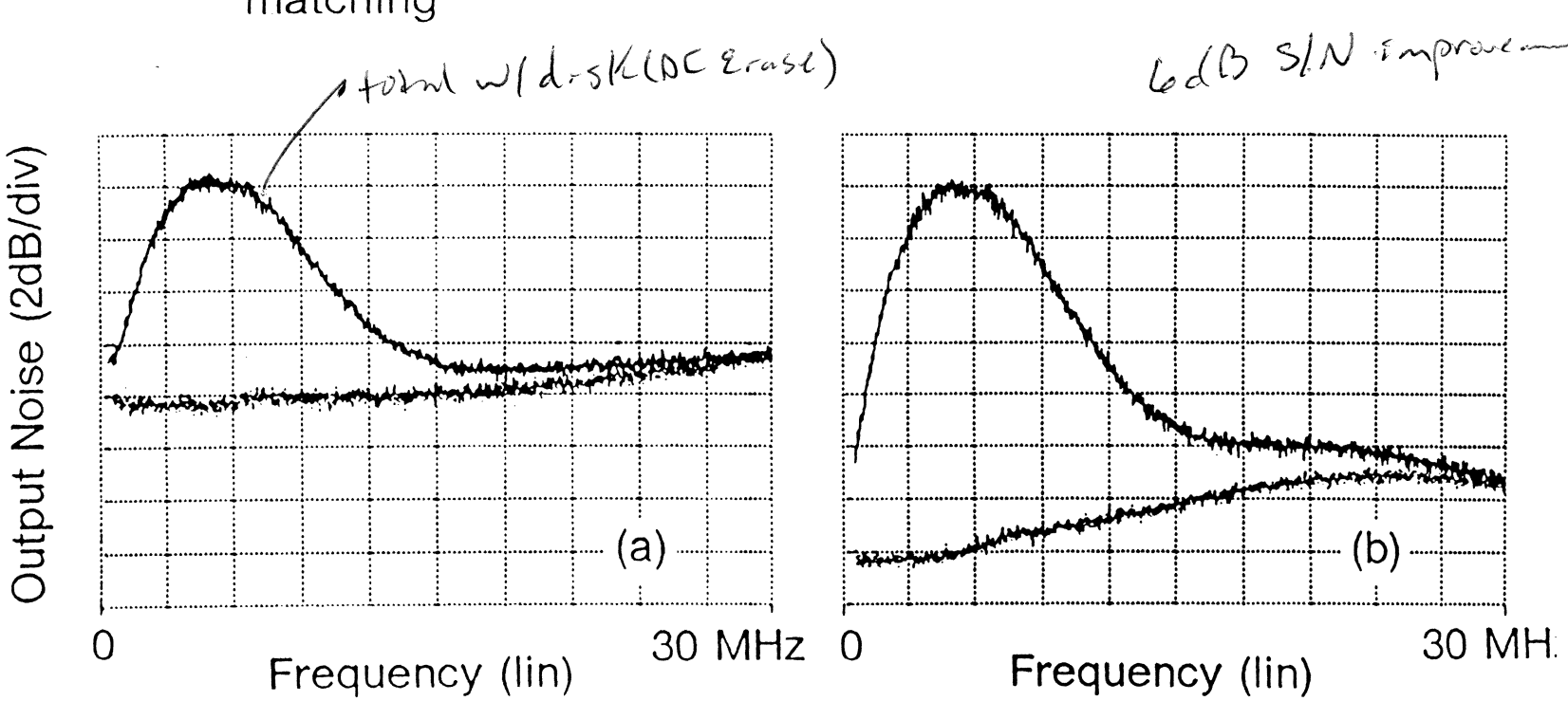

Transformer $N = 23/4$,

Total noise (top), Head and electronics noise (bottom)

Magnetic Head Instability

- **Write Instability**

  Definition: Delayed relaxation of head yoke, ***immediately after write***

- **Read Instability**

  Definition: Domain wall instability in head yoke, ***long after last write***

Relaxation after Write

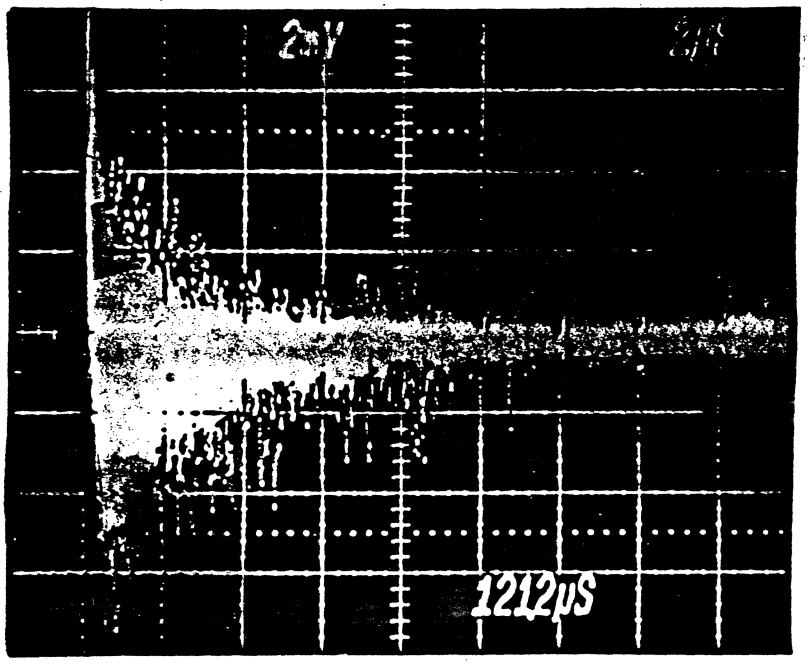

low charge
Servo problems

$I_w = 34$ mA

$t_o = 1$ μs

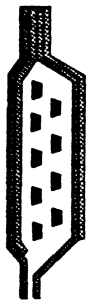

Domain Images

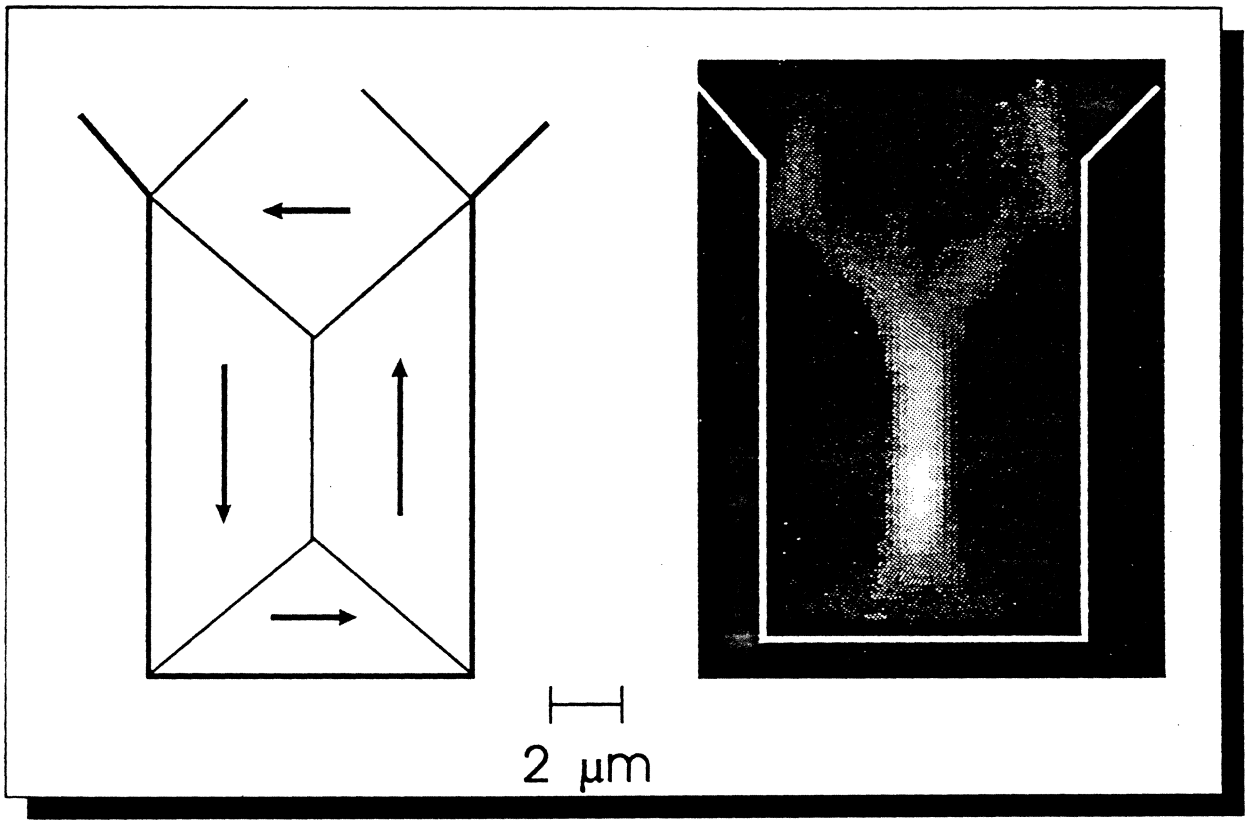

- Vertical domain wall shows biggest domain noise.

klaas.cdr

P.K. 9/9/91

MR Front-Ends

General

Front-end read/write electronics combined in a stand-alone analog integrated circuit

- Bipolar or BiCMOS technology
- Trend BiCMOS because:

  Bipolar
  - Higher currents
  - larger transconductance
  - higher gain-bandwidth product
  - lower noise (for low source resistance)
  - virtually ideal current switches
  - tolerances can be kept small
  - good V_{be} matching

  CMOS
  - virtually ideal voltage switches
  - allows low-power CMOS logic
  - very good packing density

Location

- Inside disk enclosure
- As close as possible to read/write transducers
  - Read signals small: 150 - 700 μV_{pp}
  - Write signals: require wide-band interconnections
  - Usually on the side of the head actuator arm

MR Front-End Architecture

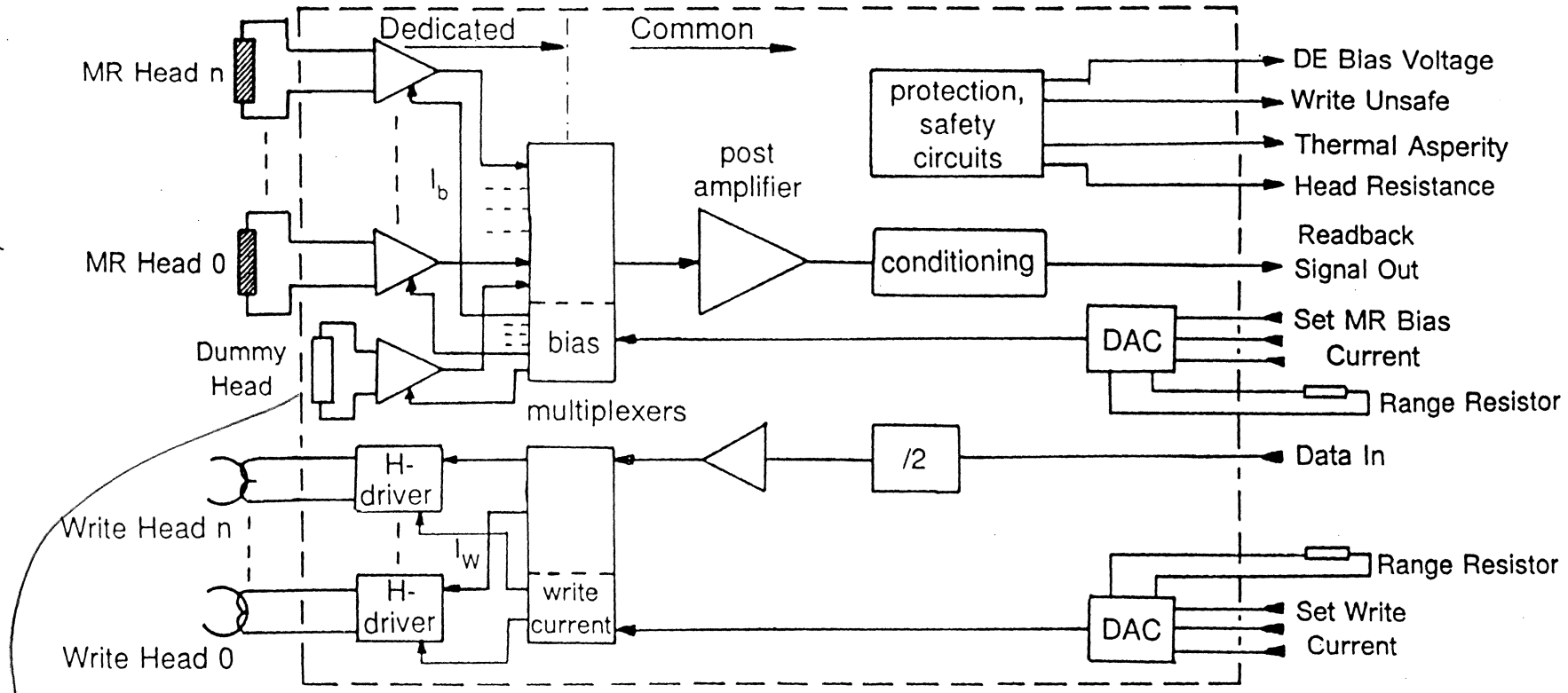

parking head so keep circuit active

MR Front-Ends

Various Design Considerations

A - MR Head Signal Amplitude

Magnetic transitions in disk cause a magnetic flux impinging on the MR sensor which produces a ΔR_{MR} which increases

1 - Linearly with track width (TW)
2 - Inversly proportional with sensor height (h)
3 - (Approximately) linearly with disk $M_r t$

low Mrt < 1 mem/c so don't overdrive corcu

Electronically detecting $\Delta R_{MR}/R_{MR}$ instead of ΔR_{MR}, therefore, makes the pre-amplifier output insensitive to variations in (1) and (2)

N.B: Especially the sensor height (defined by lapping) varies strongly

$\Delta R_{MR}/R_{MR}$ *Detection*

provides inherent or self-AGC, relieving the dynamic range requirements of the channel AGC.

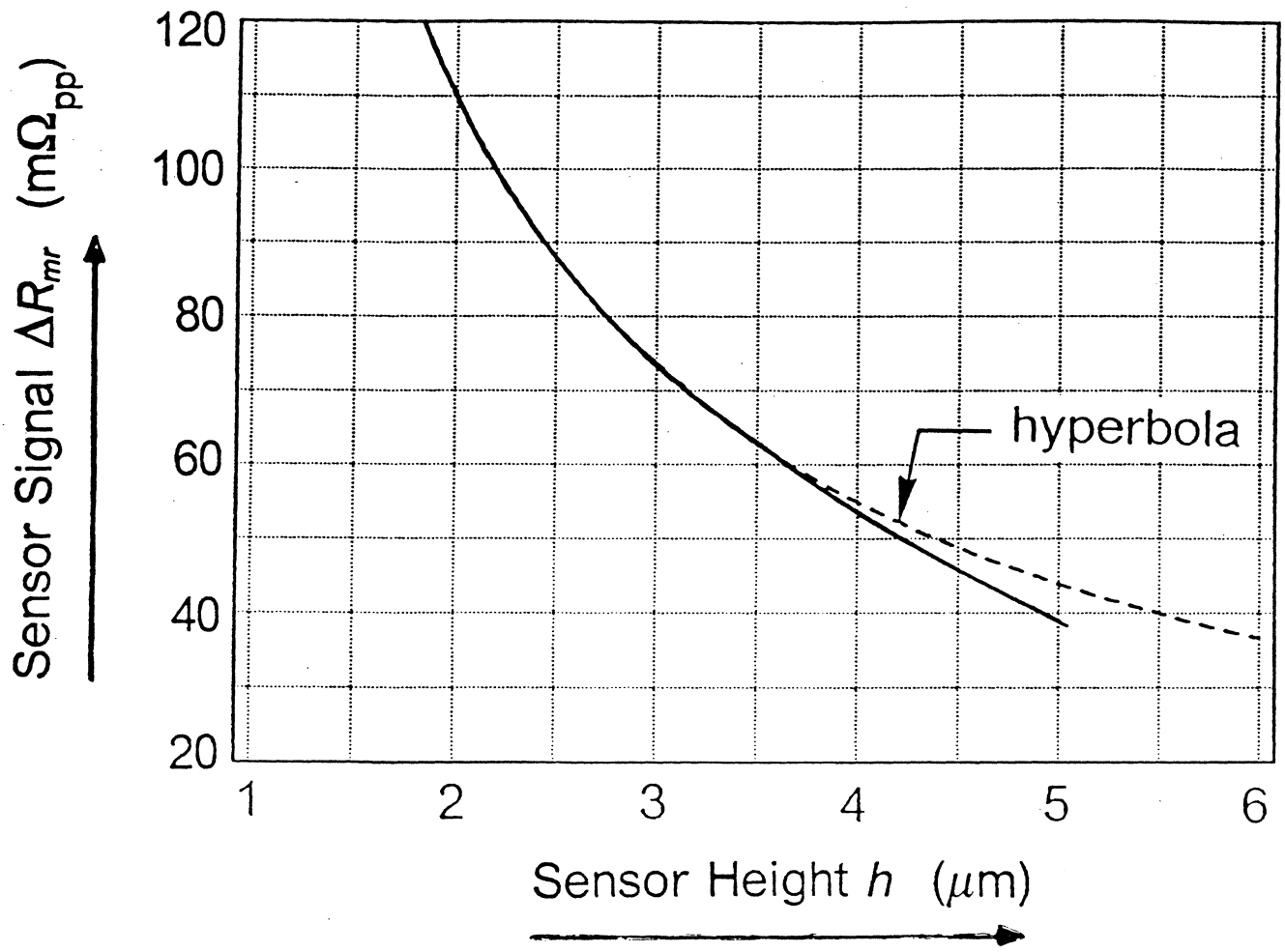

$$R_{mr} = \rho \frac{l}{th} = \alpha \frac{1}{h}$$

$$\Delta R_{mr} \simeq \beta \frac{1}{h}$$

Hence,

$$\frac{\Delta R_{mr}}{R_{mr}}$$ independent of h

MR Front-Ends

B - Biasing and Sensing Architectures

— *Four Possible Architectures*
Different forms of providing electrical bias to the MR sensor and sensing the read signals lead to four different front-end electronics architectures

— $\Delta R_{MR}/R_{MR}$ *Detection*
Only those architectures where biasing and sensing have the same physical dimension give $\Delta R_{MR}/R_{MR}$ detection
e.g. current bias & sensing.

— *Sensor Temperature/Current Density*
- MR sensor output increases with bias
- Bias limited by electromigration/interdiffusion
- Maxima for sensor current density and temperature
- For maximum head output approach these maxima as closely as possible
- Largest head-to-head variation due to sensor height *h*
- Voltage biasing allows sensor current density and temperature rise independent of *h*
- Voltage biasing allows biasing closer to the limits

$\frac{\Delta R}{R}$ & voltage sensing

MR Front-End Configurations		
Biasing	***Sensing***	
	Current $\lvert Z_{in} \rvert \ll R_{mr}$	Voltage $\lvert Z_{in} \rvert \gg R_{mr}$
Current (I_B)	$\Delta I_s = \frac{\Delta R_{mr}}{R_{mr}} I_B$	$\Delta V_s = \Delta R_{mr} I_B$
Voltage (V_B)	$\Delta I_s = -\frac{\Delta R_{mr}}{R_{mr}^2} V_B$	$\Delta V_s = \frac{\Delta R_{mr}}{R_{mr}} V_B$

overcorrected by $1/R_{mr}$

Biasing

"Constant" ≡ independent of R_{mr}

Constant Current (I_B)	Constant Voltage (V_B)
Sensor Current Density:	
$J_c = I_B \frac{1}{t\boxed{h}}$	$J_v = V_B \frac{1}{\rho l}$
Sensor Power Dissipation	
$P_c = I_B^2 R_{mr} = I_B^2 \rho \frac{l}{t\boxed{h}}$	$P_v = V_B^2 \frac{1}{R_{mr}} = V_B^2 \frac{1}{\rho} \frac{t\boxed{h}}{l}$
Sensor Temperature Rise:	
$\Delta T_c = P_c \times R_{thermal}$	$\Delta T_v = P_v \times R_{thermal}$
$\Delta T_c = I_B^2 \frac{\rho l}{th} \times \frac{gK}{2lh}$	$\Delta T_v = V_B^2 \frac{th}{\rho l} \times \frac{gK}{2lh}$
$\Delta T_c = I_B^2 \rho K \frac{g}{2t\boxed{h^2}}$	$\Delta T_v = V_B^2 \frac{K}{\rho} \frac{gt}{2l^2}$

└ no h dependence so max; current density

Paradox Illustration

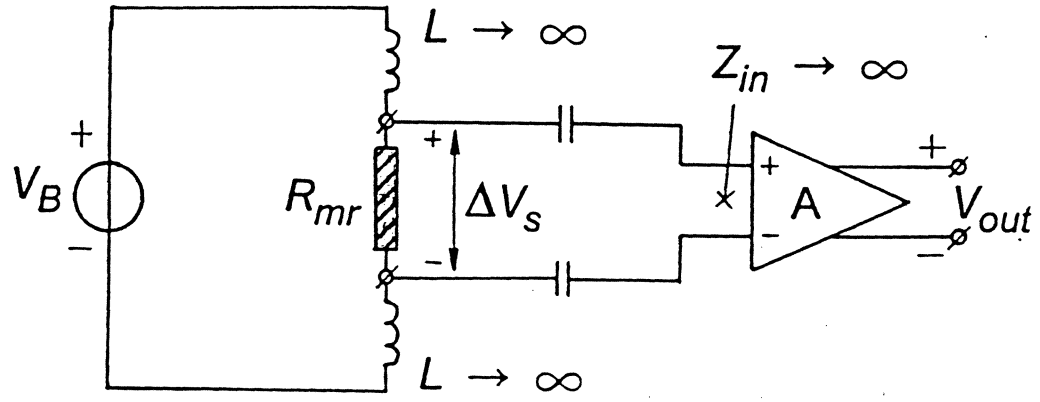

Biasing	Sensing	Sensitivity Equation
V_B	ΔV_s	$V_{out} = \frac{\Delta R_{mr}}{R_{mr}} V_B A$

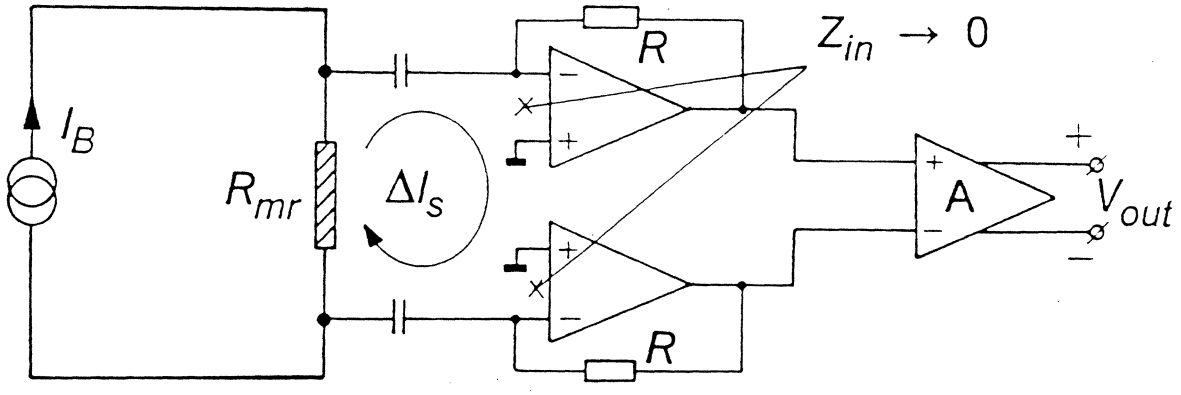

Biasing	Sensing	Sensitivity Equation
I_B	ΔI_s	$V_{out} = -\frac{\Delta R_{mr}}{R_{mr}} I_B R A$

MR Front-Ends

— *Differential Output Configuration*

Output signal is differentially coupled to the drive's circuit board.

- $Z_{out} = Z_{trans.line}$ for bandwidth
- High Z_{out} when not reading
  Smaller write-read recovery transients
  (AC coupling caps remain charged during sector servoed writing)
  Hardwired multiplex of modules into single port

MR Front-Ends

- draw more current & freq. varies

C - Amplifier Configurations

— *Differential Input Configuration*

Pre-amplifiers with a differential input exhibit high CMRR and PSRR; are more interference robust.

- o MR-to-disk potential must be zero
- o Dual power supply needed
  (DC-to-DC convertor: 80 % power efficiency, needle impulse interference, filter components)
- o Floating Disk Enclosure (Only AC grounded)
  1. Pre-amplifier biases DE at head potential
  2. DE is held at fixed DC potential, pre-amplifier biases heads at this potential.
     Needs fail safe: Customer shorting DE to ground automatically shuts off bias to MR heads

— *Single-Ended Input Configuration*

One input terminal is (virtually) grounded. No CMRR; lower PSRR.

- o Smaller package, common ground
- o Single supply voltage
- o MR head one side grounded

To not cause interference problems the DE must be designed as a *"cage of Faraday"*

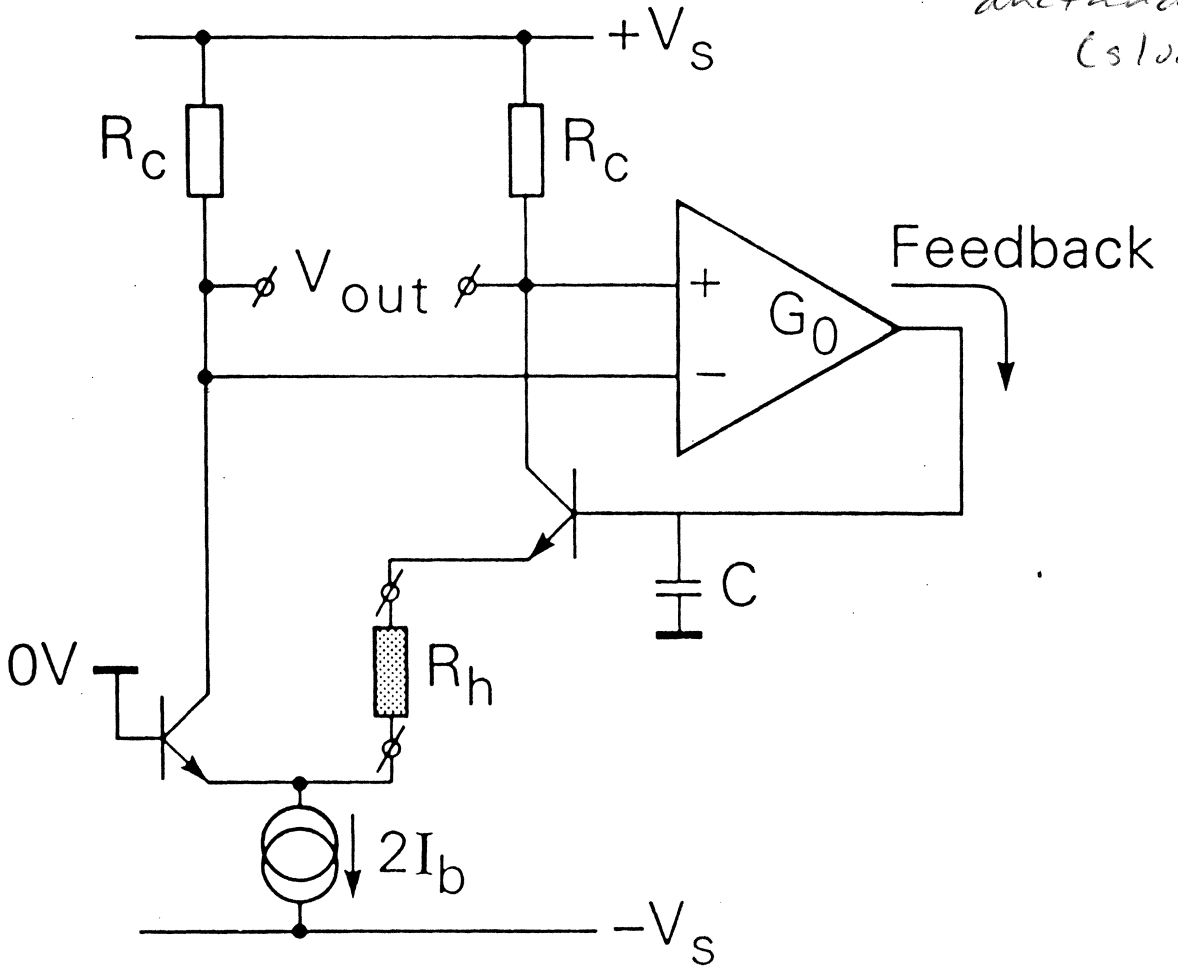

Operational Transconductance Amp.
(slowly varying)

Signal freq's
- short circuit
DC - adjusts

-78-

MR Front-Ends

D - Basic Design Examples

- Differential/Single Ended
- Voltage/Current Biasing
- Voltage/Current Sensing
- Comments

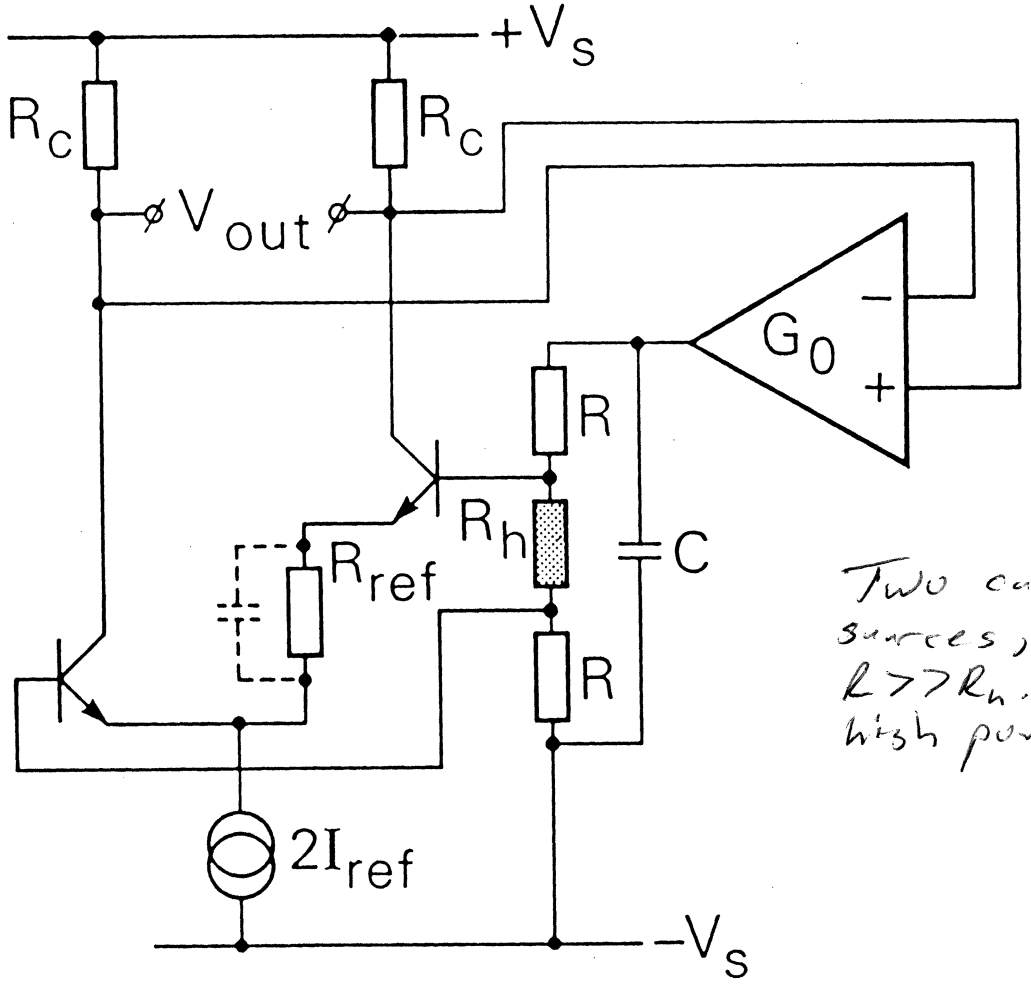

Two current sources, large $R >> R_h$. Needs high power.

Biasing	Sensing	Sensitivity Eqn.
$V_B = I_{ref} R_{ref}$	ΔV_S	$V_{out} = 2 \frac{\Delta R_{mr}}{R_{mr}} V_B \frac{R_c}{R_{ref}}$

Dual power supply
Approach (Source 70°)

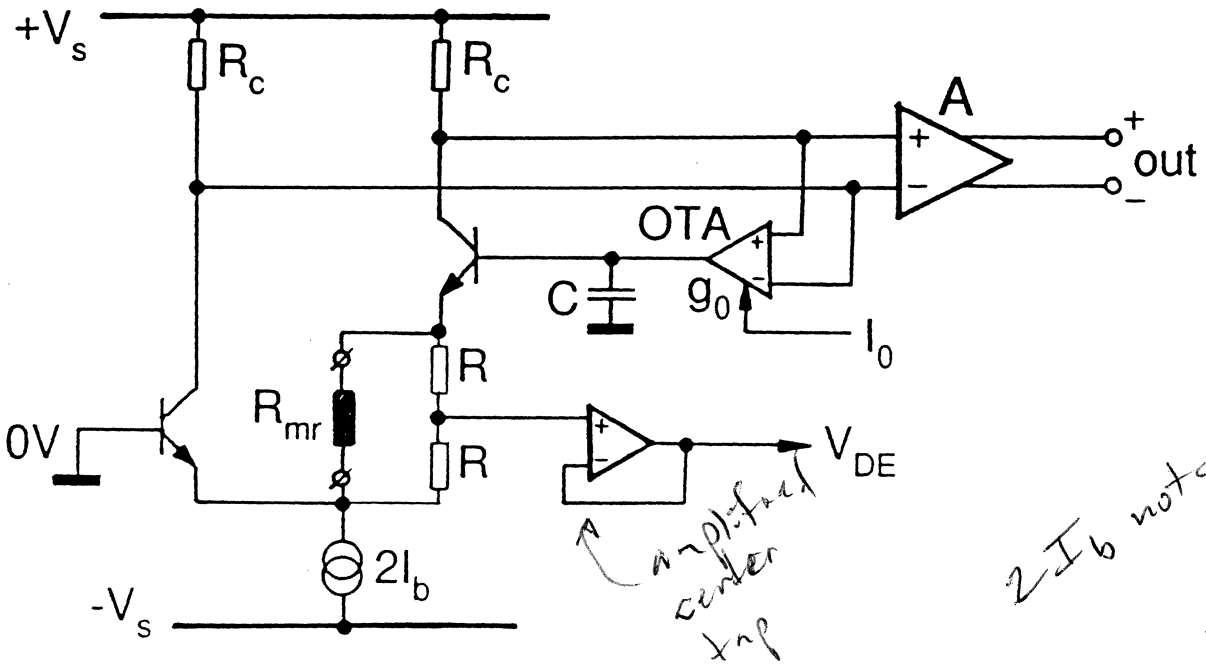

2 I_b not good.

Biasing	Sensing	Sensitivity Equation
I_B	ΔI_s	$V_{out} = 2\frac{\Delta R_{mr}}{R_{mr}} I_B A R_c$

MR Sensor in H
w/ input stage bias
Self bias

Biasing	Sensing	Sensitivity Equation
I_B	ΔI_s	$V_{out} = 2\frac{\Delta R_{mr}}{R_{mr}} I_B A R_c$

Comments:

- Differential input
- High CMRR possible
- Lowest possible sensor-disk potential
- Needs dual power supply and $2I_B$
- Low-frequency band end:

$$f_{-3dB} = \frac{1}{2\pi}\frac{2g_o R_c}{CR_{mr}}$$

- Settling time upon head switch:

$$\Delta t = C\frac{\Delta V_B}{I_{OTA,max}}$$

- Fast settle mode (enlarge I_o into OTA)
- f_{-3dB} will move up proportionally

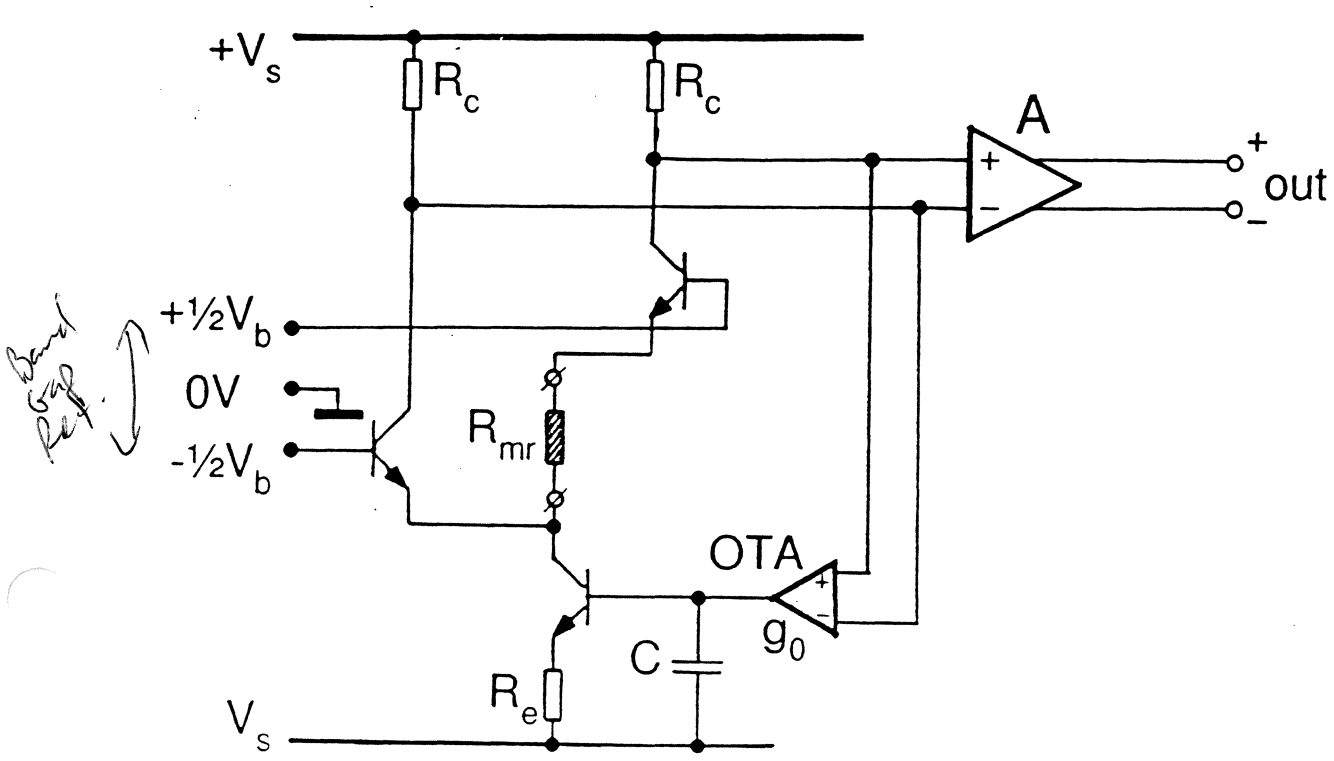

Biasing	Sensing	Sensitivity Equation
V_B	ΔI_s	$V_{out} = 2\frac{\Delta R_{mr}}{R_{mr}^2} R_c A$

Biasing	Sensing	Sensitivity Equation
V_B	ΔI_s	$V_{out} = \frac{\Delta R_{mr}}{R_{mr}^2} 2R_c A$

Comments:

- Dual supply needed
- Differential; high CMRR
- Current drain: $2I_B$
- Output proportional to $\frac{\Delta R_{mr}}{R_{mr}^2}$

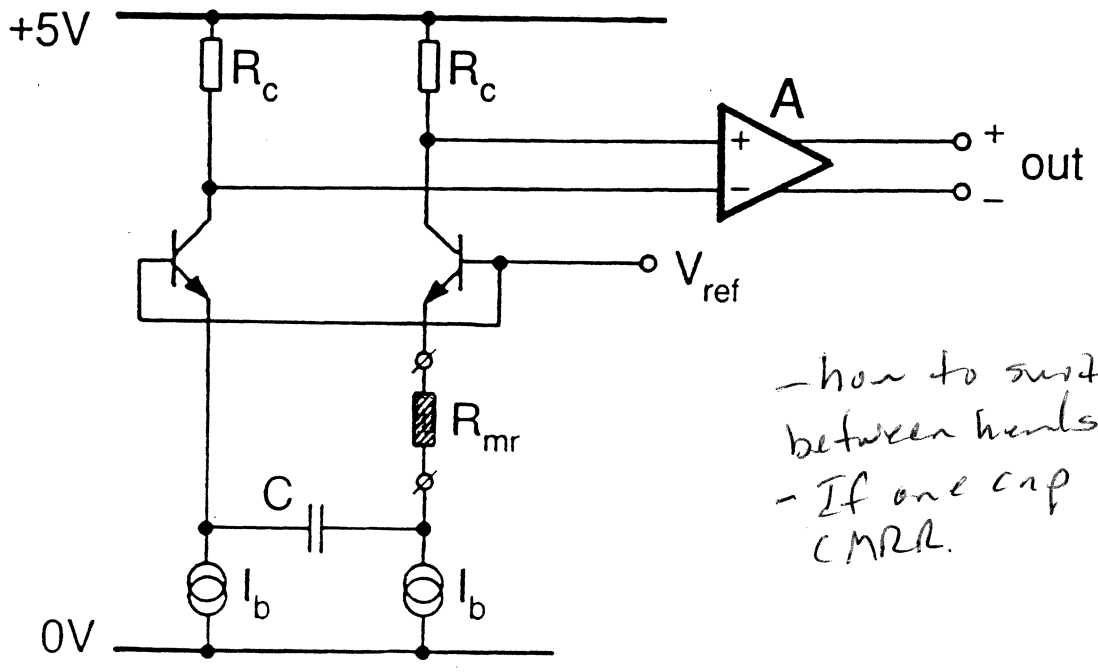

- how to switch between heads?
- If one cap lost CMRR.

Biasing	Sensing	Sensitivity Equation
I_B	ΔI_s	$V_{out} = 2 \frac{\Delta R_{mr}}{R_{mr}} I_B R_c A$

Biasing	Sensing	Sensitivity Equation
I_B	ΔI_s	$V_{out} = \frac{\Delta R_{mr}}{R_{mr}} I_B 2 R_c A$

Comments:

- AC-coupled version of previous circuit
- Does not need feedback loop
- Current drain: $2I_B$
- Settling time:

$$\Delta t = C\frac{\Delta V_B}{I_B} = C(R_{mr,max} - R_{mr,min})$$

Switch between heads

- Low-frequency band end:

$$f_{-3dB} = \frac{1}{2\pi C R_{mr}}$$

Single ended supply

Float MR @ + power supply voltage - not good!

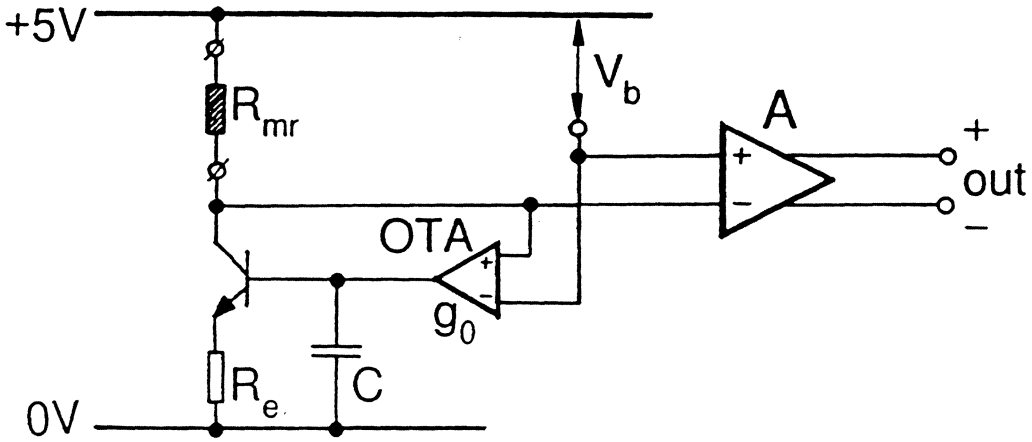

Biasing	Sensing	Sensitivity Equation
V_B	ΔV_s	$V_{out} = \frac{\Delta R_{mr}}{R_{mr}} V_B A$

Biasing	Sensing	Sensitivity Equation
V_B	ΔV_s	$V_{out} = \frac{\Delta R_{mr}}{R_{mr}} V_B A$

Comments:

- MR sensor at +5V!
  - — Conductive asperities
  - — Flash-overs
- Bias entire Disk Enclosure at +5V
  - — Customer induced shorts
  - — Detect/monitor DE potential
- Low-frequency band end:

$$f_{-3dB} = \frac{1}{2\pi} \frac{g_o R_{mr}}{C R_e}$$

one end of sensor tied to ground.

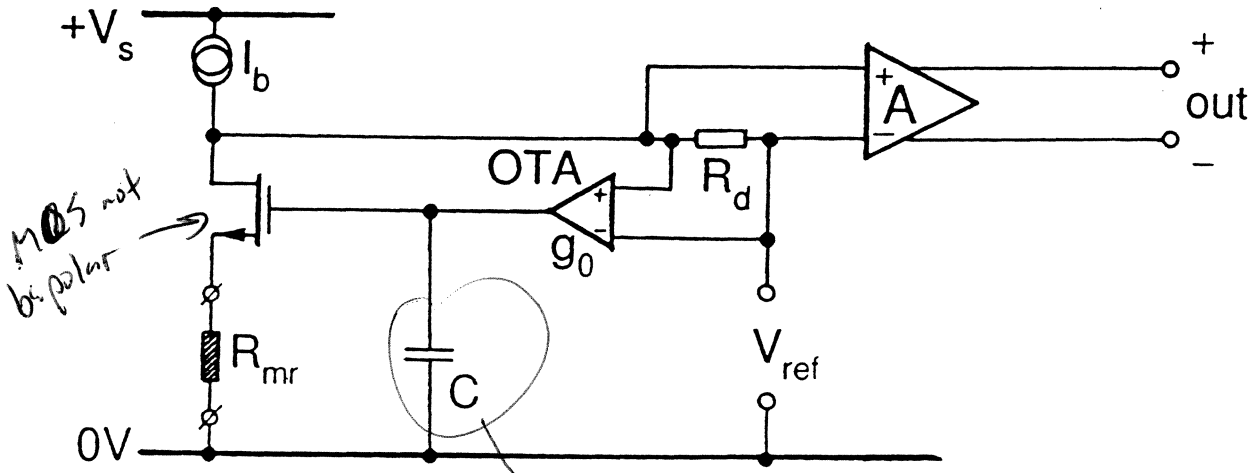

large so discrete component w/ extra parasitics

Biasing	Sensing	Sensitivity Equation
I_B	ΔI_s	$V_{out} = \frac{\Delta R_{mr}}{R_{mr}} I_B A R_d$

Biasing	Sensing	Sensitivity Equation
I_B	ΔI_s	$V_{out} = \frac{\Delta R_{mr}}{R_{mr}} I_B A R_d$

Comments:

- Single-ended input
  - No CMRR
  - Sensitive to interference pick up
  - Use Disk Enclosure as Faraday Cage

no clock into disk enclosure, no glitches fed in.

- Low-frequency band end:

$$f_{-3dB} = \frac{1}{2\pi} \frac{g_o R_d}{C R_{mr}}$$

- Dependent on R_{mr}
- Parasitic capacitance of OTA loop and other head input circuits

Parasitic Impedances

MR head is a non-self-generating transducer; it needs an electrical bias to operate

- Bias causes a DC voltage across the head ($R_{MR} \simeq 25\Omega$, $I_{Bias} \simeq 10$ mA $\rightarrow$ $V_{MR} \simeq 250$ mV)
- V_{MR} too large to apply DC-coupled gain
- Need AC coupling/by-pass capacitor in input stage

Parasitic Impedances

The AC coupling/by-pass capacitor is afflicted with parasitics (R_s, L_s) and also the head-to-electronics leads (R_l, L_l, C_l).

These parasitics can:

— reduce the available gain and bandwidth

— increase the electronics noise

— endanger the MR bias loop stability

Close proximity, good capacitors with short thick wide leads are required

Surface-Mount Capacitors

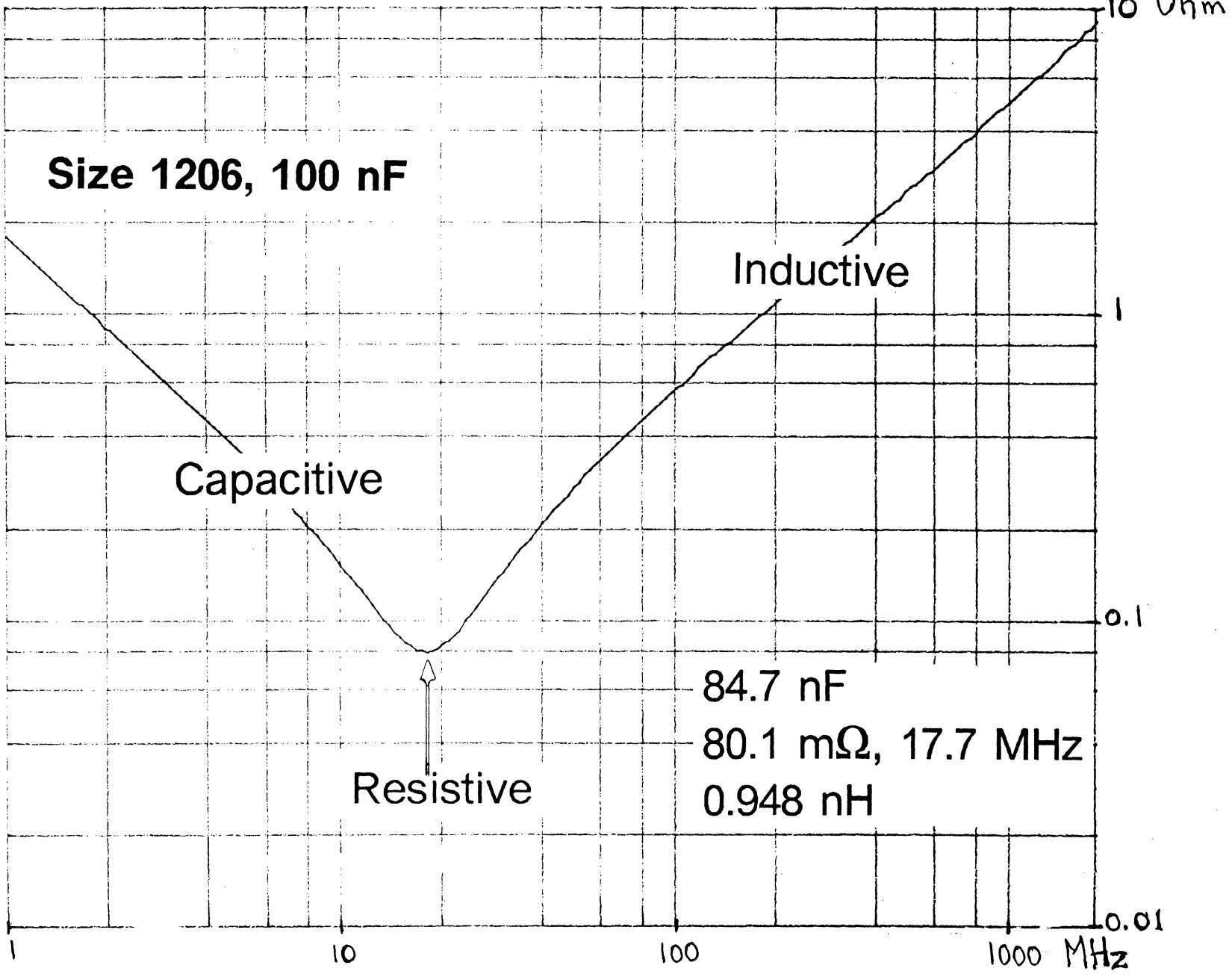

-92-

Surface-Mount Capacitors

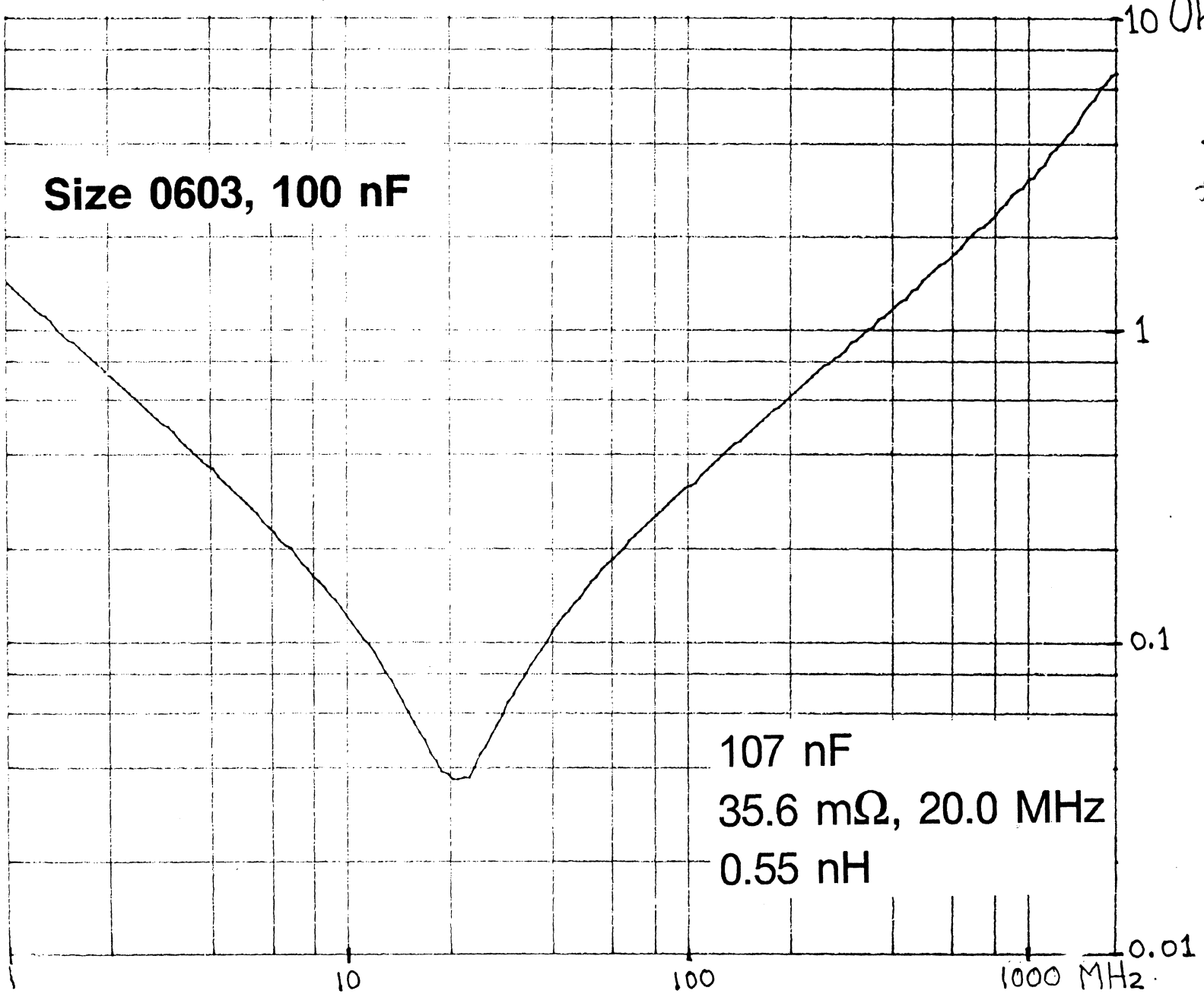

Smaller foot print

Surface-Mount Capacitors

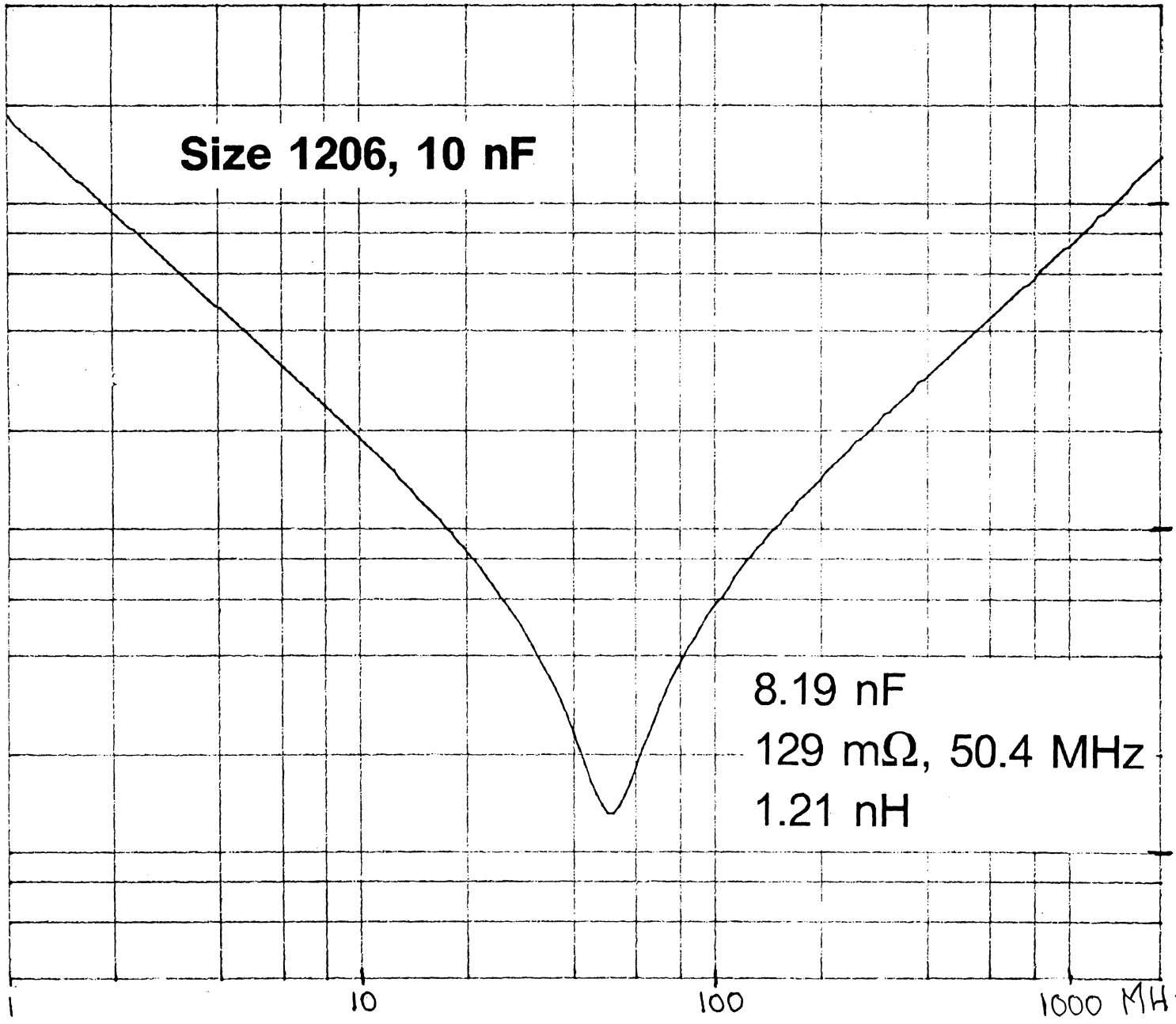

higher values, higher Q (sharper)

Surface-Mount Capacitors

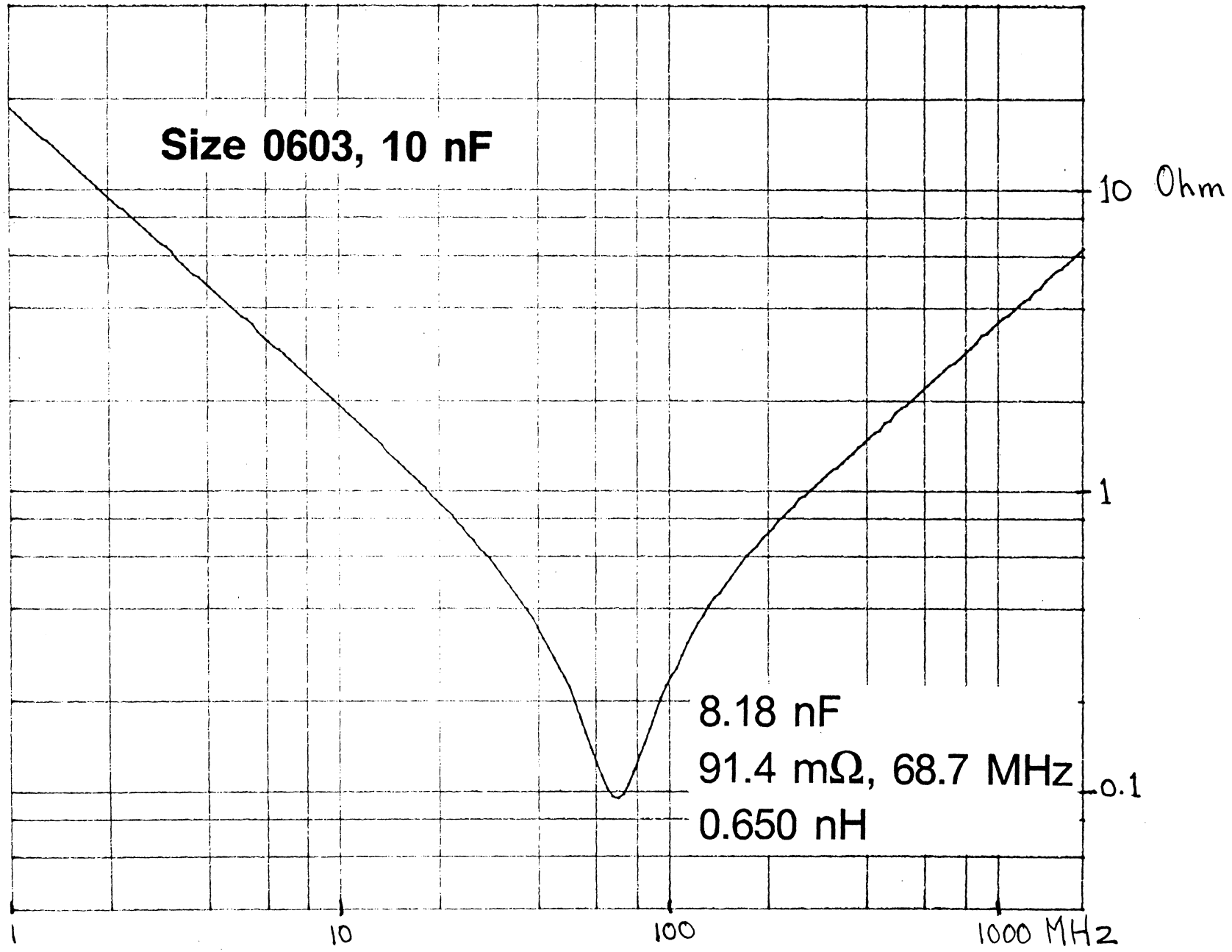

Extrinsic Gain Equalization

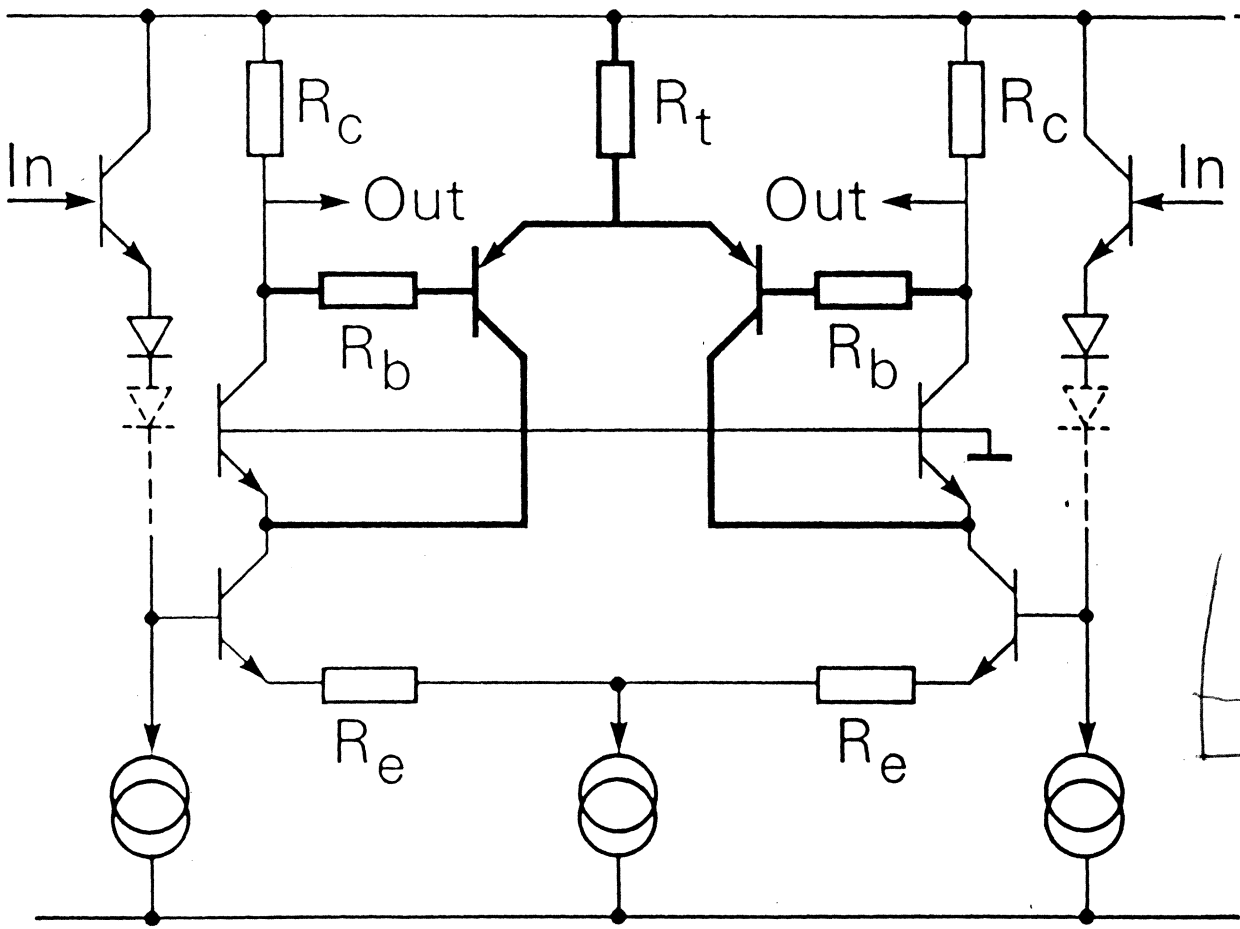

2nd stage in amp. - HF boost

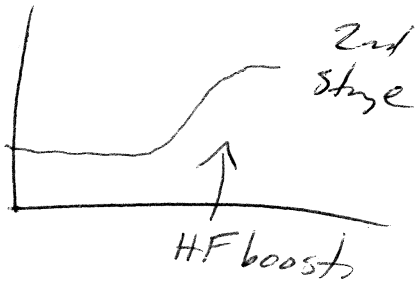

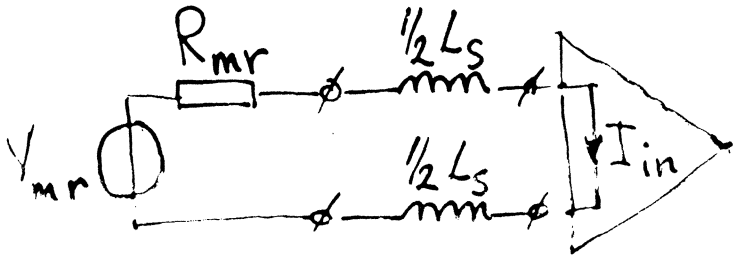

$$f_{-3dB} = \frac{L_s}{2\pi R_{mr}}$$

$$\tau = \frac{L_s}{R_{mr}}$$

$$f_{-3dB} = \frac{1}{2\pi\tau}\,\frac{R_{mr}}{2\pi L_s}$$

equalize for this attenuation - boost

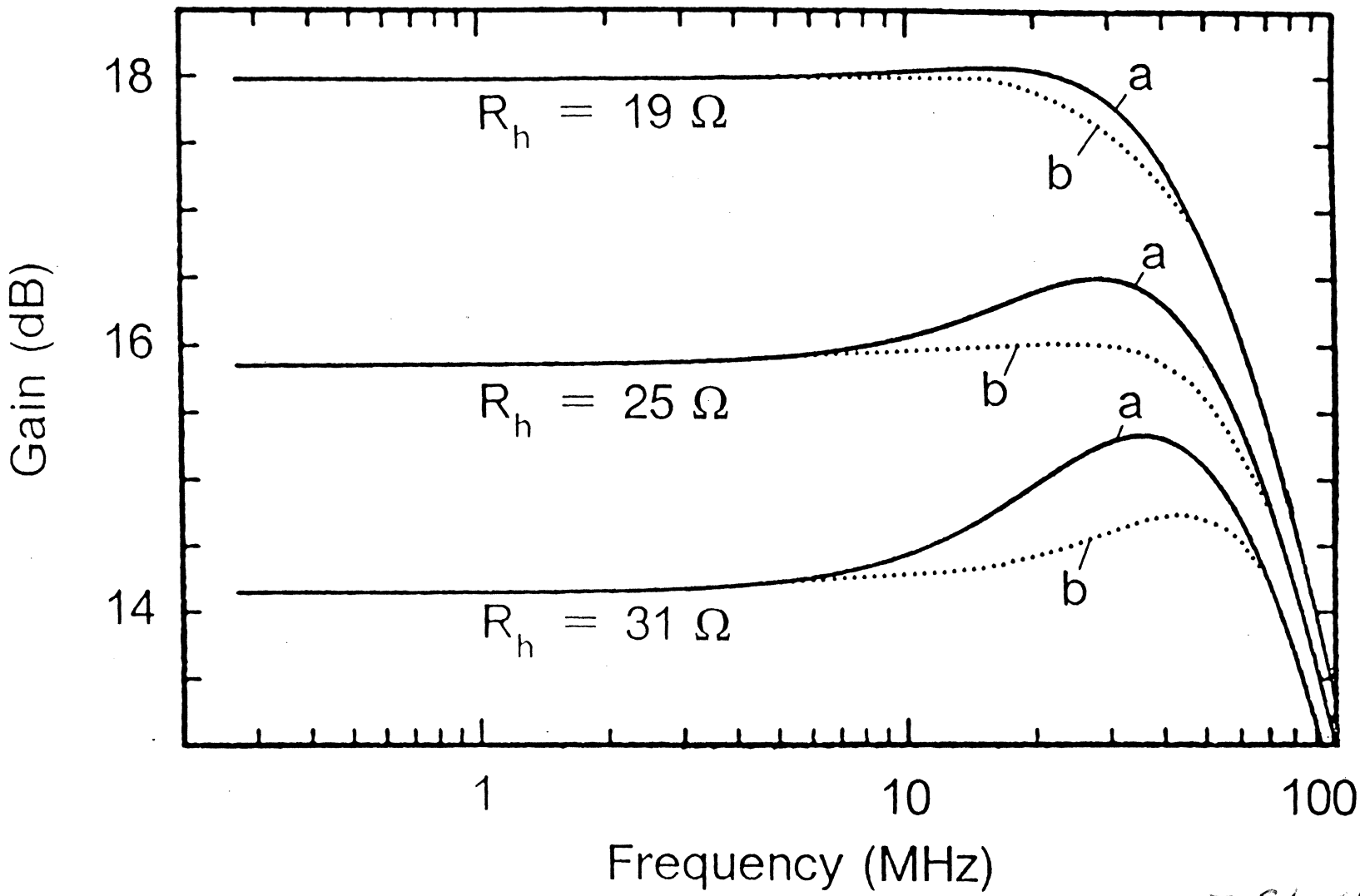

Gain depends on hand resistance

a - signal from hand resistance
b - with equalization

- small contribution to noise, increase in amp @ HF.

Design for Flexibility

Programmable Front-End Electronics

- Same module for different products
- Can be "fine tuned" to individual heads
  - — in manufacturing
  - — autonomously, when need arises (DRP)
- Easier to use in development
  (Head parameters not yet known)

data recovery procedures, beyond ECC, e.g. increase bias.

Digitally programmable/addressable via serial port

- — Individual MR head bias
- — Individual head write current
- — Write damping
- — Pre-equalization (counters lead effects)
- — Head select
- — Servo bank writing/multi-channel servo writing
- — Signal gain
- — MR bias off/on/reduced during writing
- — Select "modes of awareness" (sleep, idle, etc)

States of "Awareness"

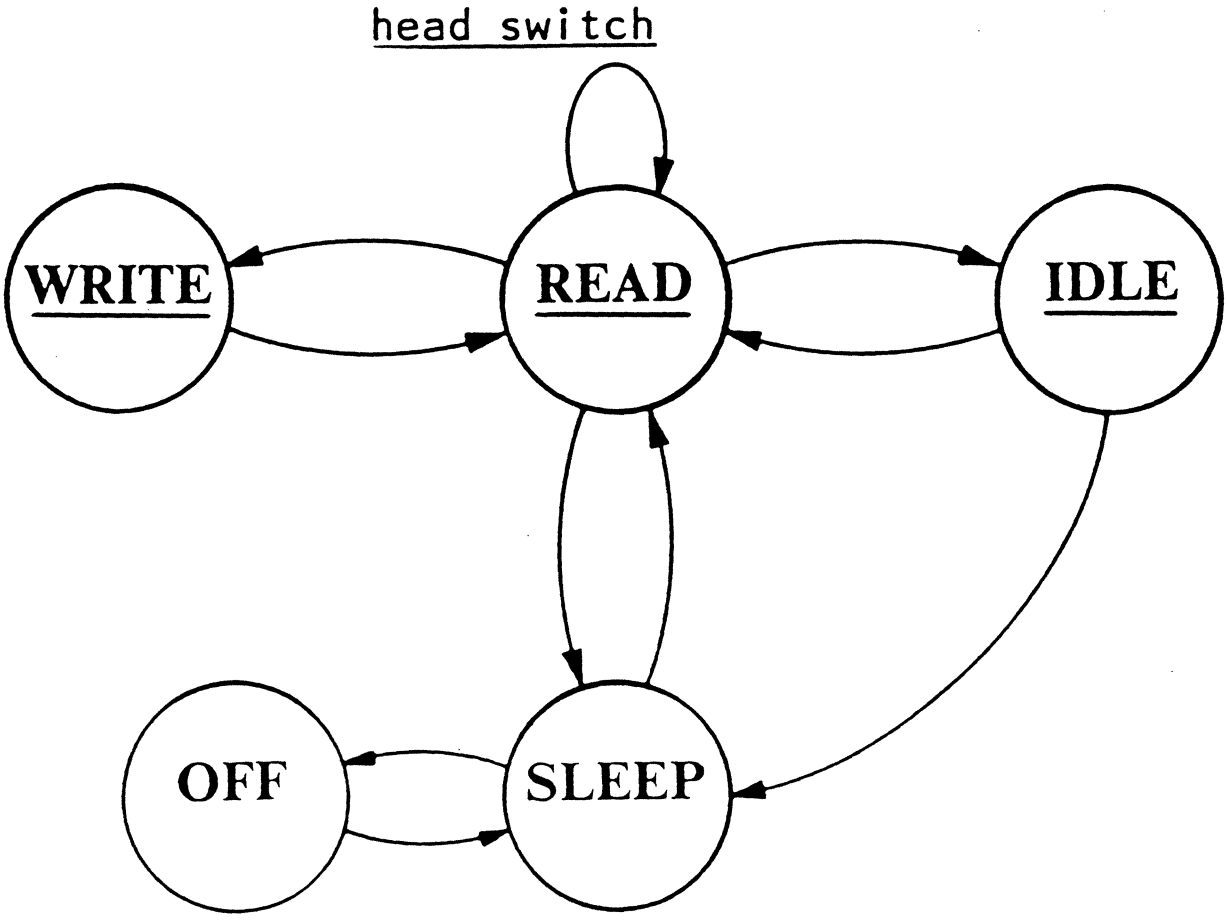

1992

Higher Data Rates, Why?

Data Rate =

$$2\pi \times \frac{RPM}{60} \times \frac{Track}{Radius} \times \frac{Linear}{Density}$$

Storage Industry Trends:

$$\textbf{\textit{Latency}} = \tfrac{1}{2} \times \frac{60}{RPM} \qquad \textbf{\textit{(down)}}$$

$$\textbf{\textit{Areal Density}} = \frac{track}{Density} \times \frac{Linear}{Density} \qquad \textbf{\textit{(up)}}$$

Conclusion:

Data rates are forced up, unless we use smaller disks (capacity loss)

Data Rate - Bandwidth

Higher Data Rates require wider signal path bandwidths.

Toughest Requirement:

- ***Write Path Bandwidth***

  — Well-defined transitions require short write current reversal times.

  — Write bandwidth much larger than read bandwidth

  — Write head/electronics interconnection becomes important

  — Reflections, standing waves, wave shapes

Goal of Study

What limits the data rate in an "industry typical" recording channel front-end?

Front-End: { *Transducer*, *Interconnect*, *AE Module* }

"All components in the Signal Path ahead of the channel chip"

A – Read Signal Path
B – Write Signal Path

**NB: Analysis should be adequate up to 1 GHz ⟹ A detailed component description is needed

Read Channel Front End

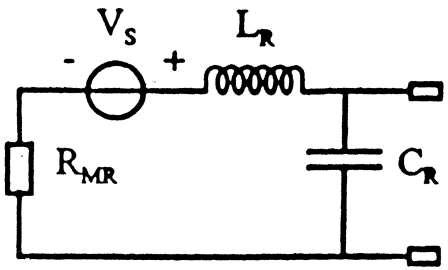

(a) MR head head

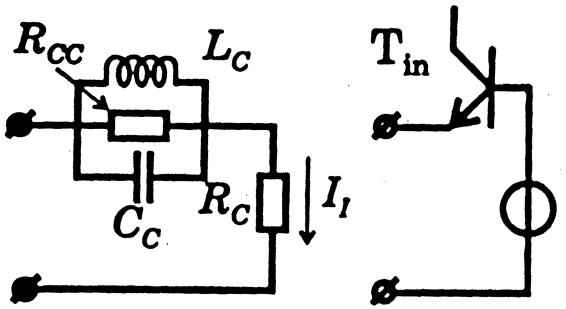

(a) Current sensing

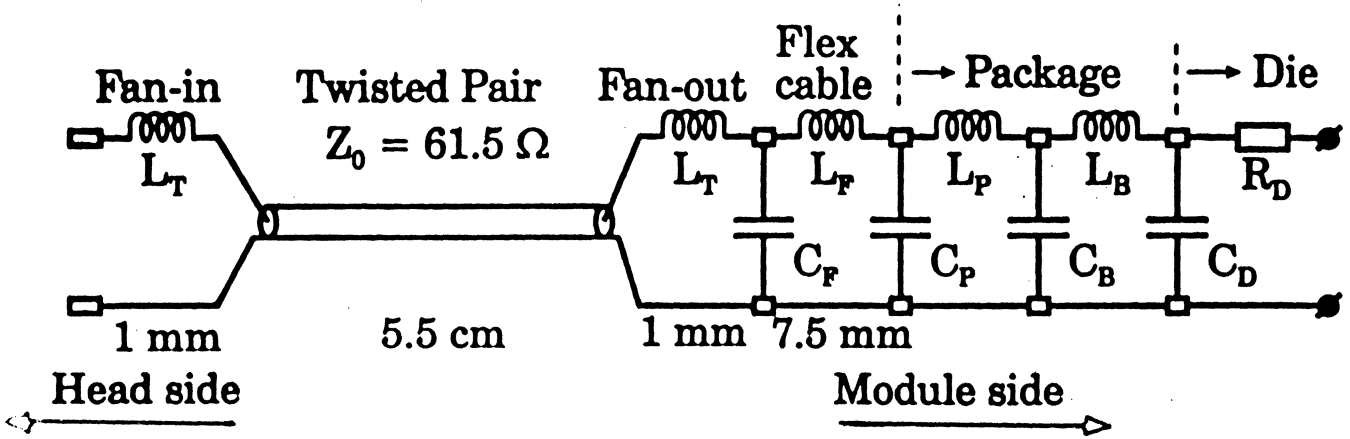

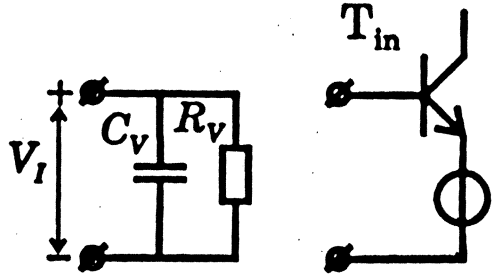

(b) Voltage sensing

Time Domain Reflectometer

Twisted Pair Characterization

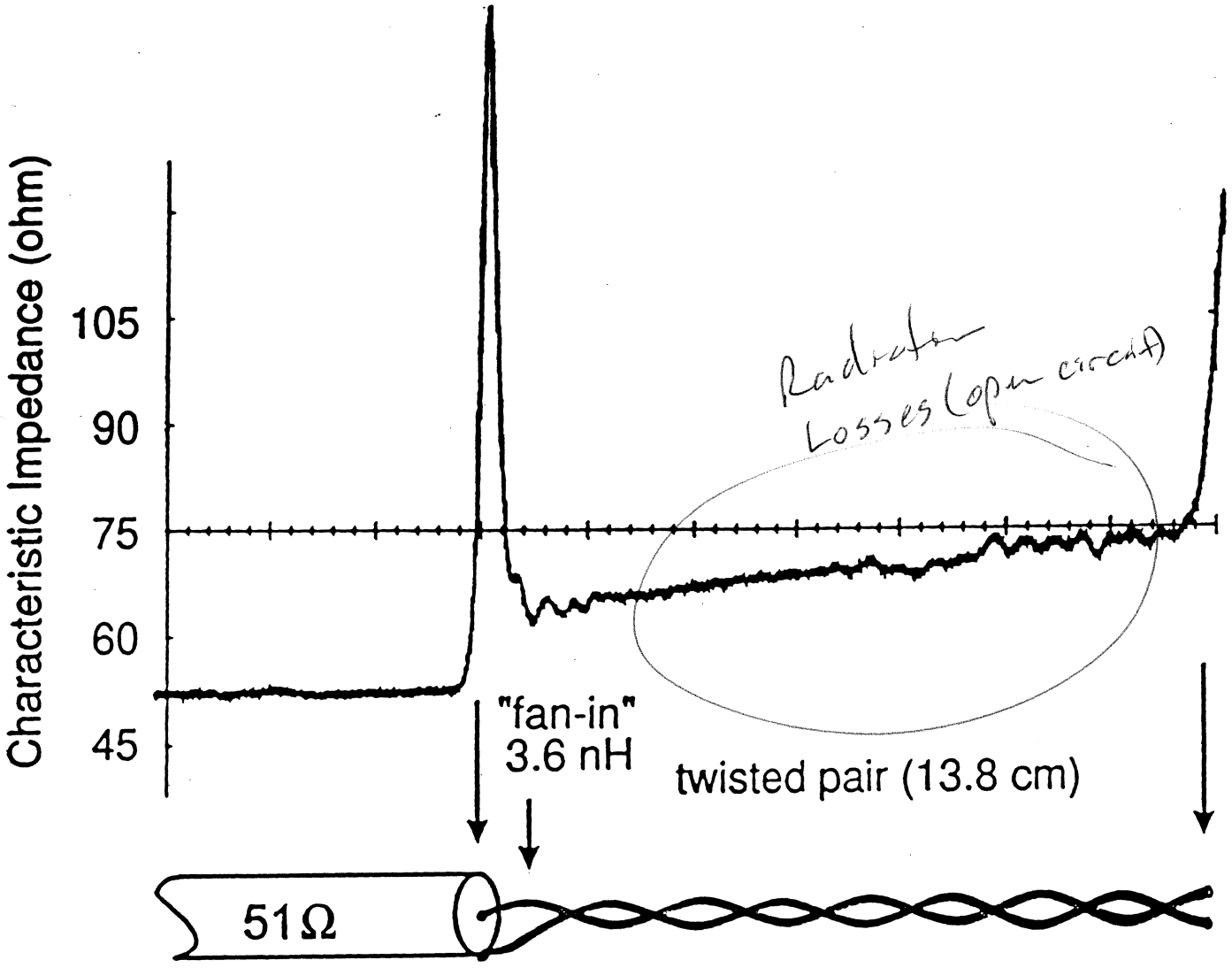

Open
14 ns
100 KS

Pre-amplifier input impedance models

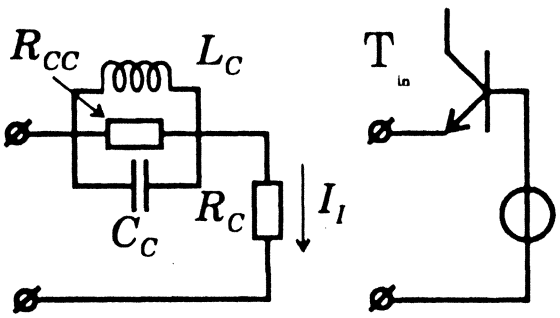

(a) Current sensing

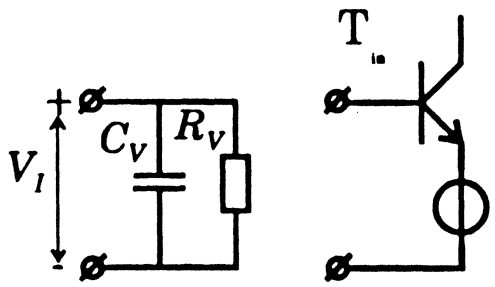

(b) Voltage sensing

Read Channel Parameter Values

- **MR Read Head**

  $15\ \Omega \leq R_{MR} \leq 45\ \Omega$, $L_R = 1$ nH,
  $C_R = 0.5$ pF, $V_S = I_{bias}\ \Delta R_{MR}$

- **Interconnect**

(a) Twisted Pair:

Gold-cladded copper wire, diameter 36 μm
Poly-urethane insulation, thickness 12 μm
One twist per mm, length 55 mm
$Z_0 = 61.5\ \Omega$, $v_p = 209 \times 10^6$ m/s, $\varepsilon_r = 2.1$, $R_S = 80.6\ \Omega/m$
Fan-in and fan-out 1 mm; $L_T = 3.6$ nH

(b) Flex cable:

Length 7.5 mm, $L_F = 15$ nH, $C_F = 0.75$ pF

(c) Package:

$L_P = 5$ nH, $C_P = 1$ pF
Bonding wire, $C_B = 0.6$ pF, $L_B = 1$ nH
Semiconductor die, $C_D = 0.5$ pF, $R_D = 0.5\ \Omega$

- **Read Pre-Amplifier**

  Single-ended input,NPN transistor area 14000 μm^2,
  $f_t = 3$ GHz, biased at 7 mA

(a) Voltage Sensing: $|Z_{in}| \gg R_{MR}$

$C_V = 14$ pF, $R_V = 500\ \Omega$

(b) Current Sensing: $|Z_{in}| \ll R_{MR}$

$C_C = 0.85$ pF, $R_{CC} = 3.5\ \Omega$, $L_C = 0.15$ nH, $R_C = 5\Omega$

Voltage Sensing Amp

Voltage transfer across MR head to preamp input leads

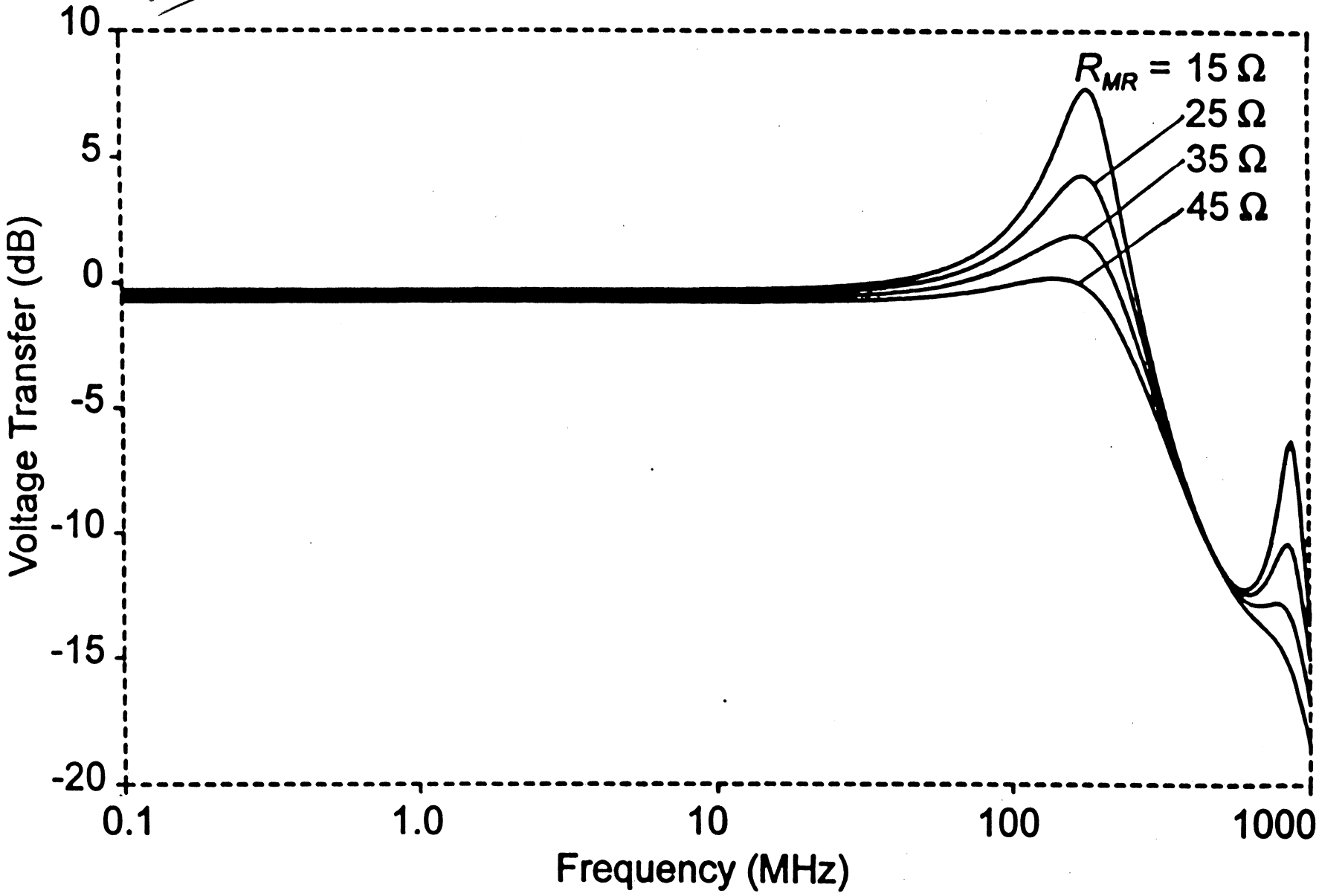

Current Sensing Amp

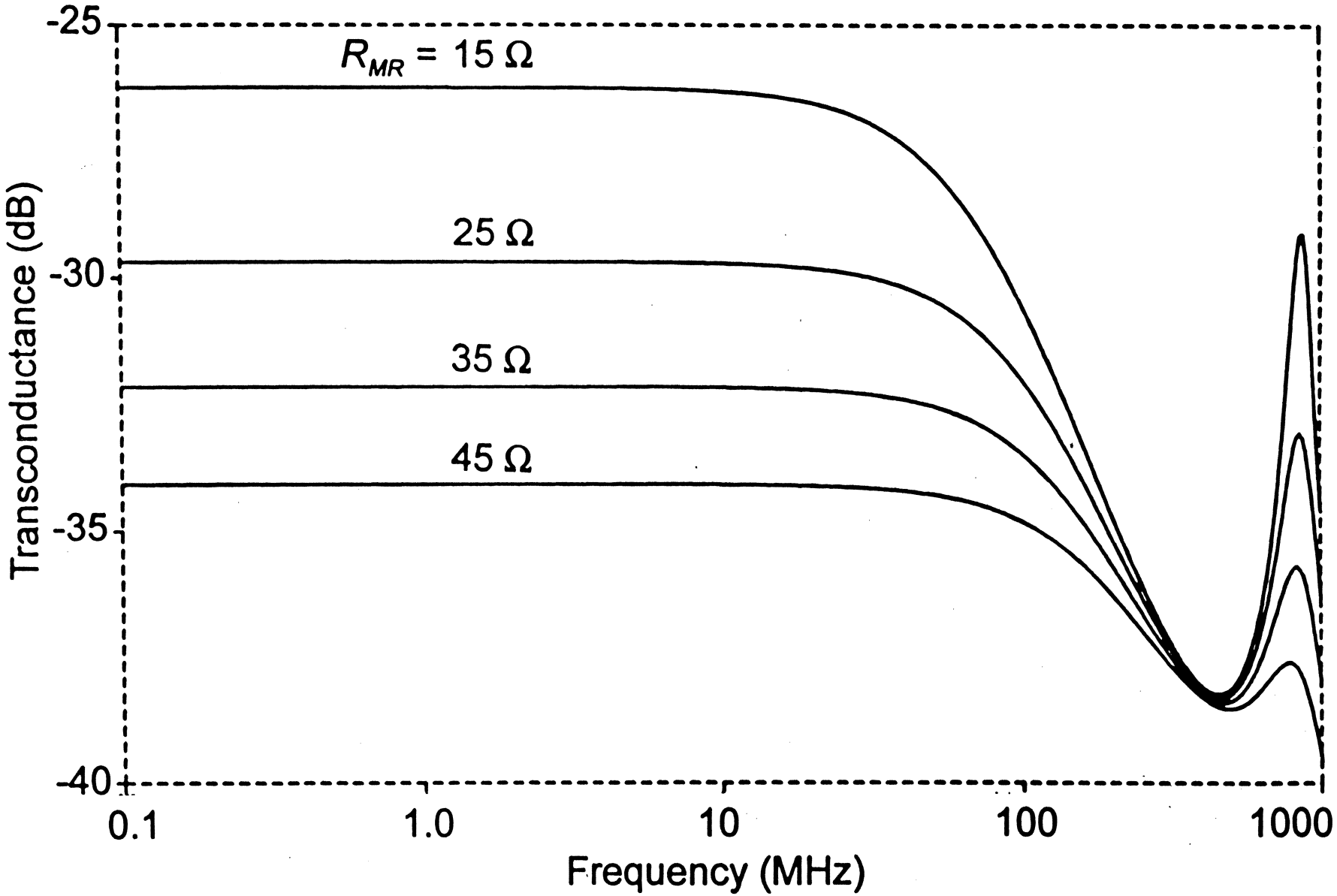

Read Bandwidth (full front-end)

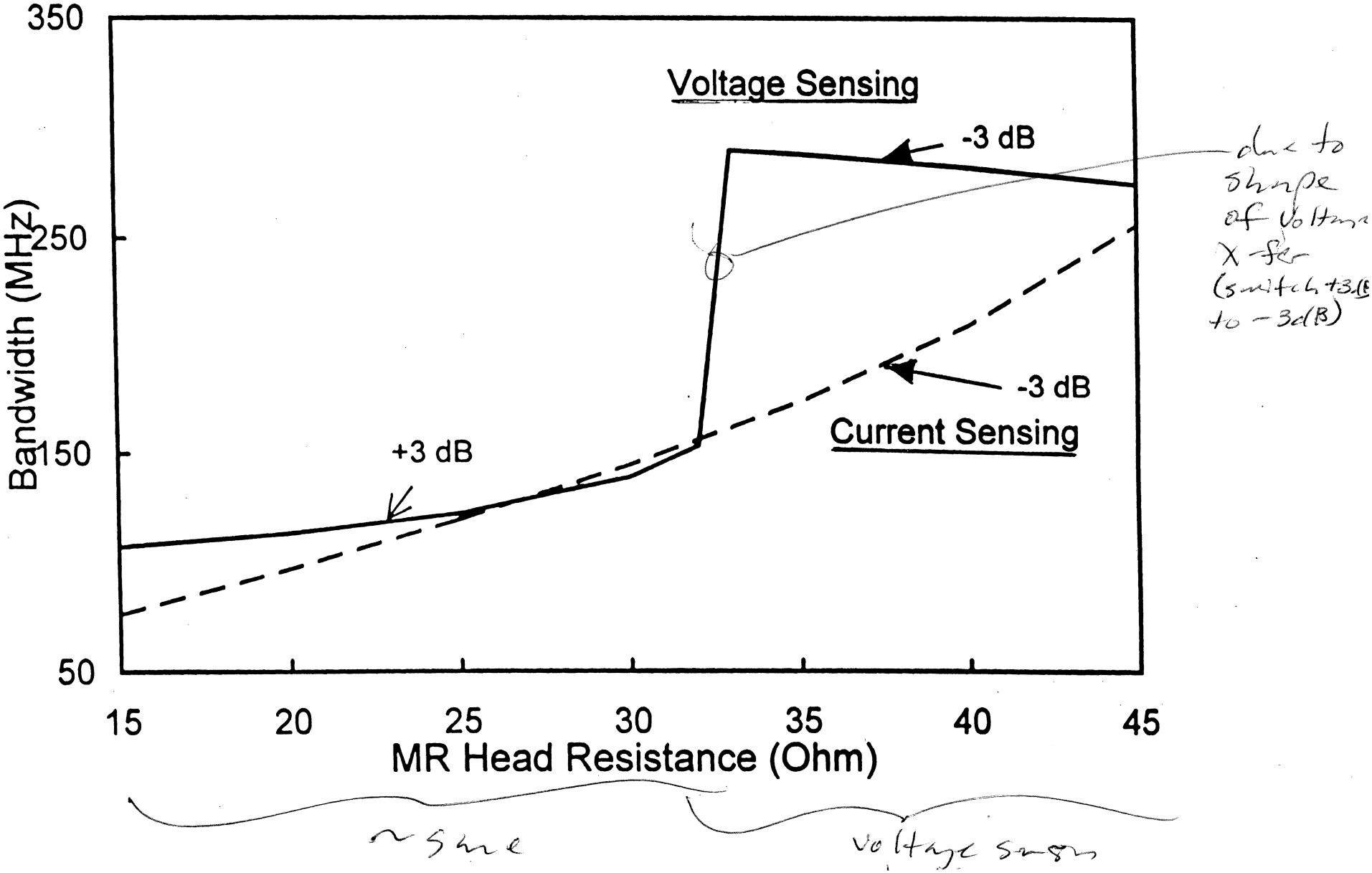

Read Bandwidth (no transmission line)

This is optomistic

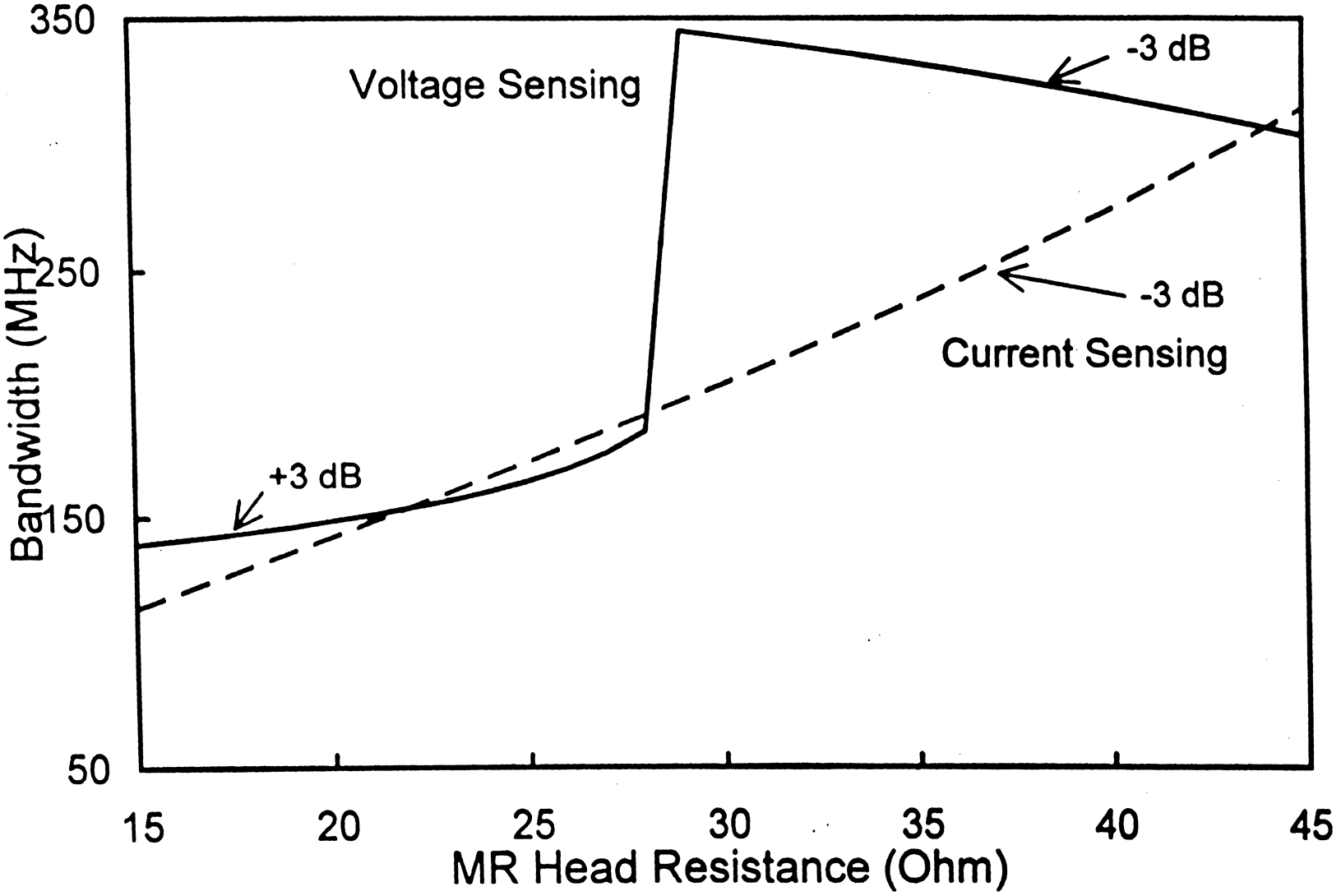

Read Bandwidth (lumped approximation)

– a little less optomistic

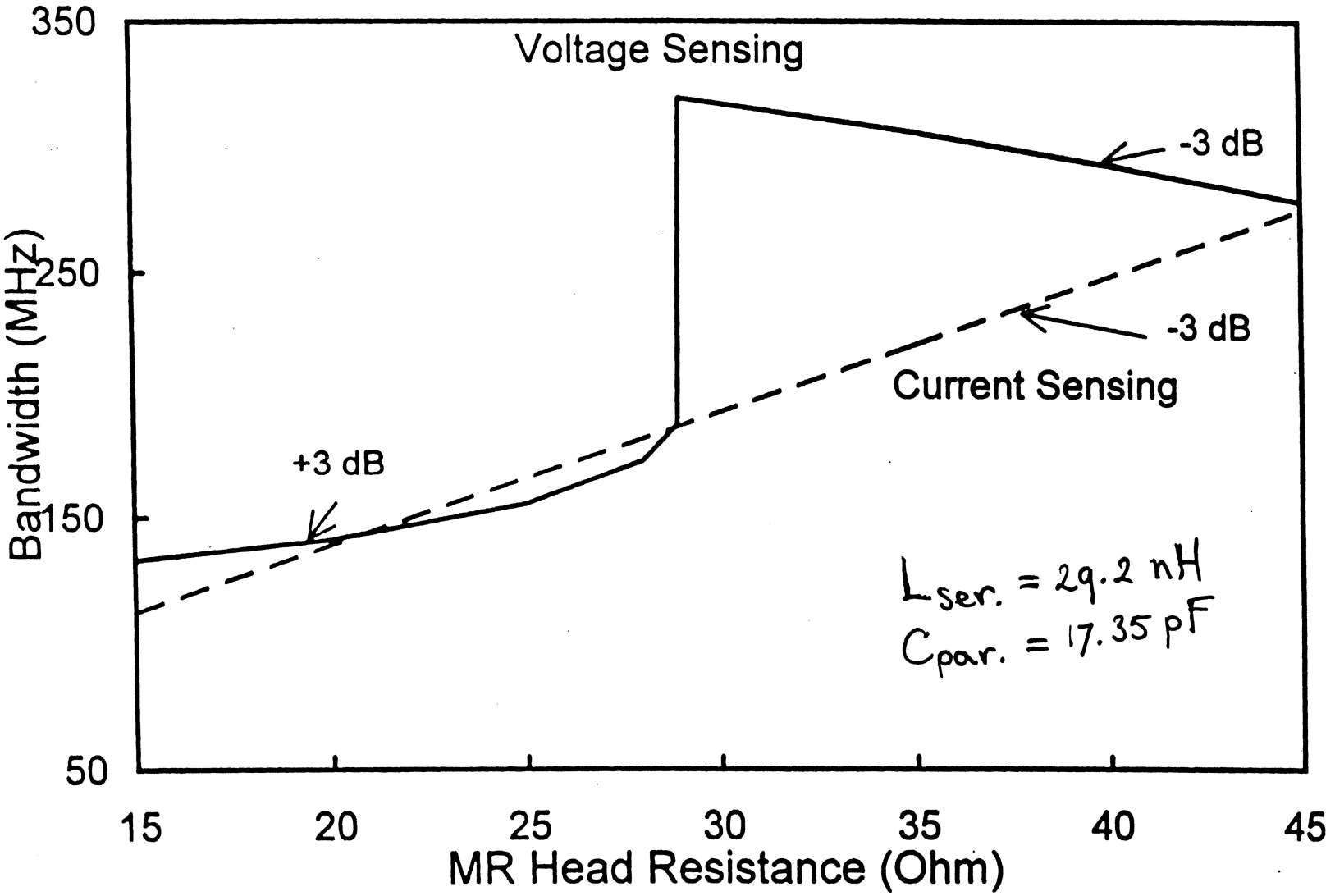

Conclusions

- **Read Path**

  - √ The bandwidth increases with increasing R_{MR}
  - √ Only for higher R_{MR} is voltage sensing better than current sensing ($> 33\ \Omega$)
  - √ Current sensing gives a better equalizable frequency response
  - √ Without transmission line the bandwidth is 50 - 75 MHz optimistic
  - √ The minimum bandwidth is 76 MHz (CS) or 108 MHz (VS)

Write Driver Dilemma

★ Limited power supply voltage: $V_s \pm x\ \%$
(e.g. 5V ± 10%)

★ Active devices in write driver output stage need voltage head room of ΔV when fully on.
(Bipolar devices $\Delta V \simeq 0.9$ V)

● Available peak-to-peak head voltage swing:

$$V_{h,pp} = 2\left\{V_s(1 - \frac{x}{100}) - 2\Delta V\right\}$$

● Also:

$$V_{h,pp} \simeq 2\left\{L\frac{dI}{dt} + IR\right\} = 4\frac{LI_W}{\tau_W} + 2I_W R_h$$

I_W peak-to-base write current
τ_W write current reversal time
R_h head series resistance
L inductance $(L = L_h + L_l)$

● Scaling $L_h = N^2 L_o$, $R_h = NR_o$, $I_W = MMF/N$

Write Driver Dilemma

- $V_{h,pp} = MMF\left\{ \frac{4L_l}{N\tau_W} + \frac{4NL_o}{\tau_W} + 2R_o \right\}$
- Smallest when $N = \sqrt{\frac{L_l}{L_o}}$ $\quad (L_h = L_l)$ head ind. = wire parasitic ind.
- Minimum is:

$$V_{h,pp} = MMF\left\{ \frac{8\sqrt{L_l L_o}}{\tau_W} + 2R_o \right\}$$

- Therefore MMF, L_l, L_o and R_o are limited to values satisfying:

$$MMF\left\{ \frac{4\sqrt{L_l L_o}}{\tau_W} + R_o \right\} \leq V_s\left(1 - \frac{x}{100}\right) - \Delta V$$

Example: Suppose $L_o = 0.8$ nH, $R_o = 1\ \Omega$, $V_s = 5$V, $x = 10\%$, $\Delta V = 0.9$V, $\tau_W = 5$ ns, $L_l = 60$ nH

★ We find $V_{h,pp} = \mathbf{5.4V}$, $I_W = \mathbf{46mA}$, $N = \mathbf{9}$, $L_h = \mathbf{65nH}$

★ For a (0,k) run-length limited code with an 8/9 code rate (where τ_W is half the closest transition spacing), we find a maximum data rate of **11.1 MB/s**

Write Driver Topologies

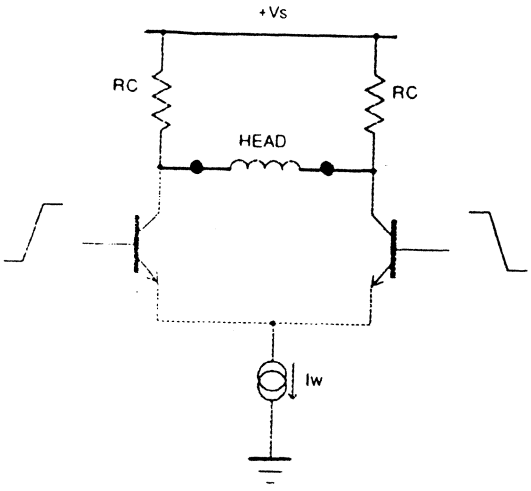

Power Inefficient
Poor Headroom

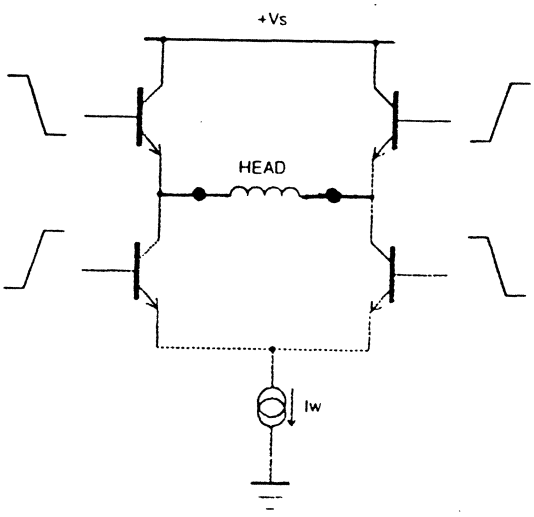

Power Efficient
Poor Headroom

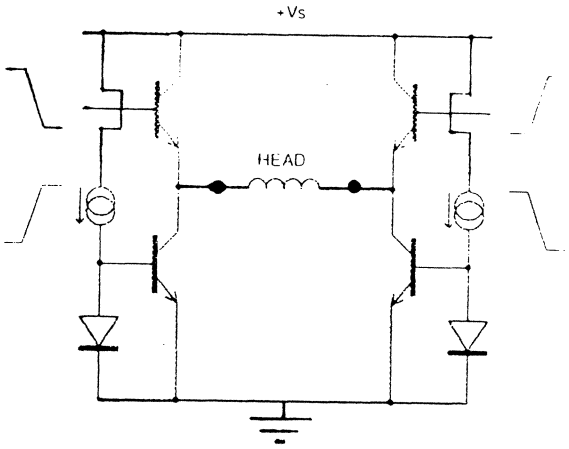

Power Efficient
Good Headroom

Write Driver Output

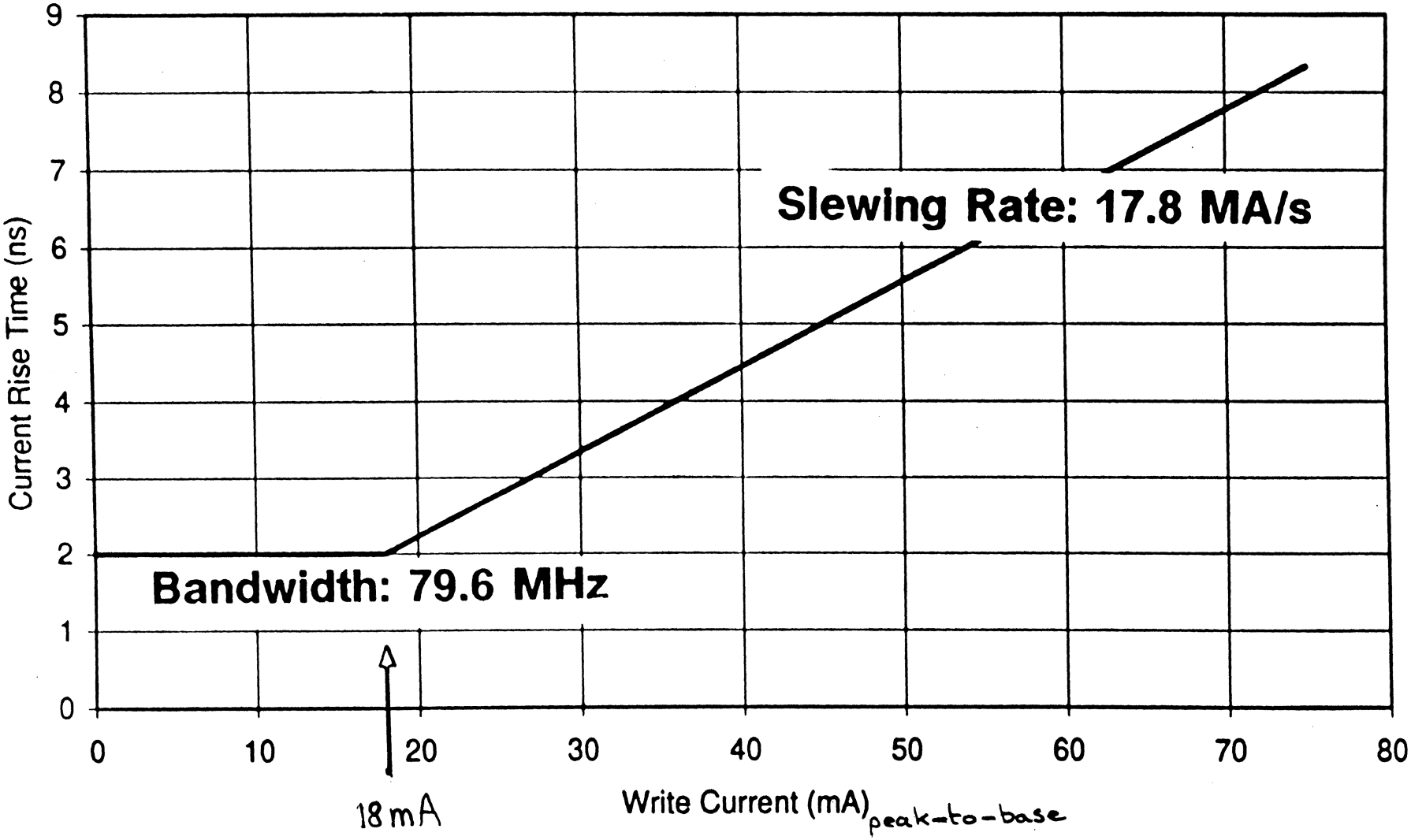

Write Channel Front End

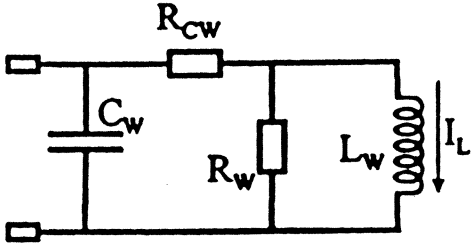

(b) Thin-film write head

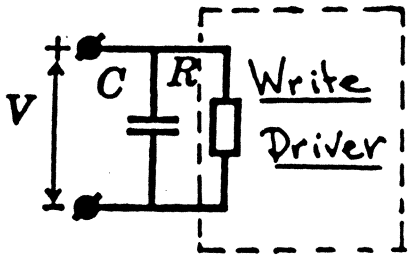

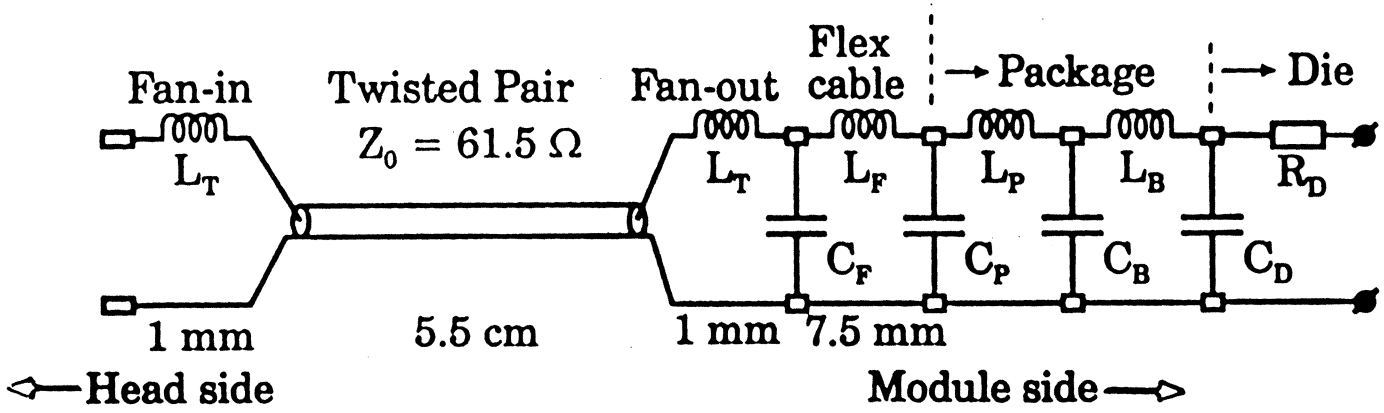

Write Head Model

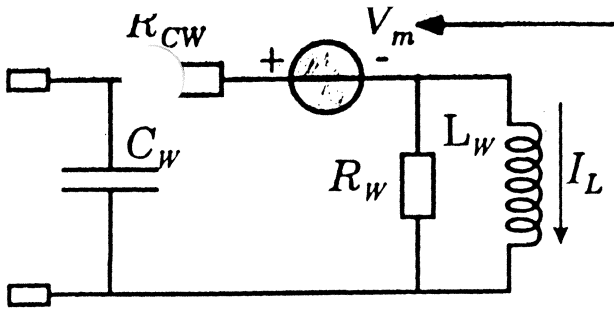

(a) Write Head Coil

$$V_m = \mu_0 NA \frac{dM(t)}{dt}$$

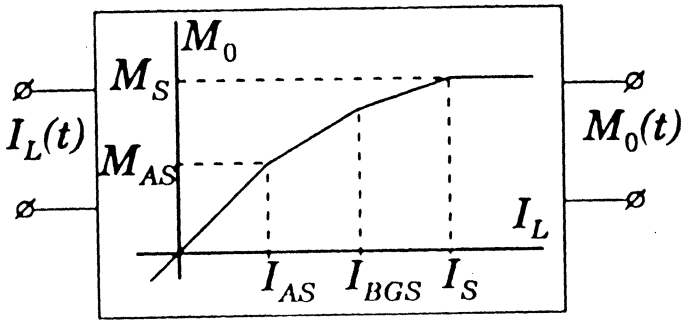

(b) I_L to M_0 Conversion

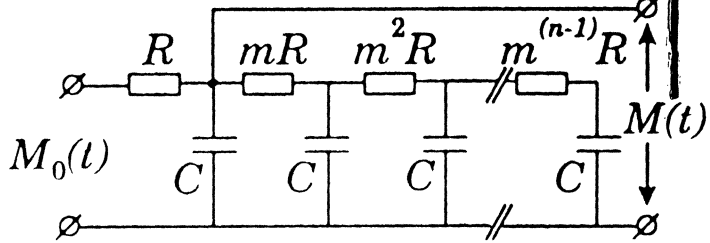

$\tau_1 = RC$ $\quad\quad$ $\tau_n = m^{(n-1)}\tau_1$

(c) Eddy Current Filter

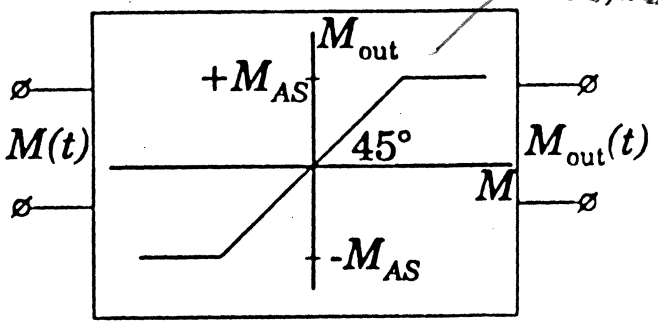

(d) Apex window

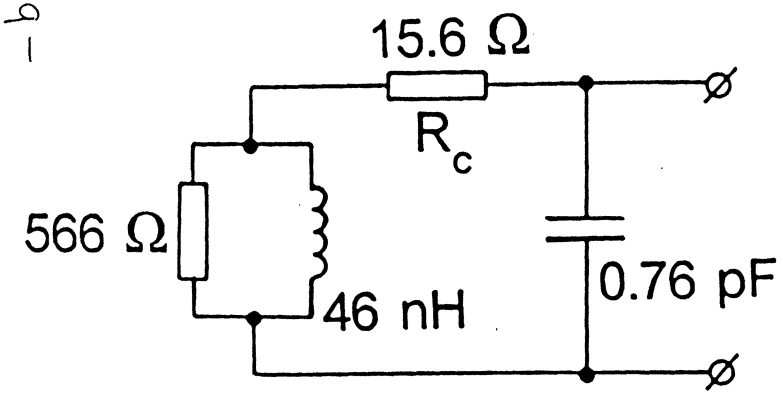

(a)

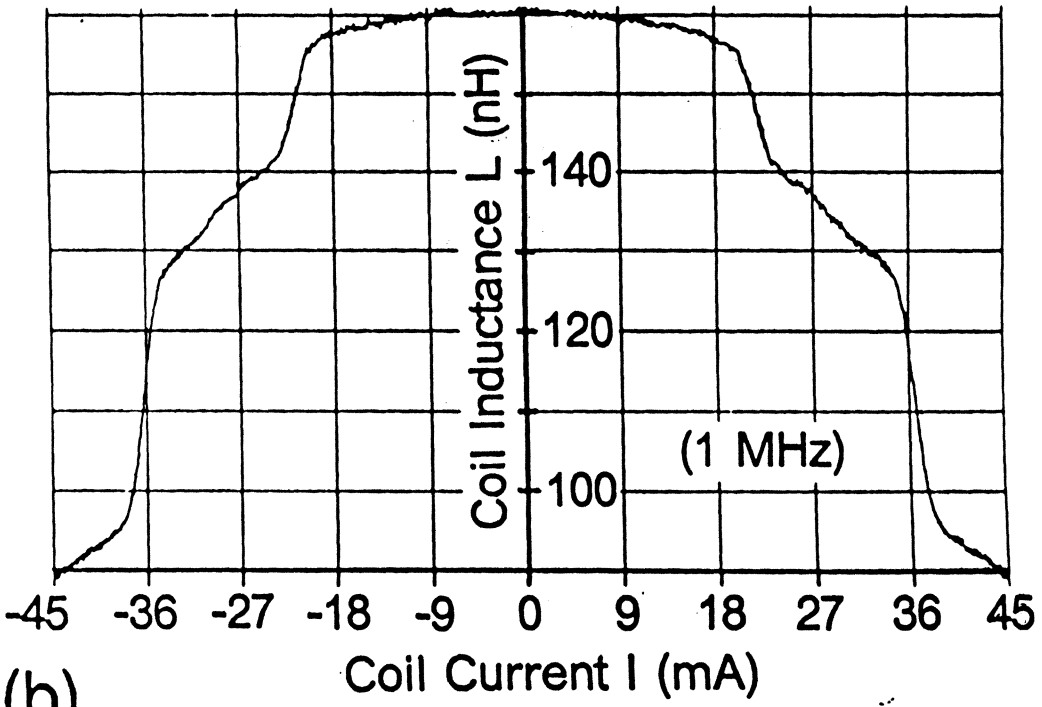

(b)

- model very close to data.

When saturated no I_w response

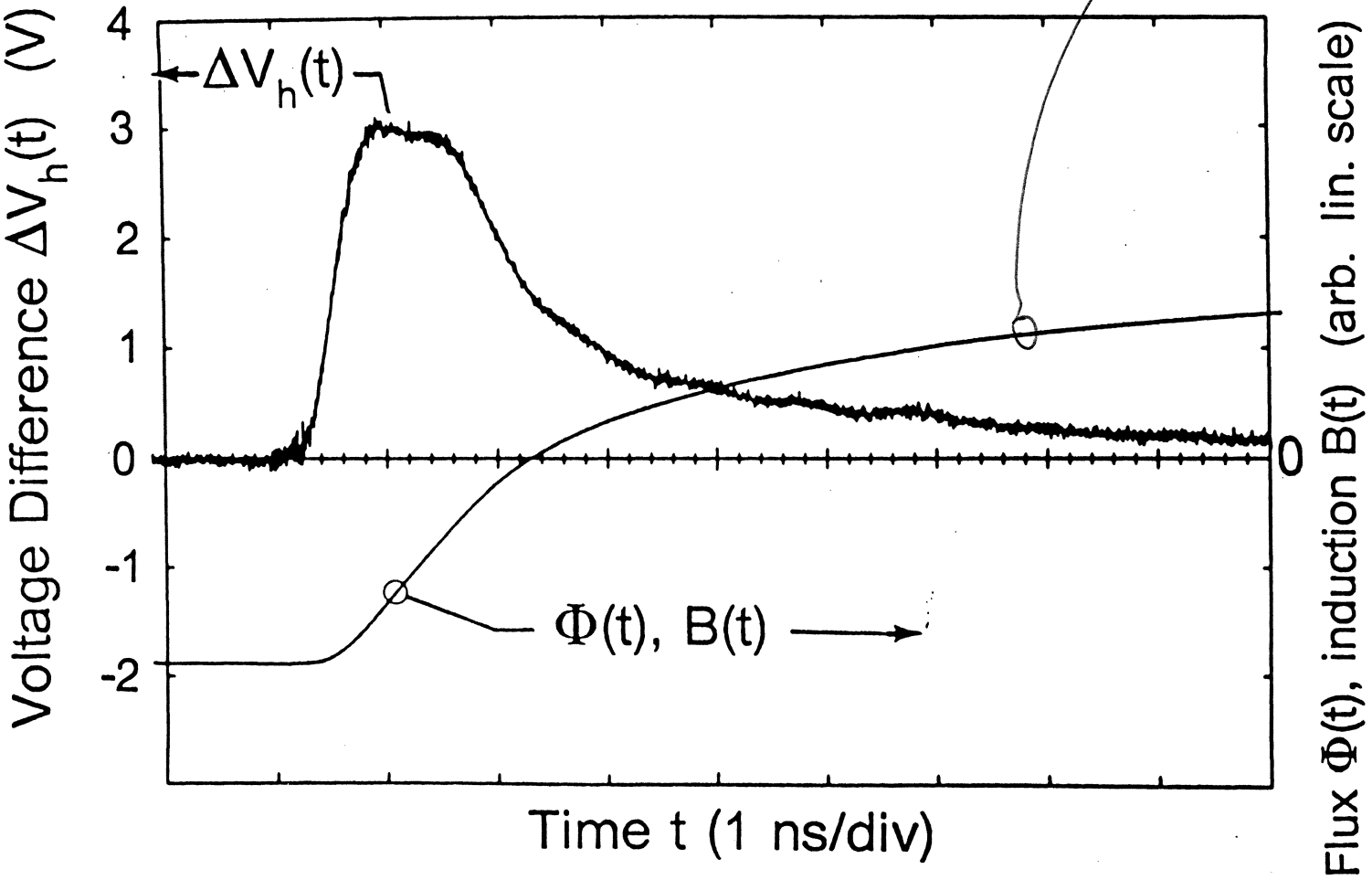
integrate
To generate M vs I curve
$\Delta V_h(t)$
$\Phi(t)$, B(t)
Voltage Difference $\Delta V_h(t)$ (V)
Flux $\Phi(t)$, induction B(t) (arb. lin. scale)
Time t (1 ns/div)
4
3
2
1
0
-1
-2
0

Measured and Calculated B(t)

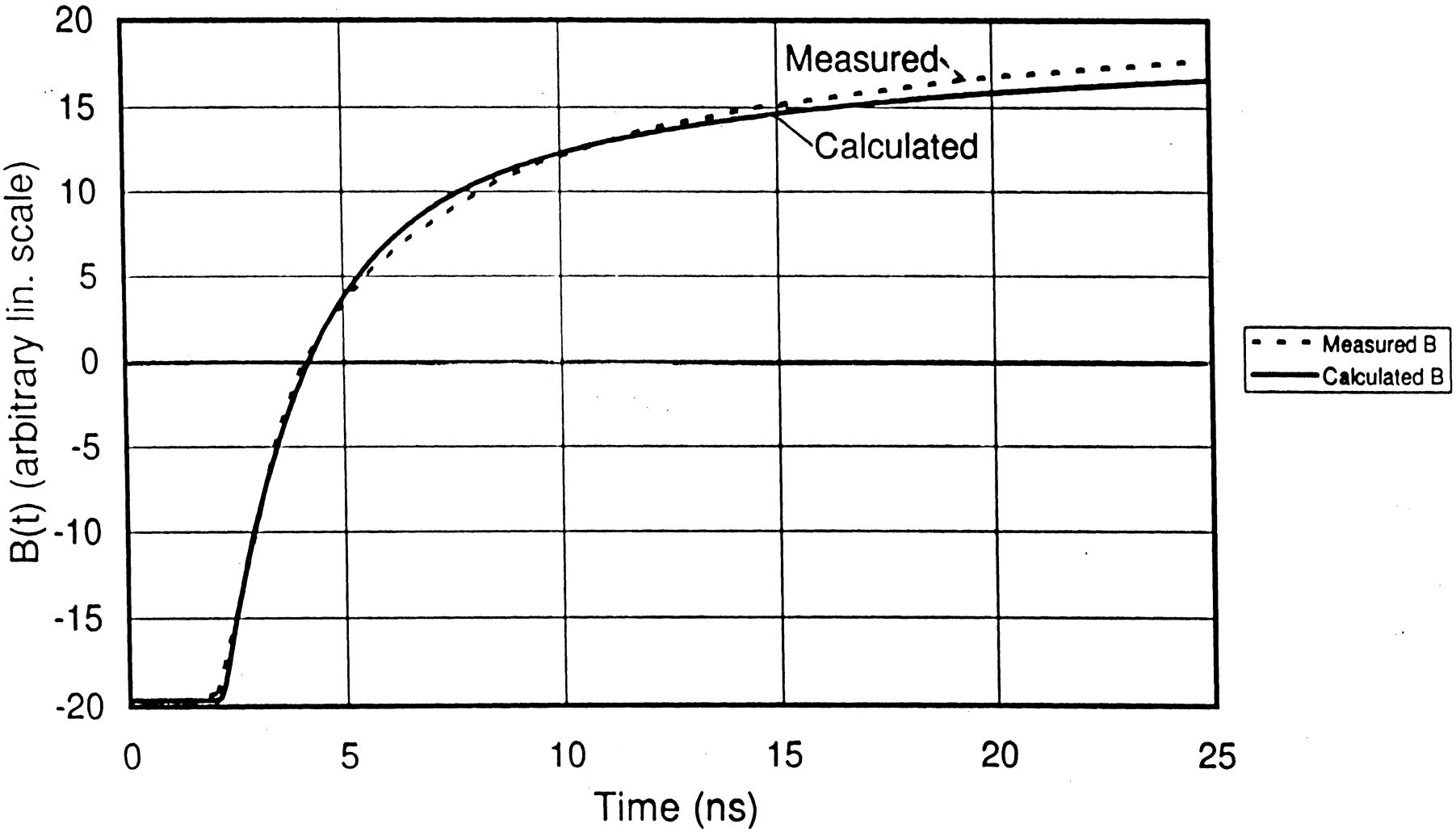

Write Channel Parameter Values

- **Write Driver**

  Differential output,NPN trnasistor area 7000 μm^2,
  f_t = 3 GHz, C = 2.5 pF, no damping resistor
  Slewing rate 18 MA/s ($I_W \geq 18$ mA)
  Bandwidth 80 MHz, Rise time 2 ns ($I_W \leq 18$ mA)

- **Inductive Write Head**

(a) Geometry:

15 turn 80/20 NiFe head
P_2W pole tip 4 μm, P_2W yoke = 60 μm
P_2T = 4.7 μm, $P_1W \gg P_2W$, P_1T = 3 μm,
yoke height 130 μm

(b) Saturated Coil Impedances:

C_W = 0.75 pF, R_W = 600 Ω, R_{CW} = 16 Ω, L_W = 50 nH

(c) Induced Voltage:

$$V_m = -N\frac{d\Phi}{dt} = -NA\frac{dB(t)}{dt}$$

N = 15, A = $P_2T \times P_2W$ yoke, NA = 4.3×10^{-9} m^2

(d) Current I_W to Induction B_0 Conversion:

$B_0 = B_{AS}$ = 0.6 T at I_W = 22 mA
$B_0 = B_{BGS}$ = 0.85 T at I_W = 36.6 mA
$B_0 = B_S$ = 1 T at I_W = 75 mA

(e) Eddy Current Filtering:

τ_1 = 2.56 ns, m = 3.16, n = 4

(f) Apex Saturation Window:

$B(t) = B_{out}(t)$ $B \leq B_{AS}$
$B(t) = B_{AS}$ $B > B_{AS}$
$B_{out}(t) \propto H_{write}(t)$

Write Coil Series Inductance

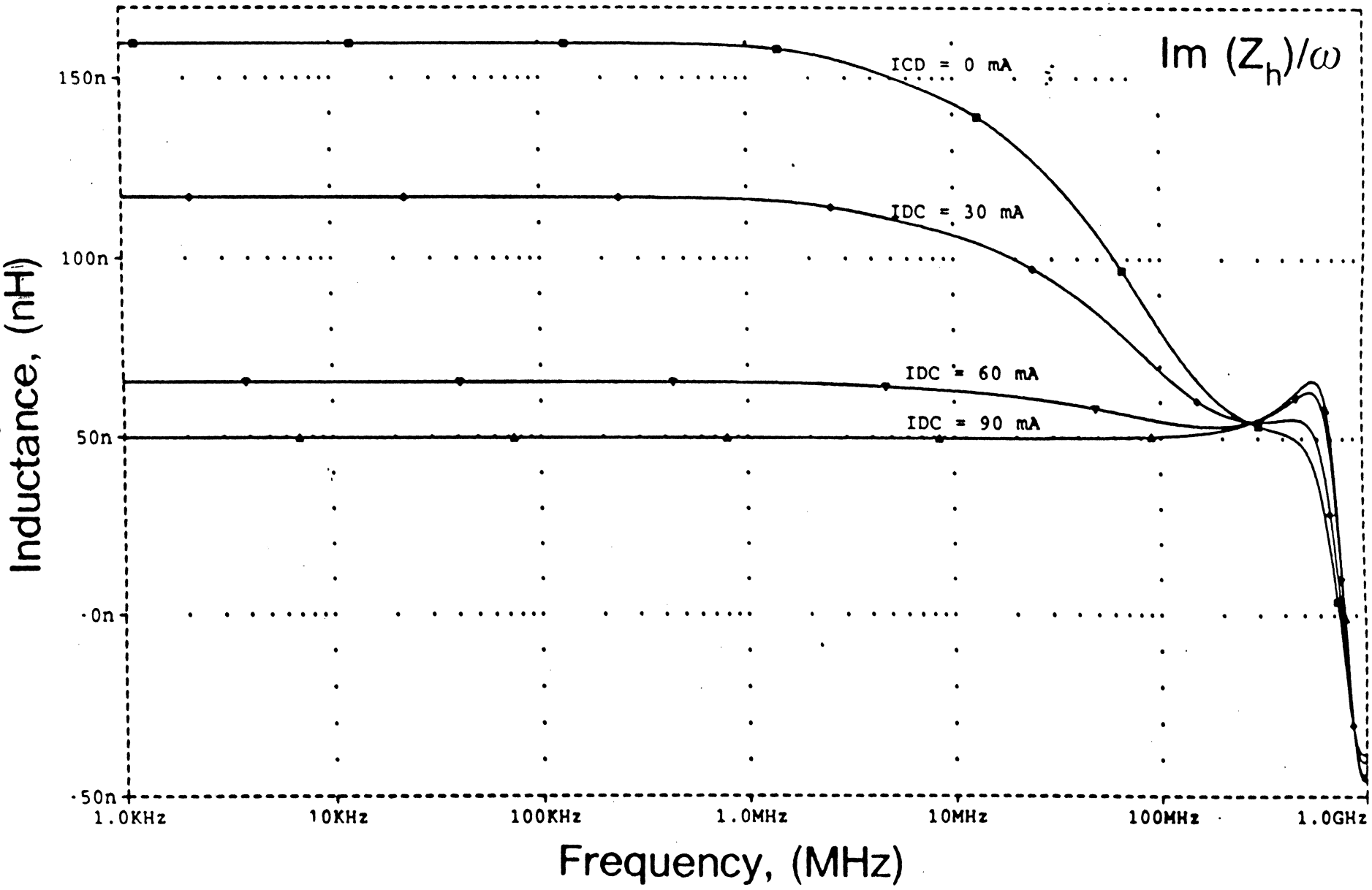

Write Channel Waveforms

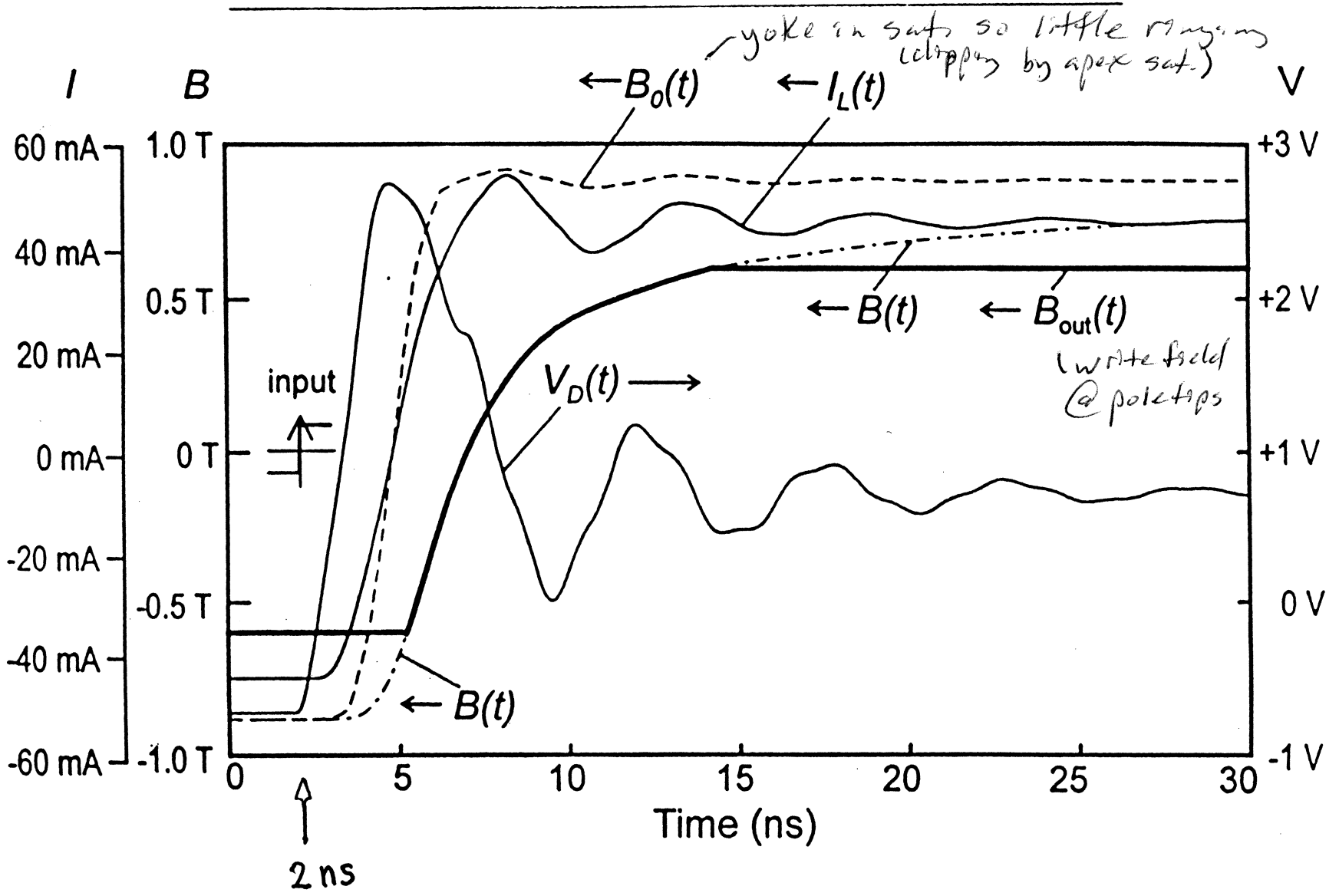

(First) Current Over/Undershoot

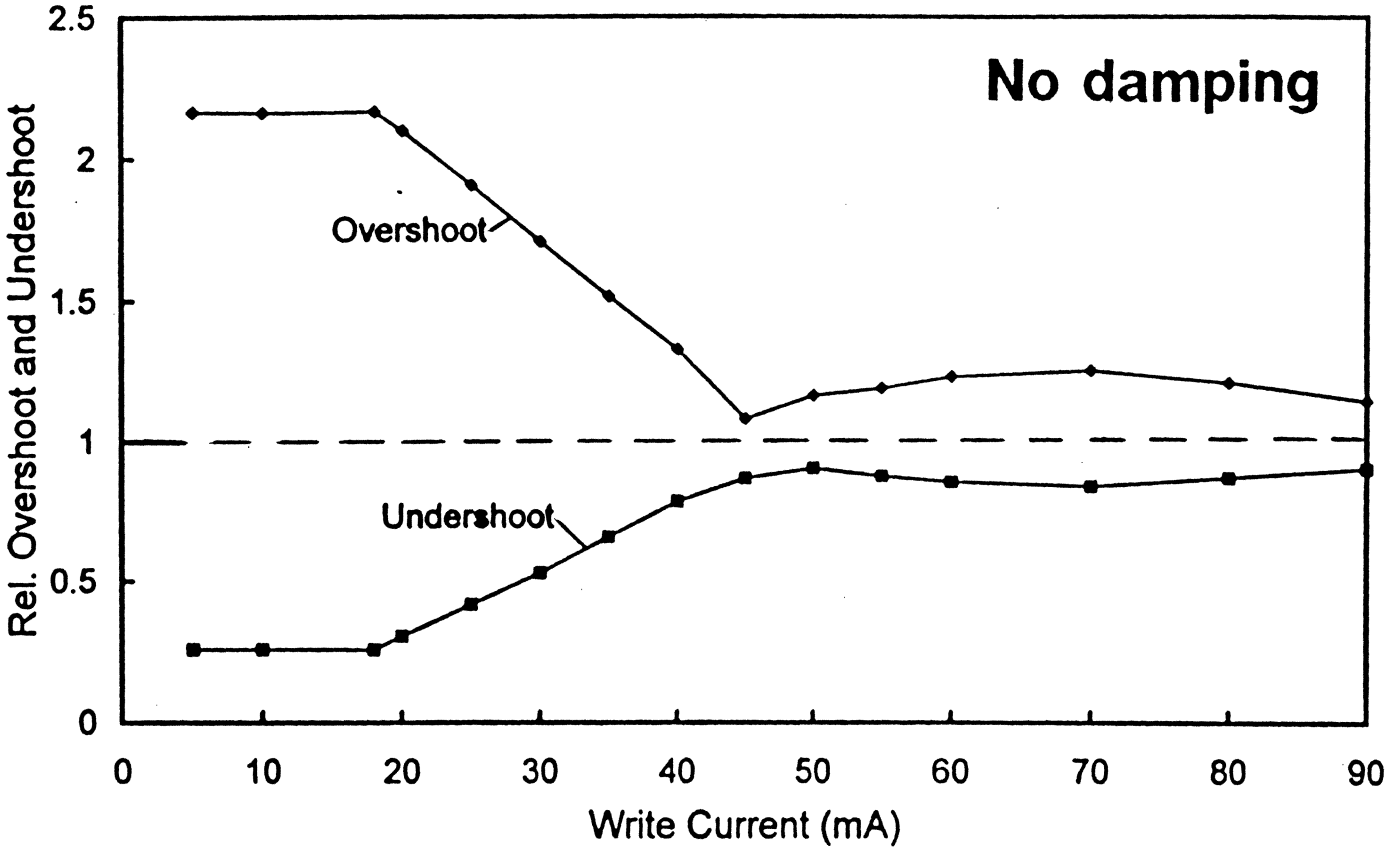

Ø-p

Write Channel Test Signals

- Square wave input
  Induction swing large enough
  Criterion: $B_{pp} > 2\,B_{min}$ (B_{AS})

- Isolated transition input
  Reversal time short enough
  Criterion: $\tau_{rev} < \tau_{max}$ $(2\,F_{W_{max}})^{-1}$

- Di-bit input
  Bit shift small enough
  Criterion: $\varepsilon < \varepsilon_{max}$ (15 %)

Peak-to-Peak Yoke Induction Swing

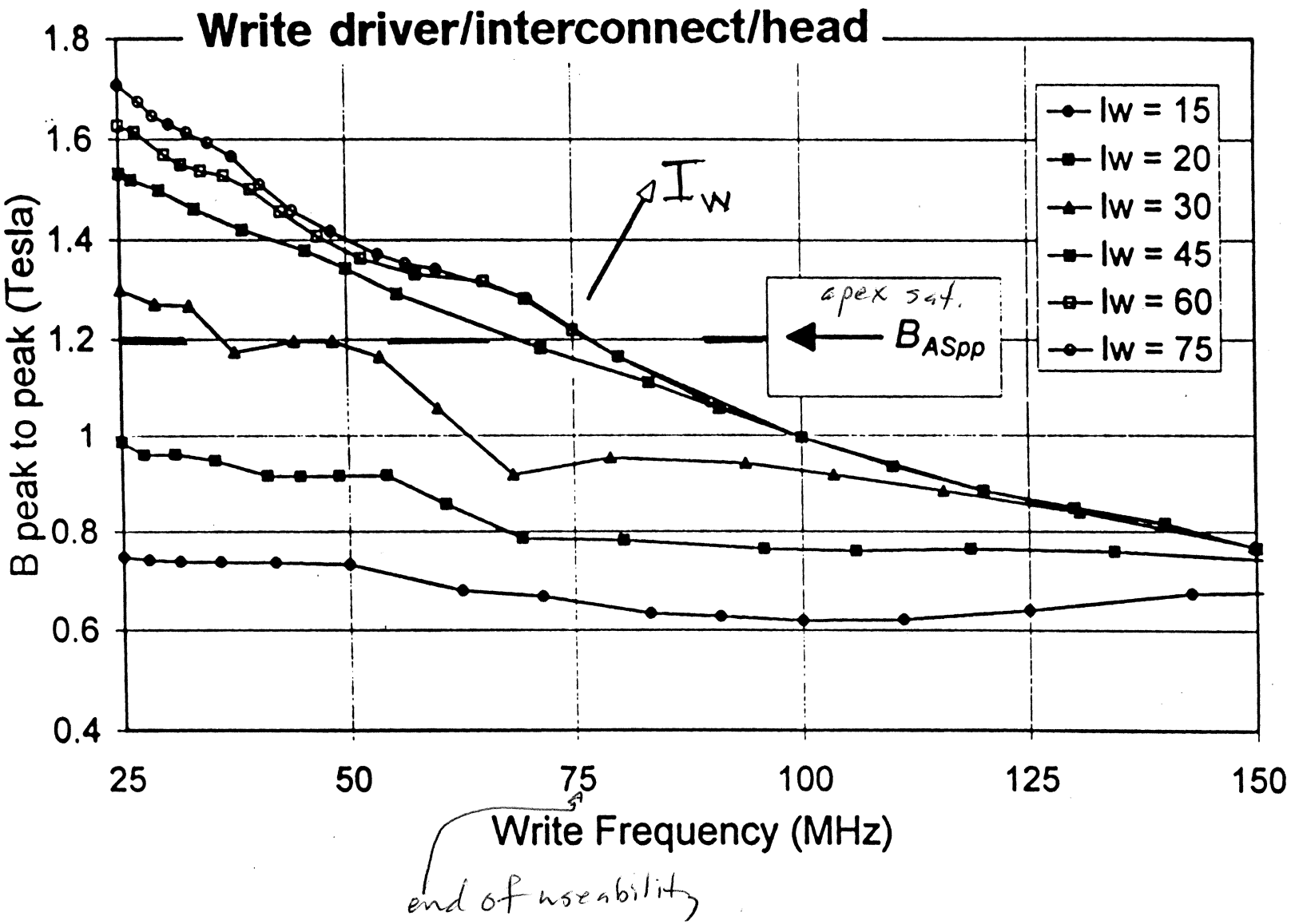

Peak-to-Peak Yoke Induction Swing

- Square waves

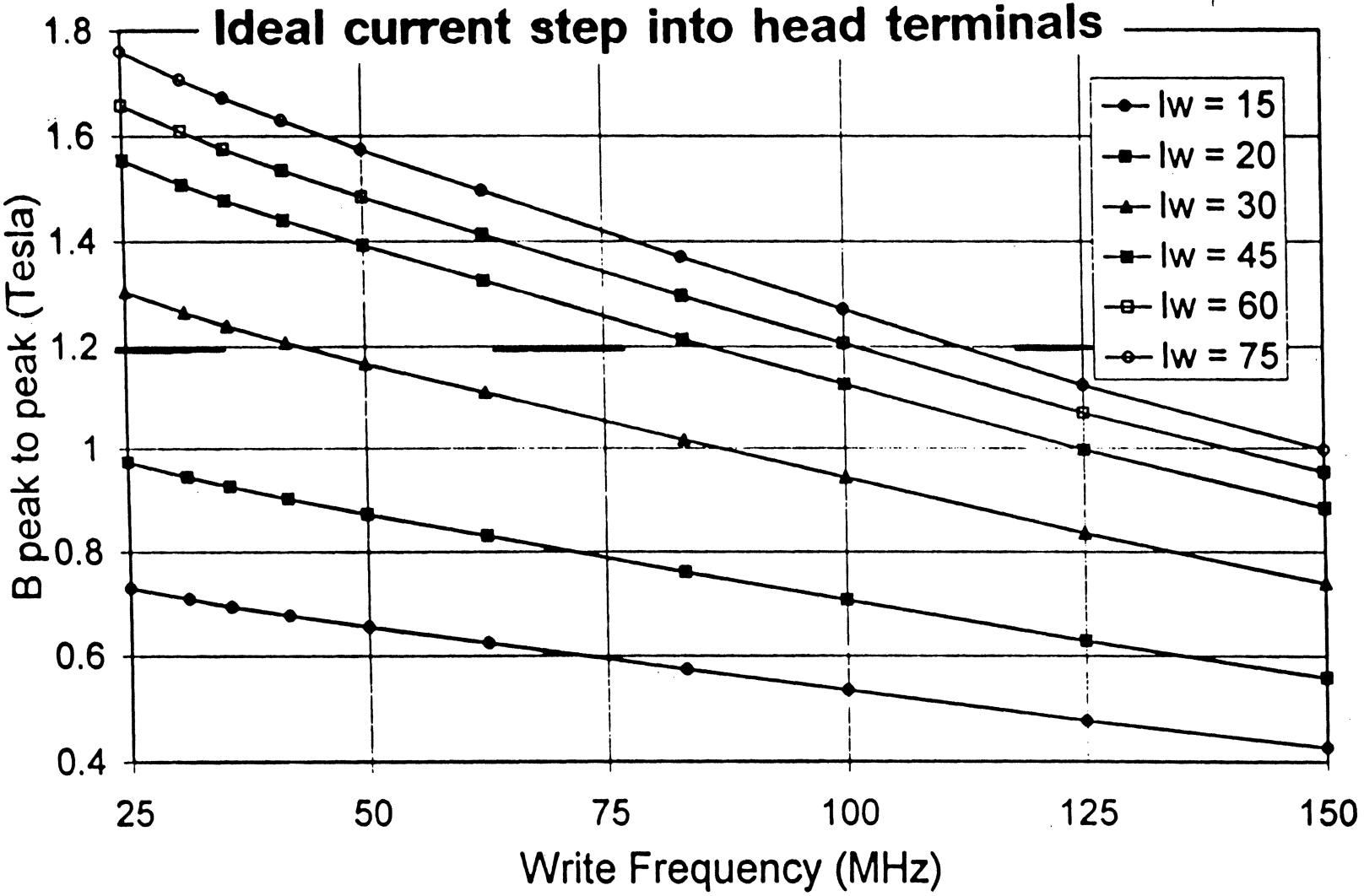

Write Field Reversal Time

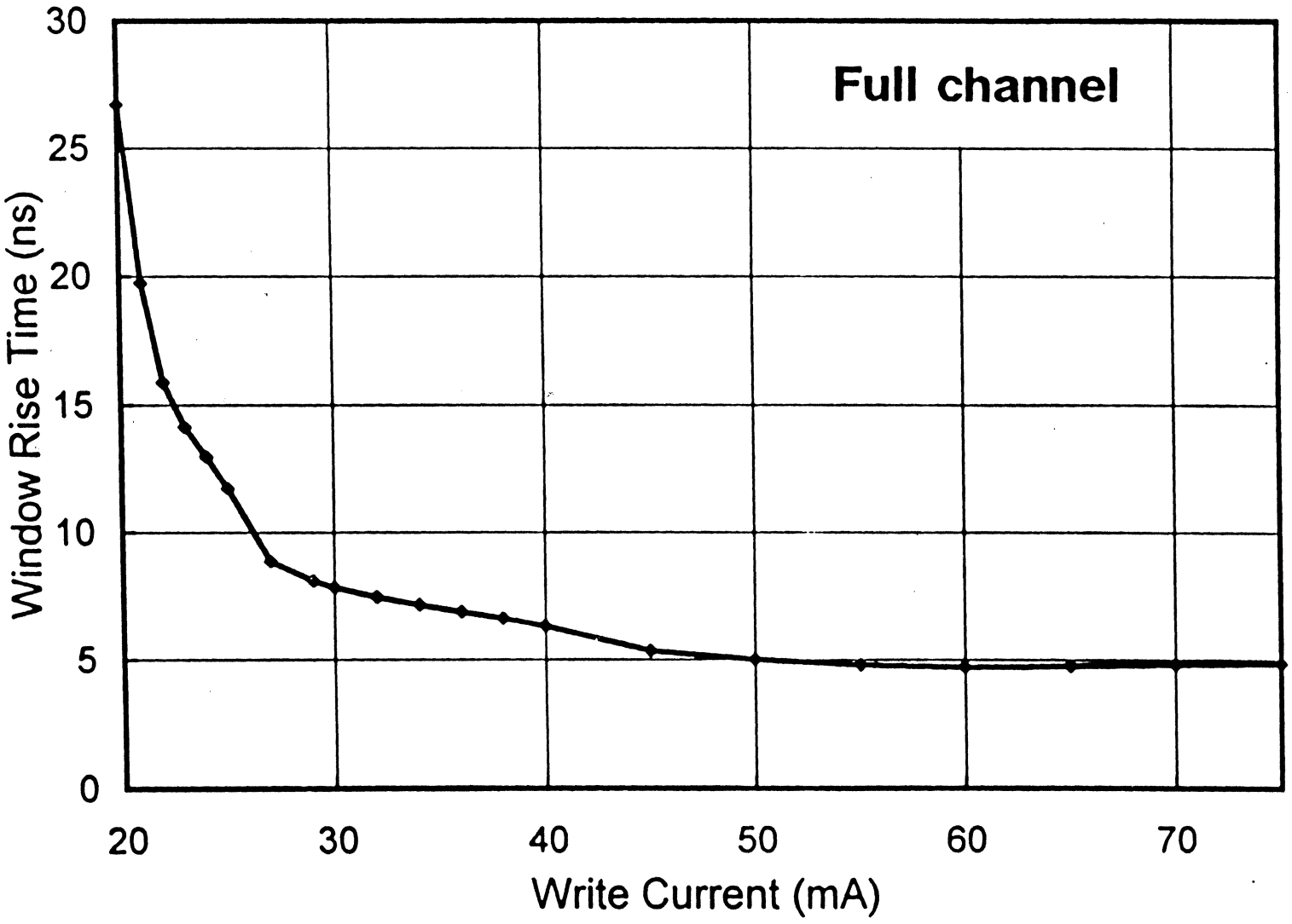

Apex sat. limited

Write Field Reversal Time

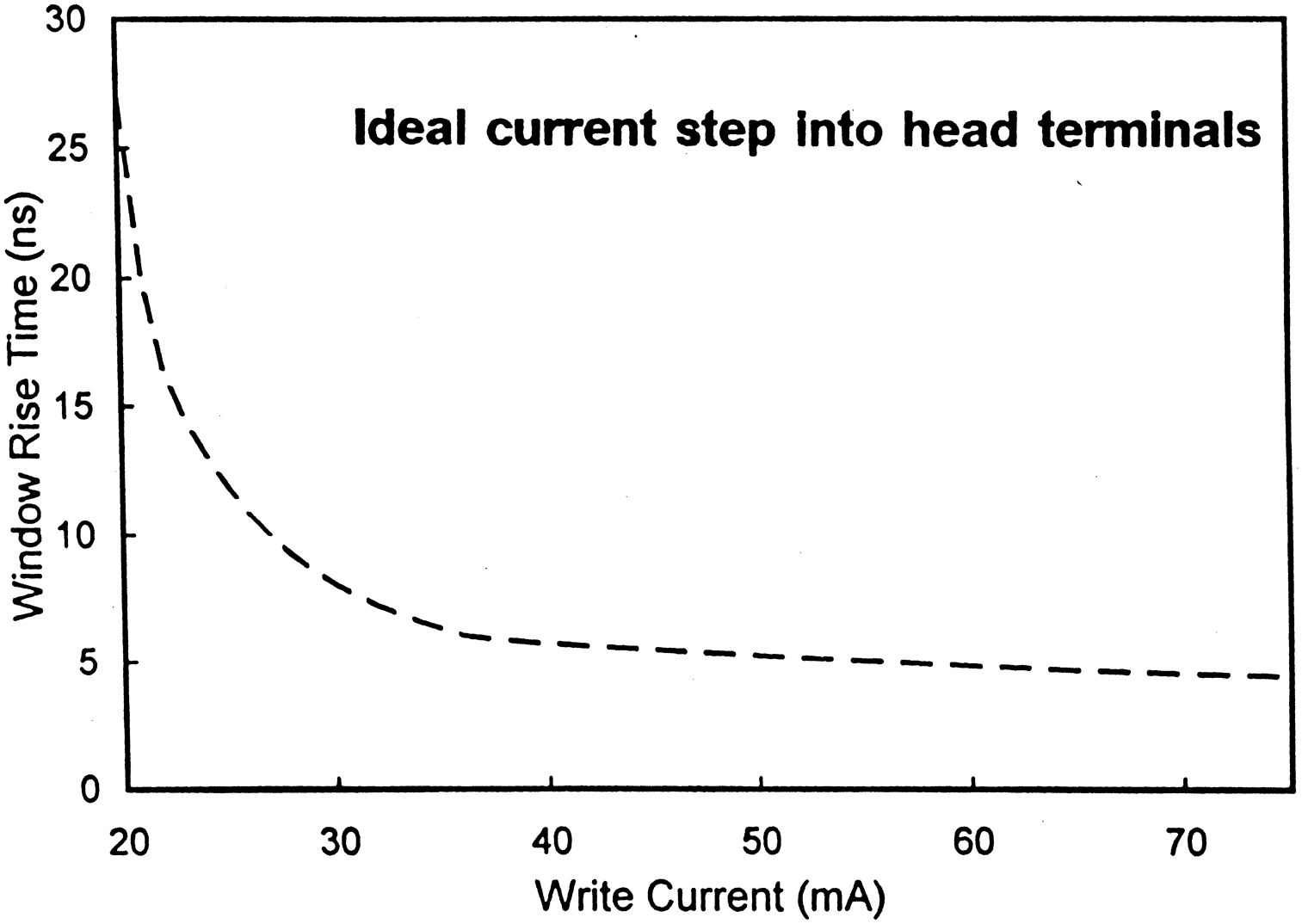

- reversal time almost totally head dependent

Pulse Compression

diff's due to compression effects (forms ft Her).

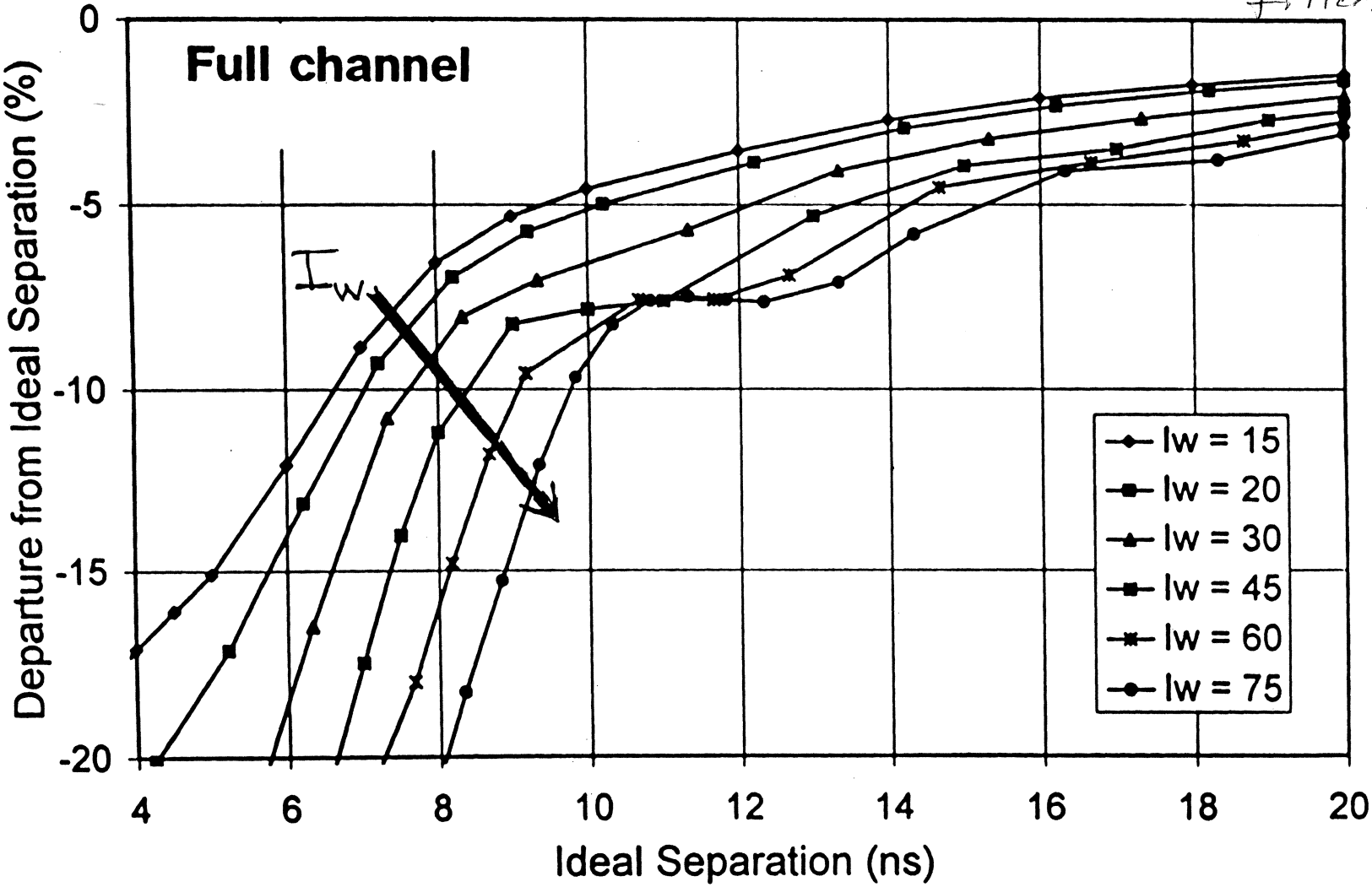

Pulse Compression

head alone.

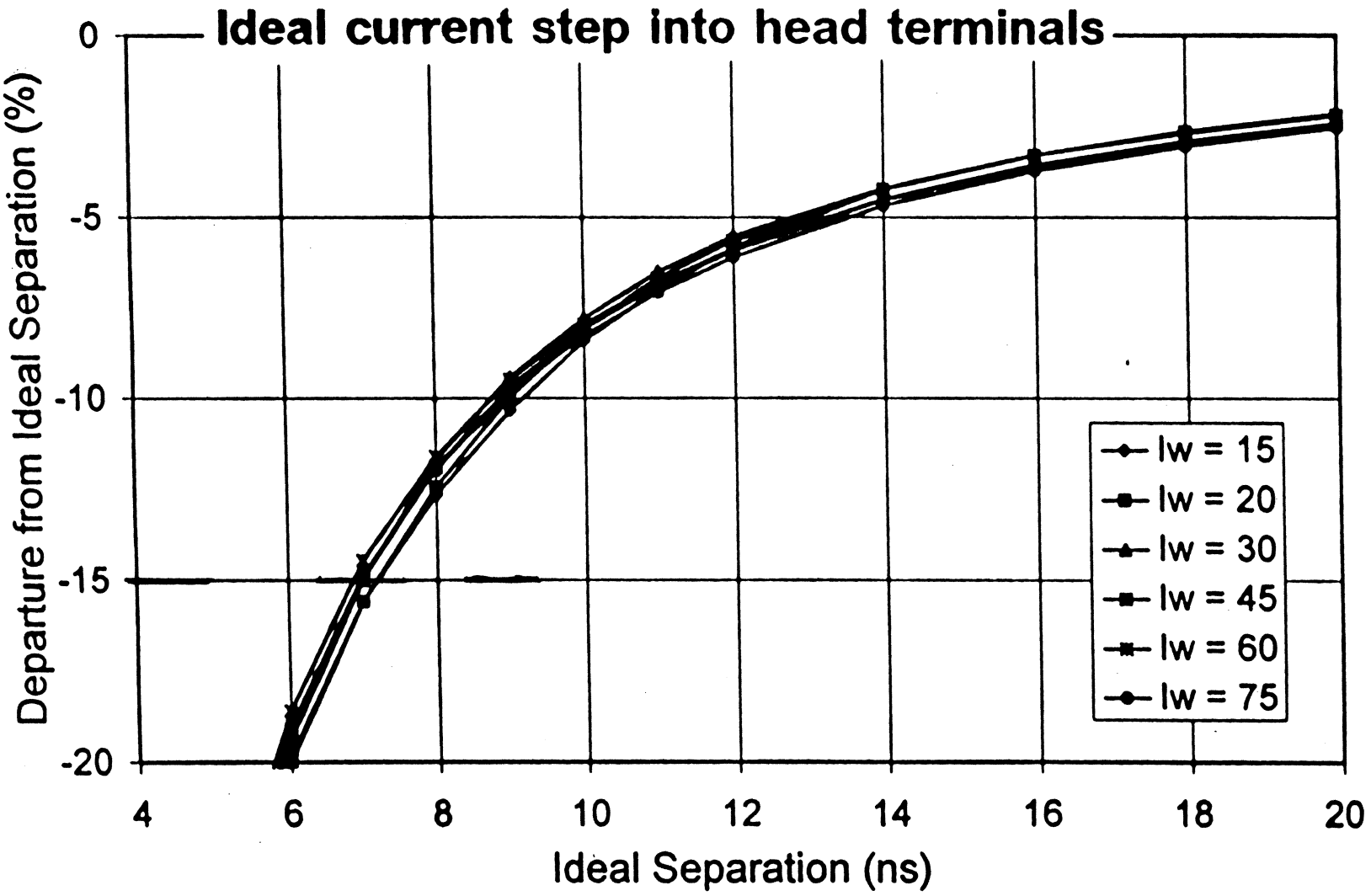

Conclusions (Cont.)

- **Write Path**

  Yoke swing $B_{pp} > 2B_{AS}$

  Transition rise time $\tau < 1/(2F_{W,max})$

  Bit shift $\varepsilon < 15\ \%$

  √ ***Full Write Path:***

  Mag. Swing and Bit Shift limited to

  $\Delta T > 7.1$ ns and $F_{W,max} < 70$ MHz

  - N.B: $I_W = 45$ mA, $\tau = 6$ ns

  √ ***Head Only:***

  Mag. Swing and Bit Shift limited to

  $\Delta T > 7.1$ ns and $F_{W,max} < 70$ MHz

  - Now: $I_W = 36$ mA, $\tau = 6.8$ ns

Final Conclusion

Therefore, the maximum data rate for this channel using a (0,k) RLL code with an 8/9 rate is 15.56 MB/s

$$(F_{W,max} = 70 \text{ MHz}, \quad \Delta T = 7.1 \text{ ns})$$

- So several systems on data rate with current technology

Finally .....

- MR heads require a well-matched disk and electronics, especially for more demanding applications:
  - — high data rates
  - — narrow trackwidths
  - — near contact operation

- Front-end must be designed as a ***system***
  - — A collection of individually optimized components makes a sub-optimal front-end
  - — Components have limited exchangeability

- Many electronic design options exist
  - — Choice depends on application
  - — Do not expect "generic" modules that serve everyone's needs

IIST

DIGITAL READ/WRITE CHANNELS FOR MAGNETIC RECORDING

Nersi Nazari

GEC Plessey Semiconductors

May 28, 1996

OUTLINE

- Signal detection theory
- Typical digital PRML chip architecture
- Testing digital PRML chips and results
- Trellis coded partial response

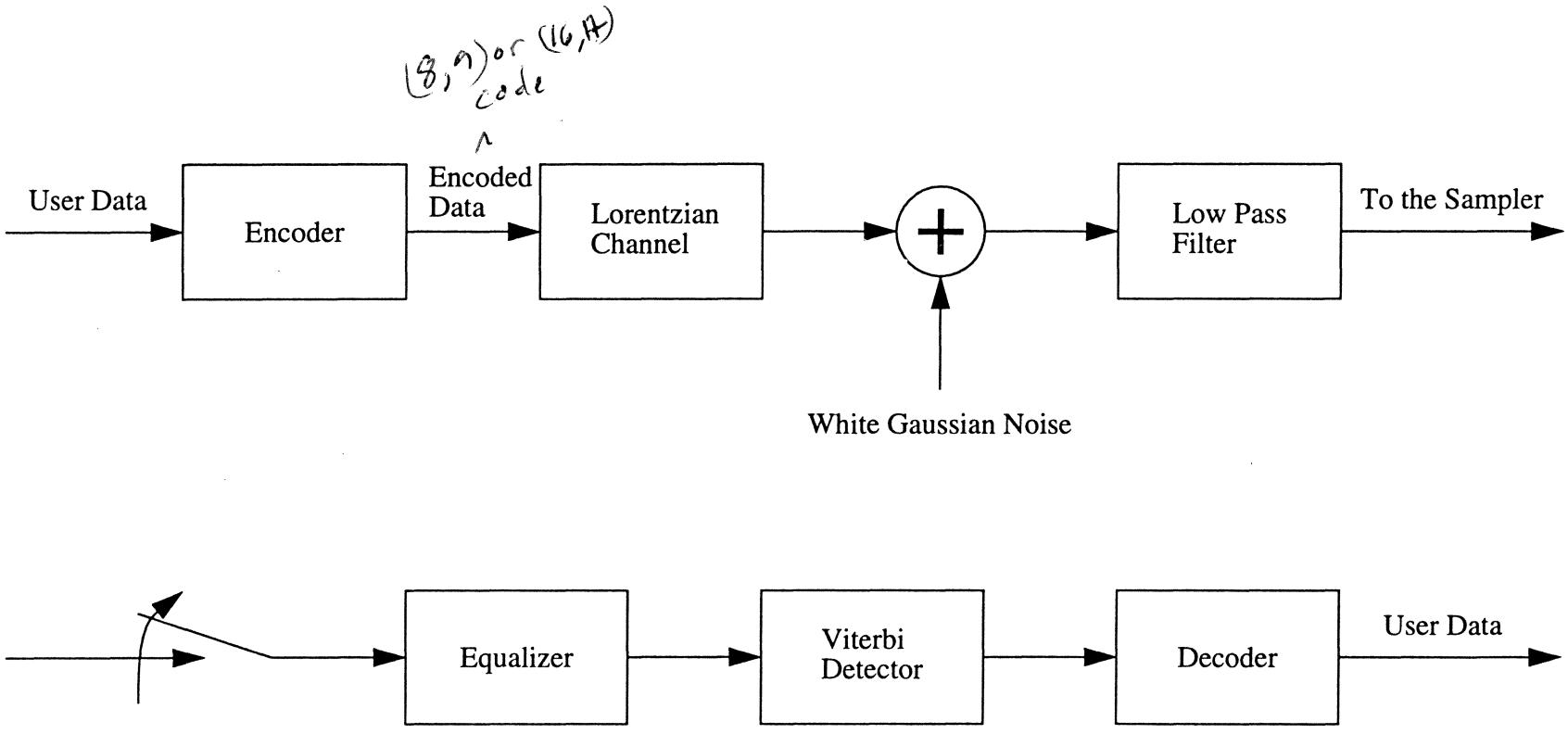

Block Diagram of the System

Signal Detection Theory

- Assume a Lorentzian Channel, then for an "isolated" transition the output voltage is

$$h(t) = \frac{1}{1 + \left(\frac{2t}{\mathrm{PW}_{50}}\right)^2},$$

where PW_{50} is the width of the pulse at 50% amplitude.

- If we needed to detect only one isolated transition, use a "matched filter" detector [1],

↳ mirror image of pulse (symmetric so same)

$$F(t) = h(-t) = h(t) \ .$$

The error probability is given by

noise floor

$$P_e = \frac{1}{2} Q\left(\sqrt{E_t / \eta_0}\right) \ ,$$

where,

$$Q(x) = \frac{1}{\sqrt{2\pi}} \int_x^\infty e^{-u^2/2} du \ ,$$

$$E_t = \int_{-\infty}^{\infty} h^2(t)\,dt = \frac{\pi}{4}\,\mathrm{PW}_{50}\ ,$$

is the energy per transition, and η_0 is the amplitude of single sided noise spectral density.

- If we need to detect a "dibit", two transition T seconds apart, the signal is

$$c(t) = h(t) - h(t-T)\ .$$

Then, the optimum detector is matched to $c(t)$ and is given by

$$F(t) = c(-t) = h(-t) - h(-t-T) \ .$$

The expression for the error probability is exactly the same as single transition, except use [2]

$$E_d = \int_{-\infty}^{\infty} c^2(t)\,dt = \frac{\pi}{2}\ \mathrm{PW}_{50}\ \frac{1}{1+S^2} \ ,$$

use E_d instead of E_t

where $S = \mathrm{PW}_{50}/T$, is the channel normalized density.

- For a "sampled" channel, such as PRML, the signal needs to pass through a low pass filter before sampling, due to sampling the energy per bit is reduced to

$$E_l = \int_{-1/2T}^{1/2T} |H(f)|^2 \, df = E_d \left[1 - e^{-\pi S}(1 + 2S^2)\right] .$$

- For a PRML channel, signal needs to be equalized to PR4 pulse shape, sequence energy at the Viterbi detector is given by [3]

$$E_v = E_l \frac{(\pi S)^3 (S^2 + 1)}{e^{\pi S} - 1 - 2S^2} \ .$$

Reference [2] shows in detail how the above equation should be modified to account for noise correlation at the Viterbi detector.

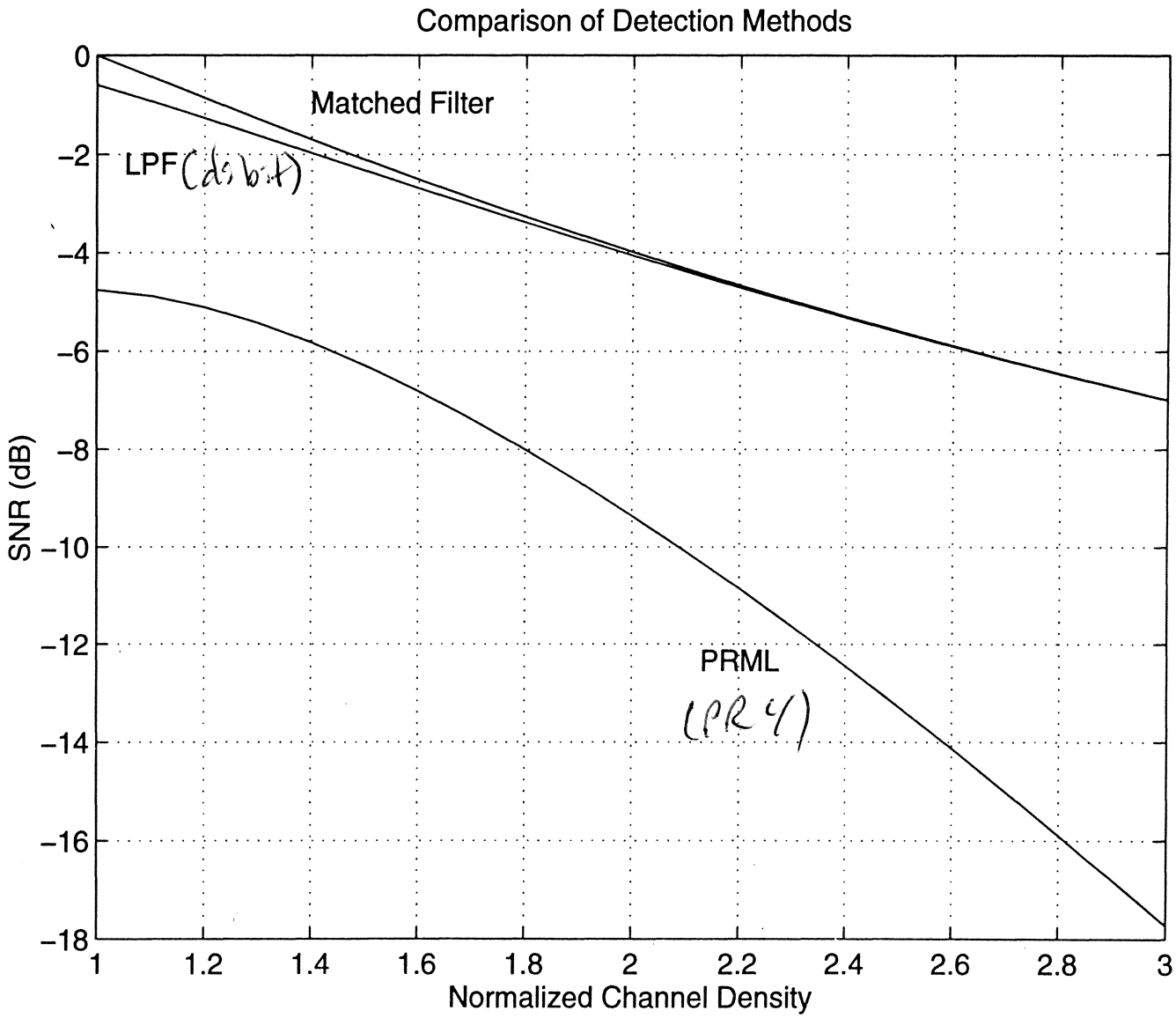
Comparison of Detection Methods
Matched Filter
LPF (d, b.t)
PRML
(PR4)
SNR (dB)
0
−2
−4
−6
−8
−10
−12
−14
−16
−18
1
1.2
1.4
1.6
1.8
2
2.2
2.4
2.6
2.8
3
Normalized Channel Density

Typical Digital PRML Architecture

- PRIV architecture
  - -- Dibit response is equalized to $1 - D^2$
  - -- Odd and even samples can be independently detected
  - -- Channel output has only three values, 0, 1, -1

detect odd/even samples independently

- 8/9 encoding
  - -- Use (0,G/I) codes such as (0,4/4)
  - -- Two transitions can be next to each other
  - -- At least one "1" sample after every G 0's
  - -- At least one "1" sample after every I 0's in odd or even subsequences

high rate - transitions adjacent to each other

- 7 pole equiripple continuous time filter
  - -- Limits noise bandwidth
  - -- Does most of channel equalization via high frequency boost
  - -- Often also has asymmetric zeros for phase equalization
  - -- Must be able to quickly change characteristics between data and servo
- 6-bit flash ADC
  - -- Distinguishing block of digital PRML channels
  - -- Besides data recovery, can be used for servo via oversampling

- Variable threshold algorithm (VTA) Viterbi detector
  - -- PRIV signal can be interleaved
  - -- Each interleave can have a trivial Viterbi detector
- 3-7 TAP DIGITAL FILTER
- Write precompensation
  - -- Necessary due to transitions written next to each other
  - -- Write close transitions farther
- Randomizer
  - -- Avoid periodic patterns
  - -- Used for reading "known" patterns

⌣: Illegal pattern
e.g.: all ϕ's for characterization of channel.

- Channel quality
  - -- Feedback from the channel for parameter optimization
  - -- Monitor health of the channel
- Digital/analog test port
  - -- Can see into the channel
  - -- Used for testing, engineering development, and manufacturing environment

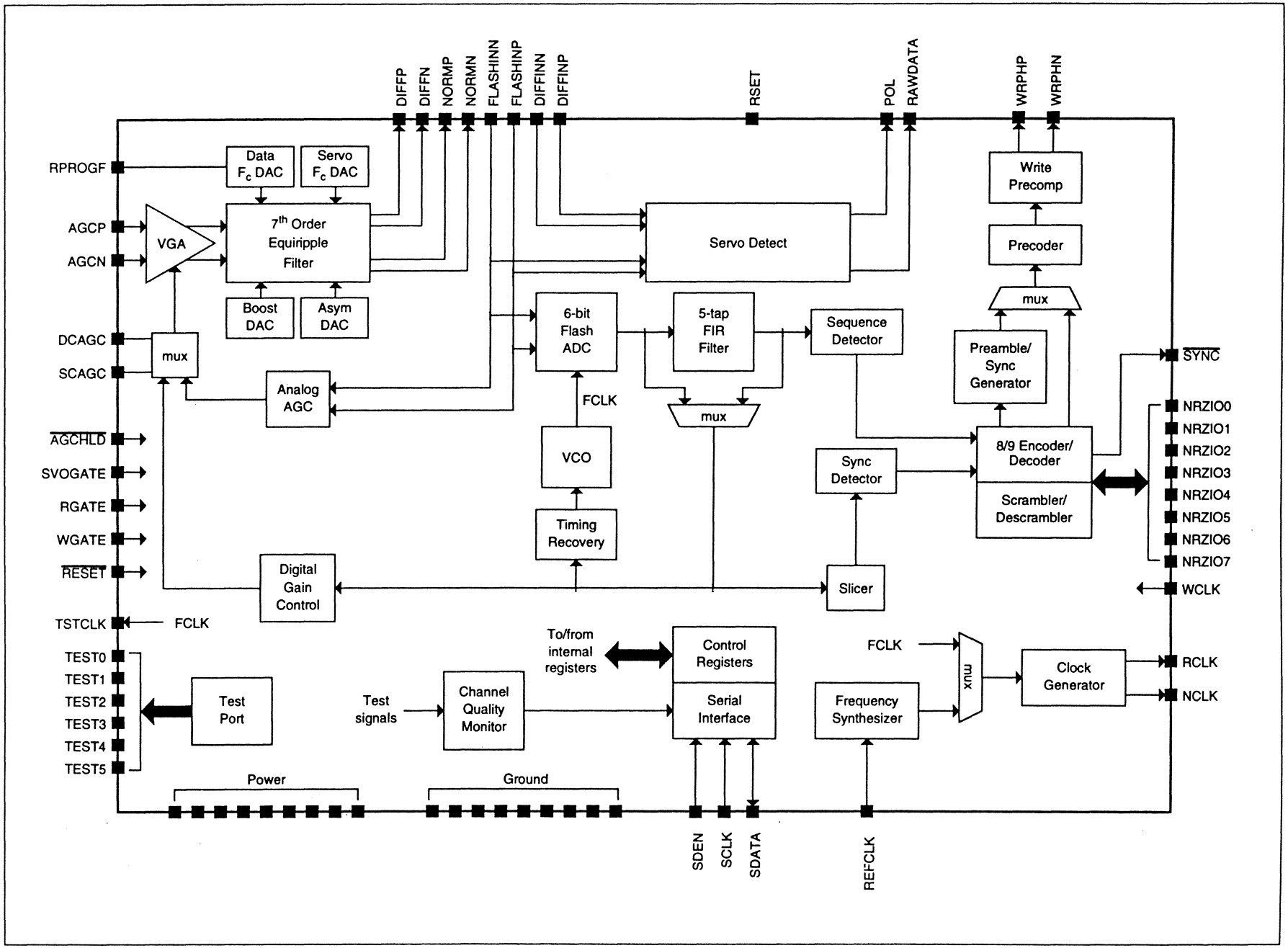
DIFFP
DIFFN
NORMP
NORMN
FLASHINN
FLASHINP
DIFFINN
DIFFINP
RSET
POL
RAWDATA
WRPHP
WRPHN
RPROGF
Data F_c DAC
Servo F_c DAC
AGCP
AGCN
VGA
7th Order Equiripple Filter
Boost DAC
Asym DAC
Servo Detect
Write Precomp
Precoder
mux
DCAGC
SCAGC
mux
Analog AGC
6-bit Flash ADC
5-tap FIR Filter
Sequence Detector
Preamble/ Sync Generator
SYNC
FCLK
mux
AGCHLD
SVOGATE
RGATE
WGATE
RESET
VCO
Timing Recovery
Sync Detector
8/9 Encoder/ Decoder
Scrambler/ Descrambler
NRZIO0
NRZIO1
NRZIO2
NRZIO3
NRZIO4
NRZIO5
NRZIO6
NRZIO7
WCLK
Digital Gain Control
Slicer
TSTCLK
FCLK
TEST0
TEST1
TEST2
TEST3
TEST4
TEST5
Test Port
To/from internal registers
Control Registers
Test signals
Channel Quality Monitor
Serial Interface
FCLK
mux
Frequency Synthesizer
Clock Generator
RCLK
NCLK
Power
Ground
SDEN
SCLK
SDATA
REFCLK

8/9 (0,4/4) PR4 VS. 2/3 (1,7) E(E)PR4

ADVANTAGES OF 8/9:

- LOWER CHANNEL DATA RATE (33%)
- HIGHER EFFECTIVE SNR (ABOUT 1 dB)
- TRIVIAL VITERBI DETECTOR
- CAN INTERLEAVE MAJOR PORTIONS OF DIGITAL LOGIC
- MORE ROBUST TIMING RECOVERY AND GAIN LOOPS

DISADVANTAGES OF 8/9:

- HIGHER FCI (50%)
  - -- CAN COPE BY OPTIMIZING THE MEDIA
  - -- CAN BE MINIMIZED BY WRITE PRECOMPENSATION
- MORE COMPLICATED ENCODER/DECODER
- IBM PATENT (FOR VENDORS WITHOUT CROSS LICENSING AGREEMENT)

ANALOG VS. DIGITAL PRML

ADVANTAGES OF DIGITAL:

- CHANNEL QUALITY MEASUREMENT
  - -- OPTIMIZATION BY SOFTWARE ON THE BENCH AND IN THE FACTORY
  - -- CHANNEL "HEALTH" MONITORING IN THE FIELD
  - -- ABILITY TO INCORPORATE FLAW SCAN, FLYING HEIGHT MONITOR, ETC.
- EXTENDABLE TO MORE ADVANCED CODING AND DETECTION SCHEMES
- REPEATABILITY/PRECISION
- HIGHER BPI (IBM INTERMAG '93)

DISADVANTAGES OF DIGITAL:

- HIGHER POWER AND LARGER SIZE DUE TO ADC

VGA

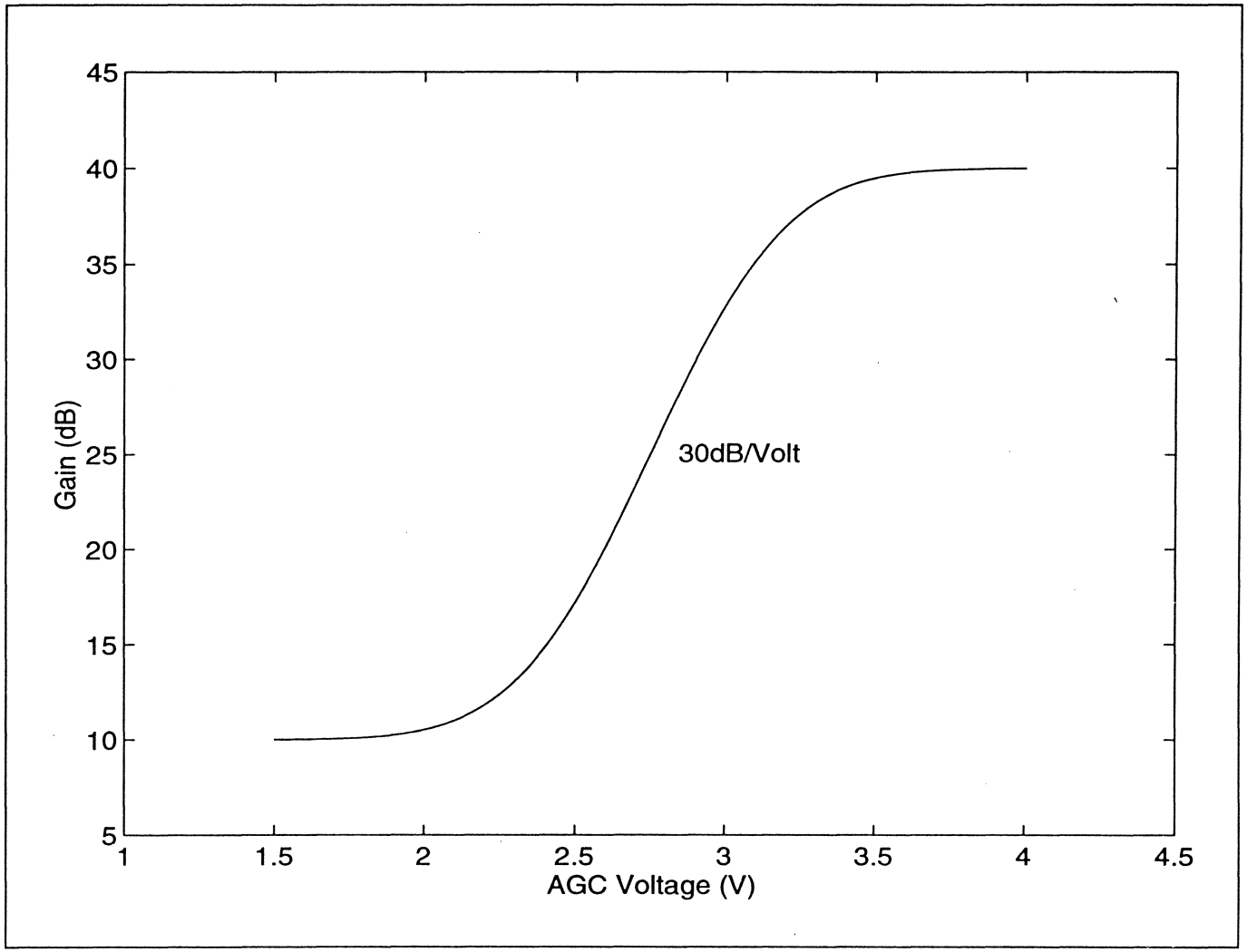
45
40
35
30
25
20
15
10
5
Gain (dB)
30dB/Volt
1
1.5
2
2.5
3
3.5
4
4.5
AGC Voltage (V)

GAIN CONTROL

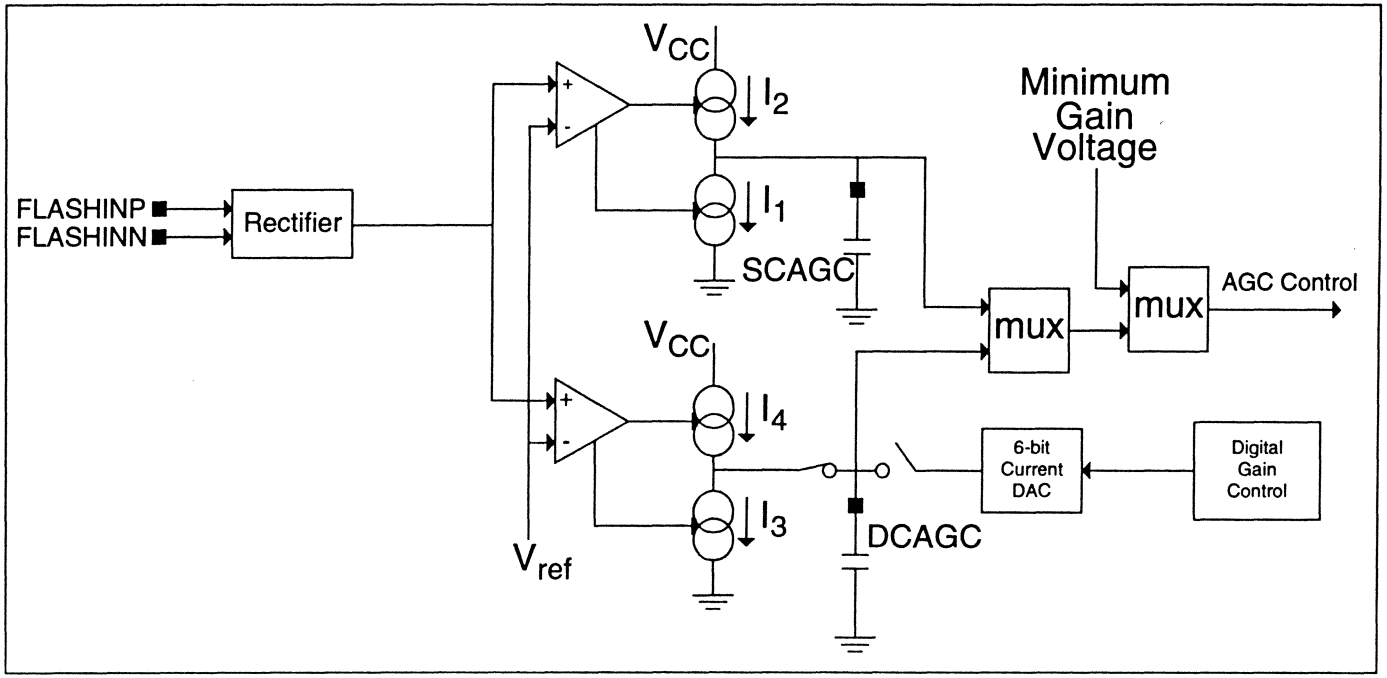

$$G_n = \hat{x}_n(y_n - x_n)\gamma$$

G_n = Gain update at time n

γ = AGC gain factor

y_n = Input value at time n

x_n = Desired value at time n

$\hat{x}_n$ = Slicer output at time n

CONTINUOUS TIME FILTER

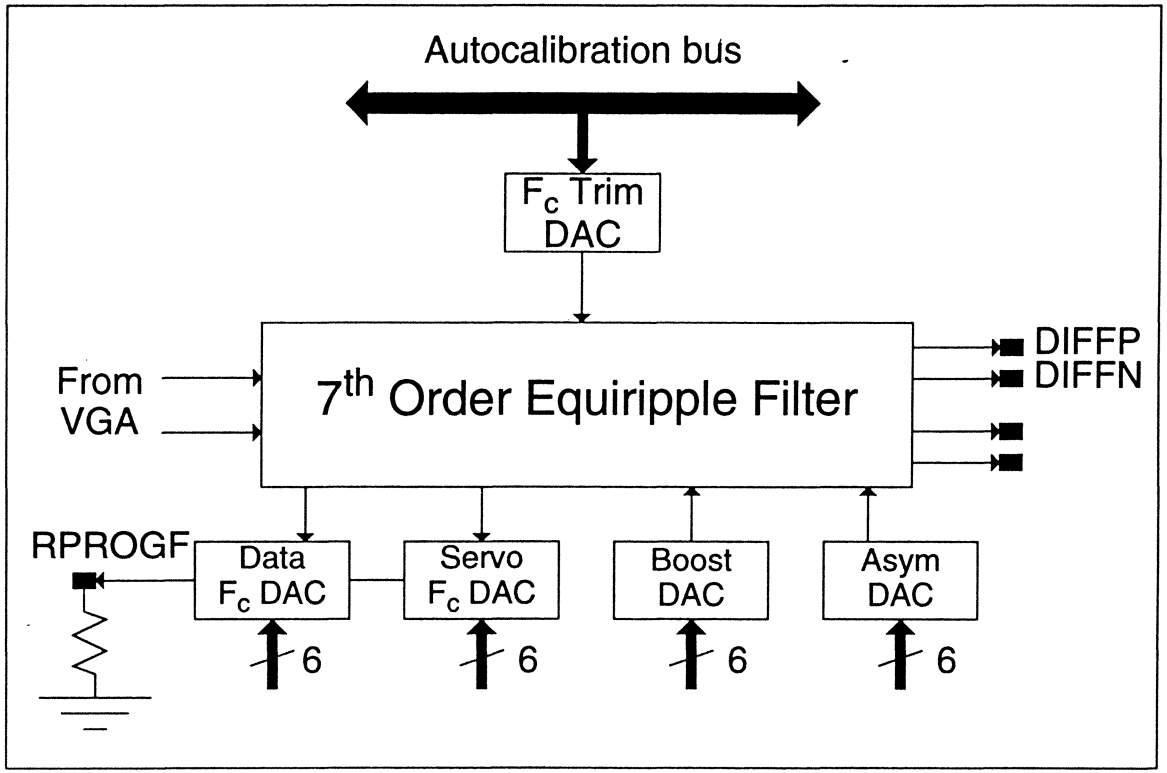

$$\frac{\left(-K_2 S^2 + K_1 S + 1\right)18}{S^7 + 5.23S^6 + 19.7S^5 + 45.9S^4 + 76.5S^3 + 84.1S^2 + 57.1S + 18}$$

ANALOG-TO-DIGITAL CONVERTER

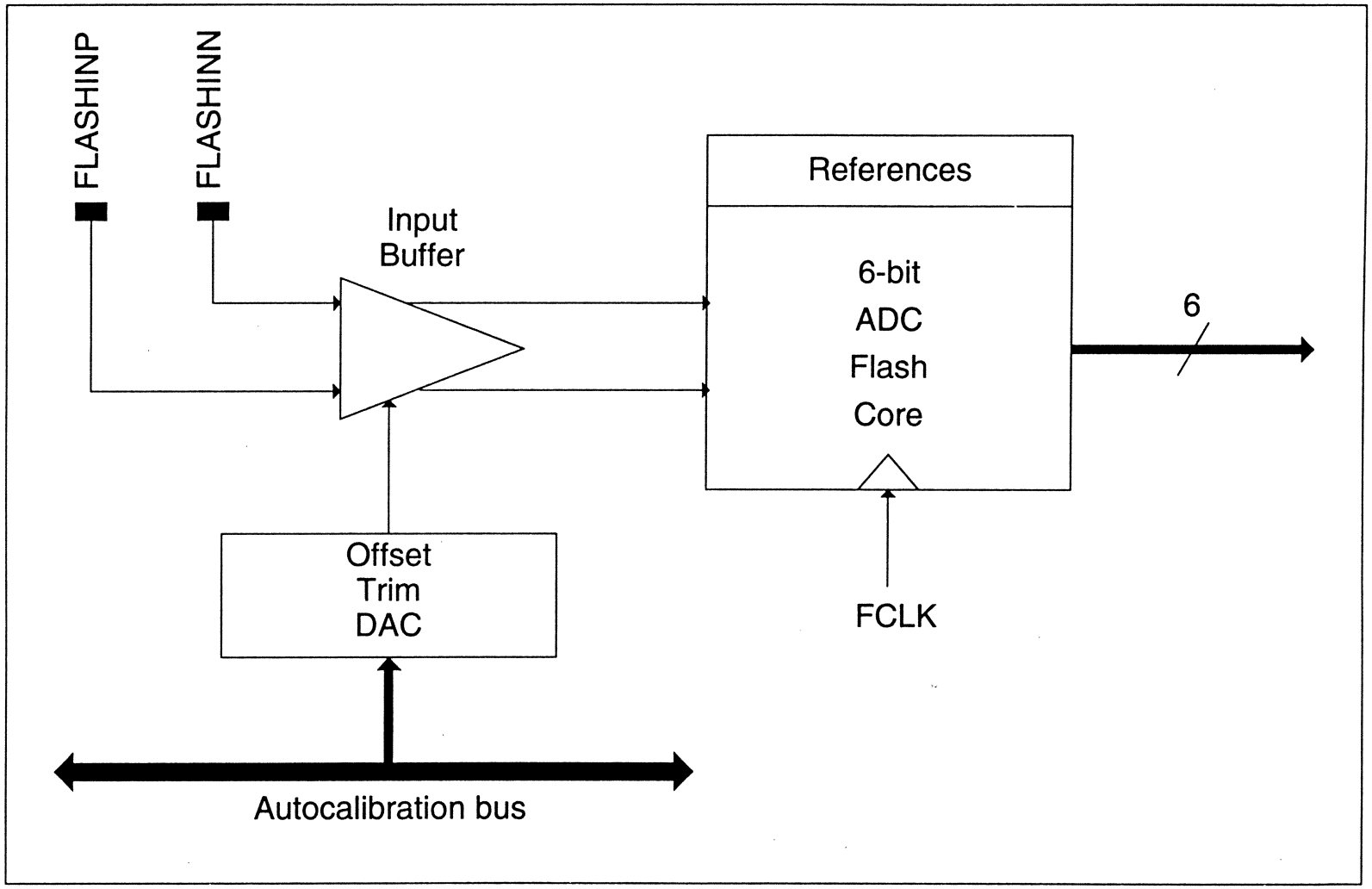

TIMING RECOVERY

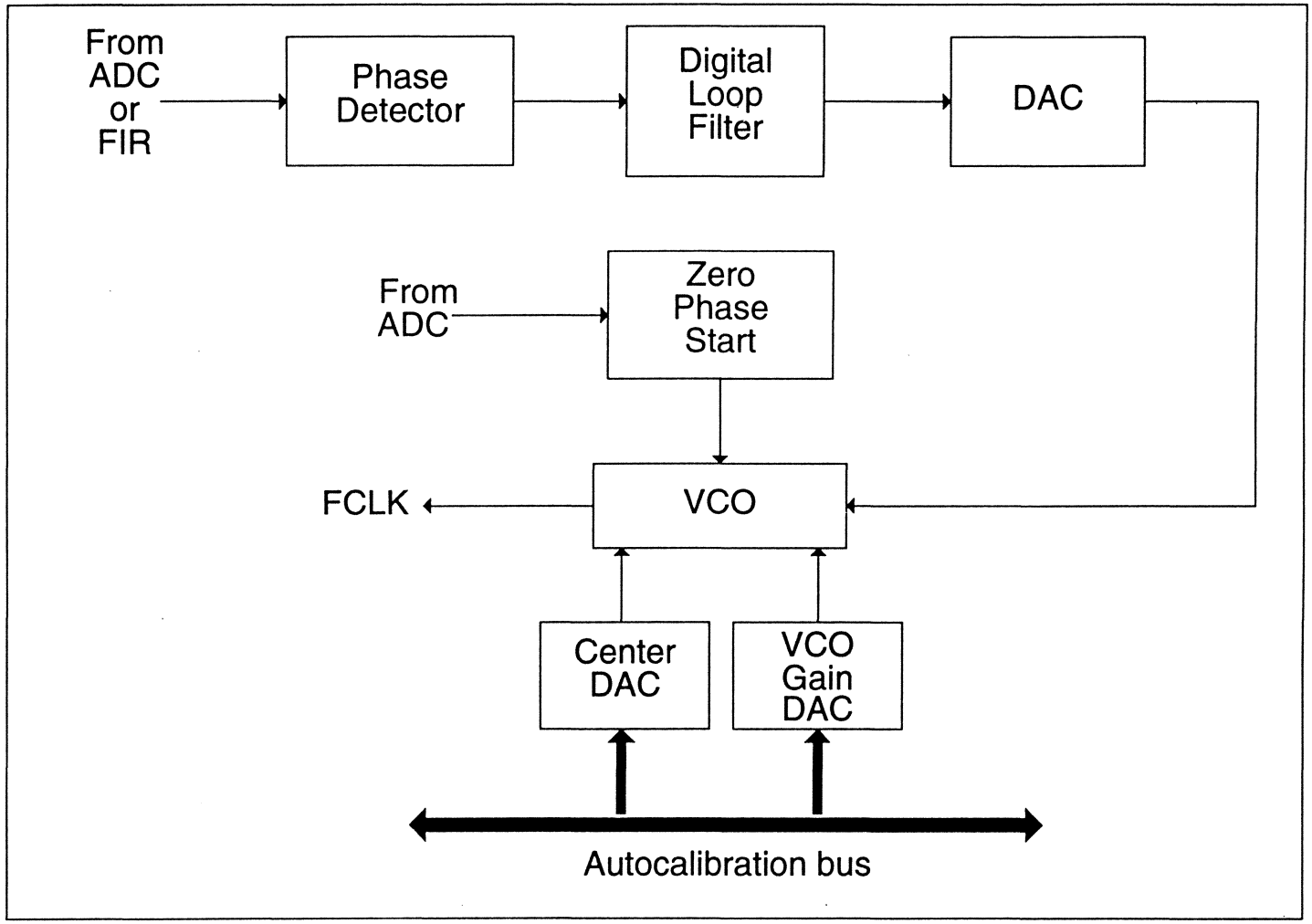

TIMING RECOVERY-cont

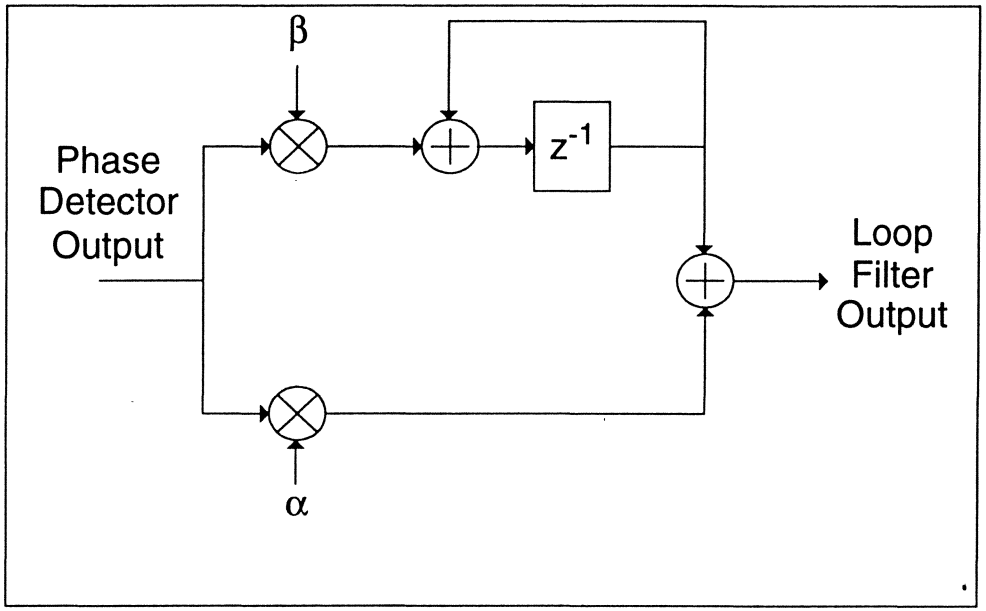

$$\Delta\tau_n = -y_n x_{n-1} + y_{n-1} x_n$$

$\Delta\tau_n$ = Phase error estimate at time n

y_n = Input value at time n

y_{n-1} = Input value at time n-1

$\hat{x}_n$ = Slicer output for y_n

$\hat{x}_{n-1}$ = Slicer output for y_{n-1}

SNR=24 dB

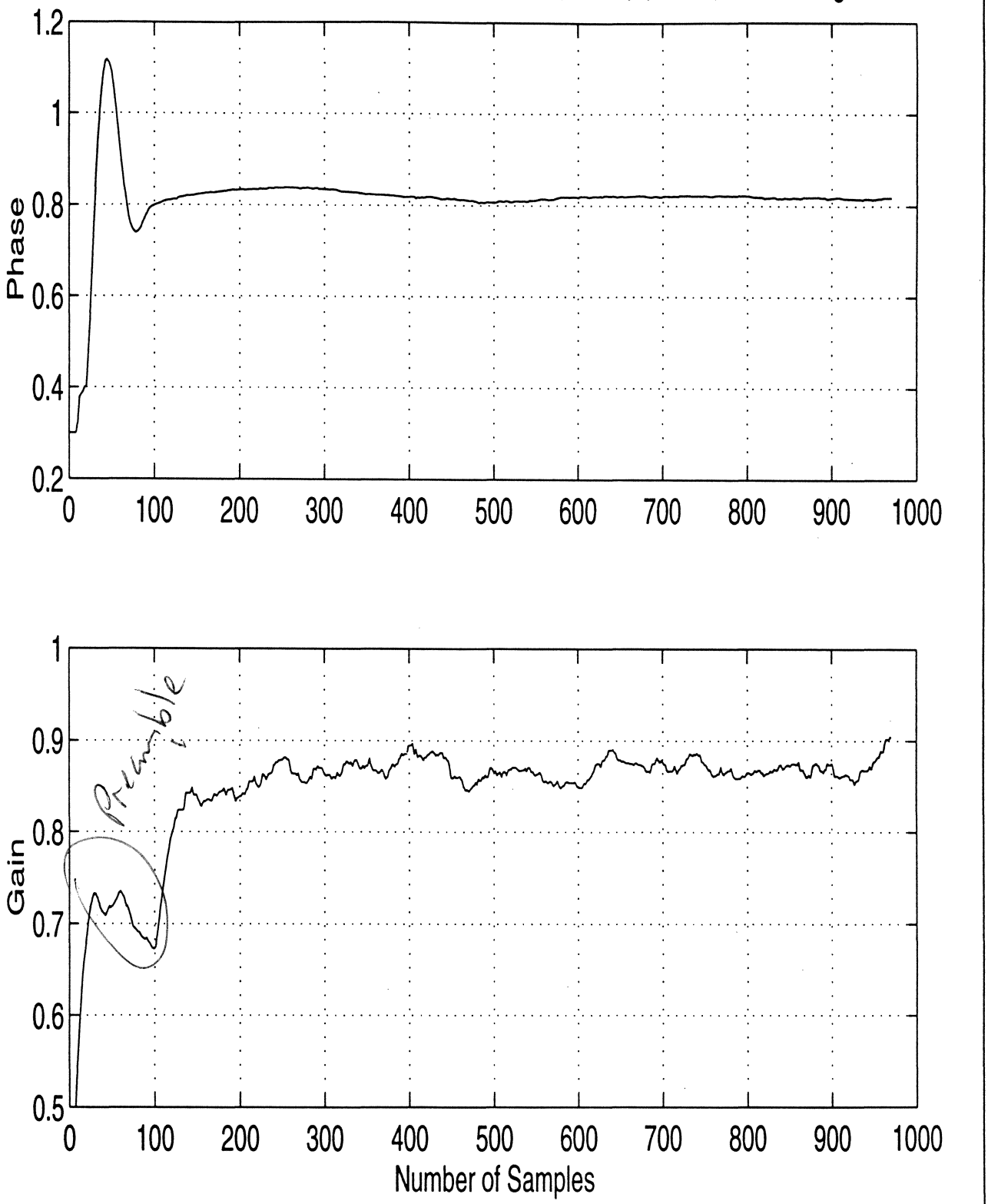
S = 2.5, Alpha = 0.025, Zeta = 0.707, Gamma = 0.02, D = 6,6, R = 4, N = 2, Margin = 0.4515
Phase
1.2
1
0.8
0.6
0.4
0.2
0
100
200
300
400
500
600
700
800
900
1000
Gain
1
0.9
0.8
0.7
0.6
0.5
Preamble
Number of Samples

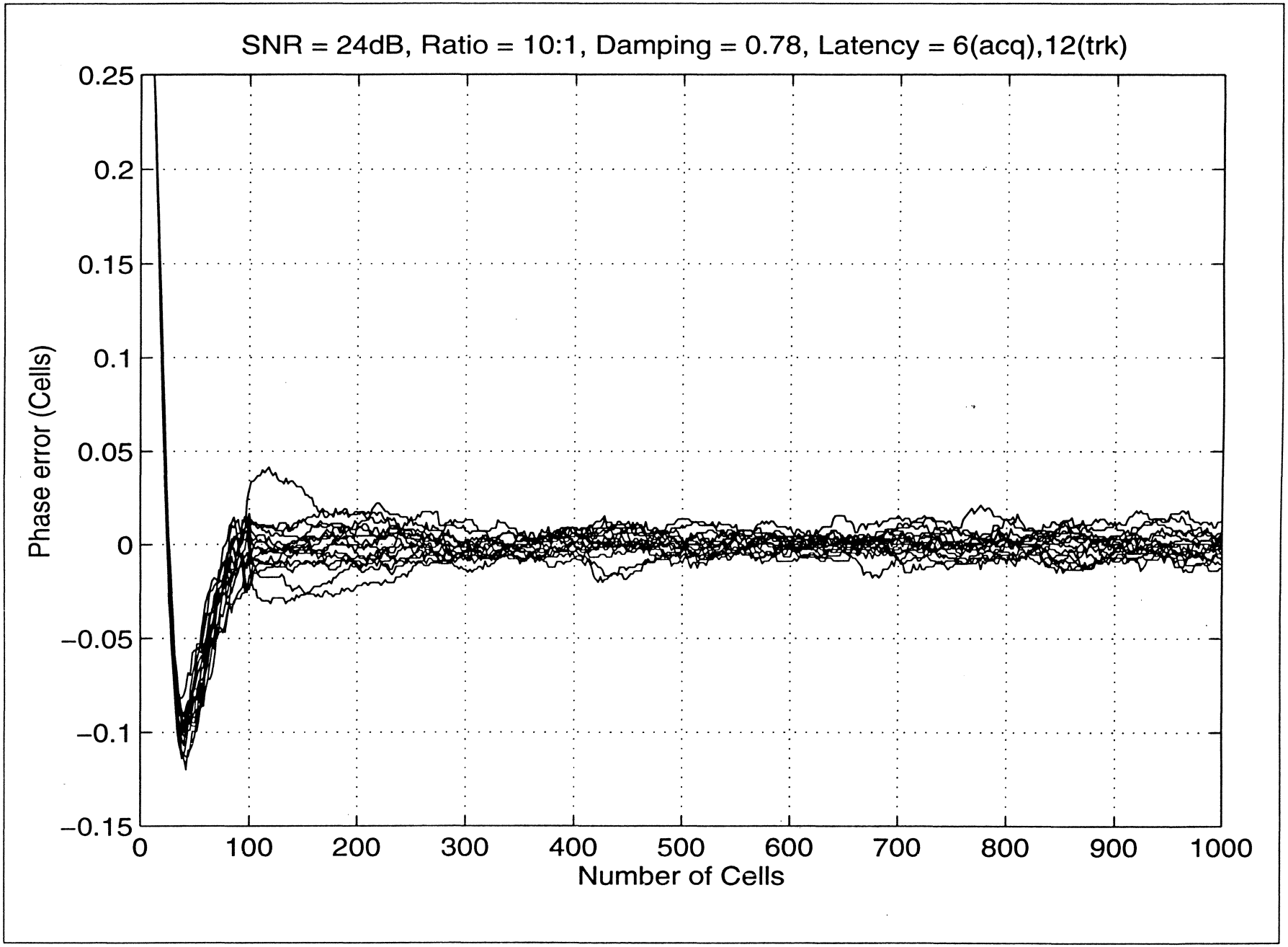
SNR = 24dB, Ratio = 10:1, Damping = 0.78, Latency = 6(acq),12(trk)
Phase error (Cells)
Number of Cells
0.25
0.2
0.15
0.1
0.05
0
−0.05
−0.1
−0.15
0
100
200
300
400
500
600
700
800
900
1000

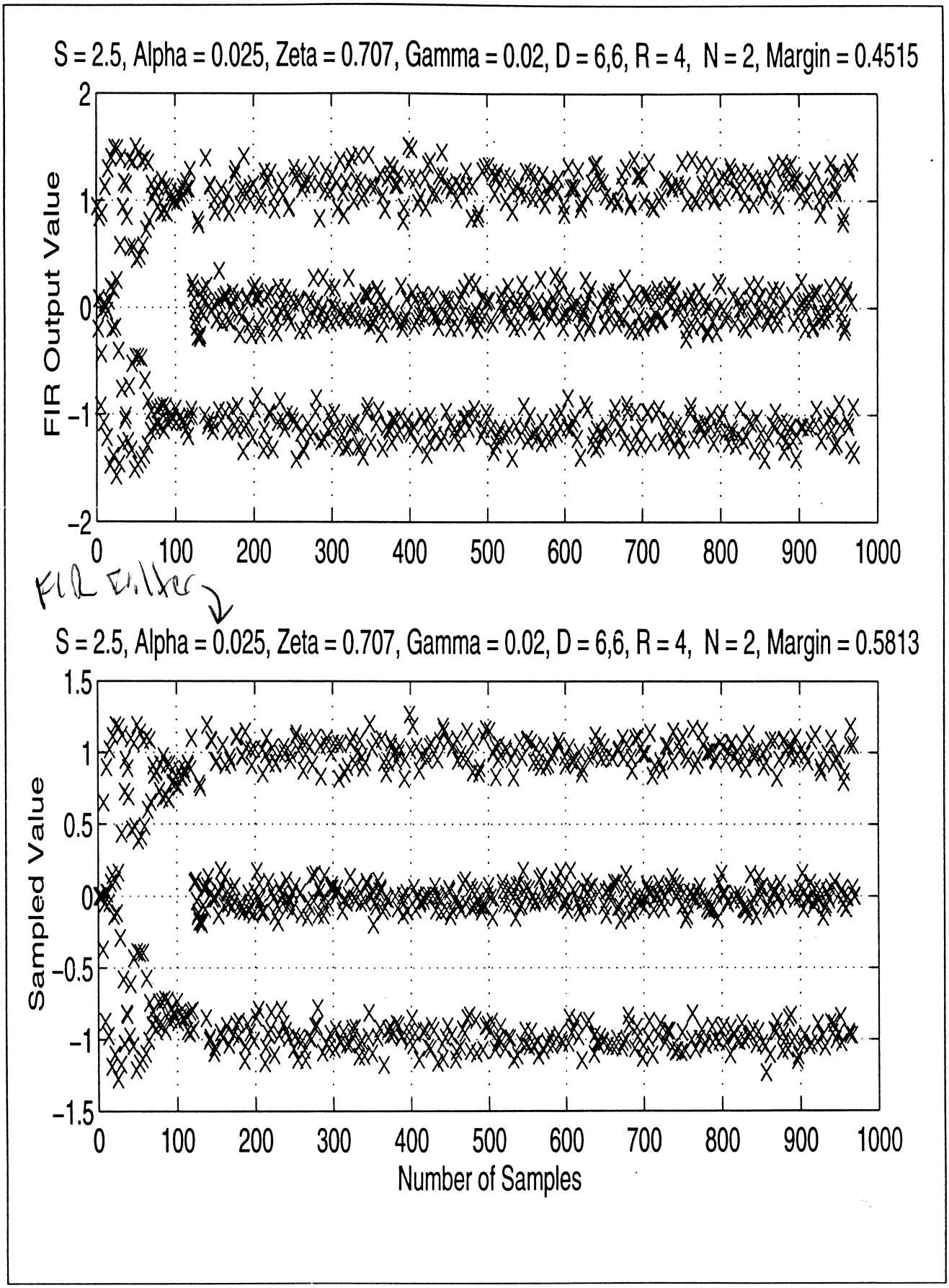
S = 2.5, Alpha = 0.025, Zeta = 0.707, Gamma = 0.02, D = 6,6, R = 4, N = 2, Margin = 0.4515
FIR Output Value
2
1
0
-1
-2
0
100
200
300
400
500
600
700
800
900
1000
FIR Filter
S = 2.5, Alpha = 0.025, Zeta = 0.707, Gamma = 0.02, D = 6,6, R = 4, N = 2, Margin = 0.5813
Sampled Value
1.5
1
0.5
0
-0.5
-1
-1.5
0
100
200
300
400
500
600
700
800
900
1000
Number of Samples

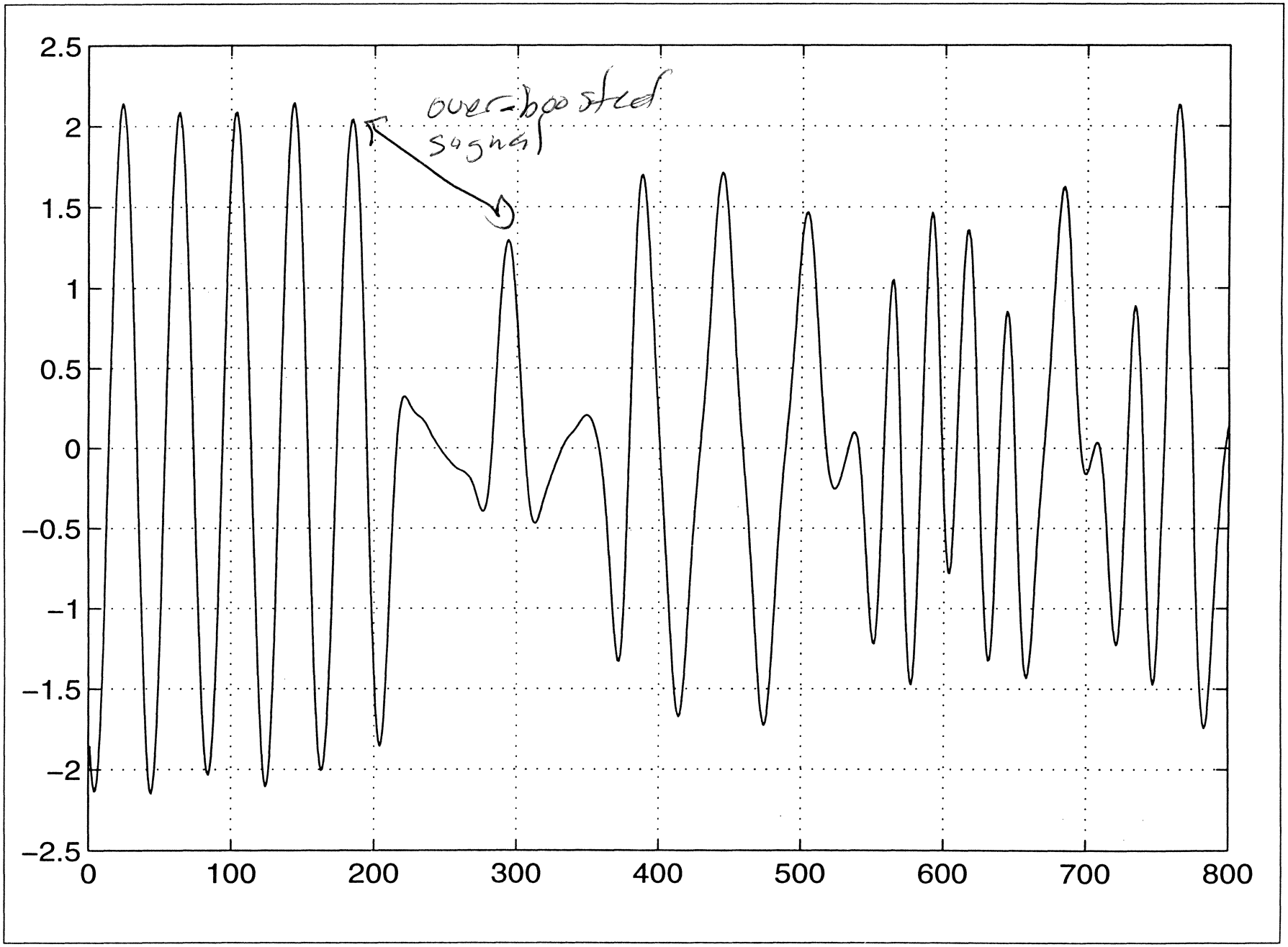
over-boosted
signal
2.5
2
1.5
1
0.5
0
−0.5
−1
−1.5
−2
−2.5
0
100
200
300
400
500
600
700
800

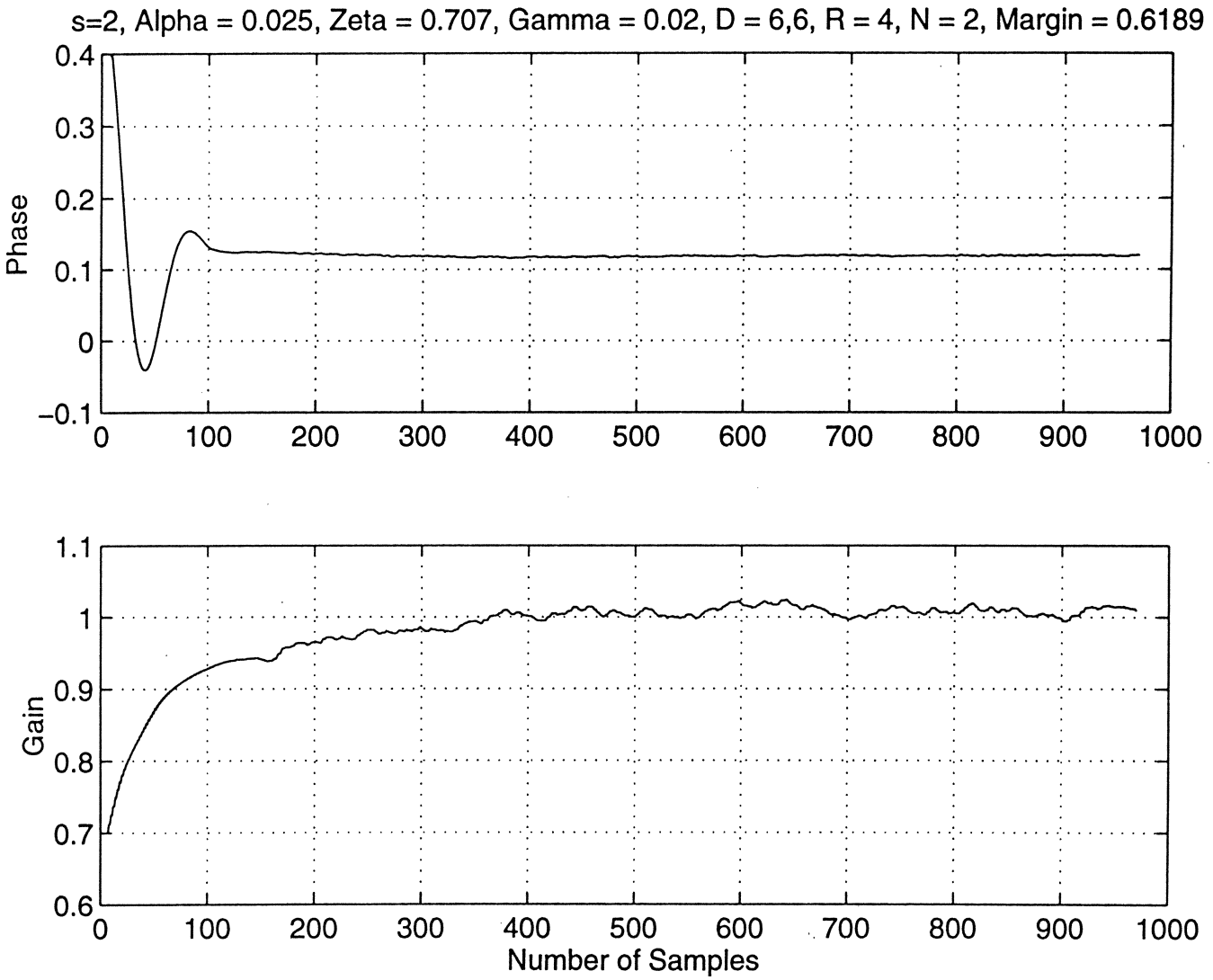
s=2, Alpha = 0.025, Zeta = 0.707, Gamma = 0.02, D = 6,6, R = 4, N = 2, Margin = 0.6189
Phase
0.4
0.3
0.2
0.1
0
−0.1
0
100
200
300
400
500
600
700
800
900
1000
Gain
1.1
1
0.9
0.8
0.7
0.6
0
100
200
300
400
500
600
700
800
900
1000
Number of Samples

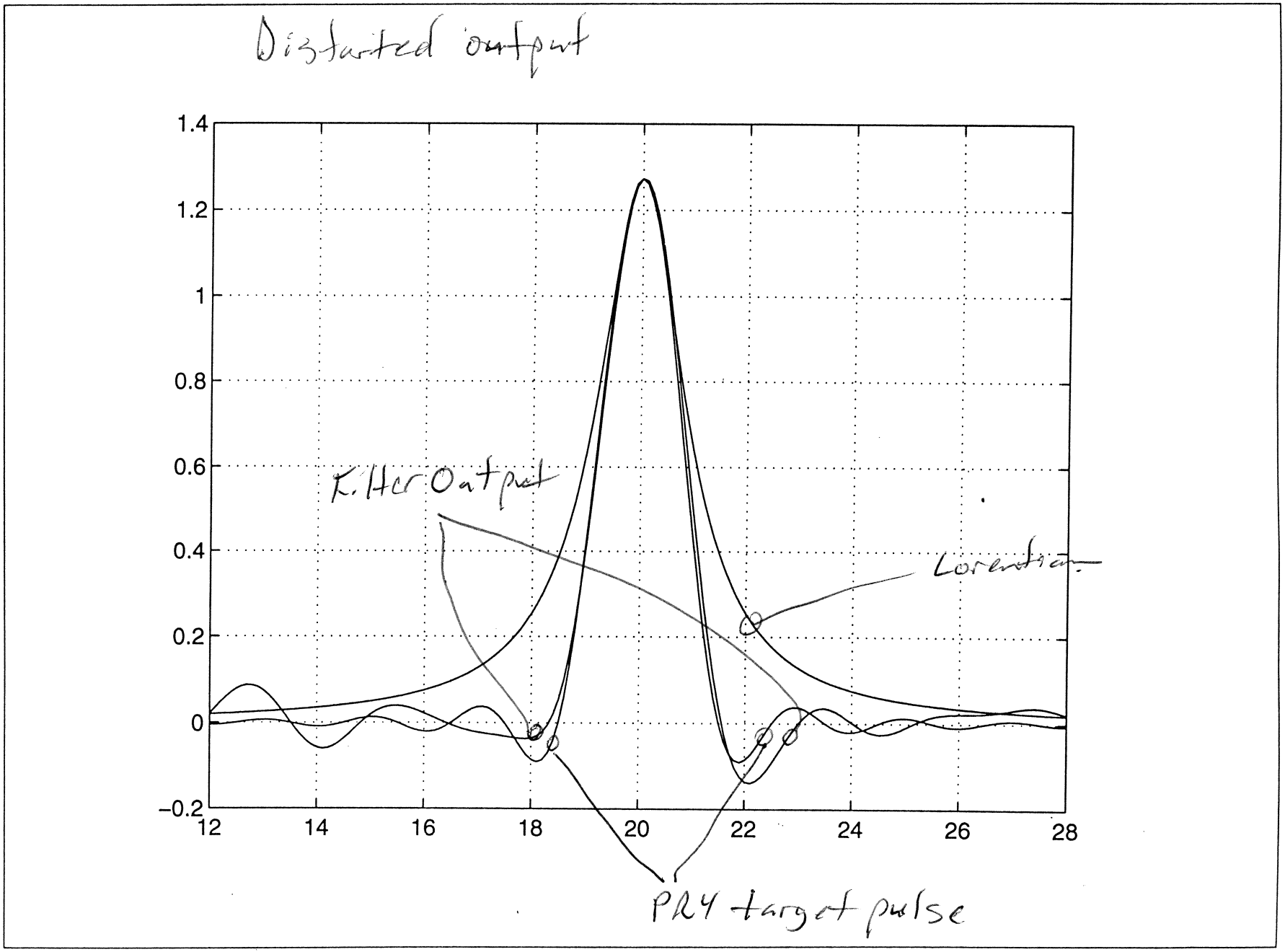
Distorted output
1.4
1.2
1
0.8
0.6
0.4
0.2
0
−0.2
12
14
16
18
20
22
24
26
28
K. Her Output
Lorentzian
PR4 target pulse

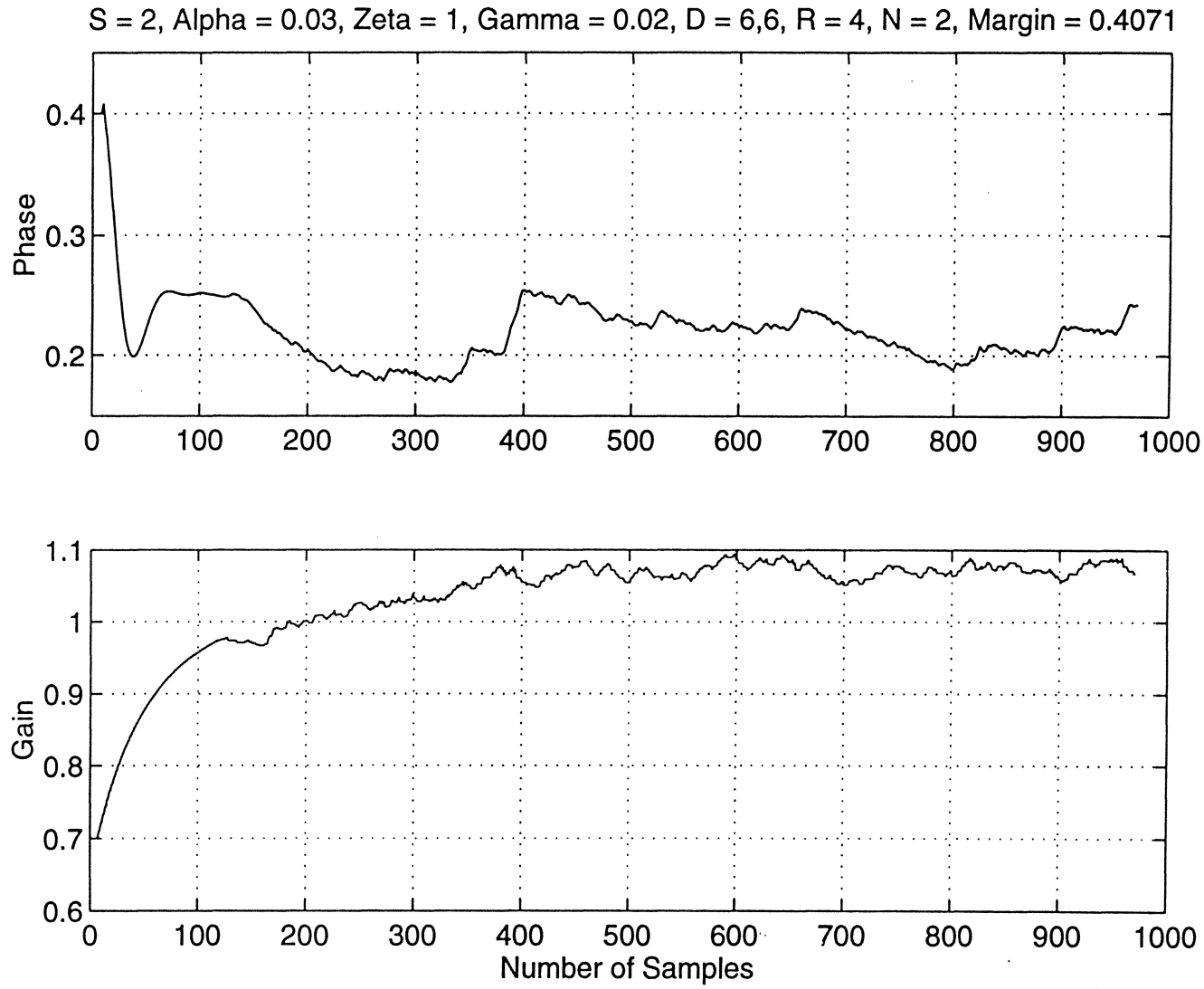

Reversed Phenomena due to phase asymmetry.

Linear filters important

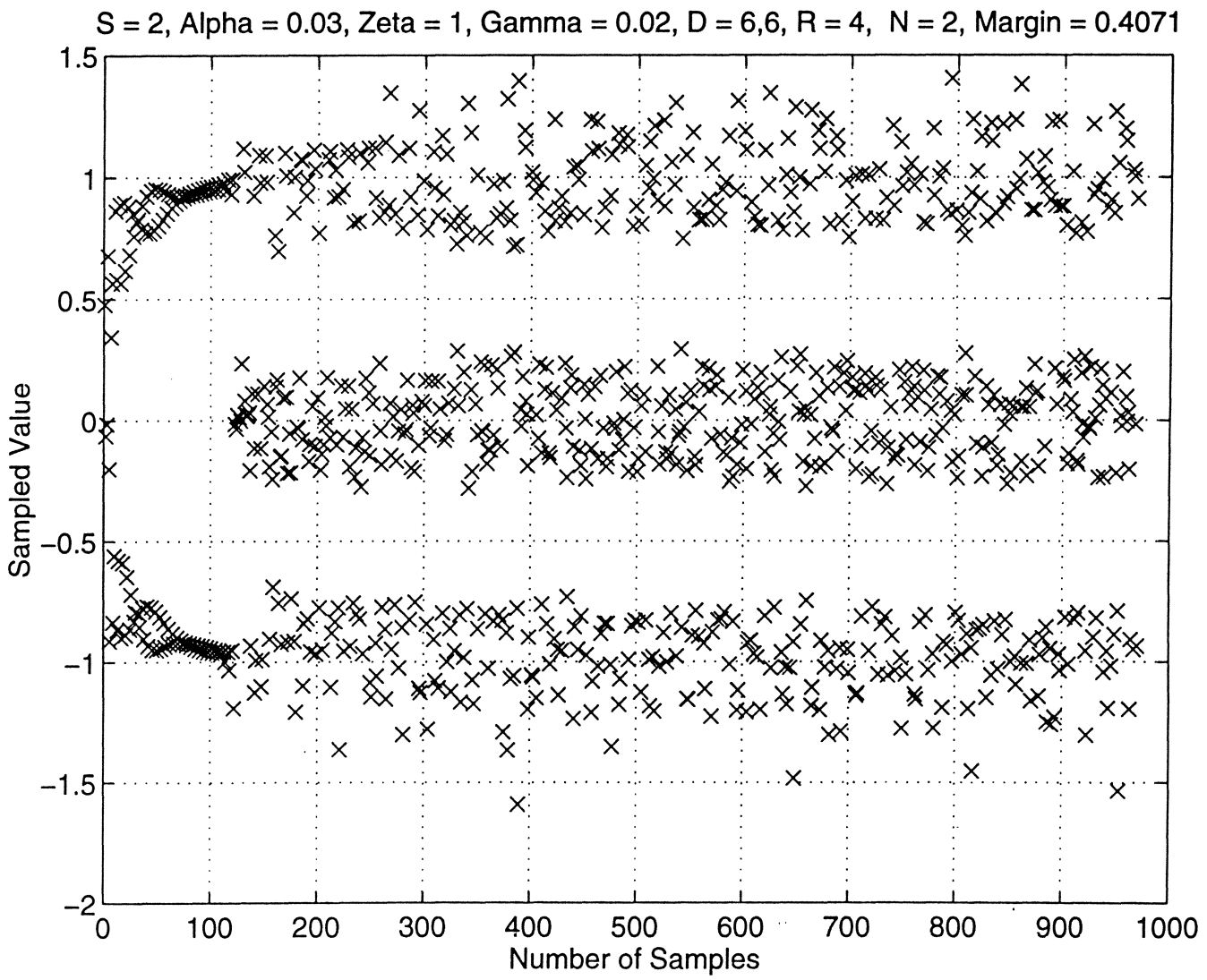
S = 2, Alpha = 0.03, Zeta = 1, Gamma = 0.02, D = 6,6, R = 4, N = 2, Margin = 0.4071
Sampled Value
Number of Samples
1.5
1
0.5
0
−0.5
−1
−1.5
−2
0
100
200
300
400
500
600
700
800
900
1000

FREQUENCY SYNTHESIZER

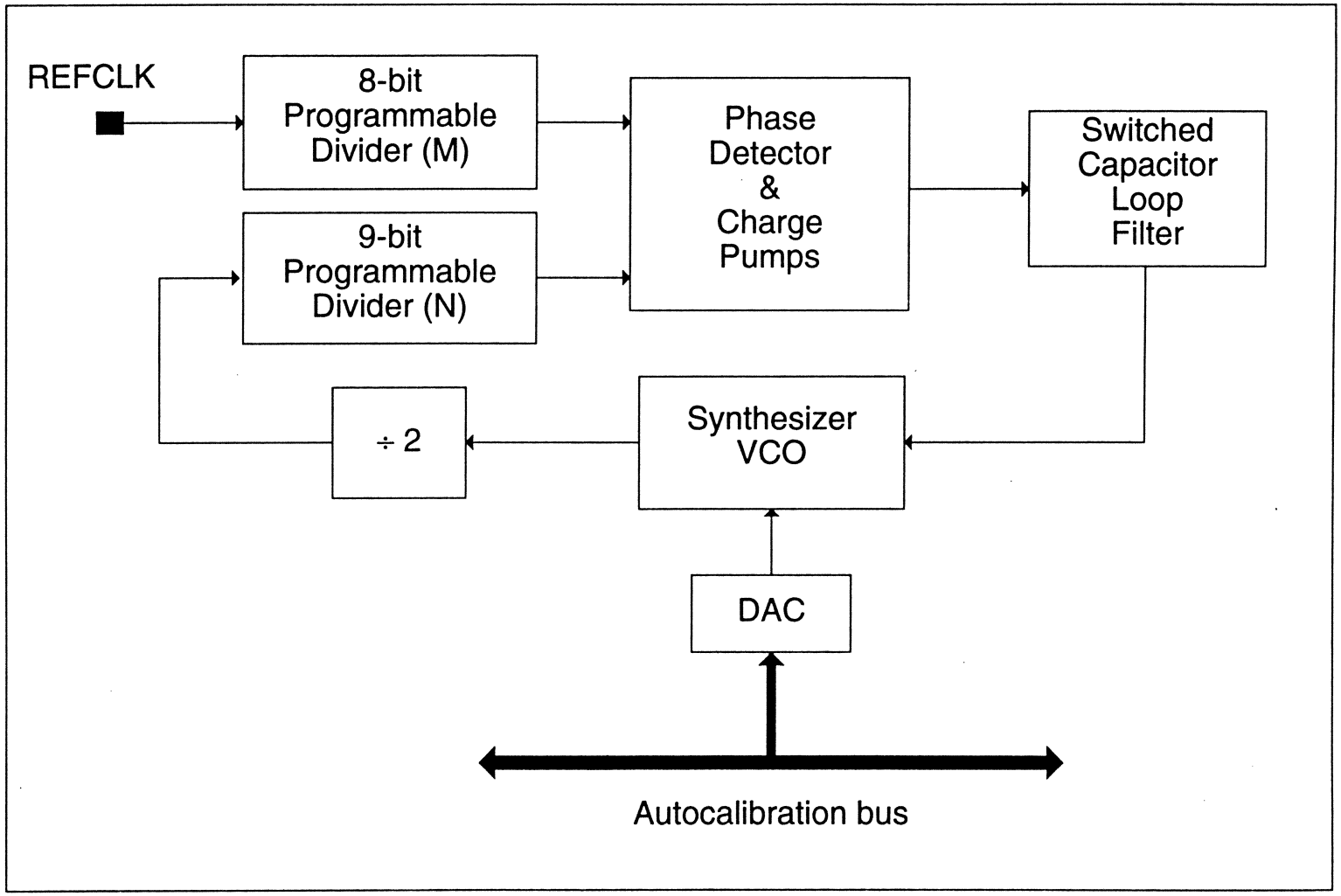

WRITE PRECOMPENSATION

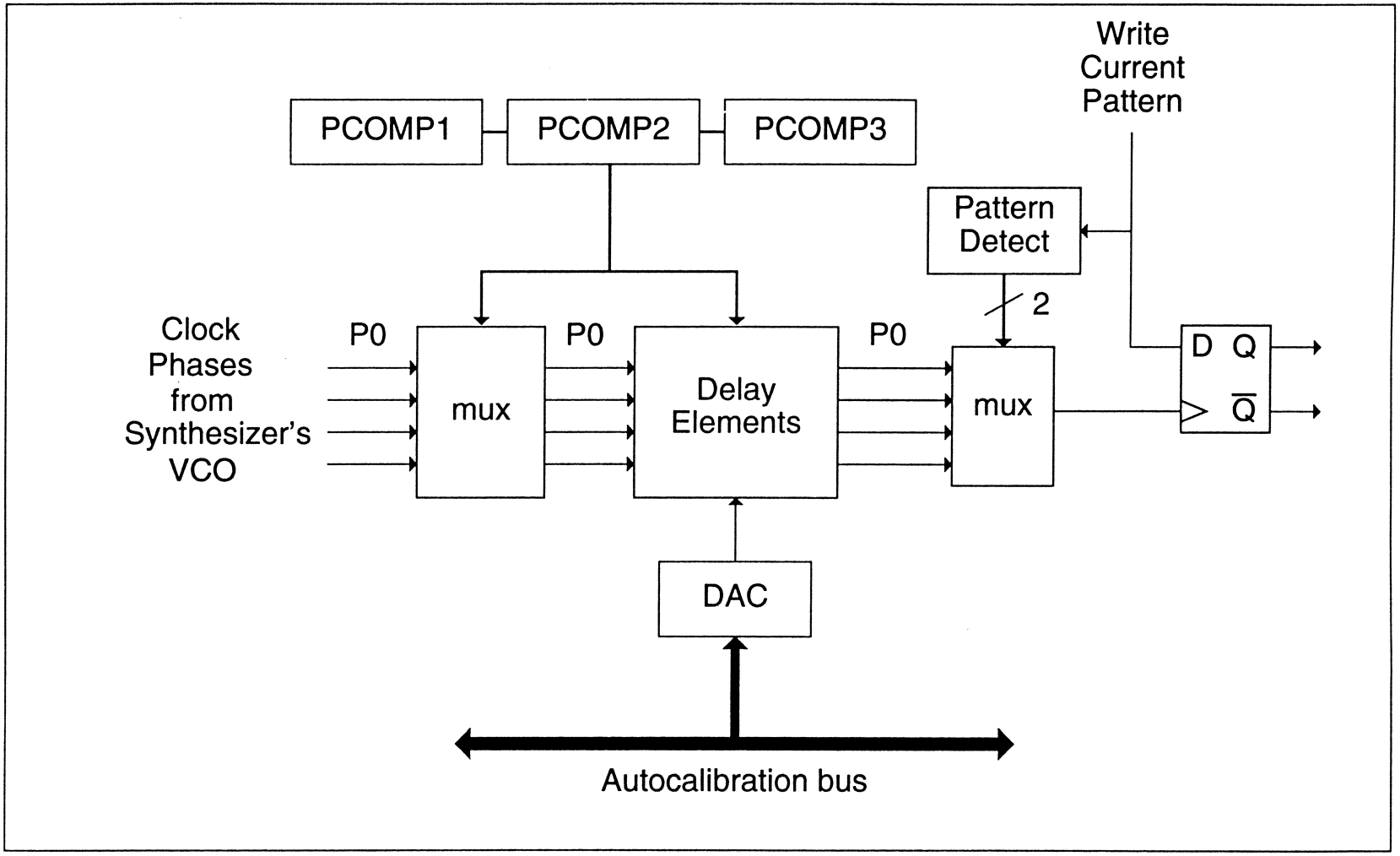

WRITE PRECOMPENSATION-cont

Write Pattern			Write Precomp
t_{-2}	t_{-1}	t_0	
N	N	T	No Precomp
T	N	T	PCOMP1
T	T	T	PCOMP2
N	T	T	PCOMP3

CHANNEL QUALITY/CALIBRATION

- QUANTITIES:
  - -- NUMBER OF ERRORS
  - -- PHASE DETECTOR OUTPUT
  - -- VCO CONTROL
  - -- AGC CONTROL
  - -- Error in +1 values
  - -- Error in -1 values
  - -- Error in 0 values
  - -- ERROR IN ALL VALUES
- MATHEMATICAL OPERATION ON THE QUANTITIES
  - -- NO OPERATION
  - -- ABSOLUTE VALUE
  - -- SQUARED VALUE
- FEATURE TO REPORT
  - -- MINIMUM
  - -- MAXIMUM
  - -- SUM

FIR FILTER

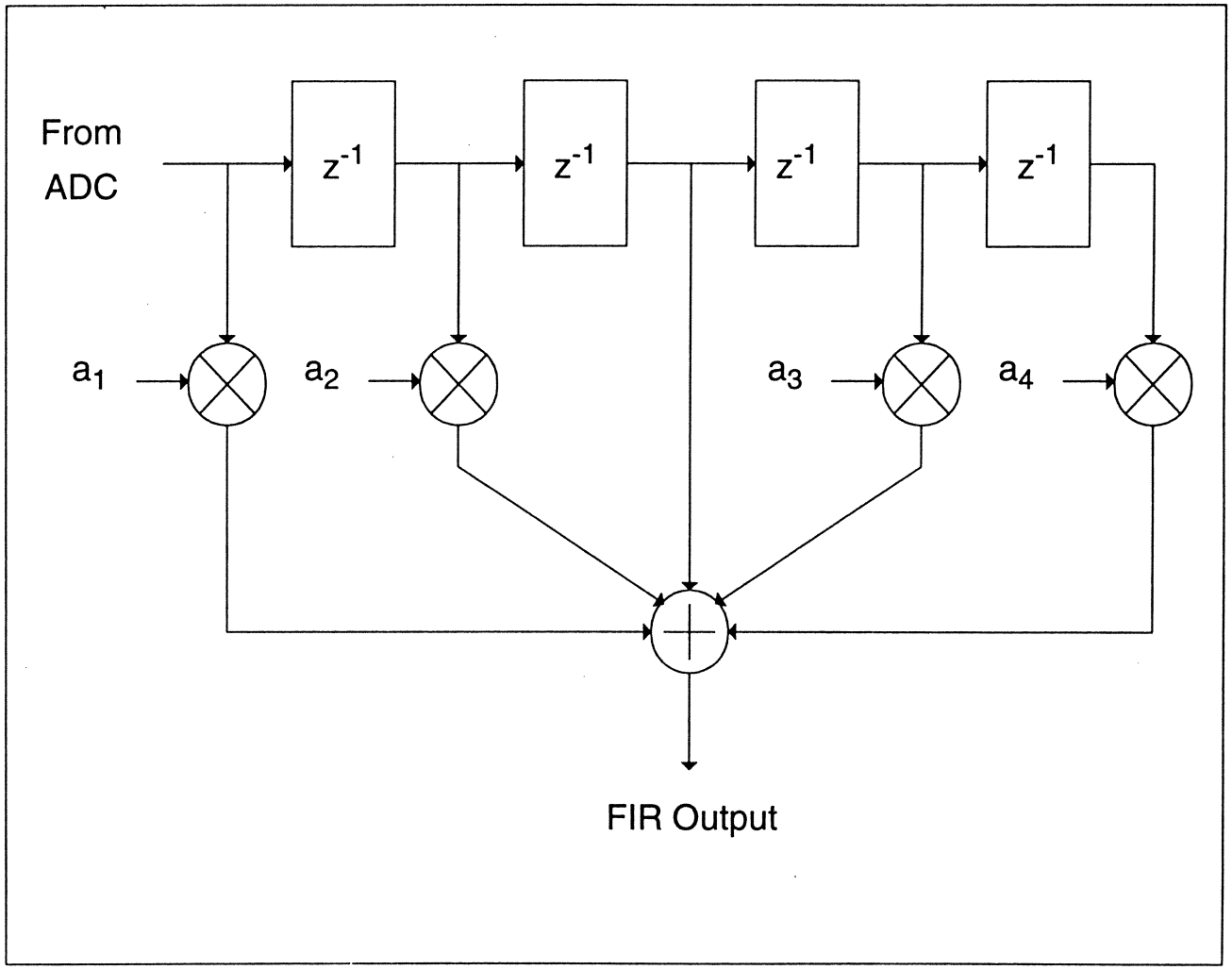

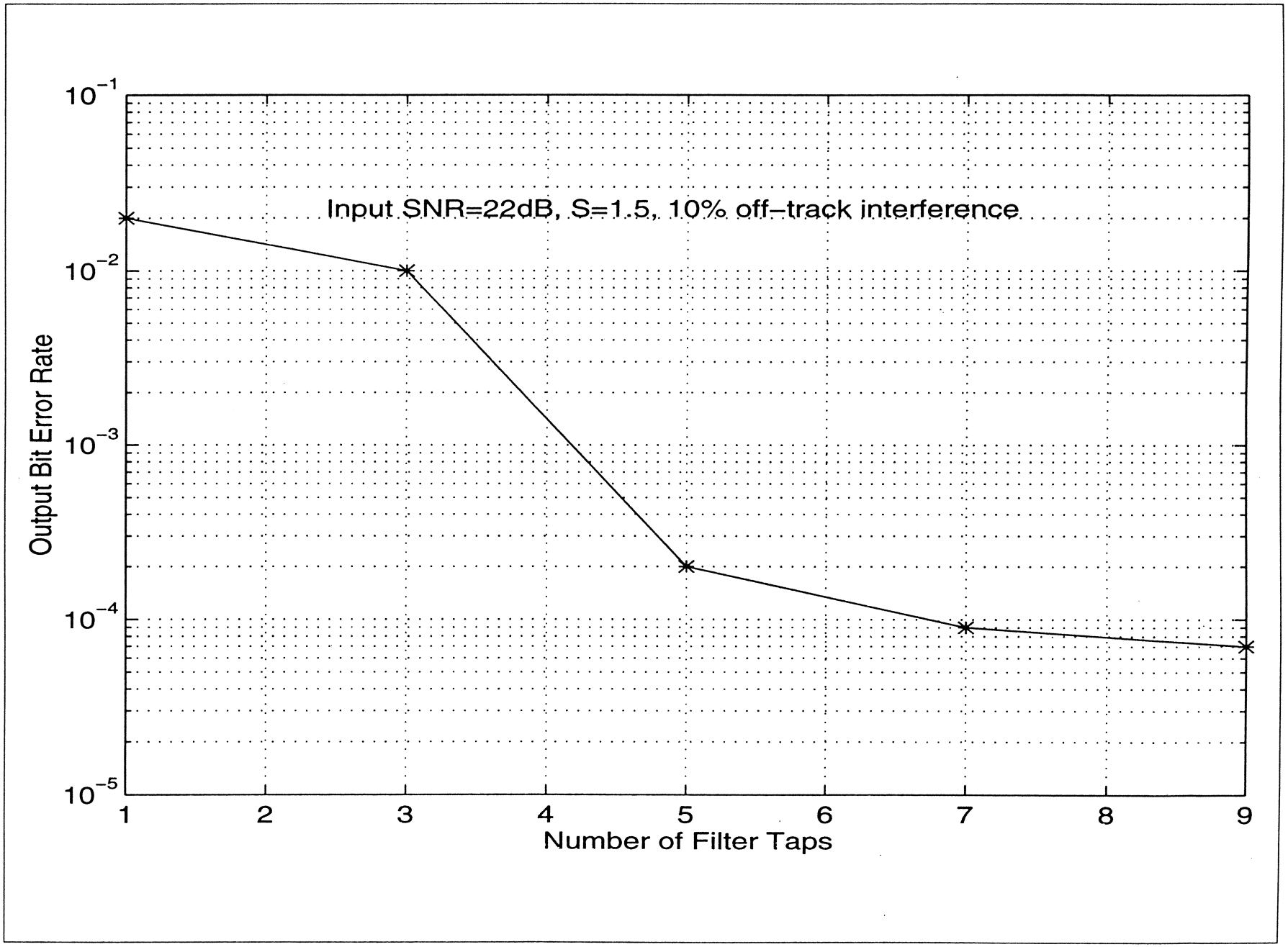
Input SNR=22dB, S=1.5, 10% off-track interference
Output Bit Error Rate
10^{-1}
10^{-2}
10^{-3}
10^{-4}
10^{-5}
1
2
3
4
5
6
7
8
9
Number of Filter Taps

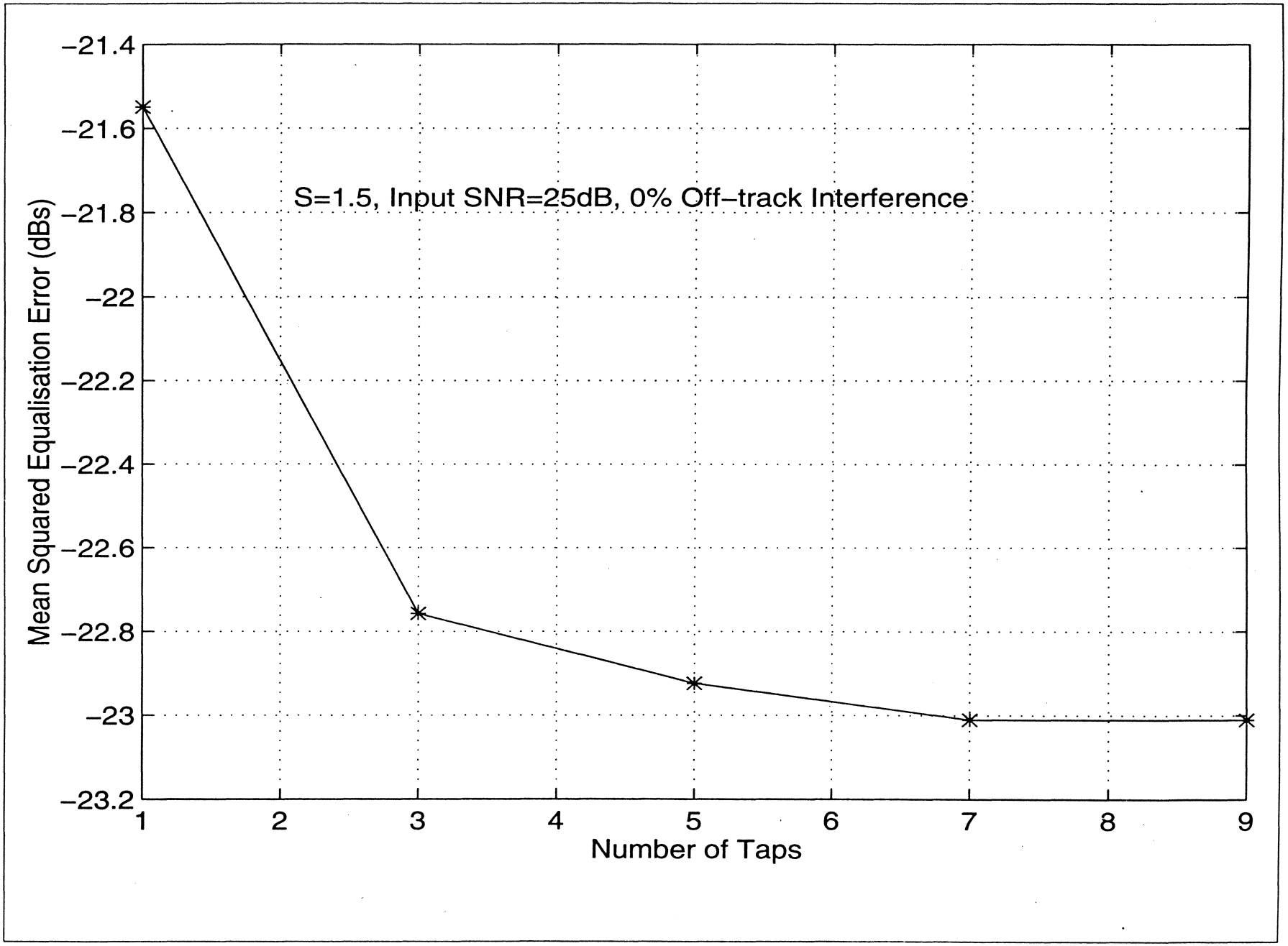
S=1.5, Input SNR=25dB, 0% Off–track Interference
Mean Squared Equalisation Error (dBs)
Number of Taps
−21.4
−21.6
−21.8
−22
−22.2
−22.4
−22.6
−22.8
−23
−23.2
1
2
3
4
5
6
7
8
9

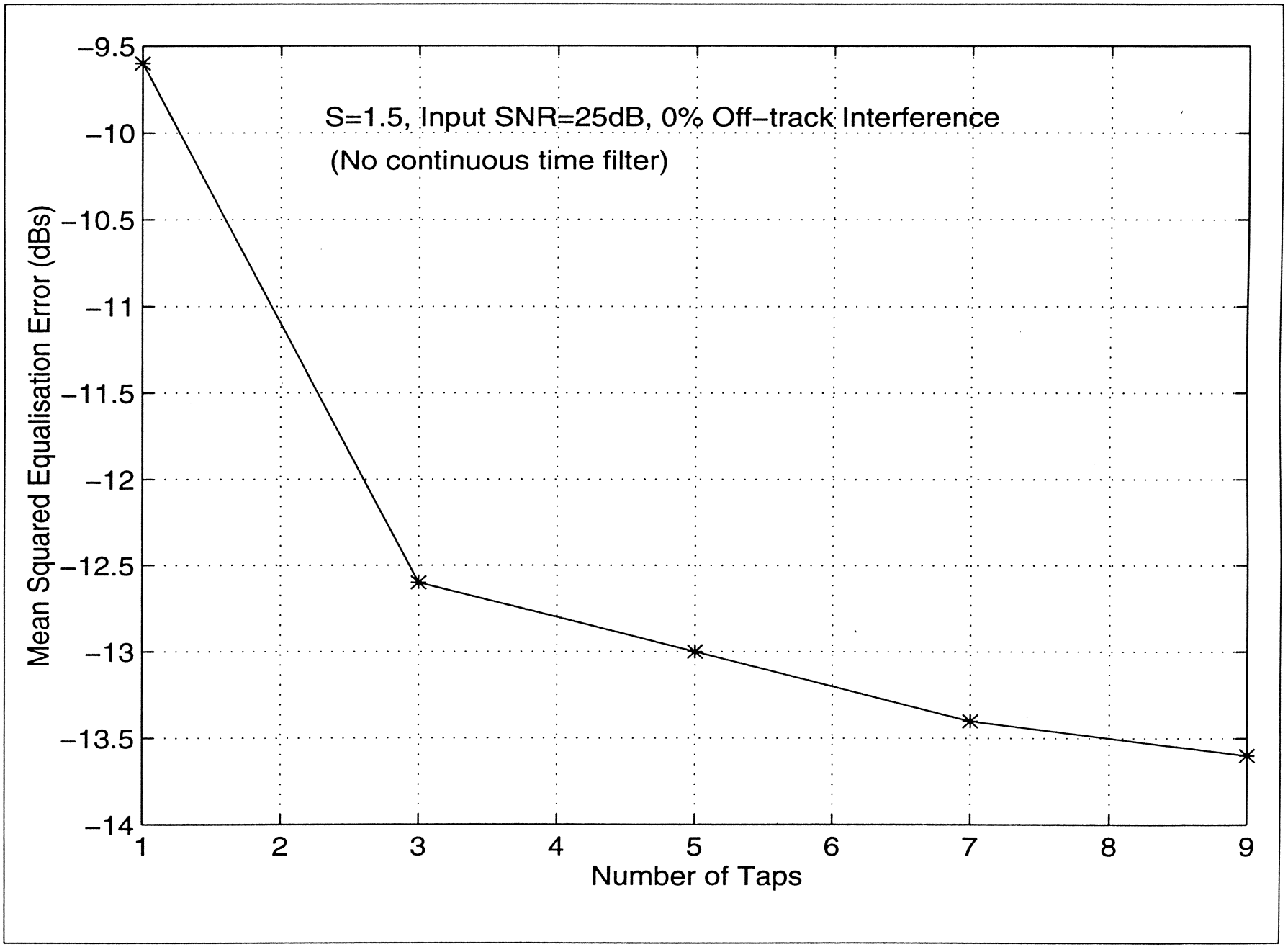
S=1.5, Input SNR=25dB, 0% Off–track Interference
(No continuous time filter)
Mean Squared Equalisation Error (dBs)
Number of Taps
−9.5
−10
−10.5
−11
−11.5
−12
−12.5
−13
−13.5
−14
1
2
3
4
5
6
7
8
9

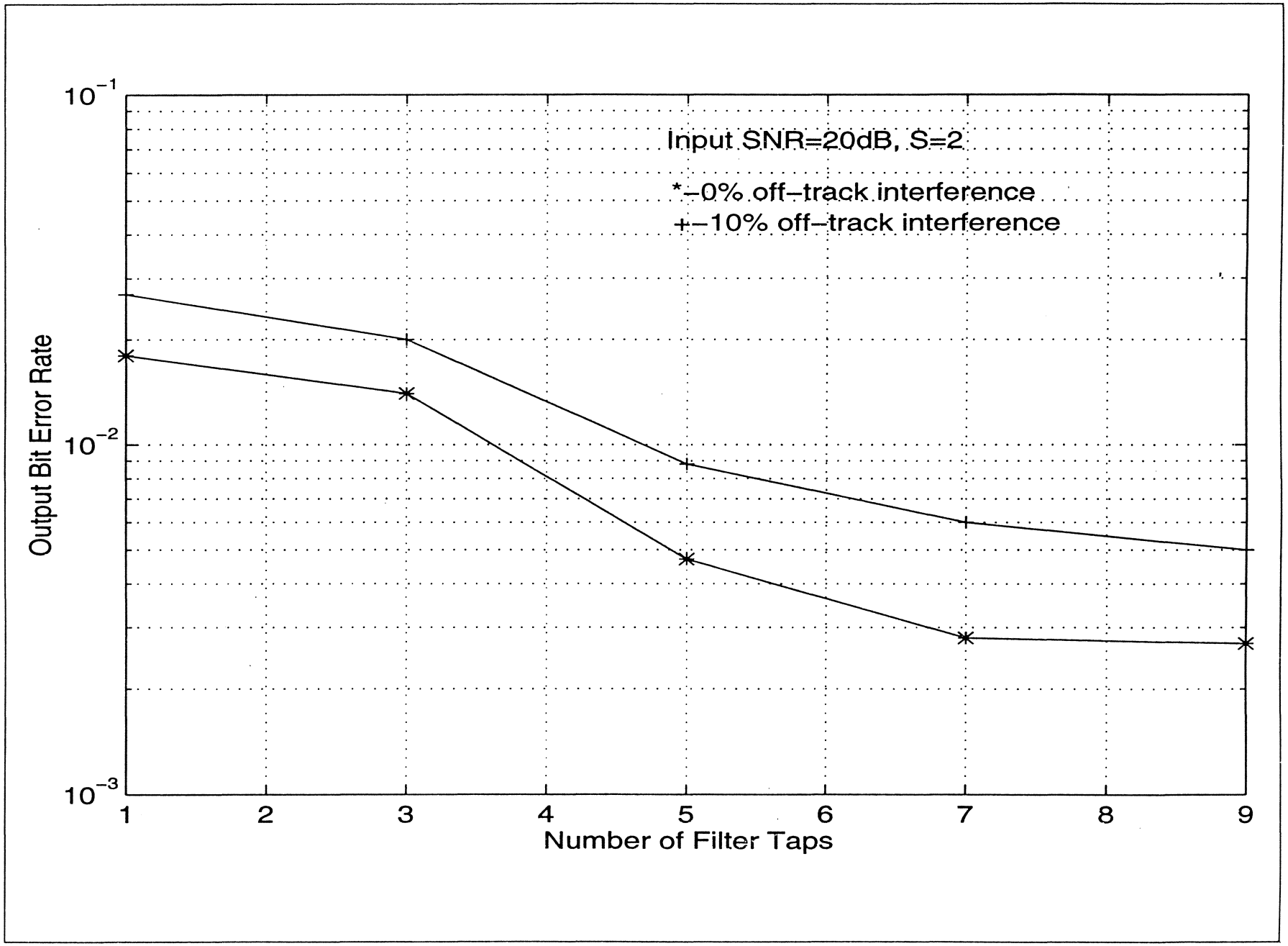
Input SNR=20dB, S=2
*–0% off–track interference
+–10% off–track interference
Output Bit Error Rate
10^{-1}
10^{-2}
10^{-3}
1
2
3
4
5
6
7
8
9
Number of Filter Taps

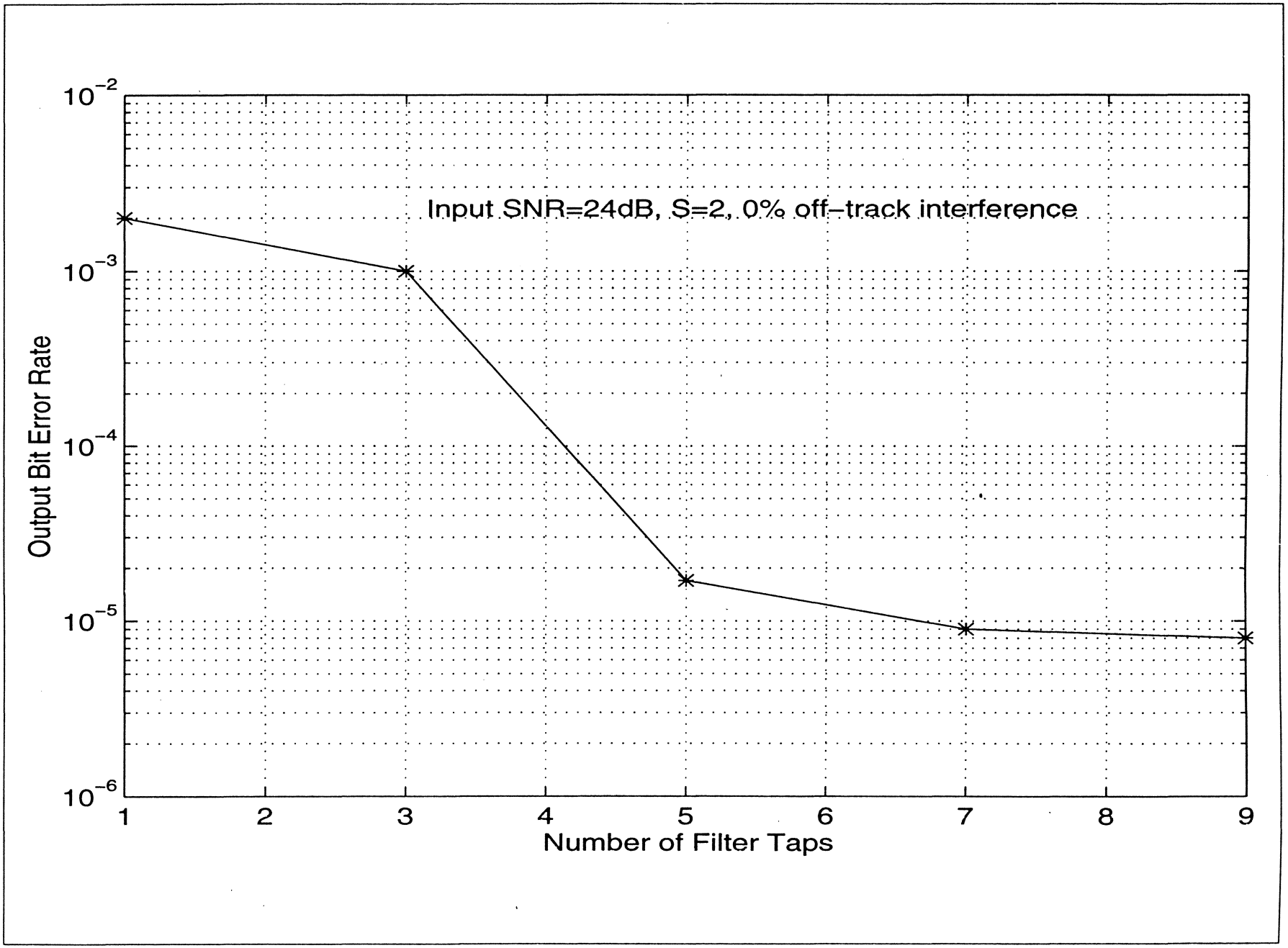
Input SNR=24dB, S=2, 0% off–track interference
Output Bit Error Rate
10^{-2}
10^{-3}
10^{-4}
10^{-5}
10^{-6}
1
2
3
4
5
6
7
8
9
Number of Filter Taps

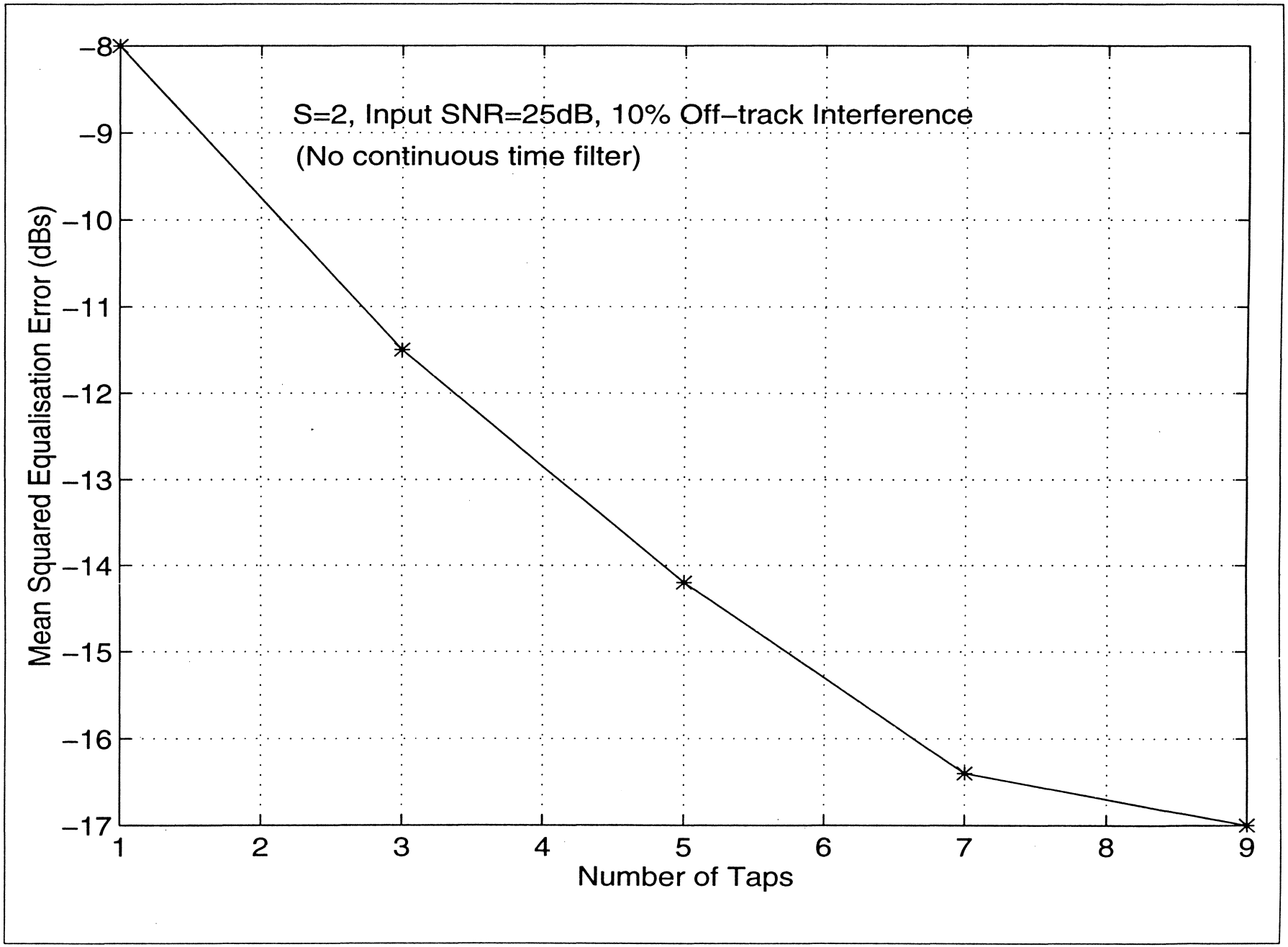
S=2, Input SNR=25dB, 10% Off–track Interference
(No continuous time filter)
Mean Squared Equalisation Error (dBs)
−8
−9
−10
−11
−12
−13
−14
−15
−16
−17
1
2
3
4
5
6
7
8
9
Number of Taps

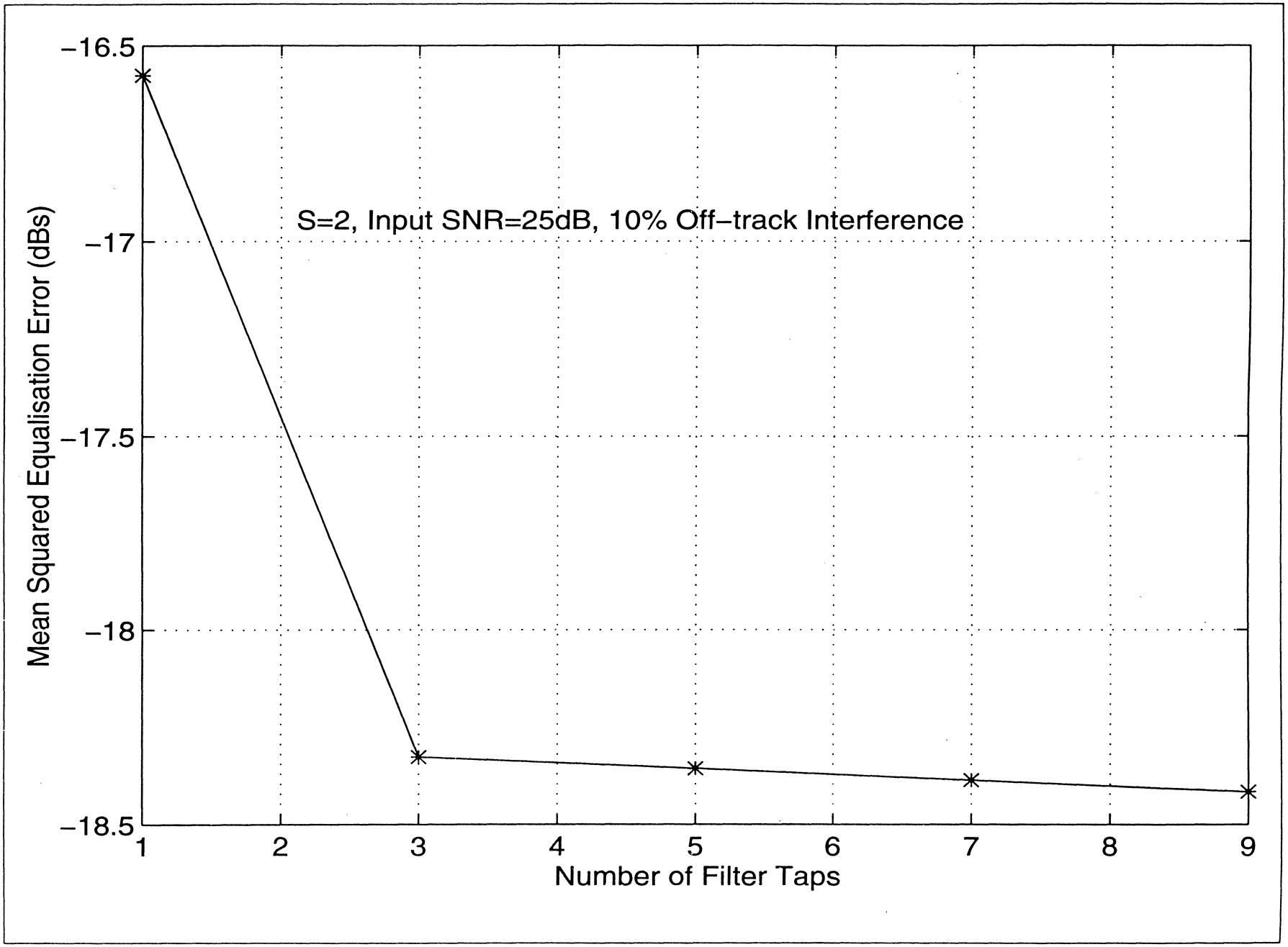
S=2, Input SNR=25dB, 10% Off–track Interference
Mean Squared Equalisation Error (dBs)
−16.5
−17
−17.5
−18
−18.5
1
2
3
4
5
6
7
8
9
Number of Filter Taps

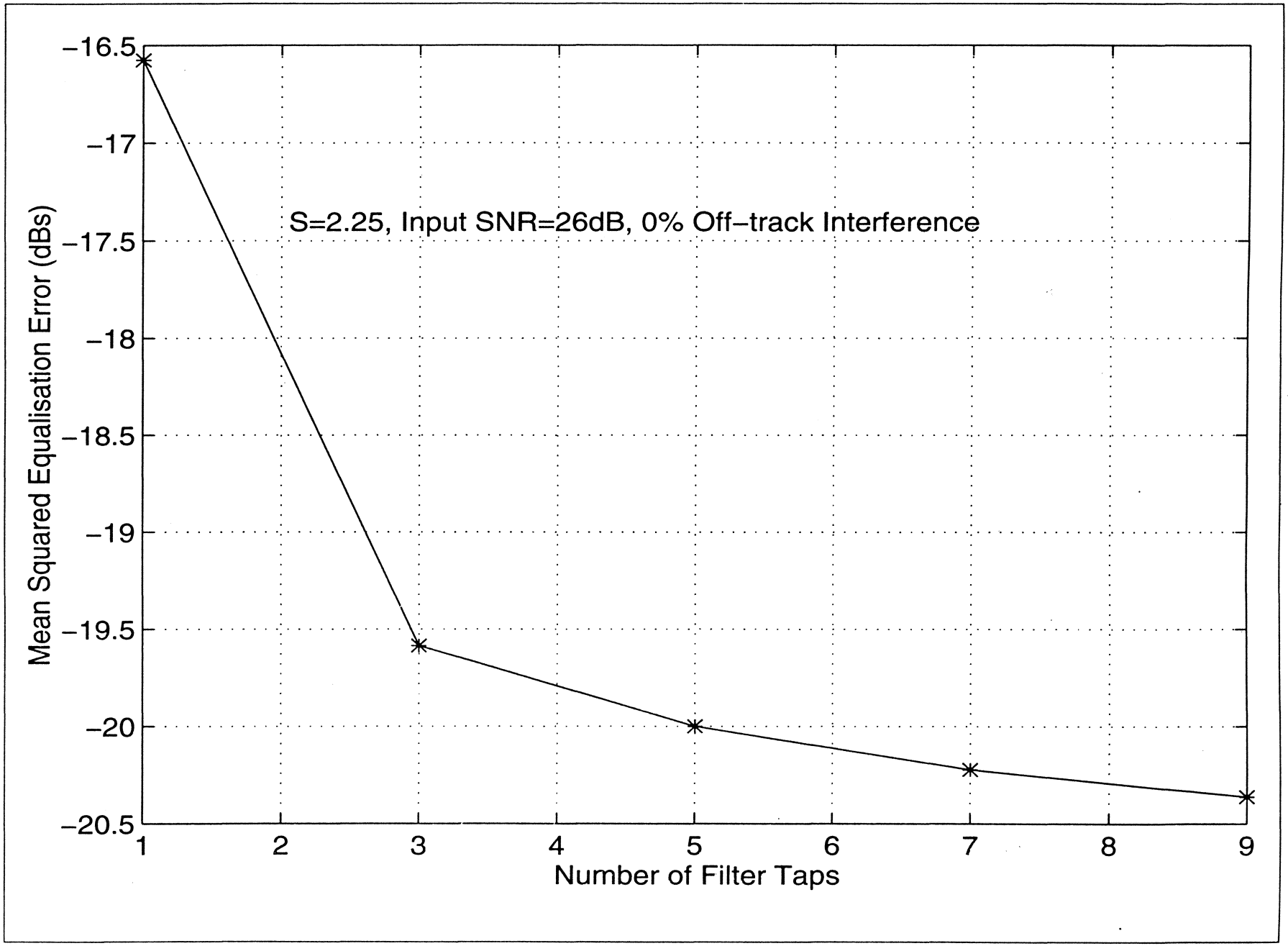
S=2.25, Input SNR=26dB, 0% Off–track Interference
Mean Squared Equalisation Error (dBs)
Number of Filter Taps
−16.5
−17
−17.5
−18
−18.5
−19
−19.5
−20
−20.5
1
2
3
4
5
6
7
8
9

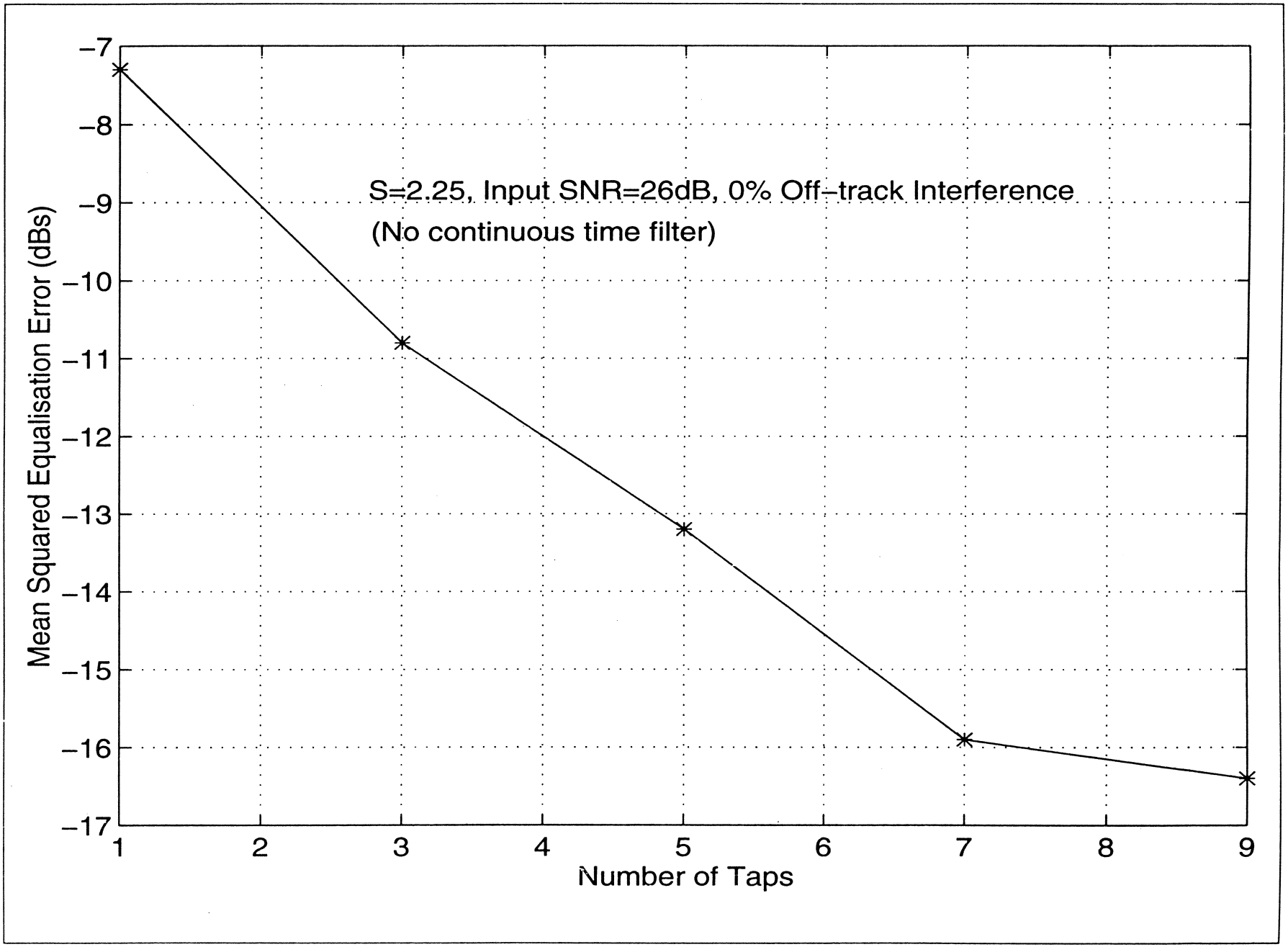
S=2.25, Input SNR=26dB, 0% Off–track Interference
(No continuous time filter)
Mean Squared Equalisation Error (dBs)
Number of Taps
−7
−8
−9
−10
−11
−12
−13
−14
−15
−16
−17
1
2
3
4
5
6
7
8
9

Phase Error. 27 Oct. 1995

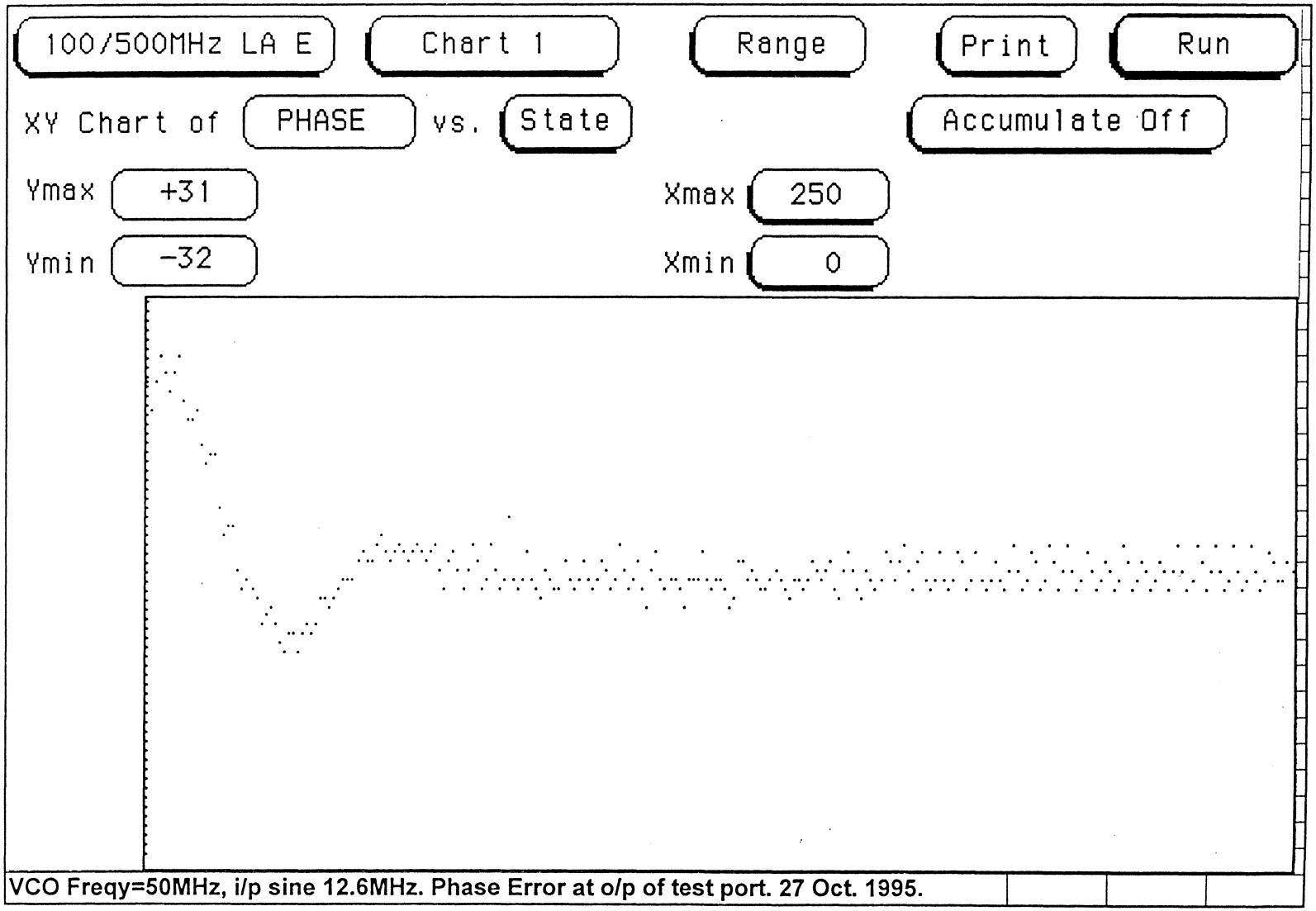

Phase Error

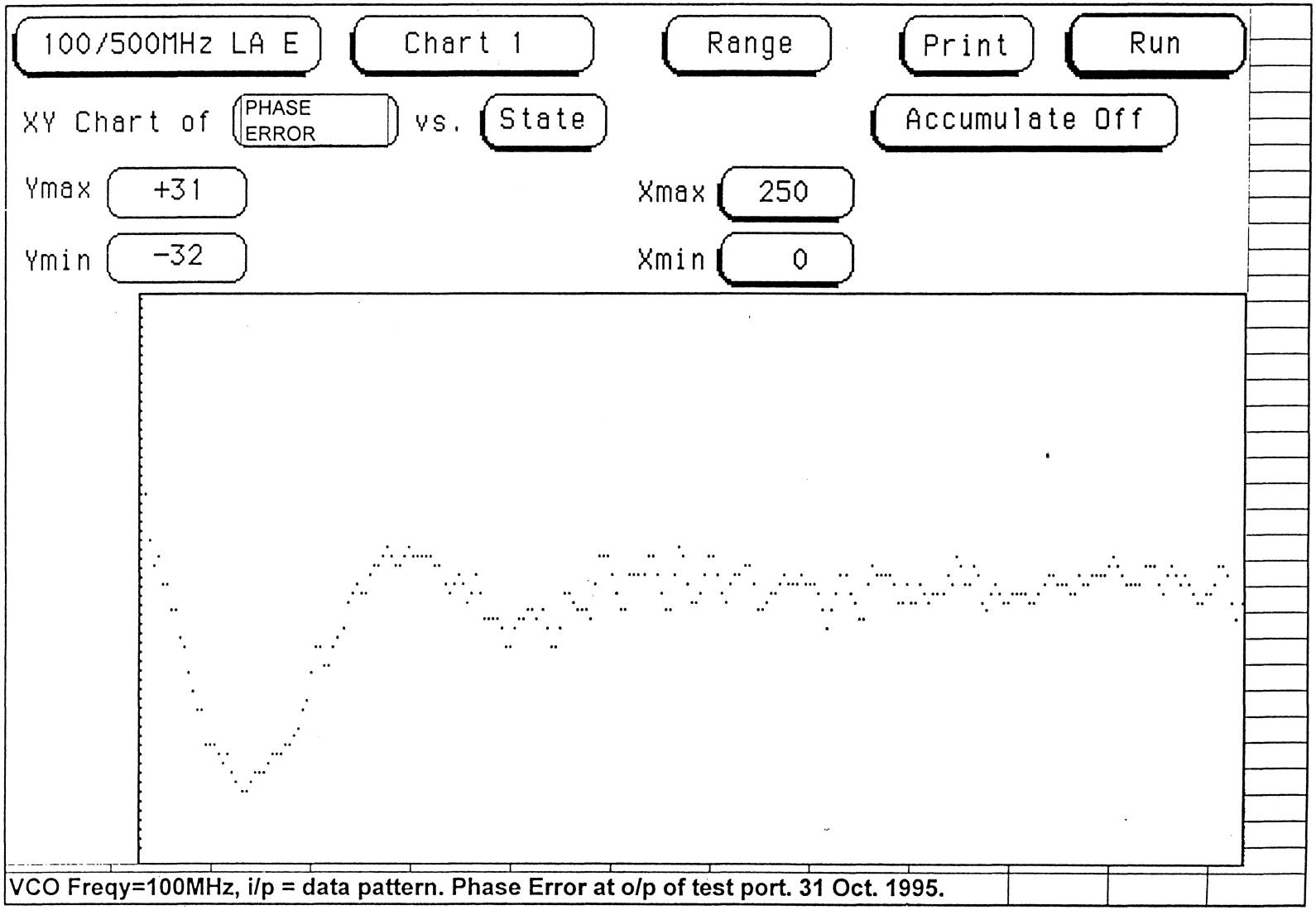
100/500MHz LA E
Chart 1
Range
Print
Run
XY Chart of
PHASE ERROR
vs.
State
Accumulate Off
Ymax
+31
Ymin
-32
Xmax
250
Xmin
0
VCO Freqy=100MHz, i/p = data pattern. Phase Error at o/p of test port. 31 Oct. 1995.

ADC(data)

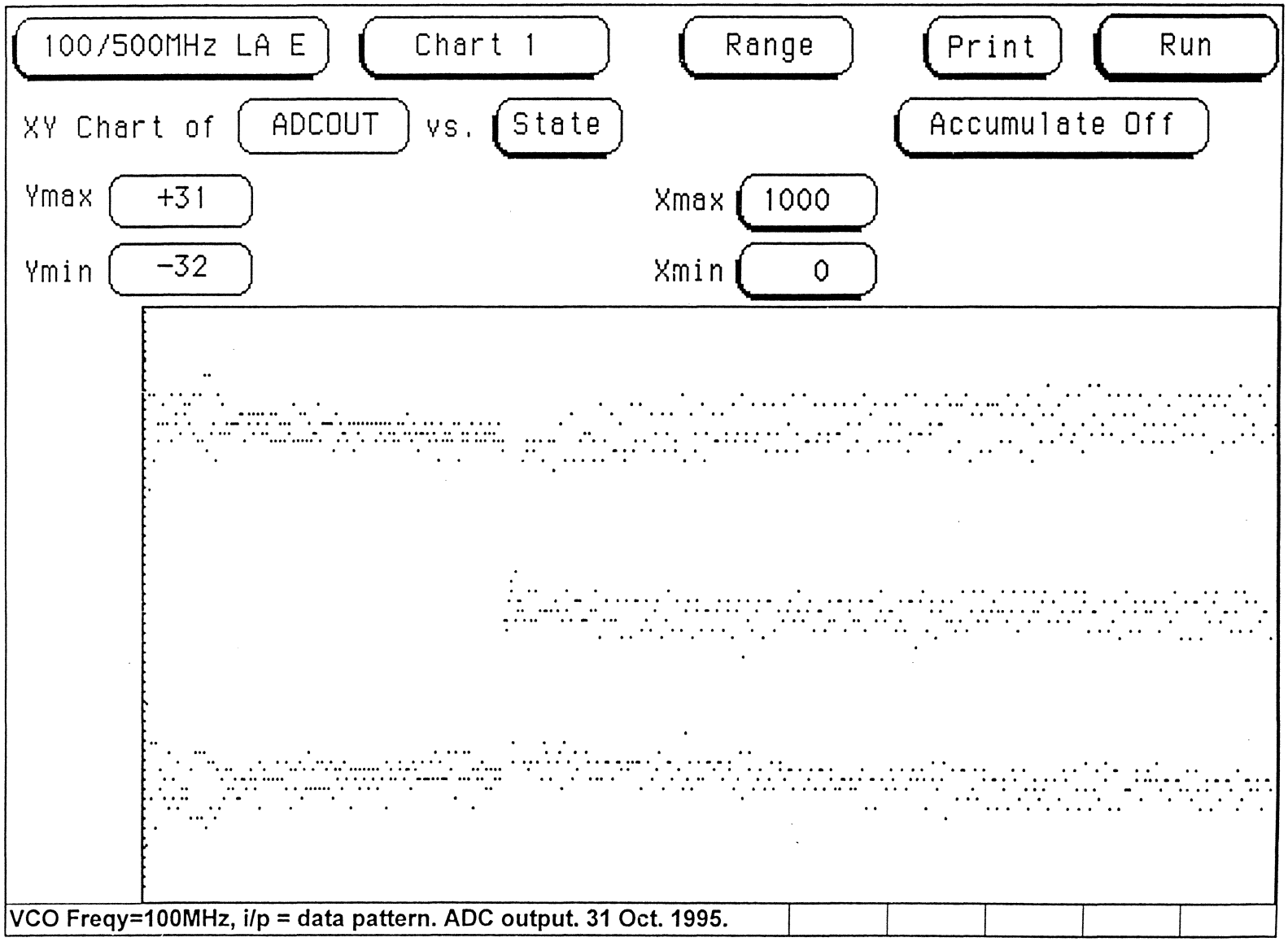
100/500MHz LA E
Chart 1
Range
Print
Run
XY Chart of
ADCOUT
vs.
State
Accumulate Off
Ymax
+31
Ymin
-32
Xmax
1000
Xmin
0
VCO Freqy=100MHz, i/p = data pattern. ADC output. 31 Oct. 1995.

Frequency Error (Zoom)

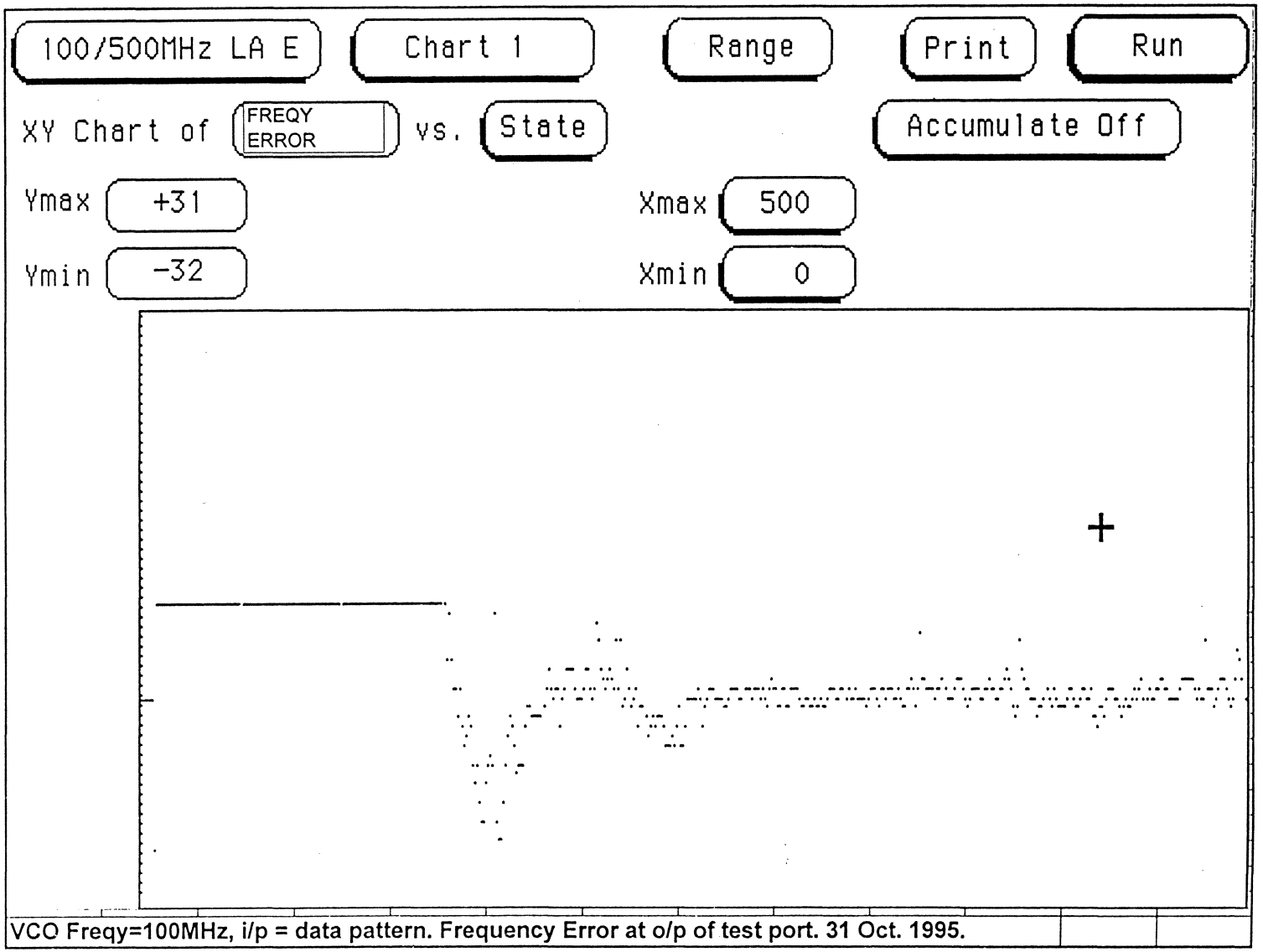

ADC(data)

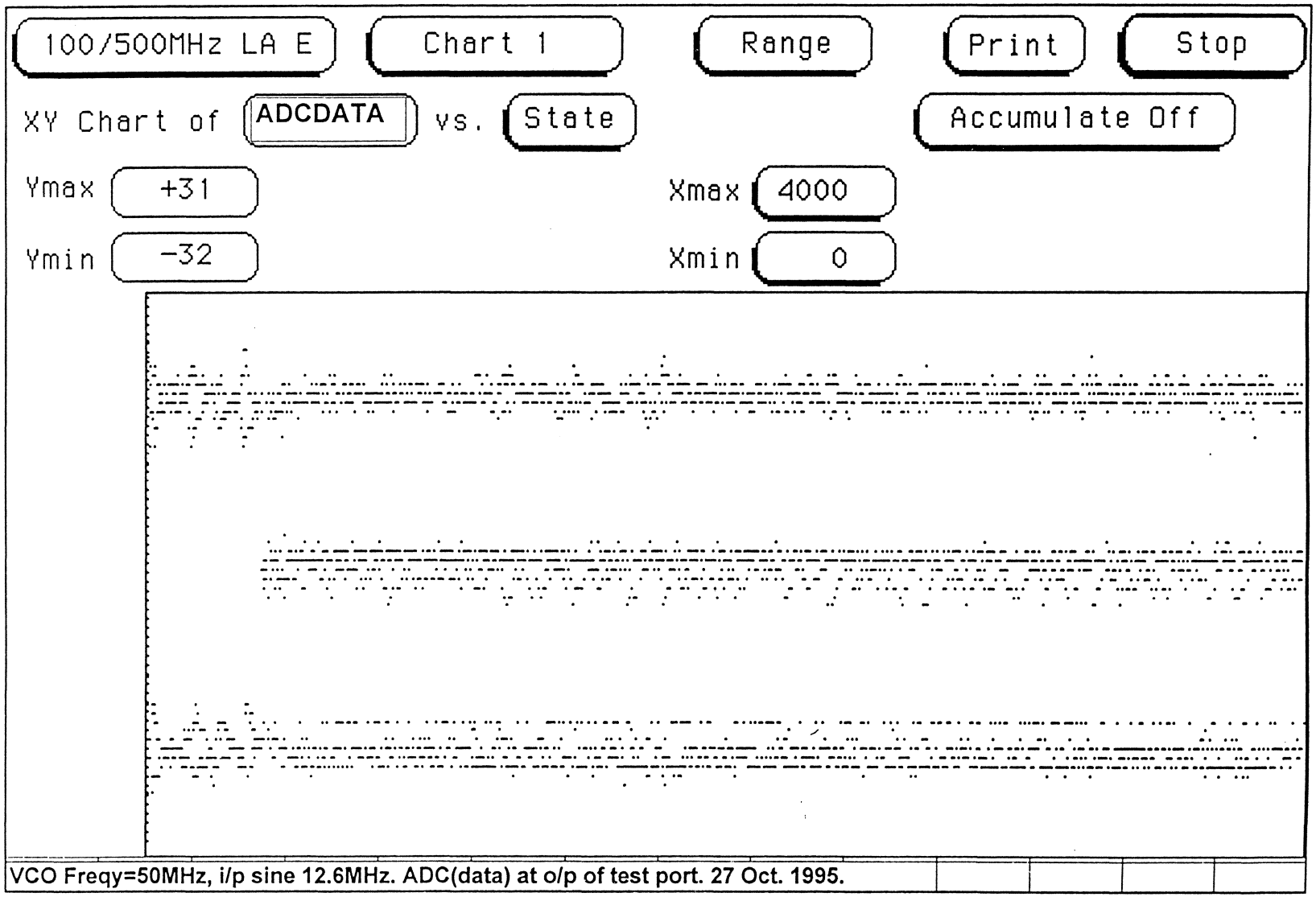
100/500MHz LA E
Chart 1
Range
Print
Stop
XY Chart of
ADCDATA
vs.
State
Accumulate Off
Ymax
+31
Xmax
4000
Ymin
-32
Xmin
0
VCO Freqy=50MHz, i/p sine 12.6MHz. ADC(data) at o/p of test port. 27 Oct. 1995.

Frquency Error. 27 Oct. 1995

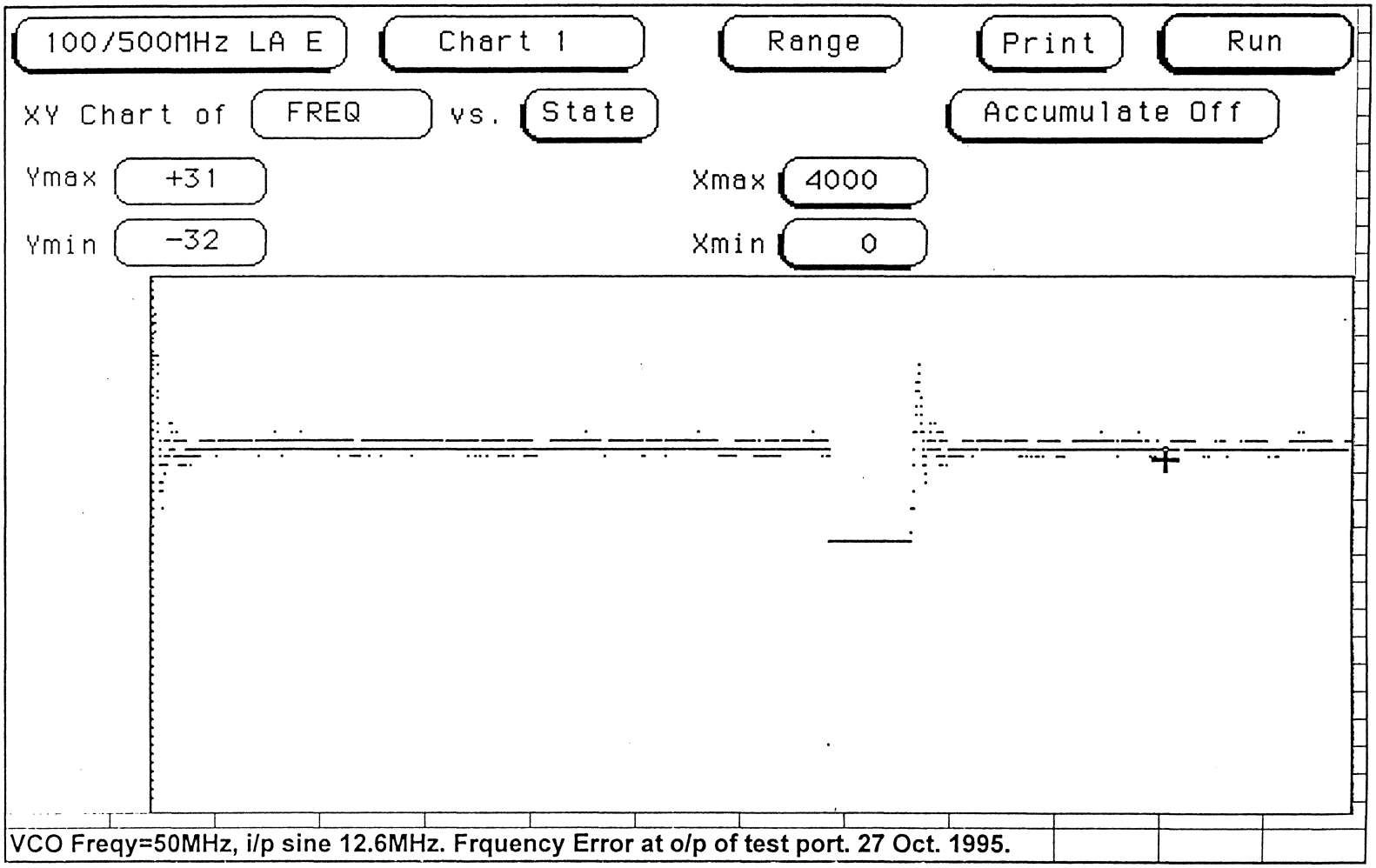

VCO Freqy=50MHz, i/p sine 12.6MHz. Frquency Error at o/p of test port. 27 Oct. 1995.

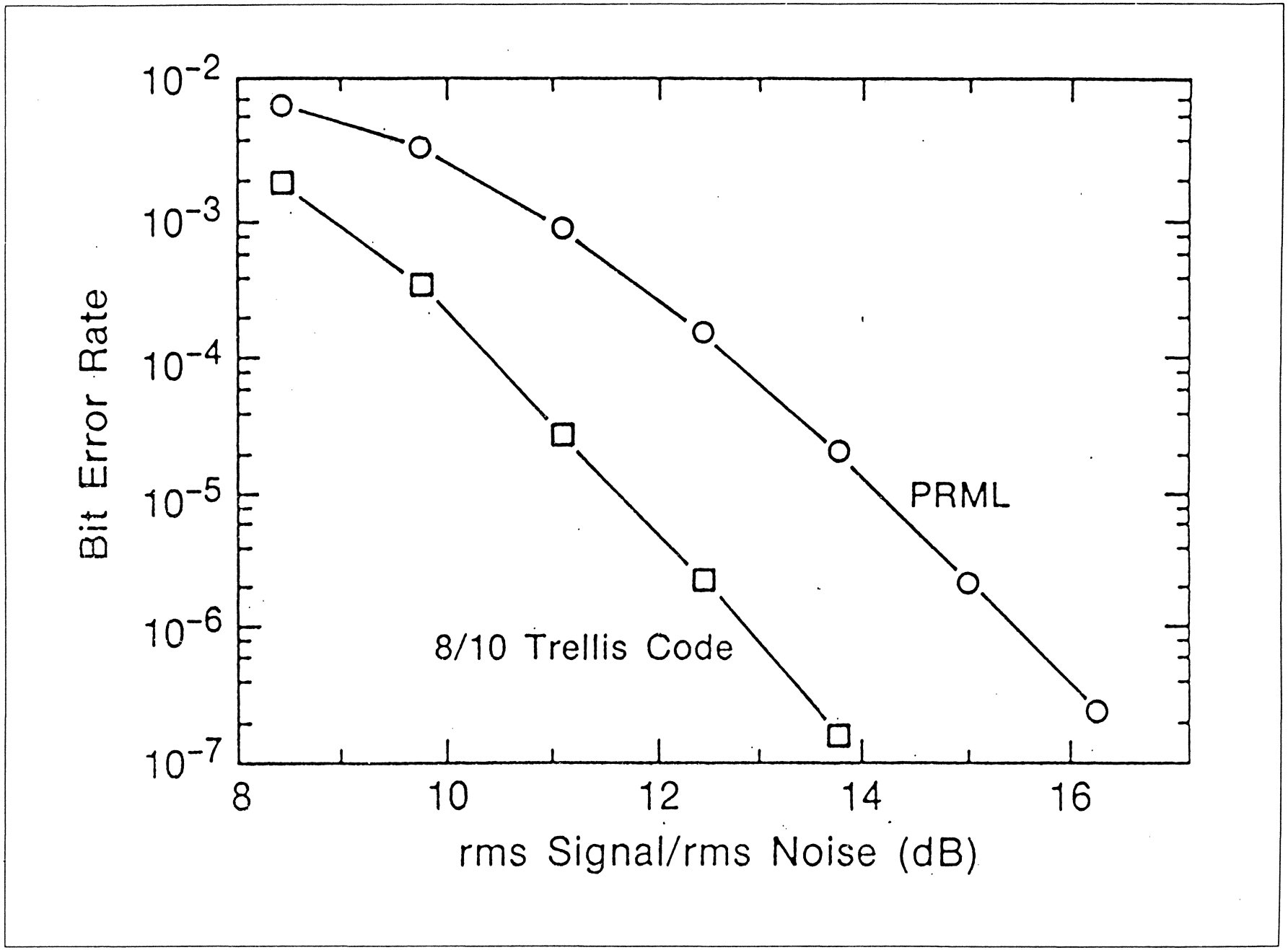
Bit Error Rate
10^{-2}
10^{-3}
10^{-4}
10^{-5}
10^{-6}
10^{-7}
8
10
12
14
16
rms Signal/rms Noise (dB)
PRML
8/10 Trellis Code

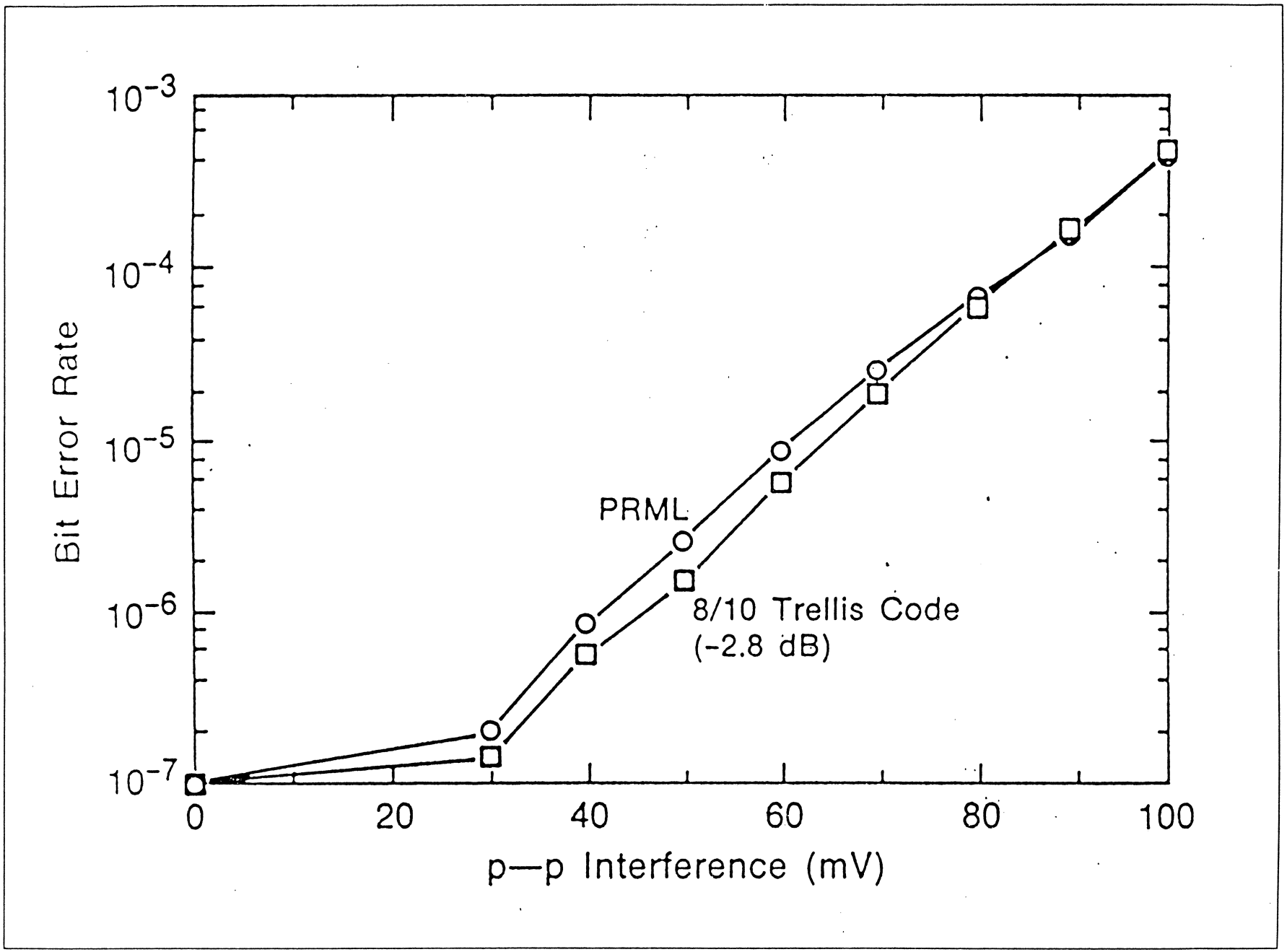
Bit Error Rate
10^{-3}
10^{-4}
10^{-5}
10^{-6}
10^{-7}
PRML
8/10 Trellis Code
(-2.8 dB)
0
20
40
60
80
100
p—p Interference (mV)

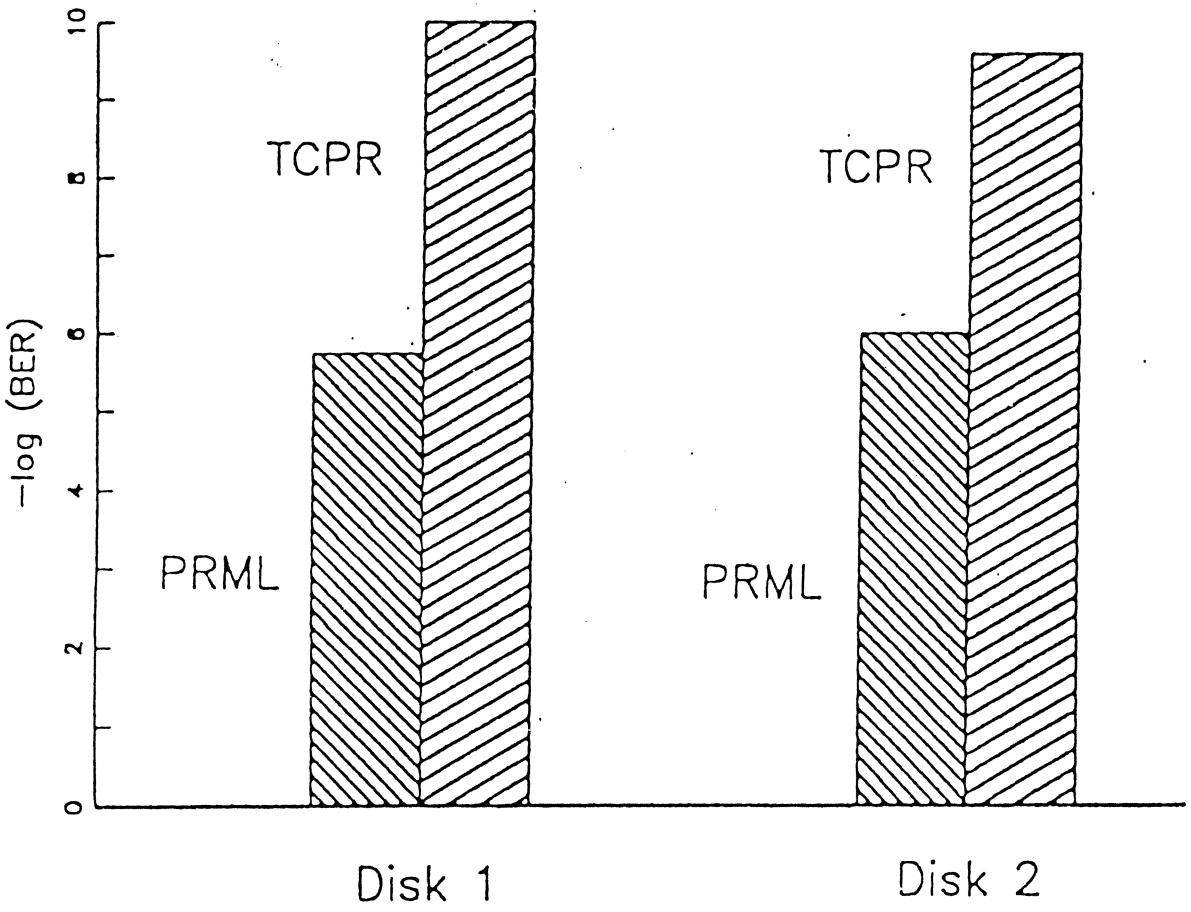
−log (BER)
0
2
4
6
8
10
TCPR
PRML
TCPR
PRML
Disk 1
Disk 2

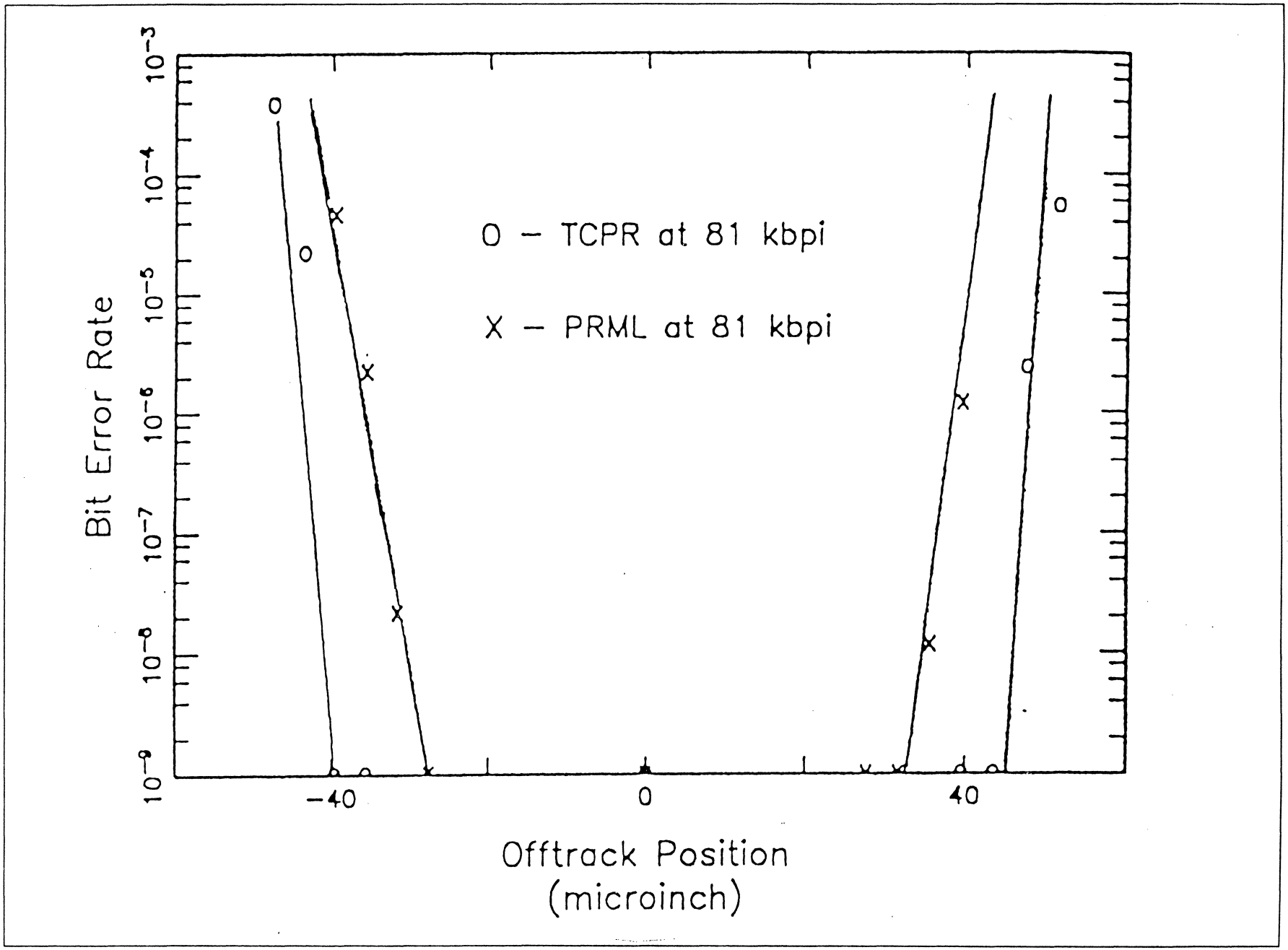
Bit Error Rate
10^{-3}
10^{-4}
10^{-5}
10^{-6}
10^{-7}
10^{-8}
10^{-9}
O – TCPR at 81 kbpi
X – PRML at 81 kbpi
−40
0
40
Offtrack Position
(microinch)

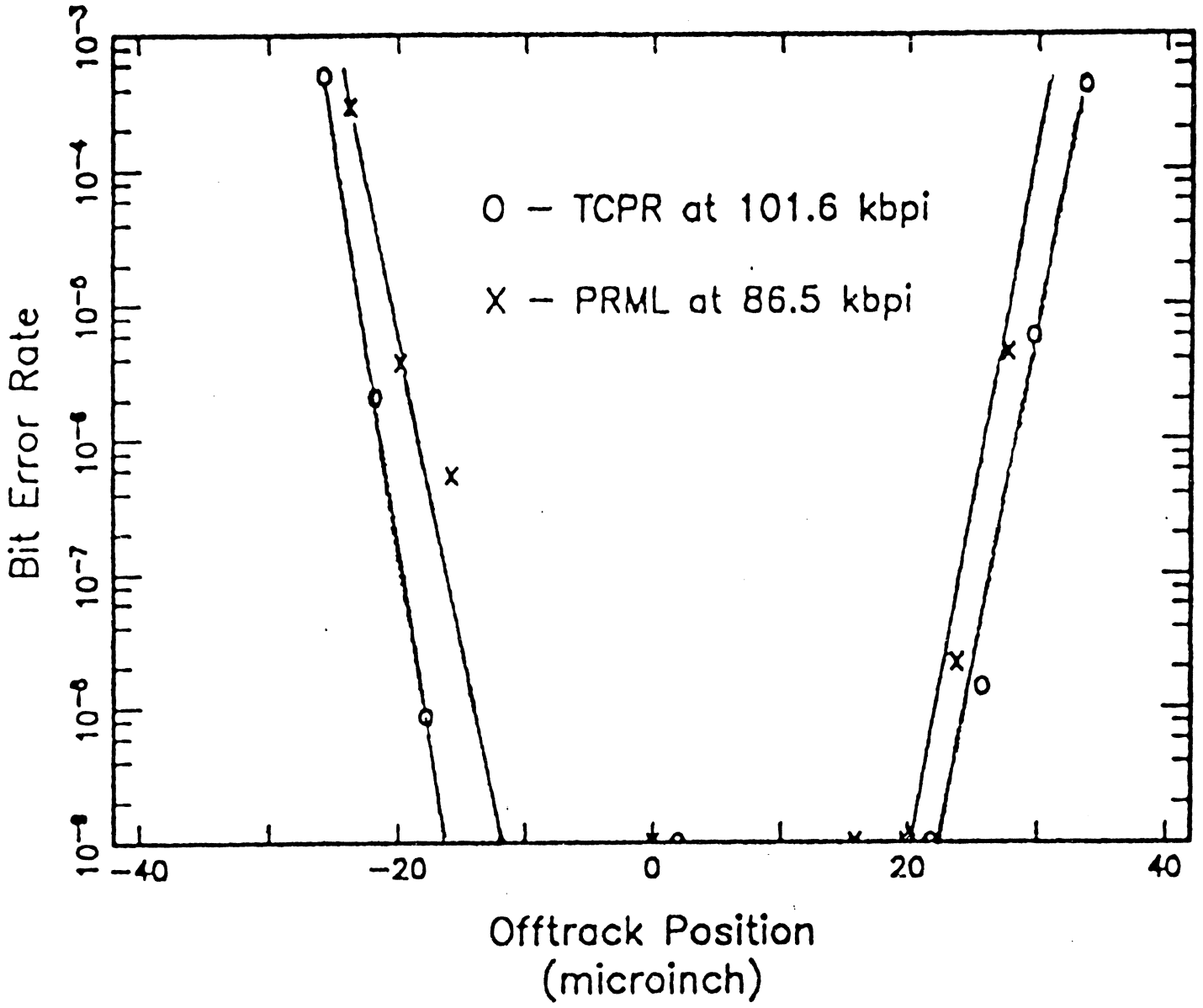
O – TCPR at 101.6 kbpi
X – PRML at 86.5 kbpi
Bit Error Rate
10^{-3}
10^{-4}
10^{-5}
10^{-6}
10^{-7}
10^{-8}
10^{-9}
−40
−20
0
20
40
Offtrack Position
(microinch)

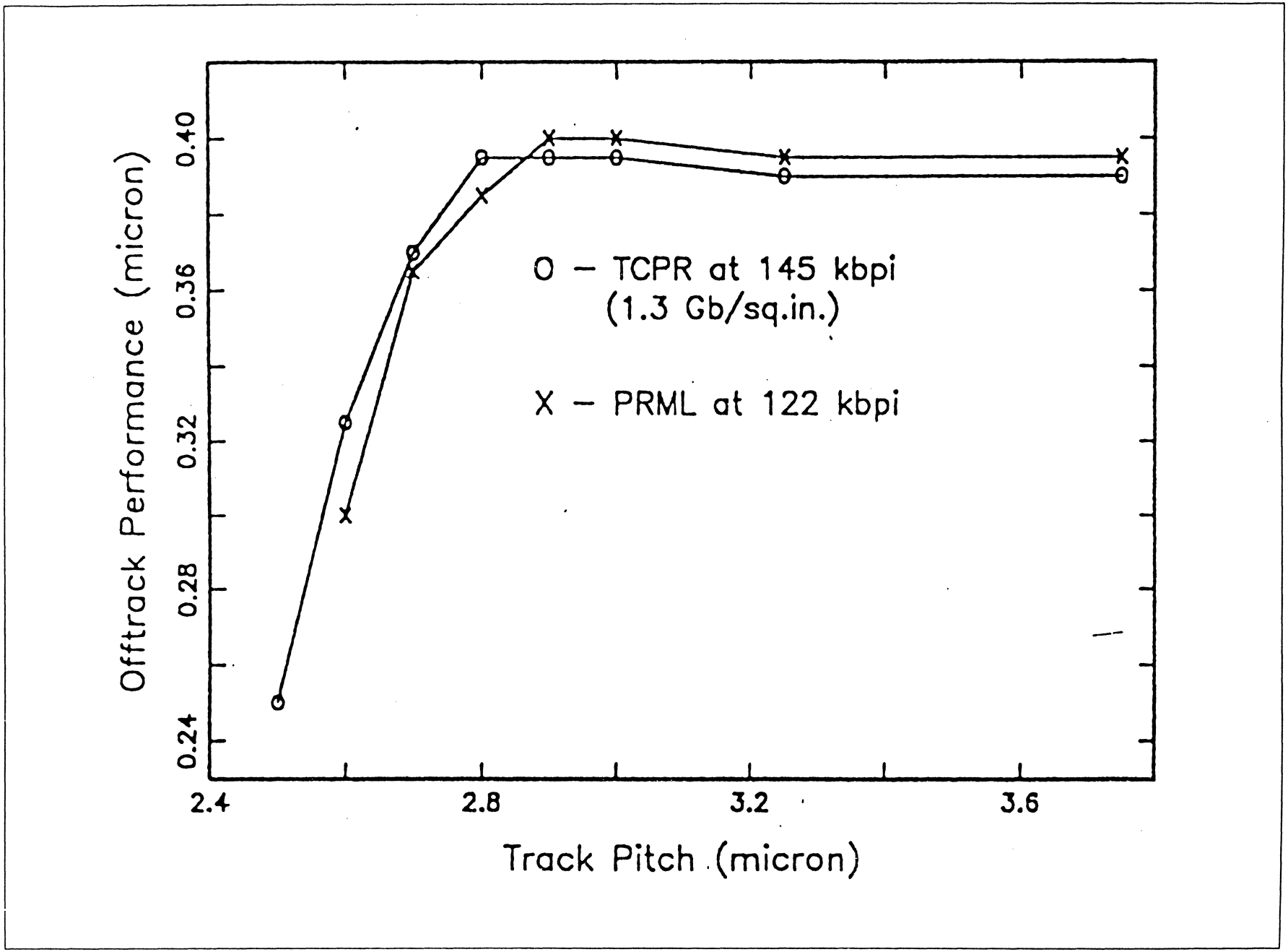
Offtrack Performance (micron)
0.24
0.28
0.32
0.36
0.40
2.4
2.8
3.2
3.6
Track Pitch (micron)
O – TCPR at 145 kbpi
(1.3 Gb/sq.in.)
X – PRML at 122 kbpi

REFERENCES

[1]. R. E. Ziemer and W. H. Tranter, *Principles of Communications*, Boston: Houghton Mifflin, 1985

[2]. R. Karabed and N. Nazari, "*Analysis of Error Sequences for PRML and EPRML Signaling Performed over Lorentzian Channel*", Submitted to IEEE 1996 Global Telecommunication Conference.

[3]. N. Nazari and C. Varanasi, "*Performance of Recording Channels Employing Partial Response Signaling*", Proceedings of IEEE 1994 Global Telecommunications Conference, pp. 1129-1133.

DIGITAL SIGNAL PROCESSING IN DISC DRIVES

INTRODUCTION/OVERVIEW

GORDON HUGHES

Seagate Technology

December 1991

DSP AND DISC DRIVE SUBSYSTEMS

- DIGITAL DATA STORAGE IS DSP

  => DIGITAL IN, DIGITAL OUT

- DRIVE EXTERNAL/INTERNAL INTERFACES ARE DIGITAL

  CONTROLLED BY DRIVE μPROCESSOR

- EXCEPT THREE CLASSICALLY ANALOG INTERNAL SERVO SYSTEMS

  => HEAD SERVO: TRACK SEEK AND POSITION HOLD

  => RECORDING (READ-WRITE) CHANNEL

  => DISC SPINDLE MOTOR SPEED SERVO

DSP HEAD TRACKING SERVO

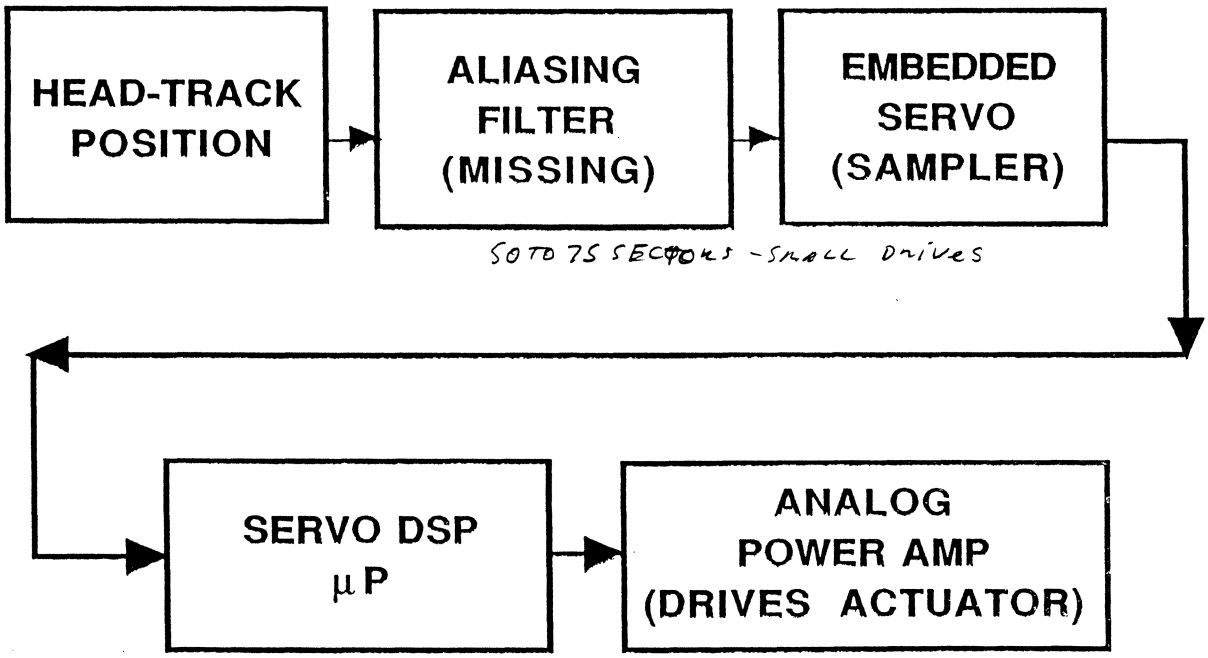

DSP READ CHANNEL

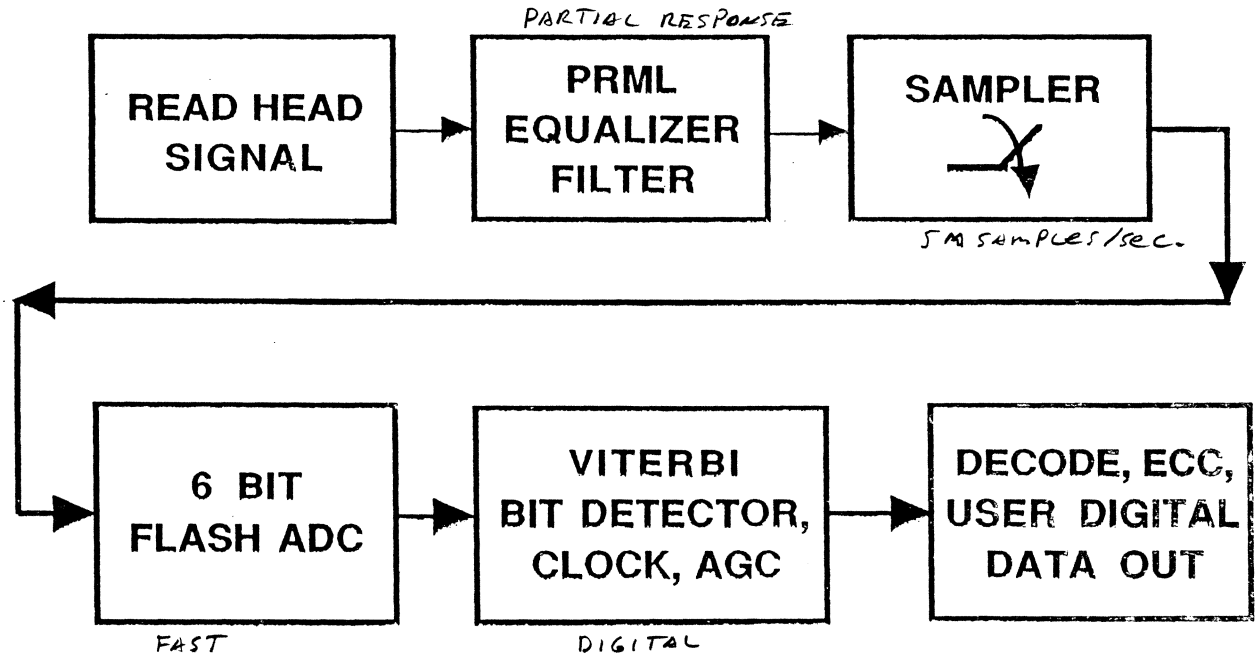

SPINDLE SPEED SERVO

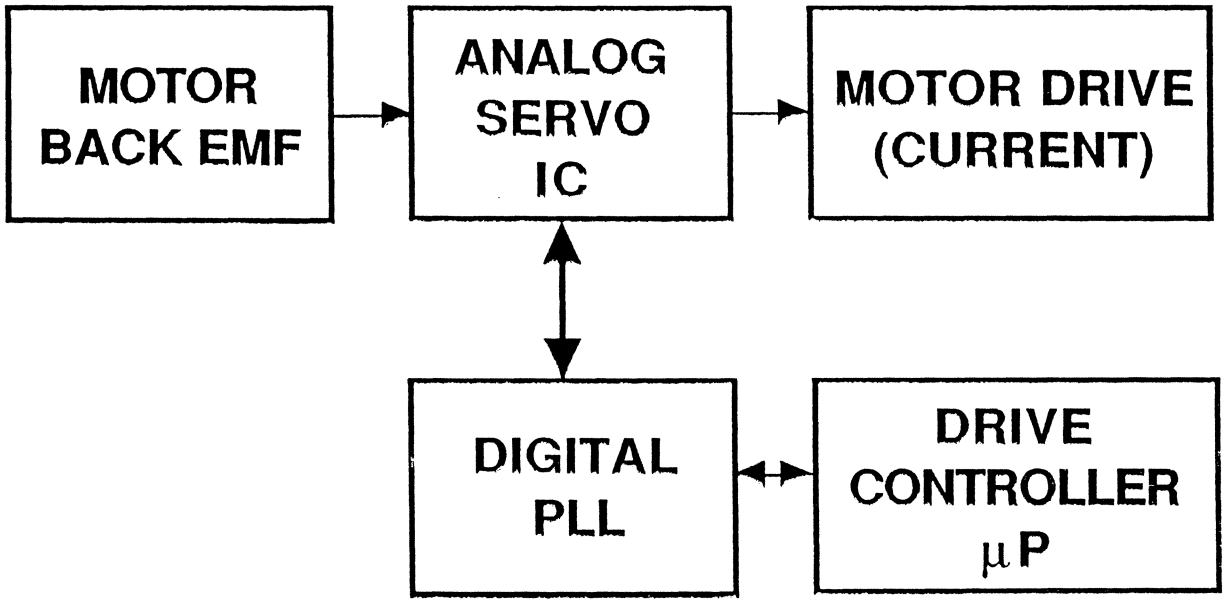

POTENTIAL DSP ADVANTAGES

- BETTER DRIVE PERFORMANCE SPECS,

  FROM TIGHTER WORST-CASE TOLERANCES TO COMPONENTS, TIME, AND TEMPERATURE.

- OR LESS STRINGENT COMPONENT TOLERANCES.

- MORE DRIVE I/O'S PER SECOND,

  FROM OFFLOADING SERVO CONTROL FUNCTIONS FROM DRIVE'S μPROCESSOR

- ADAPTIVE CONTROL ALGORITHMS,

  UTILIZING PERFORMANCE DATA,
  OVERLAPPED WITH DATA ACCESSING
  (NO OVERHEAD PENALTY)

DSP ADVANTAGES (con't)

- MANUFACTURABILITY:

  SELF CALIBRATION

  SELF TEST/DIAGNOSIS

  SELF TUNING FOR YIELD ENHANCEMENT

- DRIVE ERROR RECOVERY

  FROM OPERATING SHOCK,

  MIS-TRACKING,

  MIS-READ

- LOWER SERVO POWER CONSUMPTION,
  FROM OPTIMAL PLANT CONTROL MODELS

READ/WRITE CHANNELS

- EXAMPLE: IBM'S DSP PRML CHANNELS
  MAXIMUM LIKELYHOOD

- CONVENTIONAL CHANNEL DIGITAL ELEMENTS

  USER DIGITAL DATA INPUT

  COMPUTE AND APPEND ERROR CORRECTION CODE

  ENCODE (ENDAC)
  E

  (ANALOG WRITE-READ CHANNEL)

  DECODE (ENDAC)
  E

  DETECT AND CORRECT BURST ERRORS

  USER DIGITAL DATA OUTPUT

READ/WRITE CHANNELS (con't)

CONVENTIONAL R/W CHANNEL ANALOG ELEMENTS

- WRITE DRIVER
  - WRITE CURRENT
  - WRITE PRECOMPENSATION
- MAGNETIC RECORDING WRITE/READ PROCESS
- READ PREAMP
- READ EQUALIZATION AND NOISE FILTER
  - AGC CONTROL AND SETTING
  - BIT QUALIFIER (THRESHOLD LEVEL(S))
  - BIT TRANSITION DETECTOR
  - TIMING RECOVERY (PHASE LOCK LOOP)
  - DATA SEPARATION (TIMING SYNC)

R/W CHANNEL

DSP POTENTIAL ADVANTAGES:

- CONVENTIONAL PEAK DETECTION CHANNELS
  FACE INABILITY TO GET NECESSARY 26 dB SNR,
  AT HIGH MBITS/IN^2 AREAL DENSITIES
  100 MBITS/SQ"
  .5nV/HZ noise level INHERENT IN R/W ICs.

- ...ESPECIALLY 65 mm AND SMALLER DRIVES

- COMMUNICATIONS CHANNELS OPERATE AT 15-20 dB,
  USING HEAVY ERROR CORRECTION (10^{-4} RAW BER)
  TELEPHONE

- IBM'S SOLUTION IS DSP PRML,
  (PARTIAL RESPONSE MAXIMUM LIKELIHOOD)

- PARTIAL RESPONSE EQUALIZATION
  ALLOWS BITS TO BE PACKED CLOSER TOGETHER,
  BY ALLOWING CONTROLLED INTERFERENCE.

- A PENALTY IS THAT EQUALIZATION MUST BE PRECISE

=> USE DSP DIGITAL FILTER EQUALIZER
NEED 5% ACCURACY – TUNABLE TO COMPENSATE FOR HEAD/MEDIA VARIATIONS.

R/W CHANNEL DSP ADVANTAGES (con't)

- A SAMPLED VITERBI BIT DETECTOR IS OPTIMAL

=> A DIGITAL SIGNAL PROCESSING METHOD

PEAK LOCATION NOT COHERENT

- CLOCKING AND AGC CAN ALSO BE DONE IN THE DSP

....(PR'S HIGH BIT DENSITY DESTROYS THE PEAKS USED FOR CONVENTIONAL CLOCKING)

- DSP READ CHANNEL RESULTS IN:

  HIGHER BPI, BY USING PARTIAL RESPONSE.

  HIGHER TPI, SINCE VITERBI ALLOWS LOWER PLAYBACK AMPLITUDES (NARROW TRACKS)

- => HIGHER AREAL DENSITY (MBITS/IN^2)

  IBM IS SAYING 15-30% FOR FIRST GENERATION

  EVEN MORE LATER 150 M BITS/SQ" DENSITY

HEAD/TRACK SERVOS

- SERVO INPUT: HEAD-TRACK POSITION:
  INTEGER TRACK NUMBER (GRAY CODE),
  PLUS FRACTIONAL TRACK ERROR

- SERVO OUTPUTS:
  ACCELERATION COMMAND (ACTUATOR CURRENT),
  SEEK COMPLETE, SEEK ERROR, HEAD OFF TRACK
  IMBEDED SERVO WEDGE - NO TRACK WHILE WRITING.
- CONTINUOUS SERVO SIGNAL IN LARGER DRIVES
- SAMPLED SERVO COMMON IN SMALL DRIVES (3-5 KHZ)
- NOTE: SERVO SYSTEM SAMPLING OCCURS BEFORE ANY
  ANTI-ALIASING FILTER POSSIBLE.
  THIS CAN ALIAS HEAD FLEXURE 3-7 KHZ RESONANCE
  INTO SERVO PASSBAND.
  HEAD/GIMBEL RESONANCE
  USE NOTCH FILTER + TIGHTLY CONTROLED RESONANCE SPEC. OF HEAD ASSY.
  MEANS RESONANCE MUST BE HELD WITHIN LIMITS,
  MINIMUM RESONANCE SPEC NO LONGER ENOUGH.

PLANT MODEL ("OBSERVER")

- A POWERFUL CONCEPT FOR DSP

- CAN EFFECTIVELY ALLOW SAMPLED SERVO TO
  APPROACH SEEK/SETTLE PERFORMANCE
  OF A CONTINUOUS SERVO,
  WITHOUT THE WASTED DISC SURFACE OVERHEAD,
  AND MECH/THERMAL MISREGISTRY PENALTY.

- CAN REDUCE OFFTRACK DATA RISK
  CAUSED BY MECHANICAL SHOCK/VIBRATION

  (VALIDATE SERVO PES SAMPLES
  AGAINST OBSERVER PREDICTION)

DSP PLANT MODEL (con't)

- CONVENTIONAL LINEAR FREQUENCY DOMAIN ANALYSIS MODELS SECOND ORDER PLANT MECHANICAL SYSTEM, INCLUDING CRITICAL ARM-HEAD RESONANCES

- STATE VARIABLES ARE HEAD POSITION AND VELOCITY

- DSP TIME DOMAIN OBSERVER

  PREDICTS PRESENT STATE.

  MINIMIZES SERVO LAGS,

  ALLOWS NONLINEAR ELEMENTS.

  EXAMPLES:

    ACTUATOR FORCE CONSTANT V.S. POSITION

    HEAD-ARM SETTLING TIME VARIATIONS

DSP PLANT MODEL (con't)

- SERVO ERROR MODELS ALLOW SELF CAL/ADAPTATION:

  1) ACTUATOR FORCE CONSTANT,
     OVER TIME, TEMPERATURE, TRACK (NONLINEAR)
     DRIVE CURRENT SATURATION (NONLINEAR)

  2) ACTUATOR BIAS FORCE OVER TRACK POSITION
     (FROM HEAD FLAT CABLE, WINDAGE) (LINEAR)

  3) INDIVIDUAL HEAD THERMAL OFFSETS (LINEAR)

- REPETITIVE RUNOUT ELIMINATION POSSIBLE

  LINEAR FEEDFORWARD CONTROL,
  BY RUNOUT-LEARNING DSP FILTER

- ADAPTIVE SEEK ALGORITHM:

  MONITOR SEEK SETTLING TIME DURING DATA ACCESS
  TO MINIMIZE TOTAL SEEK TIME AND OFFTRACK

DISC SPINDLE SERVO

- **CONTROLS DISC SPIN MOTOR:**

  3-Ø BRUSHLESS PERMANENT MAGNET MOTOR,

  HAS NO FEEDBACK SENSORS (SPACE LIMITATION IN SMALL DRIVES LIMITED TO 3600 RPM BY LIMITED MOTOR TORQUE + 5V ONLY REQUIREMENT.

  (NO HALL SENSORS)

- **EXAMPLE DRIVE SPINDLE SERVO:**

  RPM IS PERFECTLY FREQUENCY LOCKED,

  USING DISC POSITION PHASE LOCK LOOP.

  POSITION NOISE SIGMA ≈ 50 NSEC — ~ NO GAP AT END OF ROTATION.

DISC SPINDLE SERVO (con't)

CONVENTIONAL DIGITAL SERVO ELEMENTS:

- A DIGITAL PHASE LOCK LOOP

- USES WRITE CLOCK CRYSTAL AS POSITION REFERENCE

- USES INPUT FEEDBACK SIGNAL FROM MOTOR BACK EMF
  MEASURED OFF THE TWO UNDRIVEN PHASES:
  THE TIMES WHEN THE PHASE VOLTAGES ARE EQUAL.
  => AN APERIODIC DIGITAL SAMPLED SIGNAL,

- GENERATES ANALOG COMMAND VOLTAGE
  TO COMMAND MOTOR ACCELERATION PUMP UP/DOWN

DISC SPINDLE SERVO (con't)

CONVENTIONAL ANALOG SERVO ELEMENTS

- START AND COMMUTATION LOGIC
- ANALOG FEEDBACK STABILIZATION LOOP
- INPUT IS DIGITAL PLL ACCELERATION COMMAND.
- OUTPUT IS SPINDLE MOTOR COIL CURRENT,
  FROM 3-Ø ANALOG POWER DRIVERS.
- INTERFACE TO DRIVE μP MINIMAL.
  POSITION PHASE ERROR CAN BE INTERROGATED.
  SPINDLE EXTERNAL SYNC SIGNAL (OPTIONAL)
- IS THIS AN ERSATZ DSP?
  ...ITS SAMPLED, PARTLY DIGITAL
  ...BUT SAMPLING TIMES ARE APERIODIC,

Discrete-time and Digital Signal Processing

David G. Messerschmitt

Electrical Engineering and Computer Science

University of California at Berkeley

Discrete-time and digital signal processing are increasingly prevalent, due to many factors. Increasingly, analog signal processing is employed only at the very highest speeds where digital solutions are not available.

Objectives:

- **What are the differences and similarities between discrete-time and continuous-time? How do we convert between the two?**
- **What are the differences and similarities between digital and analog?**
- **What are the advantages and disadvantages of digital and discrete-time?**

Electrical Engineering and Computer Science

University of California at Berkeley

Typical Configuration

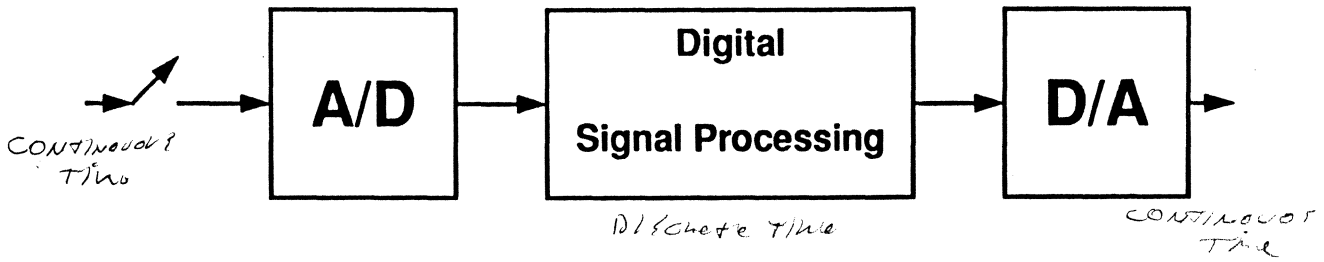

Oversimplified!

Basic elements:

- **Sampler to convert continuous-time to discrete-time**
- **Analog-to-digital converter to convert from analog to digital**
- **Signal processing implemented in the digital and discrete-time domain**
- **Digital-to-analog converter to convert from digital to analog**

Also required are anti-aliasing and reconstruction low-pass filters

Electrical Engineering and Computer Science

University of California at Berkeley

Comparison of Continuous- and Discrete-Time Signals

Different time variables: $x(t)$ **and** $x[n]$

Both can be periodic:

- $x(t+T) = x(t)$
- $x[n+N] = x[n]$

Sinusoids exist (and are very important):

- $x(t) = \cos(\omega_0 t)$
- $x[n] = \cos(\lambda_0 n)$

Continuous-time (but not discrete-time) sinusoids are always periodic:

- $\cos\left(\omega_0 \cdot \left(t + \frac{2\pi}{\omega_0}\right)\right) = \cos(\omega_0 \cdot t)$
- $\cos(\lambda_0 \cdot (n+N)) = \cos(\lambda_0 \cdot n)$ for $\lambda_0 = \frac{2\pi}{N} \cdot k$

Electrical Engineering and Computer Science

University of California at Berkeley

Why Discrete-Time Sinusoids are Not Always Periodic

Represent sinusoid as real part of complex exponential $e^{j\omega_0 t}$ or $e^{j\lambda_0 n}$:

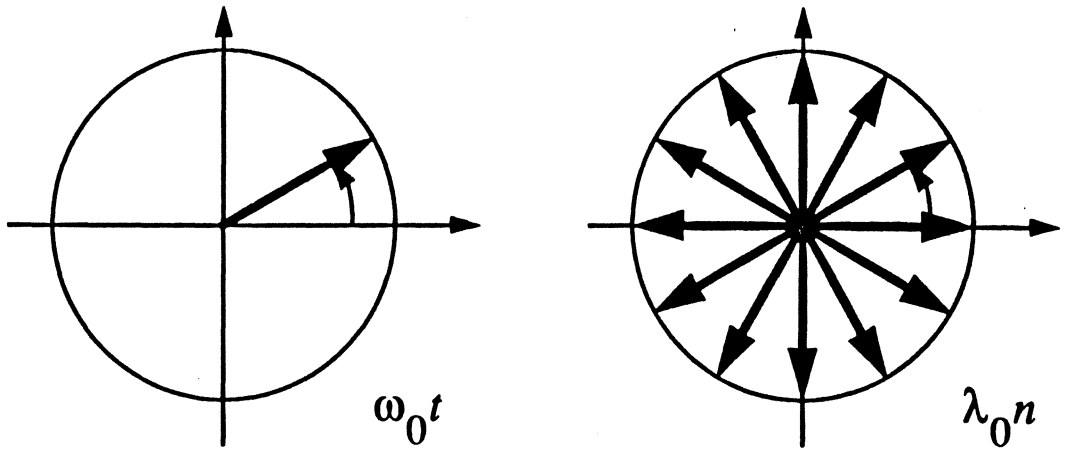

Discrete-time vector moves in discrete steps, only retraces the same points for specific values of λ_0

Electrical Engineering and Computer Science

University of California at Berkeley

Discrete-Time Sinusoids Are Periodic in Frequency

When we increase the frequency by 2π, a discrete-time sinusoid does not change:

- $\cos\left((\lambda_0 + 2\pi) \cdot n\right) = \cos(\lambda_0 \cdot n)$

The interesting range of frequencies is an interval of length 2π

- $\lambda_0 \in [-\pi, \pi]$

This is a form of frequency aliasing

For example, frequency $\lambda_0 = 2\pi$ results in the same samples as frequency $\lambda_0 = 0$ (d.c.)

Electrical Engineering and Computer Science

University of California at Berkeley

Some Examples of Frequency Aliasing

$$\cos(\omega_0 t) \xrightarrow[n \cdot T]{} \cos(\lambda_0 \cdot n)$$

$$\lambda_0 = \omega_0 \cdot T$$

Increasing λ_0 by 2π (ω_0 by $\frac{2\pi}{T}$) results in the same samples!

Sampling is not reversible: many input continuous-time signals can result in the very same samples!

Normal response is to limit input frequencies to half the sampling rate: $|\omega_0| < \frac{\pi}{T}$

Electrical Engineering and Computer Science

University of California at Berkeley

Some Examples of Frequency Aliasing

Several continuous-time waveforms have the same samples:

$$x_1(kT) = x_2(kT) = x_3(kT)$$

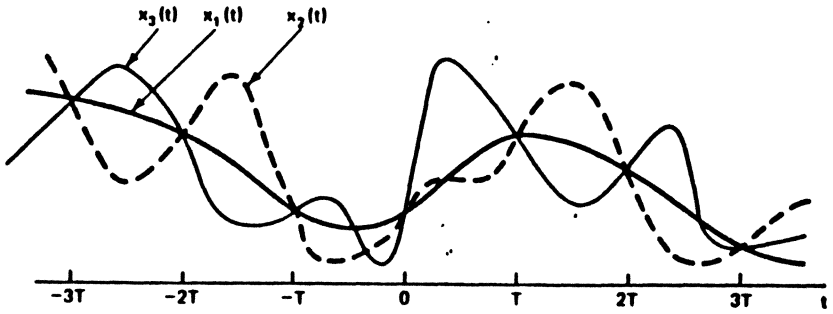

However, there is only one waveform bandlimited to $\frac{\pi}{T}$ with that set of samples (the others all have higher frequency components)

LIMIT TO BW < 1/2 SAMPLE RATE

NYQUIST RATE = 1/2 SAMPLE RATE.

Electrical Engineering and Computer Science

University of California at Berkeley

Some Examples of Frequency Aliasing

Need 3 samples / period for correct Recode

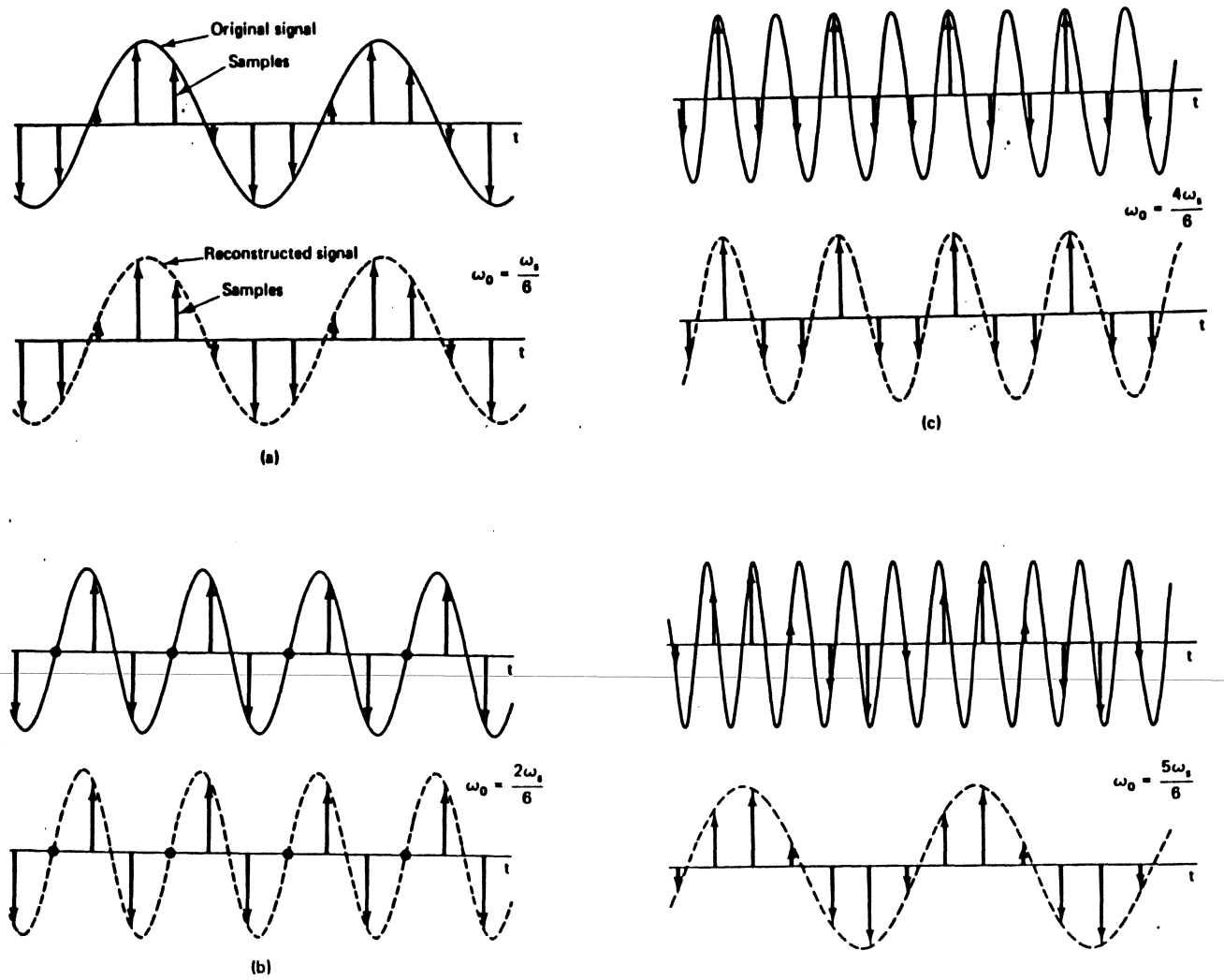

Electrical Engineering and Computer Science

University of California at Berkeley

Digital Filters (LTI Systems)

LINEAR TIME INVARIENT

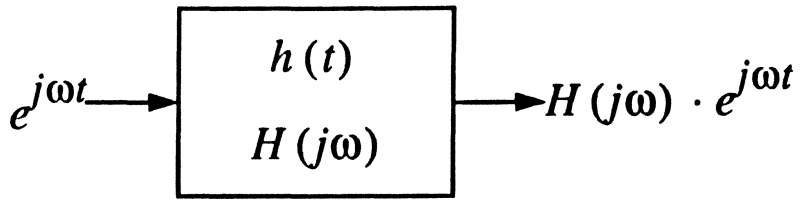

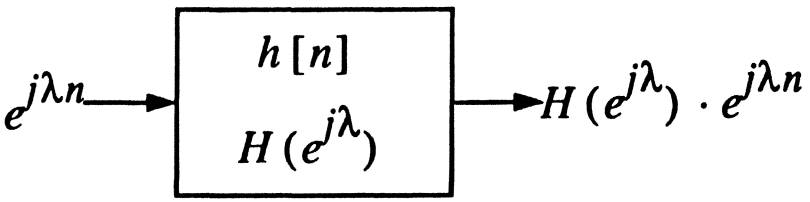

These functions $H(j\omega)$ and $H(e^{j\lambda})$ are known as the frequency response, $h(t)$ and $h[n]$ are the impulse responses

Input complex exponentials of a given frequency result in output complex exponential at the same frequency

Equivalent effect on sinusoids is an amplitude and phase shift

$H(e^{j\lambda})$ is periodic in 2π: Only range $|\lambda| < \pi$ is of interest

Electrical Engineering and Computer Science

University of California at Berkeley

Two Types of Implementable Digital Filters

Finite impulse response (FIR):

- $$y[n] = \sum_{k=0}^{M} b_k \cdot x[n-k]$$

- $$H(e^{j\lambda}) = \sum_{k=0}^{M} b_k \cdot e^{-j\lambda k}$$

Infinite impulse response (IIR):

- $$y[n] = \sum_{k=0}^{M} b_k \cdot x[n-k] - \sum_{k=1}^{N} a_k \cdot y[n-k]$$

- $$H(e^{j\lambda}) = \frac{\sum_{k=0}^{M} b_k \cdot e^{-j\lambda k}}{\sum_{k=0}^{N} a_k \cdot e^{-j\lambda k}}$$

Electrical Engineering and Computer Science

University of California at Berkeley

Continuous-Time Filter Implemented in Discrete Time

Sample, preceded by anti-alias lowpass filter:

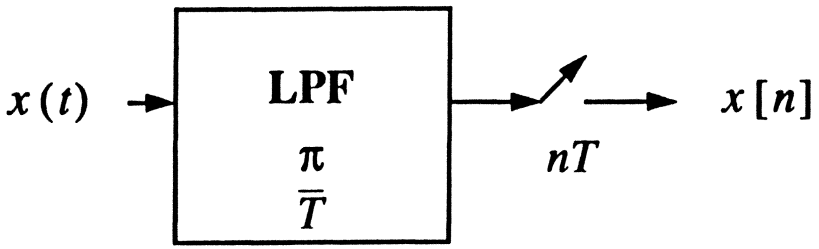

Discrete-time filter:

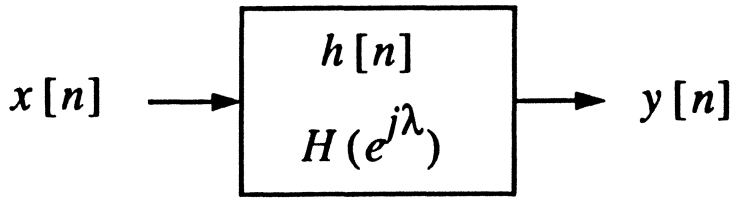

Electrical Engineering and Computer Science

University of California at Berkeley

Continuous-Time Filter Implemented in Discrete Time (Con't)

Reconstruct continuous-time signal:

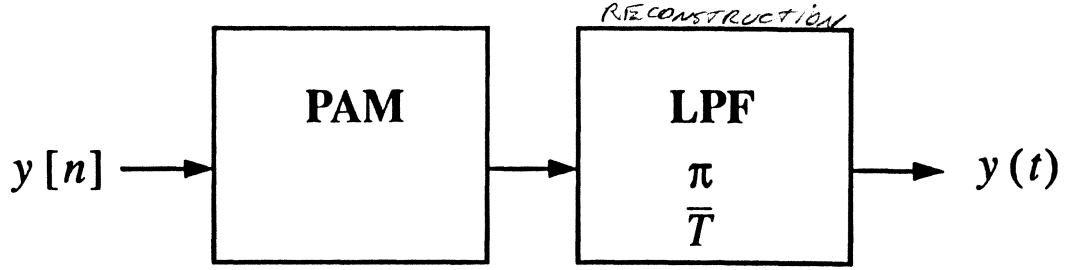

APERTURE "DROOP" CAN BE COMPENSATED WITH GAIN BOOST NEAR NYQUIST RATE.

Pulse-amplitude generator produces sequence of pulses amplitude-modulated by $y[n]$

Lowpass filter reconstructs continuous-time signal by interpolation

Within the bandwidth $\frac{\pi}{T}$, $H(j\omega) = H(e^{j\lambda T})$

Electrical Engineering and Computer Science

University of California at Berkeley

Quantization Distortion

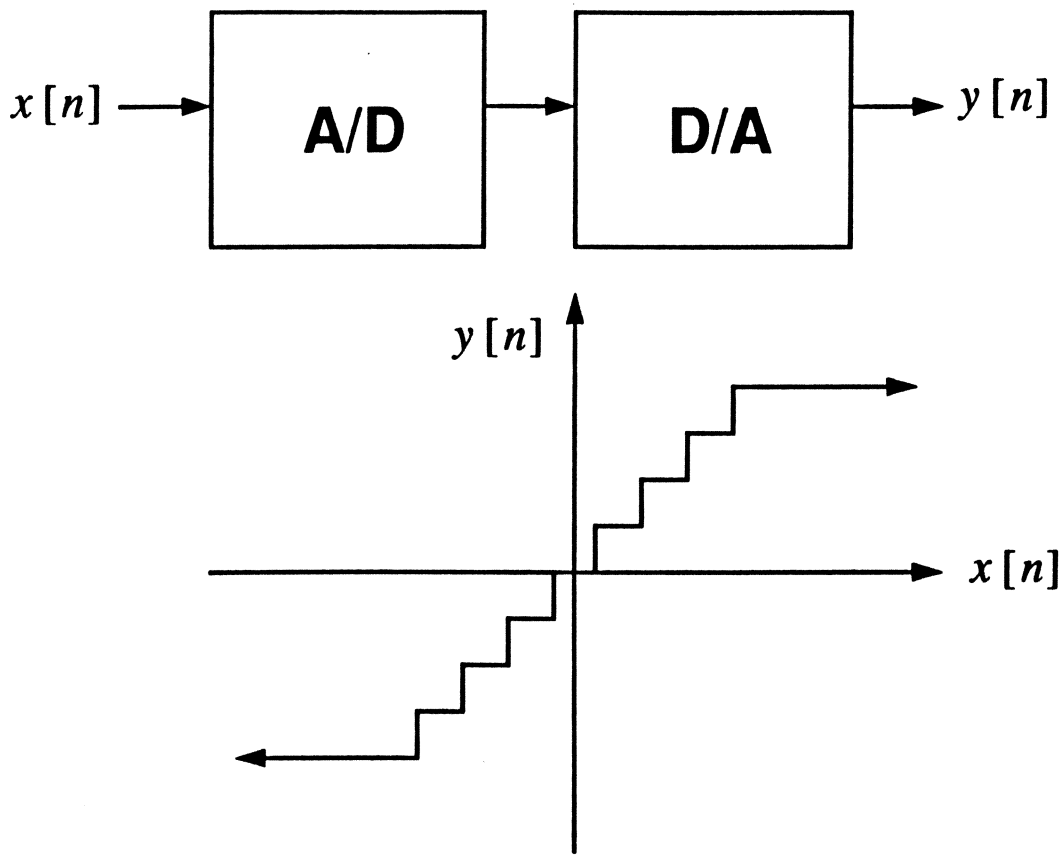

For K bit quantizer, there are 2^K quantization intervals, with overload point at $2^{K-1} \cdot \Delta$ with step-size Δ

Electrical Engineering and Computer Science

University of California at Berkeley

Quantization Distortion is Often Modeled as Additive White Noise

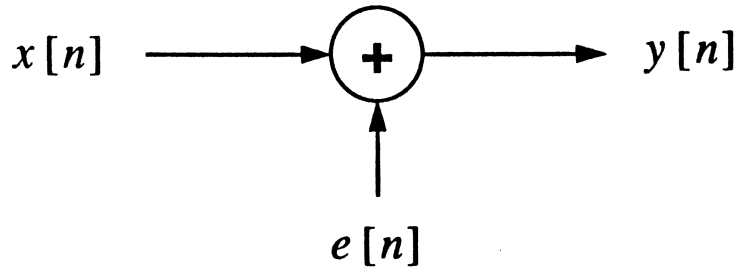

The successive samples of "quantization error" are approximately uncorrelated if the input signal is "random"

For step-size Δ, the quantization error power is approximately $\frac{\Delta^2}{12}$, or easily related to K and the overload point

In contrast to thermal noise, quantization distortion goes away when the signal is absent!

Electrical Engineering and Computer Science

University of California at Berkeley

Effect of Quantization Error

Added quantization noise at A/D converter: a price to be paid for A/D conversion

- Control by adjusting precision (number of bits)

Roundoff errors in internal computations

- Control by adjusting precision of internal arithmetic, which is typically greater than input/output

Overflow problems due to overload point of quantizer

- Limits dynamic range
- Scaling is big issue in fixed point arithmetic
- Floating point arithmetic increases the dynamic range dramatically

Change in filter frequency response due to quantization of coefficients

- Coefficient quantization normally taken account of in filter design

Electrical Engineering and Computer Science

University of California at Berkeley

Some Advantages of Digital Systems

Highest-density IC technologies (based on DRAMs) are primarily digital: poor or non-existent capacitors, etc.

Regenerative property of digital systems is extremely important in storage and transmission applications (avoids the "multiple generation problem" of analog)

Accuracy can be increased arbitrarily by increasing the precision of the arithmetic

Accuracy is forever: no component drift or temperature variations

Digital systems are deterministic: testing and fault detection are much easier

Design abstraction makes complexity easier to manage, reduces designer skill level required (analog designers difficult to find)

- Programmable solutions

Much more complex algorithms are feasible

Electrical Engineering and Computer Science

University of California at Berkeley

Design Abstraction in Digital Systems

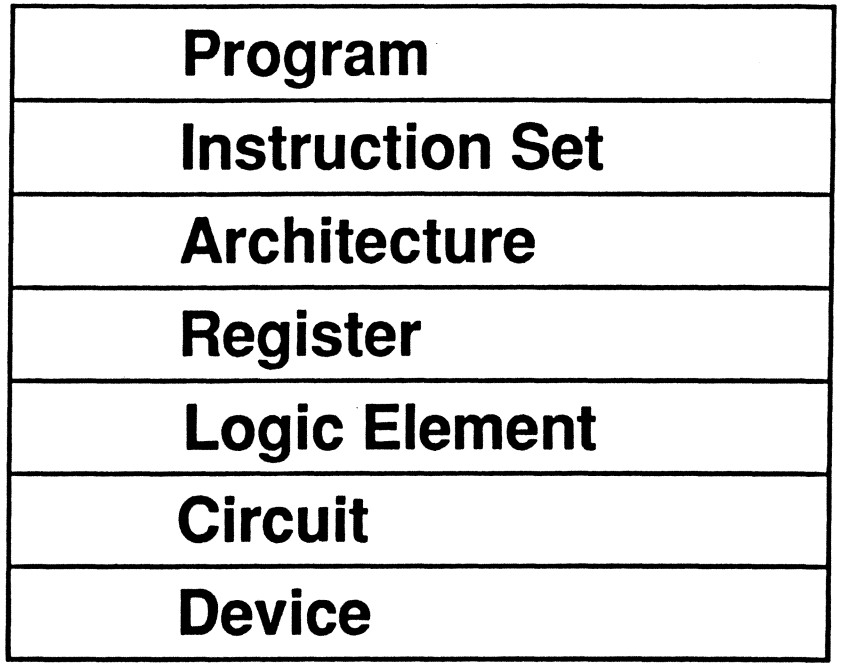

Typically designers are split into three semi-independent groups: logic/circuit/device, instruction set/architecture/register, programmers

Much higher complexity designs become feasible

Electrical Engineering and Computer Science

University of California at Berkeley

Some Disadvantages of Digital Discrete-Time Systems

In a continuous-time world, A/D/A conversion incurs an extra cost

Quantization error is incurred at the A/D converter and internal to the computations (although it can be controlled to whatever extent necessary)

Highest-speed systems must be implemented in analog

- A/D converters and multipliers are typical bottlenecks
- Example: microwave RF

Design effort expended in finite precision issues (quantization, dynamic range)

Synchronization is major issue, particularly as the signal propagation times increase in relation to the clock cycle

Some Examples of DSP Commercial Applications

Digital compact disk

Compressed digital television (NTSC, HDTV)

Digital television receivers

Digital audio broadcast

Digital transmission and switching in telephony

Digital cellular telephone

Voiceband data modems

Compressed video conferencing

Digital Filters

December 14, 1991

Hemant K. Thapar

IBM Corporation
San Jose, California
Telephone 284-0308

TOPICS

- Why Consider Digital Filters
- Filter Design Problem
- Digital Filter Design Tools
- Digital Filter Design Methods
- Applications

1. WHY CONSIDER DIGITAL FILTERS

- Component tolerances (Accuracy)
- End-of-life component tolerances (Reproducibility)
- Implementation of Time-Varying Filters

  Presettable filters

  Adaptive filters
- Size
- Power Dissipation
- Control of transient response

Analog and Digital Components

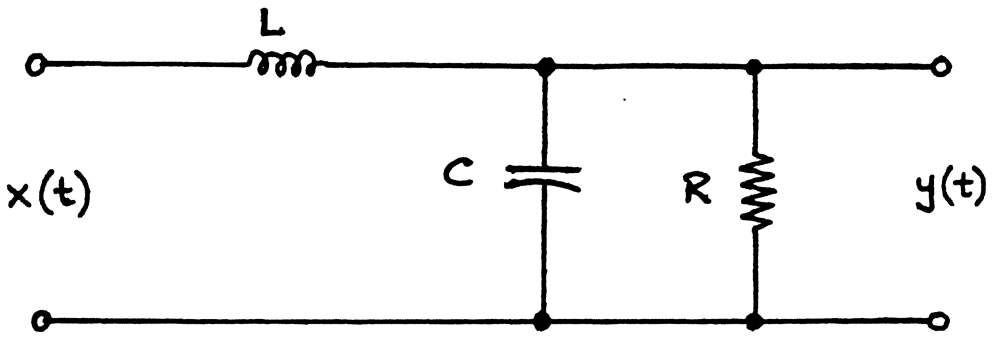

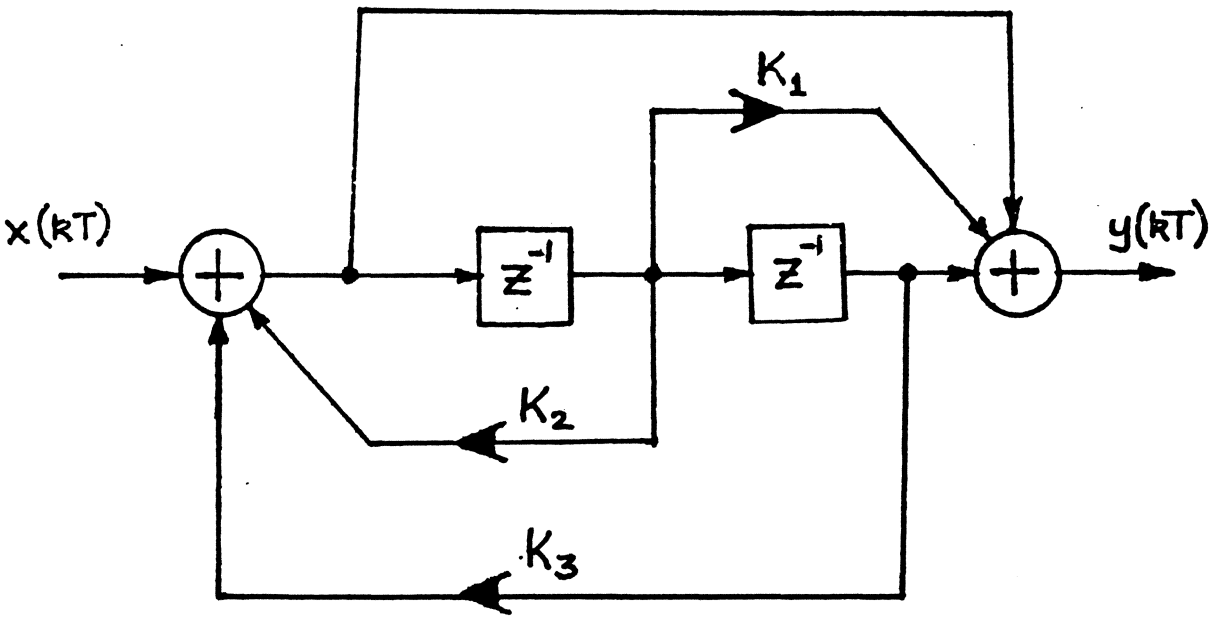

A Second-order Bandpass Filter

TOPICS

- Why Consider Digital Filters
- Filter Design Problem
- Digital Filter Design Tools
- Digital Filter Design Methods
- Applications

2. FILTER DESIGN PROBLEM

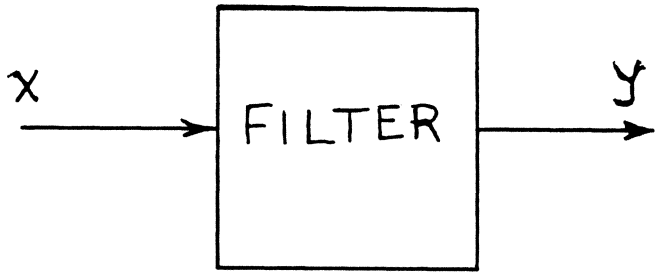

Motivation

- Improve quality of the output signal:

  Remove noise, interference, and distortion.

- Process or extract information from the input:

  Estimation and prediction.

- Some notion of frequency discrimination is involved:

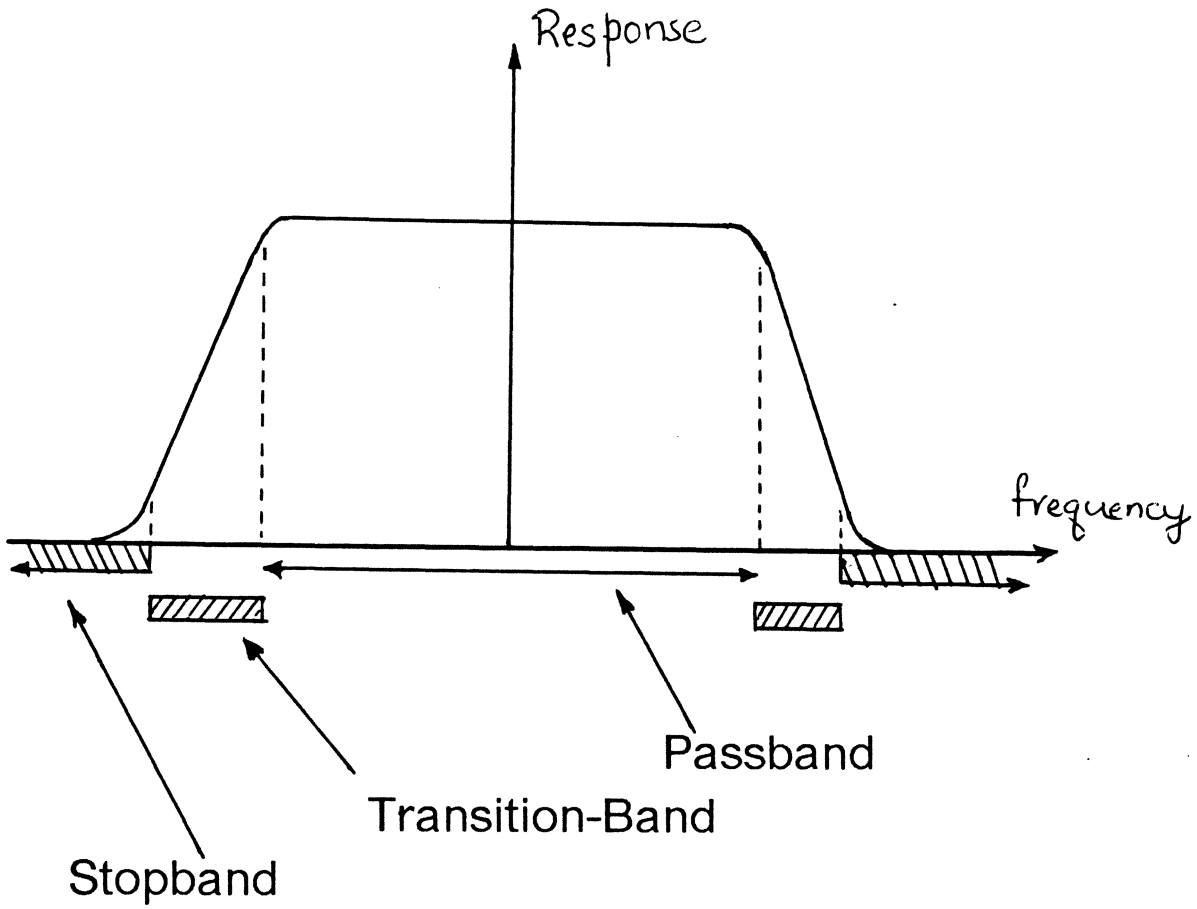

- Linkage between time-domain and frequency-domain behavior:

$$y(n) = \frac{1}{2\pi} \int_{-\pi}^{\pi} Y(\omega) d\omega$$

Analog and Digital Frequencies

- Sampling of the analog signal

$$x_a(t) = A\cos(\Omega t + \theta)$$

produces

$$x(kT) = A\cos(\Omega kT + \theta) \triangleq A\cos(\omega k + \theta)$$

- Ω rad/ sec $\Leftrightarrow$ $\omega = \Omega T$ *rad/sample*
- Relationship between analog and digital frequencies:

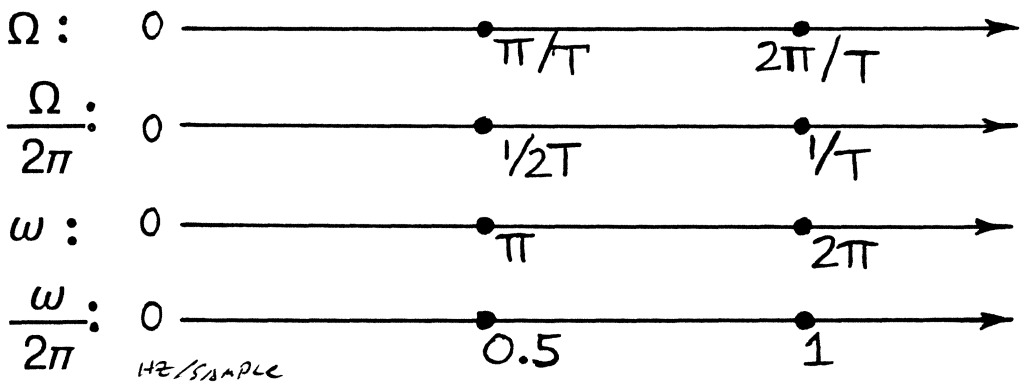

- When the Nyquist sampling theorem is satisfied, the digital frequency is always less than π radians; that is

$$\omega = \Omega T < \pi$$

TOPICS

- Why Consider Digital Filters
- Filter Design Problem
- Digital Filter Design Tools
- Digital Filter Design Methods
- Applications

3. Filter Design Tools

- Restrict the allowed structures to:

  Non-Recursive Filters

  Recursive Filters

Non-Recursive Filters

- Output is formed by linearly combining a sequence of inputs:

$$y_k = \sum_{i=-N}^{N} a_i x_{k-i}$$

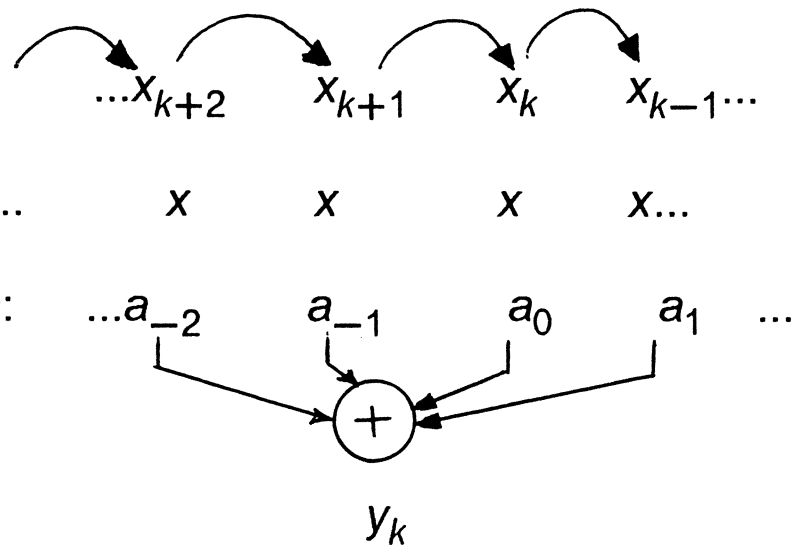

Example: $a_{-1} = 0.8, \quad a_0 = 1, \quad a_1 = 0.6$

$$\Rightarrow \quad y_k = 0.8x_{k+1} + x_k + 0.6x_{k-1}$$

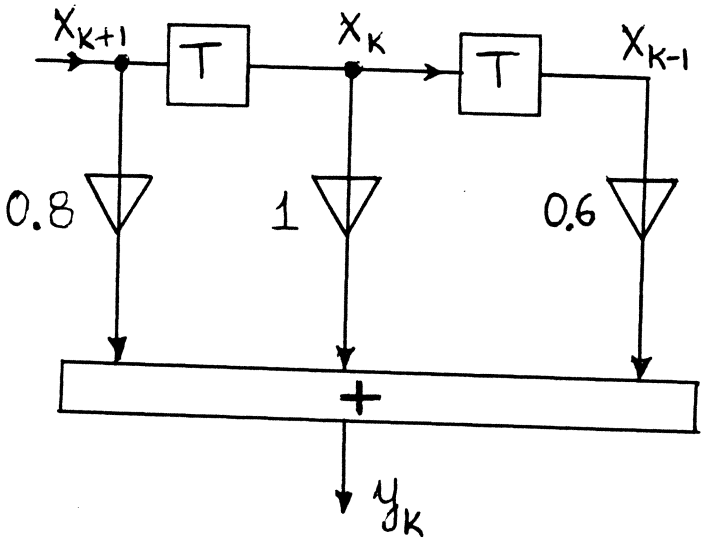

Recursive Filters

UNSTABLE - SINUSOIDAL OUTPUT UNDESIRABLE

- Output is formed by linearly combining sequences of inputs and previous outputs:

$$y_k = \sum_{i=0}^{N} a_i x_{k-i} + \sum_{l=1}^{M} b_l y_{k-l}$$

- Output at time k depends upon the previous outputs. Therefore, initial conditions must be known before the output due to the first input can be computed.

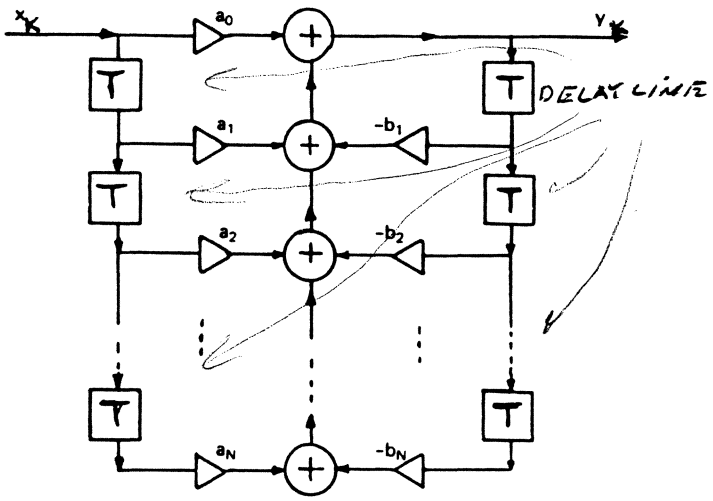

CAN NOT BE OPTIMIZED.

Unit Pulse Response

- Response for a unit pulse input, defined as:

$$x_k = \begin{cases} 1 & , k = 0 \\ 0, & otherwise \end{cases}$$

Nonrecursive Filters: VERY STABLE, CAN BE OPTIMIZED

$$h_k \triangleq y_k = \sum_{i=-N}^{N} a_i x_{k-i}$$

$$= a_k$$

- The unit pulse response is a finite sequence of (2N + 1) terms. Such filters are, therefore, often referred to as FINITE IMPULSE RESPONSE (FIR) filters.

Recursive Filters:

$$h_k \triangleq y_k = \sum_{i=0}^{N} a_i x_{k-i} + \sum_{l=1}^{M} b_l y_{k-l}$$

- Even though there are a finite number of a_ks, the second term can continue to generate an output long after the first term is zero. Such filters are, therefore, often referred to as INFINITE IMPULSE RESPONSE (IIR) filters.

Properties

- Homogeneity and Superposition:

$$\text{if} \quad x_k \Rightarrow y_k \quad \text{and} \quad s_k \Rightarrow r_k$$

$$\text{then} \quad fx_k + gs_k \Rightarrow fy_k + gr_k$$

- Shift-invariance:

$$\text{if} \quad x_k \Rightarrow y_k \quad \text{then} \quad x_{k-l} \Rightarrow y_{k-l}$$

- Filters that admit homogeneity, superposition, and shift-invariance are referred to as linear, time-invariant (LTI) filters.
- Input-Output of such filters can be defined by the discrete-time convolution:

$$y_k = \sum_{i=-\infty}^{\infty} x_i h_{k-i}$$

Structures

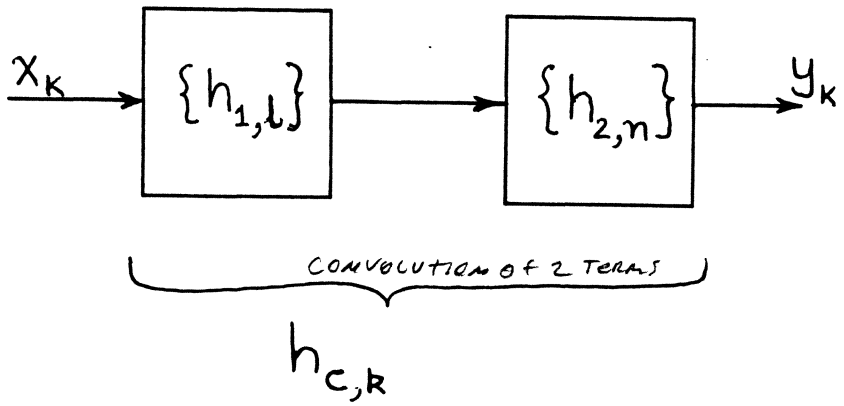

- Cascade: $h_{C,k} = \sum_{l=-\infty}^{\infty} h_{1,l} h_{2,k-l}$

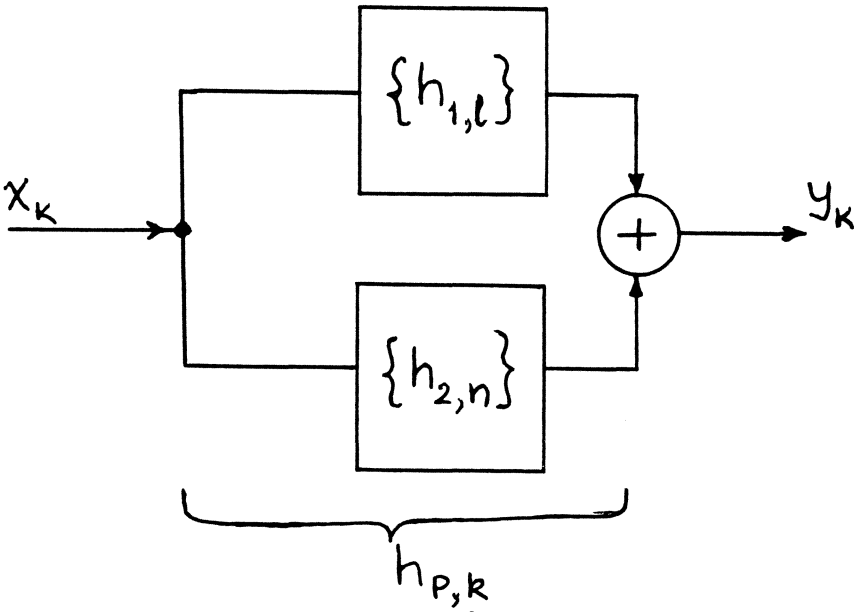

- Parallel: $h_{P,k} = h_{1,k} + h_{2,k}$

Eigenfunctions

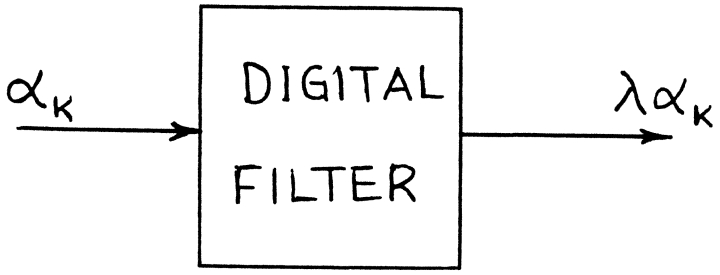

- Def: α_k is an eigenfunction of the digital filter iff the application of α_k produces the scaled output $\lambda\alpha_k$. λ is referred to as the eigenvalue.

$$\lambda\alpha_q = \sum_{j=-\infty}^{\infty} h_q - \alpha_{k=i}$$

Eigenfunction 1:

$$a_k = \exp(j\omega k) = \cos(\omega k) + j \sin(\omega k)$$

produces an output

$$\exp(j\omega k)\left[\sum_{l=-\infty}^{\infty} h_l e^{-j\omega l}\right]$$

- $H(\omega) = \sum_{l=-\infty}^{\infty} h_l e^{-j\omega l}$ is referred to as the frequency response of the digital filter. Note that h_l uniquely determines $H(\omega)$.
- H(ω) is, in general, complex, and may be written as

  $H(\omega) = | H(\omega) | e^{\phi(\omega)}$

  Then, if the input is $\cos \omega k$, the output is given by $| H(\omega) | \cos(\omega k + \phi)$.

Eigenfunction 2:

$$a_k = z^k$$

produces an output

$$z^k \left[\sum_{l=-\infty}^{\infty} h_l z^{-l} \right]$$

- $H(z) = \sum_{l=-\infty}^{\infty} h_l z^{-l}$ is referred to as the transfer function of the digital filter. Note that h_l uniquely determines $H(z)$.

- $Y(z) = H(z) X(z)$

  $Y(z) = \cdots + y_0 + y_1 z^{-1} + y_2 z^{-2} + y_3 z^{-3} + \cdots$

  $y(k) = \{ \cdots y_0 \; y_1 \; y_2 \; y_3 \cdots \}$

Z-transform and Frequency Response

- $H(\omega) = H(z)\big|_{z=\exp(-j\omega)} = \sum_{l=-\infty}^{\infty} h_l e^{-j\omega l}$
- Geometrical interpretation

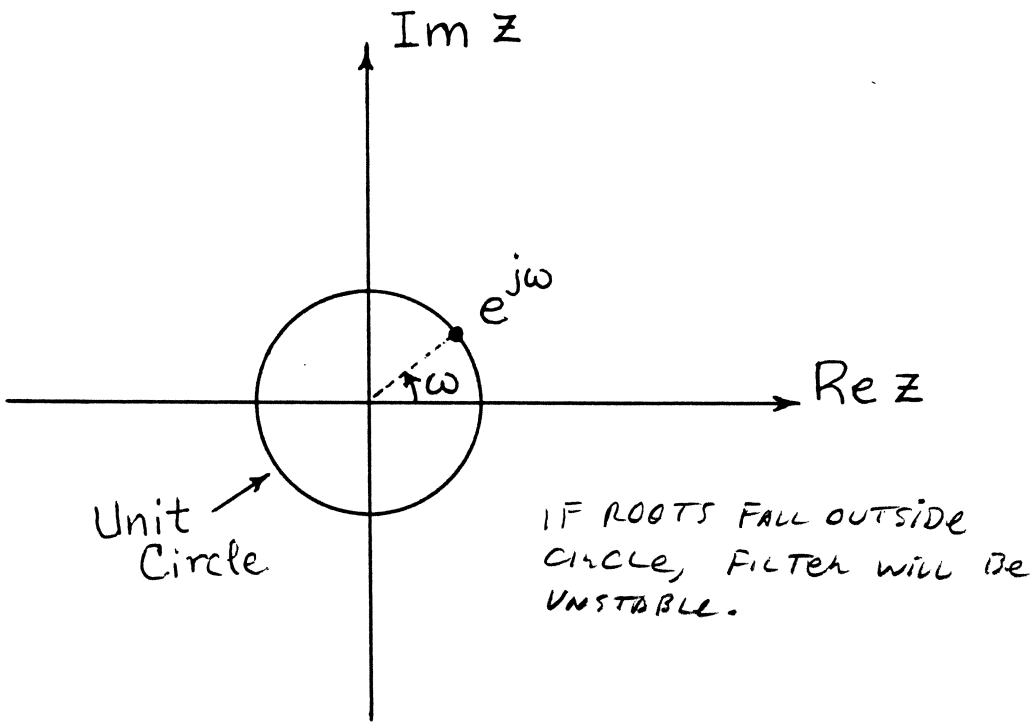

- Frequency response for digital filters is periodic in 2π.

An Example

$h_{-1} = 1, \quad h_0 = 2, \quad h_1 = 1$

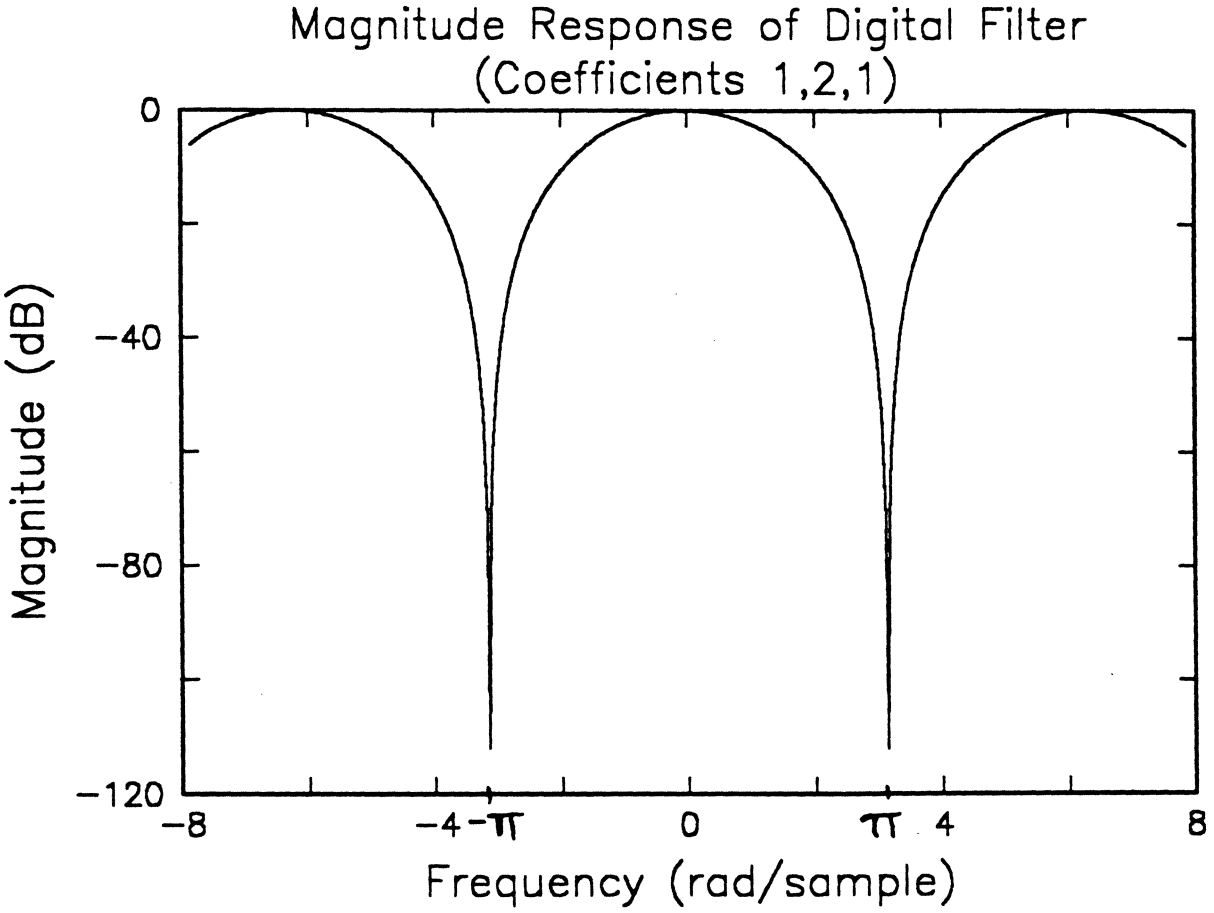

Frequency Response of FIR and IIR Filters

- FIR Filters

$$H(\omega) = \sum_{l=-N}^{N} a_l e^{-j\omega l}$$

- Recursive Filters

$$H(\omega) = \frac{\sum_{i=0}^{N} a_i e^{-j\omega i}}{1 - \sum_{m=1}^{M} b_m e^{-j\omega m}}$$

Cascade and Parallel Forms

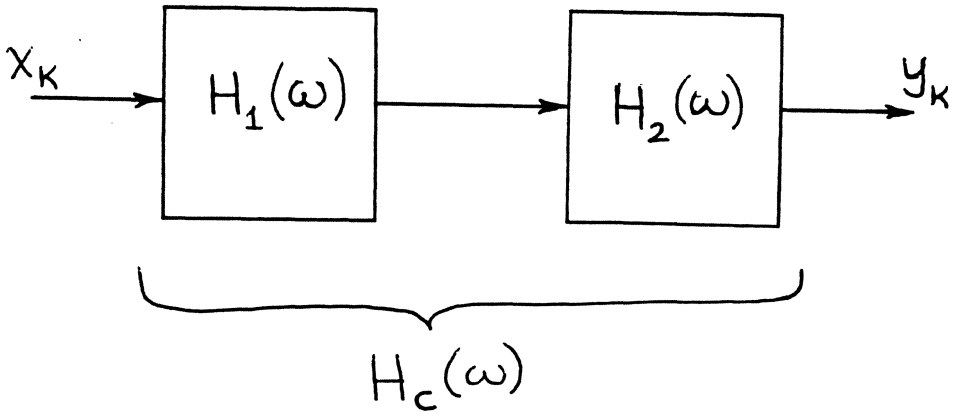

- Cascade: $H_C(\omega) = H_1(\omega)H_2(\omega)$

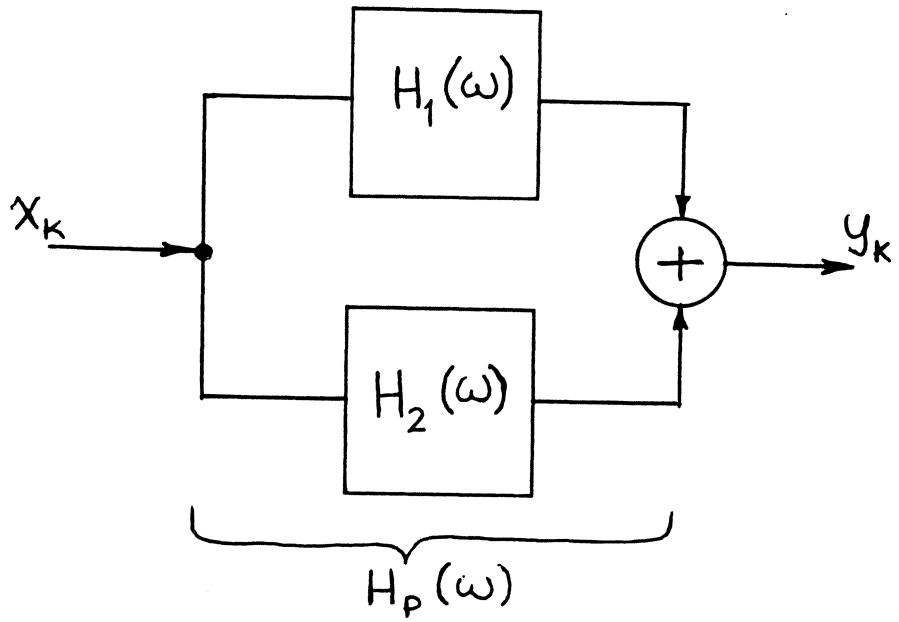

- Parallel: $H_P(\omega) = H_1(\omega) + H_2(\omega)$

COMPLEX NUMBERS — TAKE CARE IF CIRCUIT IS TO WORK.

TOPICS

- Why Consider Digital Filters
- Filter Design Problem
- Digital Filter Design Tools
- Digital Filter Design Methods
- Applications

4. Filter Design Methods

Fourier Series

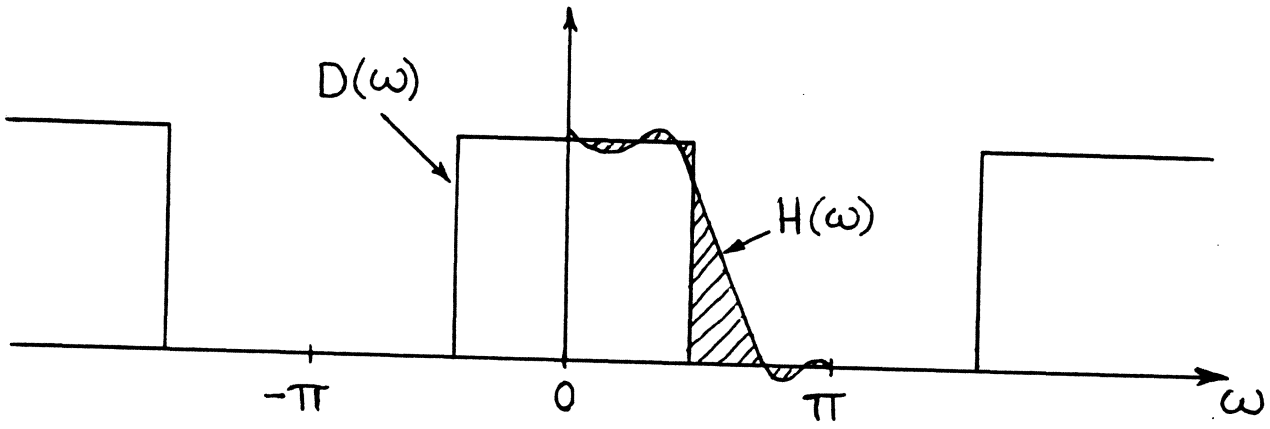

Error: $E(\omega) = D(\omega) - H(\omega)$

Squared – error: $\varepsilon = \int_{-\pi}^{\pi} |E(\omega)|^2 d\omega$

$$\min \varepsilon \Rightarrow h_k = \frac{1}{2\pi} \int_{-\pi}^{\pi} D(\omega) e^{j\omega k} d\omega$$

- The h_k sequence generates the smallest integral squared-error than any other response.
- Each h_k is computed independently; value of one term does not affect the other.
- Set $a_k = h_k$.
- Truncation error is given by:

$$\varepsilon_T = \int_{-\pi}^{\pi} | D(\omega) |^2 d\omega - 2\pi \sum_{i=-N}^{N} | a_i |^2$$

An Example

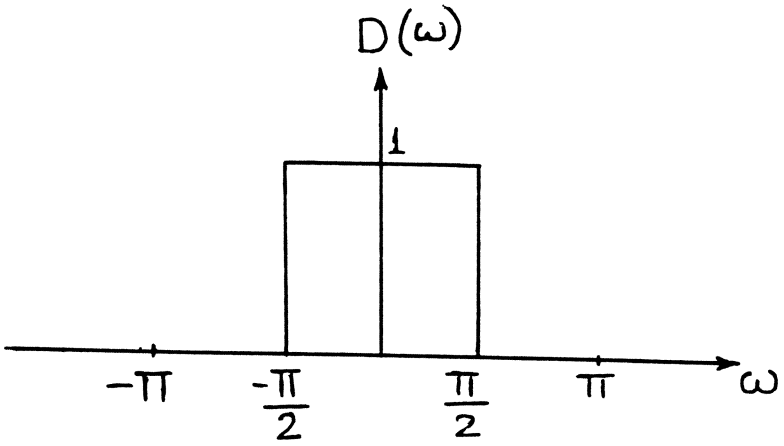

$$h_k = \frac{1}{\pi k} \sin\left(\frac{\pi k}{2}\right), \quad h_0 = 0.5$$

Frequency Response as a function of N

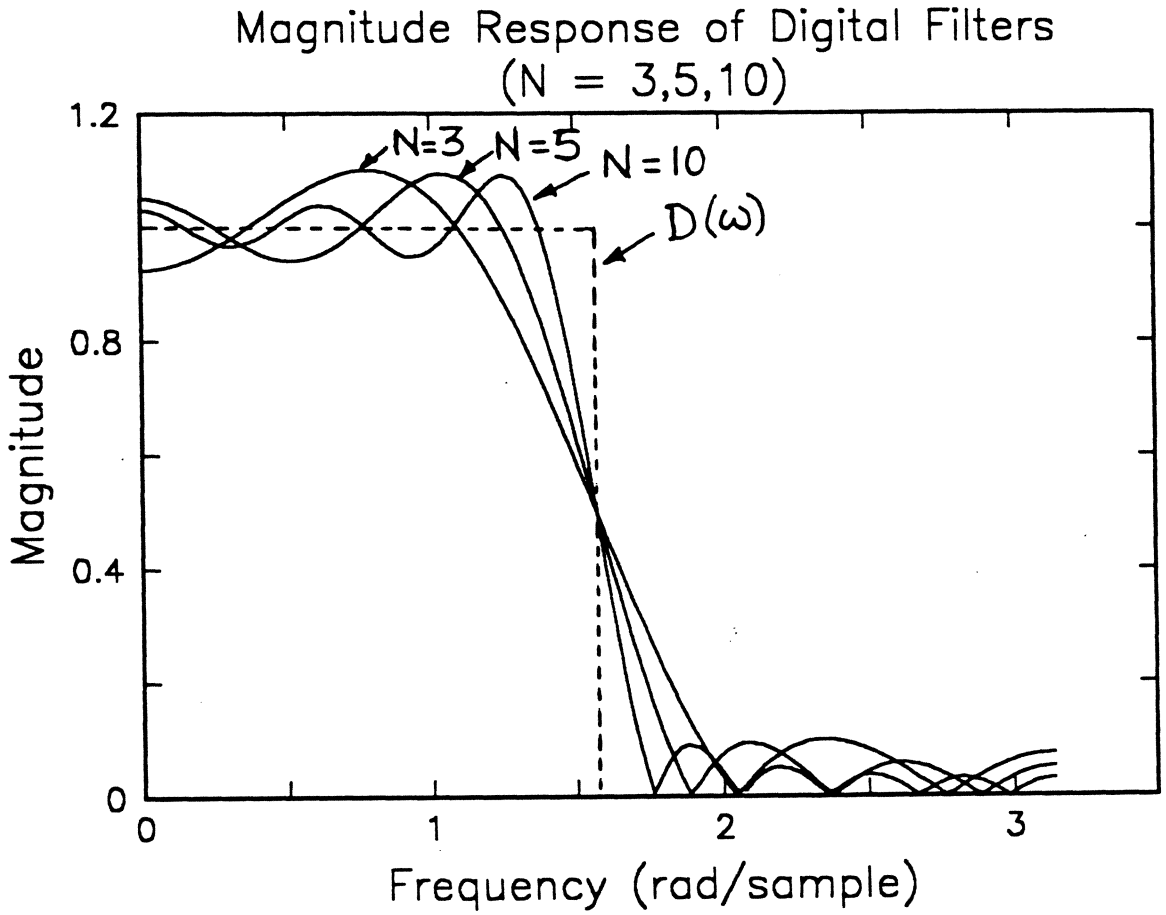

Frequency Response as a function of N

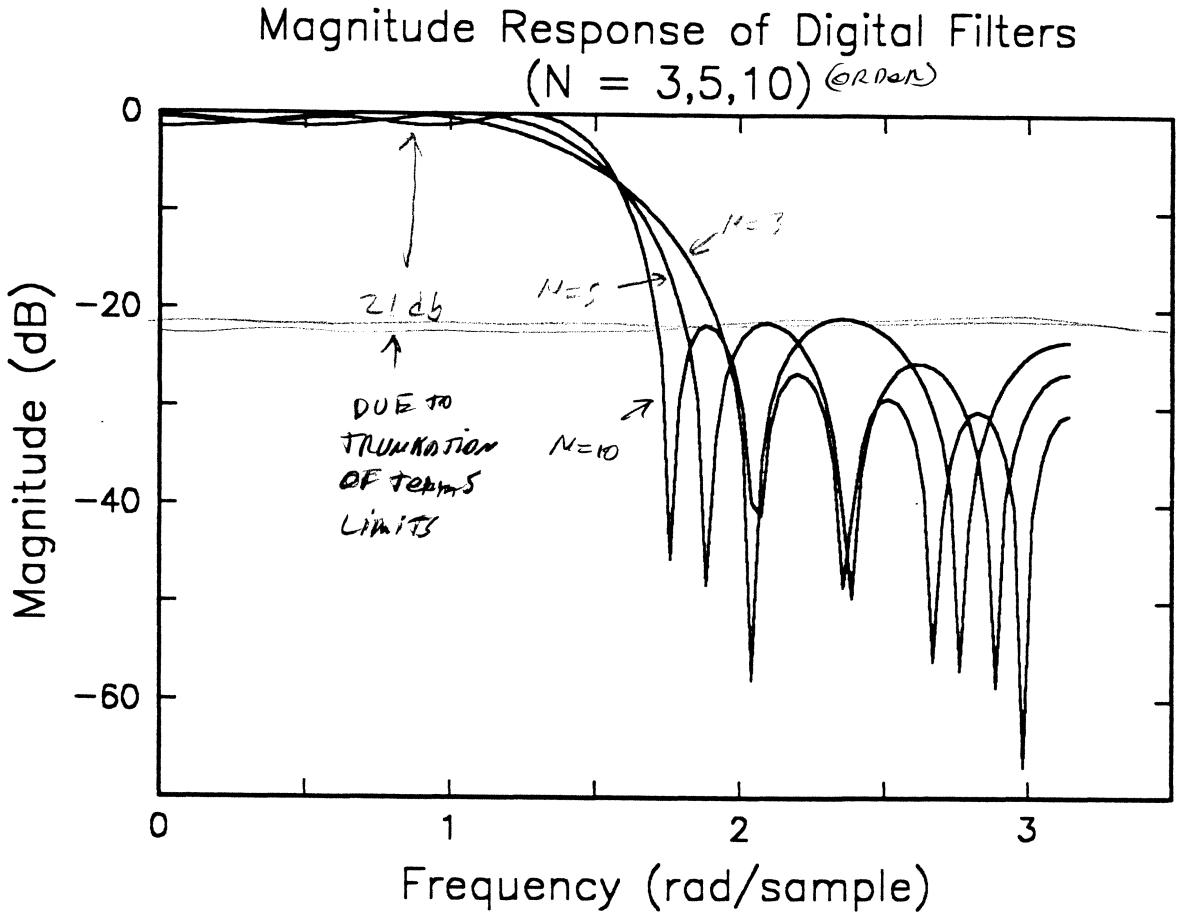

Windowing

- Rectangular Window

Low-pass Filter Coefficients based on the Fourier Series Method

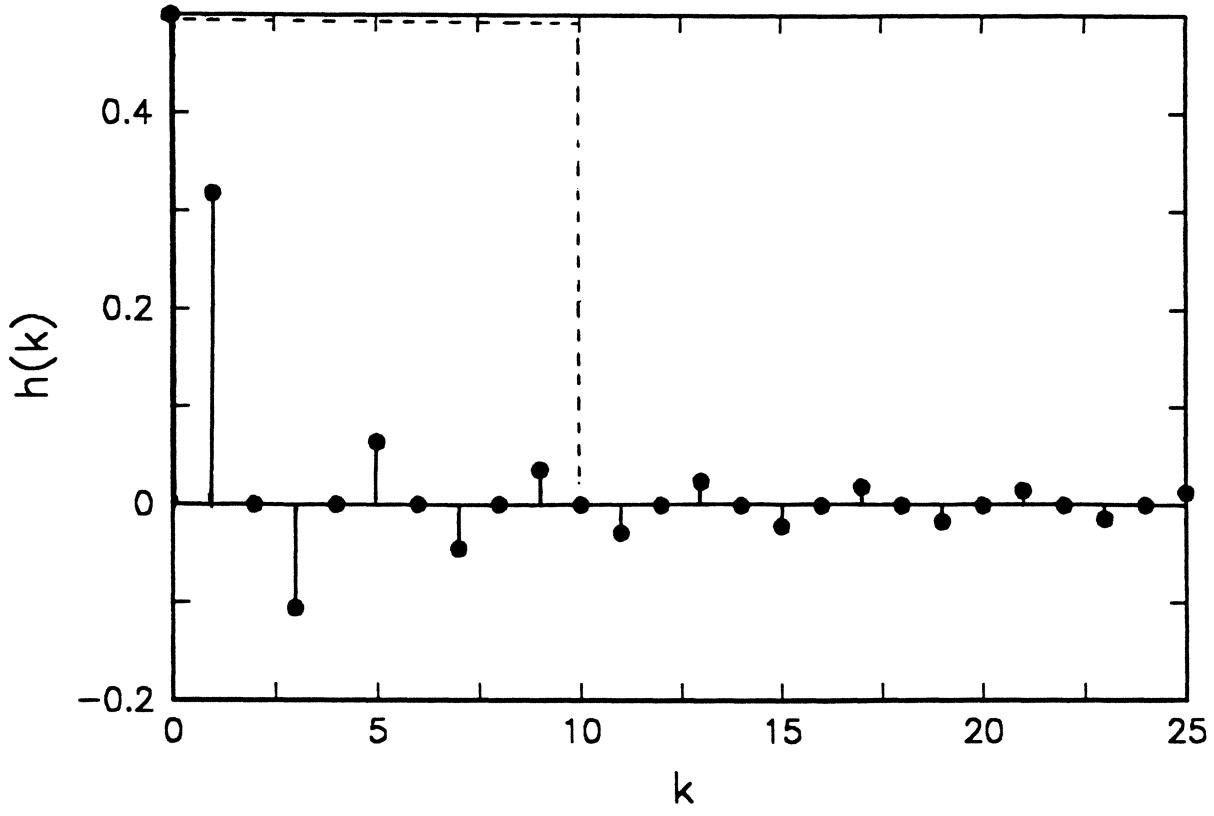

- Other windowing functions are used to achieve more desirable control of passband ripple and/or stopband attenuation.

$$a_K = w_K \, h_K$$

↑ WINDOW FUNCTION COEF.

Commonly-used Windowing Functions

- Rectangular:

$$w(k) = 1$$

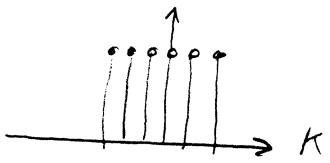

- Triangular:

$$w(k) = 1 - \frac{|k|}{M+1}, \quad M = 2N+2$$

- Hann:

$$w(k) = \frac{1}{2}\left(1 + \cos\frac{2\pi k}{M}\right), \quad M = 2N+2$$

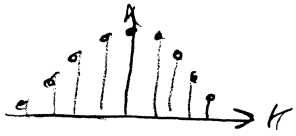

- Hamming:

$$w(k) = 0.54 + 0.46\cos\frac{2\pi k}{M}, \quad M = 2N+2$$

- Blackman:

$$w(k) = 0.42 + 0.5\cos\frac{2\pi k}{M} + 0.08\cos\frac{4\pi k}{M}, \quad M = 2N+2$$

- Kaiser:

$$w(k) = \begin{cases} I_0\left[\beta\sqrt{1-\left(\frac{k}{(2N+1)/2}\right)^2}\right] \Big/ I_0(\beta) & ; -N \le k \le N \\ 0 & , \text{otherwise} \end{cases}$$

where

$$I_0(z) = 1 + \sum_{m=1}^{\infty}\left[\frac{(z/2)^m}{m!}\right]$$

Filter Transformations

Low-pass	$h_{LP}(k)$

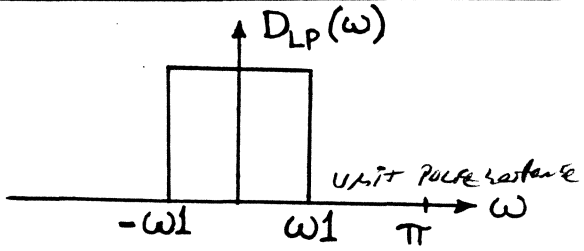

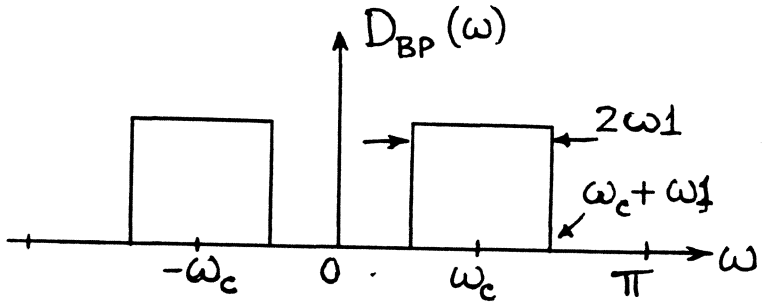

- Band-pass $2h_{LP}(k)\cos(\omega_c k)$

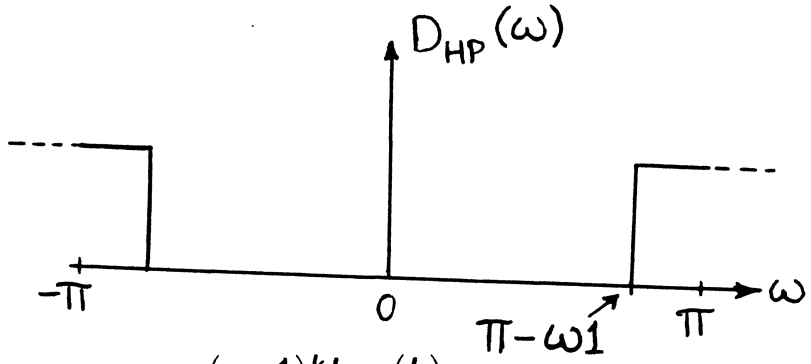

- High-pass $(-1)^k h_{LP}(k)$

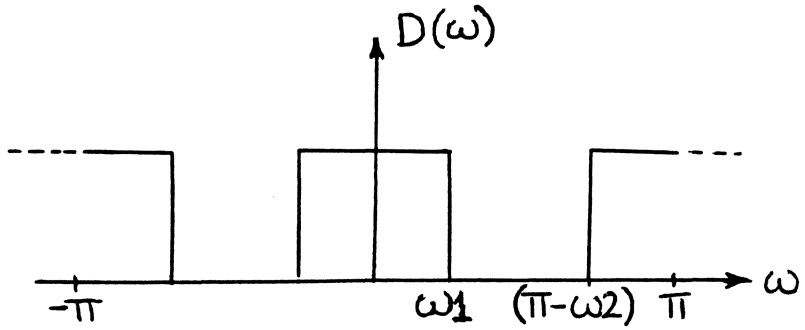

- Notch $h_{LP,\omega 1}(k) + (-1)^k h_{LP,\pi-\omega 2}$

An Example

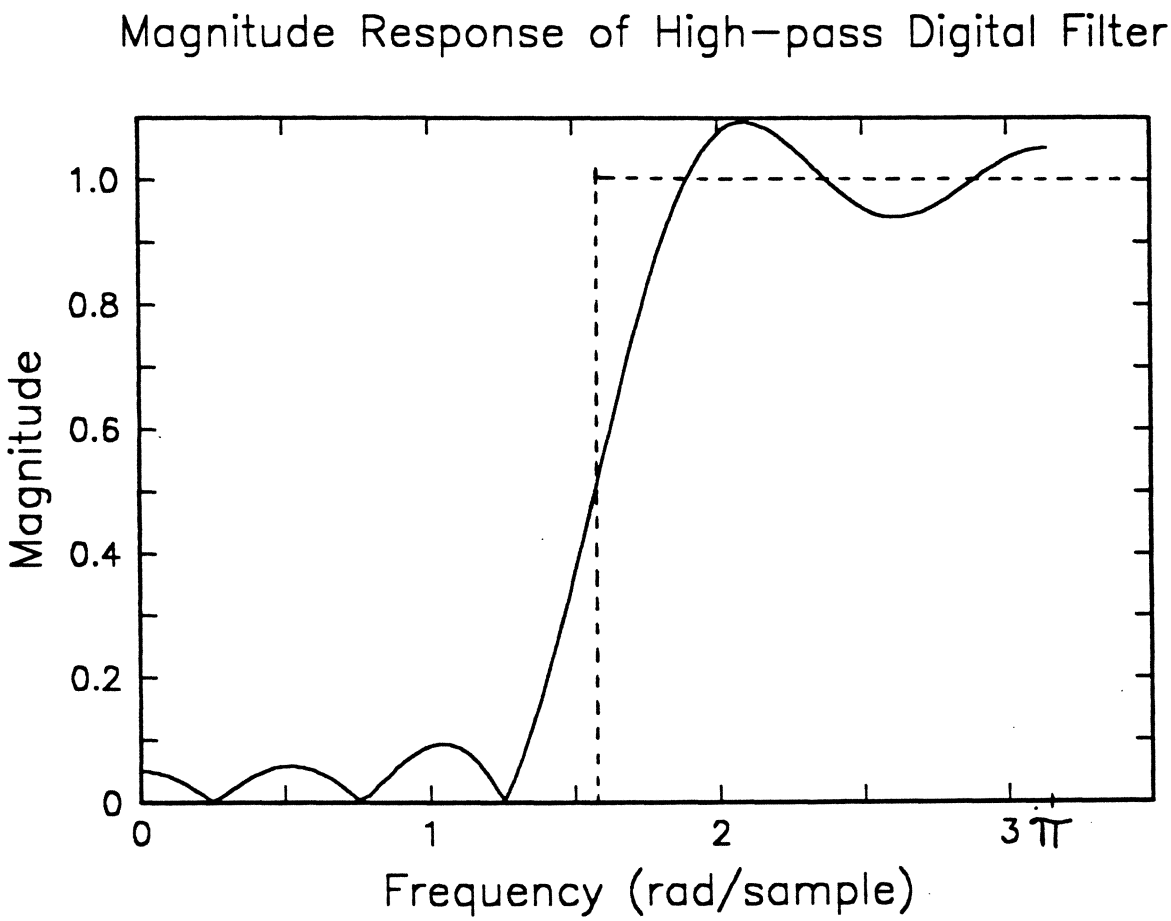

Low-pass Coefficients: 0.064 1.6E-17 -0.11 -1.6E-17 0.32 0.5 0.32 -1.6E-17 -0.11 1.6E-17 0.064
High-pass Coefficients: -0.064 1.6E-17 0.11 -1.6E-17 -0.32 0.5 -0.32 -1.6E-17 0.11 1.6E-17 -0.064

Time-Domain Design Method

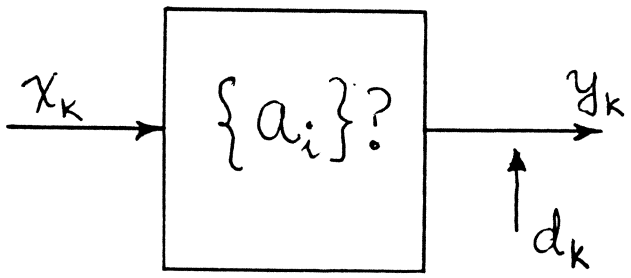

- Input sequence, x_k, and the desired output sequence, d_k are known; the problem is to determine a_k.
- Define

$$\underline{a} = [\ a_{-N}\ \ a_{-N+1}\ \ \dots\ \ a_N]$$

$$\underline{d} = [\ d_0\ \ d_1\ \ \dots\ \ d_p],, \qquad p \geq 2N+1$$

$$\underline{x} = [\ x_{-N}\ \ x_{-N+1}\ \ \dots\ \ x_{p+N}],.$$

- Set-up p + 1 equations of the form

$$\begin{bmatrix} x_{-N} & x_{-N+1} & \cdots & x_N \\ x_{-N+1} & x_{-N+2} & \cdots & x_{N+1} \\ \vdots & & & \\ x_{p-N} & x_{p-N+1} & \cdots & x_{p+N} \end{bmatrix} \begin{bmatrix} a_{-N} \\ a_{-N+1} \\ \vdots \\ a_N \end{bmatrix} = \begin{bmatrix} d_0 \\ d_1 \\ d_2 \\ \vdots \\ d_p \end{bmatrix}$$

$$\triangleq \underset{\sim}{H} \qquad \underline{a}^T \qquad \underline{d}^T$$

- Use least-squares solution to the over-determined system of equations to obtain

$$\underline{a}_{OPT}{}^{T} = (\underset{\sim}{H}^{T}\underset{\sim}{H})^{-1}\underset{\sim}{H}^{T}\underline{d}^{T}$$

- The above equation is of the form

$$\underline{a}_{OPT} = \underset{\sim}{\Phi}^{-1}\underline{\xi}$$

Adaptive Filtering

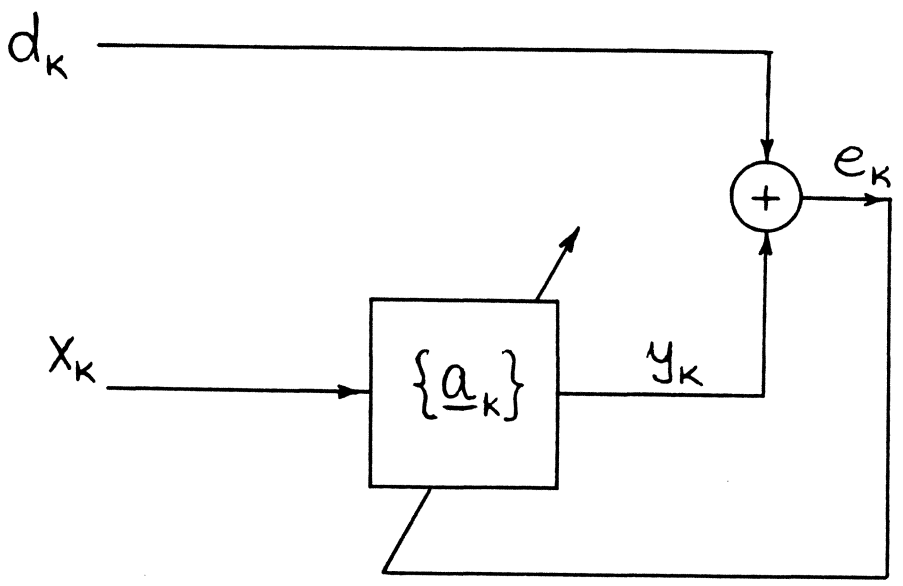

Application	x	d
System Identification	Known Data	Output Signal
Equalization	Distorted Signal	"Known" Data
Prediction	Past Input	Present Input

Commonly-used Approach

- Minimize the mean-squared error between the desired output, d, and a linear combination of the input, x; that, is:

$$E[e_k^2] = E[(d_k - y_k)^2] = E[(d_k - \sum_i a_i x_{k-i})^2]$$

- The above error criterion defines a convex surface for the mean-squared error as a function of the tap weights:

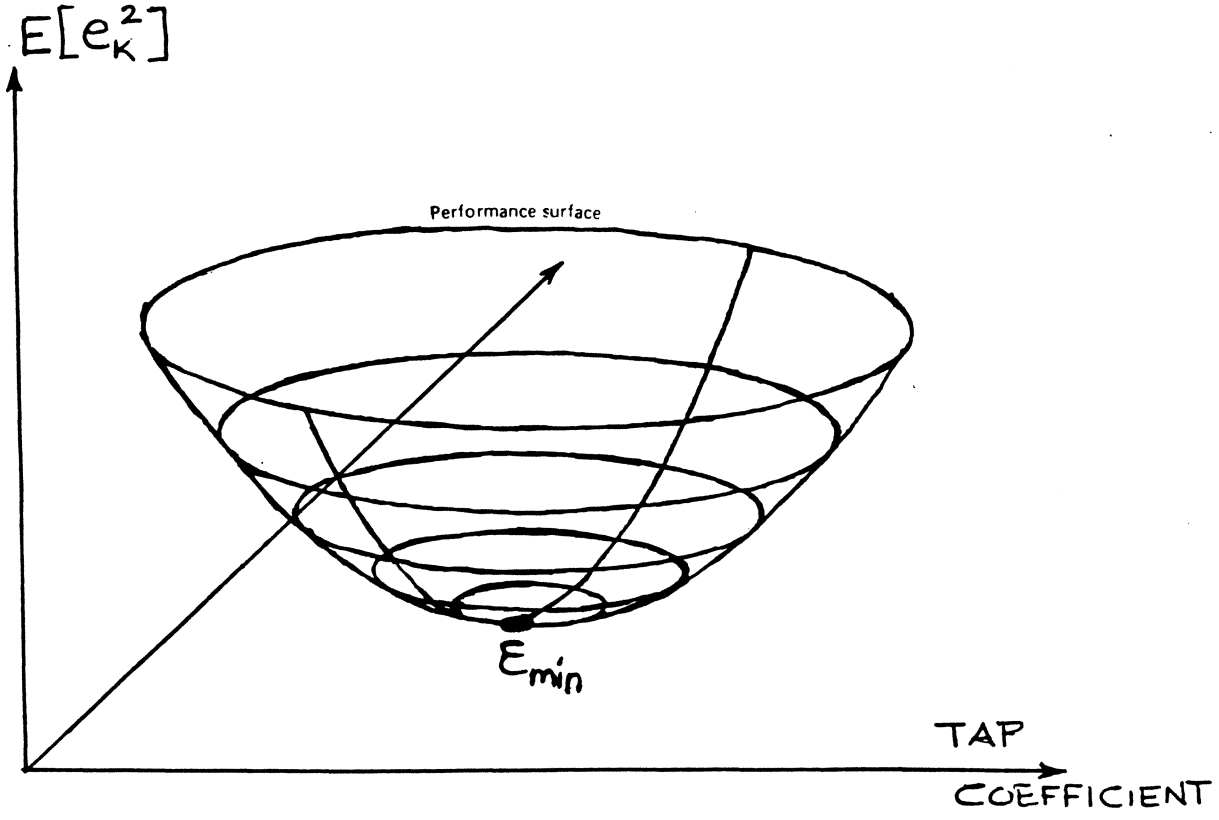

- The adaptive filter starts with an initial guess on the coefficients, $\underline{a}_0$, and progressively moves down the well using:

$$\underline{a}_k = \underline{a}_{k-1} - \beta \nabla_{\underline{a}_k} E[e_k^2]$$

- In practice, the gradient of the instantaneous squared-error is substituted for the mean squared-error, resulting in the following adaptive algorithm (most commonly referred to as the LMS algorithm):

$$\underline{a}_k = \underline{a}_{k-1} + 2\beta e_k \underline{x}_k$$

- The LMS algorithm is the most commonly-used algorithm in real-time adaptive filtering.

TOPICS

- Why Consider Digital Filters
- Filter Design Problem
- Digital Filter Design Tools
- Digital Filter Design Methods
- Applications

5. Applications in Digital Storage

- Recording Channel Identification
- Equalization
- Timing and Gain Control
- Digital servo

Recording Channel Identification

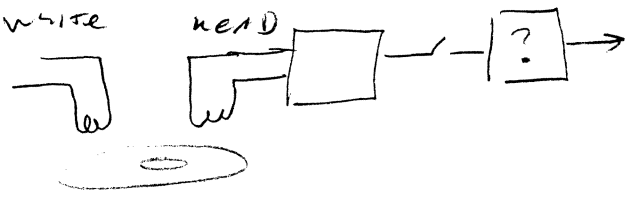

- Input Sequence

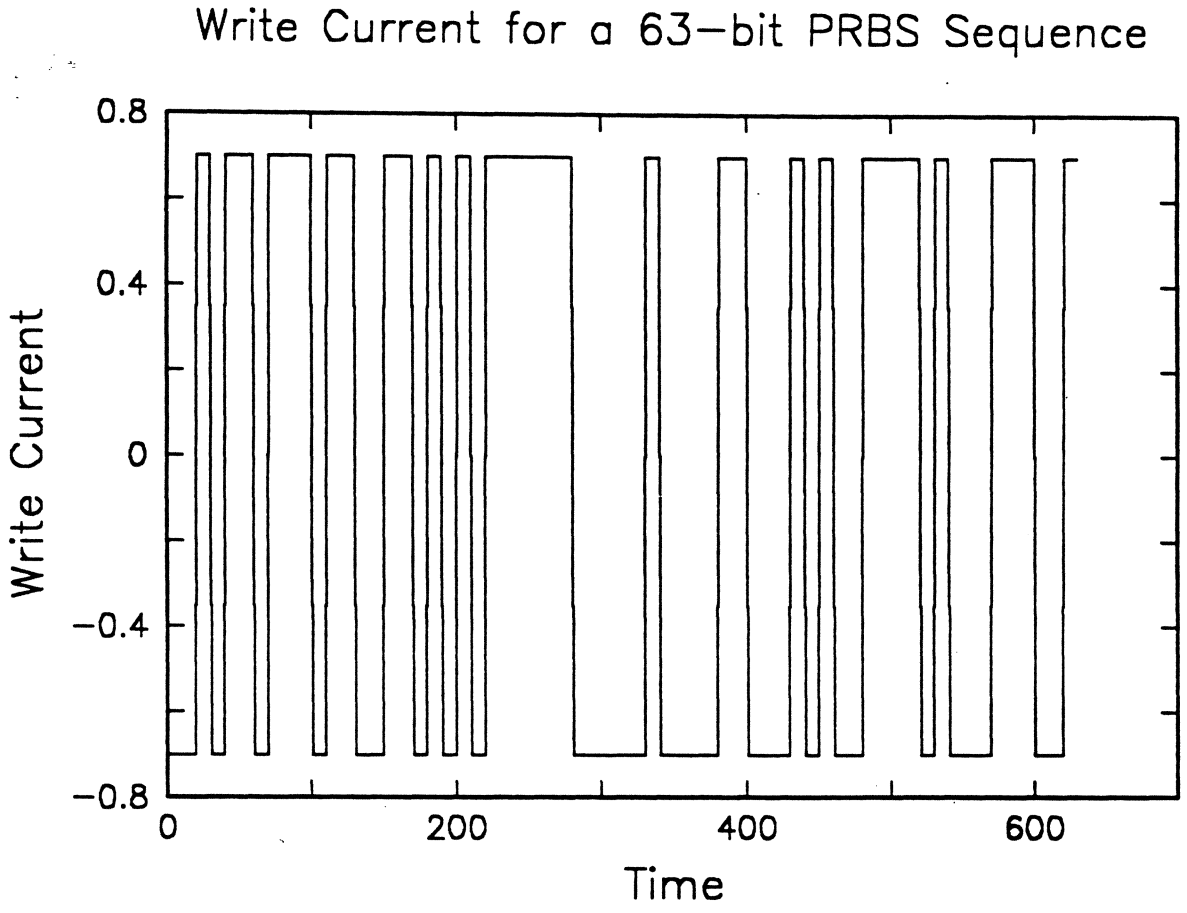

- Averaged Output Waveform

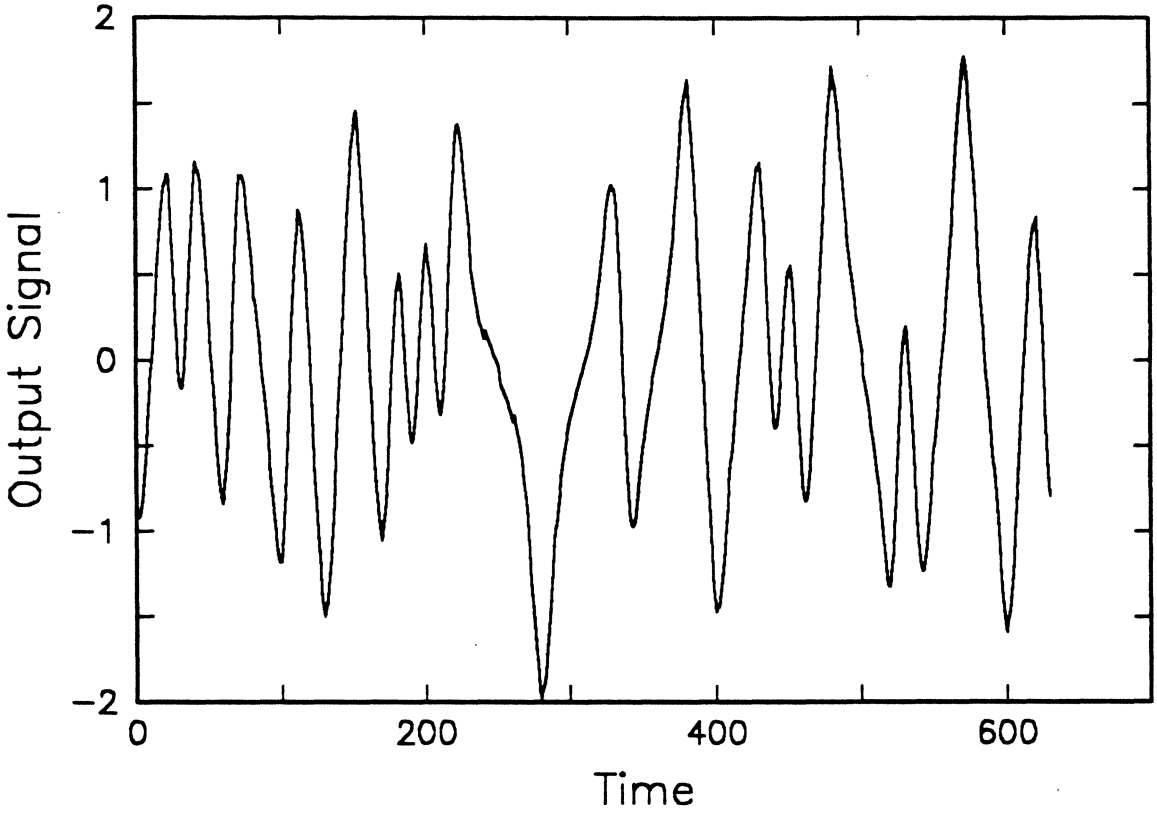

- Identified Pulse Response

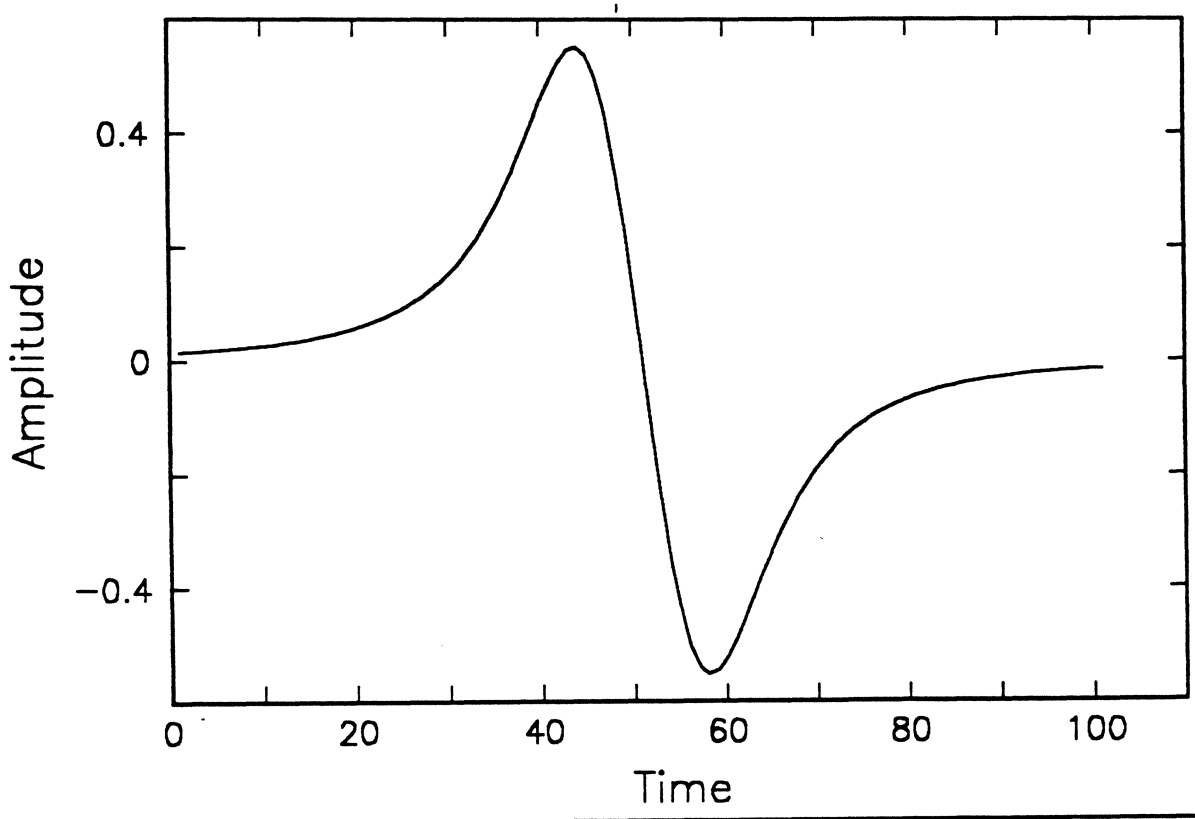

Equalization

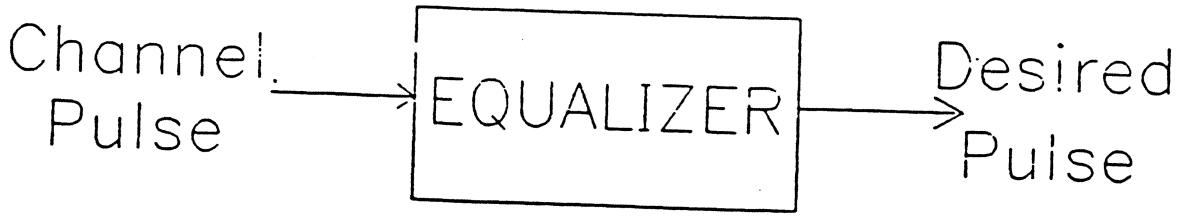

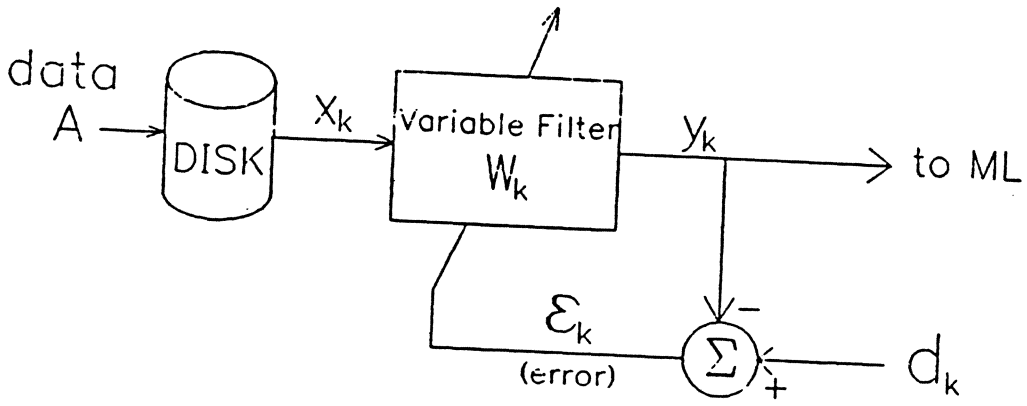

6. SUMMARY

- Why consider digital filters:

  Component tolerances (Accuracy)

  End-of-life component tolerances (Reproducibility)

  Implementation of Time-Varying Filters

  Size

  Power Dissipation

  Control of transient response

  Design abstraction

- Pitfalls in digital filter design:

  Relationship between analog and digital frequencies

  Direction of sample shifting

  Aliasing

  Finite precision and arithmetic

  Step-size selection

A/D AND D/A CONVERTERS IN HDD SYSTEMS:

- Servo Channel Requirements/Solutions
  - High Capacity Drives
  - Small Size Drives
- Technology options for a possible read – channel architecture.

BILL HUNT
ANALOG DEVICES
DEC '91.

"DEDICATED V'S EMBEDDED SERVO"

Complete embedded servo front end for HDD

Trends in HDD servo electronics: a) New demodulator techniques

ii) Embedded servo vs dedicated surface

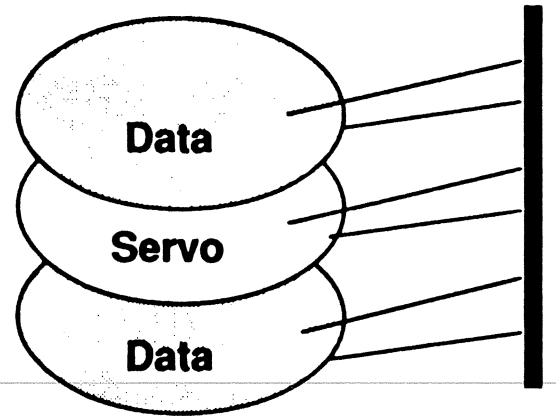

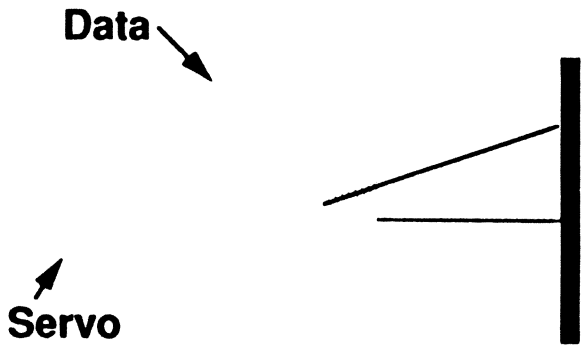

- 3 platters => 6 surfaces
  use 5 for data, 1 for servo
- surfaces mechanically linked
- continuous position f/back

- 1 platter => 2 surfaces
  interleave data and servo
- no registration problems
- sampled position f/back

GENERIC BLOCK DIAGRAM FOR CLASSICAL LARGE CAPACITY/SMALL SIZE HDD'S

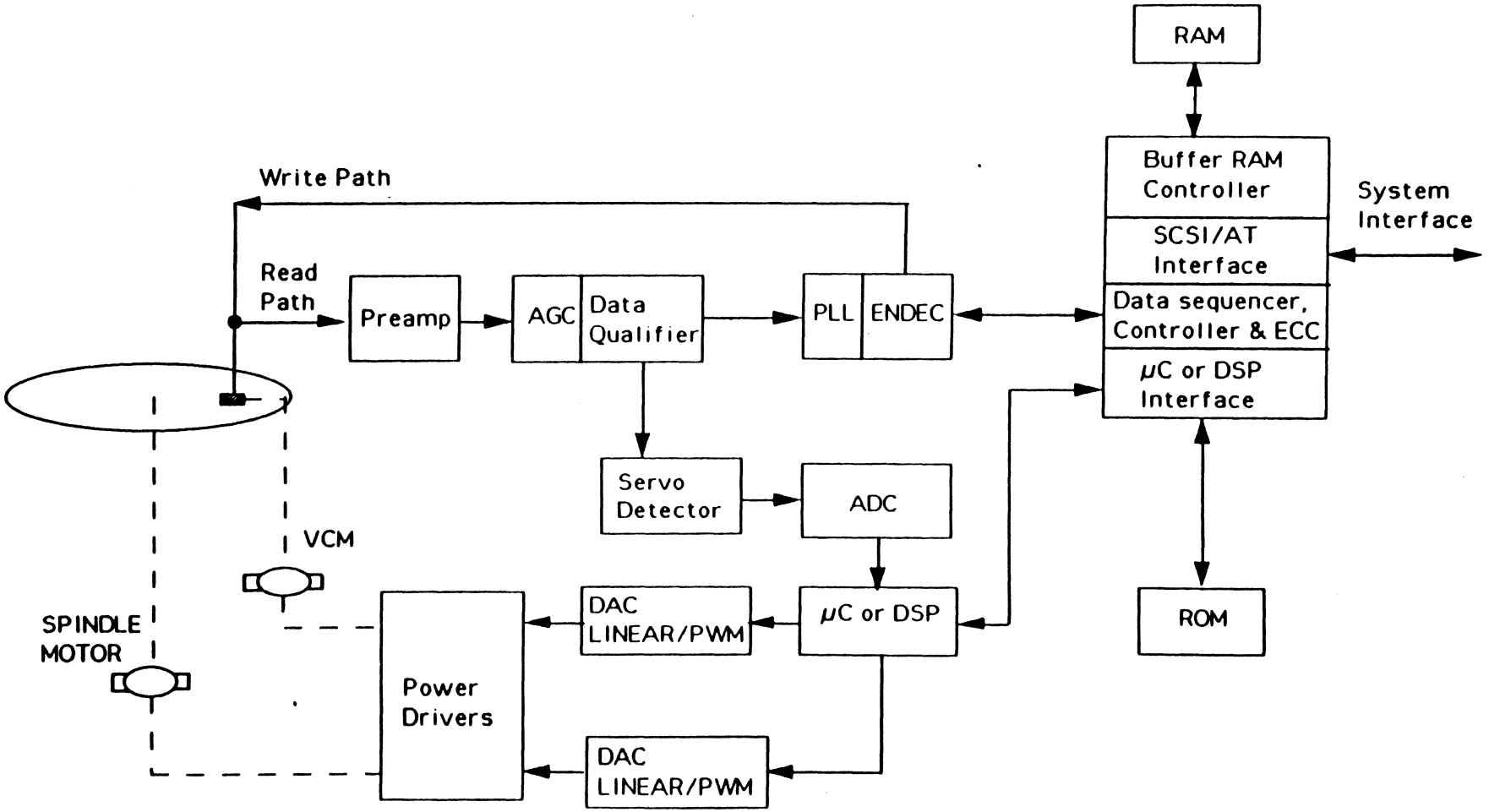

"CAPACITY"

– a possible classification

HIGH CAPACITY: > 300 MBYTE

- Size 5 1/4" to 3 1/2 x 1"
- Capacity 300 Mb – > 1Gb
- Access time: 10 mSEC
- Transfer rate: > 15 MB/S
- Improved Reliability (ELF)/(MTTF)
- Reducing cost

SMALL SIZE < 100M BYTES

- Size 3 1/2" to 2 1/2" to 1.8"
- Capacity 20 to 100 mb
- Low power
- "Zero" power in power down mode
- Lower supply voltage (smaller batteries) 3V
- Improved Reliability (ELF)/(MTTF)
- Reducing Cost

"LARGE" DRIVE:

system requirements

- Power control OF VCM/Spindle Motors
- For increasing capacity
  - An increase in T.P.I.
  - An increase in data transfer rate
- Dedicated/Hybrid servo.
- Reduced access time requires adaptive servo control.
- More measurement of system parameters required.
- More control of system parameters.
- Increased integration to reduce foot print.
- Reduced costs.

3.5" DRIVES — 'LARGE' CAPACITY

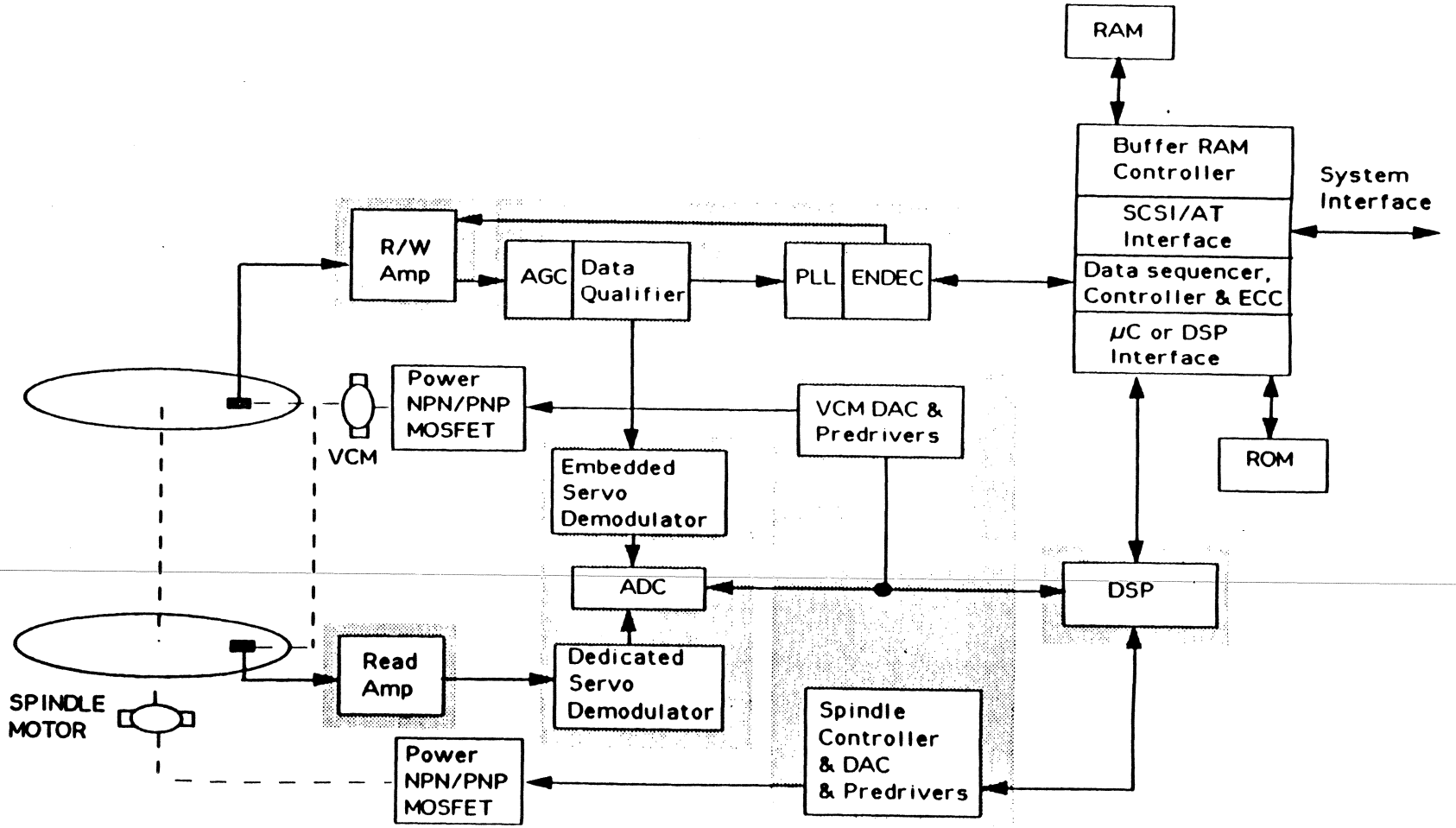

'LARGE' DRIVE: TECHNOLOGY REQUIREMENTS

- **+ 5V/+12v operation (+12 V to drive motors) ± 10%.**
- **Increased T.P.I.**
  - More resolution on VCM control (> 10 bits).
  - More resolution on position sensing (> 8 bits).
- **Maximise Channel S/N Ratio Use 'Bias' referenced signals.**
- **Dedicated/Hybrid servo control:**
- **Reduced Access Time**
  - Faster through – put through servo demod. channel.
  - Faster ADC conversion time. equivalent.
  - Faster processing uP/DSP.
  - Adaptive control bandwidth; AGC, rectifier discharge rate..
- **Fast interface speed for high speed uP's/DSP.**
- **Integration to give smaller foot print.**
  - Multiple small pin count SMD's (SOIC).
  - Single large pin count SMD's (PQFP).
- **Functional integration:**

  Include power pre – drivers; loop control element; with VCM DAC.

Typical 3.5"/5.25" Medium/High Performance HDD
300 MBytes
45,000 BPI
15 MB/S Transfer
15 mS Access Time

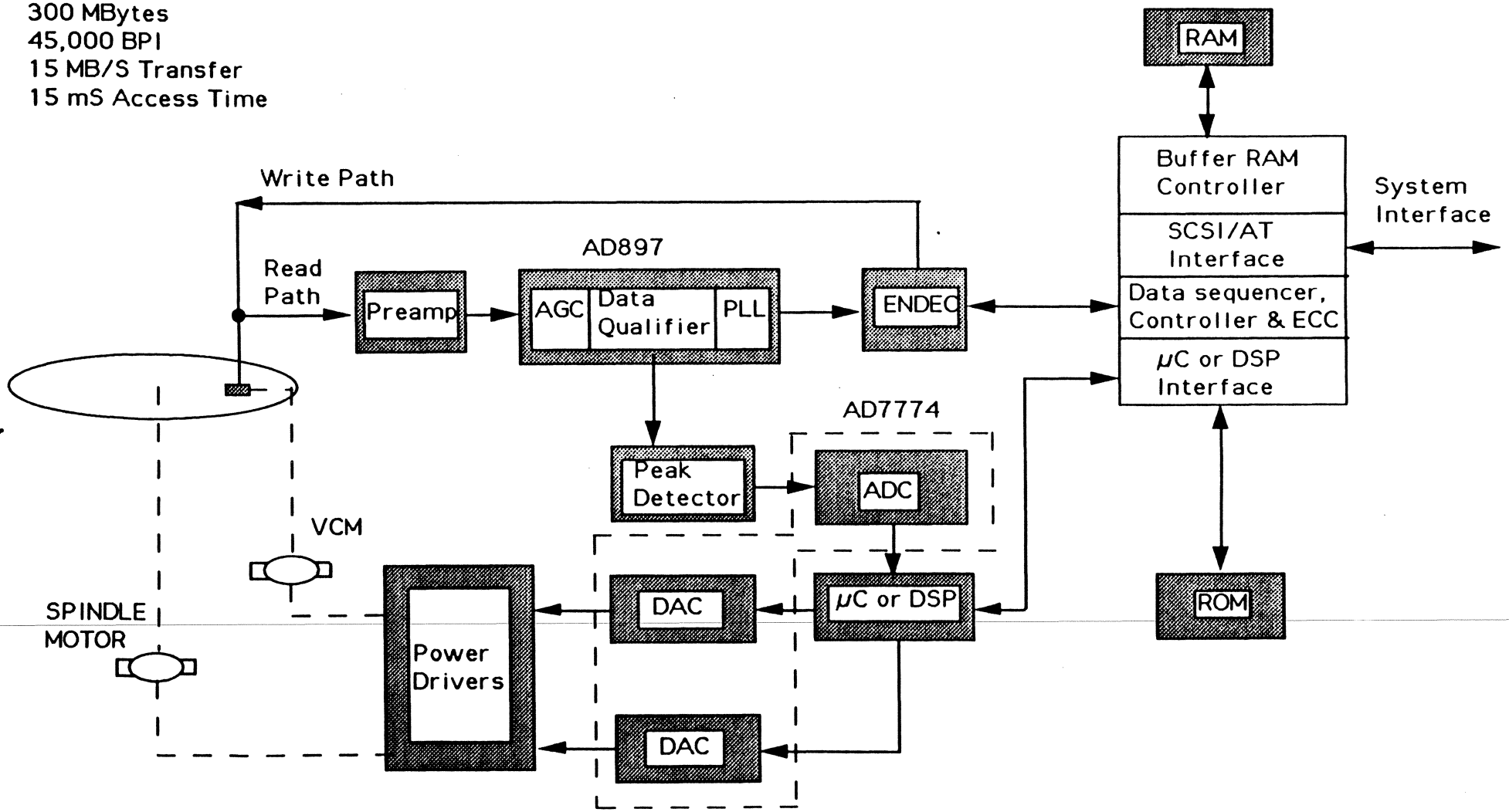

AD7774 FUNCTIONAL BLOCK DIAGRAM

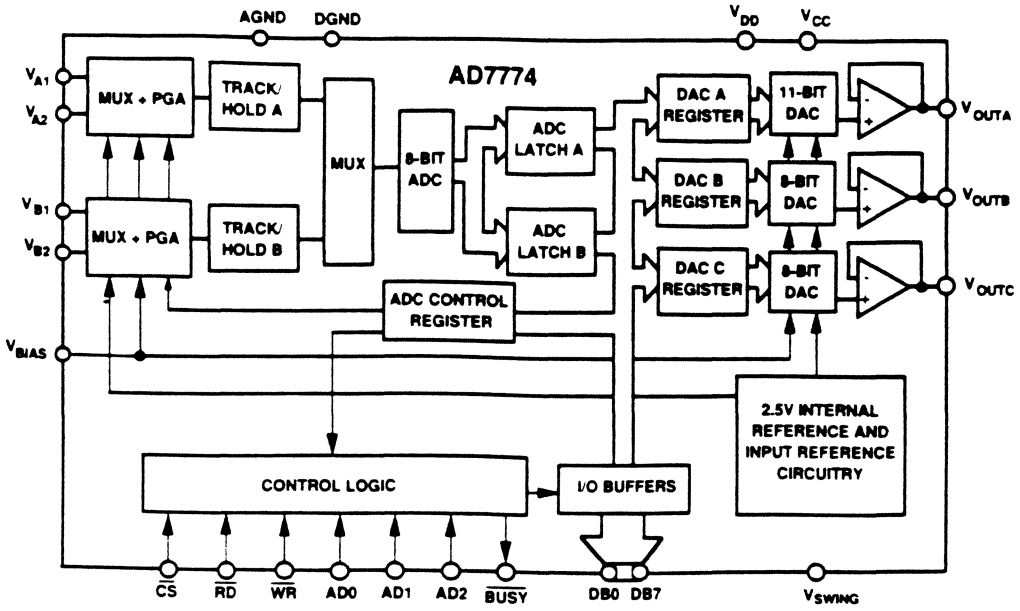

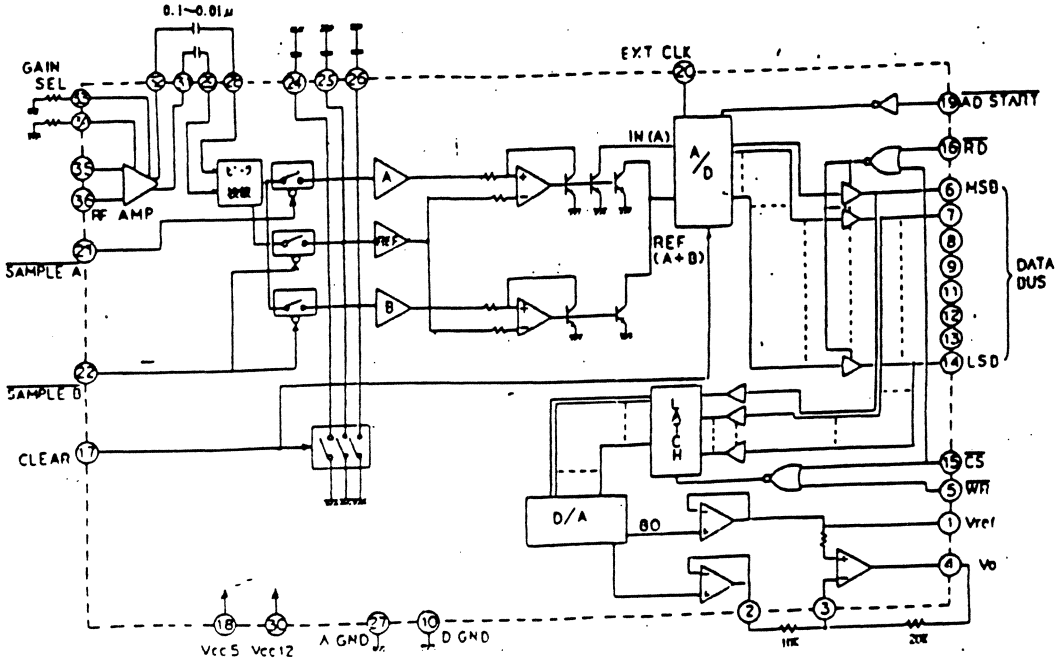
0.1~0.01μ
GAIN SEL
RF AMP
SAMPLE A
SAMPLE B
CLEAR
EXT CLK
IN(A)
A/D
REF (A+B)
AD START
RD
MSB
DATA BUS
LSB
CS
WR
Vref
Vo
D/A
BO
LATCH
Vcc5
Vcc12
A GND
D GND
11K
20K

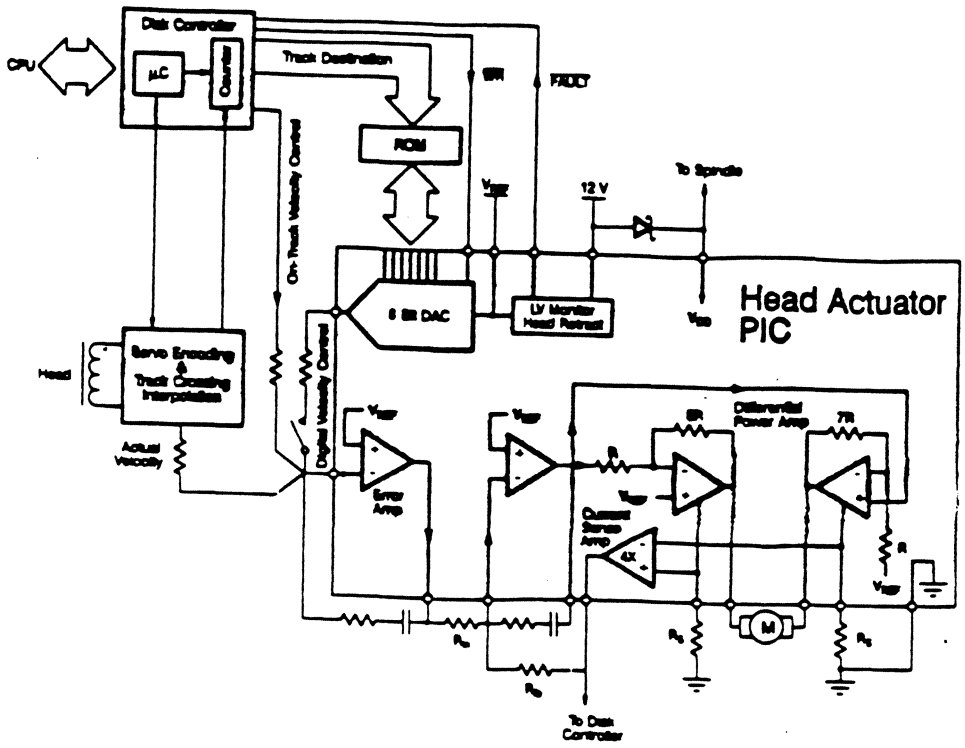

Fig. 1. HDD head-positioning servo system.

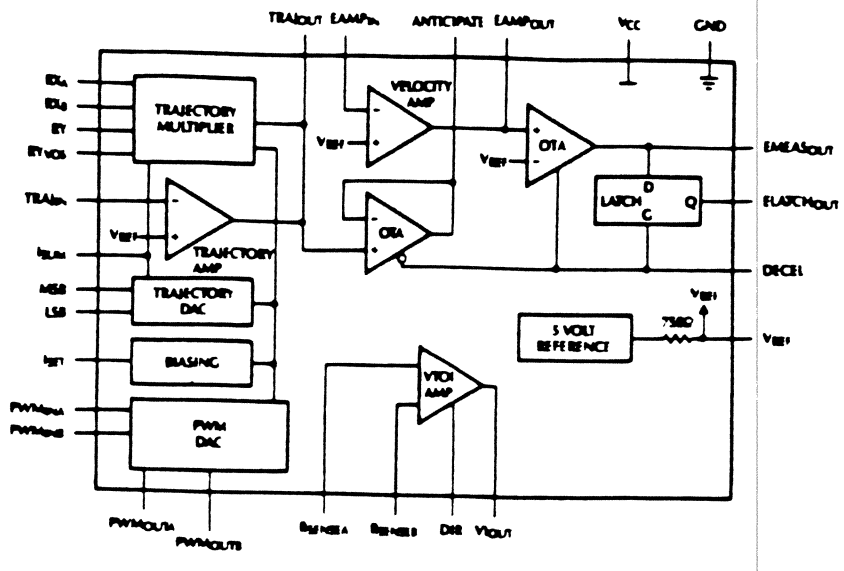
TRAJOUT
EAMPIN
ANTICIPATE
EAMPOUT
VCC
GND
TRAJECTORY MULTIPLIER
VELOCITY AMP
OTA
OTA
LATCH
D
C
Q
TRAJECTORY AMP
TRAJECTORY DAC
BIASING
5 VOLT REFERENCE
VTOI AMP
PWM DAC
DIR

'SMALL' SIZE

SYSTEM REQUIREMENTS:

- Reducing size 3 1/4 to 2 1/2 to 1.8".
- For increasing capacity to 80 mb.
  - an increase in T.P.I.
  - an increase in data transfer rate.
- Single platter.
- Power save mode for portable PC's (Laptop/notebooks).
- Low volume battery.
- Low – Low cost.

'SMALL' SIZE

Technology Requirements:

- For reduced size to < 1.8"
  - Component height reduction
  - Foot print reduction
- Embedded servo technique – single platter.
- Increased capacity by BPI/TPI increase, requiring more bandwidth/resolution (> 10 bits).
- Power save requires power down mode to < 1% normal.
- Minimize normal power drain to maximize life of fixed size battery.
- 5V only operation reducing to 3V ± 10%.
- Fast Interface speed for high speed uP's/DSP.
- Integration of additional functions.
  - Power drivers/devices and control circuits for VCM.
  - Servo demodulation spindle control functions.
- SMD packaging SOIC/PQFP for small foot print.
- TSOP/TPQFP for low (thin) packages.

Complete embedded servo front end for HDD

Demodulator channel block diagram

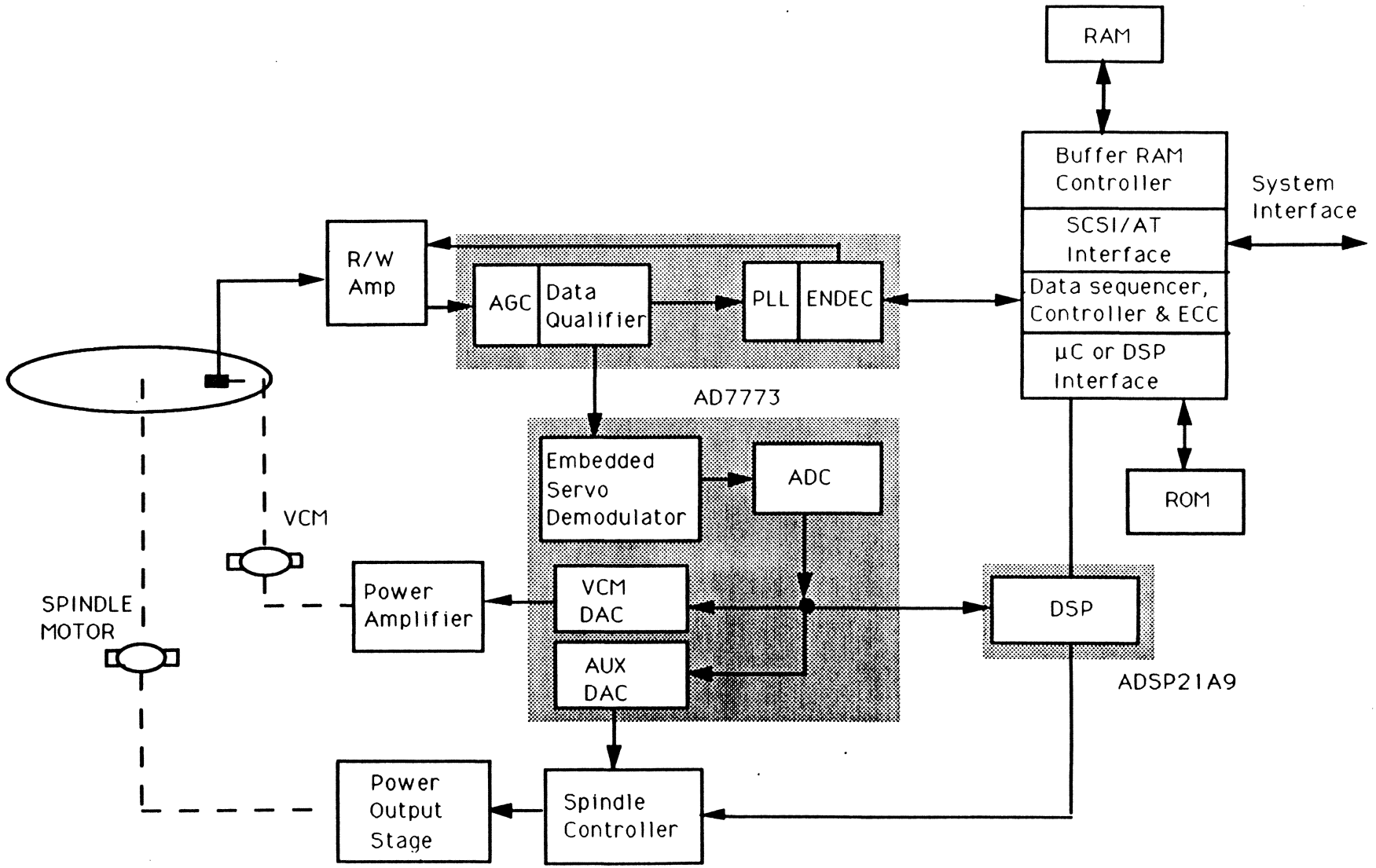

DEC '91 16-Nov-91

Complete embedded servo front end for HDD

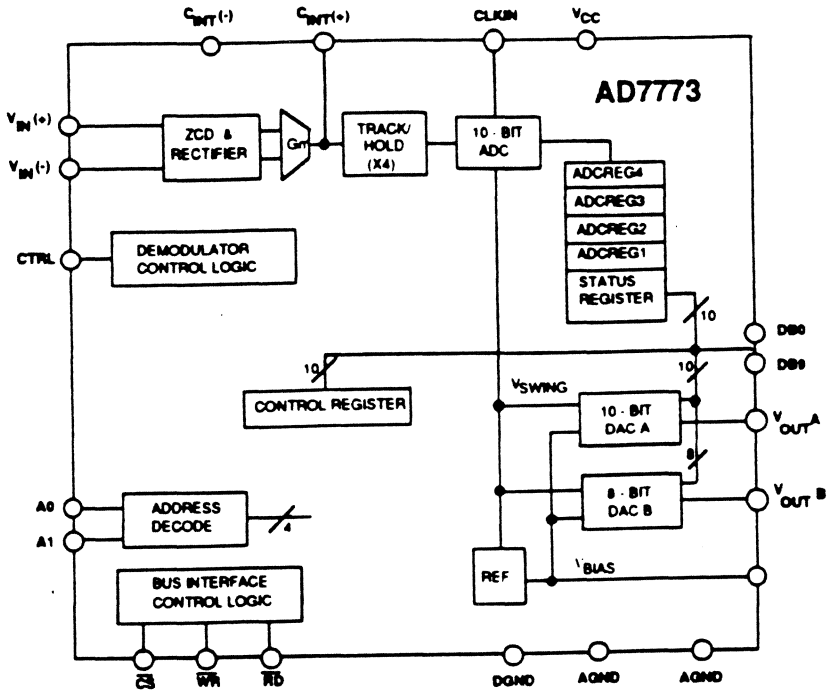

DEC '91 16-Nov-91

- Embedded Servo Demod.
- BICMOS Technology
- 10 Bit Resolution DAC (VCM) + ADC
- Area detect for increased noise immunity
- 'MOTEL' Interface
- 5V operation + 10%
- Power Down option
- On chip ref.
- Gated/Signal Sync'd mode (ZCD)
- Additional 8 bit DAC – for spindle control
- 5MHz signal input allowed
- 2.1 uSEC conversion time per acquired burst.
- Software control # of bursts, # cycles/burst.
- 28 SOIC /32 pin TSOP

BLOCK DIAGRAM

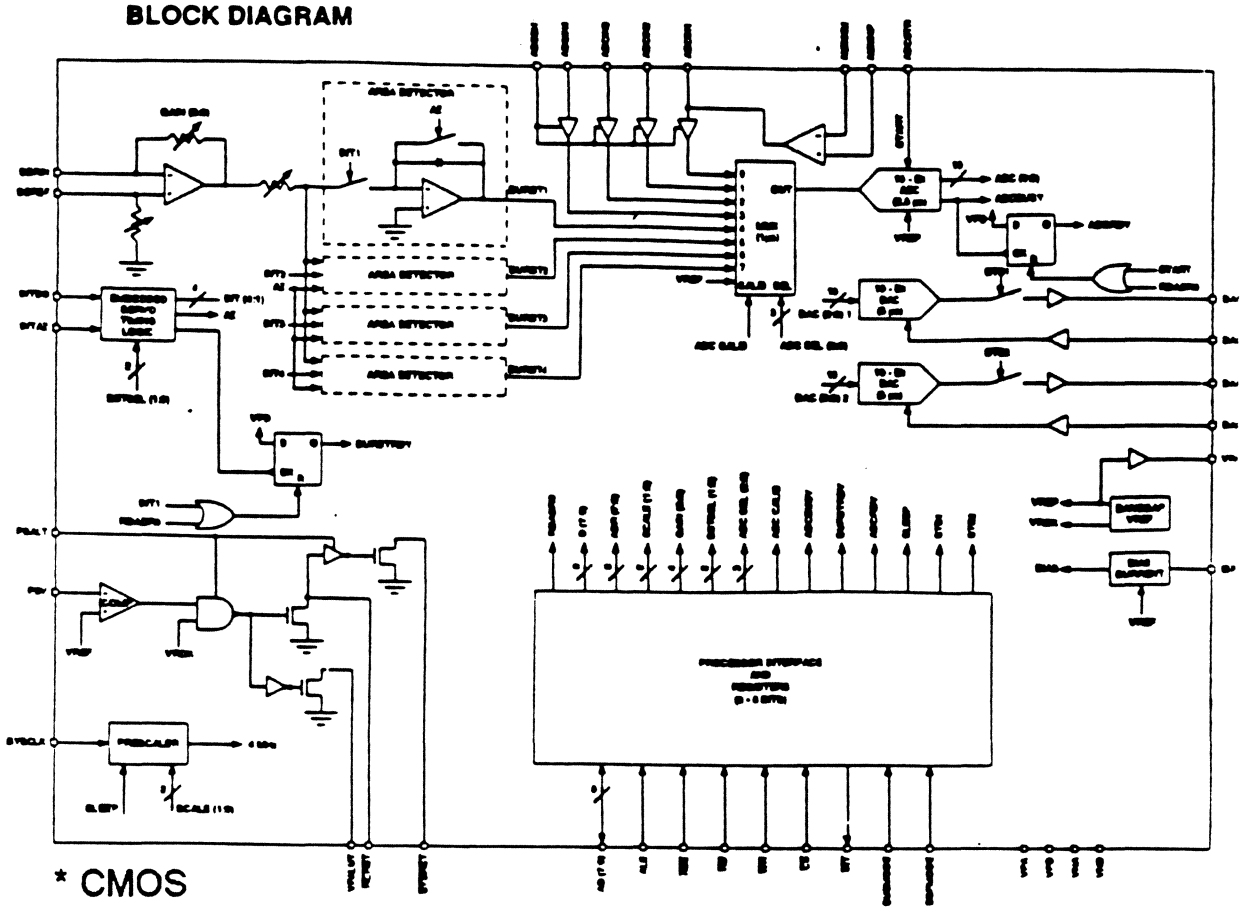

* CMOS
* 5V + 5%
* 8 CH 10 bit ADC 2.5 uSEC.
* Two 10 bit DAC's
* Area Detection
* PGA, software control
* Gated control of integration
* # bursts software control
* Voltage fault detection
* On chip ref.
* Motel Interface
* 44 SOIC

SMALL DRIVE

Further Integration : Options:

* Merge A/D and D/A function with DSP/uP – (1)

* Merge A/D & D/A function with
  - VCM Power Control
  - All Spindle Control Functions
  - Programmable servo timing control

  (Servo demod. merged with Read Channel – (2)

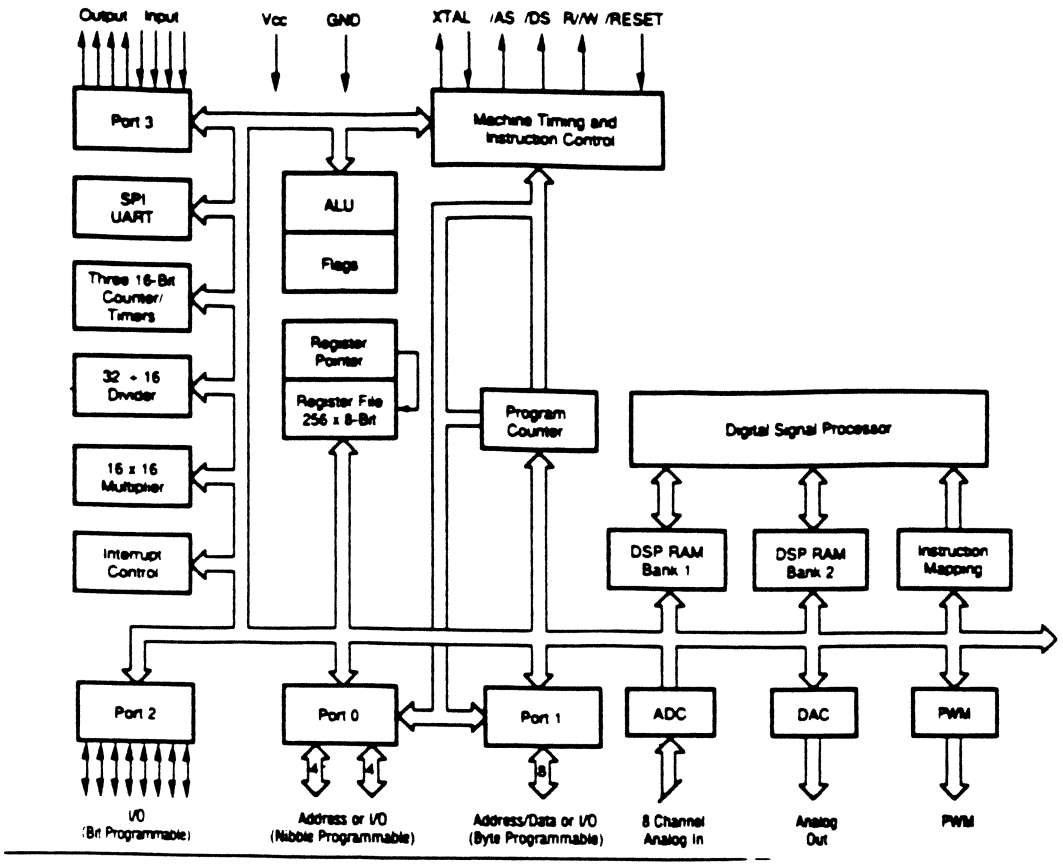
Output
Input
Vcc
GND
XTAL
/AS
/DS
R/W
/RESET
Port 3
Machine Timing and Instruction Control
SPI UART
ALU
Flags
Three 16-Bit Counter/ Timers
Register Pointer
32 ÷ 16 Divider
Register File 256 x 8-Bit
Program Counter
Digital Signal Processor
16 x 16 Multiplier
DSP RAM Bank 1
DSP RAM Bank 2
Instruction Mapping
Interrupt Control
Port 2
Port 0
Port 1
ADC
DAC
PWM
I/O (Bit Programmable)
Address or I/O (Nibble Programmable)
Address/Data or I/O (Byte Programmable)
8 Channel Analog In
Analog Out
PWM

2.5" Future Integration (1992)
4/5 Chips
80 MBytes
45,000 BPI
15 MB/S Transfer
19 mS Access Time

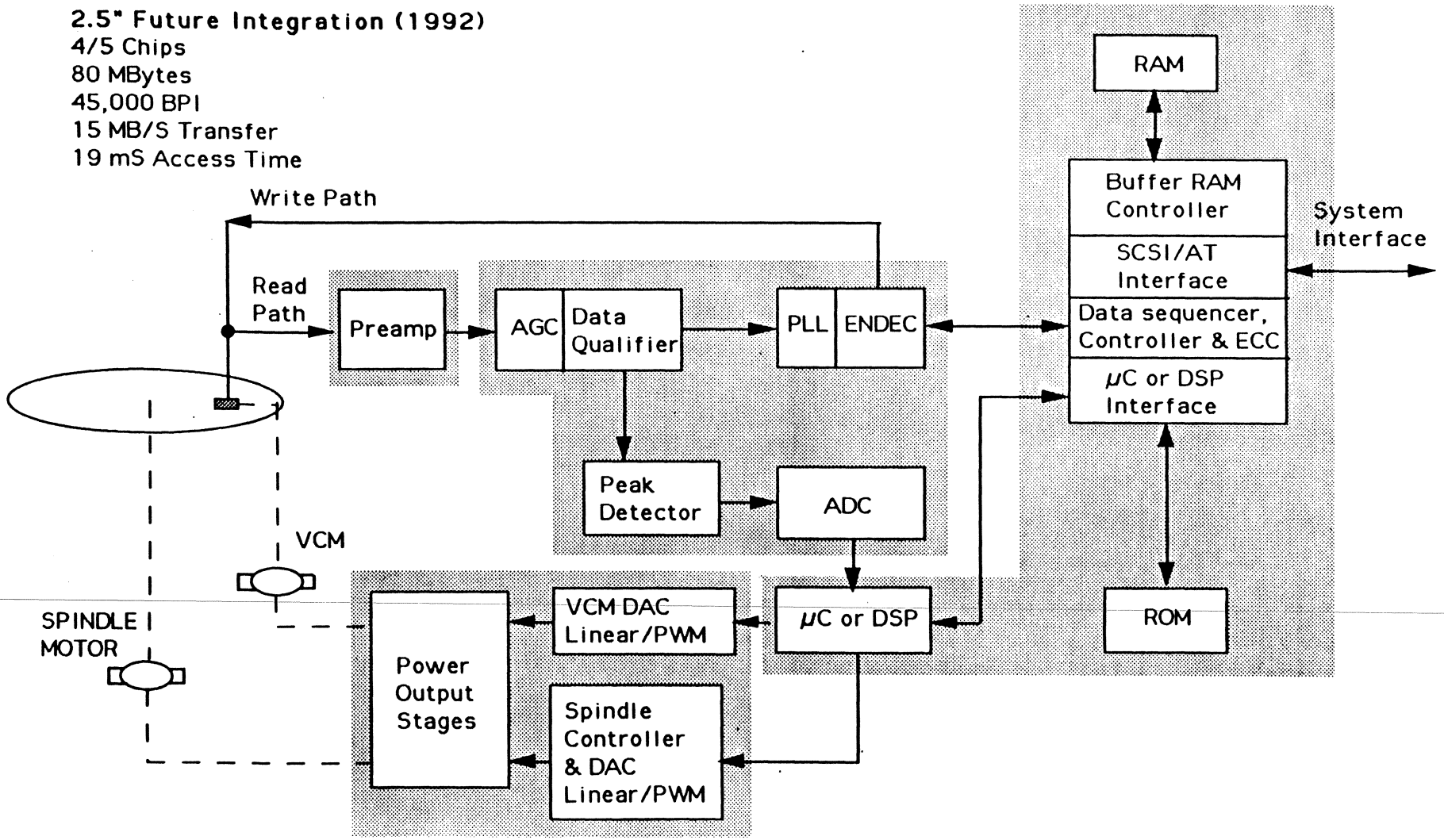

ANALOG DEVICES

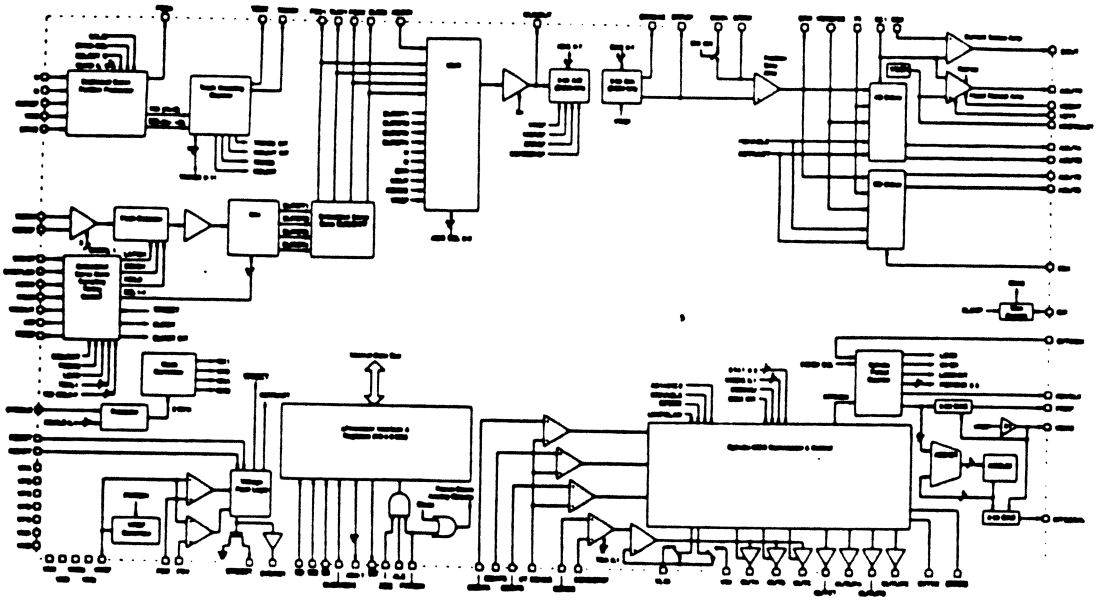

BLOCK DIAGRAM
SSI 32H4631

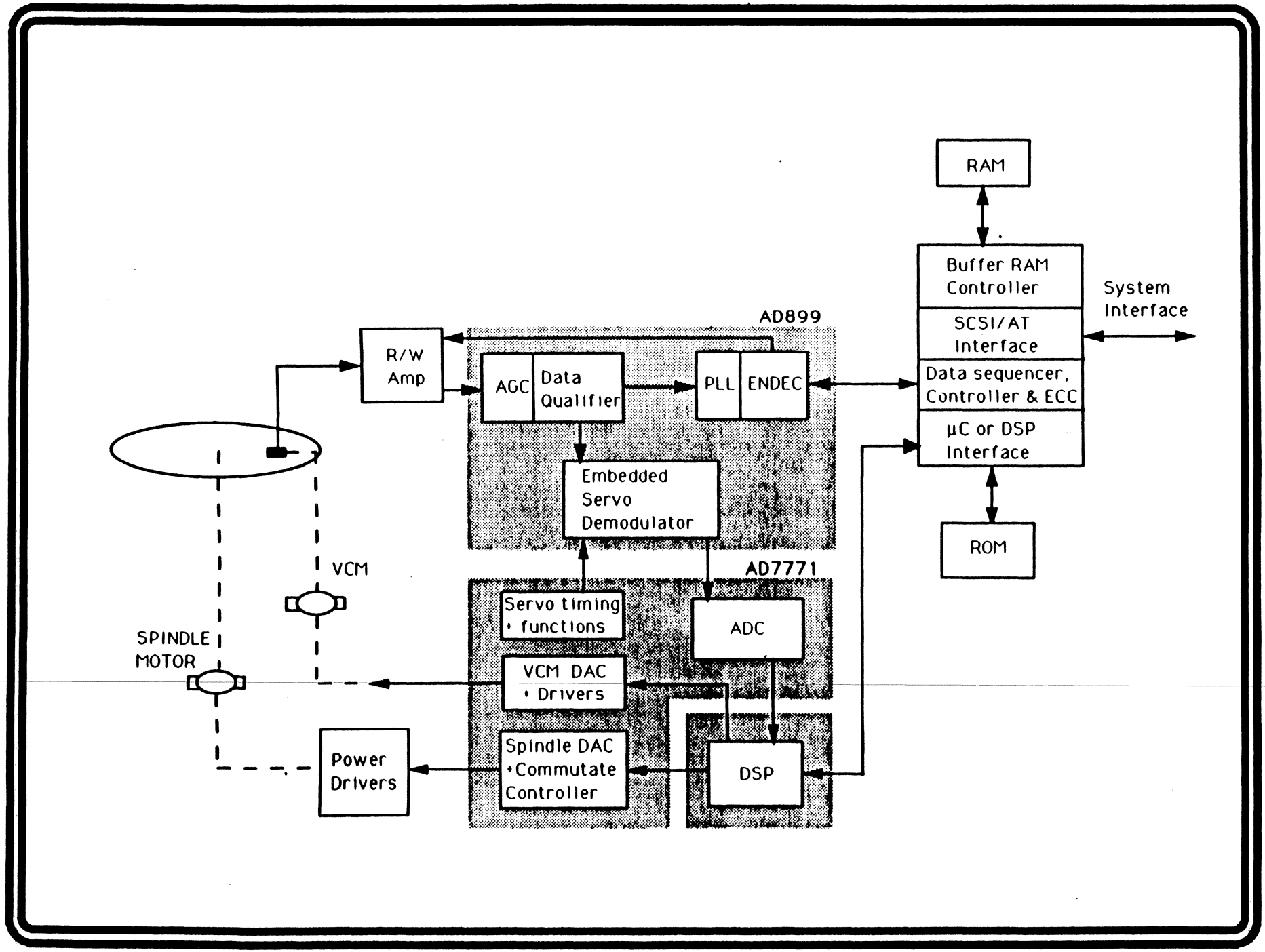
RAM
Buffer RAM Controller
System Interface
SCSI/AT Interface
Data sequencer, Controller & ECC
µC or DSP Interface
ROM
AD899
R/W Amp
AGC
Data Qualifier
PLL
ENDEC
Embedded Servo Demodulator
AD7771
Servo timing + functions
ADC
VCM DAC + Drivers
Spindle DAC +Commutate Controller
DSP
VCM
SPINDLE MOTOR
Power Drivers

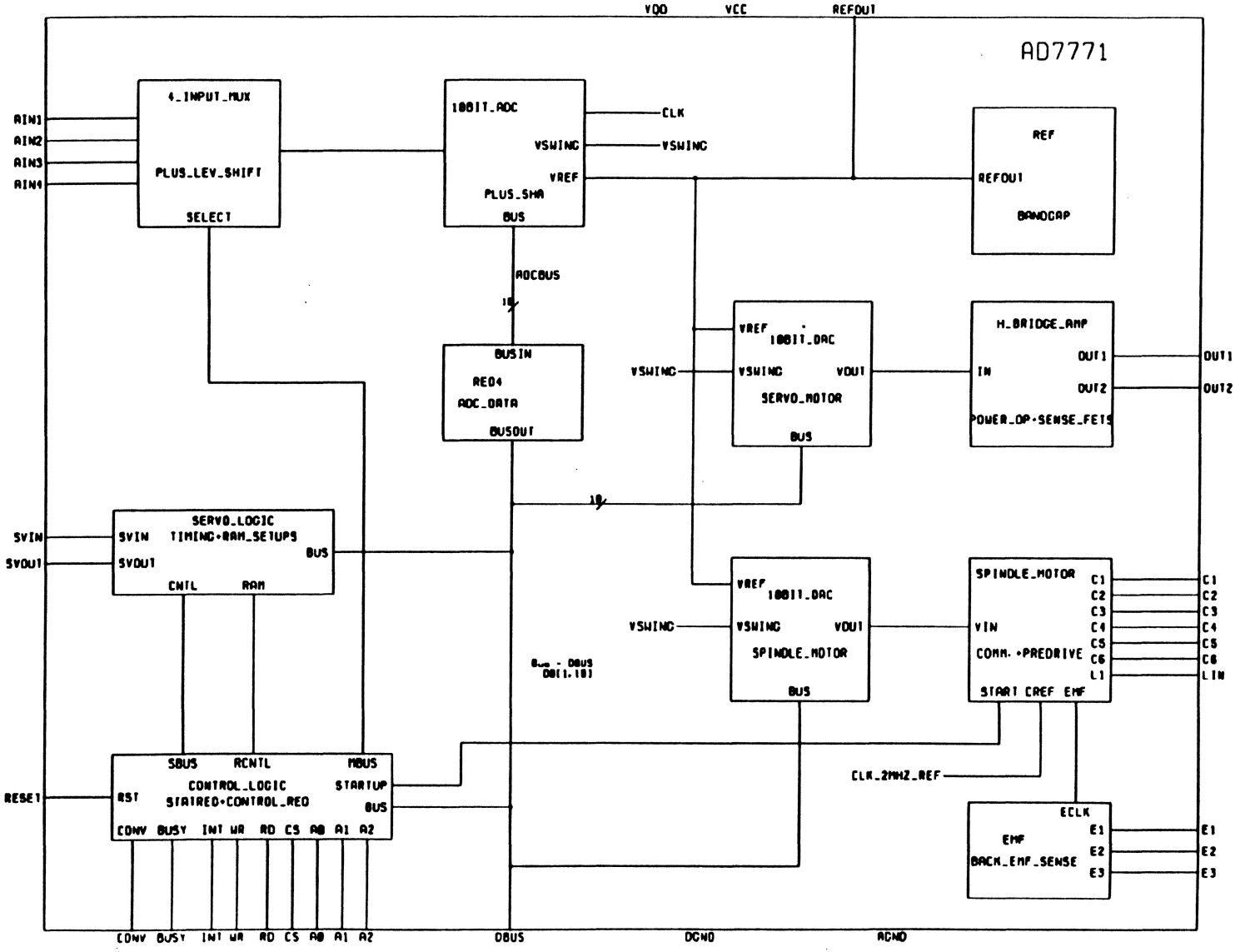
AD7771
VDD
VCC
REFOUT
AIN1
AIN2
AIN3
AIN4
4_INPUT_MUX
PLUS_LEV_SHIFT
SELECT
10BIT_ADC
CLK
VSWING
VREF
PLUS_SHA
BUS
REF
REFOUT
BANDGAP
ADCBUS
16
BUSIN
REG4
ADC_DATA
BUSOUT
VREF
10BIT_DAC
VSWING
VOUT
SERVO_MOTOR
BUS
H_BRIDGE_AMP
OUT1
IN
OUT2
POWER_OP-SENSE_FETS
SVIN
SVOUT
SERVO_LOGIC
TIMING+RAM_SETUPS
CNTL
RAM
SPINDLE_MOTOR
C1
C2
C3
C4
C5
C6
L1
VIN
COMM.+PREDRIVE
START CREF EMF
CLK_2MHZ_REF
ECLK
EMF
BACK_EMF_SENSE
E1
E2
E3
RESET
SBUS
RCNTL
MBUS
CONTROL_LOGIC
STATRED+CONTROL_REG
RST
STARTUP
CONV BUSY INT WR RD CS A0 A1 A2
DBUS
DGND
AGND

SMALL DRIVES

FUTURE:

- 3V Operation
- Smaller motors
- Lower power drive < 250 mA (included on chip)
- CMOS
- Single chip embedded servo?
- Semiconductor Memories!!

ADC FOR PRML CHANNEL

– TECHNOLOGY OPTIONS

PROPOSED ADC SPECIFICATION

Resolution:		6 Bits
Accuracy:	Target	5.8 ENOB EFFECTIVE NUMBER OF BITS
Sampling Rate:		72 MSPS
Error Rate:		10 E – 10
Input Bandwidth:		5.8 ENOB to 25 MHZ
		5.0 ENOB to 50 MHZ (1.4 NyQuist)
Input Signal Range:		1.5 Vpp differential
		+/– 375 mV about 2.5V
Input Capacitance		5 PF Differential

Jitter	< 40 PS
PSRR	< 30db at 30 MHZ
Assumed Driving Impedance:	100 ohms
Power Supply:	5V ± 10%
Power Dissipation	200 mW total
	100 mW for comparators
Temperature Range	0°to 70° C Ambient
	0° to 125° C Junction Temp.
Package	Surface Mount: (SOIC/PQFP)

KEY COMPARATOR SPEC'S DEDUCED FROM ADC SPEC

- Error Rate (ER).
- Input signal bandwidth (B.W.).
- Power dissipation (per comparator) (P.D.).
- L.S.B. size/input signal range.

COMPARATOR EVALUATION

- Bipolar, CMOS, BICMOS circuits studied.

- Relationships between technology/P.d/ER/BW established.

BIPOLAR RESULTS:

- > 5 GHZ devices will meet 72 msps rate.
- Power dissipation is marginal.
- Dynamic range good.
- > 100 MHZ input bandwidth possible.
- Good tolerance of temp/supply variations.
- Major problem with ECL to CMOS/TTL conversion.
- Can be extended to higher resolution.

CMOS RESULTS:

- Technology $\leqslant$ 1u meets 72 Msps rate.
  (No auto zero cycle).
- Power dissipation just O.K.
- Marginal on input bandwidth, sharp break – off.
- Concern on dynamic range, comparator offset.
- Solves the level shift problem.
- More sensitive to temp/supply variations than bipolar.

BICMOS:

- Needs $\leq$ 1u CMOS Technology.
- Needs good bipolar device $\geq$ 5GHz.
- Meets power requirements.
- Input bandwidth to > 100 MHZ possible.
- Dynamic range O.K., due to low offset.
- Good tolerance to supply/temp variations.
- Possible to increase resolutions.

— Best Choice for Target Spec.

DAC's FOR SMALL DRIVES OPERATING AT 3V.

- What's the best architecture?
- Assume Fine Line CMOS technology:
  - (a) String Dac:
    - 2^N Switches (256/1024)
    - Poly Resistor string
    - Guaranteed monotonic to resolution
    - 7/8 bits accurate
    - Vout range; 0 to Vref
    - Static output
    - Needs high impedance load
    - Not very fast

CMOS DIGITAL-ANALOG AND ANALOG-DIGITAL CONVERTERS

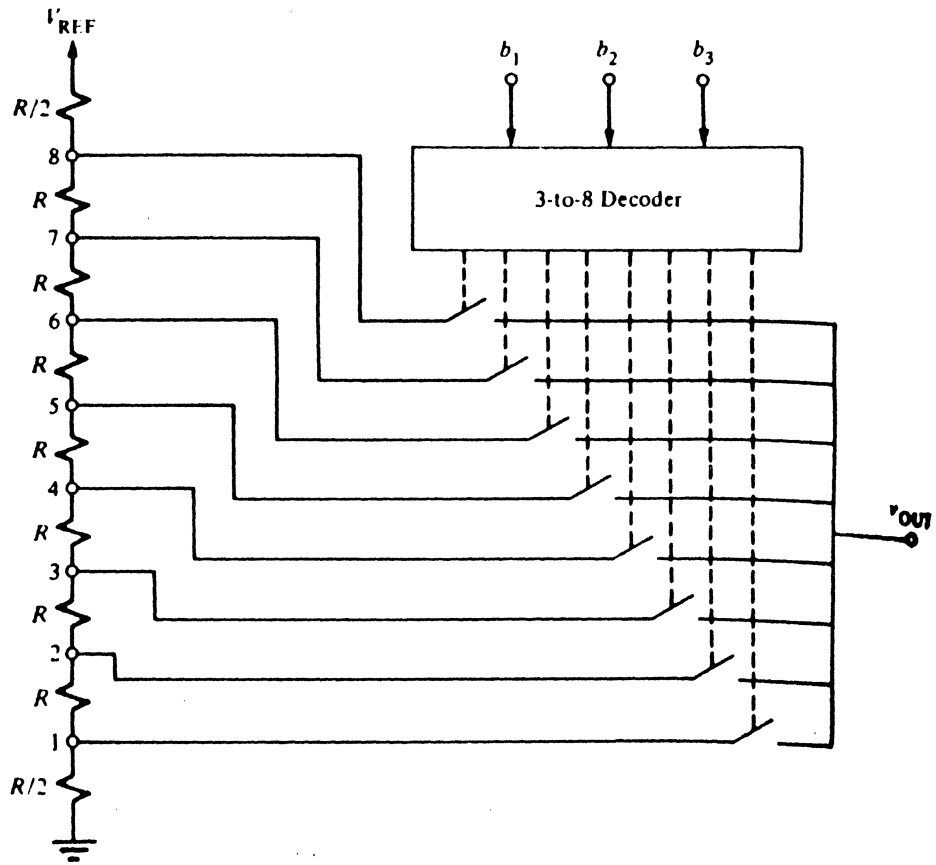

C

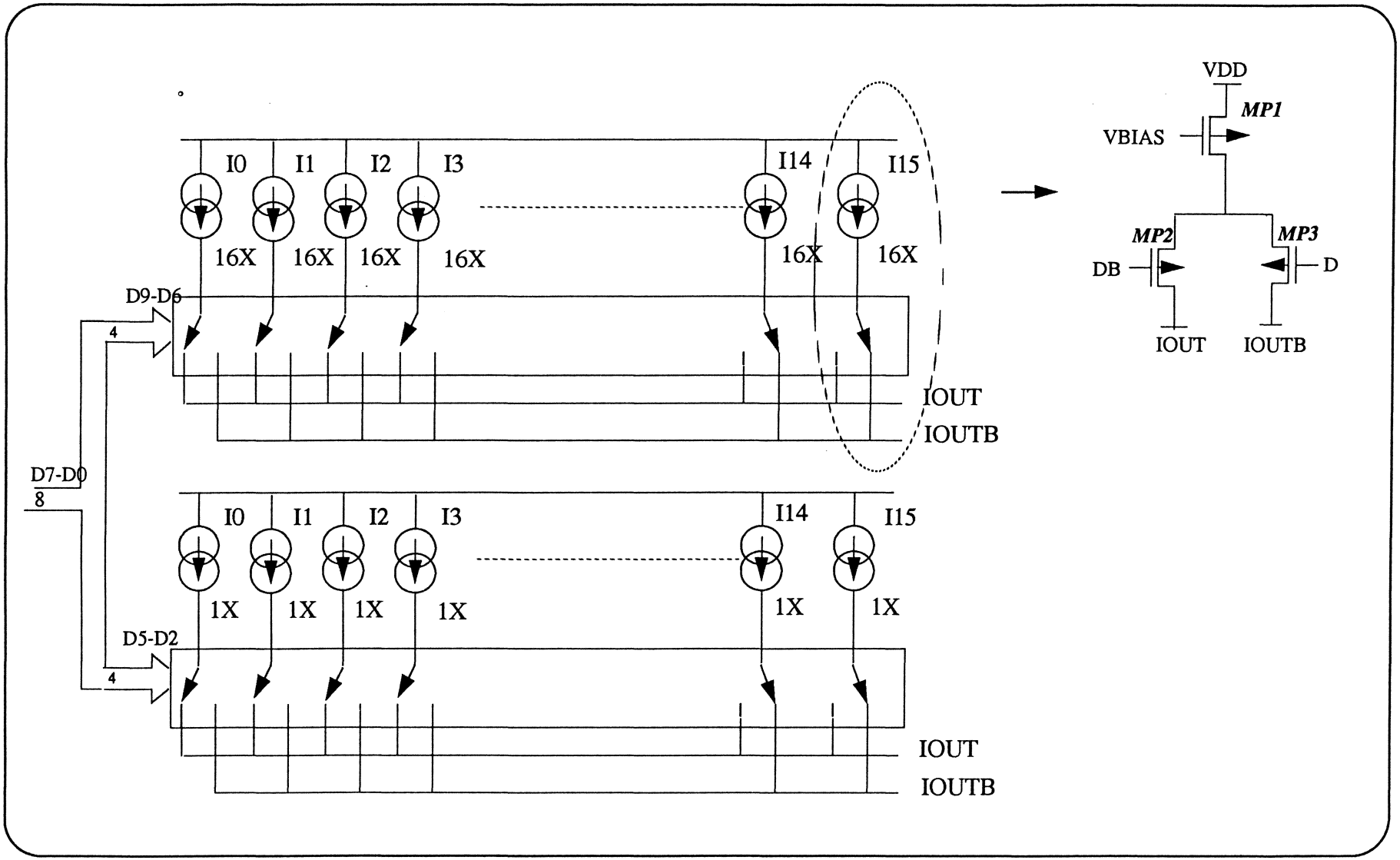
I0
I1
I2
I3
I14
I15
16X
16X
16X
16X
16X
16X
D9-D6
4
IOUT
IOUTB
D7-D0
8
I0
I1
I2
I3
I14
I15
1X
1X
1X
1X
1X
1X
D5-D2
4
IOUT
IOUTB
VDD
MP1
VBIAS
MP2
MP3
DB
D
IOUT
IOUTB

D

(b) – Current Source DAC
(e.g. RAM DAC)

- Can be very fast
- Limited voltage output range (0 – 1.5V).
- 10 bits monotonicity possible
- 8/9 bits accurate
- Static output
- Could be calibrated.

(c) Switch Cap DAC

- C – 2C architecture or variations there of
- Dynamic output for fixed input code
- Needs post filtering
- Needs poly – poly caps. for 10 bits monotonicity
- Could be calibrated.

3 bit DAC

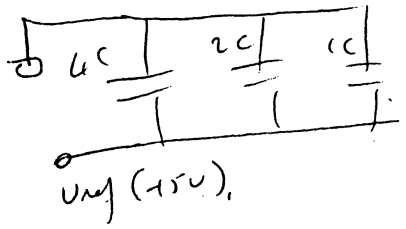
4C
2C
1C
Vref (+5V)

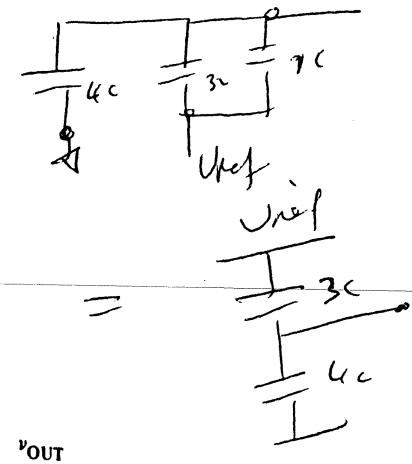
4C
2C
1C
Vref
Vref
3C
4C

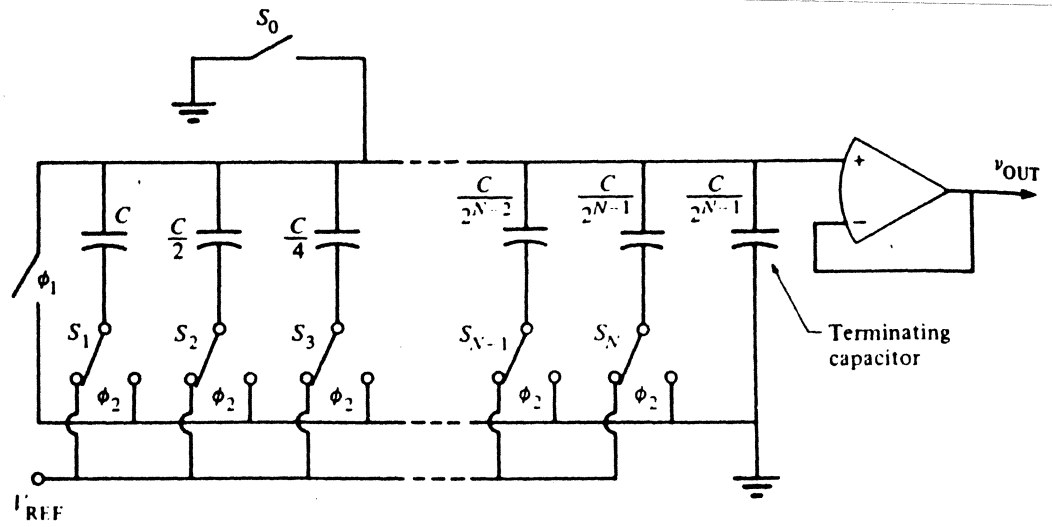
S_0
C
$\frac{C}{2}$
$\frac{C}{4}$
$\frac{C}{2^{N-2}}$
$\frac{C}{2^{N-1}}$
$\frac{C}{2^{N-1}}$
ϕ_1
S_1
S_2
S_3
S_{N-1}
S_N
ϕ_2
V_{OUT}
Terminating capacitor
I_{REF}

(a)

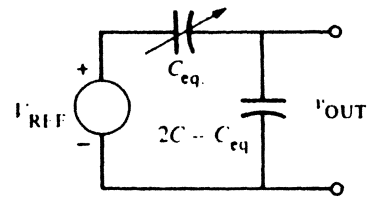
C_{eq}
I_{REF}
$2C - C_{eq}$
V_{OUT}

(d) (P.W.M) DAC

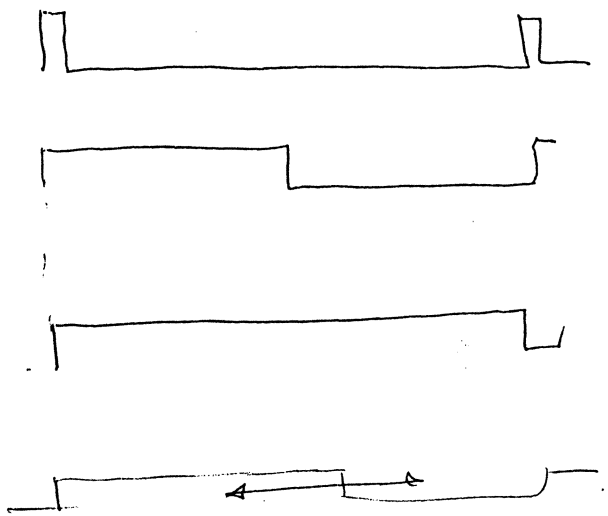

- 10 bits in 100uSEC possible
- Dynamic output
- Needs post filtering
- Small size.

- Choice of architecture should consider complete function not just D/A function i.e. follow on amplifiers; power drivers etc..
- Adjustment required to zero – out accumulated offsets in the DAC/Driver chain.

– Use Calibration

But when can we calibrate??

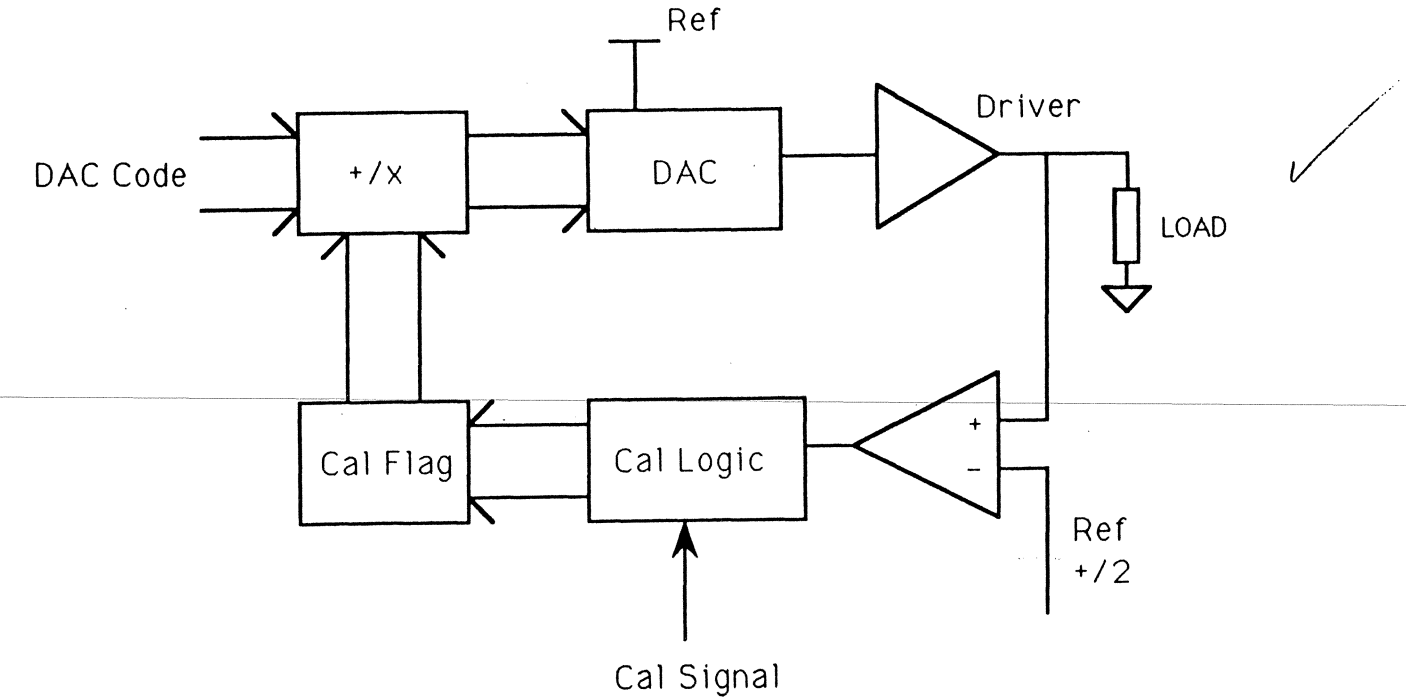

ADC'S for Small Drives operating at 3V

- What's the best architecture?
- Assume fine line CMOS Technology

(a) SAR Technique:

- Efficient in area
- Low Power Consumption
- Limited in conversion speed
  (1 uSEC at 8 bits, 3 uSEC at 10 bits)
- Use string DAC/Switch Cap. DAC/ Current Source DAC.
- Sampled data comparator design
- 9 bits no missed codes possible
- 7/8 bits accurate
- Could be calibrated.

SUCCESSIVE APPROXIMATION A/D CONVERTER ENCODER

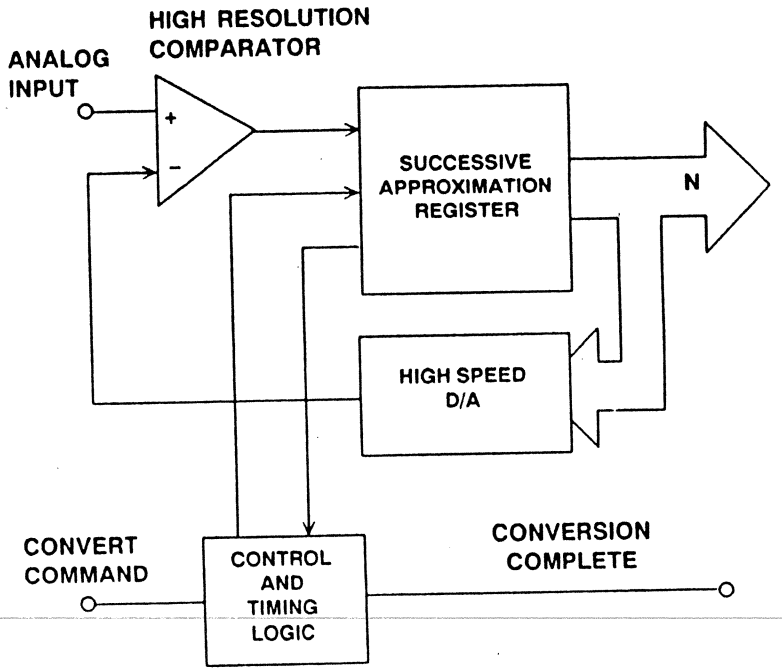

Figure 4.2

10.6.4. K

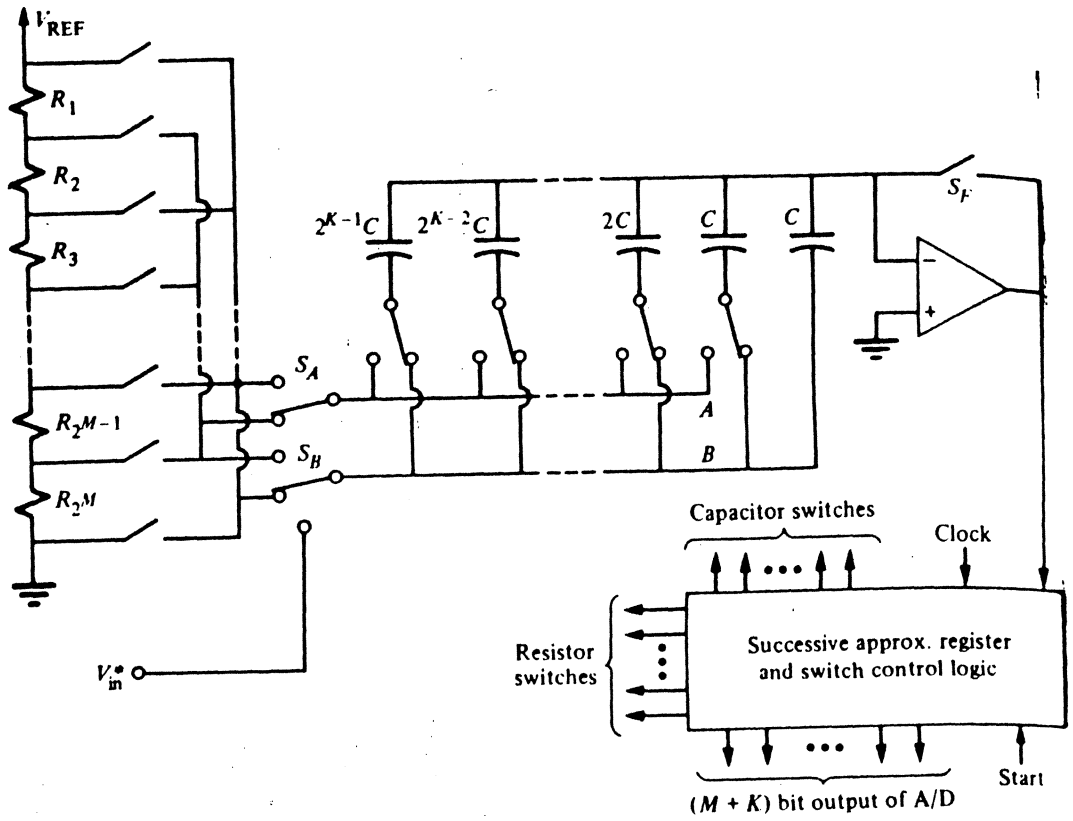
V_{REF}
R_1
R_2
R_3
R_{2^M-1}
R_{2^M}
S_A
S_B
V_{in}^*
$2^{K-1}C$
$2^{K-2}C$
$2C$
C
C
S_F
A
B
Capacitor switches
Clock
Resistor switches
Successive approx. register and switch control logic
Start
$(M + K)$ bit output of A/D

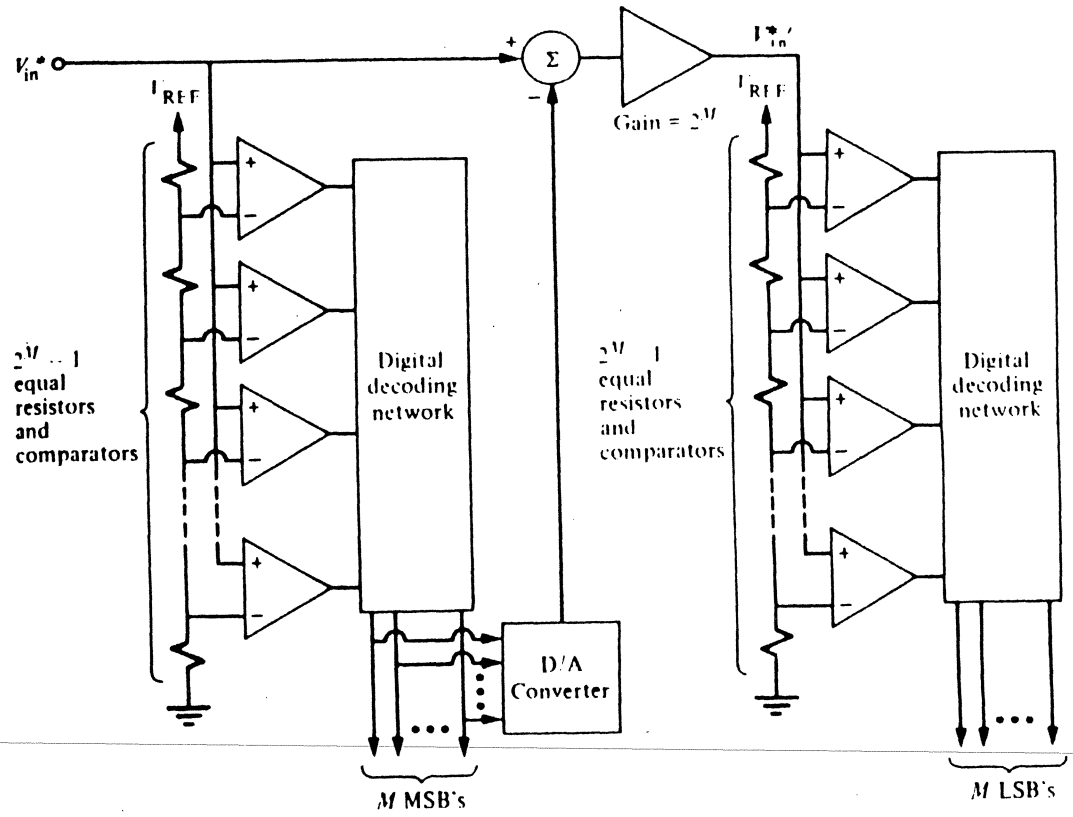
V_{in}^*
I_{REF}
Σ
+
−
Gain = 2^M
I_{in}^*
I_{REF}
$2^M - 1$ equal resistors and comparators
Digital decoding network
D/A Converter
M MSB's
$2^M - 1$ equal resistors and comparators
Digital decoding network
M LSB's

(b) Flash – Flash technique:

- Achieves faster conversion time (200/400 nSEC).
- Greater power consumption
- Larger in area
- 8 bits (4 + 4)/10 bits (5 + 5) resolution
- 7/8 bits accurate
- Sensitive to noise.

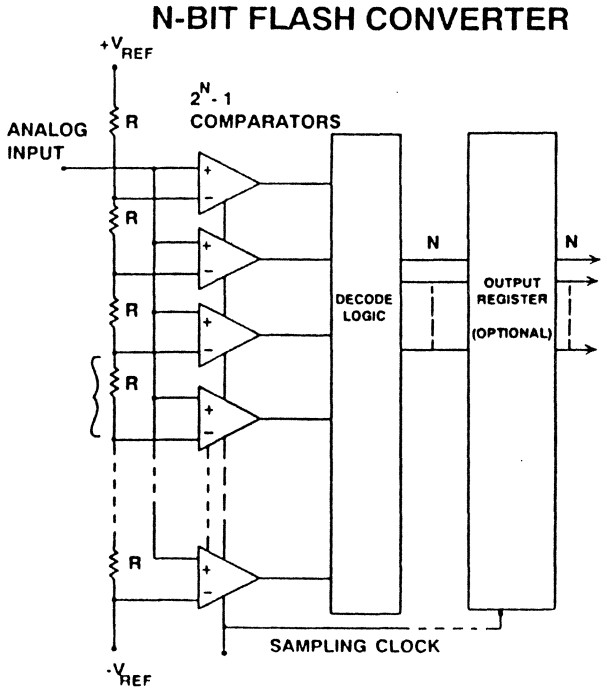
N-BIT FLASH CONVERTER
+V REF
2^N - 1
COMPARATORS
ANALOG
INPUT
R
R
R
R
R
N
N
DECODE
LOGIC
OUTPUT
REGISTER
(OPTIONAL)
SAMPLING CLOCK
-V REF

Figure 4.4

- Choice of architecture should consider complete function not just the A/D function, i.e. pre conditioning stages etc..
- With small signal span offsets become a problem.
  - Use calibration
  - when can we calibrate?

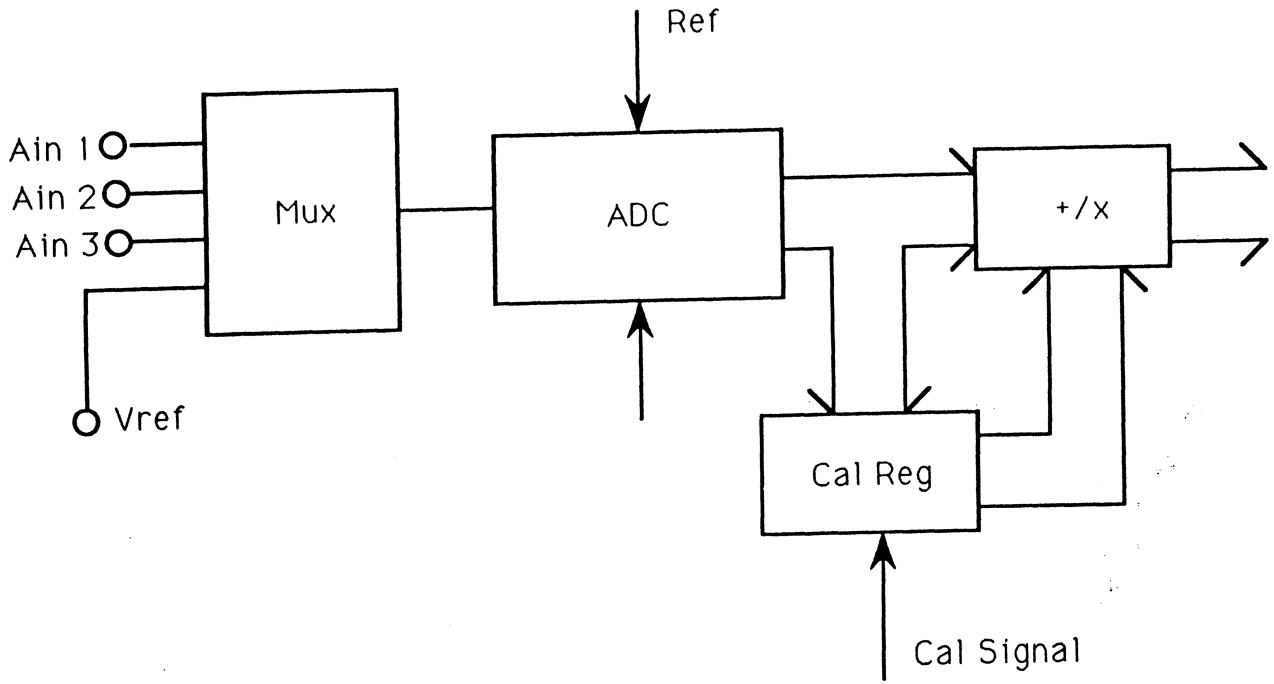

(c) Full Flash Technique:

- Very fast (50/100 nSEC)
- Power consumer
- large in area
- 8 bit resolution upper limit due to size
- Sensitive to noise

MAGNETIC CHANNEL CHARACTERISTICS

EDGAR M. WILLIAMS
READ-RITE CORPORATION

- ○ Recorded Magnetization Patterns
- ○ Zig-Zag Transitions in Thin Films
- ○ Mathematical Approximations of Transitions
- ○ Estimation of the Transition Parameter
- ○ Write Field Gradient Limits on Transitions
- ○ Writing at High Transition Densities
- ○ Time-Domain Asymmetry and Overwrite
- ○ Readback Pulses and Transition Shape
- ○ Readback Pulse Shape and Head Geometry
- ○ Pulse Interference and Amplitude Spectra
- ○ Pulse Shape Influence on Complex Data Patterns
- ○ Pulse Shape Influence on Peak Shift
- ○ Head and Medium Noises
- ○ Influence of Noise and Interference on Error Rate

IEEE TRANSACTIONS ON MAGNETICS, VOL. MAG-19, NO. 5, SEPTEMBER 1983
(p.1600-1604)

OBSERVATION OF RECORDED MAGNETIZATION PATTERNS BY ELECTRON HOLOGRAPHY

K. Yoshida, T. Okuwaki, N. Osakabe, H. Tanabe
Y. Horiuchi, T.Matsuda, K.Shinagawa
A. Tonomura and H. Fujiwara.

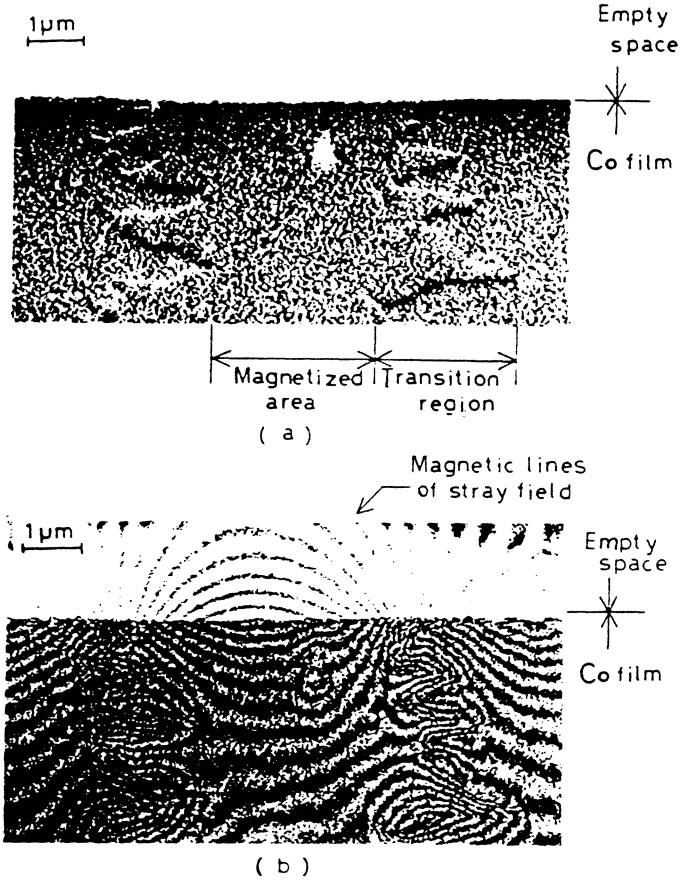

Fig. 5. Recorded magnetization pattern on a Co film (film thickness=45nm, coercivity=27kA/m, saturation induction=1.1T). A bit length is 5μm. (a) Lorentz micrograph. (b) Interference micrograph.

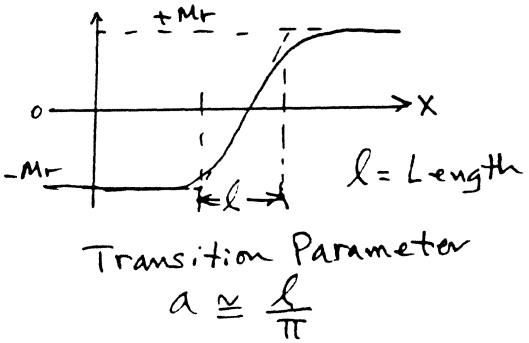

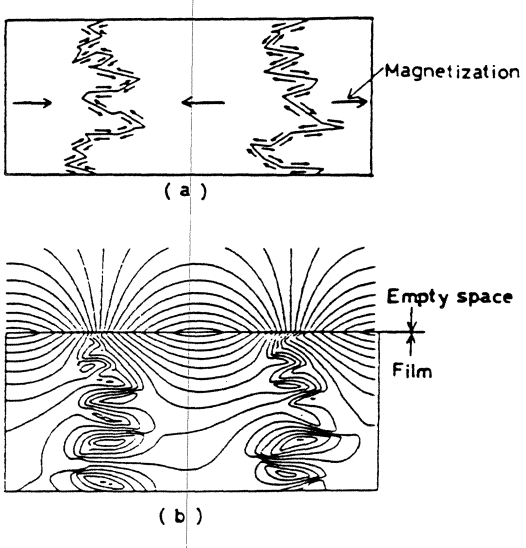

Fig. 6. Calculated interference image.
(a) Presumed magnetization distribution.
(b) Calculated interference image using the model of (a).

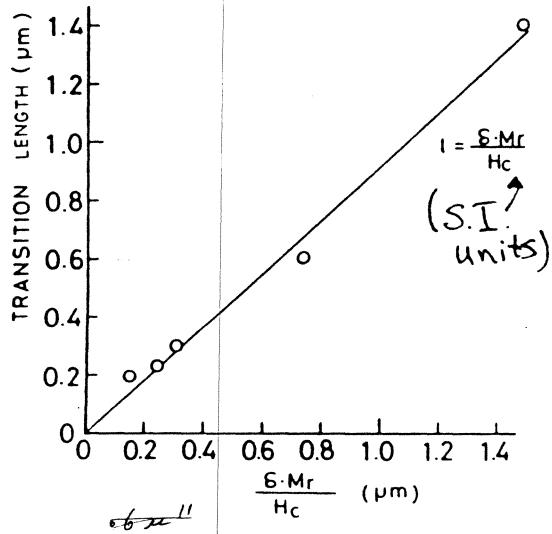

Fig. 7. Transition length as a function of $\delta M_r/H_c$.

IEEE TRANSACTIONS ON MAGNETICS, VOL. MAG-22, NO. 5, SEPTEMBER 1986 (p.889-891)

Zigzag Transition Profiles, Noise, and Correlation Statistics in Highly Oriented Longitudinal Film Media

by

T. C. Arnoldussen

H. C. Tong

International Business Machines Corporation
General Products Division
San Jose, California

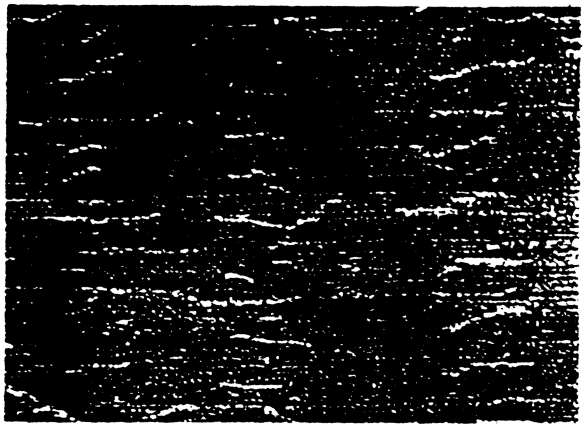

Figure 1: Lorentz micrograph of 300 fr/mm track. Track direction is left to right.

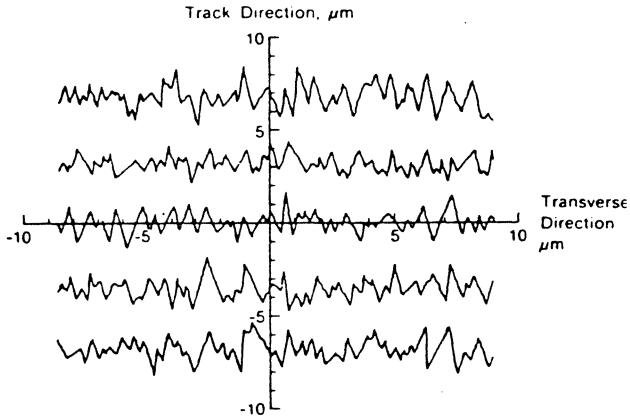

Figure 2: Digitized zigzags.

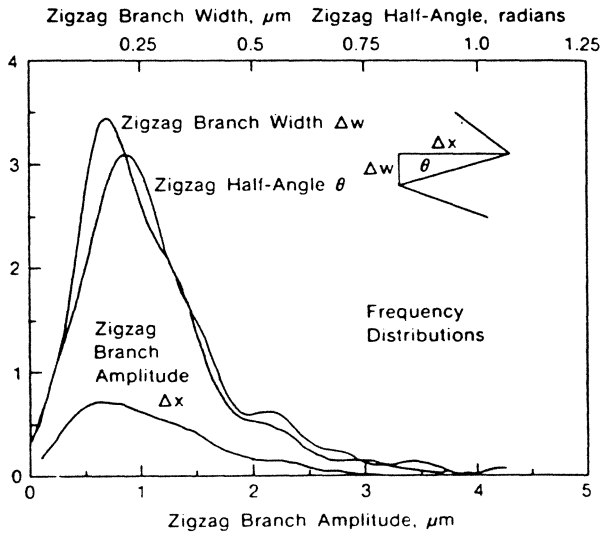

Figure 5: Zigzag dimensional distributions.

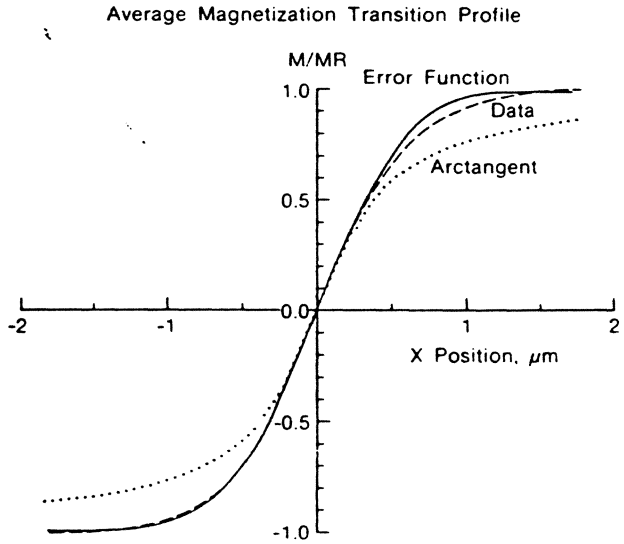

Figure 3: Composite magnetization transition profile.

ROS CAMP CURVE USED TO MODEL

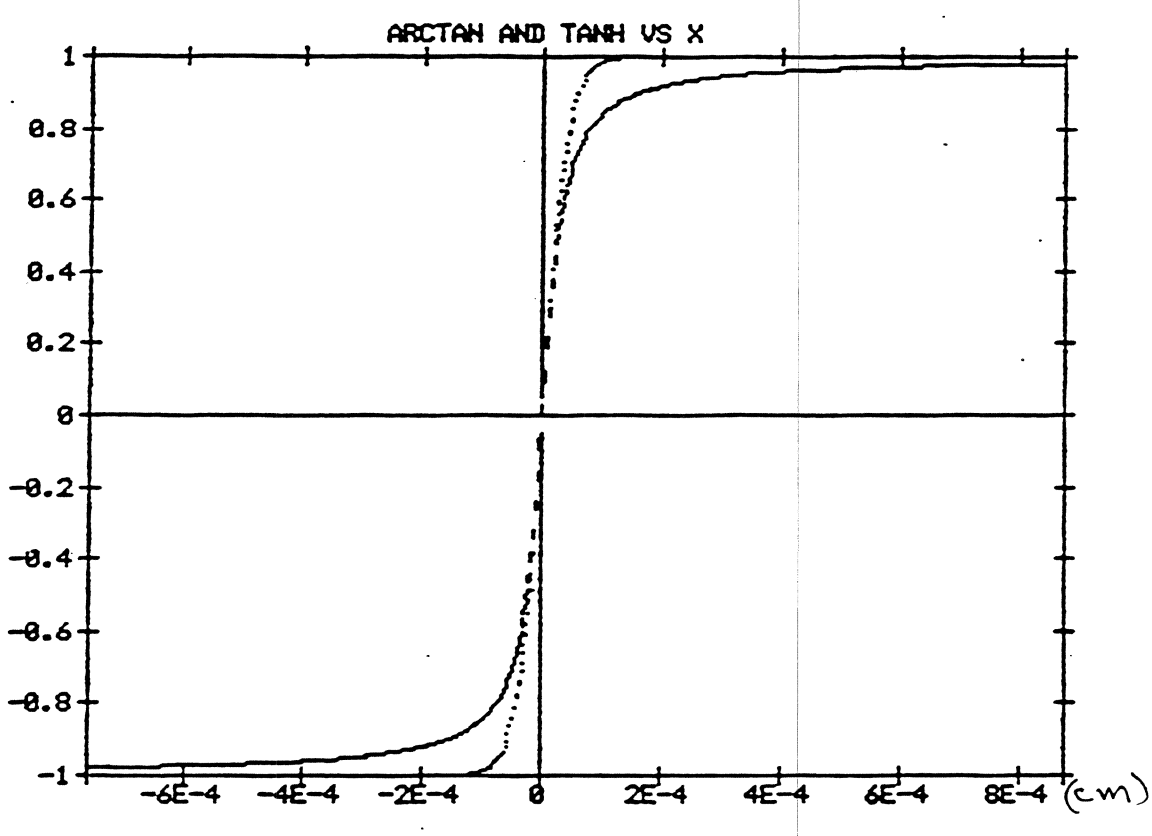

$a = 0.253\,\mu$

$$\frac{2}{\pi}\tan^{-1}\left(\frac{x}{a}\right) \quad \& \quad \tanh\left(\frac{2x}{\pi a}\right)$$

THE WRITTEN TRANSITION

Ref.: M.L. Williams & R.L. Comstock, PROC. A.I.P. Conf. on Magnetism & Magnetic Materials, 1971.

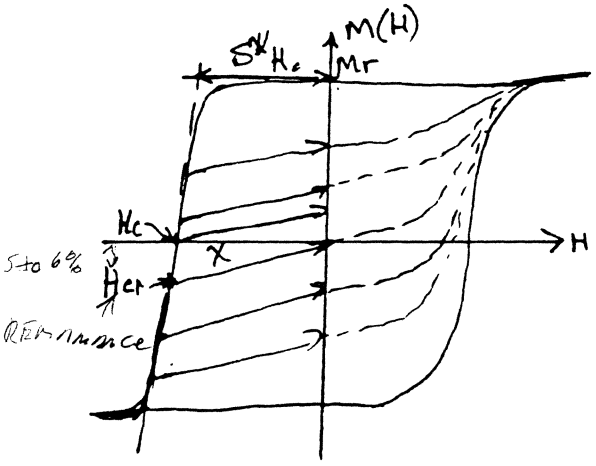

$$\left.\frac{dM}{dx}\right|_{x=0} = \frac{dM}{dH}\left(\frac{dH_h}{dx} + \left.\frac{dH_d}{dx}\right|_{H=H_{cr}}\right)$$

① $M(x) = \frac{2M_r}{\pi}\tan^{-1}\left(\frac{x}{a}\right)$

② Demagnetizing Field Gradient

$$\left.\frac{dH_d}{dx}\right|_{H=H_{cr}} = -\frac{4M_r\delta}{a_1^2}$$

(δ = magnetic film thickness)

Intermediate Transition:

$$\frac{a_1}{r} = \frac{y(1-S^*)}{\pi Q} + \left\{\left[y(1-S^*)/\pi Q\right]^2 + (2M_r\delta/H_c)(2y/Q_r)\right\}^{1/2}$$

$$r = 1 - \chi(1-S^*)H_c/M_r, \quad \chi = M_r/4H_c$$

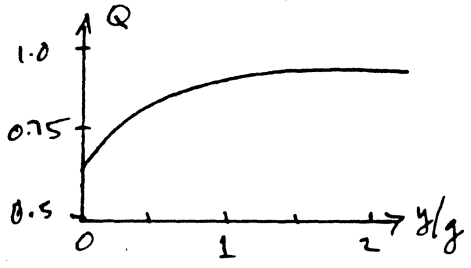

Assumes $\frac{dH_h}{dx}$ is at maximum

$\therefore \frac{dH_h}{dx} = Q\frac{H_c}{y_r}$

↑ SPACING FROM GAP &

Final Transition:

$$a_2 = \frac{a_1}{2r} + \left[(a_1/2r)^2 + 2\pi\chi\delta a_1/r\right]^{1/2}$$

$a_2 > a_1$ (i.e. transition broadens after leaving write field)

Head-Limited Transition:

$$a_h = \frac{H_c}{\frac{dH_h}{dx}} \quad (\text{at } H_x = H_{cr})$$

E. Williams
12/7/91

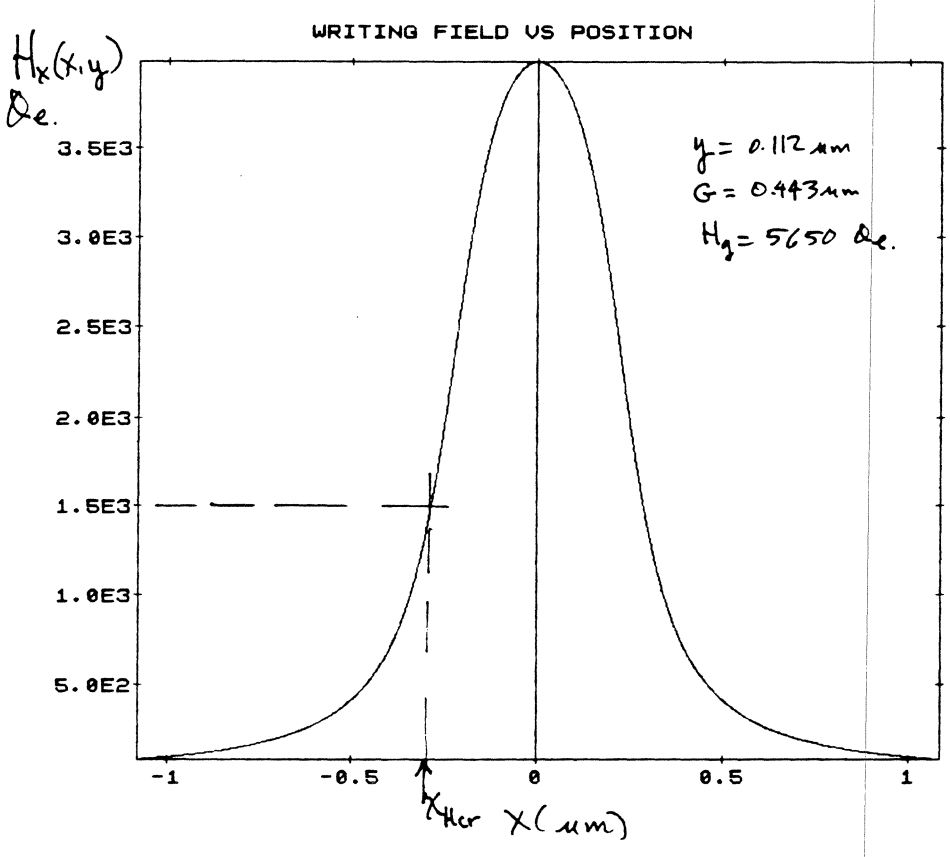

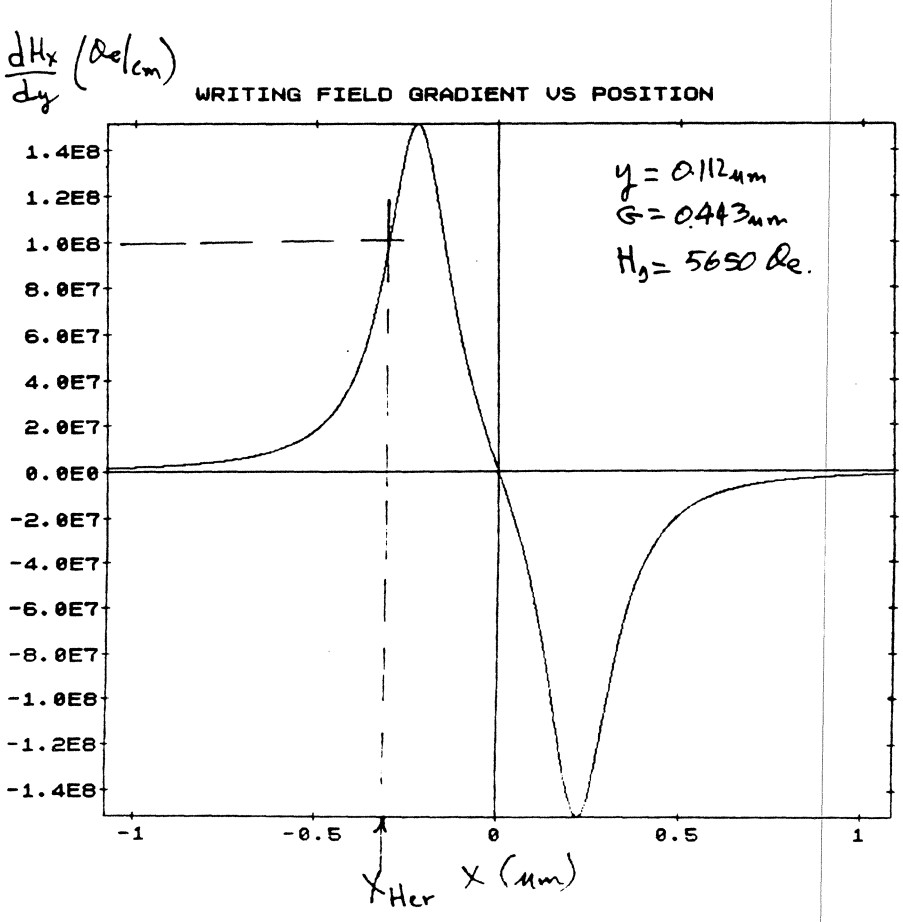

E M Williams
12/7/91

Transition Parameter vs Coercivity

Write Gradient and Medium-limited

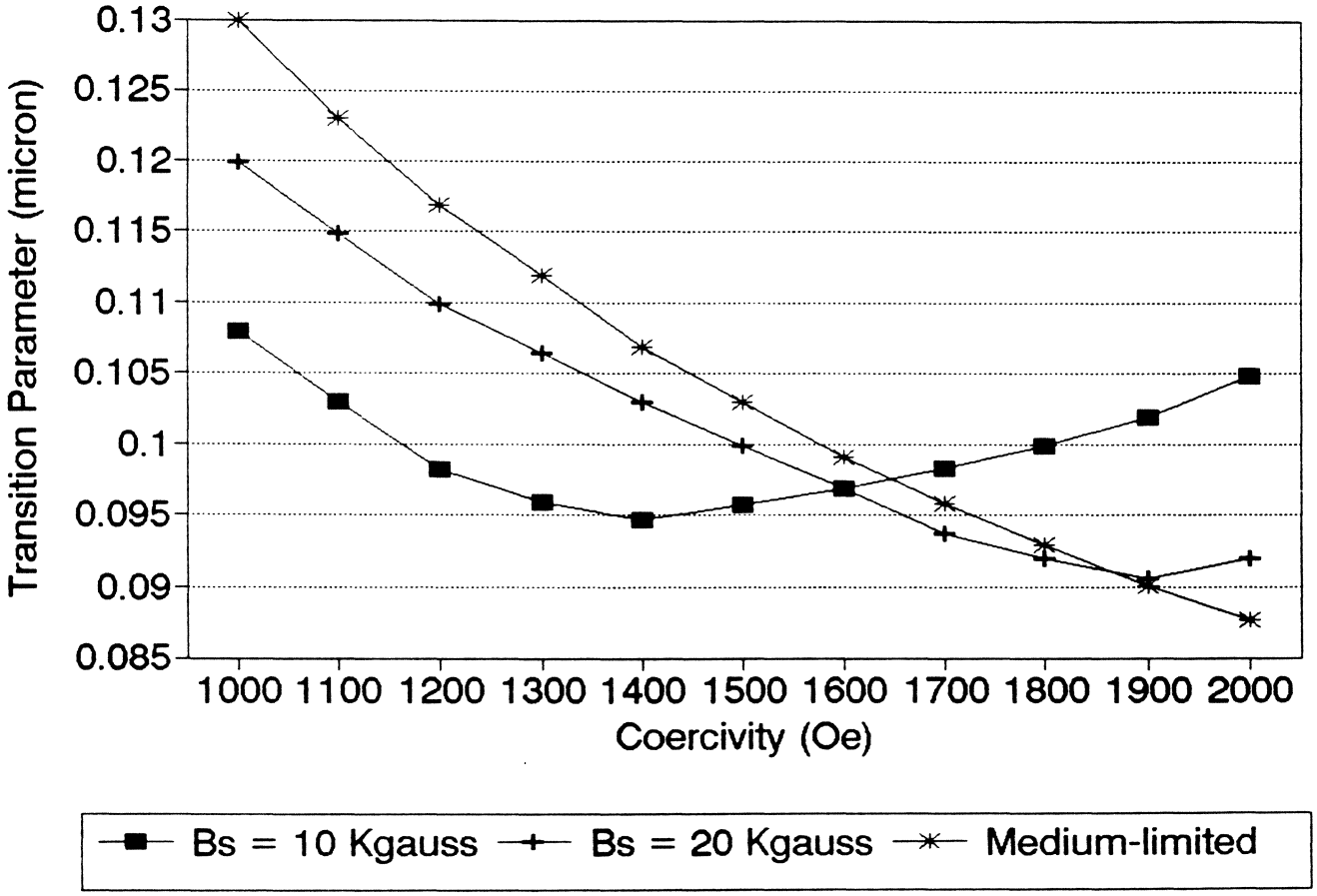

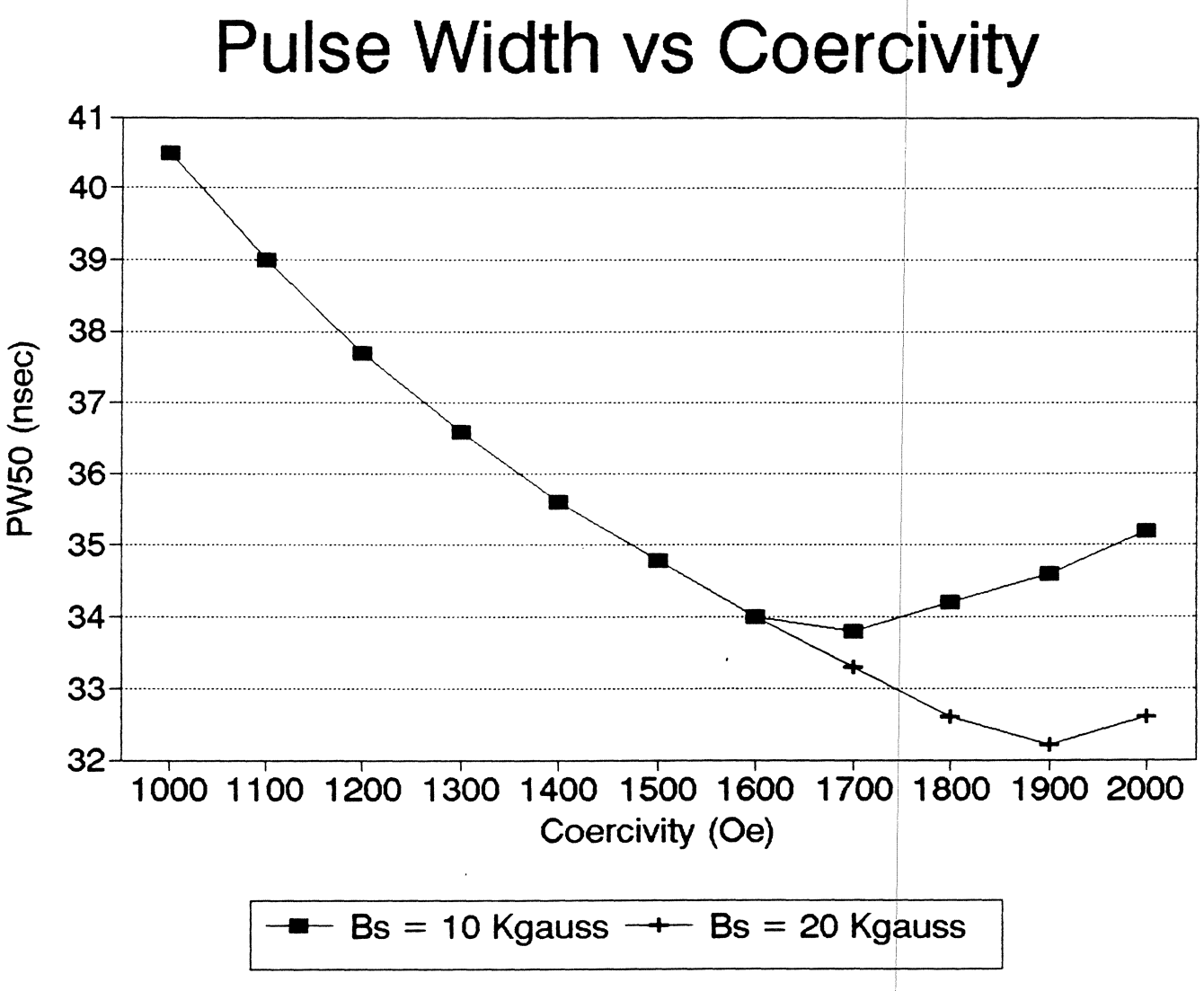
Pulse Width vs Coercivity
PW50 (nsec)
41
40
39
38
37
36
35
34
33
32
1000 1100 1200 1300 1400 1500 1600 1700 1800 1900 2000
Coercivity (Oe)
Bs = 10 Kgauss
Bs = 20 Kgauss

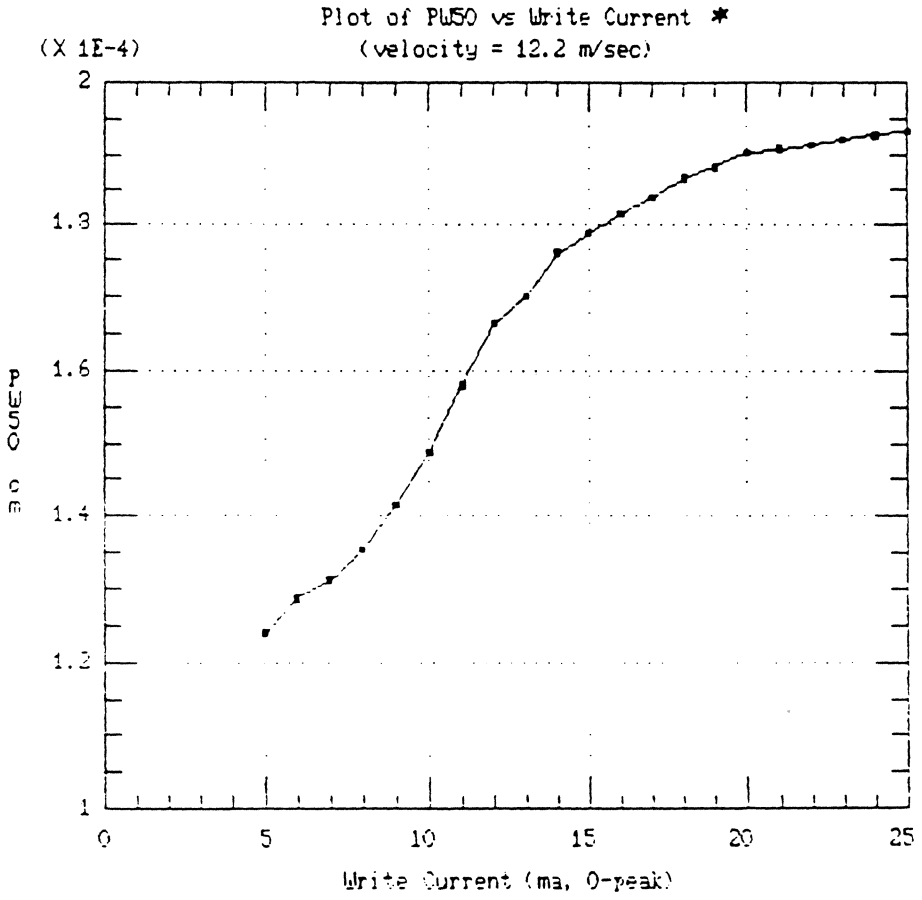

Thin Film Head : P1/G/P2 ≅ 3.2/0.5/3.2 μm ; 32 turns

Thin Film Disk: M_r = 750 emu/cc ; H_c = 1100 Oe ;
δ = 650 Å ; S^* = 0.90
overcoat = 350 Å

Fly Height ≅ 0.225 μm

* Head over-lapped: throat ≈ 1.53 μm
to demonstrate
gradient limitations

E. M. Williams
Read-Rite Corp.

19/24

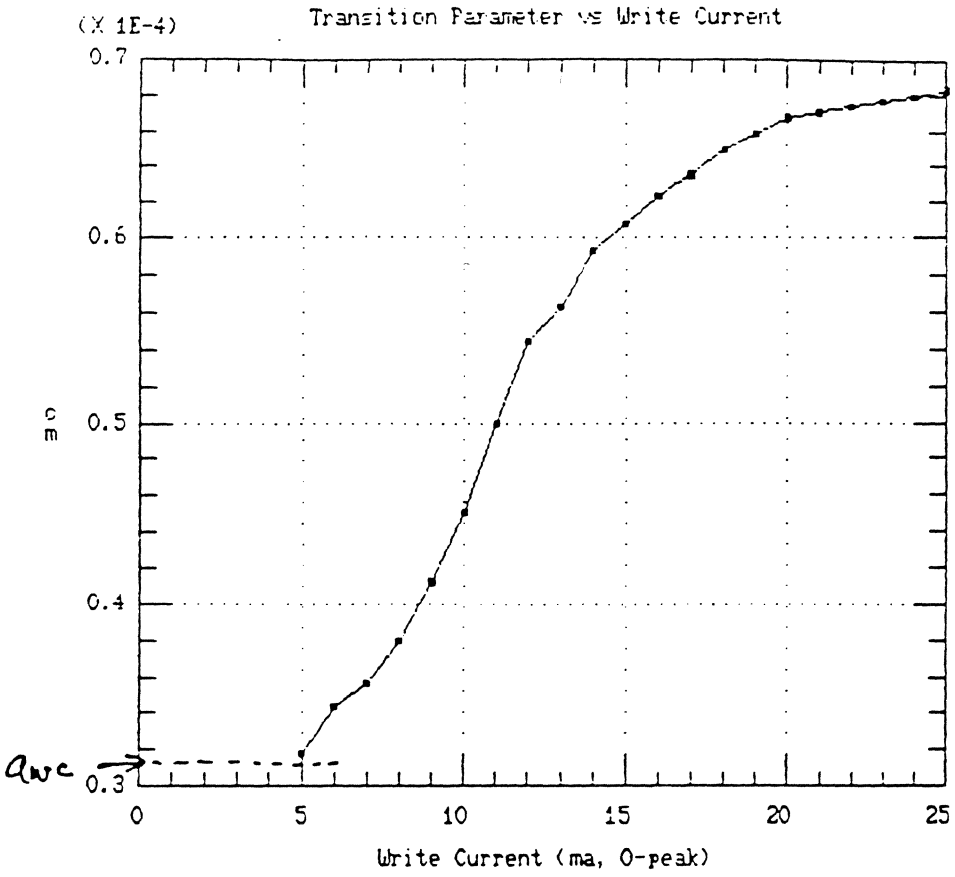

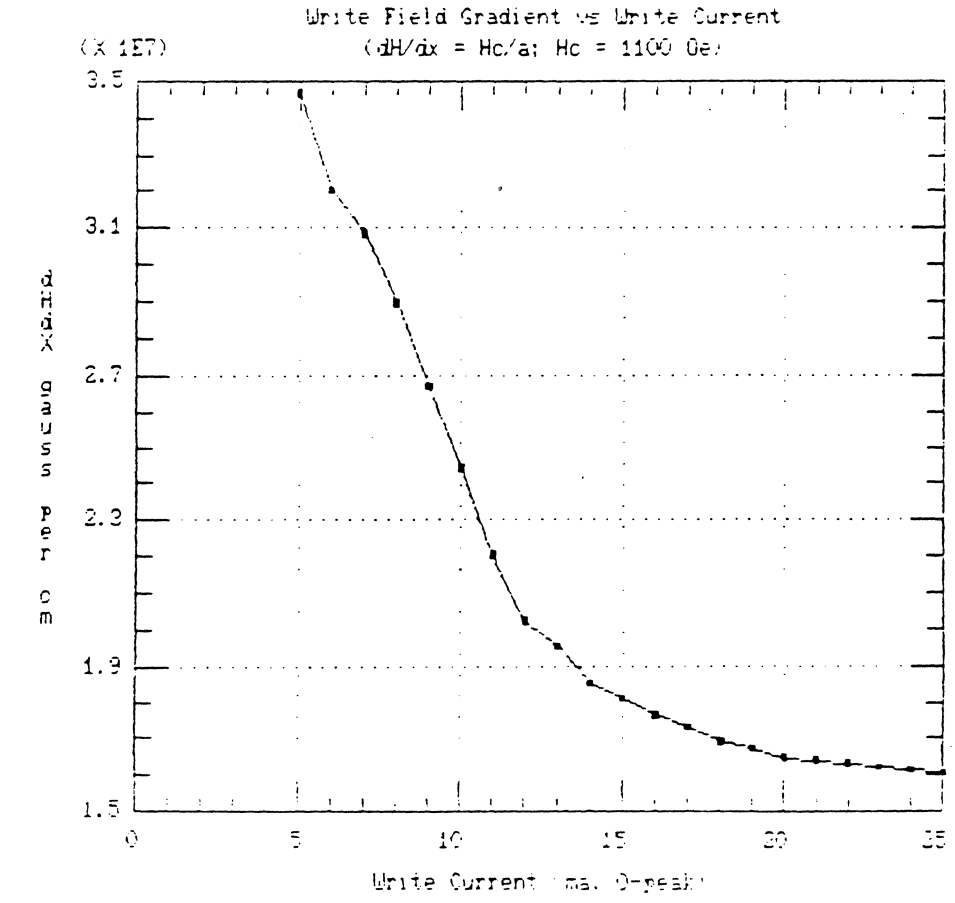

Deconvolved Parameter:

$$a = \left[\frac{PW50^2 - g^2}{4}\right]^{1/2} - d$$

d = fly. ht.

Medium-limited transition parameter (Williams-Comstock):

$a_{wc} \simeq 0.31$ μm

Gradient is computed from experiment, under the assumption that transition parameter is limited by head field gradient.

"a" is the deconvolved value

E.M. Williams
Read-Rite Corp.
2/0/24

WRITING AT HIGH TRANSITION DENSITIES

○ Partial erasure of previously written transitions (sometimes called "non-linear writing effects").

○ Writing occurs near the trailing edge of the gap.

○ Gap edge saturation exacerbates partial erasure effects (writing field spreads and write gradient decreases).

○ Transition Density

$$\text{Density} = 1/(T_{min} \times \text{Velocity})$$

○ Partial erasure of previous transition is likely if

$$\text{Density} \approx 2/G \qquad (G = \text{gap length})$$

$$\text{or} \quad T_{min} \approx G/(2 \times \text{Velocity})$$

○ Simple Example:

Velocity = 6 meters/sec (236 in/sec)

G = 0.40 μm

For $T_{min} \approx$ 33 nsec, partial erasure may occur.

○ Effective gap length increases when writing with excessive write current.

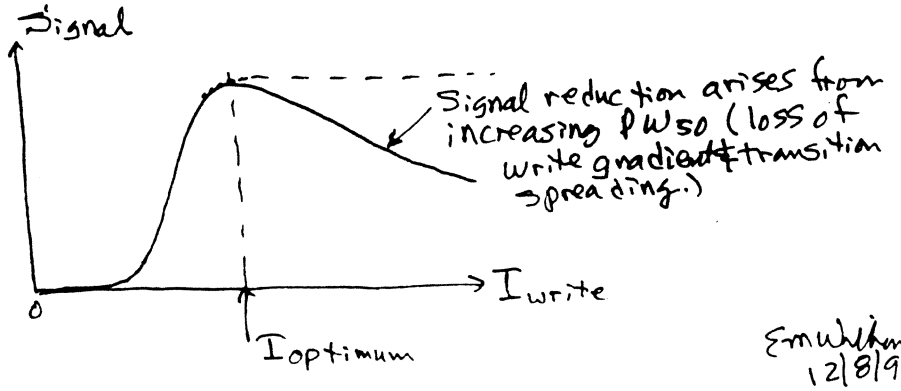

Em Williams
12/8/91

TIME-DOMAIN NATURE OF OVERWRITE

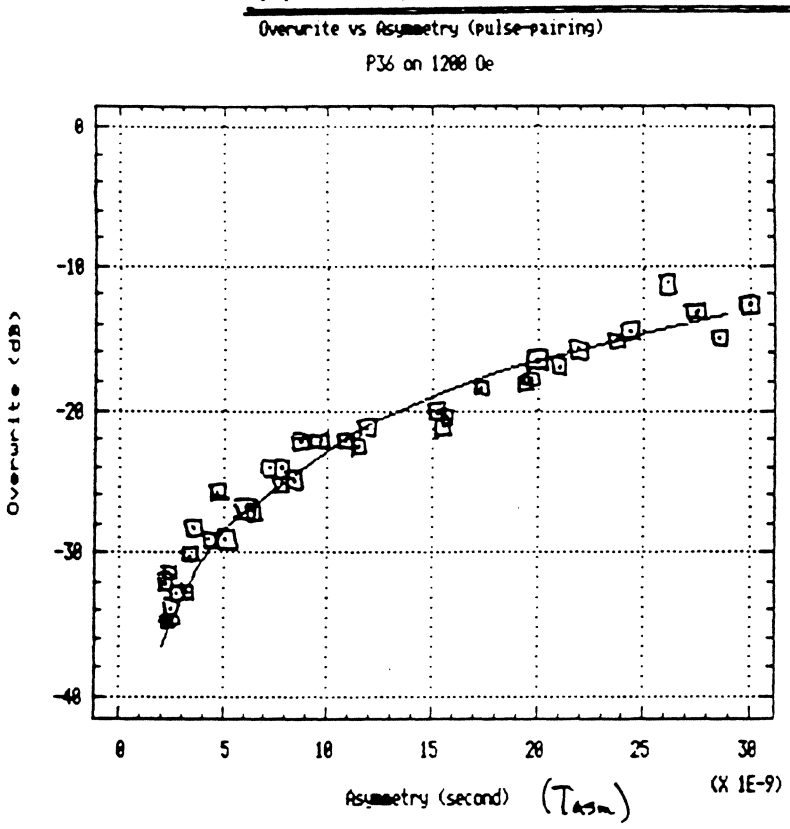

(pulse-pairing)

⊡-⊡ R&D Gazik Experiments at Read-Rite

—— Computed from $OW = 20\log\sin\phi$
5 MHz ; T_0 = 4ns ; H_c = 1200 Oe
R = 0.45 (95%) ; $T_{asm} = 4T_{wo}$

$$OW(dB) = 20\log_{10}\left(\frac{\pi f \cdot R \cdot T_{asm}}{2}\right)$$

E. M. Williams
6/14/88
Read-Rite

$$\text{Write-induced Phase-shift} = T_{wo} = \frac{T_{asym}}{4}$$

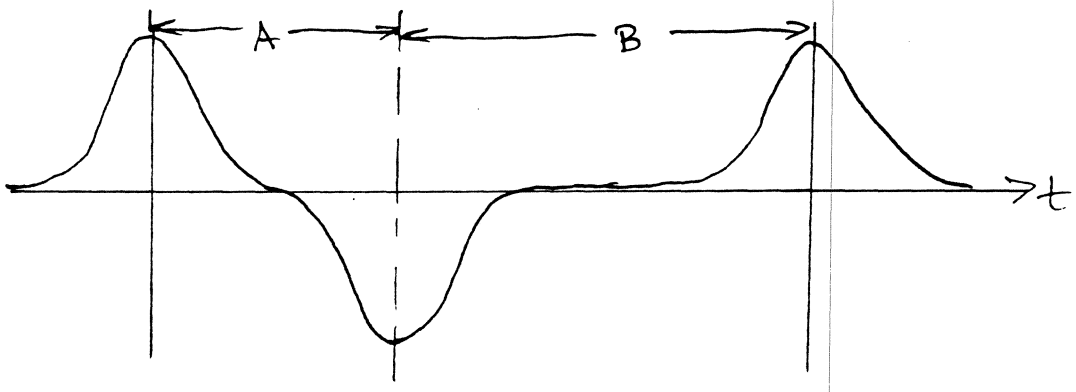

$T_{asym} \triangleq B - A$

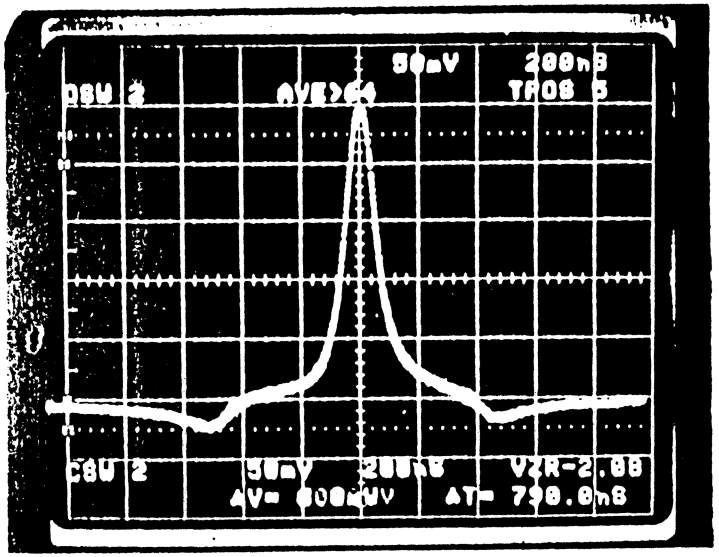

M38 #415403-137 on Delta 1100 ; 300 in/sec
Filter 2 (20 MHz)

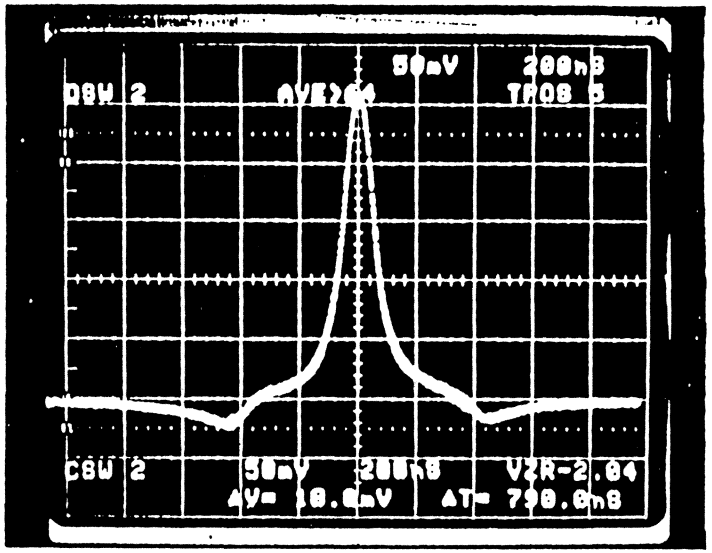

M38 #415984-369 on Delta 1100 ; 300 in/sec
Filter 2 (20 MHz)

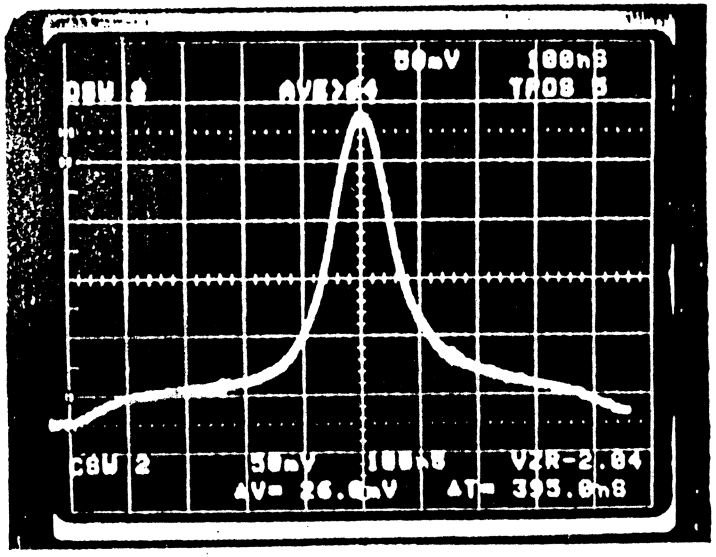

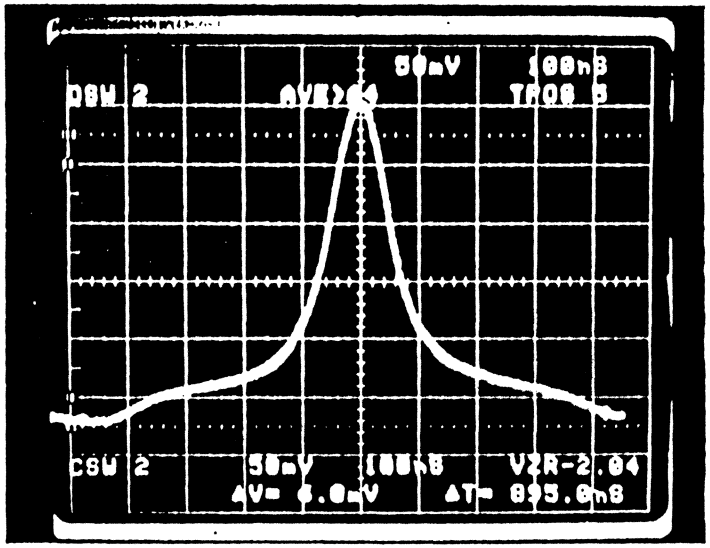

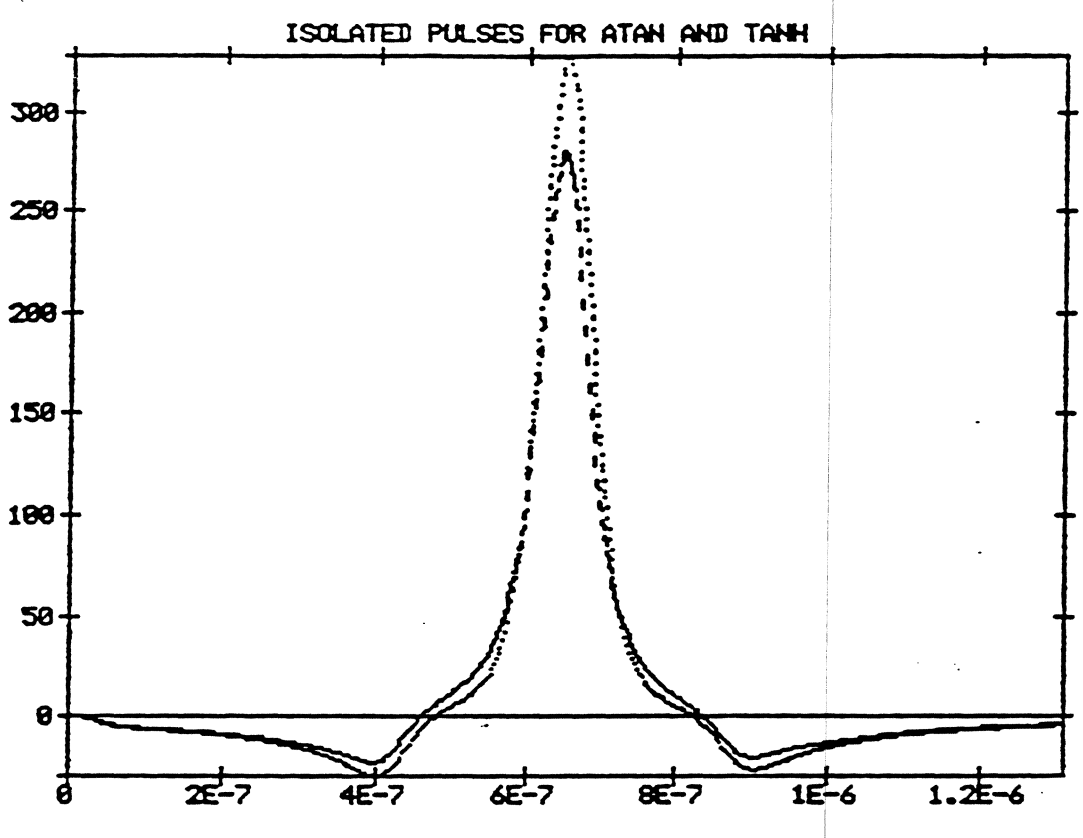

	$\frac{2}{\pi}\tan^{-1}\left(\frac{x}{a}\right)$	$\tanh\left(\frac{2x}{\pi a}\right)$	TFH Experiment
PW50	1.02 mm	1.06 mm	1.03 mm
PW25	1.70	1.61	1.61
PW10	2.70	2.33	2.66
$PW50/PW25$	0.60	0.66	0.65
$PW50/PW10$	0.38	0.46	0.43

See also Noyan et al, ~~IEEE~~ Trans. Magn., MAG-24, 1811-1813, Mar (1988).

Middleton, B.K, ~~IEEE~~ Trans. Magn., MAG-27, 3563-3569, Jul (1991).

E M Williams
12/7/91

Isolated Pulses vs Time

F1/6/F2: TFH and Ferrite Geometries

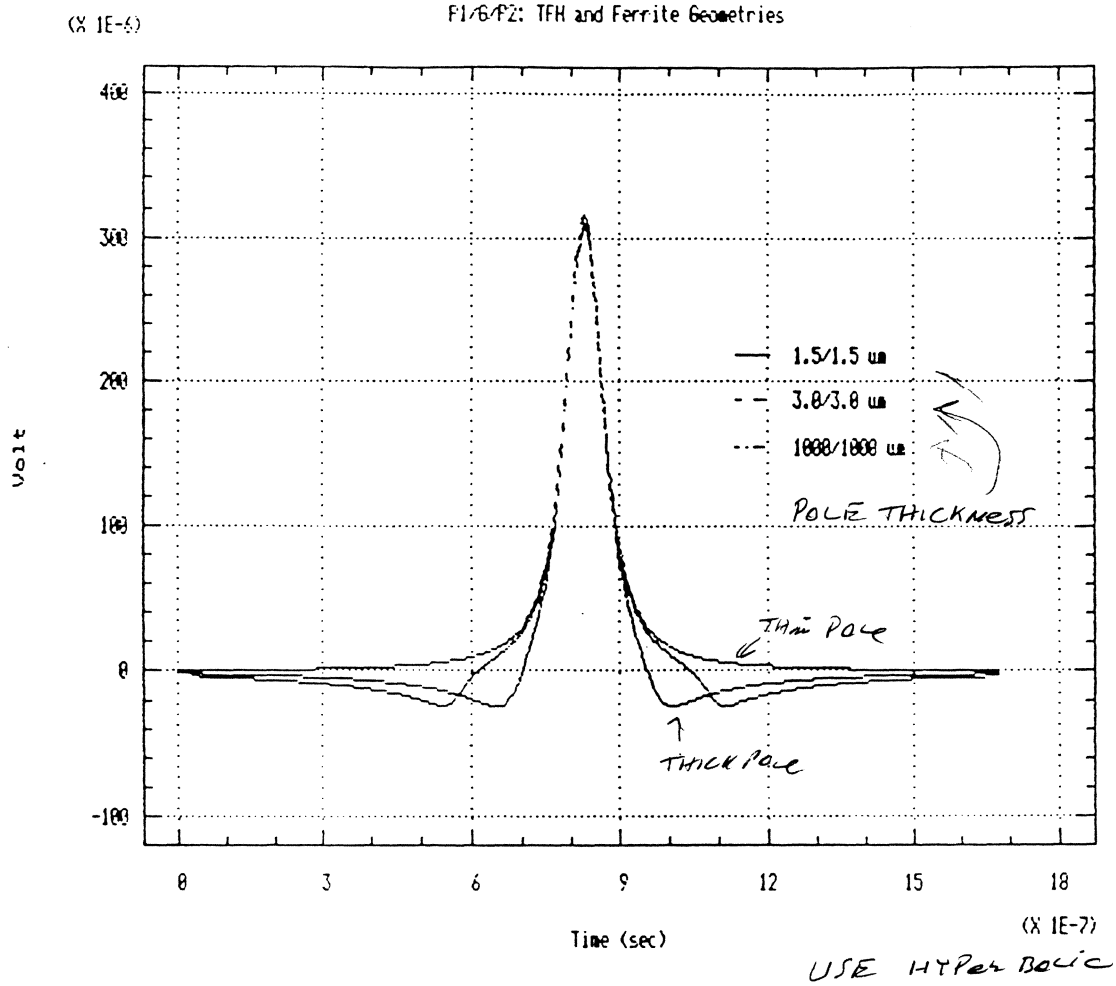

PW50 = 92 nsec

V = 1200 cm/sec

USE HYPER BOLIC TANGENT FOR MODELING NOT ARCTANGENT

Normalized Signal vs Linear Density
Poles: Inf.; 4.5; 3; 1.5 um

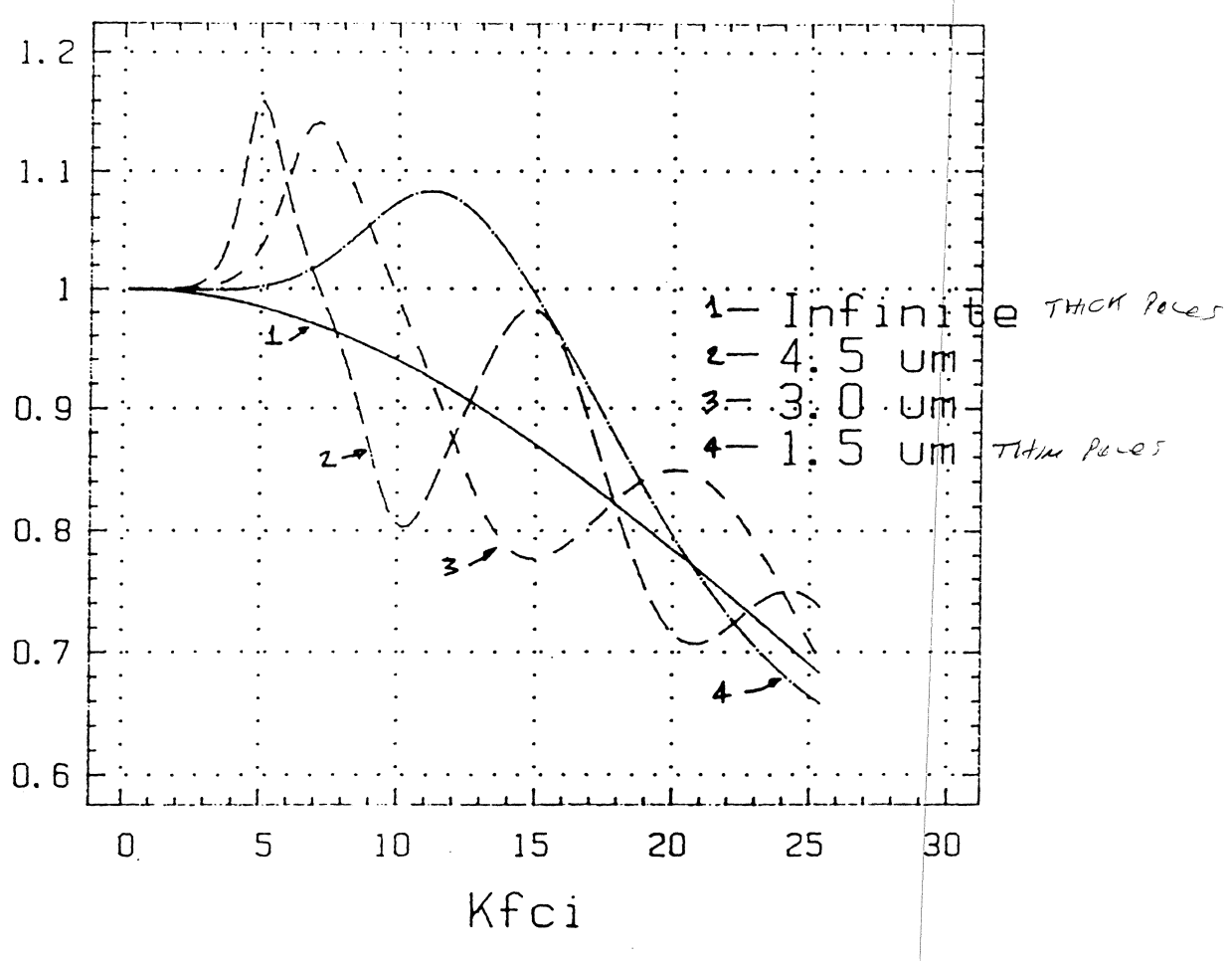

Normalized Signal vs Density
(Thin, Thick, Asymmetric Poles)

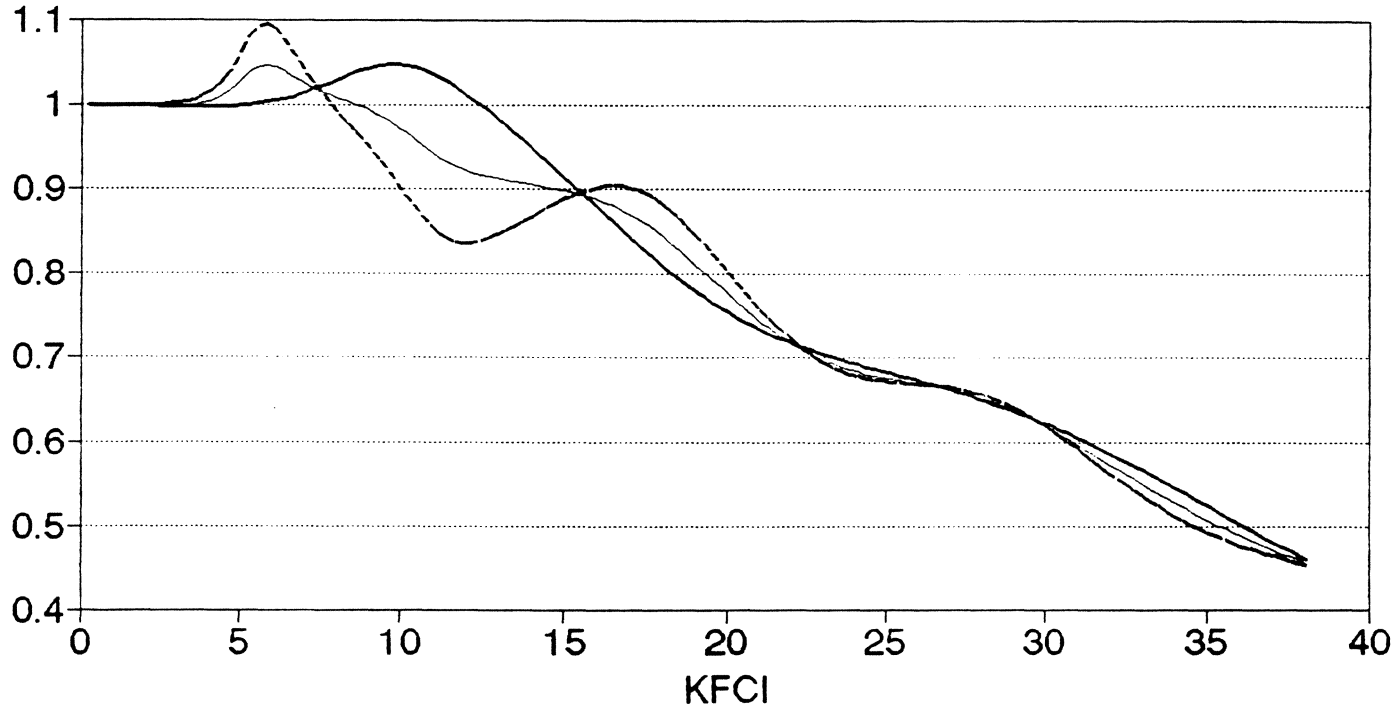

—— P1/P2 = 2/2 micron ····· P1/P2 = 4/4 micron —— P1/P2 = 2/4 micron

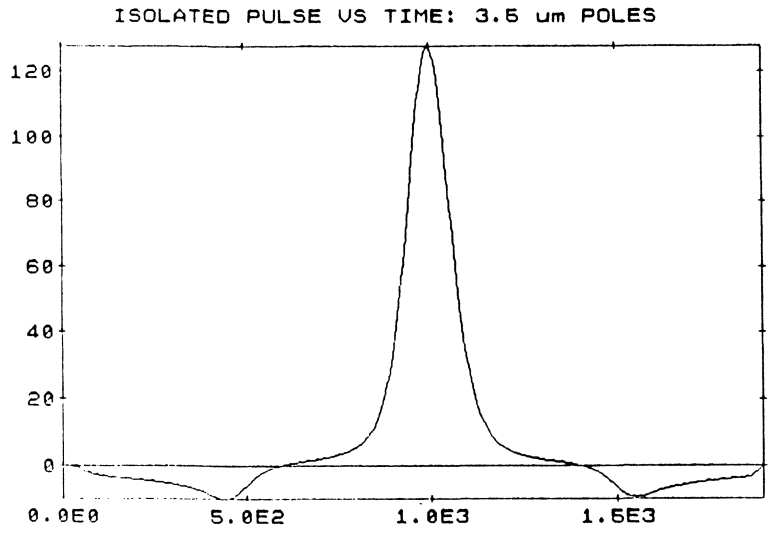
ISOLATED PULSE VS TIME: 3.5 um POLES
120
100
80
60
40
20
0
0.0E0
5.0E2
1.0E3
1.5E3

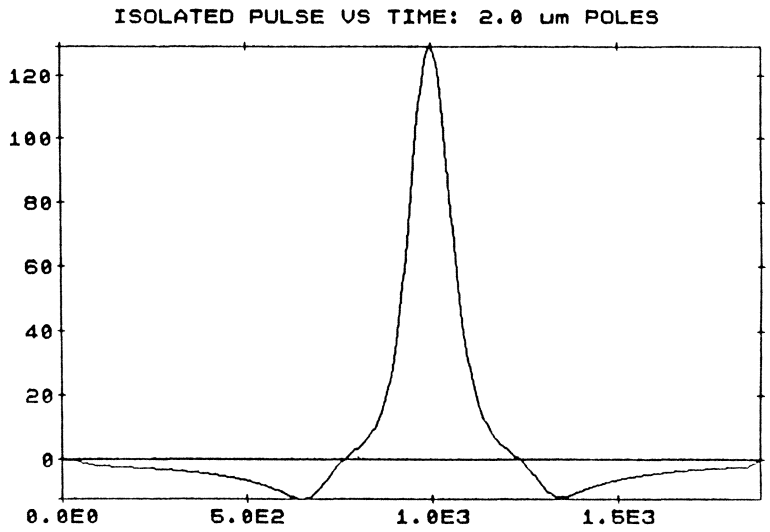
ISOLATED PULSE VS TIME: 2.0 um POLES
120
100
80
60
40
20
0
0.0E0
5.0E2
1.0E3
1.5E3

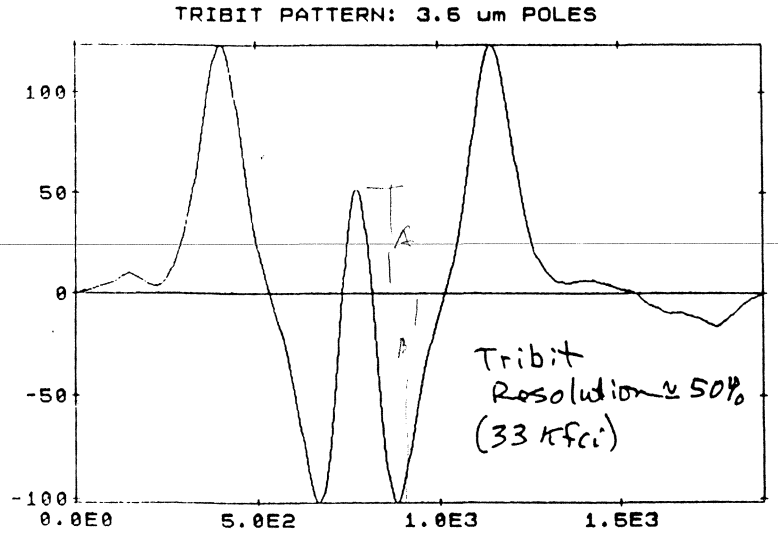
TRIBIT PATTERN: 3.6 um POLES
100
50
0
-50
-100
0.0E0
5.0E2
1.0E3
1.5E3
Tribit
Resolution ≃ 50%
(33 kfci)

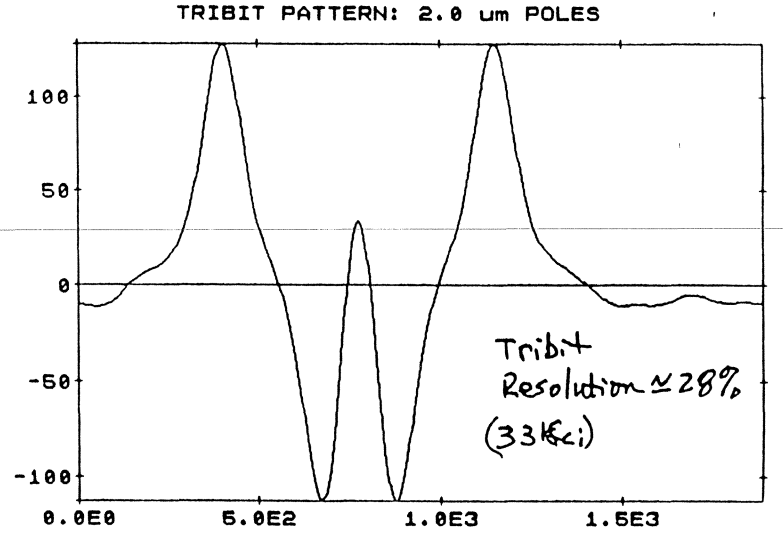
TRIBIT PATTERN: 2.0 um POLES
100
50
0
-50
-100
0.0E0
5.0E2
1.0E3
1.5E3
Tribit
Resolution ≃ 28%
(33 kfci)

E M Williams

Dibit Peakshift vs Linear Density

(X 1E-9) P1/G-P2: TFH and Ferrite Pole Geometries (2,7) RLL

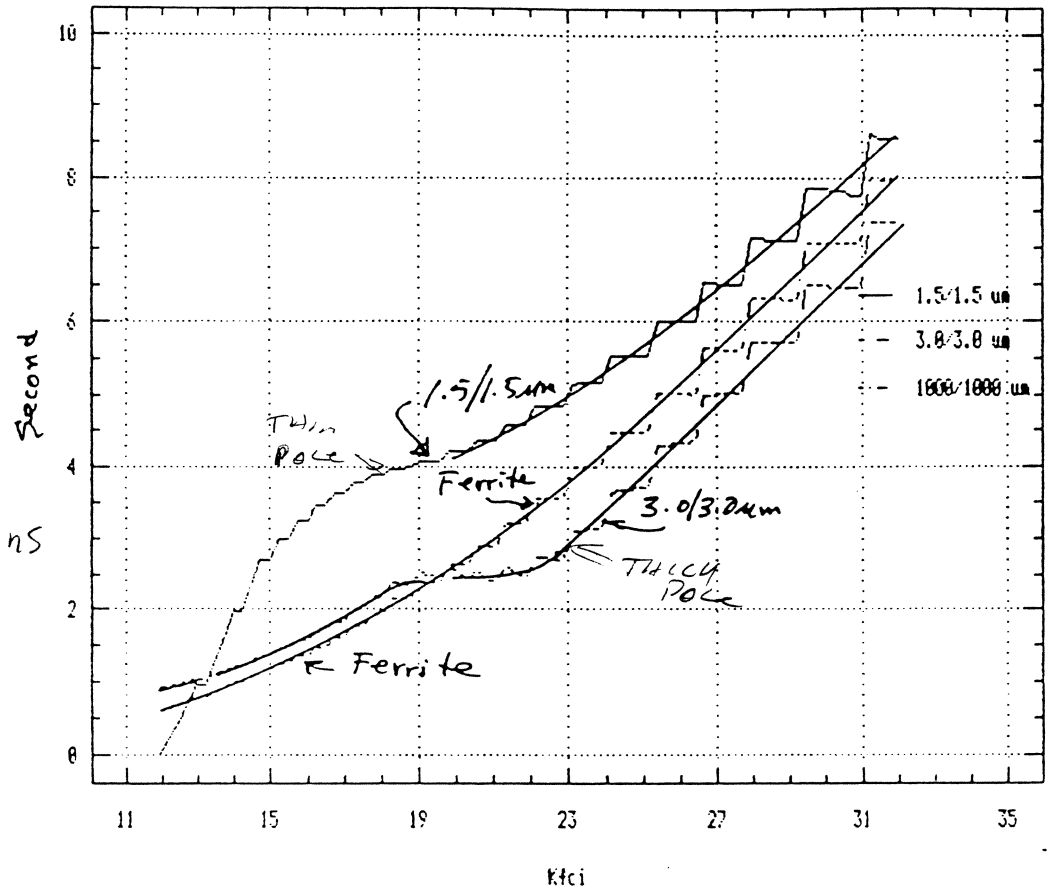

Velocity = 1200 cm/sec

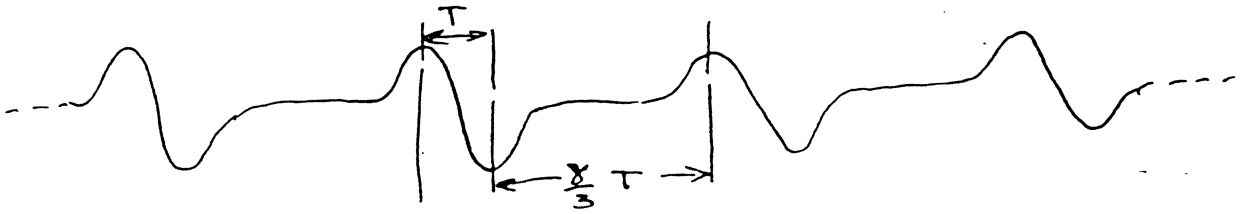

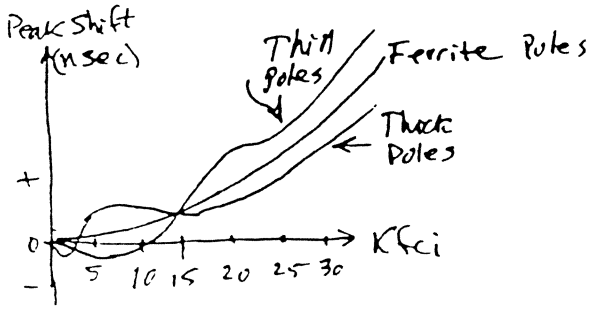

E M Williams

Random Data IBM encoded

Window = ± 27.8 nsec (43.7 Kbpi ; 12 Mb/sec)

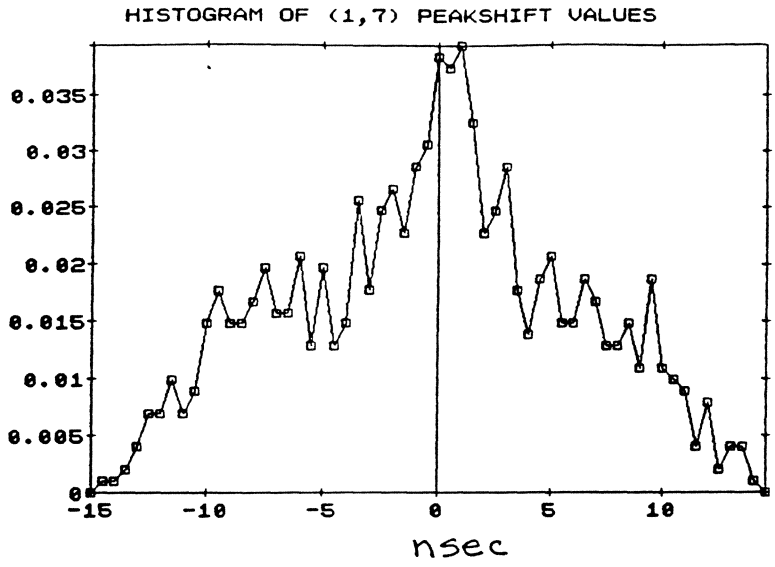

P1|G|P2
3.5/0.40/3.5 um
THICK POLE

931 transitions
$\bar{x}$ = -0.41 nsec
σ = 6.19 "
Max = 14.8 "
Min = -14.6 nsec

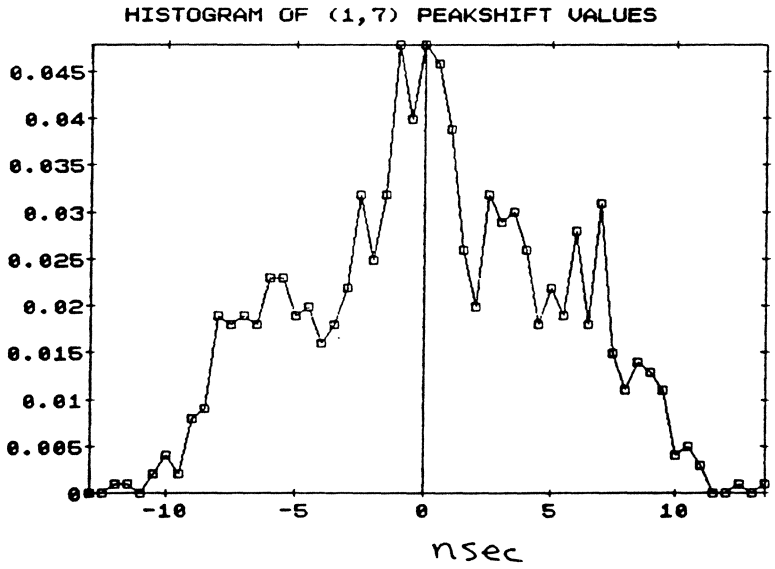

P1|G|P2
2.0|0.4|2.0 um
THIN POLE
929 transitions
$\bar{x}$ = 0.102 nsec
σ = 4.88 "
Max = 13.3 "
Min = -12.5 nsec

REMOVE UNDER SHOOT

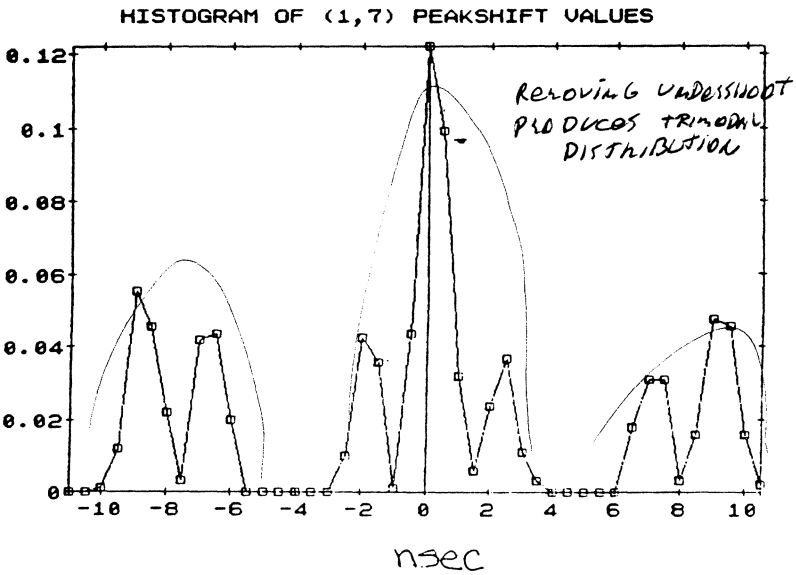

P1|G|P2
∞/0.40/∞ um
927 transitions
$\bar{x}$ = -0.31 nsec
σ = 5.82 "
Max = 10.2 "
Min = -10.0 nsec

E Williams

Head, Preamp & Medium Noises

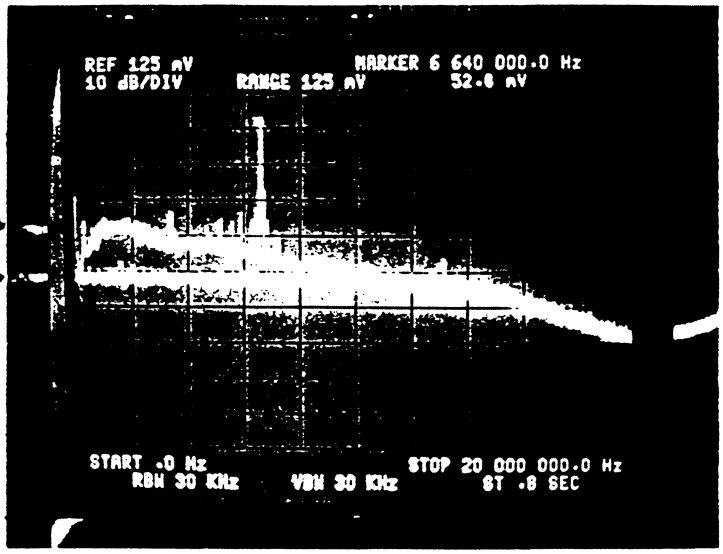

TRANSITION NOISE

$5.8 \frac{nV}{\sqrt{Hz}}$

$1.1 \frac{nV}{\sqrt{Hz}}$

Disk "A" (Thin Film)

28 Kfci

Signal ≅ 190 mV (p-p)

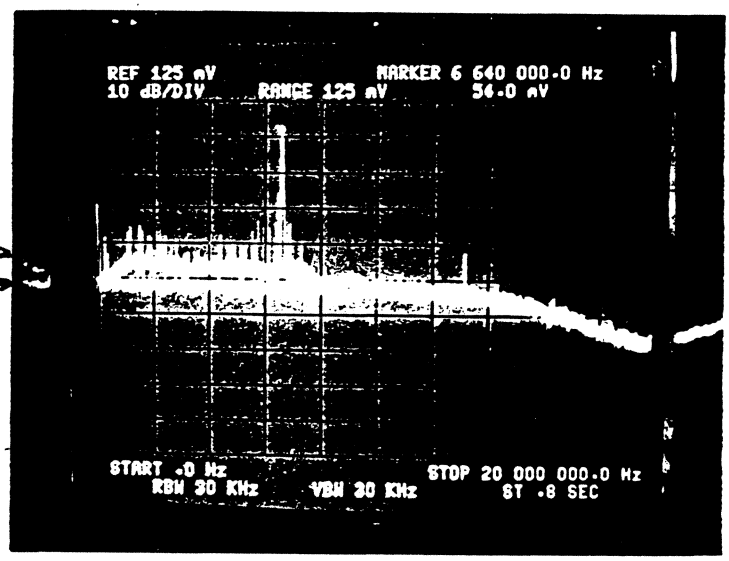

$2.5 \frac{nV}{\sqrt{Hz}}$

$1.1 \frac{nV}{\sqrt{Hz}}$

INTRINSIC

Disk "B" (Thin Film)

28 Kfci

Signal ≅ 194 mV (p-p)

Head Noise Spectral Density $N_h \approx 0.56$ nV/$\sqrt{Hz}$

Preamp " " " $N_p \simeq 0.95$ nV/$\sqrt{Hz}$

Head + Preamp = $[N_h^2 + N_p^2]^{1/2} \simeq 1.1$ nV/$\sqrt{Hz}$

$$E.R. = 1 - erf(z) = erfc(z) ,$$
$$where\ z = SNR\frac{T_W}{PW50} .$$

If $T_{asym} = 0$ & ISI shift $= 0$, then

$$T_W = T_{WSNR} = \frac{4.57\ PW50}{SNR} .$$

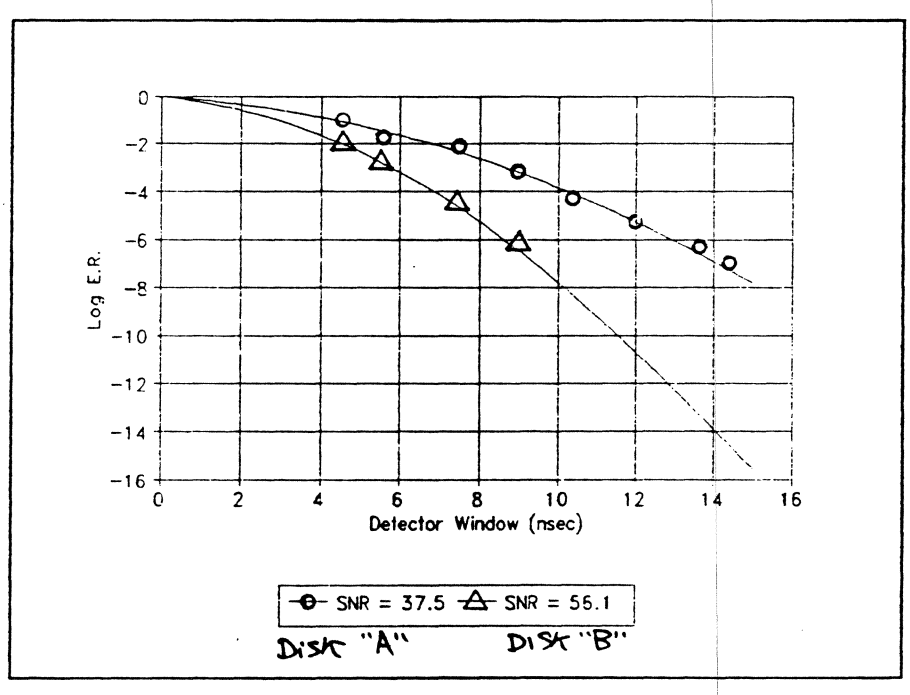

Figure 5: Log_{10} E.R. vs Detector Window Size

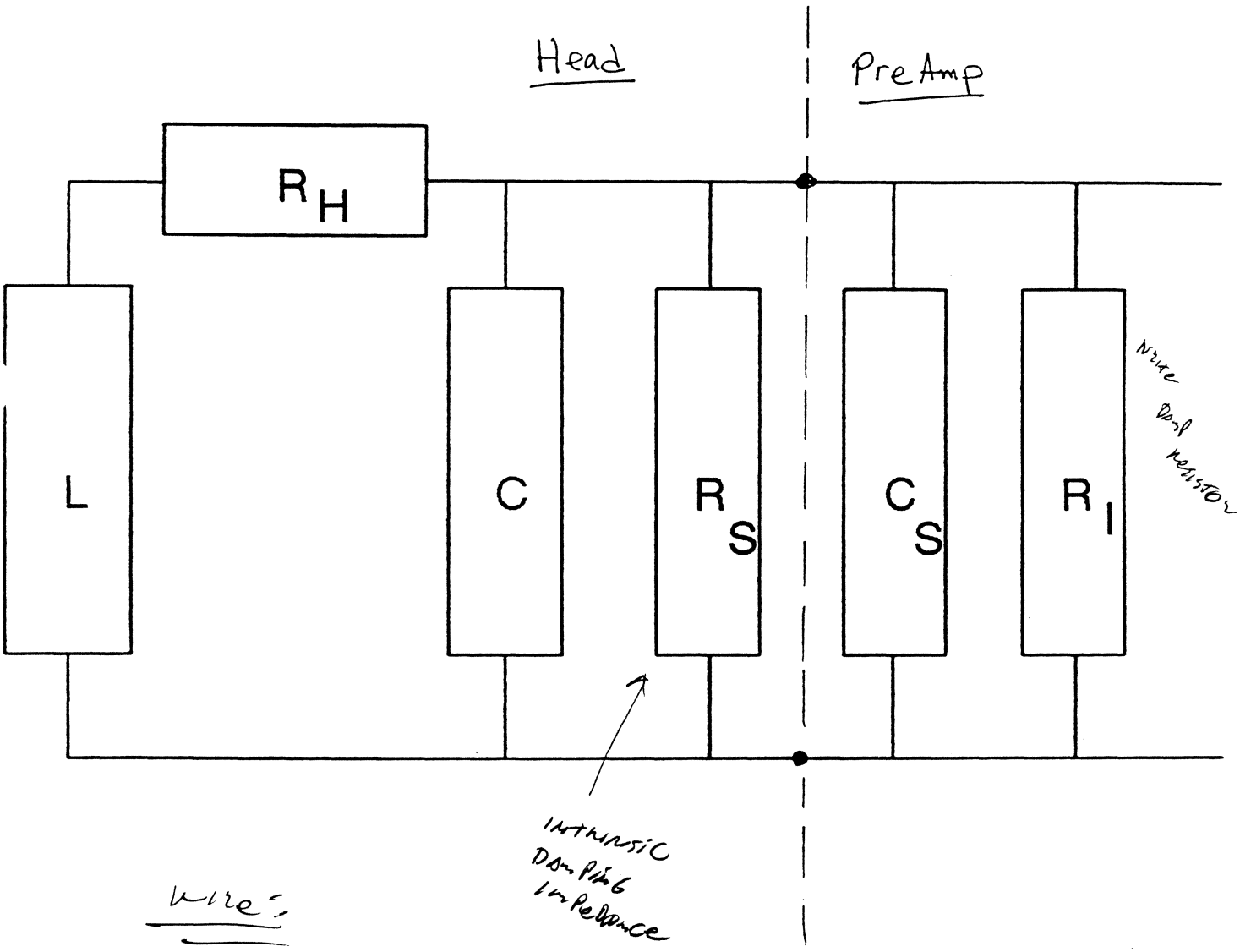

Wire:

20nH / ~~inch~~ cm Length

.8pF / cm of Length

E.M. Williams

Table 1: Electrical Properties of Inductive Heads

Head Type	$R_H(\Omega)$	$R_S(\Omega)$	L(nH)	C(pF)	f_R(MHz)
TFH (30-turn)	31.0	292	475	5.2	101.3
TFH (42-turn)	45.0	417	825	5.0	78.4
MIG (34-turn)	4.4	2805	1580	5.0	56.8
Mini-Composite	6.0	3410	4200	5.2	33.9
Mini-Monolithic	6.0	5410	14000	6.0	17.4

If a head is loaded by a preamplifier differential input resistance (R_I) and input capacitance (C_S), the real part of the total impedance is

$$Re[Z] = \frac{R_p}{D}[(R_H)(R_H+R_P) + (\omega L)^2], \quad (2)$$

where the terms R_P and D are defined by the relations

$$R_p = \frac{R_S R_I}{R_S+R_I} \quad (3)$$

$$D = [R_H+R_P-J(\omega^2)]^2+[F\omega]^2 \quad (4)$$

and F and J are given by

$$F = L + [R_H R_P(C+C_S)], \quad (5)$$

$$J = R_P L (C+C_S). \quad (6)$$

When a head is loaded by a preamp (assume R_I = 750Ω and C_S = 20 pF), Re[Z] changes substantially; Figure 2 is a plot for the heads in Table 1, and resonant frequencies are reduced by the input capacitance of the preamp.

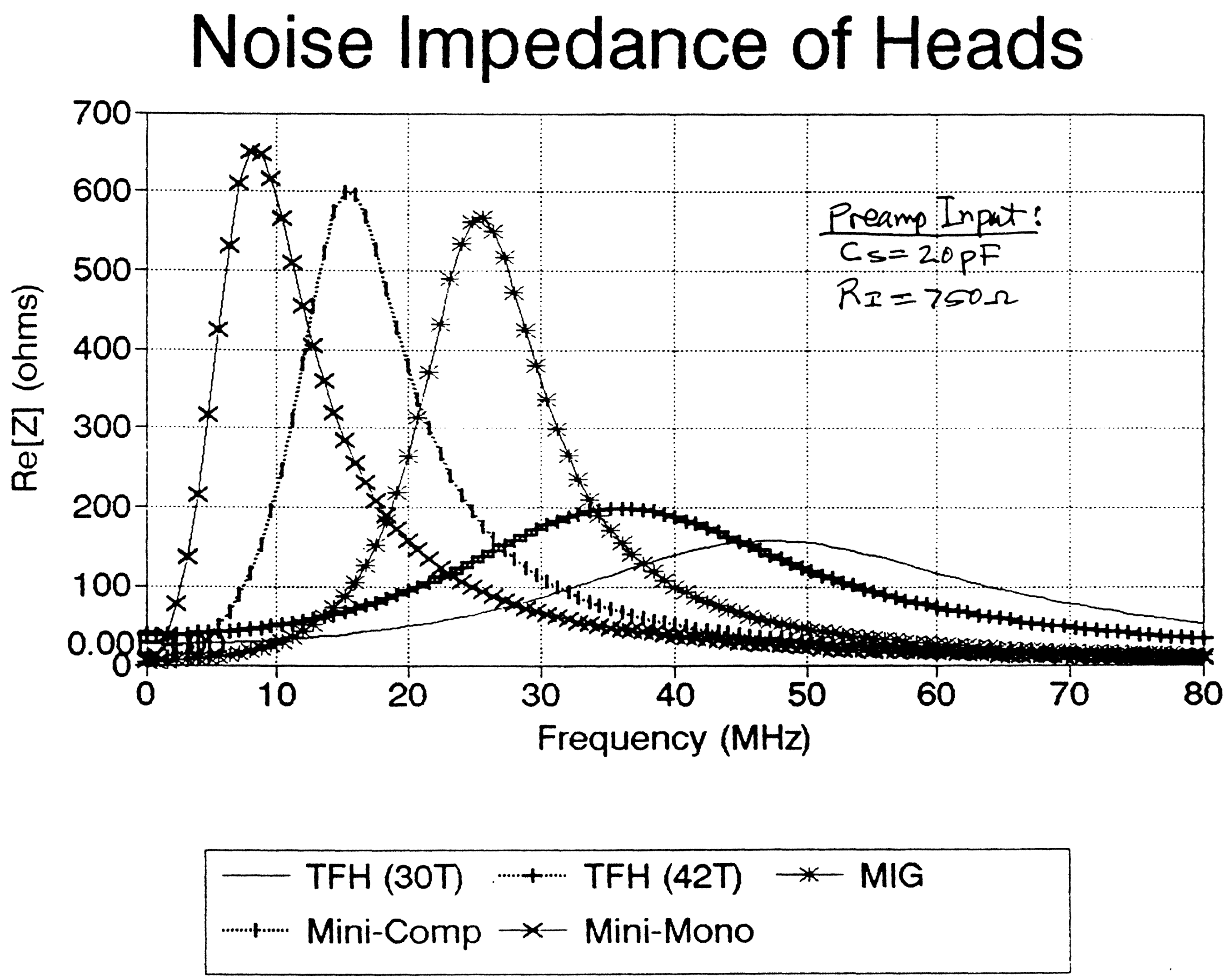
Noise Impedance of Heads
Re[Z] (ohms)
Frequency (MHz)
0
100
200
300
400
500
600
700
0
10
20
30
40
50
60
70
80
Preamp Input:
Cs = 20pF
RI = 750Ω
TFH (30T)
TFH (42T)
MIG
Mini-Comp
Mini-Mono

S. Williams

TIMING WINDOW and MARGIN BUDGET

$$\text{Error Rate} = \text{erfc}(z)$$

$$z \cong (SNR/PW50)(Tw - Tp - Two)$$

$Tp \cong 0$ for symmetric patterns (1111, 1010, etc.)

$Two \cong 0$ for any pattern written on same pattern

$$\text{erfc}(4.50) \cong 1E\text{-}10 \text{ Error Rate}$$

(NOTE:
$4.50 \cong \frac{6.36134}{\sqrt{2}}$
where 6.36134 is the argument for the normal probability function)

$$Tw10 = (4.50\ PW50/SNR) + Tp + Two$$

$$= TwSNR + Tp + Two$$

$$= \text{Noise} + \text{Pattern} + \text{Write-induced Shifts}$$

SNR is pk-pk signal to RMS noise ratio

SMW
READ-RITE

DETECTOR WINDOW (MARGIN) TESTING

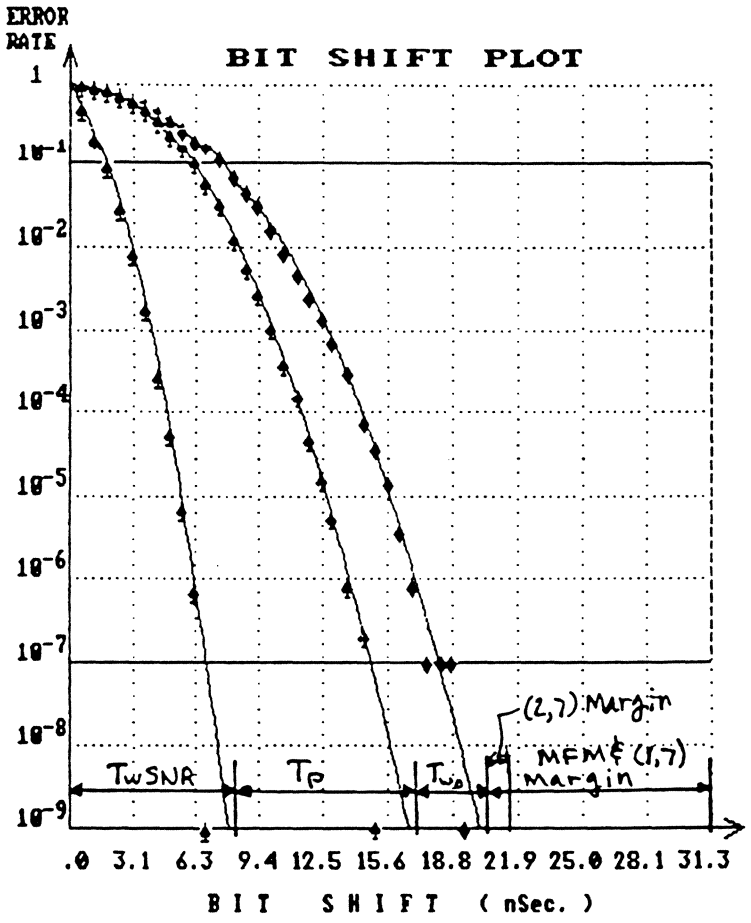

TRAK HD PTRN ZERO S THRS

♦ 1145 0 B6D9 20.0 I 49.8 B6D9 on DC Erase
FILTER 1 15mA 125nS F
♦ 1145 0 B6D9 16.6 I 49.8 B6D9 on B6D9
FILTER 1 15mA 125nS F
♦ 1145 0 FFFF 7.8 I 49.8 FFFF on FFFF
FILTER 1 15mA 125nS F

T_{w10} = Timing window at 10^{-10} B.E.R.
= $T_{wSNR} + T_p + T_{wo}$

T_{wSNR} = Noise-induced shift
T_p = Pattern-induced "
T_{wo} = Write-induced "

♦ Ir:= .999669
ID: P38/K1200
11/21/88 08:52:50

Error Rate = $\operatorname{erfc}(z)$

$z \cong \frac{SNR}{PW50}(T_w - T_p - T_{wo})$ where $\left(SNR: \frac{P\text{-}P}{rms}\right)$

For E.R. = 10^{-10}; $z_{10} \cong 4.50$

$\therefore T_{w10} \cong \frac{4.50\ PW50}{SNR} + T_p + T_{wo} = T_{wSNR} + T_p + T_{wo}$

$\left(T_{wo} \cong \frac{T_{asym}}{4}\right)$

The Read/Write Channel:

Opportunities for Digital Signal Processing

Tom Howell
Quantum Corporation

IIST
December 1991

Outline

1. Review of Peak Detection
2. Sampling Detection
3. Gain and timing control
4. Equalization
5. Performance

Outline

1. *Review of Peak Detection*
2. Sampling Detection
3. Gain and timing control
4. Equalization
5. Performance

Digital Magnetic Recording Channel

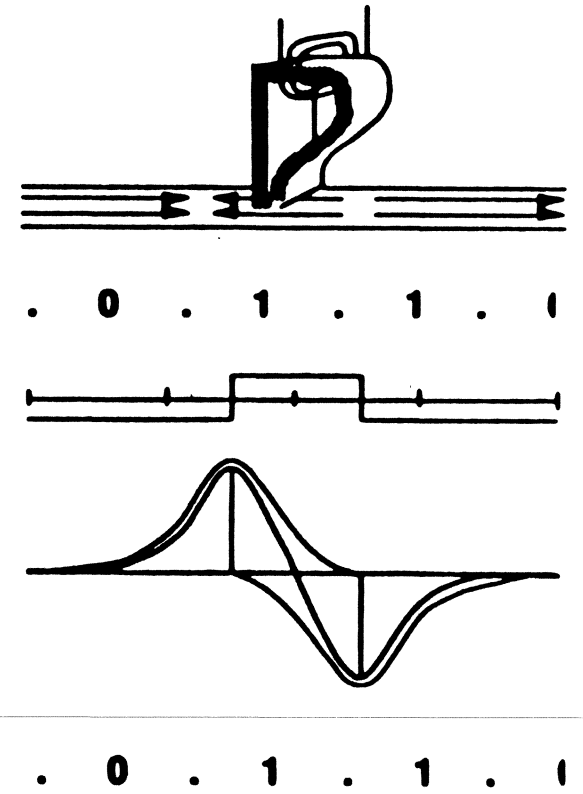

Causes of bit detection errors

- **Random noise**
- **Pulse crowding (1's close together)**
- **Loss of clock synchronization (1's far apart)**

Comparison of RLL (D,K) Constraints

Data:	1		1		0		0	
FM:	1	1	1	1	0	1	0	1
MFM:	1	0	1	0	0	1	0	1
(2,7):	1	0	0	1	0	0	0	0
(1,7):	1	0	1	0	0	0		

FM → MFM → (2,7) Same clock, reduced pulse crowding

(1,7) vs (2,7) Involves trade-offs

Outline

1. Review of Peak Detection
2. *Sampling Detection*
3. Gain and timing control
4. Equalization
5. Performance

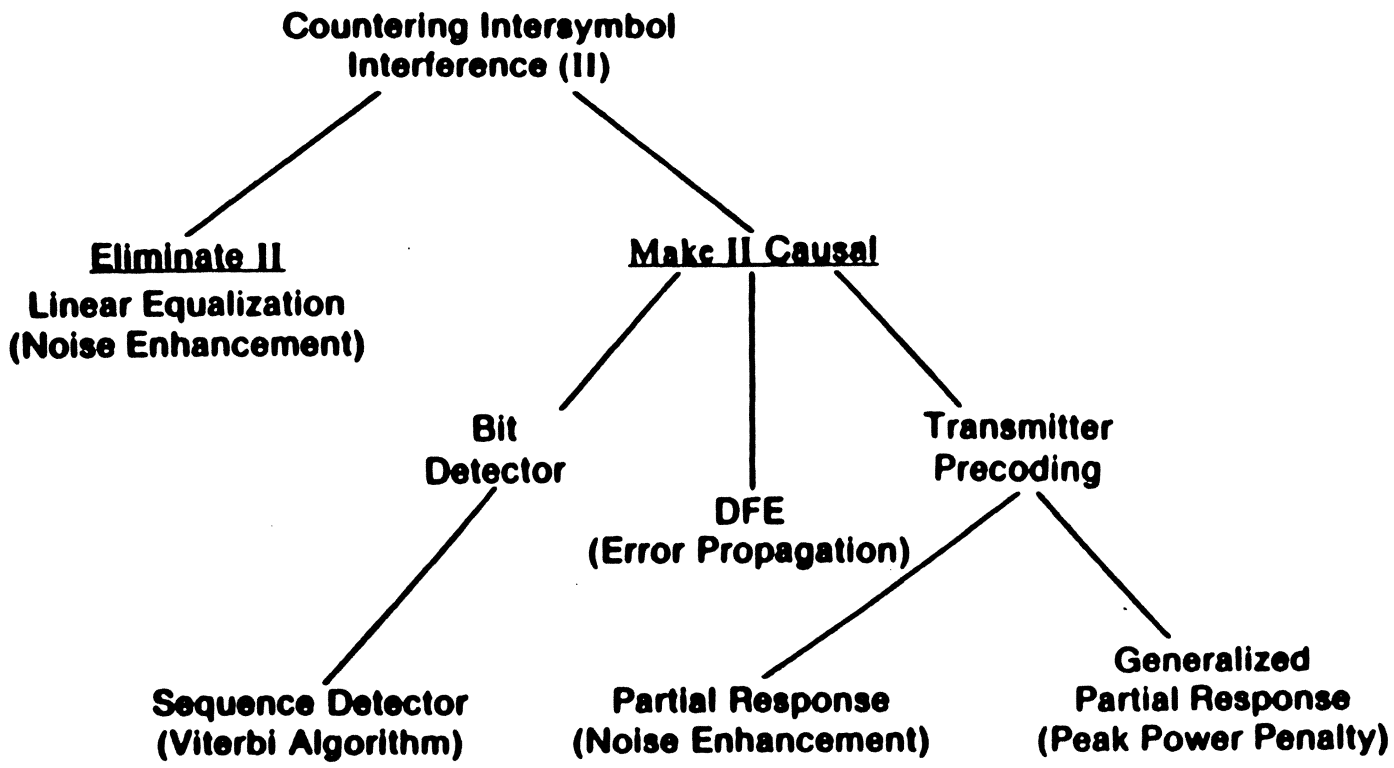

Figure 1. Summary of available methods of countering intersymbol interference in sampling detectors.

Zero-Forcing Equalization

- Equalize step response to:

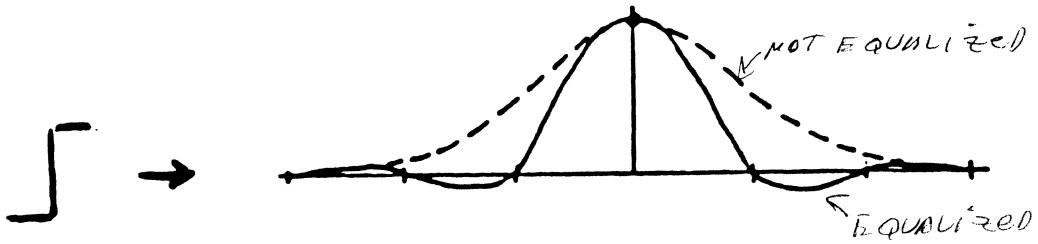

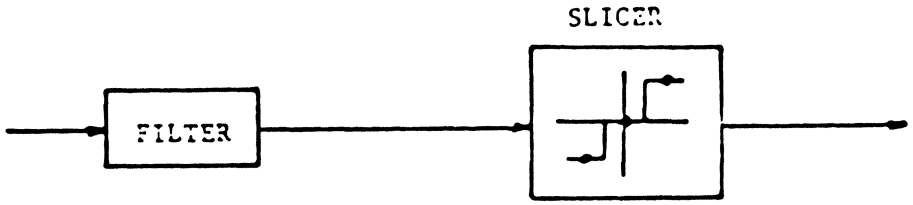

- limited by noise enhancement

Zero-Forcing Equalization

- Equalize NRZ bit response to:

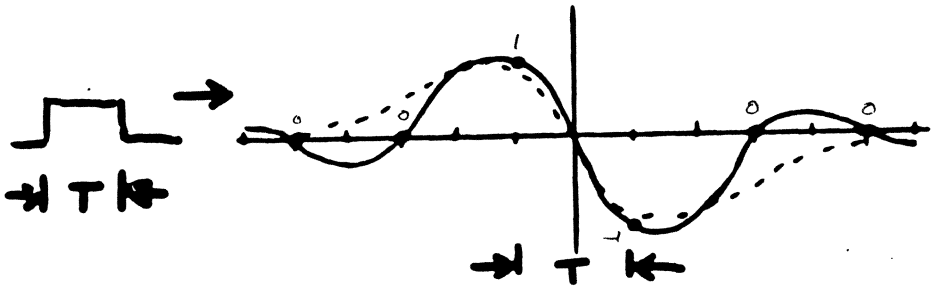

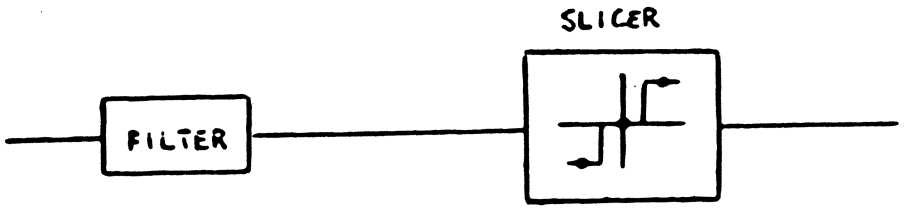

- limited by noise enhancement

Decision Feedback Equalization

- Equalize NRZ bit response to: BETTER ~~SNR~~

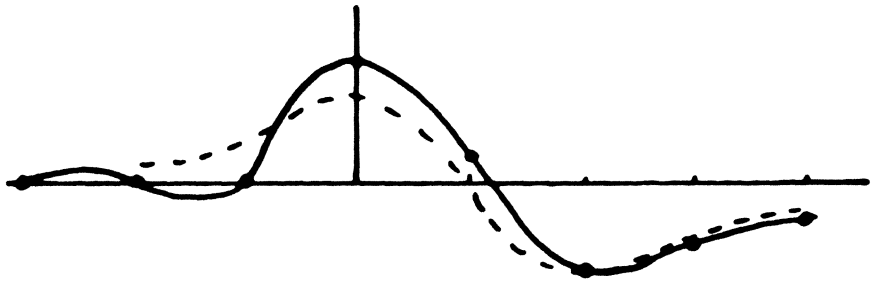

PRODUCES MUCH LESS ERRORS; LENGTH OF ERRORS LONG-

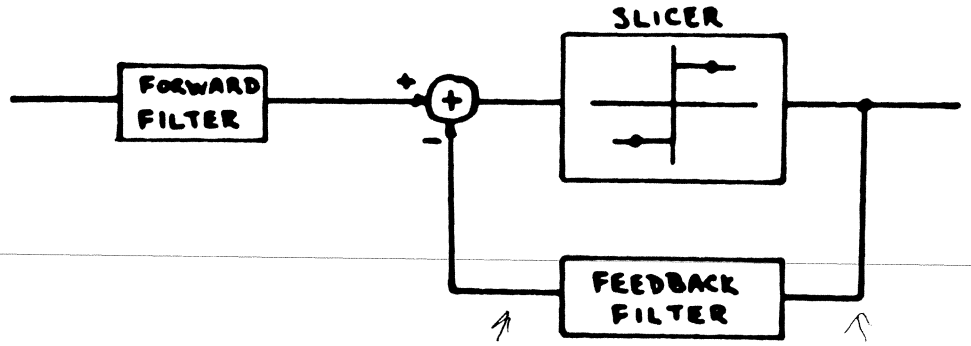

- subject to error propagation

Partial Response

- Equalize NRZ bit response to:

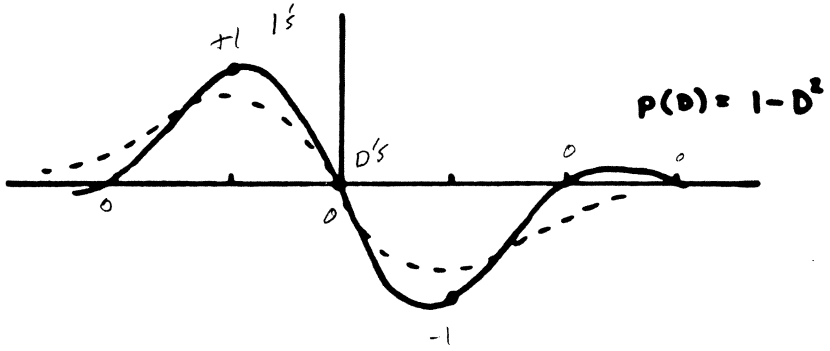

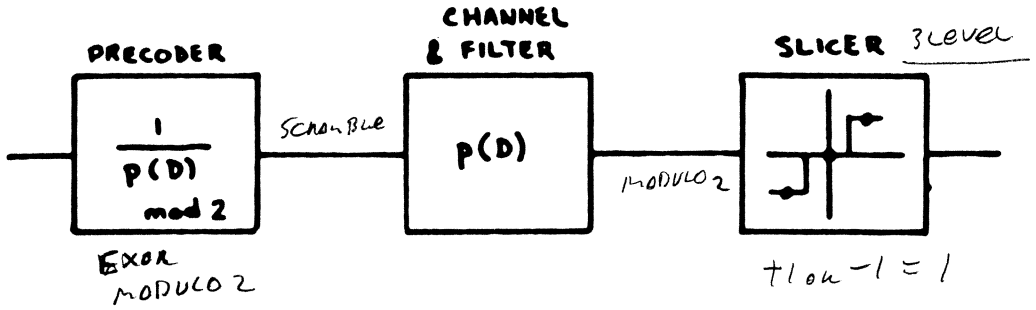

- no error propagation
- less noise enhancement than ZFE or Flat
- more noise enhancement than DFE

3db of noise immunity compared to Peak Detection METHOD - (Twice as much noise)

Maximum Likelihood Sequence Detector

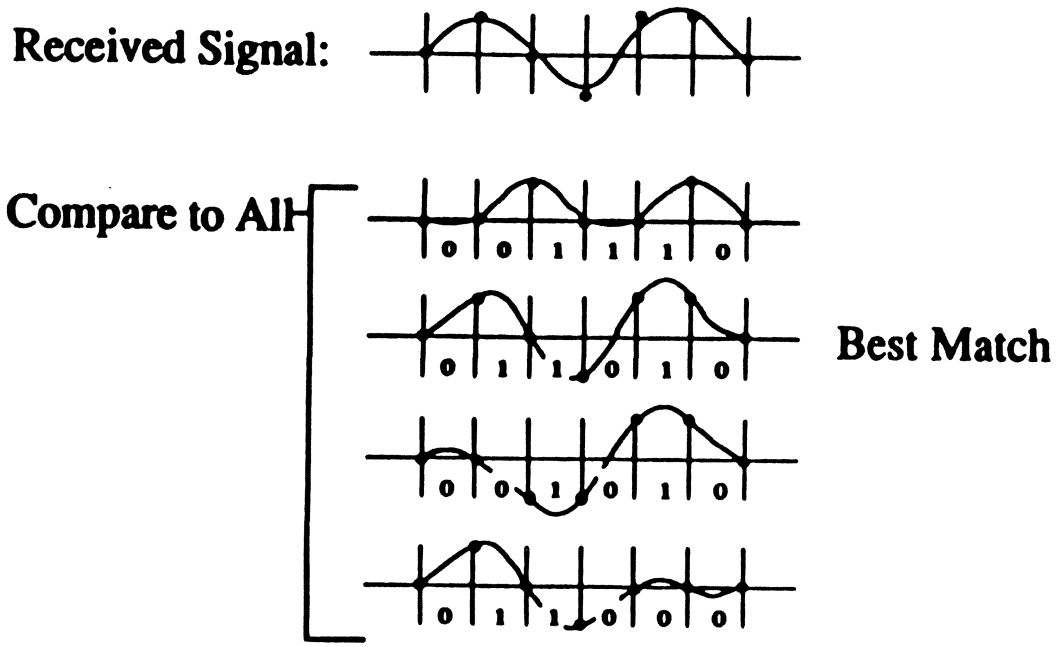

Most likely information sequence:

. . . 0 1 1 0 1 0 . . .

Trellis Diagram

1010

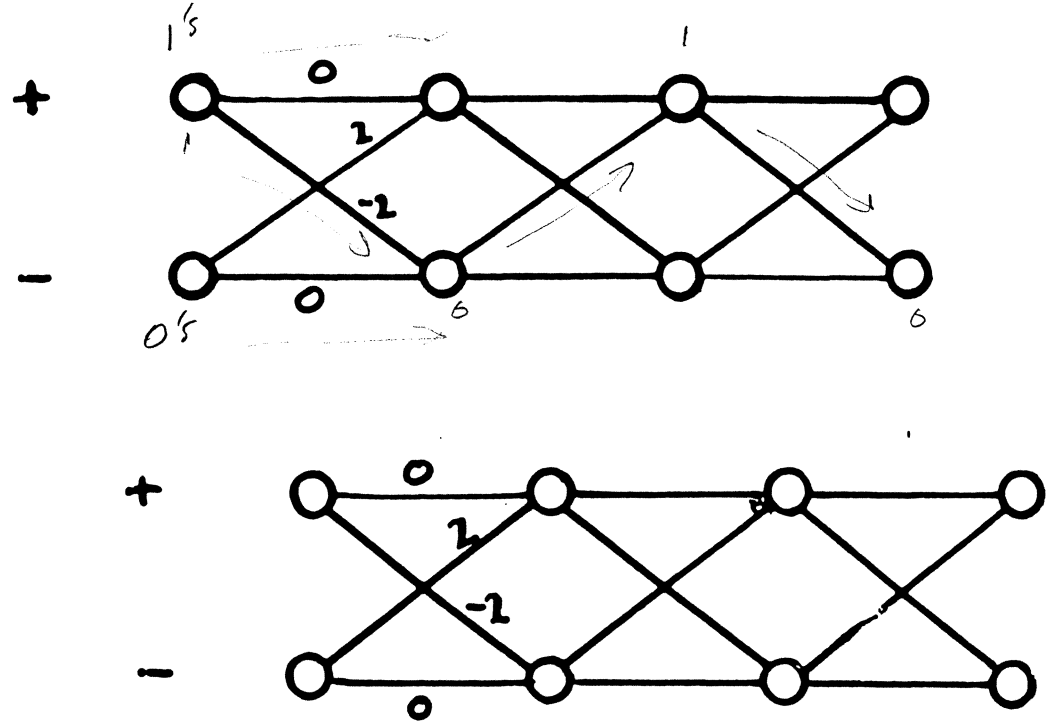

Viterbi Algorithm Path Metrics

y_n = INPUT SAMPLE, SUBTRACT IDEAL SAMPLE VALUE

SQUARE

ACCUMULATING SUM OF SQUARES

$$J_n(+1) = \min \{J_{n-2}(+1) + (y_n - 0)^2, J_{n-2}(-1) + (y_n - 2)^2\}$$

$$J_n(-1) = \min \{J_{n-2}(+1) + (y_n + 2)^2, J_{n-2}(-1) + (y_n - 0)^2\}$$

The Recursive Algorithm

$$DJ_n = \begin{cases} y_n + 1 \text{ if } +1 < (DJ_{n-2} - y_n) & \leq \\ DJ_{n-2} \text{ if } -1 < (DJ_{n-2} - y_n) < +1 & = \\ y_n - 1 \text{ if } (DJ_{n-2} - y_n) < -1 & \geq \end{cases}$$

Example:

1 0 0 0 1 1 1 0

Viterbi Detector Metric Calculation

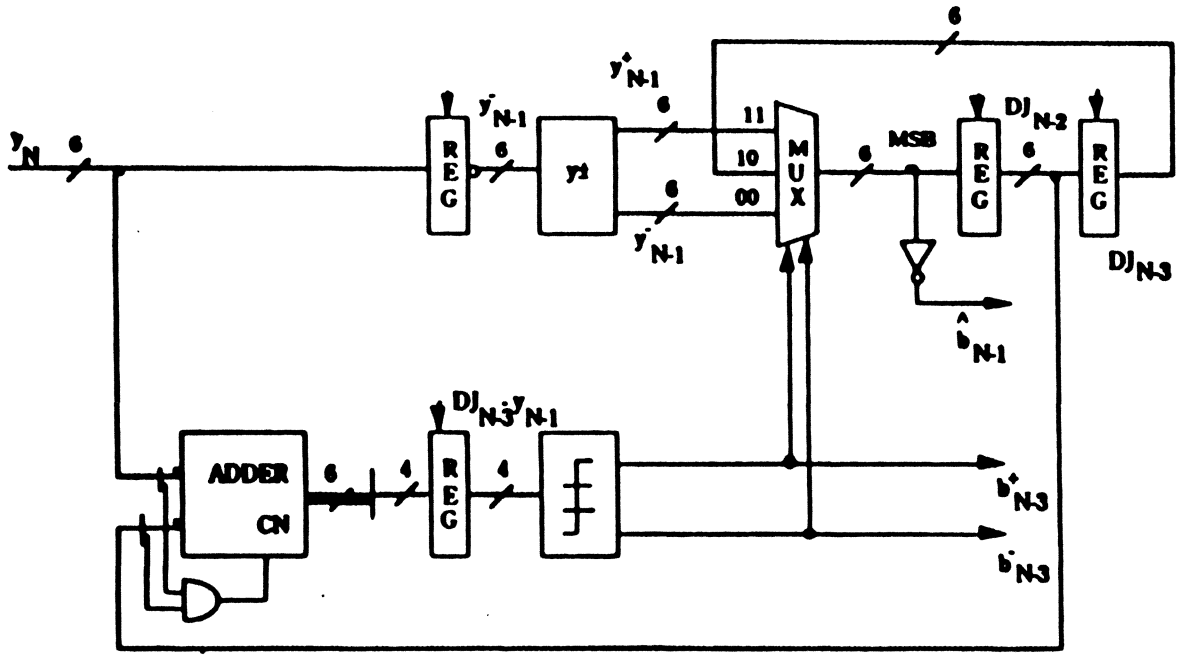

Two's complement representation is used.
Most significant bit (MSB) is at the top or left.

Path Memory

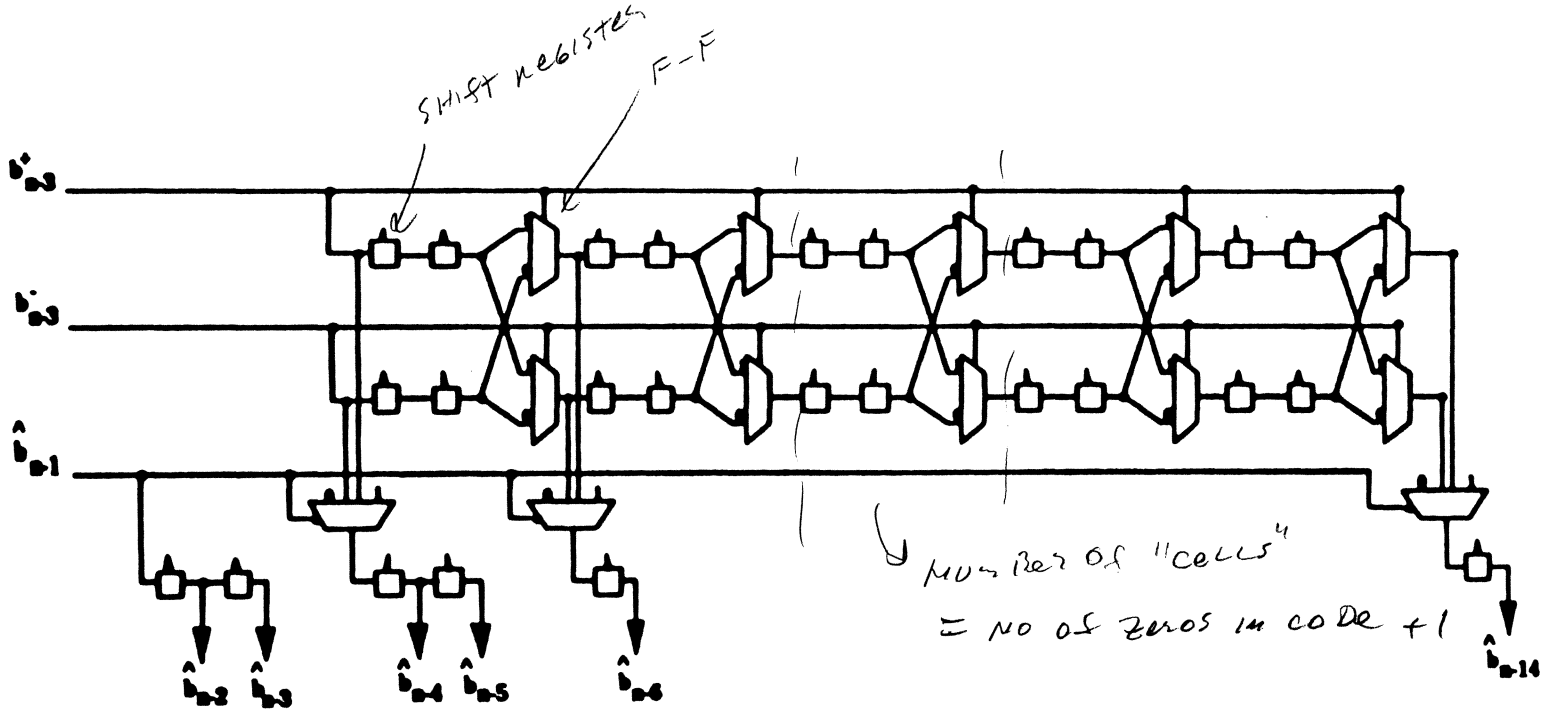

Outline

1. Review of Peak Detection
2. Sampling Detection
3. *Timing and gain control*
4. Equalization
5. Performance

Timing and Gain Control

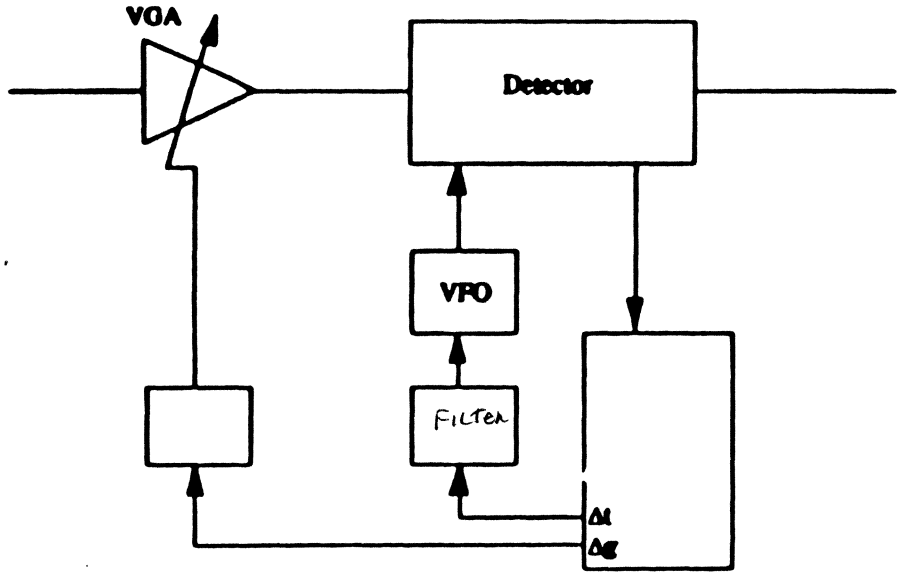

Timing and Gain Control for PRML

$$\hat{y}_n = \hat{a}_n - \hat{a}_{n-2}$$

$$\hat{\dot{y}}_n = \hat{y}_{n+1} - \hat{y}_{n-1}$$

$$e_n = y_n - \hat{y}_n$$

$$\Delta g_n = e_n \hat{y}_n$$

$$\Delta\tau_n = e_n \hat{\dot{y}}_n$$

$$\Delta T_{n+1} = \Delta T_n + \tau \Delta\tau_n$$

$$\tau_{n+1} = t_n - \beta\Delta\tau_n - \Delta T_n$$

$$g_{n+1} = g_n - \gamma g \Delta g_n$$

Example:

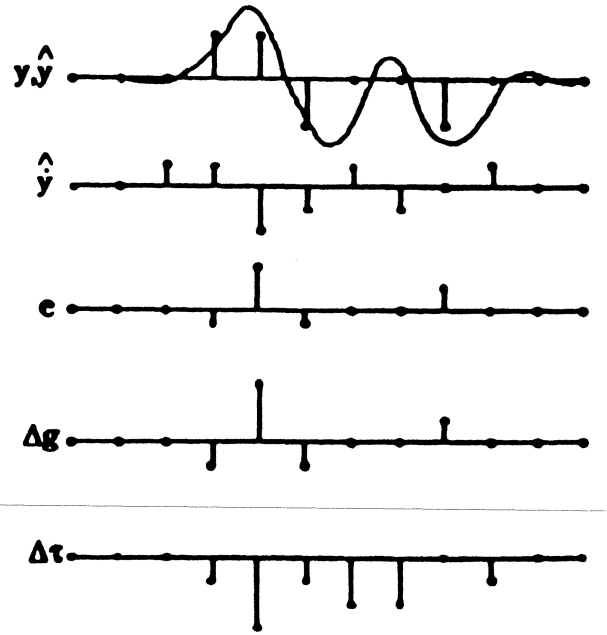

Sample values are constant

Peak Detect & Delay Lines

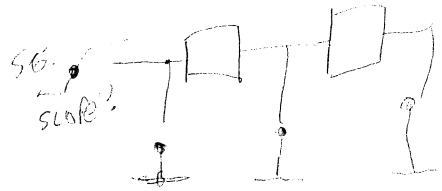

Filtering the Error Signals

CHARGE COUPLED LOGIC Implementation!

$$\varepsilon_{n+1} = \varepsilon_n - \gamma \Delta\varepsilon_n$$

DIGITAL

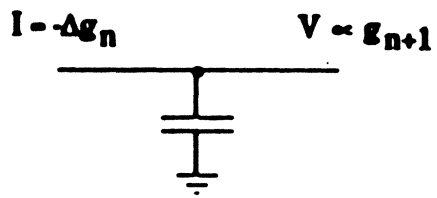

ANALOG

$$\Delta T_{n+1} = \Delta T_n + \zeta \Delta\tau_n$$

$$\tau_{n+1} = \tau_n - \beta\Delta\tau_n - \Delta T_n$$

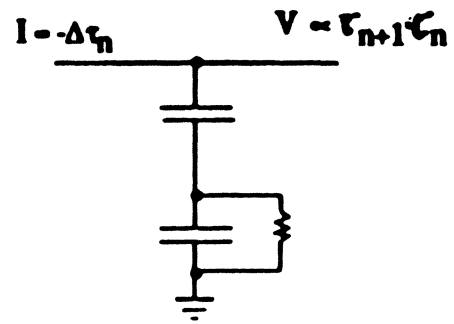

Outline

1. Review of Peak Detection
2. Sampling detection
3. Gain and timing control
4. *Equalization*
5. Performance

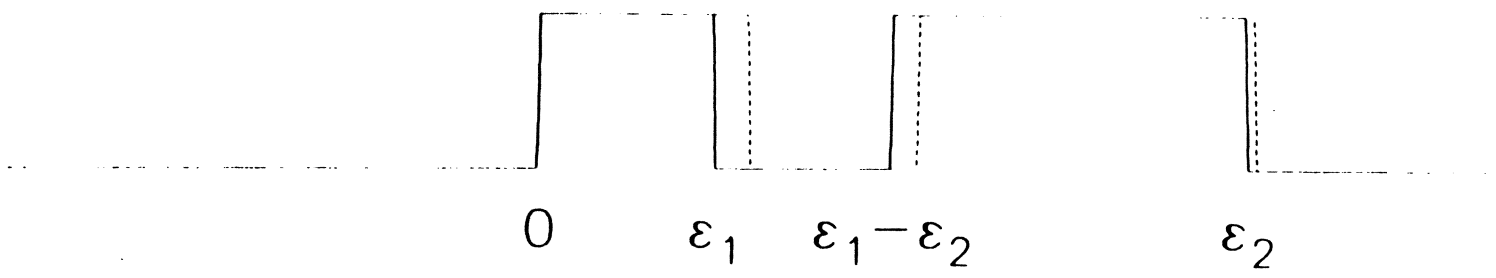

- Nominal write current

  Precompensated write current

HOWELL D EC126327 May 7, 1990 at 16:08:15 by GDFUGT (V-90.033)

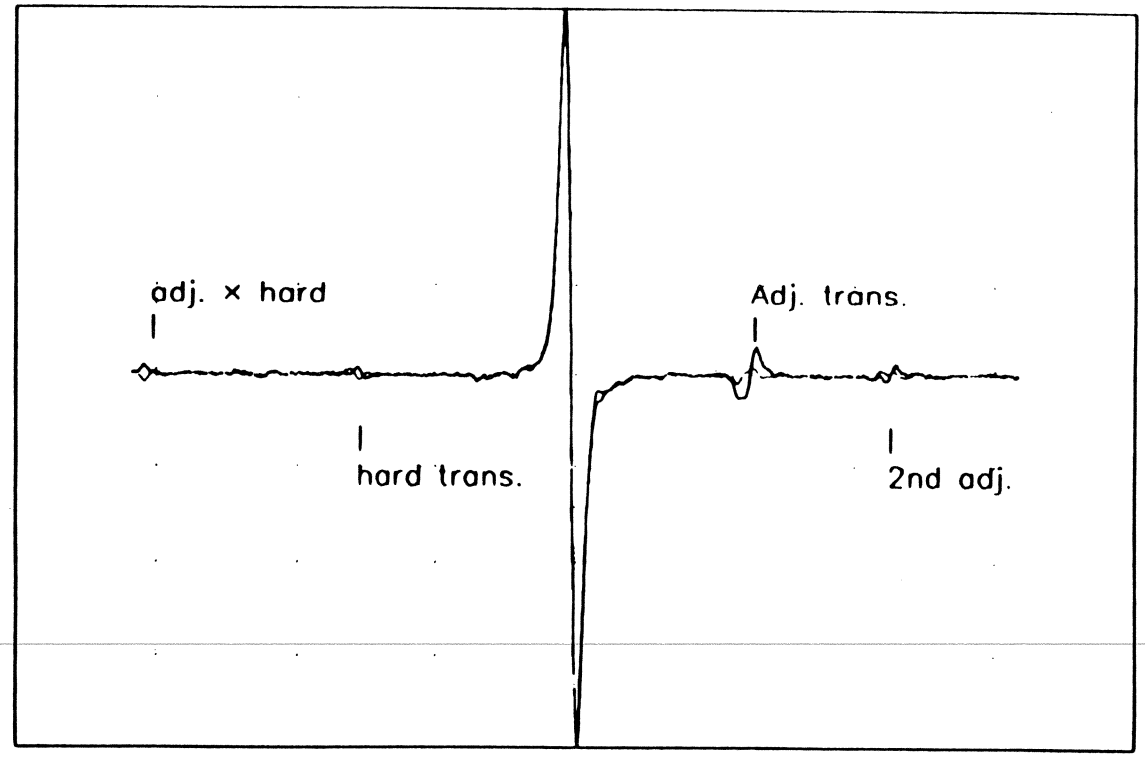

Time (bit periods)

Class IV (Modified Duobinary)

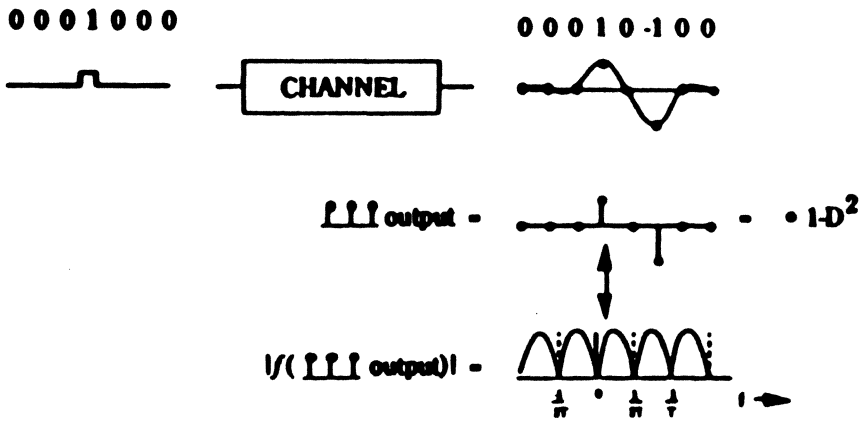

$$f(\text{output} \bullet 1\text{-}D^2) = 1\text{-}e^{iw2T}$$

$$= e^{iwT}\ 2i \sin wT$$

$$= e^{i2\pi fT}\ 2i \sin 2\pi fT$$

↑ DELAY FUNCTION

3-level output: $y_n = -2, 0, 2$

Sampled NRZ BIT Responses

1 - 6 Feedback Taps

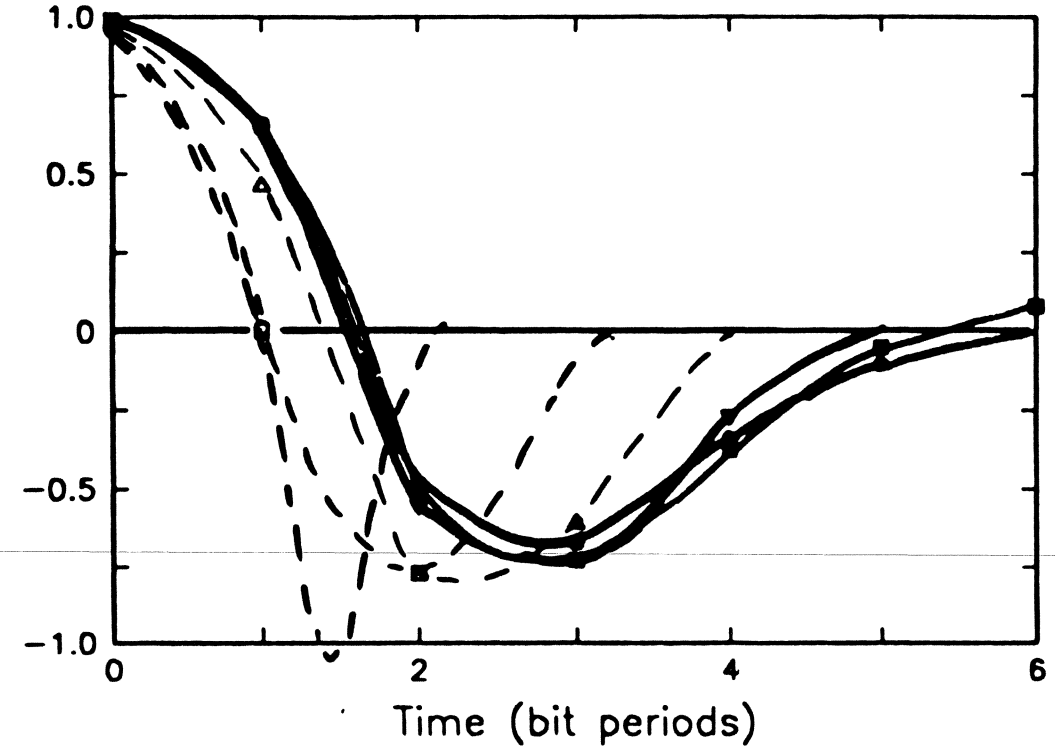

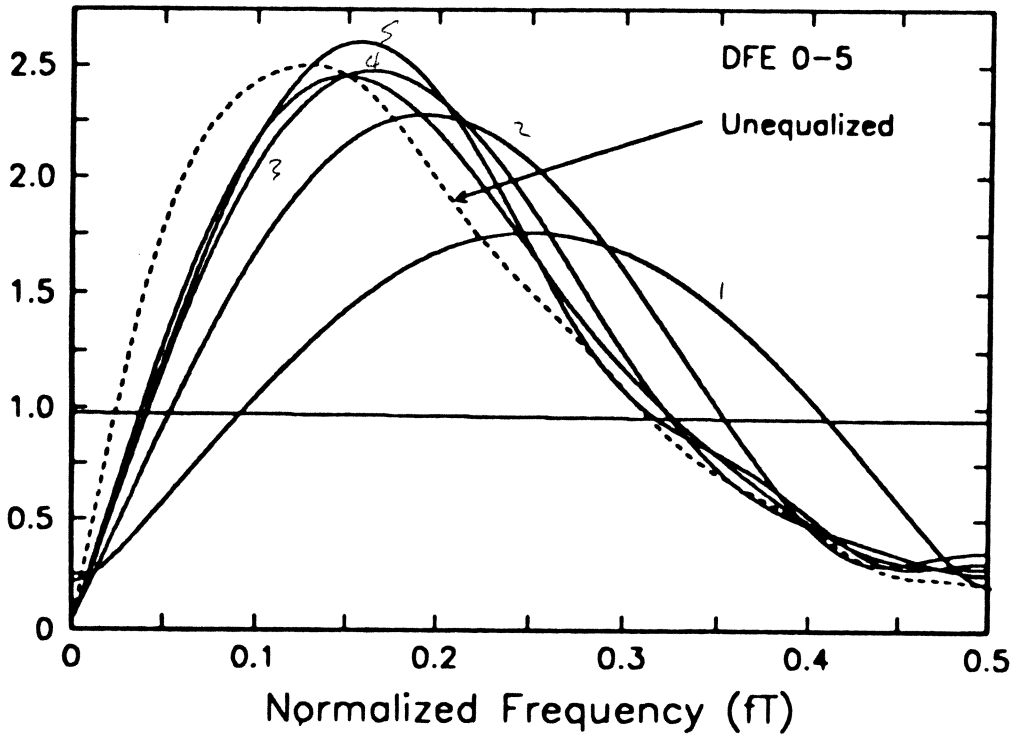
DFE 0-5
Unequalized
2.5
2.0
1.5
1.0
0.5
0
0
0.1
0.2
0.3
0.4
0.5
Normalized Frequency (fT)

HOWELL D UNEPRBS3 January 24, 1990 at 17:48:00 by GDFTRN (V-88.322)

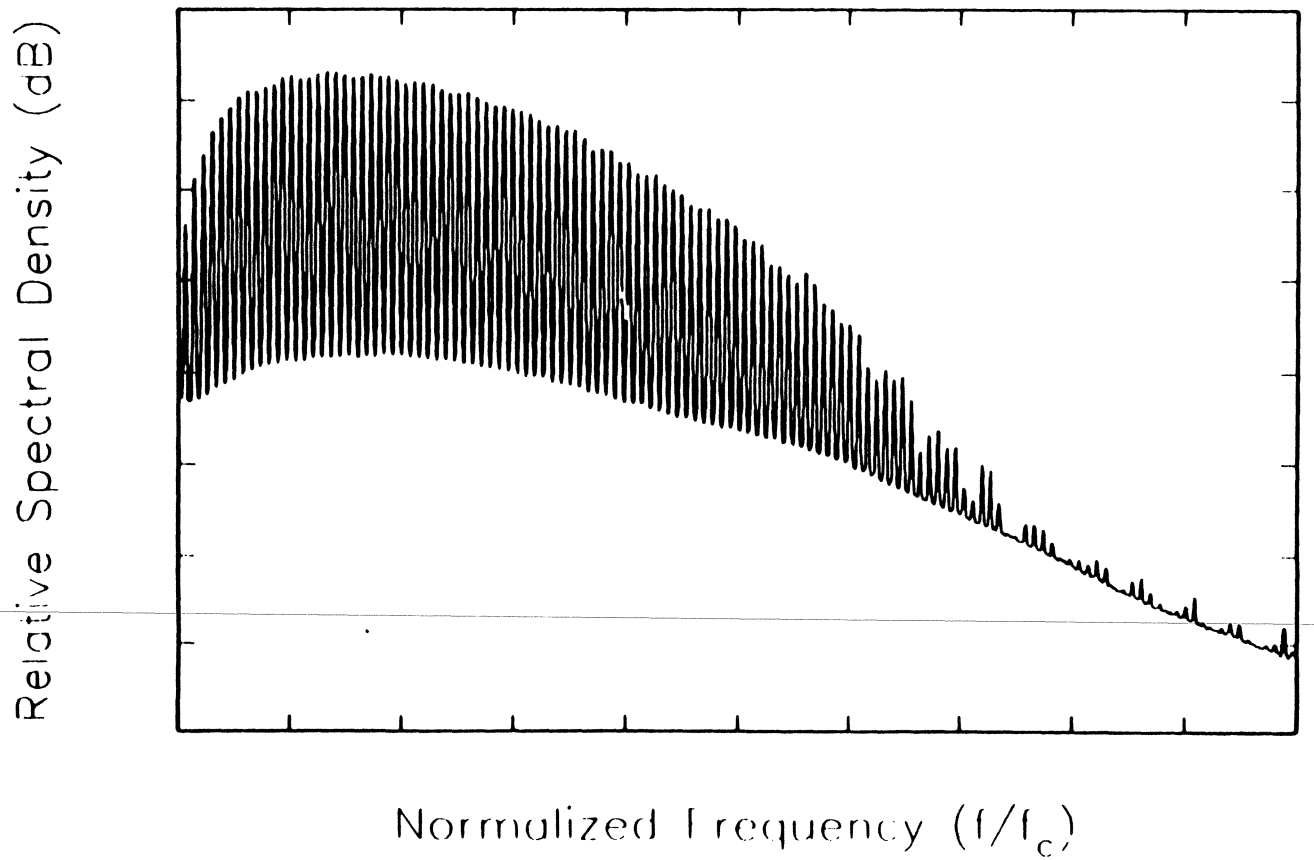

HOWELL D EQUPRBS3 January 24, 1990 at 17:48:16 by GDFTRN (V-88.322)

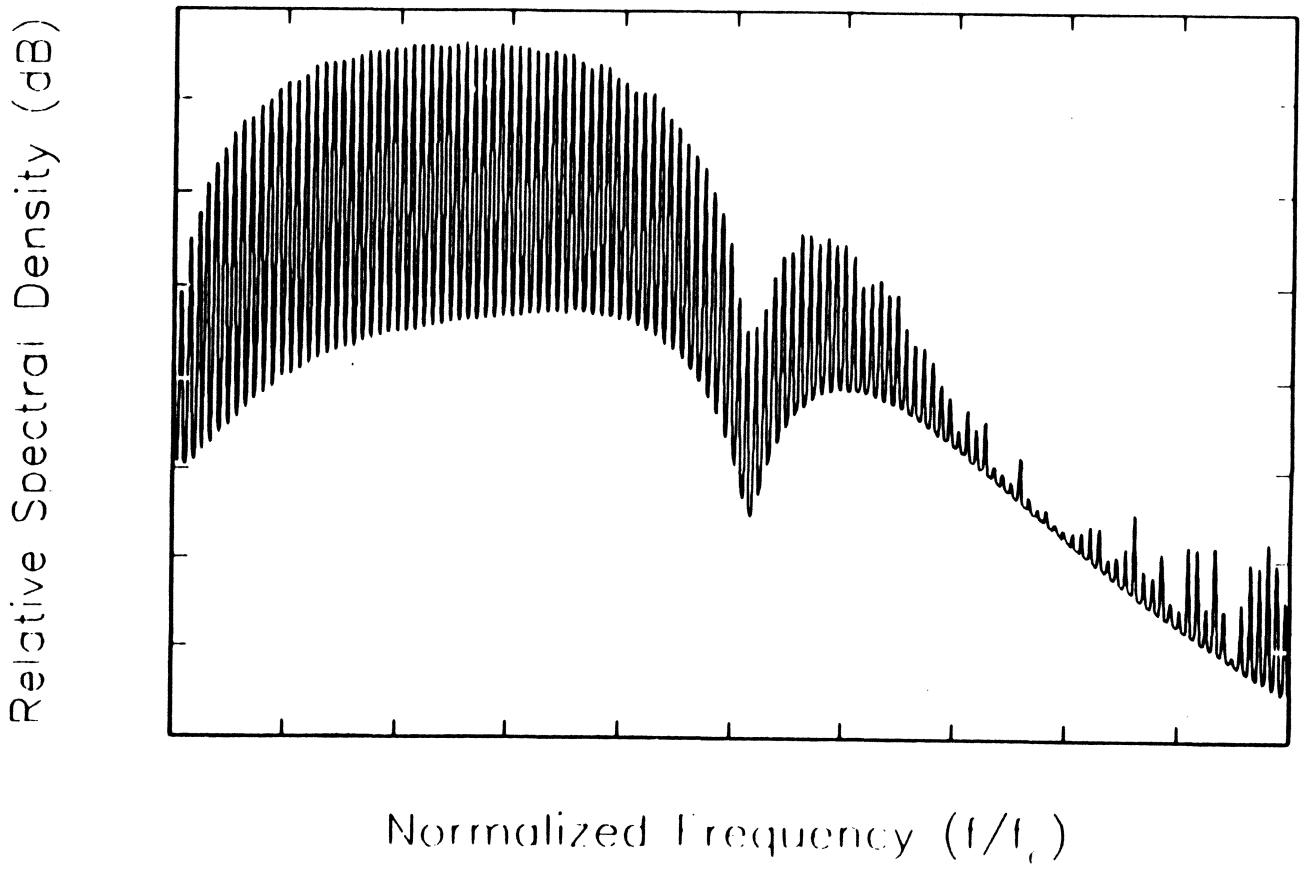

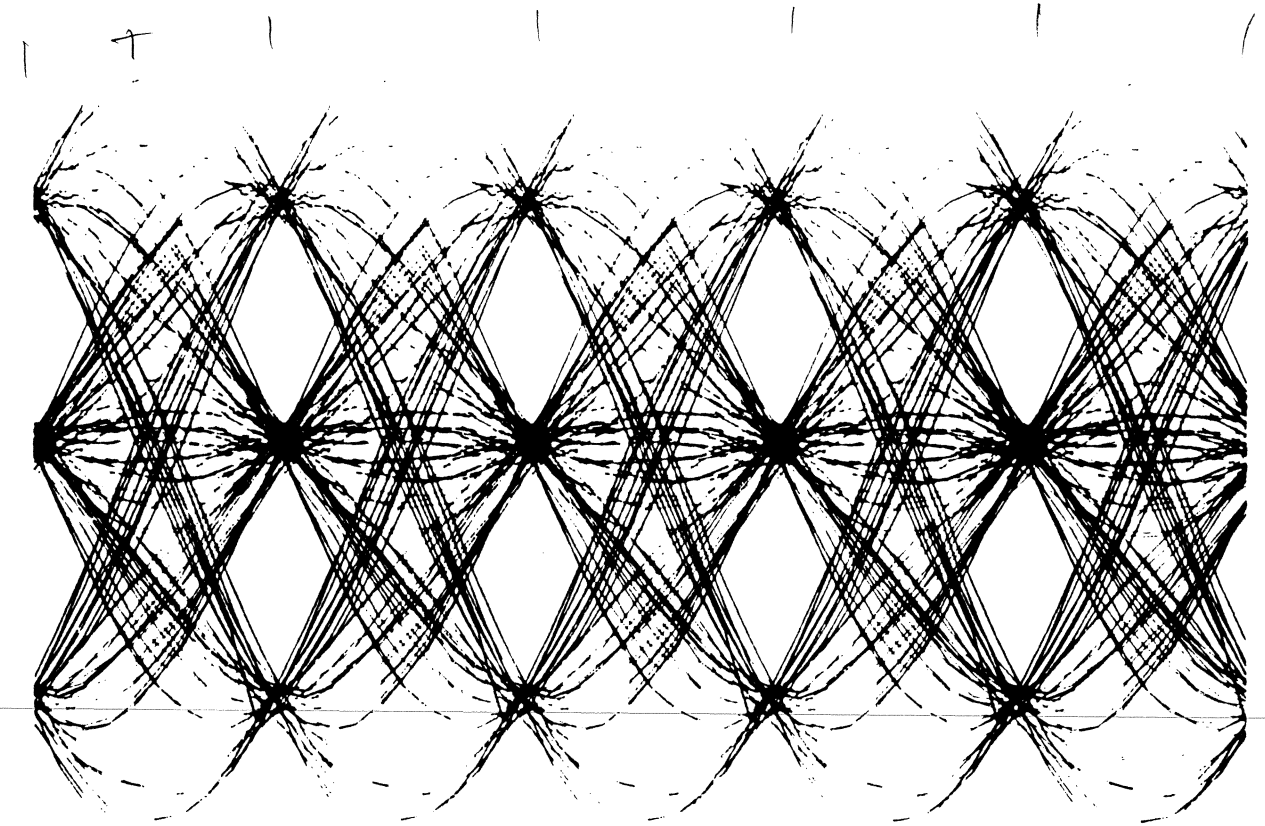

5T

6001 Equalizer response
to wide Band Input

Implementation

1. R-L-C Network

$$H(w) = \frac{N(z)}{d(z)} = \frac{\pi(z-z_j)}{\pi(z-P_j)}\Bigg|_{z=iw}$$

2.

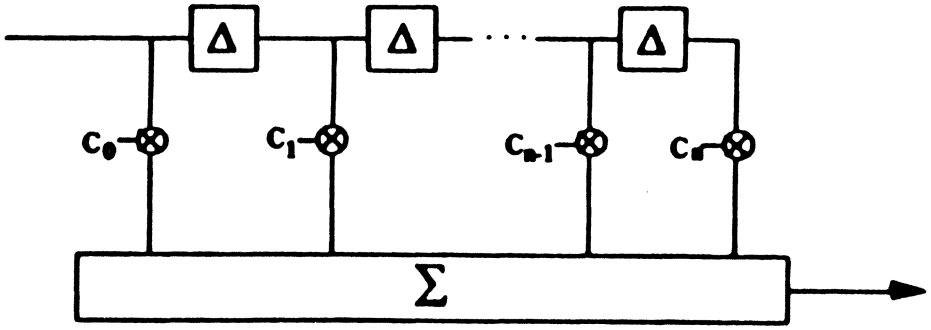

$$H(w) = f\left(\sum_k c_k \delta(t-k\Delta)\right)$$

Outline

1. Review of Peak Detection
2. Sampling Detection
3. Gain and timing control
4. Equalization
5. *Performance*

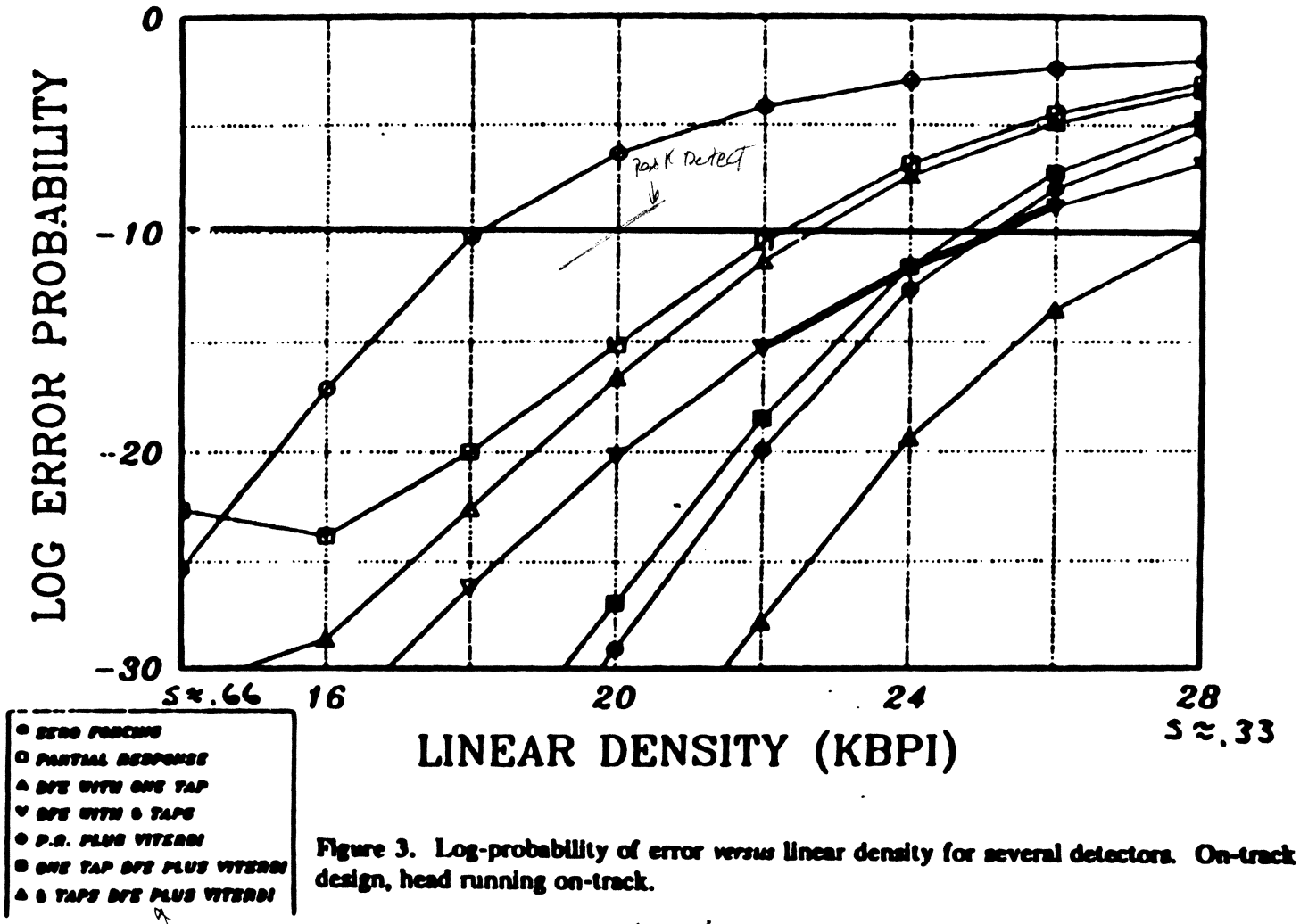

Figure 3. Log-probability of error *versus* linear density for several detectors. On-track design, head running on-track.

Performance of Channel Alternatives

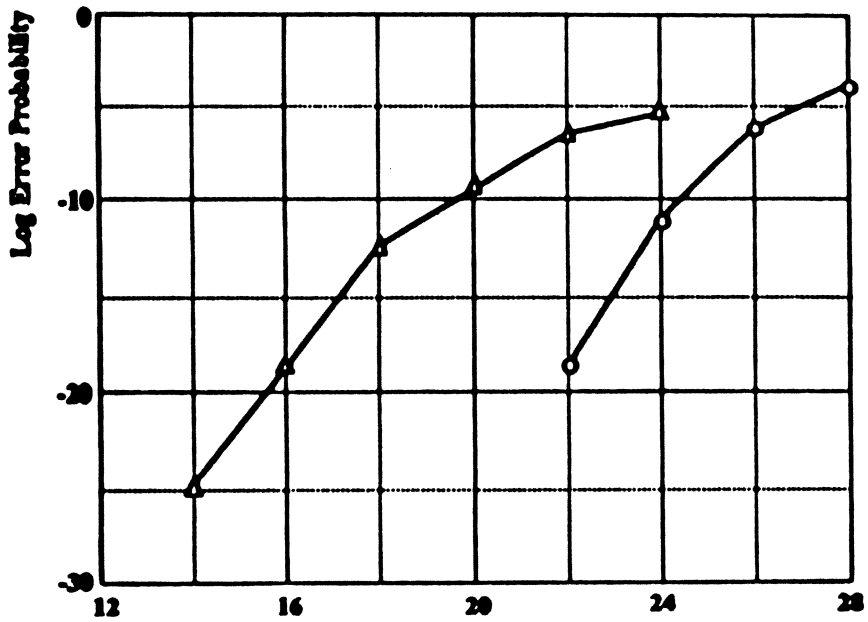

Model Results On-Track

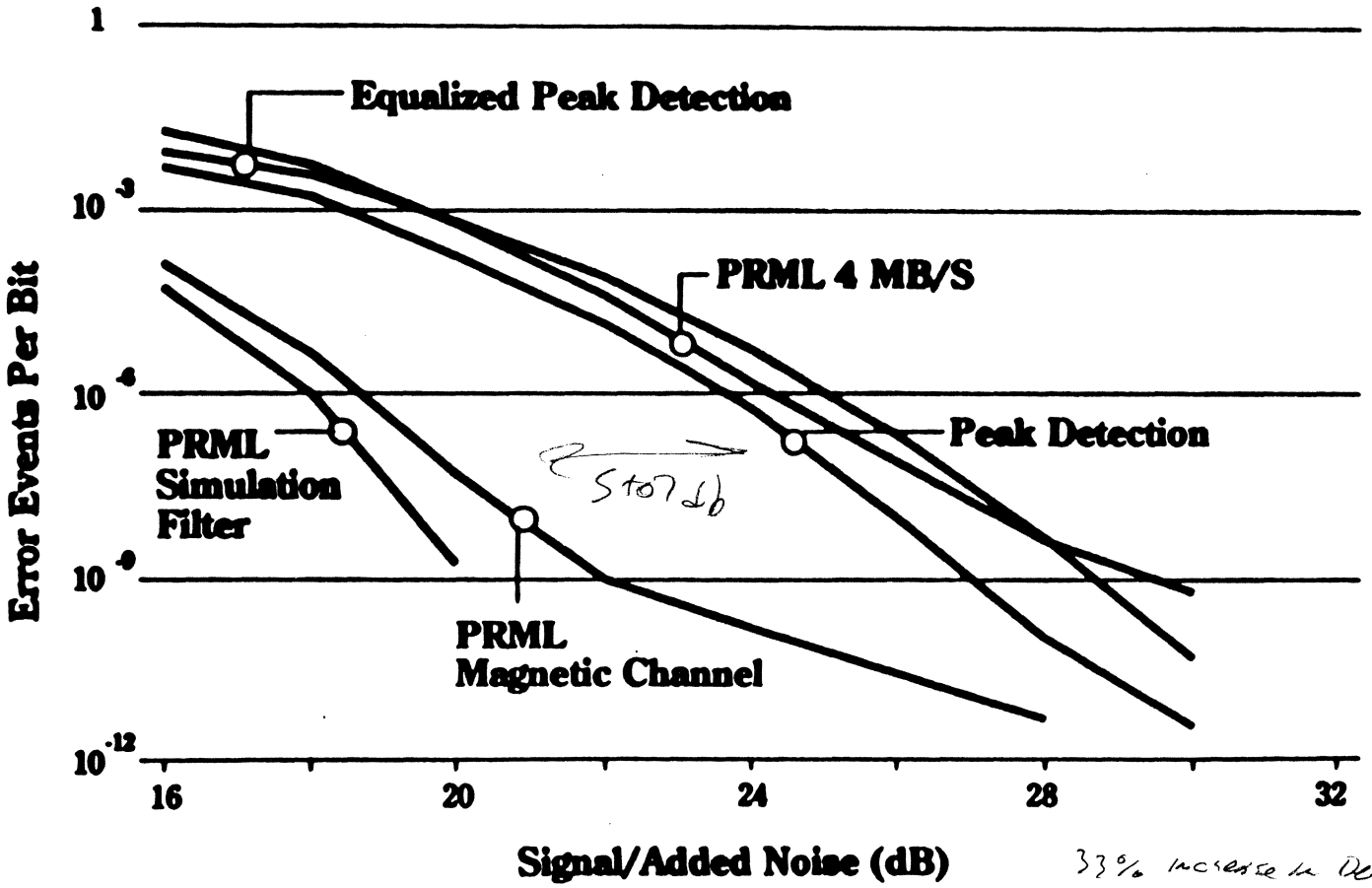

33% increase in Density
at same Error Rate.

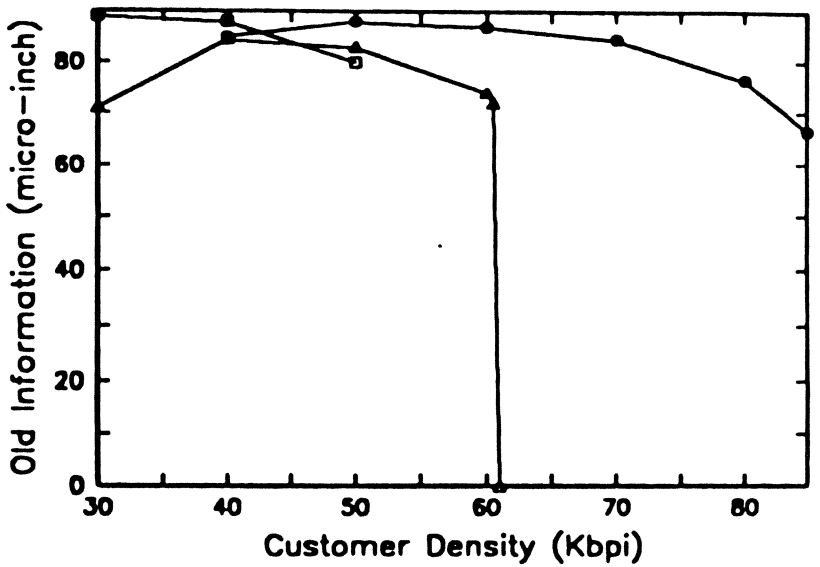

Figure 35. Old information versus linear density on MR head film disk. ○ = PRML, □ = (1,7) peak detection without equalization, △ = (1,7) peak detection with equalization.

Conclusions

Best aternatives are PRML and DFE

<u>Compared wtith the best peak detector, they offer:</u>

- **25 - 40% linear density improvement at the same error rate and noise level or...**
- **5 - 7 dB more noise tolerance at the same linear density and error rate or...**
- **Several orders of magnitude improvement in on-track error rate at given linear density and noise.**

CODING FOR PARTIAL-RESPONSE CHANNELS

PAUL H. SIEGEL

IBM RESEARCH DIVISION
ALMADEN RESEARCH CENTER
SAN JOSE, CALIFORNIA

OUTLINE

- Digital recording channel
- Constrained codes for PRML
- Trellis codes for PRML

DIGITAL DATA RECORDING (SCHEMATIC)

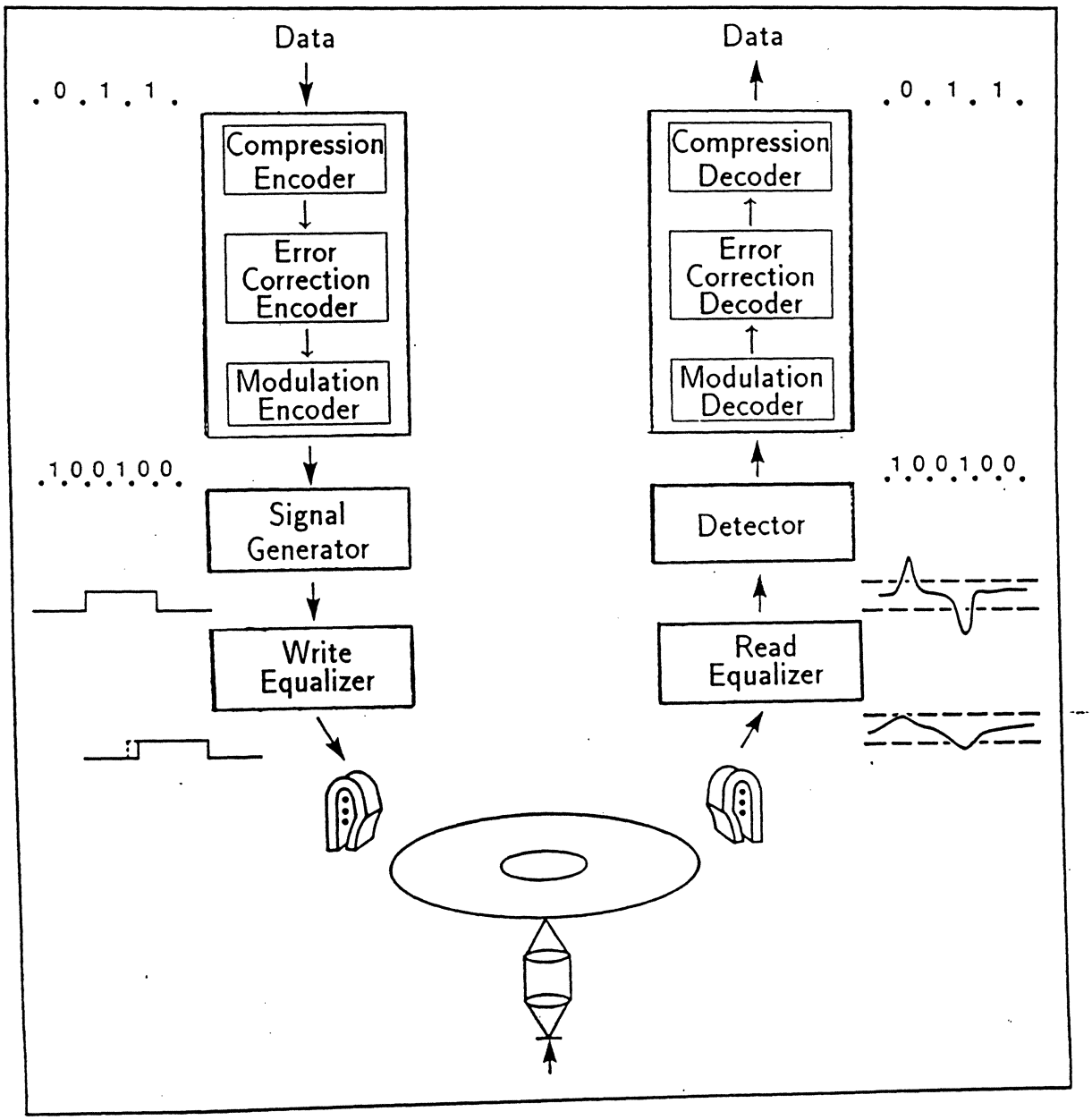

Configuration of Codes

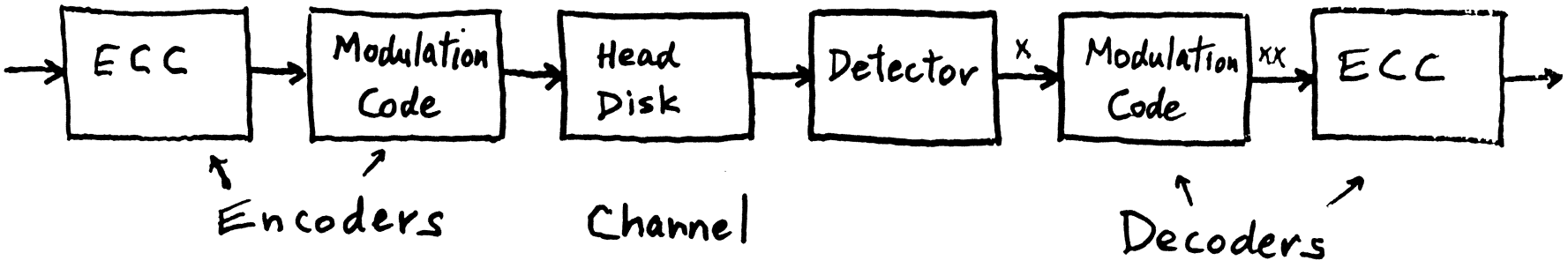

Modulation Code

Matches recording signal characteristics to channel bandwidth, detection method, read/write electronics, timing and tracking servo requirements

Error Correction Code

Detects and corrects data detection errors

PRML Channel

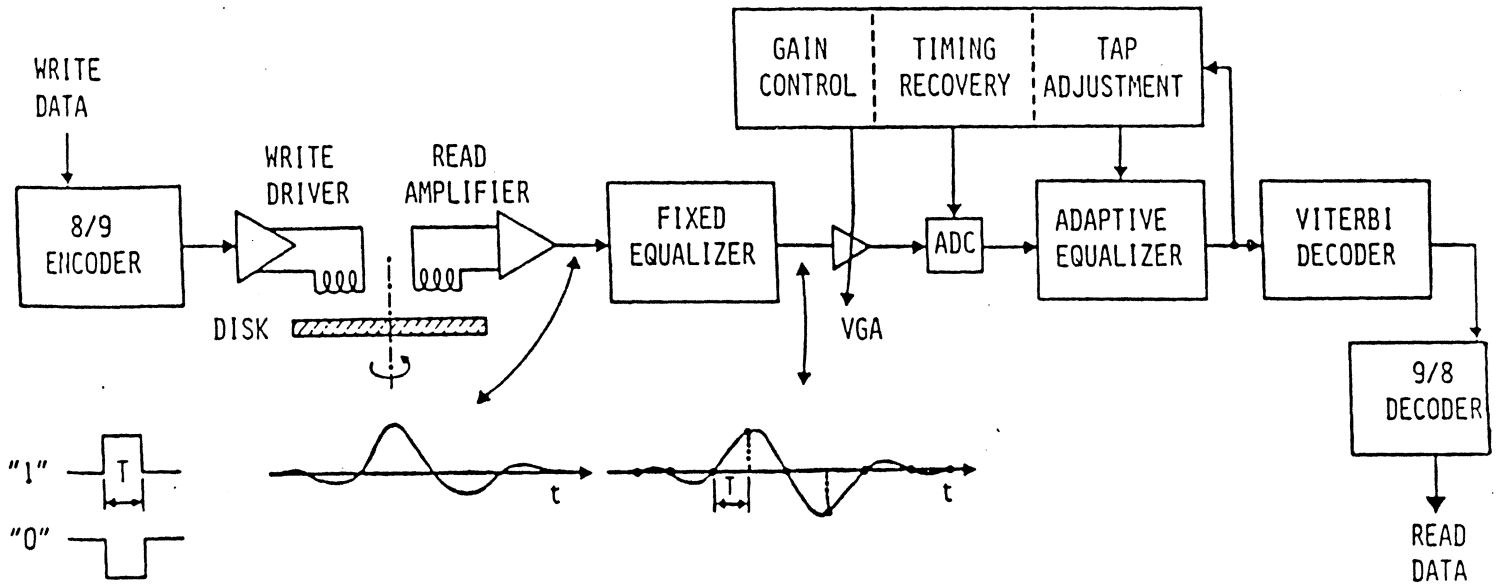

PRML: PARTIAL-RESPONSE CLASS-IV SIGNALING
with MAXIMUM-LIKELIHOOD SEQUENCE DETECTION

- 30% linear density advantage over (2,7) peak detection

Digital Recording Channel

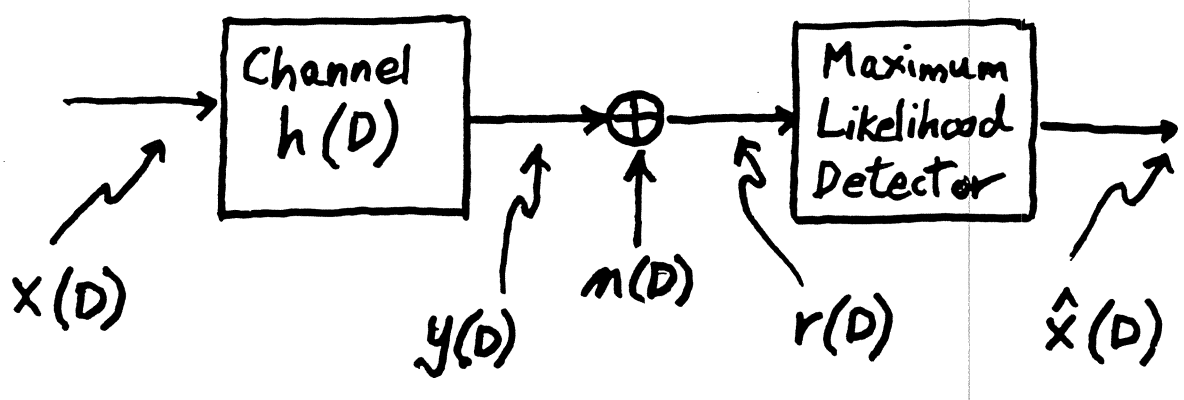

- Binary channel input

$$x(D) = \sum_{j=0}^{\infty} x_j D^j \quad ; \quad x_j \in \{0,1\}$$

- Channel linear filter model

$$h(D) = \sum_{j=0}^{N} h_j D^j \quad ; \quad \{h_j\}_0^N = \text{impulse response}$$

$$y(D) = x(D)\, h(D)$$

- Additive, i.i.d. Gaussian noise

$$n(D) = \sum_{j=0}^{\infty} n_j D^j \quad ; \quad n_j \sim N(0,\sigma^2)$$

Partial-Response Filter Model for Recording Channels

- Magnetic recording
- Transfer polynomial
  - $h(D) = 1 - D$

  $(y_n = x_n - x_{n-1})$

  "Dicode"
- Transfer function

  $H(f) = j2T \sin \pi f T$

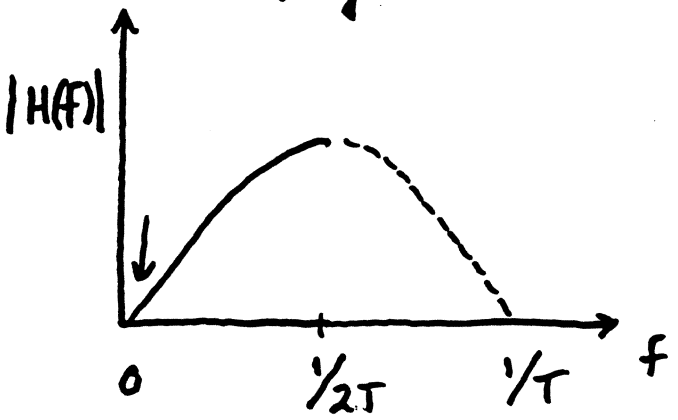

- $h(D) = \begin{cases} (1-D)(1+D) \\ (1-D)(1+D)^2 \end{cases}$

$y_n = \begin{cases} x_n - x_{n-2} \\ x_n + x_{n-1} - x_{n-2} - x_{n-3} \end{cases}$

$\begin{cases} \text{"PR4"} \\ \text{"EPR4"} \end{cases}$

$H(f) = \begin{cases} j2T \sin 2\pi f T \\ j4T \cos \pi f T \sin 2\pi f \end{cases}$

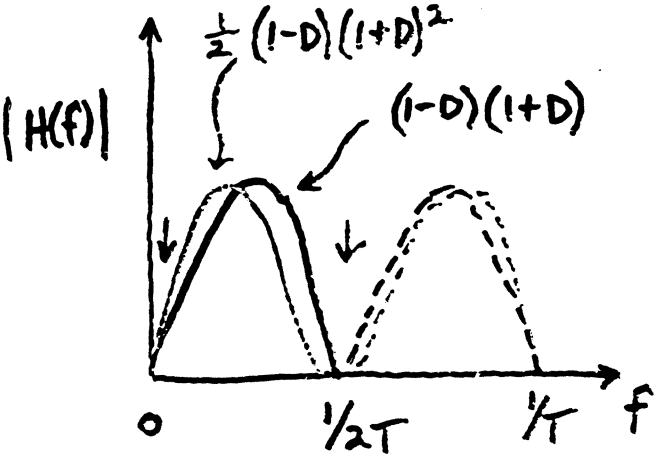

PR Models (cont.)

- Magnetic recording - step responses
  - Dicode: $h(D) = 1 - D$

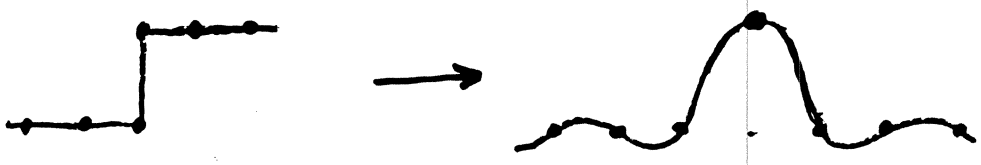

- PR4: $h(D) = (1-D)(1+D) = 1 - D^2$

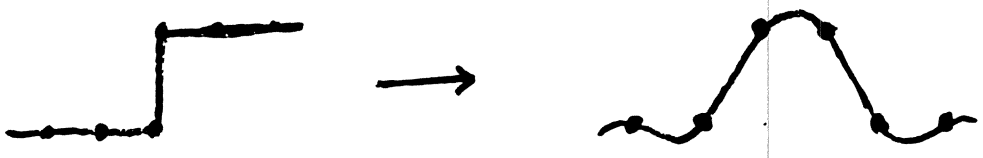

- EPR4: $h(D) = (1-D)(1+D)^2 = 1 + D - D^2 - D^3$

PR Filter Models (cont.)

- Optical recording

- Transfer polynomial

$$h(D) = \begin{cases} 1 + D \\ (1+D)^2 \end{cases}$$

- Transfer function

$$H(F) = \begin{cases} 2T \cos \pi f T \\ 4T \cos^2 \pi f T \end{cases}$$

$$y_n = \begin{cases} x_n + x_{n-1} \\ x_n + 2x_{n-1} + x_{n-2} \end{cases}$$

$$\begin{cases} \text{"PR1"} \\ \text{"PR2"} \end{cases}$$

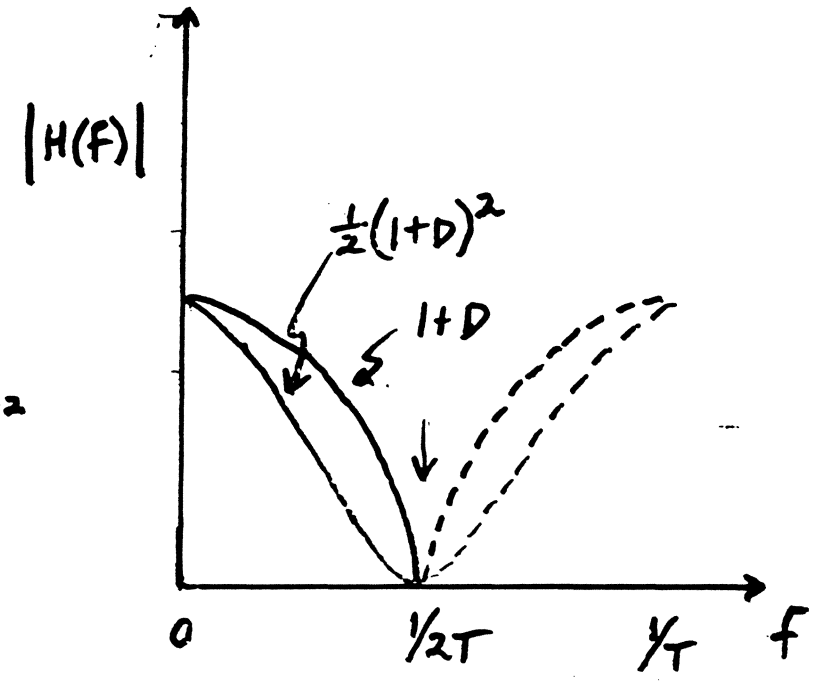

PR Models (cont.)

- Optical recording - pulse responses
  - PR 1 (duobinary): $h(D) = 1+D$

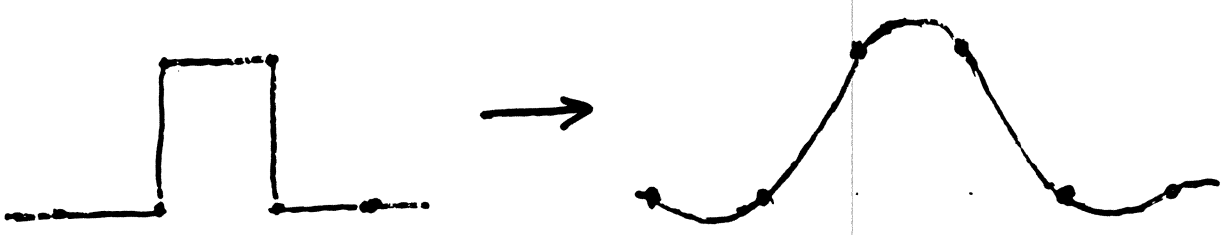

  - PR 2 : $h(D) = (1+D)^2$

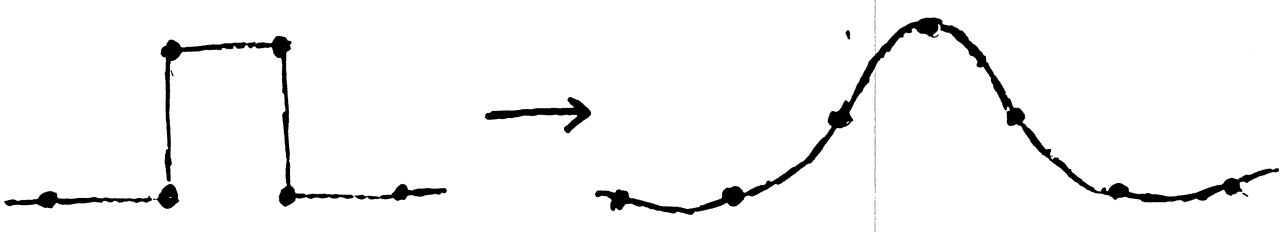

EYE DIAGRAM FOR PR4

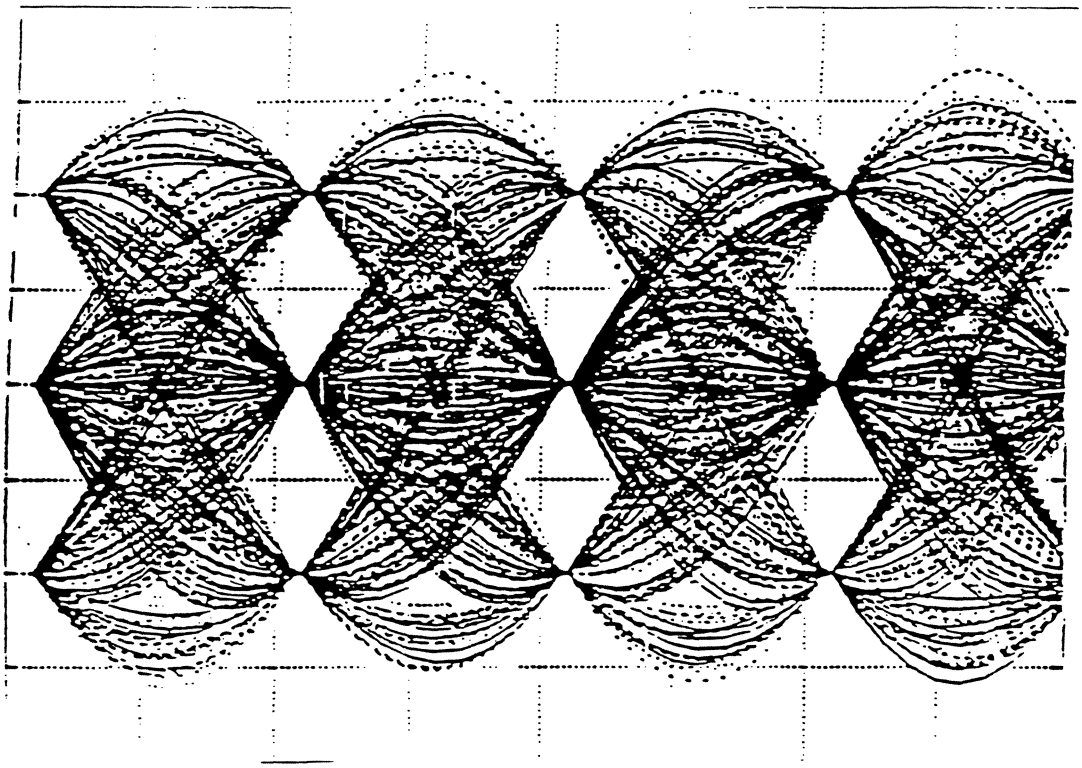

- 3 nominal sample values

EYE DIAGRAM FOR EPR4

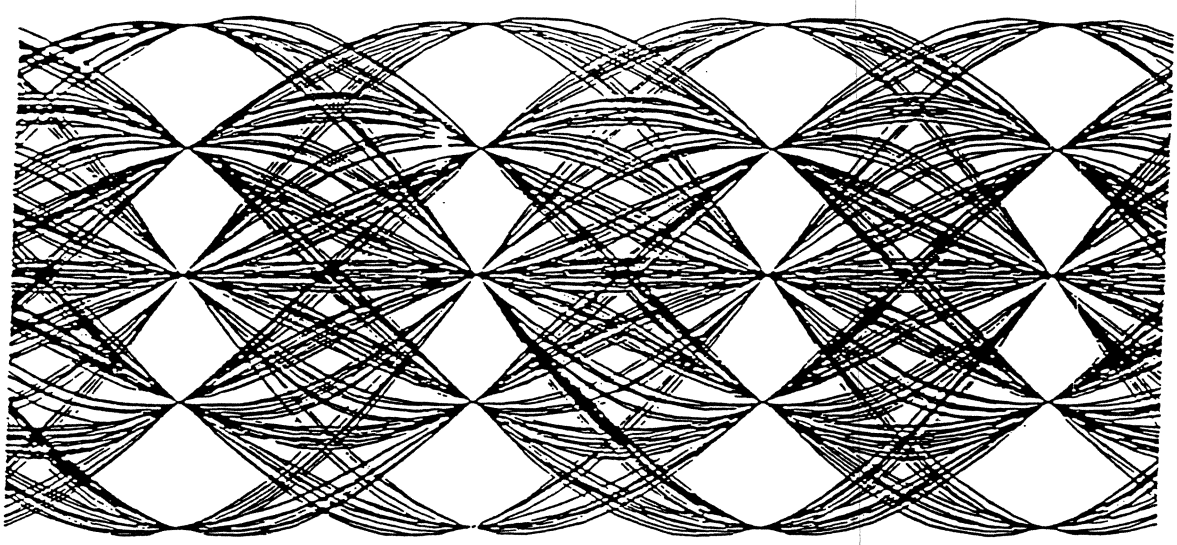

- 5 nominal sample values

DETECTION

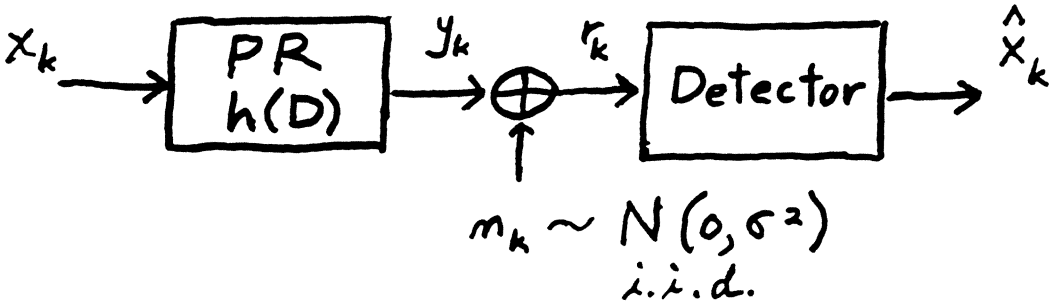

Received samples: $r_k = y_k + n_k$

- Maximum Likelihood (ML) detector

$$\max_{\underline{x}} \; p(\underline{r} \mid \underline{x})$$

likelihood function

ML is optimal detector

- ML $\Longleftrightarrow$ Minimum-Distance decoding

$$\max_{\underline{x}} \; p(\underline{r} \mid \underline{x}) \Longleftrightarrow \min_{\underline{x}} \sum_k (r_k - y_k)^2$$

Maximum-Likelihood Detection (Schematic)

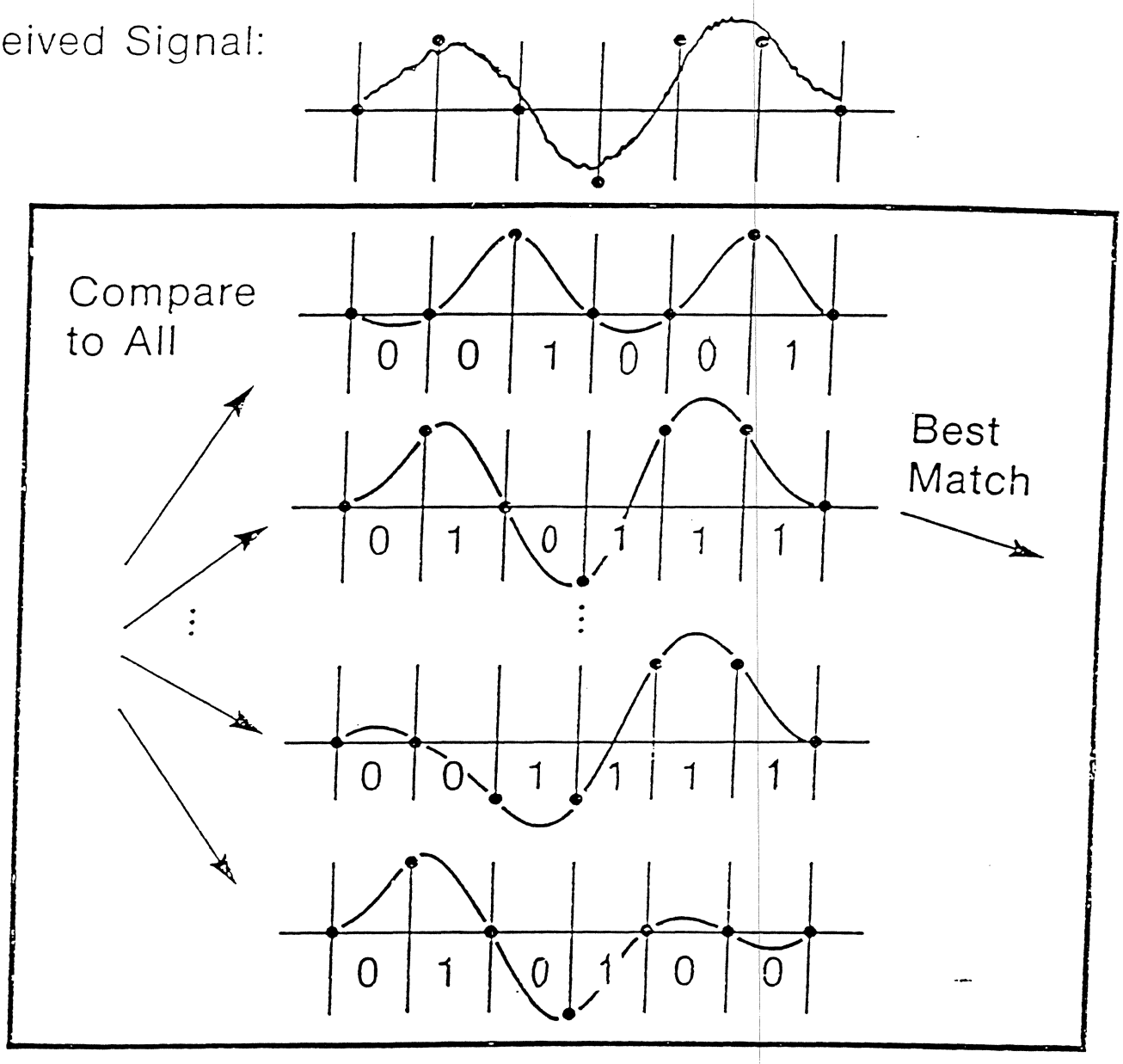

Most likely information sequence:

. . . 0 1 0 1 1 1 . . .

The Viterbi Algorithm (VA)

- Recursive solution of ML detection (dynamic programming)
- Trellis representation of PR channel (Forney)

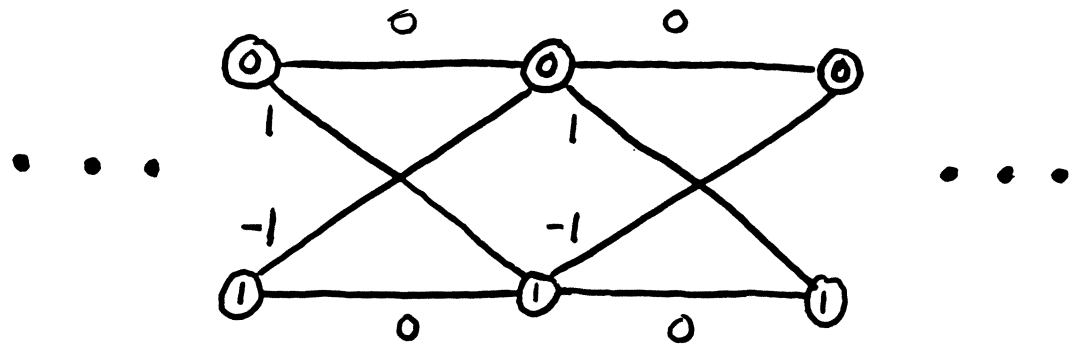

"Dicode" channel: $h(D) = 1 - D$

- Trellis-based architecture

Trellis state $\longrightarrow$ Add-Compare-Select processor (ACS)

PR Trellises

- PR4 (interleaved dicode)

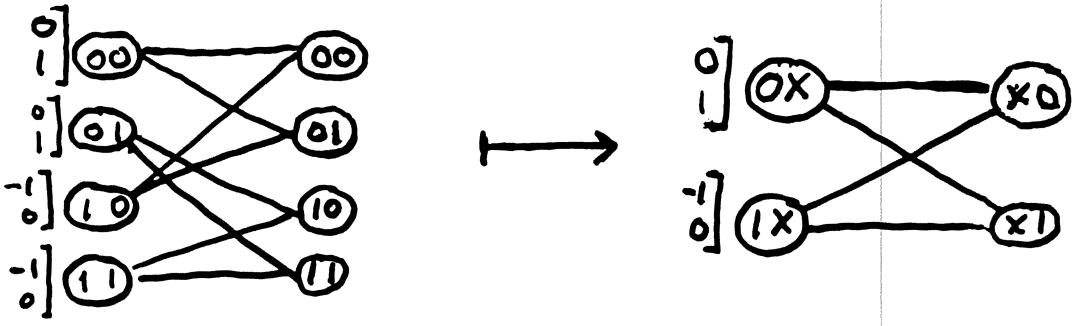

- EPR4

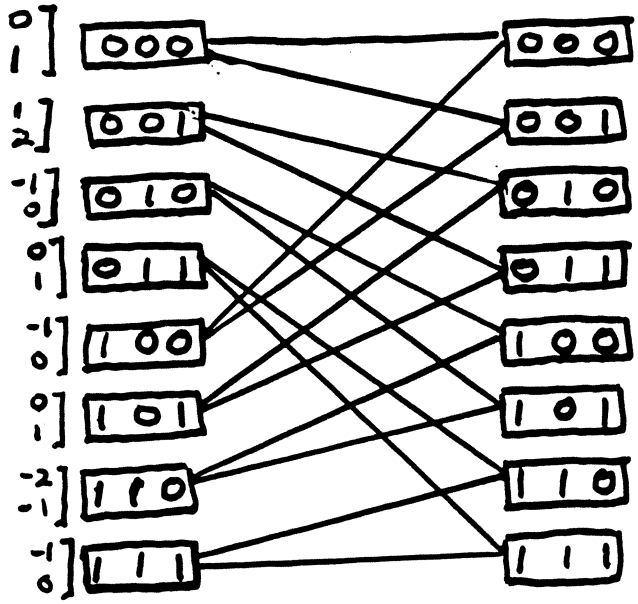

Improved PR model ⇒ larger detector complexity

VA Performance

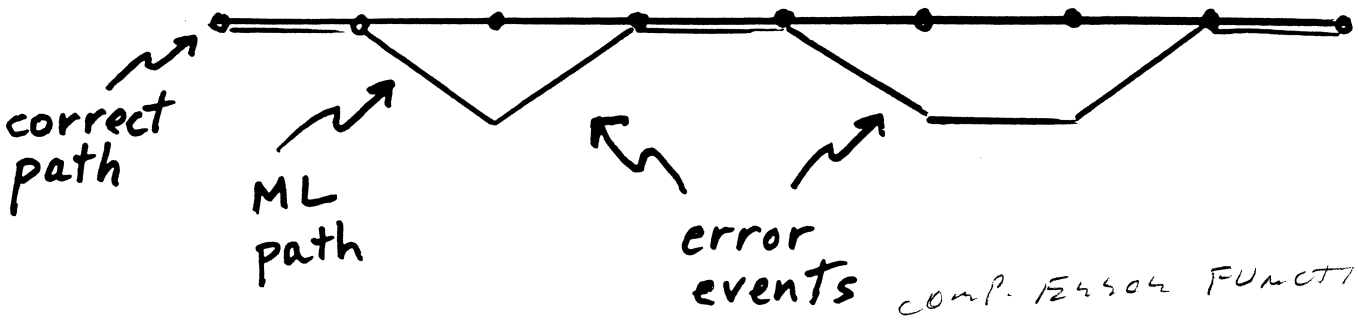

COMP. ERROR FUNCTION

$$P_e \approx N\, Q\left(\frac{d_{free}}{2\sigma}\right)$$

where N = "error coefficient"

d^2_{free} = minimum distance between any two trellis sequences differing by 1 error event

and

$$Q(x) = \frac{1}{\sqrt{2\pi}} \int_x^\infty e^{-\frac{s^2}{2}}\, ds$$

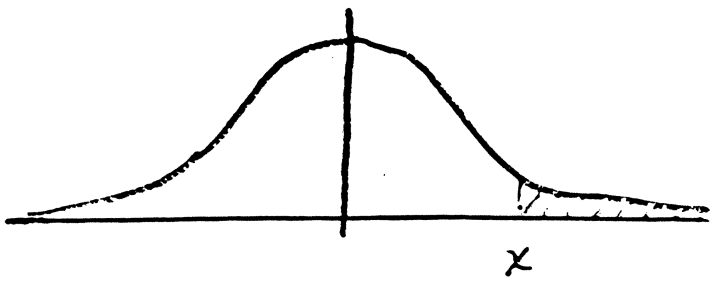

VA Performance Example

- $h(D) = (1-D)$

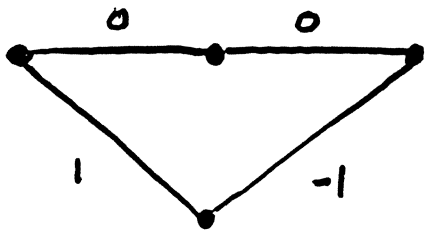

$$d^2_{free} = 2$$

$$N = 2$$

$$P_e^{VA} \approx 2\,Q\left(\frac{\sqrt{2}}{2\sigma}\right)$$

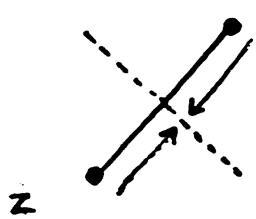

$$\frac{d_{free}}{2} = \frac{\sqrt{2}}{2}$$

- Compare to threshold detection (TD)

$$P_e^{TD} \approx \frac{3}{2}\,Q\left(\frac{1}{2\sigma}\right)$$

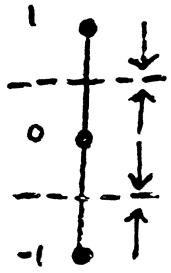

$$\frac{d}{2} = \frac{1}{2}$$

- VA is <u>3 dB</u> <u>better</u> than TD

VITERBI ALGORITHM

- Difference-metric formulation

Extension	*Condition*	*Update*
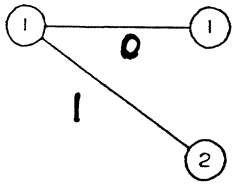	$DM_k \leq 2y_{k+1} - 1$	$DM_{k+1} = 2y_{k+1} - 1$
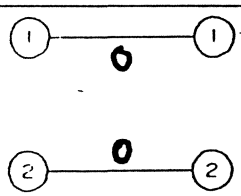	$2y_{k+1} - 1 < DM_k < 2y_{k+1} + 1$	$DM_{k+1} = DM_k$
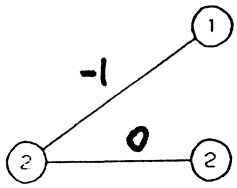	$2y_{k+1} + 1 \leq DM_k$	$DM_{k+1} = 2y_{k+1} + 1$

(0, G/I) CONSTRAINED CODES FOR PRML

PRECODING CONVENTIONS
(peak detection)

- NRZI: $\left(\frac{1}{1 \oplus D}\right)$

  0 ⟶ no transition

  1 ⟶ ± transition

- (d, k) constraints

  $d \leq$ # consecutive 0's $\leq k$

  d reduces intersymbol-interference

  k provides timing/gain information

- (1, 7) example

  1 0 1 0 0 0 0 0 0 0 1 0 0 1 0 1 . . .

Precoding Conventions (PRML)

- Interleaved NRZI (INRZI): $\frac{1}{1 \oplus D^2}$

  $0 \longrightarrow 0$ sample

  $1 \longrightarrow \pm 1$ sample

- $(0, G/I)$ constraints

  $d = 0$ (no ISI problem)

  G = Global k constraint (timing/gain)

  I = Interleaved k constraint (Viterbi path memory)

(0,G/I) = (0,4/4)

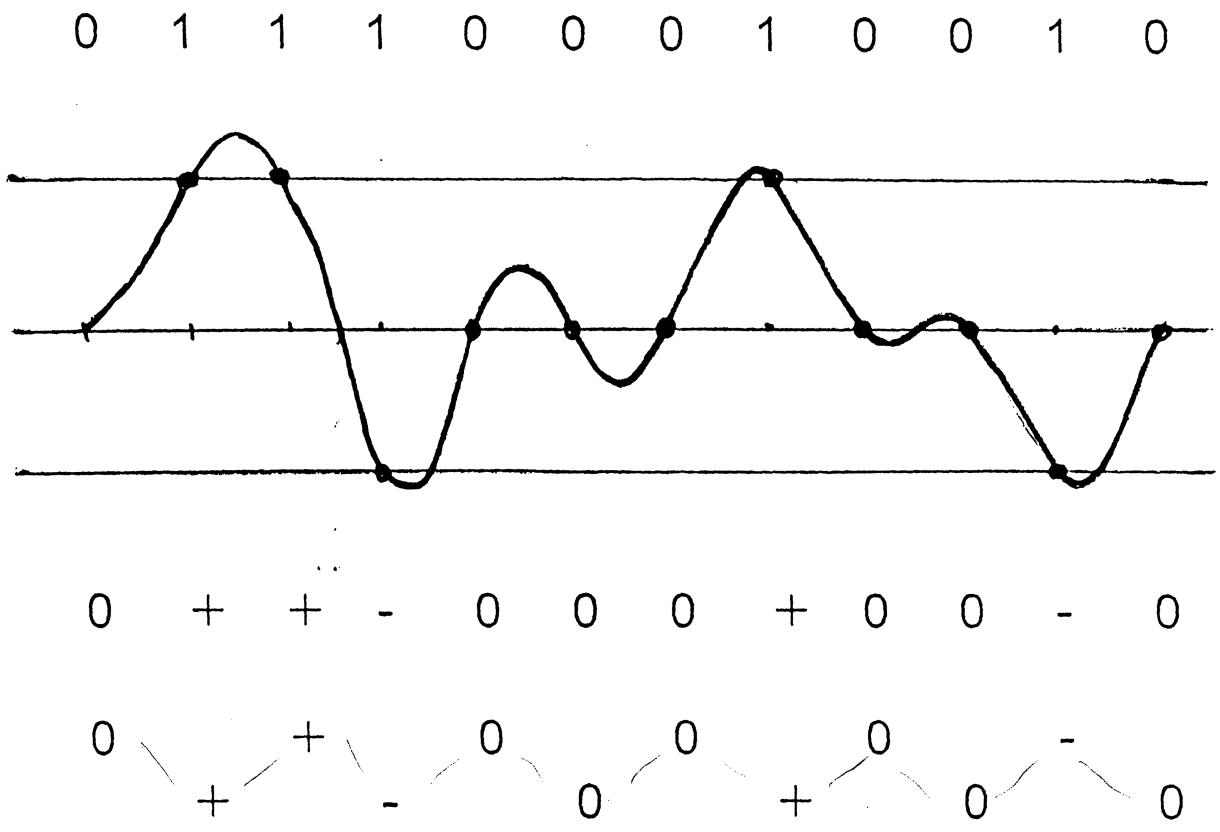

Sliding-Block Codes

- Finite-state encoder

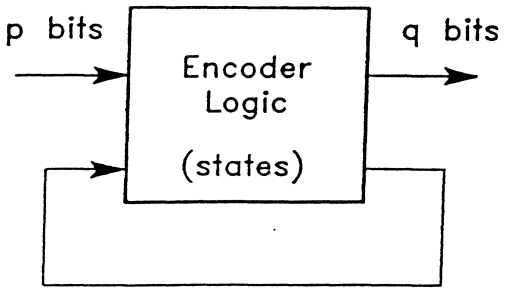

- Sliding-block decoder

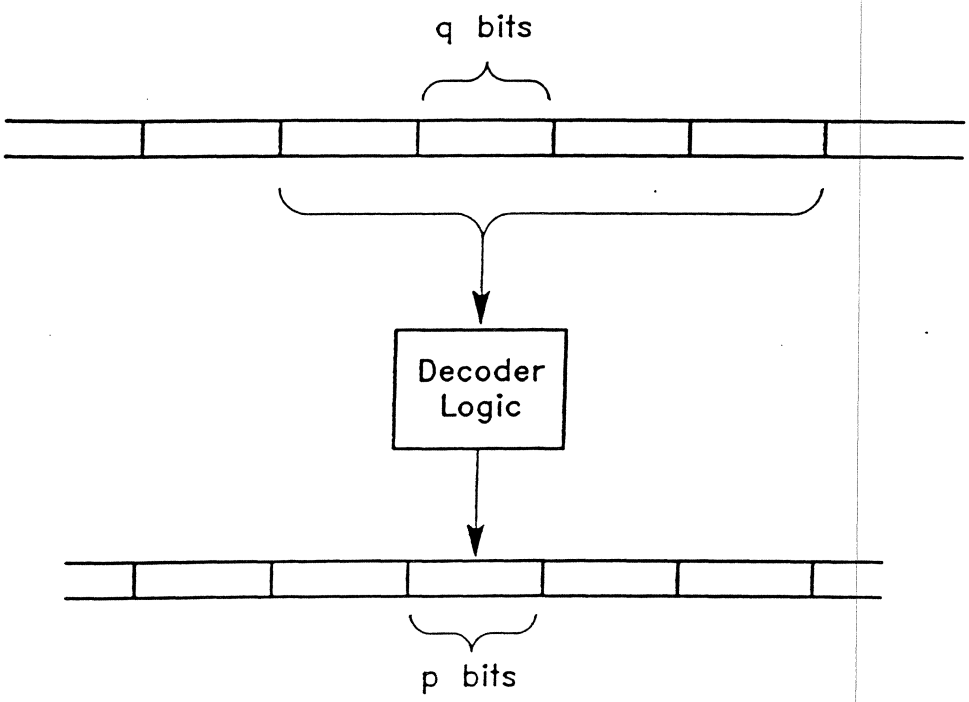

- Practical code construction methods

Sliding-Block (0,G/I) Codes

(0,G/I)	Capacity	Rate	Efficiency (%)	Encoder States	Decoder Window
(0,4/4)*	0.961	8/9	92.4	1	1
(0,4/3)	0.939	8/9	94.6	3	1
(0,3/6)*	0.944	8/9	94.1	1	1
(0,3/5)	0.941	8/9	94.4	2	1
(0,3/4)	0.934	8/9	95.1	3	2
(0,3/3)	0.915	8/9	97.0	4	2

x 9 for # of bits

* Originally found by J. Eggenberger

$(0, G/I) = (0, 4/4)$

- Optimal list of 279 9-bit words (in decimal)

73	116	183	225	268	310	361	402	438	479
75	117	185	227	269	311	363	403	439	481
76	118	186	228	270	313	364	406	441	483
77	119	187	229	271	314	365	407	442	484
78	121	188	230	281	315	366	409	443	485
79	122	189	231	282	316	367	410	444	486
89	123	190	233	283	317	369	411	445	487
90	124	191	235	284	318	370	412	446	489
91	125	195	236	285	319	371	413	447	491
92	126	198	237	286	329	372	414	451	492
93	127	199	238	287	331	373	415	454	493
94	146	201	239	289	332	374	417	455	494
95	147	203	241	291	333	375	419	457	495
97	150	204	242	292	334	377	420	459	497
99	151	205	243	293	335	378	421	460	498
100	153	206	244	294	345	379	422	461	499
101	154	207	245	295	346	380	423	462	500
102	155	210	246	297	347	381	425	463	501
103	156	211	247	299	348	382	427	466	502
105	157	214	249	300	349	383	428	467	503
107	158	215	250	301	350	390	429	470	505
108	159	217	251	302	351	391	430	471	506
109	177	218	252	303	353	393	431	473	507
110	178	219	253	305	355	395	433	474	508
111	179	220	254	306	356	396	434	475	509
113	180	221	255	307	357	397	435	476	510
114	181	222	265	308	358	398	436	477	511
115	182	223	267	309	359	399	437	478	

$G=4$: ≤ 2 0's at beginning/end
≤ 4 consecutive 0's inside

$I=4$: ≤ 2 0's at beginning/end in <u>each</u> interleave
≤ 4 consecutive 0's inside in <u>each</u> interleave

TRELLIS-CODED PRML

- Objectives and tradeoffs
- Example - Interleaved Biphase
- Design techniques
  - Precoded convolutional codes
  - Matched-spectral-null codes

TRELLIS CODING

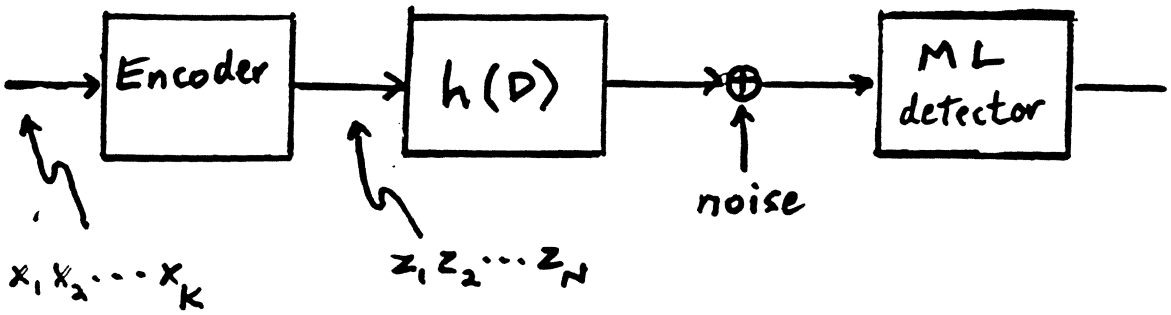

Binary symbols $\Rightarrow N > K$

- Why use coding?
  - Reduce P_e
  - Tolerate larger σ

  } • off-track capability
  • areal density
  • component yield
  • fly height relaxation

- Coding approach
  - Increase d_{free} with structured redundancy (trellis)
  - Enhance ML detector
- Costs
  - Code rate loss
  - Code/detector complexity

TRELLIS-CODED MODULATION

HISTORICAL BACKGROUND

- Shannon (1948): Use structured waveforms for efficient utilization of signal power and limited channel bandwidth.

- Elias, Massey, Viterbi, Forney, et al. (1960's): Convolutional codes for binary, memoryless channel

- Ungerboeck (1981): Trellis-coded modulation (TCM) for multi-level, memoryless channel.

- Wolf-Ungerboeck (1986): TCM for binary, partial-response channels $h(D) = 1 \pm D^N$ using convolutional codes.
  [Also, Calderbank-Heegard-Lee (1986)]

- Karabed-Siegel (1988): New TCM for binary, PR channels
  - Convolutional codes + inner codes
  - Matched-Spectral-Null codes
- TCM for multi-level, PR channels ...

Trellis Code Design Problem

- Replace selected digital blocks in PRML channel

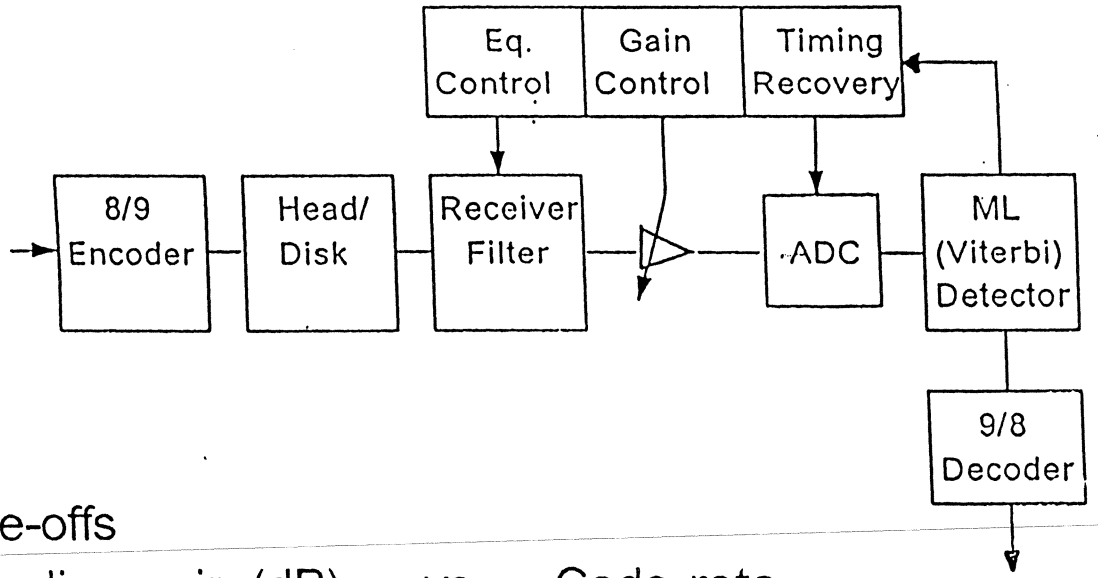

- Trade-offs

  Coding gain (dB) vs Code rate
  Encoder/decoder complexity
  Viterbi detector complexity

Trellis Code Example

- Interleaved Biphase (IB) Code

  Rate: 1/2 (2:4)

  Encoder: $xy \rightarrow xy\bar{x}\bar{y}$

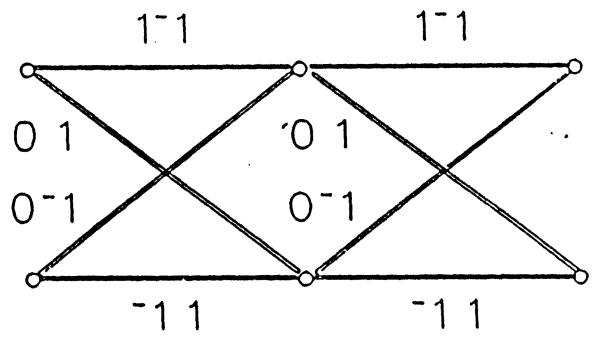

- Coding gain 4.8 dB

$$d^2_{free} = 6 \qquad \left(10 \log_{10} \frac{6}{2} = 4.8\right)$$

- Complexity 4 $\left(\frac{\#\ \text{edges}}{\text{stage}}\right)$

IB/DICODE PERFORMANCE (simulated)

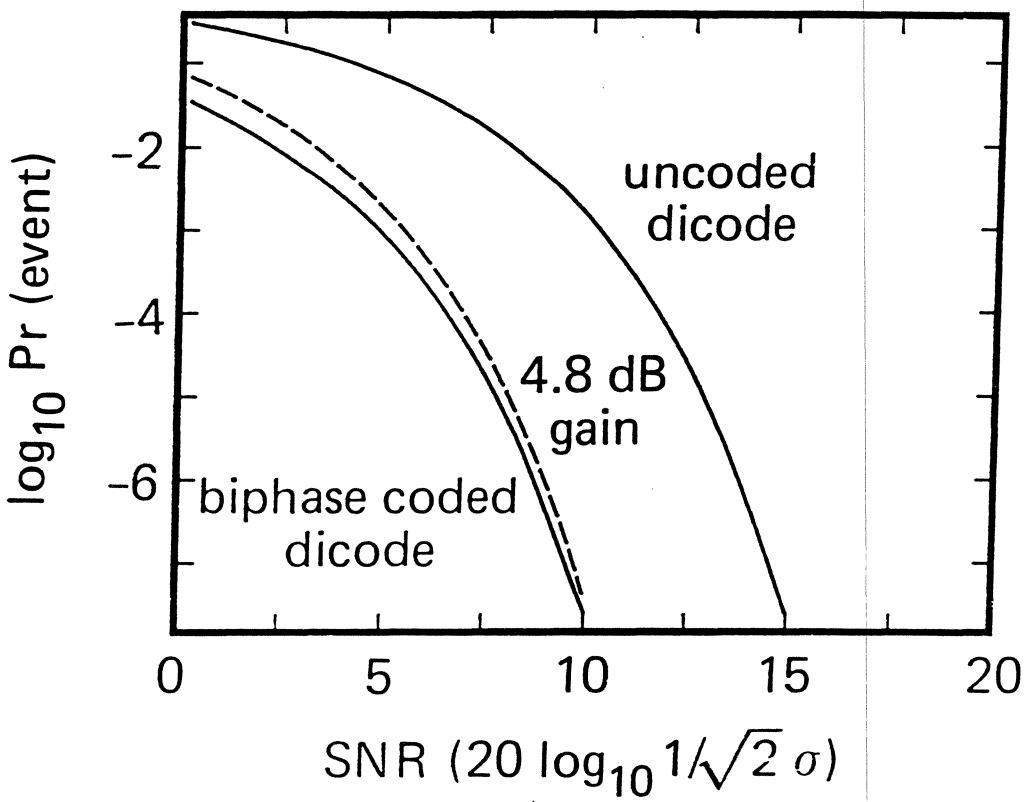

- Additive white gaussian noise

$$n_i \sim N(0, \sigma^2)$$

Increasing Areal Density

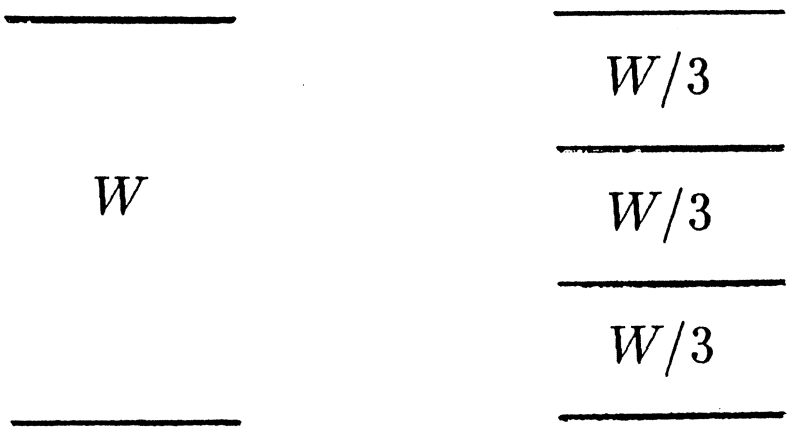

- Reduce trackwidth by 3: costs 4.8 dB
- Rate 1/2 IB code: gains 4.8 dB
- Net areal density: 1.7 (70% increase)
  $3 \times (1/2) \times (9/8) \simeq 1.7$
- Same P_e

TRACK CUTTING

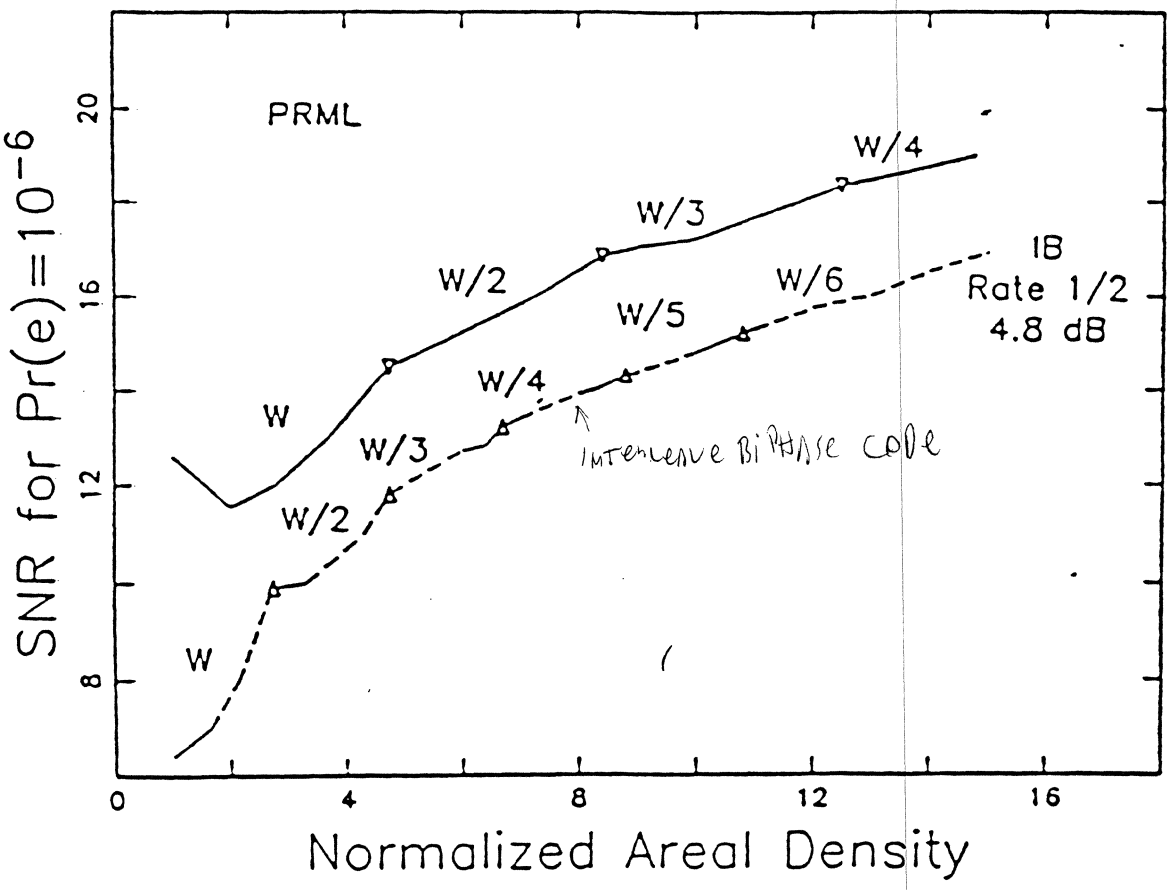

- IB areal density gains > 70%
  - Low rate ⇒ very narrow tracks

TRACK CUTTING (cont.)

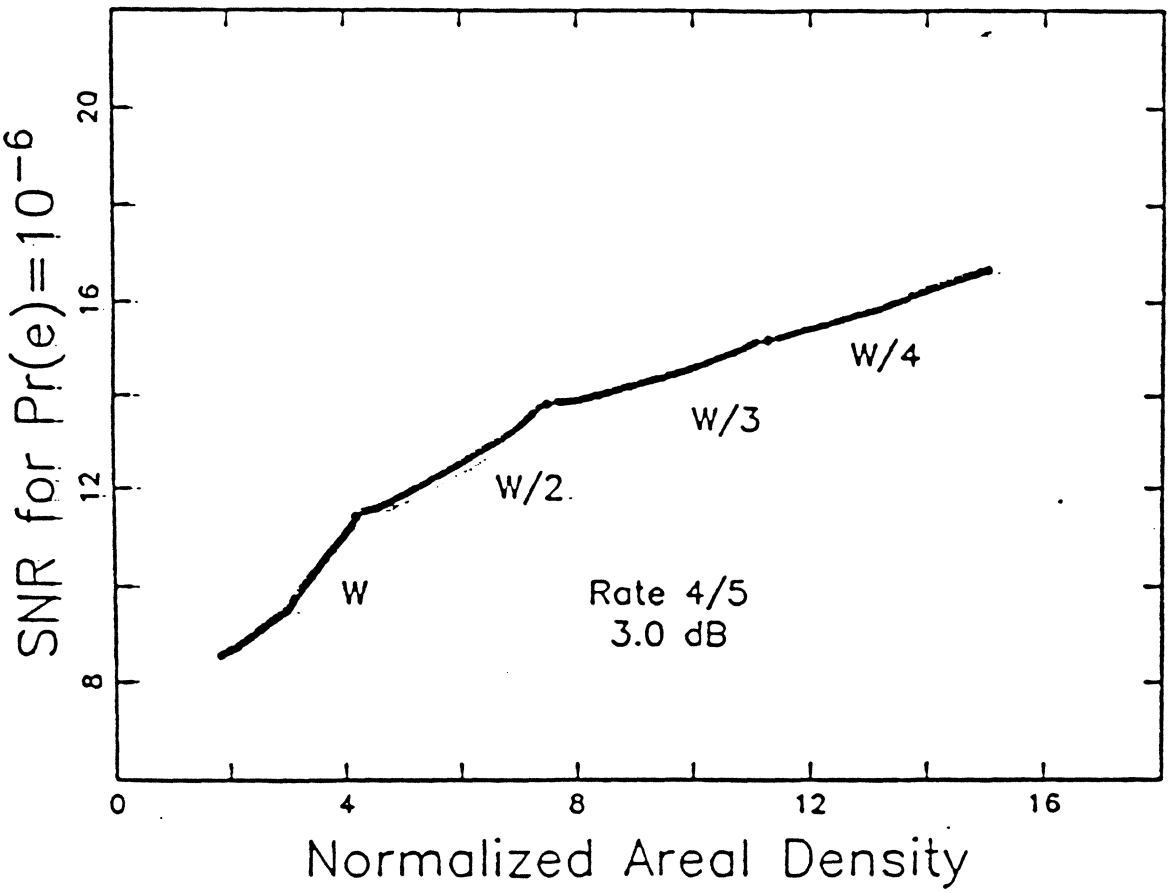

- Rate 4/5, gain 3 dB
  - Same density gains
  - Wider tracks

Wolf-Ungerboeck Codes

- Use known binary convolutional codes (designed for memoryless channel)
- Neutralize PR channel memory via precoding
- Add coset sequence to limit runs of zero samples

Convolutional Codes

- Linear Feed-Forward Shift Register Encoder

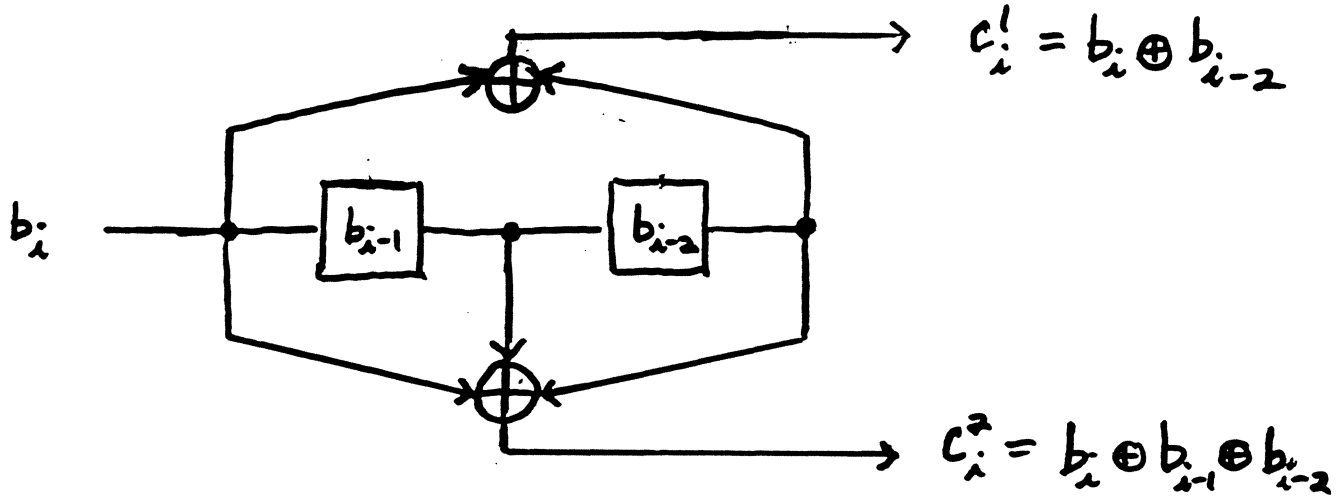

0,0,0,0,0,0. } $d^H = 1$ ⟶ $d^H = 5$ { 00.00.00.00.00.00.
0,0,1,0,0,0. } { 00.00.11.01.11.00.

- State-diagram representation

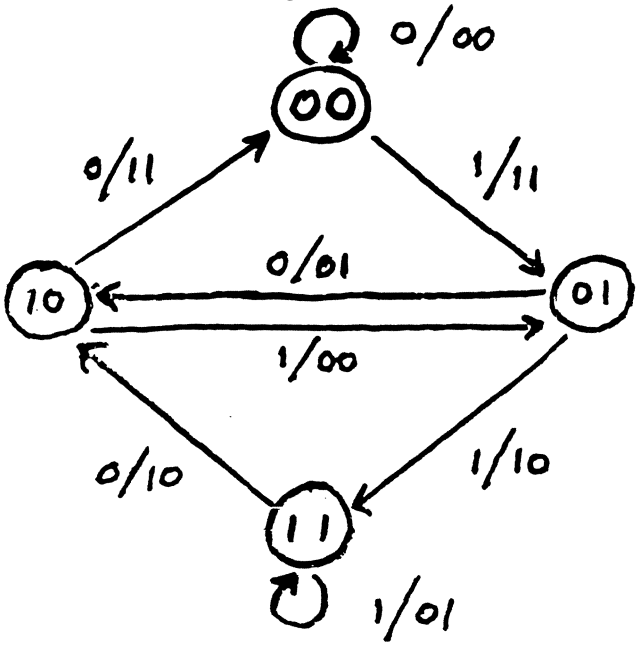

$d^H_{free} = 5$

Decoding Convolutional Codes

- Trellis representation

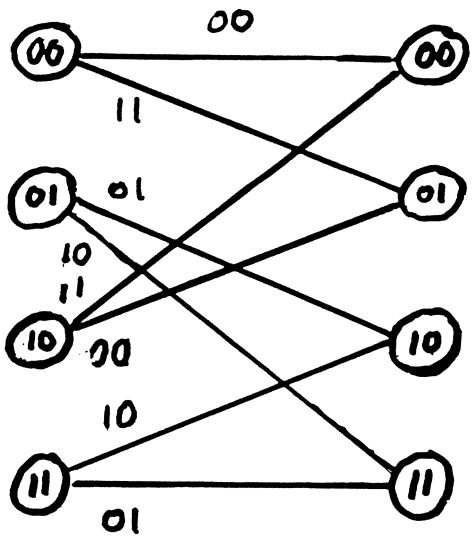

- ML decoding via VA

- Optimal codes

Maximize d_{free}^{H}

for given rate $R = \frac{k}{N}$

and complexity M (total encoder memory)

Optimal Code Tables

- Best codes found by computer search
- Examples [ref. Lin-Costello]

		M	States (2^M)	d_{free}^H
Rate $\frac{1}{2}$				
		2	4	5
	*	6	64	10
Rate $\frac{2}{3}$				
		4	16	5
		10	1024	10
Rate $\frac{3}{4}$				
		5	32	5
		6	64	6
Rate $\frac{4}{5}$				
from [Daut, et al.]		3	8	3

CONVOLUTIONAL CODES FOR PR $h(D) = (1 \pm D^N)$

- PR channel memory can destroy good d^H_{free} at channel input
- Solution (W-U): Use <u>precoder</u> to neutralize channel memory

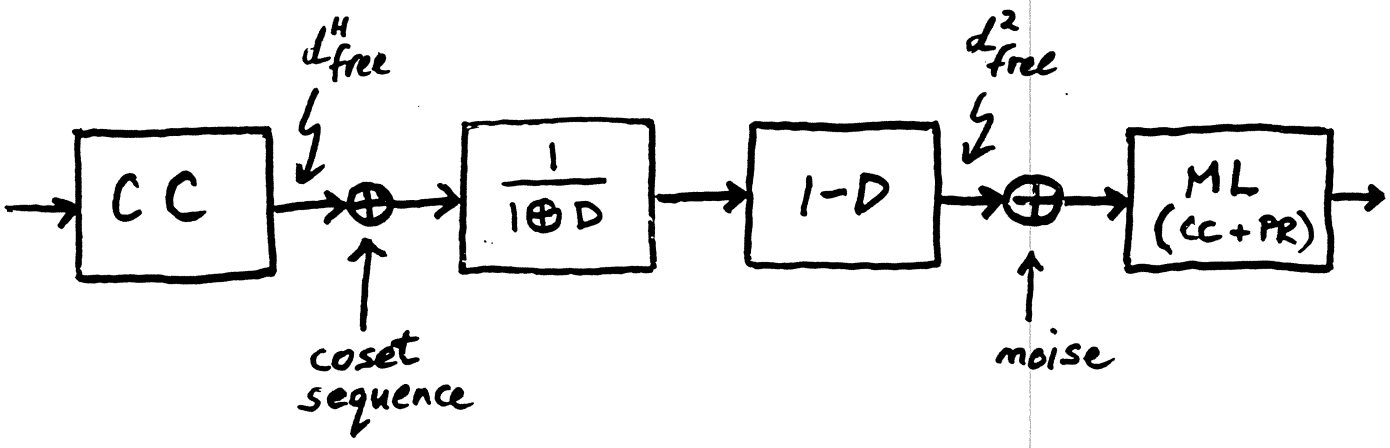

- Precoder effect:

$$0 \longmapsto 0$$
$$1 \longmapsto \pm 1$$

$$d^2_{free} \geq \begin{cases} d^H_{free} & \text{if } d^H_{free} \text{ is even} \\ d^H_{free}+1 & \text{if } d^H_{free} \text{ is odd} \end{cases}$$

[see also C-H-L & Hole]

Precoded PR (cont.)

- Coset sequence limits maximum run of zero outputs (timing/gain)
- ML decoder trellis has $\underline{2^{M+1}}$ states (usually - not always, e.g. see * in table)
- Gains smaller than in memoryless channel (for given rate and decoder complexity)

"Full response"	PR $(1 \pm D)$
$R = \frac{3}{4}$, $M = 6$, $d^H_{free} = 6$	$R = \frac{3}{4}$, $M+1 = 6$, $d^2_{free} = 6$
$C.G. = 10 \log_{10} \boxed{\frac{d^H_{free}}{1}}$	$C.G. = 10 \log_{10} \boxed{\frac{d^2_{free}}{2}}$
≈ 7.8 dB	≈ 4.8 dB
$A.C.G. = C.G. + 10 \log_{10} R$	$A.C.G = C.G. - 10 \log_{10} R$
≈ 6.5 dB	≈ 3.5 dB

W-U CODE EXAMPLE
(for 1-D channel)

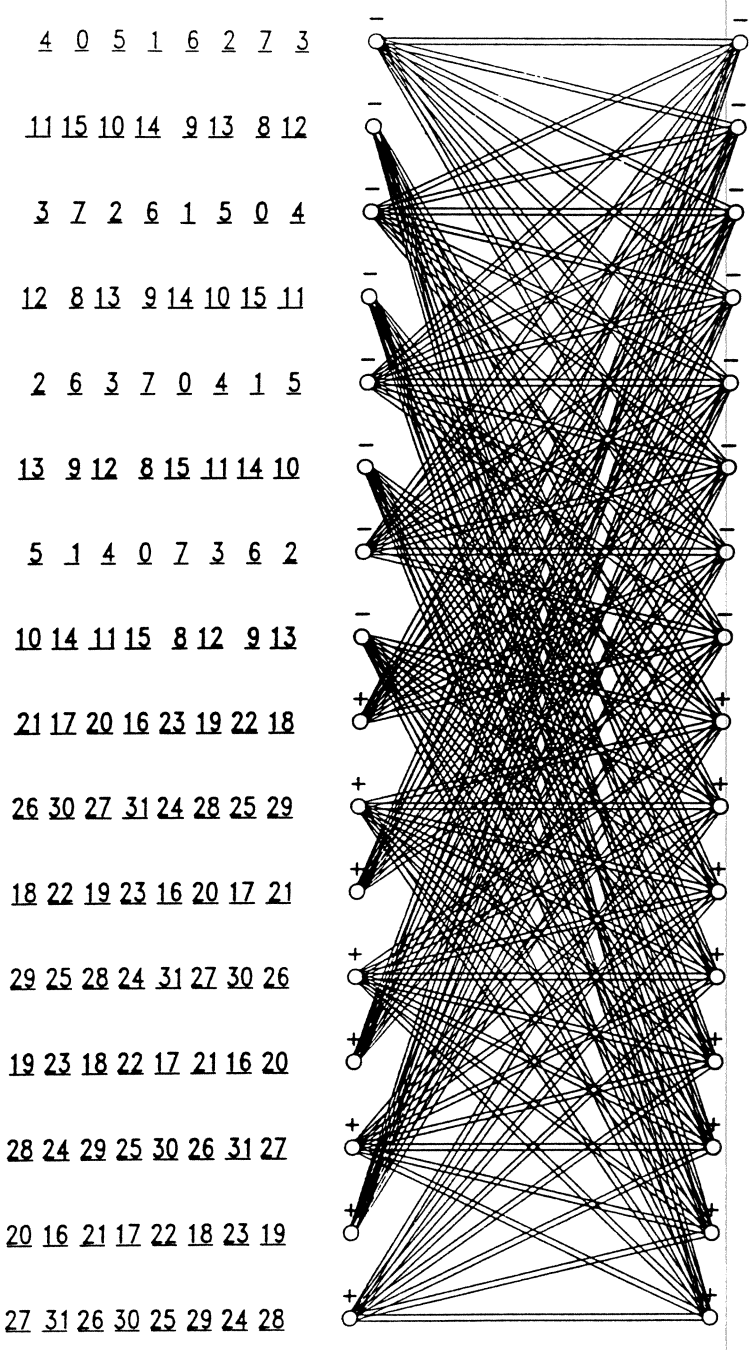

- Rate 4/5, gain 3 dB
- (0, G/I) = (0, 44/22) when interleaved

W-U Code Example (cont.)

- Detector edge labels

− to −		+ to −		− to +		+ to +	
0	$10\bar{1}00$ $1\bar{1}01\bar{1}$	16	$00\bar{1}00$ $0\bar{1}01\bar{1}$	8	00100 $010\bar{1}1$	24	$\bar{1}0100$ $\bar{1}10\bar{1}1$
1	$1\bar{1}1\bar{1}0$ $1000\bar{1}$	17	$0\bar{1}1\bar{1}0$ $0000\bar{1}$	9	$01\bar{1}10$ 00001	25	$\bar{1}1\bar{1}10$ $\bar{1}0001$
2	$01\bar{1}00$ $0001\bar{1}$	18	$\bar{1}1\bar{1}00$ $\bar{1}001\bar{1}$	10	$1\bar{1}100$ $100\bar{1}1$	26	$0\bar{1}100$ $000\bar{1}1$
3	$001\bar{1}0$ $0100\bar{1}$	19	$\bar{1}01\bar{1}0$ $\bar{1}100\bar{1}$	11	$10\bar{1}10$ $1\bar{1}001$	27	$00\bar{1}10$ $0\bar{1}001$
4	$0010\bar{1}$ $010\bar{1}0$	20	$\bar{1}010\bar{1}$ $\bar{1}10\bar{1}0$	12	$10\bar{1}01$ $1\bar{1}010$	28	$00\bar{1}01$ $0\bar{1}010$
5	$01\bar{1}1\bar{1}$ 00000	21	$\bar{1}1\bar{1}1\bar{1}$ $\bar{1}0000$	13	$1\bar{1}1\bar{1}1$ 10000	29	$0\bar{1}1\bar{1}1$ 00000
6	$1\bar{1}10\bar{1}$ $100\bar{1}0$	22	$0\bar{1}10\bar{1}$ $000\bar{1}0$	14	$01\bar{1}01$ 00010	30	$\bar{1}1\bar{1}01$ $\bar{1}0010$
7	$10\bar{1}1\bar{1}$ $1\bar{1}000$	23	$00\bar{1}1\bar{1}$ $0\bar{1}000$	15	$001\bar{1}1$ 01000	31	$\bar{1}01\bar{1}1$ $\bar{1}1000$

Inner Codes

- Use simple inner code to exploit channel memory (Karabed-Siegel, Immink)

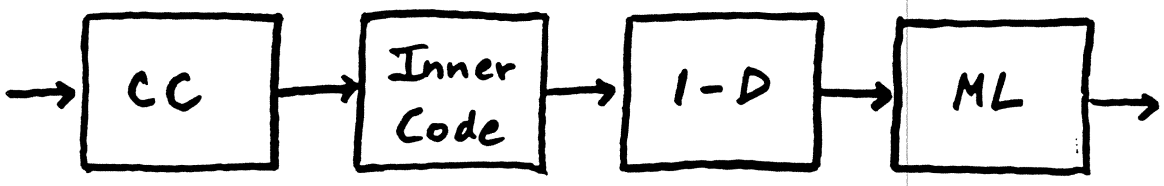

	Rate	Inner Code	Zero Runlength
(W-U)	$R=1$	$\frac{1}{1 \oplus D}$	CC dependent
(IC1)	$R=\frac{1}{2}$	$x \longmapsto x\bar{x}$ (biphase)	1
(IC2)	$R=\frac{2}{3}$	$xy \longmapsto xy\bar{y}$	2

- IC1 and IC2 give robust coding gain.

Inner Codes (cont.)

- Gains from IC1 and IC2 (for any convolutional code)

IC1:

$$d^2_{free} \geq 4 d^H_{free} + 4$$

$$R_{cc/IC} = \frac{1}{2} R_{cc}$$

IC2:

$$d^2_{free} \geq 2 d^H_{free}$$

$$R_{cc/IC} = \frac{2}{3} R_{cc}$$

- Example using IC2

$R_{cc} = \frac{3}{4}$, $M = 3$, $d^H_{free} = 5 \Longrightarrow$

$R_{cc/IC} = \frac{3}{6}$, states = 16, $d^2_{free} = 10$

Compare to w-u: $R = \frac{1}{2}$, states = 64, $d^2_{free} = 10$

Matched-Spectral-Null Codes

- Code design method based on general theorem

Significant coding gain results if:

$$\left\{\begin{array}{l}\text{null frequencies}\\ \text{in code power}\\ \text{spectrum}\end{array}\right\} = \left\{\begin{array}{l}\text{null frequencies}\\ \text{in channel frequency}\\ \text{response}\end{array}\right\}$$

- Sliding-block code design

- Reduced-complexity detector trellis

MSN Examples

- Biphase code

$h(D) = 1 - D$

C.G. = 4.8 dB

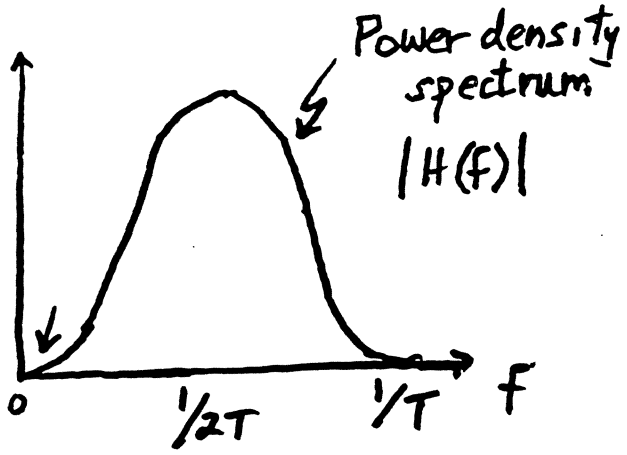

- Interleaved Biphase

$$h(D) = \begin{cases} (1-D)(1+D) & \text{(PR4)} \\ (1-D)(1+D)^2 & \text{(EPR4)} \end{cases}$$

C.G. = 4.8 dB

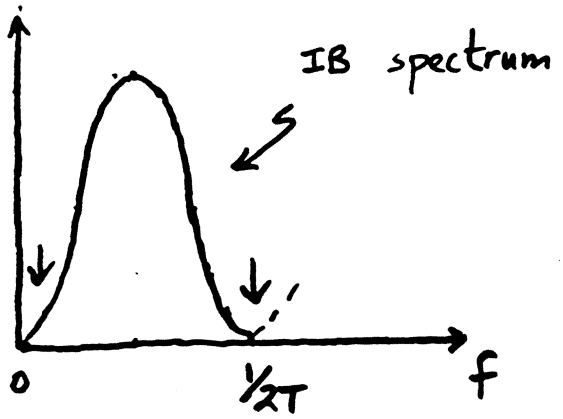

- Even Mark Modulation

$$h(D) = \begin{cases} 1+D & \text{(PR1)} \\ (1+D)^2 & \text{(PR2)} \end{cases}$$

$$\text{C.G.} = \begin{cases} 3\ \text{dB} \\ 4\ \text{dB} \end{cases}$$

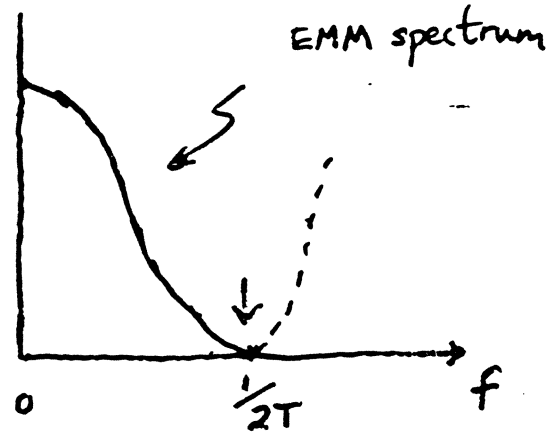

Matched Spectral Null Codes (cont.)

- Magnetic recording partial-responses

Interleaved Biphase

PR4: 4.8 dB
EPR4: 4.8 dB

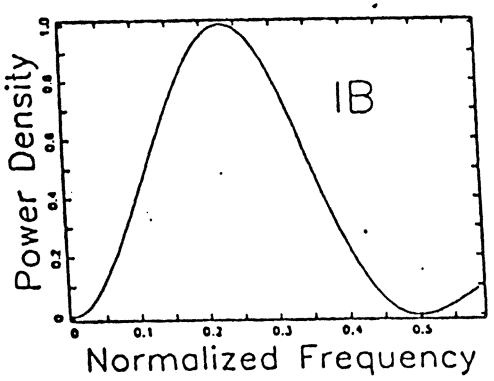

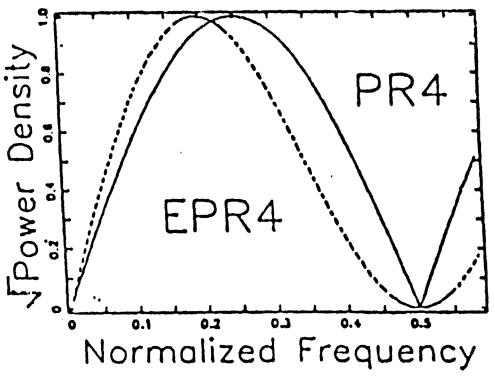

- Optical recording partial-responses

EMM

PR1: 3 dB
PR2: 4 dB

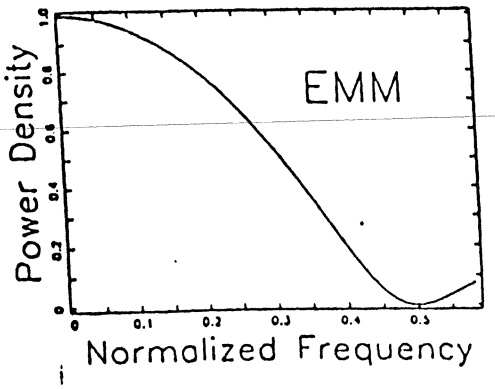

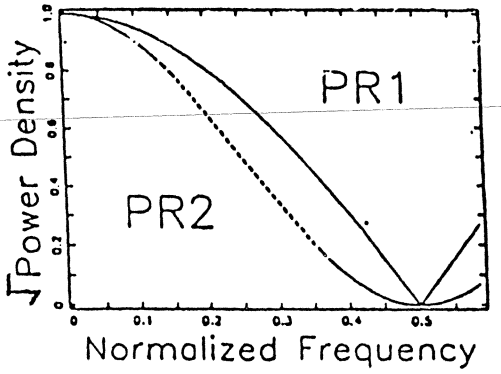

EVEN-MARK-MODULATION (EMM)

- Asymmetric RLL constraint for optical recording
- Marks must be <u>even</u> in length

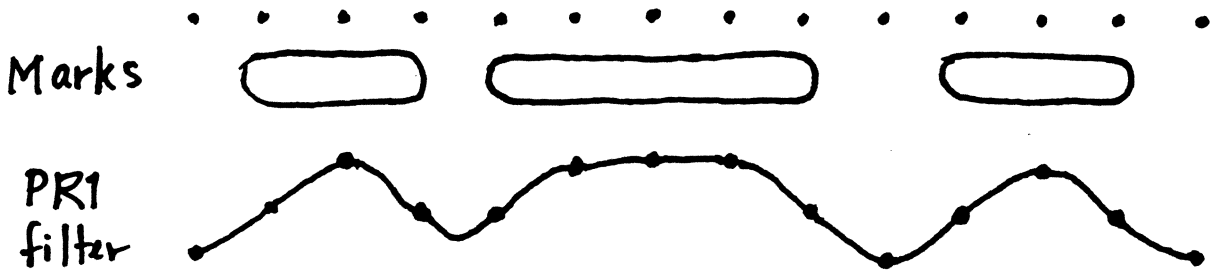

- EMM constraint diagram

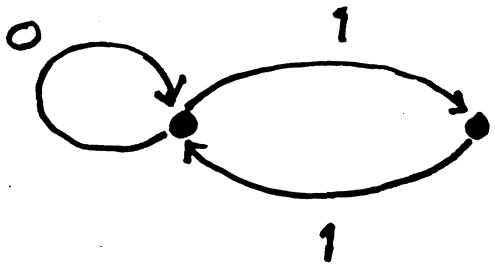

$$C = \log_2 \frac{1+\sqrt{5}}{2} \approx .69$$

- Rate 2/3 code possible

EMM Code

Rate 2:3 encoder

Data b_1/b_2 State $s_1s_2s_3$	00	01	10	11
000	011/000	011/001	110/000	110/001
001	001/100	001/101	110/010	011/110
010	000/000	000/011	111/100	111/101
011	001/100	001/101	111/100	111/101
100	100/000	100/001	101/100	101/101
101	111/000	111/001	100/010	111/111
110	000/000	000/001	111/100	111/101
111	000/000	000/001	111/100	000/010

Table entries = "codeword/next state"

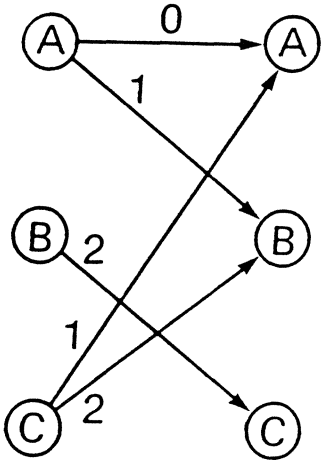

Detector trellis
EMM/PR1

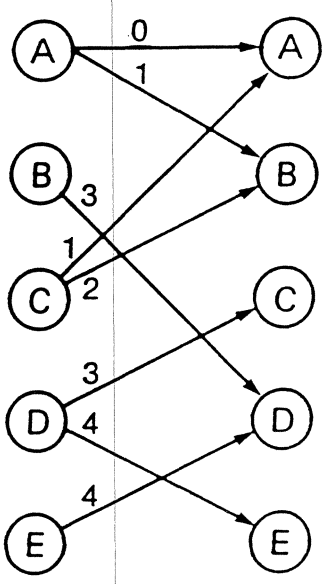

Detector trellis
EMM/PR2

EMM/PR1 PERFORMANCE
(simulated)

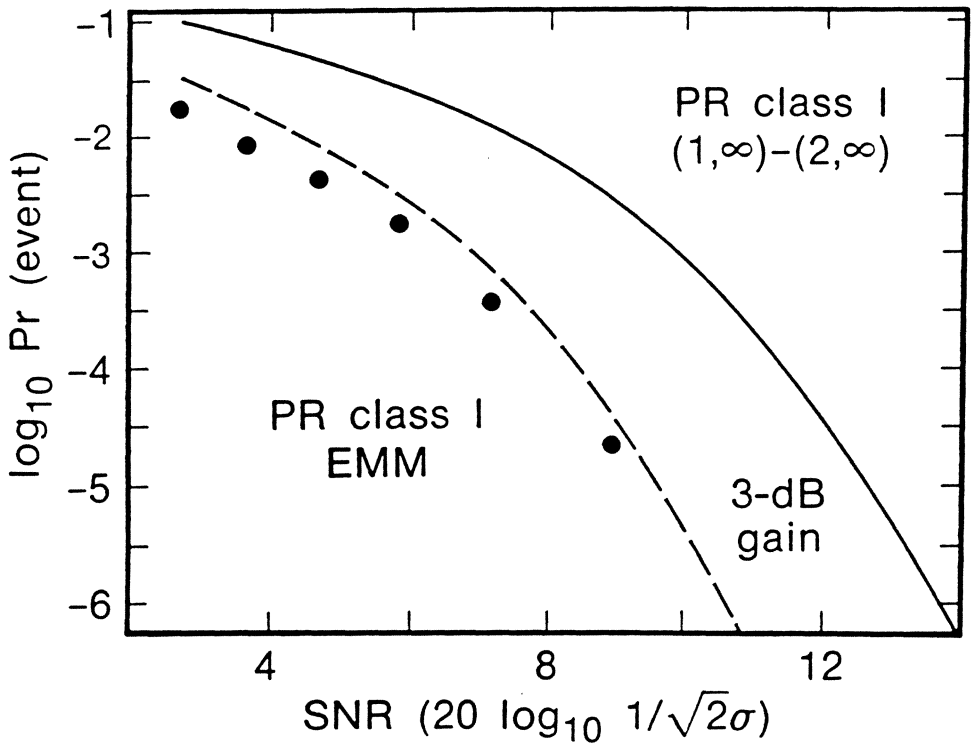

- Additive white gaussian noise

$$n_i \sim N(0, \sigma^2)$$

EMM/PR2 PERFORMANCE (simulated)

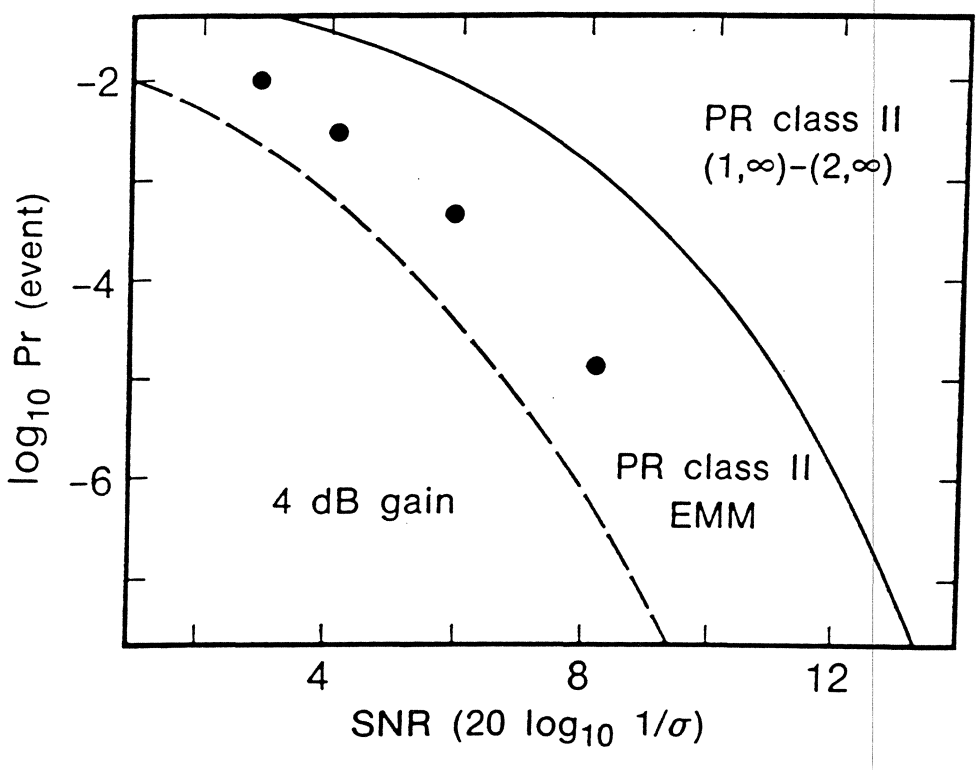

- Additive white gaussian noise

$$n_i \sim N(0, \sigma^2)$$

MSN Code Example (for 1-D)

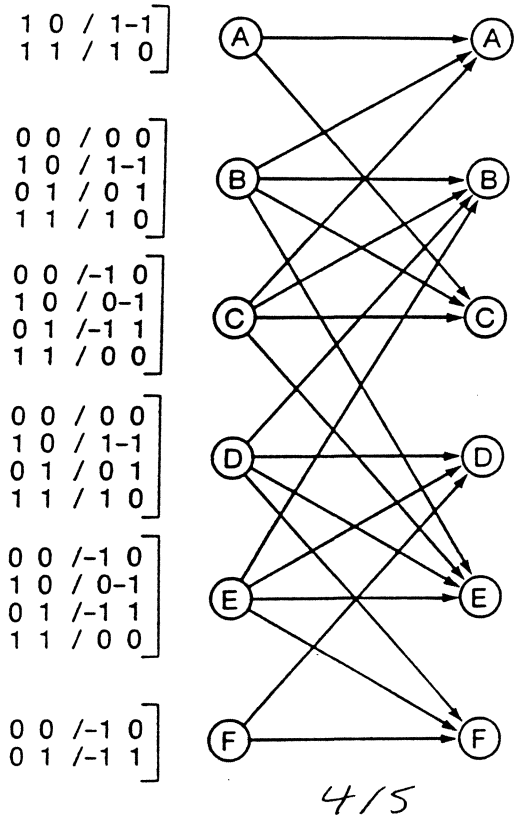

- Rate 8/10, gain 3dB
- (0, G/I) = (0, 10/5) when interleaved
- Reduced complexity trellis
- 2-state encoder, block decoder

TRELLIS CODE PERFORMANCE
(simulation)

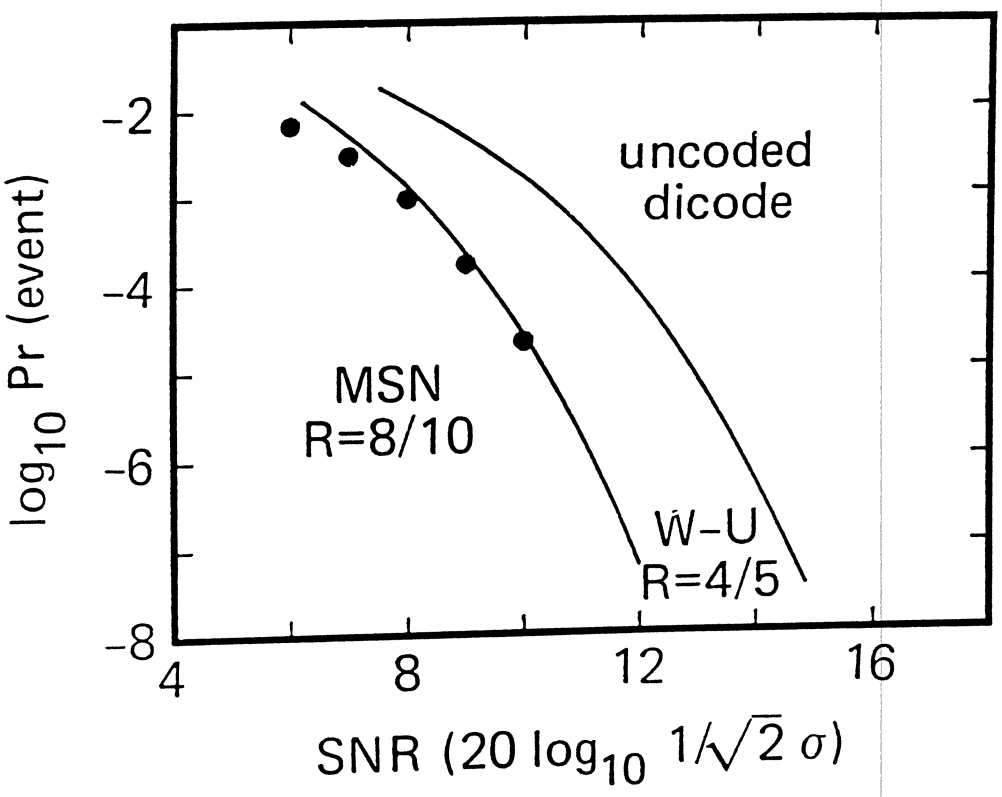

- Confirms 3dB coding gain with AWGN

MSN Coding Gain

- Order-K null at $f = \frac{k}{mT}$

$$S(f) = S^{(1)}(f) = \cdots = S^{(2K-1)}(f) = 0$$

$S(f)$: power spectrum

- Theorem (sketch for $f = 0$, binary code)

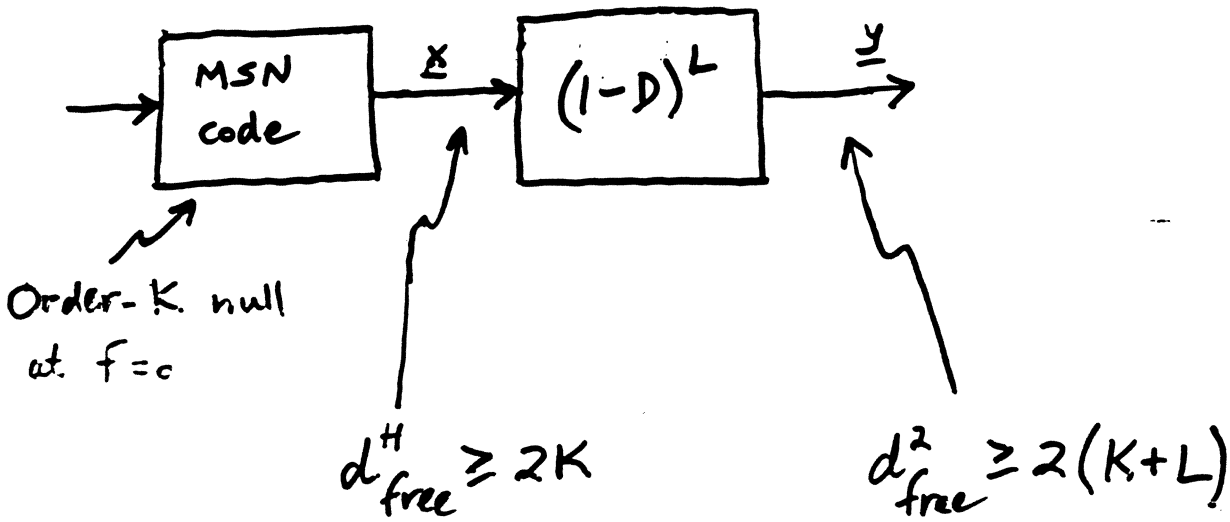

- Generalizes to multilevel codes

MSN Code Design

- "Canonical diagram" representation of sequences with order-K null(s).

$f=0$, $K=1 \Rightarrow G_0'$

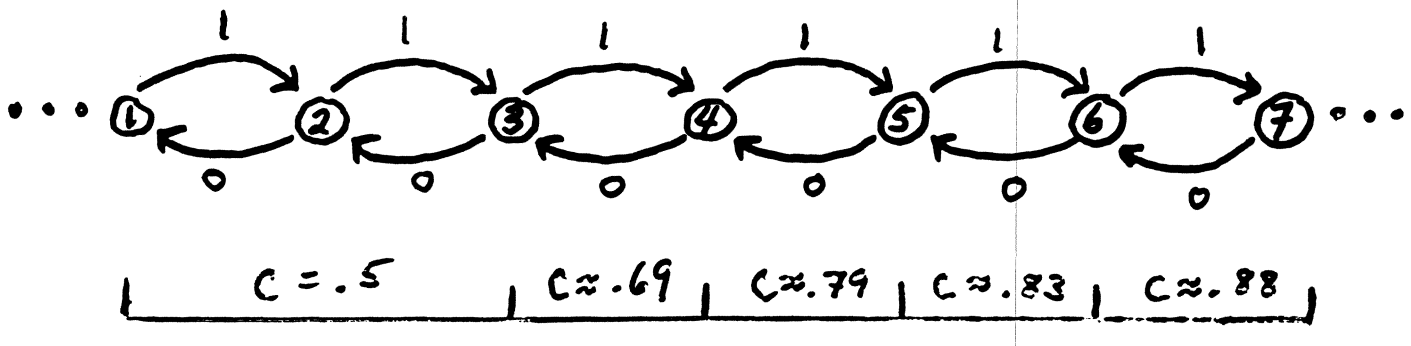

- Sliding block code construction
  - Choose desired rate R
  - Pick subdiagram $S \subset G_0'$ with $R < C_S$
  - Apply sliding block code algorithm [A-C-H, K-M]

Reduced Complexity MSN Detector Trellis

- Detector trellis derived from spectral null constraint, not from actual encoder.

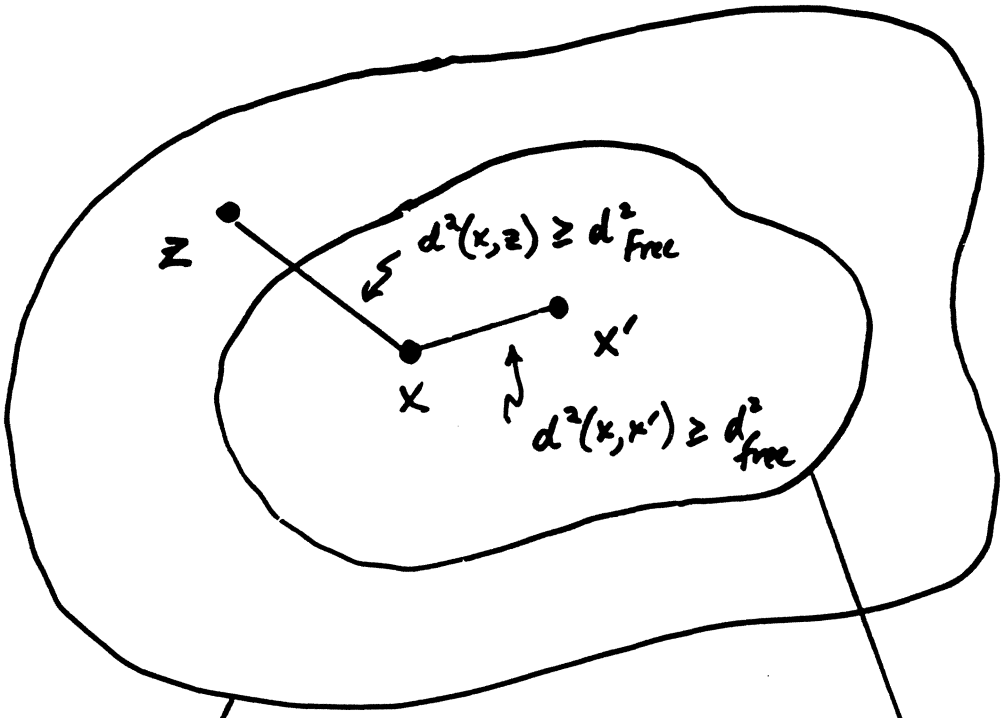

- spectral null sequences
  - 6 states
  - 20 edges
  - 2 symbols/edge

MSN code sequences
- 4 states
- 1024 edges
- 10 symbols/edge

VLSI DESIGN FOR RATE 8/10 MSN CODE

- ARCHITECTURE
- LAYOUT
- FUNCTIONAL EVALUATION

(Chip designer: Prof. C. B. Shung)

Chip Block Diagram

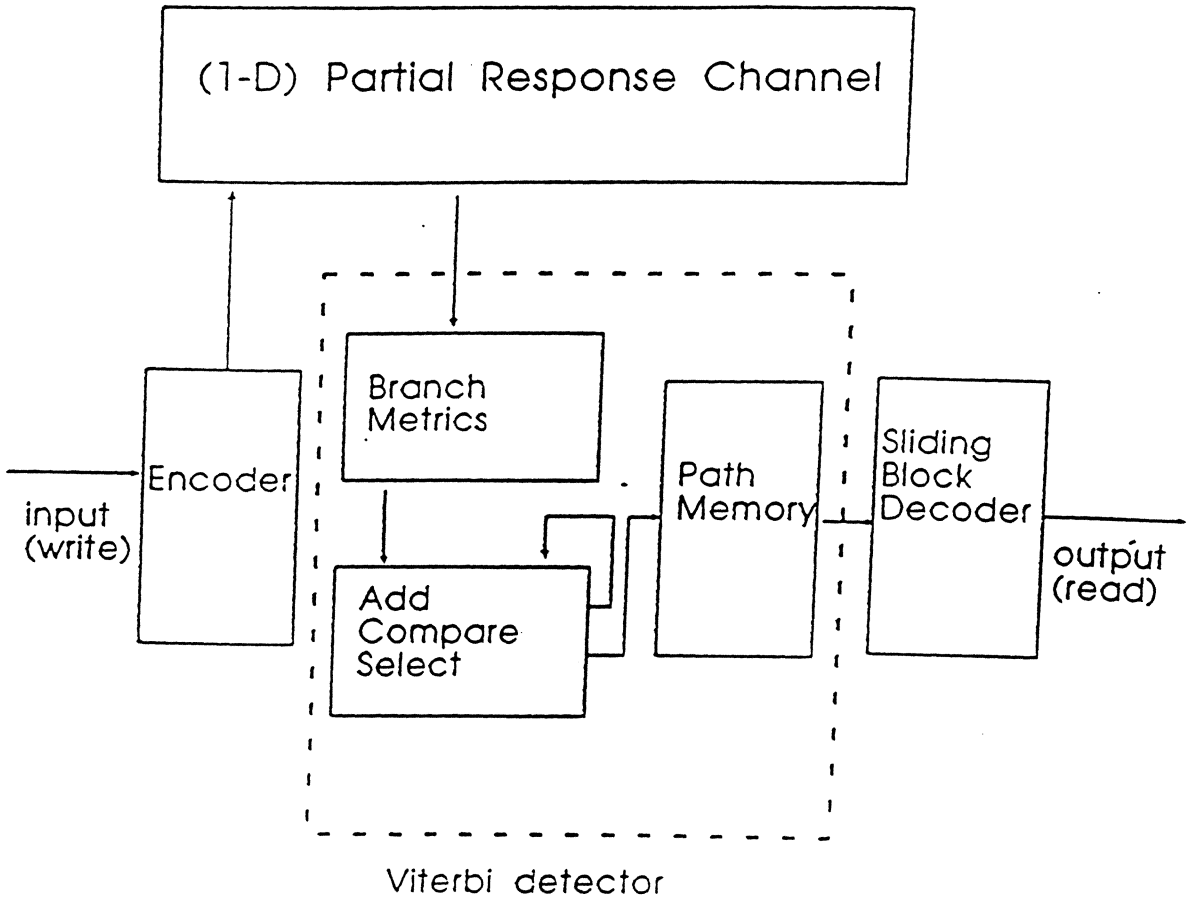

- Main architectural features
  - Modulo metric normalization
  - Pipelined ACS architecture

CHIP APPLICATION TO PRML

Write Channel

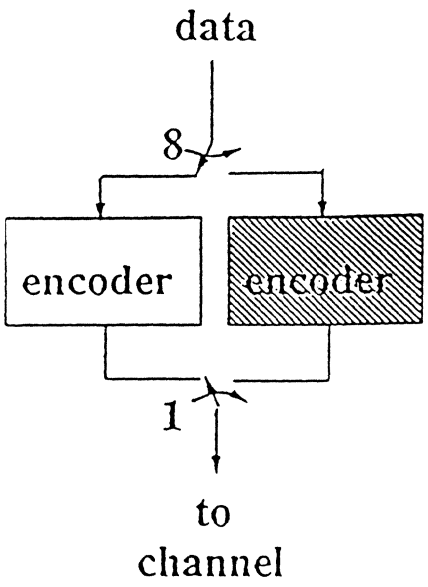

Read Channel

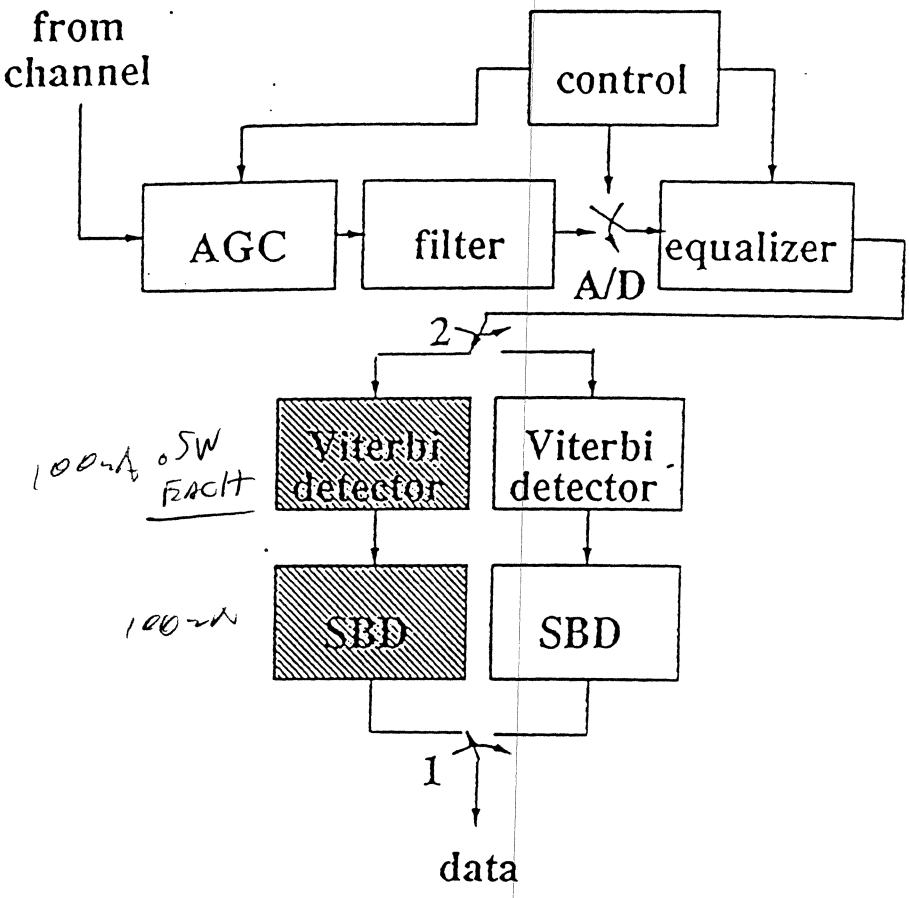

- 2 chips interleaved for PR4

MSN Trellis in Chip

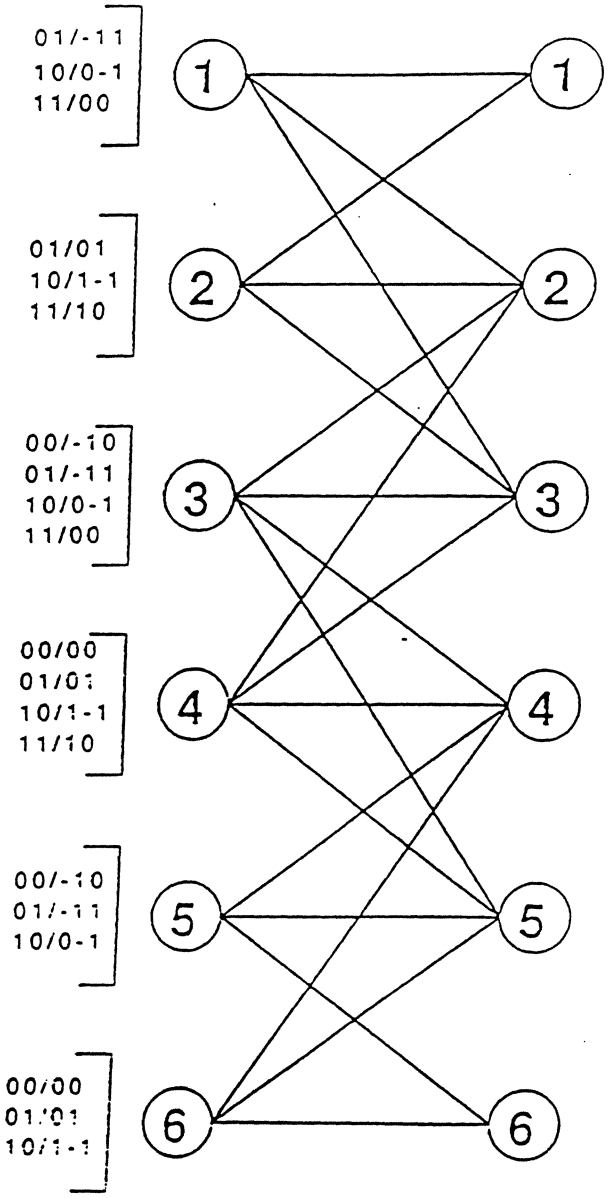

- Variation on trellis shown earlier

TRELLIS EMULATION VIA PIPELINING

01/	−1 1
10/	0 −1
11/	0 0
00/	−1 0

01/	0 1
00/	0 0
11/	1 0
10/	1 −1

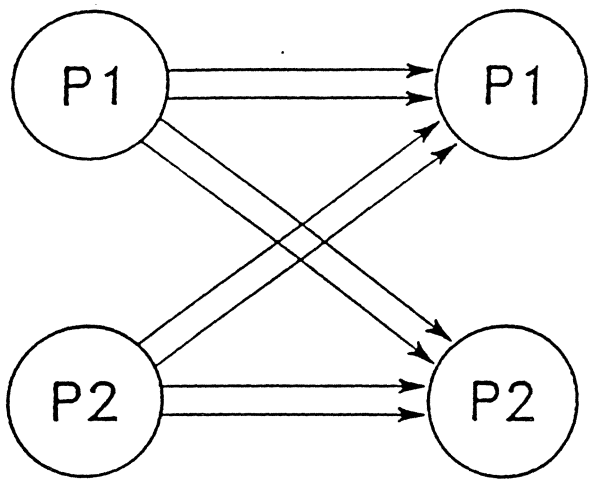

- 2-state trellis that emulates 6-state MSN trellis.

Pipelined ACS Circuit

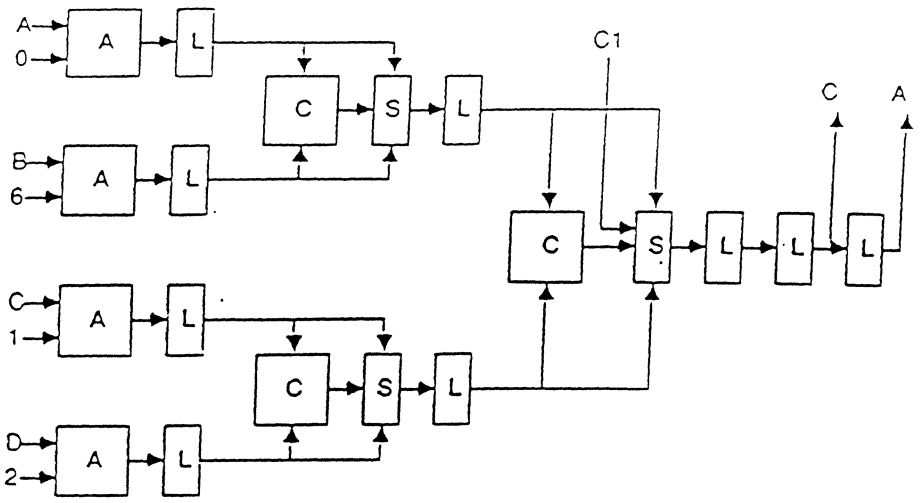

ACS1

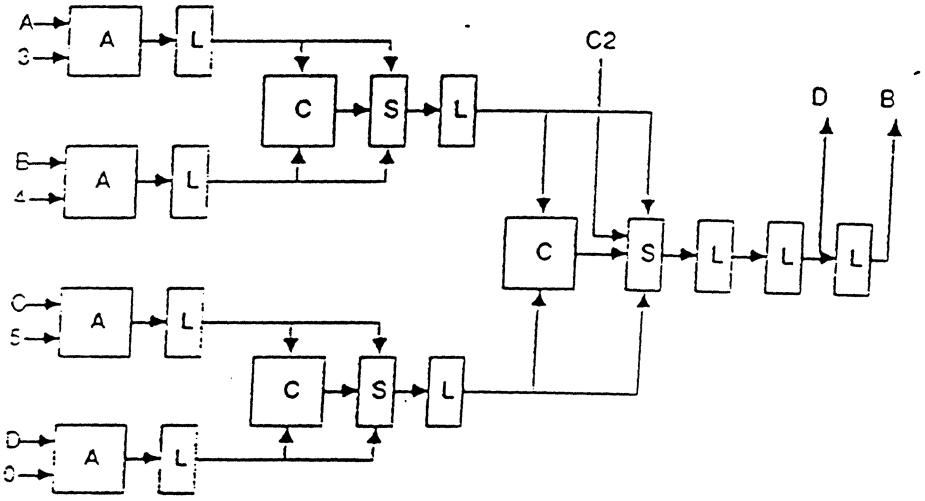

ACS2

- Legend

  A = adder
  C = comparator
  S = selector
  L = latch

Pipelined State Schedule

ACS Schedule

Stage T+1	Stage T	Stage T−1	
7 5 3 1	7 5 3 1	7 5 3 1	← P1
6 4 2 8	6 4 2 8	6 4 2 8	← P2

METRIC RENORMALIZATION (CONVENTIONAL APPROACH)

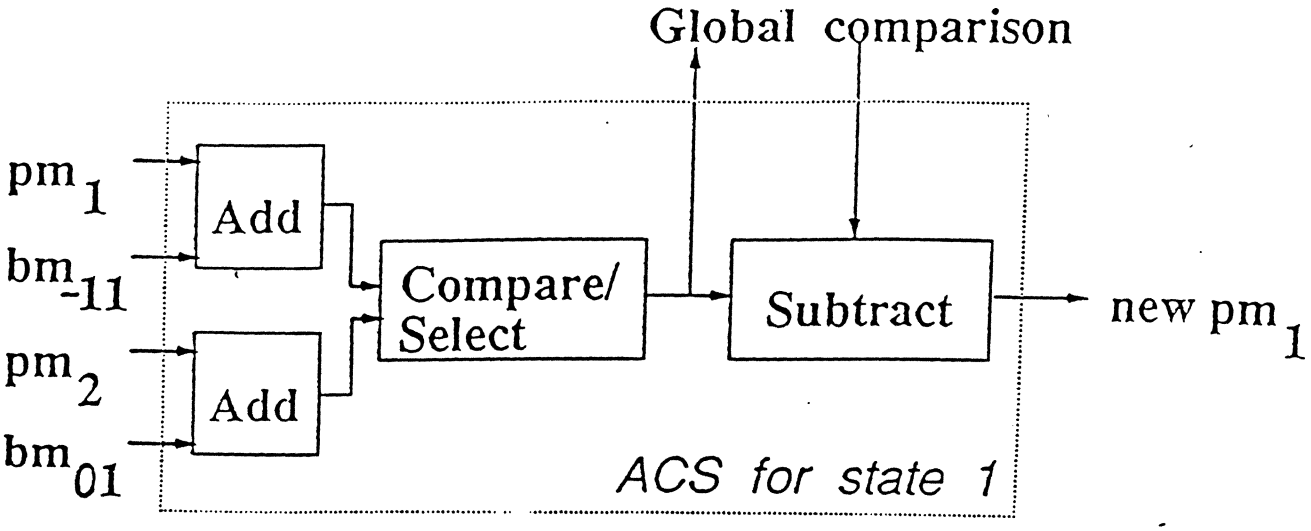

MODULO NORMALIZATION

- Two's-complement arithmetic
- Uses bound Δ on path metric differences

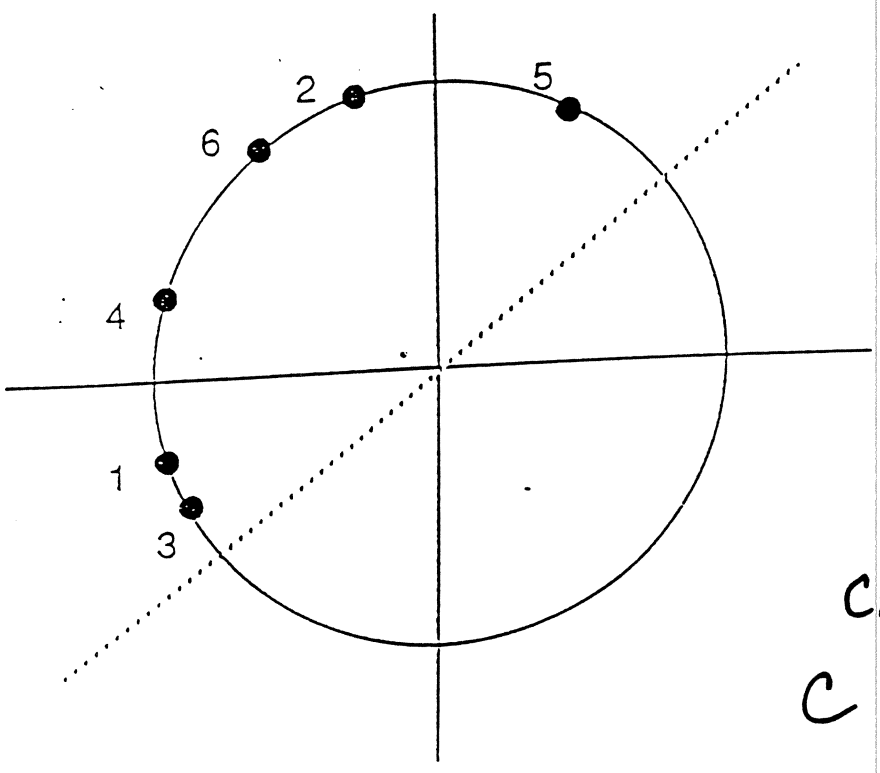

Circumference

$C = 2\Delta$

- Local and regular
- Compatible with pipelined ACS architecture

PERFORMANCE EVALUATION
(experimental set-up)

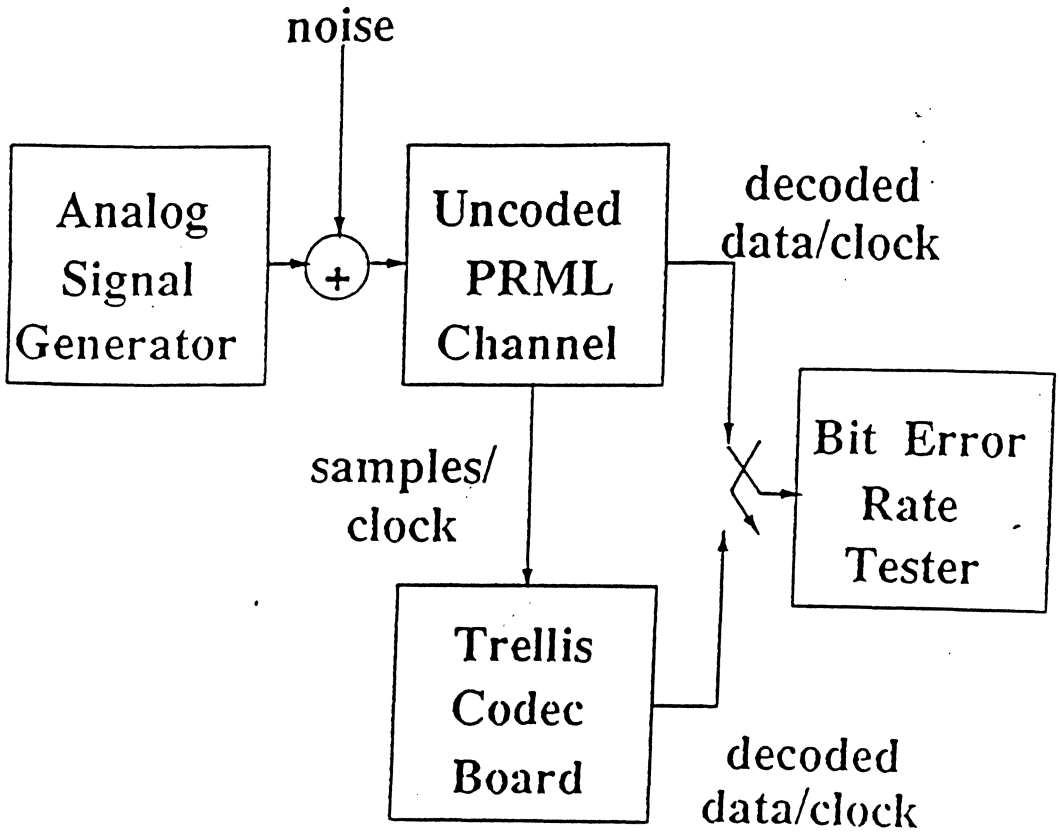

5 1W = 5 x 2.604/4

Measured Bench-Test Results

- MSN-coded PR vs. PRML
- Synthesized PR waveforms
- Injected AWGN

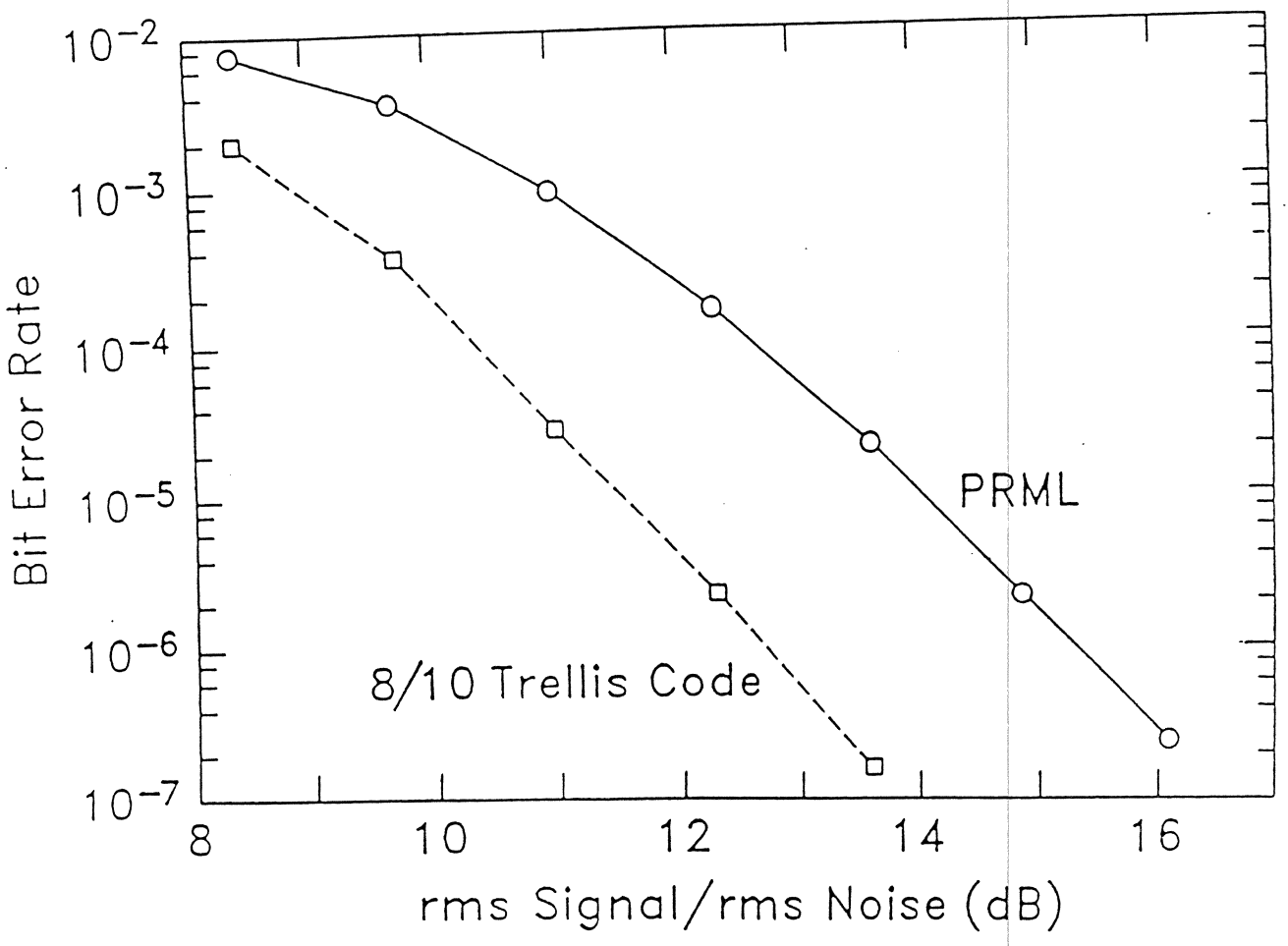

TRELLIS CODE CHIP FLOORPLAN

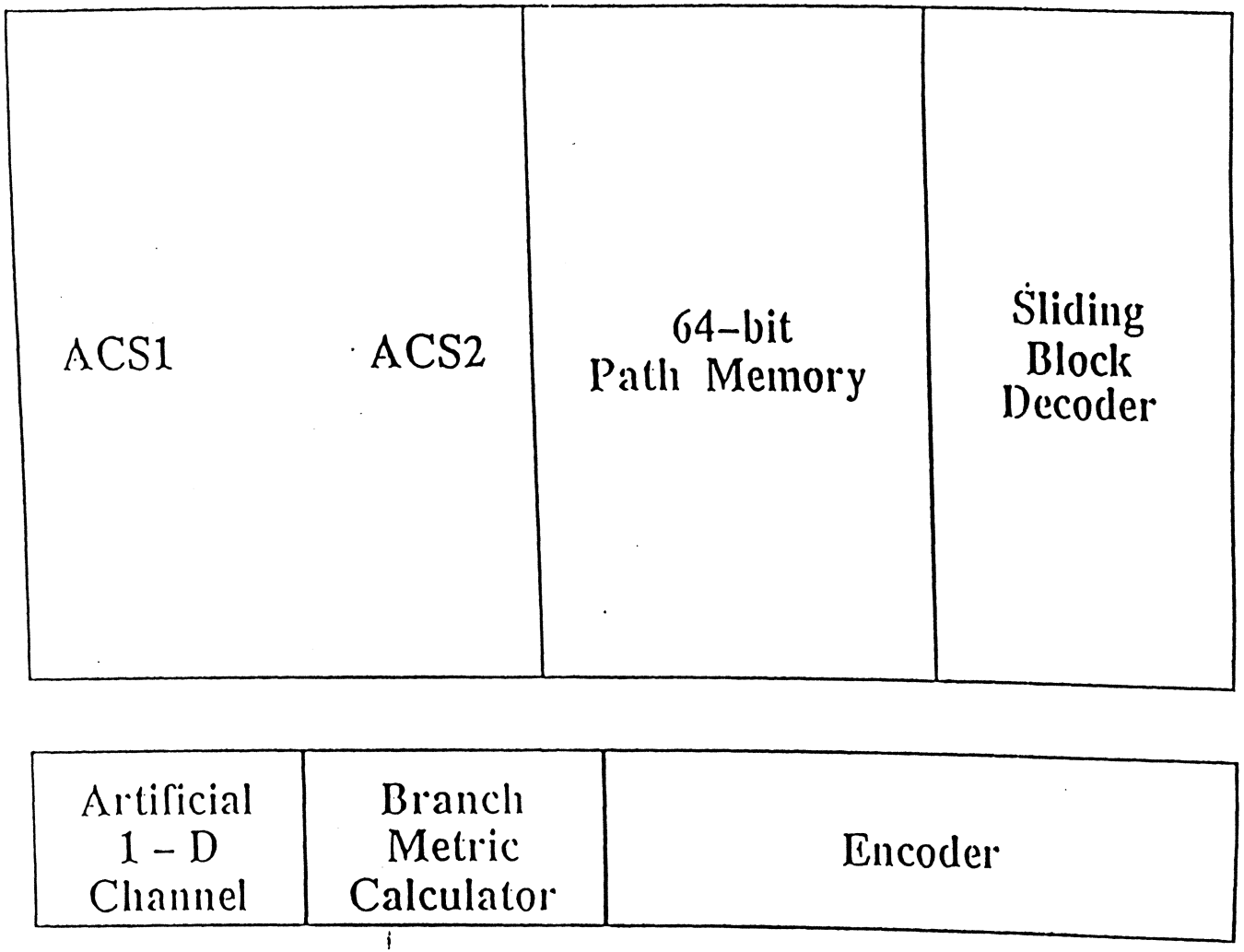

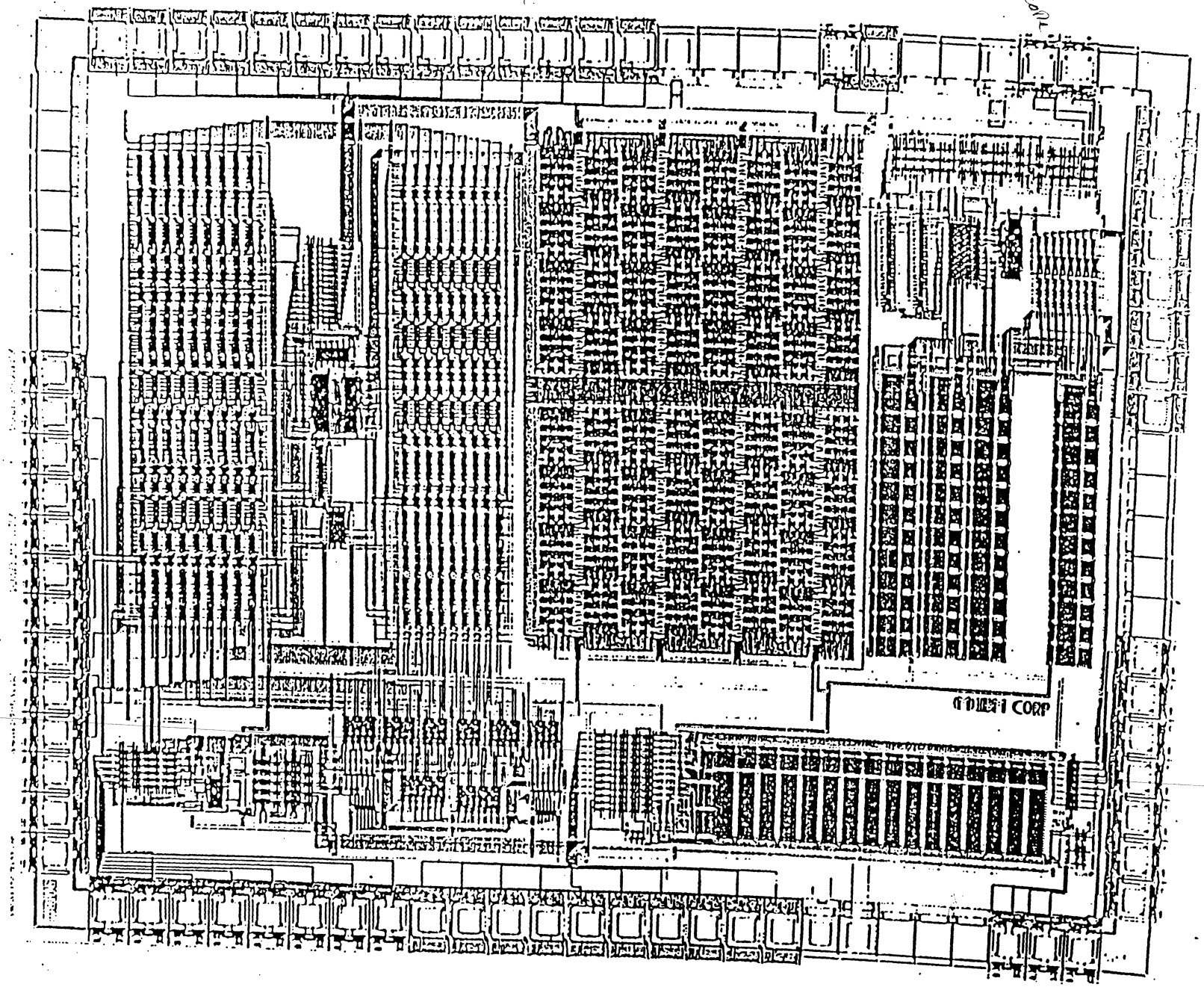

TRELLIS CHIP MICROGRAPH

SELECTED REFERENCES

Coding for Partial Response Channels

Partial-Response Channels

[1] A. Lender, "Correlative level coding for binary data transmission," *IEEE Spectrum,* vol. 3, no. 2, p. 104, 1966.

[2] E.R. Kretzmer, "Generalization of a technique for binary data transmission," *IEEE Trans. Comm. Tech.,* vol. COM-14, p. 67., 1967.

[3] P. Kabal and S. Pasupathy, "Partial-response signaling," *IEEE Trans. Comm.,* vol. 23, no. 9, pp. 921-934, September 1975.

[4] H. Kobayashi and D.T. Tang, "Application of partial-response channel coding to magnetic recording systems," *IBM J. Res. Dev.,* vol. 14, pp. 368-375, July 1970.

[5] H. Thapar and A. Patel, "A class of partial response systems for increasing storage density in magnetic recording," *IEEE Trans. Magnetics,* vol. MAG-23, no. 5, pp. 3666-3668.

Maximum-Likelihood Decoding/Viterbi Algorithm

[6] A. J. Viterbi, "Error bounds for convolutional codes and an asymptotically optimum decoding algorithm," *IEEE Trans. Information Theory,* vol. IT-13, pp. 260-269, April 1967.

[7] G.D. Forney, Jr., "The Viterbi algorithm," *Proc. of the IEEE,* vol. 61, pp. 268-278, March 1973.

[8] G.D. Forney, Jr., "Maximum likelihood sequence detection in the presence of intersymbol interference," *IEEE Trans. Info. Th.,* vol. IT-18, no. 3, pp. 363-378, May 1972.

[9] B. Shung, P. Siegel, G. Ungerboeck, and H. Thapar, "VLSI architectures for metric normalization in the Viterbi algorithm," *Proceedings of IEEE Int. Conf. on Commun. (ICC'90),* paper 347.4, pp. 1723-1728, April 1990.

[10] B. Shung, H-D. Lin, P. Siegel, and H. Thapar, "Area-efficient architectures for the Viterbi algorithm," *Proceedings of Globecom'90,* paper 901.5, pp. 1787-1793, December 1990.

[11] B. Shung, H-D. Lin, R. Cypher, P. Siegel, and H. Thapar, "Area-efficient architecture for the Viterbi algorithm, parts I and II," to appear in *IEEE Transactions on Communications.*

[12] P. Siegel, B. Shung, T. Howell, and H. Thapar, "Exact bounds on Viterbi detector path metric differences," IBM RJ 8091, *Proceedings of 1991 IEEE Int. Conf. on Acoustics, Speech, and Signal Processing (ICASSP'91),* paper 1743, May 1991.

PRML - Performance and Implementation

[13] H. Kobayashi, "Application of probabilistic decoding to digital magnetic recording systems," *IBM J. Res. Dev.,* vol. 15, no. 1, pp.64-74, January 1971.

[14] R.W. Wood and D.A. Petersen, "Viterbi detection of class IV partial response on a magnetic recording channel," *IEEE Trans. Comm.,* vol. COM-34, pp.454-461, May 1986.

[15] F. Dolivo, "Signal processing for high density digital magnetic recording," *Proc. COMPEURO 89,* Hamburg, W. Germany, May 1989.

[16] H. Thapar and T. Howell, "On the performance of partial response maximum likelihood and peak detection methods in digital magnetic recording," *Digests of the 1991 Magnetic Recording Conference (MRC'91),* paper D-1, June 1991.

[17] R. Kost and W. Zhang, "A comparison of maximum likelihood and peak detection performance for digital magnetic recording," *Digests of the 1991 Magnetic Recording Conference (MRC'91),* paper E-1, June 1991.

[18] J. Hong, R. Wood, and D. Chan, "An experimental 180 Mb/s PRML magnetic recording channel," *Digests of the 1991 Magnetic Recording Conference (MRC'91),* paper D-2, June 1991.

[19] J. Coker, R. Galbraith, G. Kerwin, J. Rae, and P. Ziperovich, "Implementation of PRML in a rigid disk drive," *Digests of the 1991 Magnetic Recording Conference (MRC'91),* paper D-3, June 1991.

[20] J. Coker, R. Galbraith, G. Kerwin, "Implementation of PRML in a rigid disk drive," *Digests of the 1991 Magnetic Recording Conference (MRC'91),* paper D-3, June 1991.

[21] R. Cideciyan, F. Dolivo, R. Hermann, W. Hirt, and W. Schott, "A PRML system for digital magnetic recording," to appear in *Journal on Selected Areas in Communications, Special Issue on Signal Processing and Coding for Recording Channels,* 1992.

[22] R. Spencer and P. Hurst, "Analog implementations of sampling detectors," *Digests of the 1991 Magnetic Recording Conference (MRC'91),* paper B-5, June 1991.

Constrained Codes for PRML

[23] B. Marcus and P. Siegel, "Constrained codes for PRML," IBM Research Report RJ 4371, July 1984.

[24] B. Marcus and P. Siegel, "Constrained codes for partial response channels," *Beijing Int. Workshop on Info. Th.,* pp. DI1.1-DI1.4, July 1988.

[25] J. Eggenberger and A. Patel, "Method and apparatus for implementing optimum PRML codes," U.S. Patent 4,707,681, November 1987.

[26] B. Marcus, A. Patel, and P. Siegel, "Method and apparatus for implementing a PRML code," U.S. Patent 4,786,890, November 1988.

[27] P. Siegel, "Recording codes for PRML," *Digests of the 1991 Magnetic Recording Conference (MRC'91),* paper F-2, June 1991.

[28] M. Melas and P. Sutardja, "Signalling for peak power limited magnetic channels," *Digests of the 1991 Magnetic Recording Conference (MRC'91),* paper F-4, June 1991.

[29] B. Marcus, P. Siegel, and J. Wolf, "A tutorial on finite-state modulation codes for data storage," to appear in *Journal on Selected Areas in Communications, Special Issue on Signal Processing and Coding for Recording Channels,* 1992.

Convolutional Codes - Tables

[30] S. Lin and D.J. Costello, Jr., *Error Control Coding: Fundamentals and Applications,* Englewood Cliffs, New Jersey: Prentice-Hall, 1983.

Trellis-Coded Modulation

Ungerboeck Codes

[31] G. Ungerboeck, "Channel coding with multilevel/phase signals," *IEEE Trans. Info. Th.*, vol. IT-28, pp. 55-67, January 1982.

[32] G. Ungerboeck, "Trellis-coded modulation with redundant signal sets: Parts 1 and 2," *IEEE Comm. Mag.*, vol. 25, no. 2, pp. 5-21, February 1987.

Convolutionally-Coded Partial-Response

[33] J.K. Wolf and G. Ungerboeck, "Trellis coding for partial-response channels," *IEEE Trans. Comm.*, vol. COM-34, no. 8, pp. 765-773, August 1986.

[34] A.R. Calderbank, C. Heegard, and T.A. Lee, "Binary convolutional codes with application to magnetic recording," *IEEE Trans. Info. Th.*, vol. IT-32, no. 6, pp. 797-815, November 1986.

[35] E. Zehavi, "Coding for magnetic recording," Ph.D. Dissertation, Univ. California San Diego, February 1987.

[36] K.A.S. Immink, "Coding techniques for the noisy magnetic recording channel: A state-of-the-art report," *IEEE Trans. Comm.*, Vol. COM-37, no. 5, pp. 413-419, May 1987.

[37] E. Zehavi and J. Wolf, "On saving decoder states for some trellis codes and partial response channels," *IEEE Trans. Comm.*, vol. COM-36, no. 2, pp. 222-224, February 1988.

[38] K. Hole, "Punctured convolutional codes for the 1-D partial-response channel," *IEEE Trans. Info. Th., Special Issue on Coding for Storage Devices*, vol. 37, no. 3, pt. II, pp. 808-817, May 1991.

[39] R. Karabed and P. Siegel, "Matched spectral null trellis codes for partial response channels, part I: Low rate concatenated codes," *Abstracts of Int. Symp. Info. Th.*, Kobe, Japan, pp. 142-143, June 1988.

[40] R. Karabed and P. Siegel, "Improved trellis codes for partial-response channels," U.S. Patent 4,808,775, issued December 19, 1989.

Matched-Spectral-Null Codes

[41] R. Karabed and P. Siegel, "Matched spectral null trellis codes for partial response channels, part II: High rate codes with simplified Viterbi detectors," *Abstracts of Int. Symp. Info. Th.*, Kobe, Japan, pp. 142-143, June 1988.

[42] R. Karabed and P. Siegel, "Even-Mark Modulation for Optical Recording," *Proceedings of the 1989 International Conference on Communications*, vol. 3, Boston, Massachusetts, pp. 1628-1632, June 1989.

[43] R. Karabed and P. Siegel, "Even-Mark Modulation for Optical Recording," U.S. Patent 4,870,414, September 1989.

[44] R. Karabed and P. Siegel, "Matched spectral null trellis codes for partial response channels," U.S. Patent 4,888,779, December 1989.

[45] R. Karabed and P. Siegel, "Matched spectral null codes for partial response channels," *IEEE Trans. Info. Th., Special Issue on Coding for Storage Devices*, vol. 37, no. 3, pt. II, pp. 818-855, May 1991.

[46] G. Pierobon, "Codes for zero spectral density at zero frequency," *IEEE Trans. Info. Th.*, vol. IT-30, pp. 425-429, March 1984.

[47] B. Marcus and P. Siegel, "On codes with spectral nulls at rational submultiples of the symbol frequency," *IEEE Trans. Info. Th.*, vol. IT-33, no. 4, pp. 557-568, July 1987.
[48] C.M. Monti and G.L. Pierobon, "Codes with a multiple spectral null at zero frequency," *IEEE Trans. Info. Th.*, vol. 35, no. 2, pp. 463-471, March 1989.
[49] K.A.S. Immink and G. Beenker, "Binary transmission codes with higher order spectral zeros at zero frequency," *IEEE Trans. Info. Th.*, vol. 33, no. 3, pp. 452-454, May 1987.
[50] R. Adler, D. Coppersmith, and M. Hassner, "Algorithms for sliding-block codes," *IEEE Trans. Info. Th.*, vol. IT-29, no. 1, pp. 5-22, January 1983.
[51] R. Karabed and B. Marcus, "Sliding-block coding for input-restricted channels," *IEEE Trans. Info. Th.*, vol. 34, no. 1, pp. 2-26, January 1988.
[52] C. Shung, P. Siegel, G. Ungerboeck, and H. Thapar, "VLSI architectures for metric normalization in the Viterbi algorithm," *Proc. of Int. Conf. Comm. (ICC'90)*, pp. 1723-1728, April 1990.
[53] B. Shung, P. Siegel, H. Thapar, R. Karabed, "A 30MHz trellis codec chip for partial response channels," *Digests of Int. Solid States Cir. Conf. (ISSCC'91)*, vol. 34, paper TP 8.1, February 1991.
[54] B. Shung, P. Siegel, H. Thapar, R. Karabed, "A 30 MHz trellis codec chip for partial-response channels," *IEEE Journal of Solid-State Circuits, Special Issue on Analog and Signal Processsing Circuits*, vol. 26, no. 12, pp. 1981-1987, December 1991.
[55] H. Thapar, J. Rae, B. Shung, R. Karabed, and P. Siegel, "On the performance of a rate 8/10 matched spectral null code for class-4 partial response (digest)," to be presented at Intermag'92.

Related Readings

[56] L. Carley, "Comparison of computationally efficient forms of FDTS/DF against PR4-ML," *Digests of the 1991 Magnetic Recording Conference (MRC'91)*, paper E-4, June 1991.
[57] J. Moon, "Discrete-time modeling of transition noise dominant channels and study of detection performance," *Digests of 1991 Magnetic Recording Conference (MRC'91)*, paper E-5, June 1991.
[58] A. Patel, "A new digital signal processing channel for data storage products," *Digests of the 1991 Magnetic Recording Conference (MRC'91)*, paper E-6, June 1991.
[59] J. Wolf, "Coding for partial response channels," *Digests of the 1991 Magnetic Recording Conference (MRC'91)*, paper F-1, June 1991.
[60] K. Knudson, J. Wolf, and L. Milstein, "Producing soft-decision information at the output of a class IV partial response detector," *Proc. of IEEE Int. Conf. on Commun. (ICC'91)*, June 1991.
[61] P. Siegel and J. Wolf, "Modulation and coding for information storage," *IEEE Communications Magazine*, December 1991.

Cambrian
Integrated Test Solutions

Cambrian Systems Inc.,
47600 Westinghouse Drive
Fremont, CA 94539
(415) 490-9001
FAX (415) 490-9006

CHARACTERIZATION OF DISK DRIVE COMPONENTS USING DSP TECHNIQUE

AVTAR SINGH

CAMBRIAN SYSTEMS, INC.

CONTENTS

1. INTRODUCTION

- Analog Signal Process (ASP) based ATE
    - Head tester
        - Parametric tester
        - Phase margin tester
        - Time interval analyzer
    - Disk Certifier
        - MP, EP, MOD tester
        - Window margin tester
    - Glide tester
    - Flying height tester
        - Digital
            - Average flying height measurement
            - Dynamic flying height measurement
        - Analog
    - et el
- Digital Signal Process (DSP) based ATE

2. PARAMETRIC TESTING

(A) TRACK AVERAGE AMPLITUDE

- ANALOG SIGNAL PROCESSING CAN PROVIDE AVERAGE TAA.

DSP APPROACH CAN PROVIDE

- AVERAGE TAA
- POSITIVE / NEGATIVE MODULATION
- CONTRIBUTION DUE TO MISREGISTRATION OF READ HEAD
- CONTRIBUTION DUE TO SPINDLE JITTER, AXIAL & RADIAL NON-REPEATABLE RUN OUT.

(B) O/W MEASUREMENT

- ASP TECHNIQUE USES BAND PASS FILTER OR SPECTRUM ANALYZER.

DSP APPROACH CAN PROVIDE

- DSP USE FFT ANALYSIS
- CONTRIBUTION DUE TO SPINDLE JITTER & RUN OUT
- CONTRIBUTION DUE TO MISREGISTRATION OF READ HEAD.

20MBIT/SEC TESTER CLOCK RATE
NEED MORE MEMORY IN DSP TEST SYSTEM THAN ANALOG METHODS

(C) NOISE MEASUREMENT

HEAD NOISE

- JOHNSON THERMAL NOISE
- BARKHAUSEN NOISE
- MAGNETIC DOMAIN INSTABILITY
  - AMPLITUDE MEASUREMENT
  - PULSE WIDTH MEASUREMENT PW 2.5
  - HEAD BIAS TECHNIQUE BIAS current $\leq$ 3% of I_w UNSTABLE HEAD $\approx$ 2%

MEDIA NOISE

- SA TECHNIQUE
- TRUE-RMS VOLTMETER TECHNIQUE
- REVERSE DC ERASE TECHNIQUE
- MEDIA EDGE NOISE

(D) WAVE SHAPE ANALYSIS

- PULSE WIDTH
- UNDERSHOOT
- ASYMMETRY
- SPECTRUM
- RISE / FALL TIMING
- NON-LINEAR RESPONSE

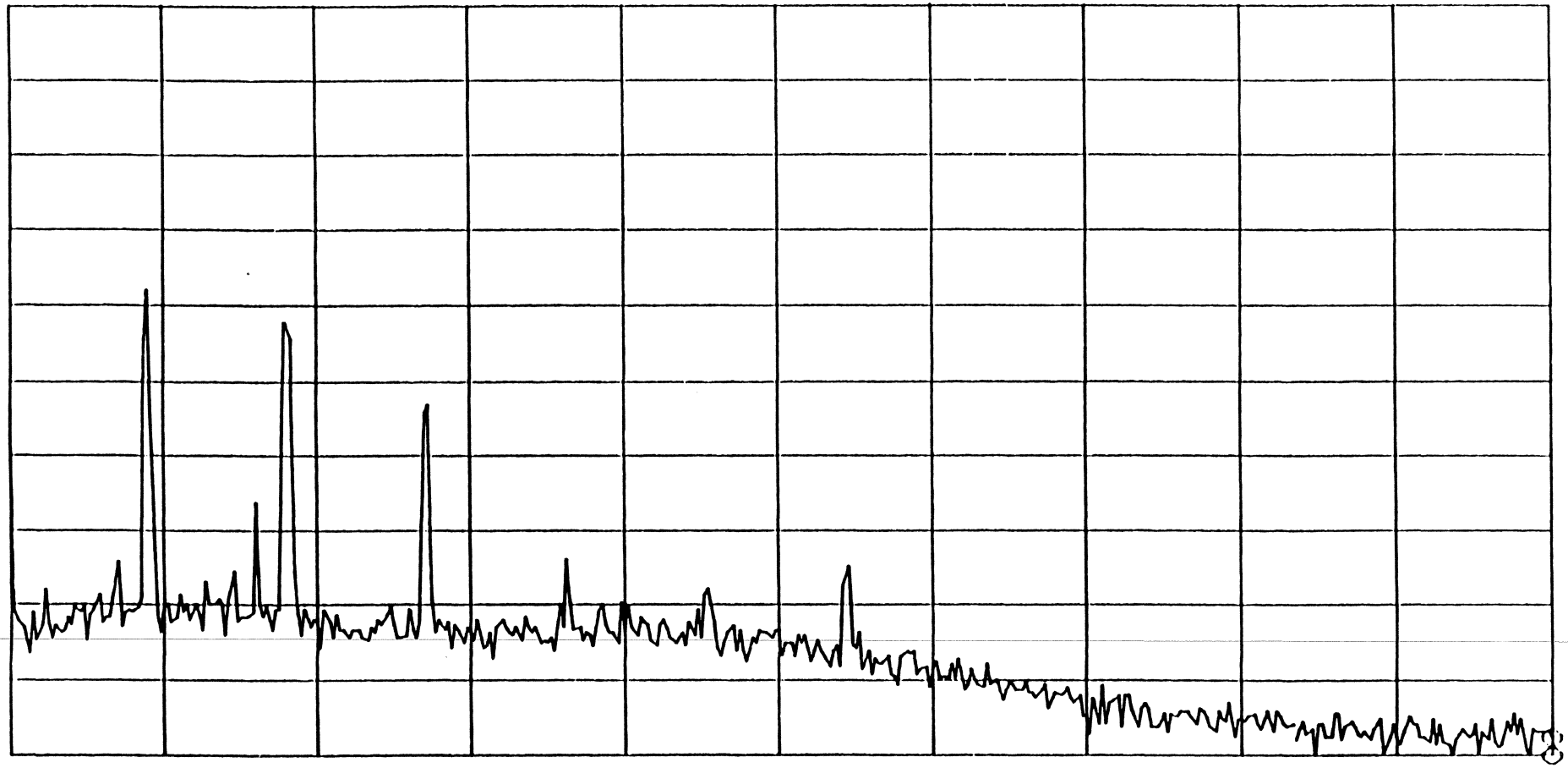

Fig. 1. Transition Noise of Medium.

3. TOTAL TIMING ERROR

I . HEAD / MEDIA / PREAMP NOISE

II. INTER SYMBOL INTERFERENCE

III. PEAK SHIFT DUE TO HARD TRANSITION EFFECT

IV INTER TRACK INTERFERENCE

V NON-LINEAR DISTORTION

I. HEAD / MEDIA / PREAMP NOISE

Peak Shift based on SNR

Simple approximation

$$Te = [\ Ts/4.2]\ \sqrt{-\log_{10}(4.2 * Pe\ )}\ /\ SNR$$

where

$$10^{-22} < Pe < 10^{-3}$$

Ts = Time period for highest frequency

Te = timing error

Pe = error probability per bit

SNR = signal to noise ratio (rms to rms)

Let us say SNR = 30

5 MHz Freq

T_e = 4.8 ns

G.H.Hughes & R.K.Schmidt, " On noise in digital recording", IEEE Trans Mag, Vol. MAG-12, No.6 pp 752.

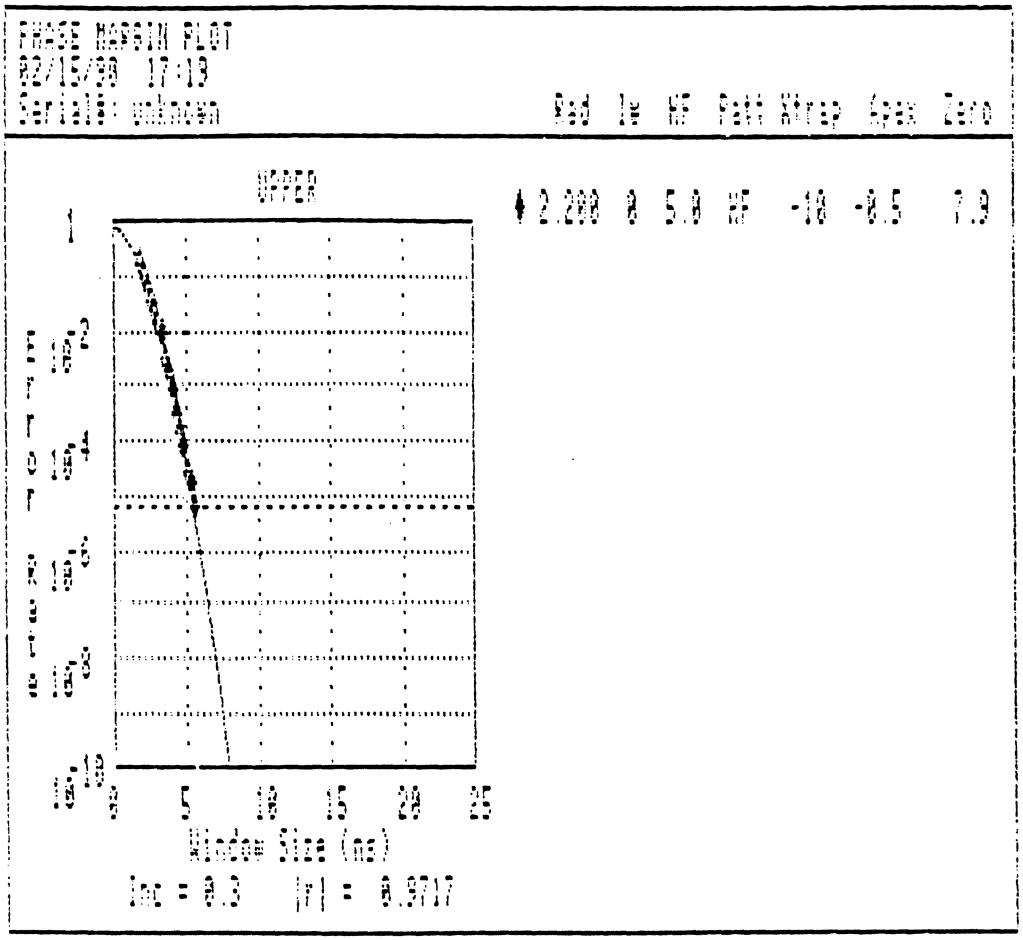

Fig 3 : Phase margin plot for (1,1) MFM pattern.

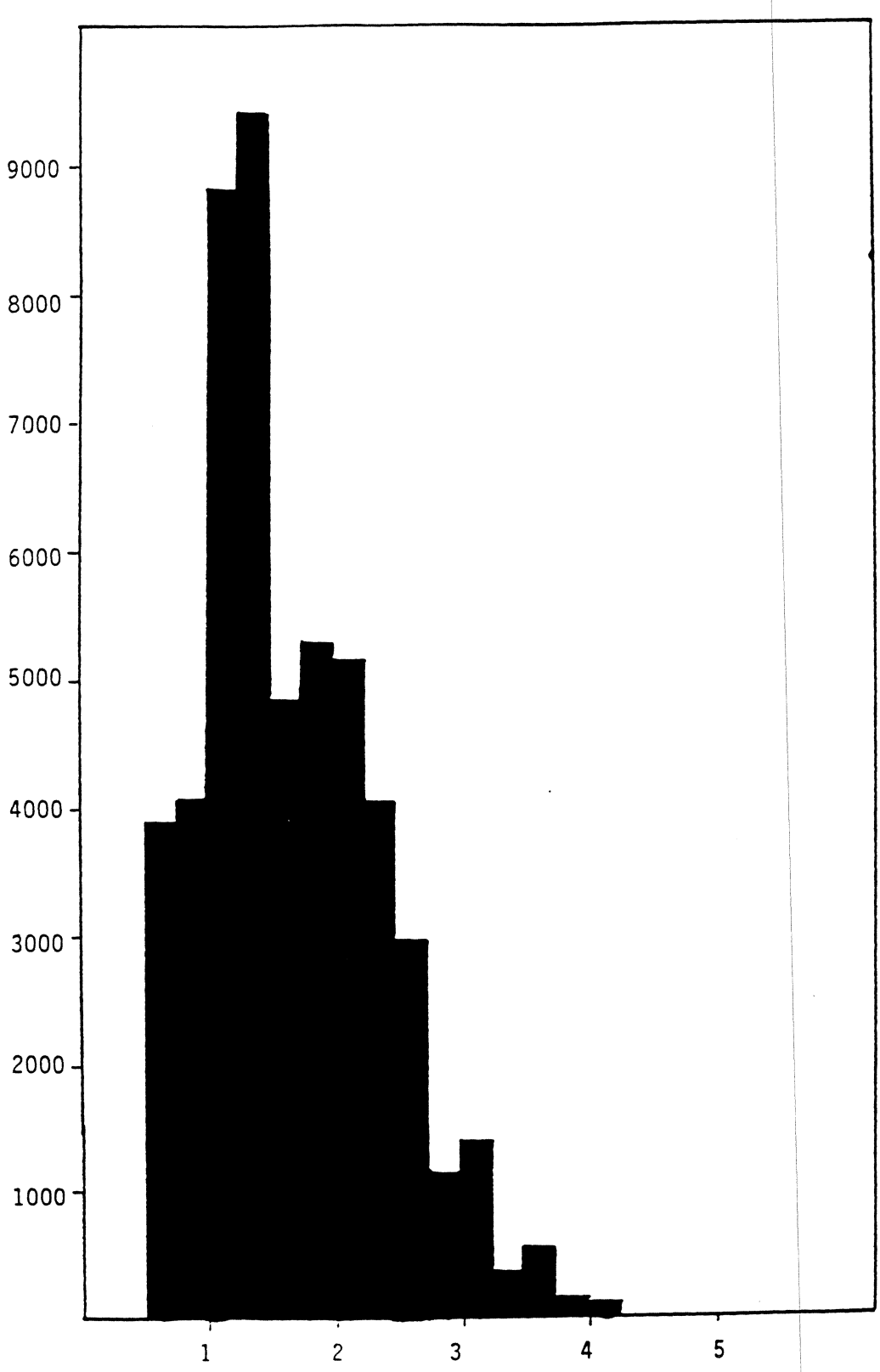

Fig 4 : Peak shift distribution for (1,1) MFM pattern.

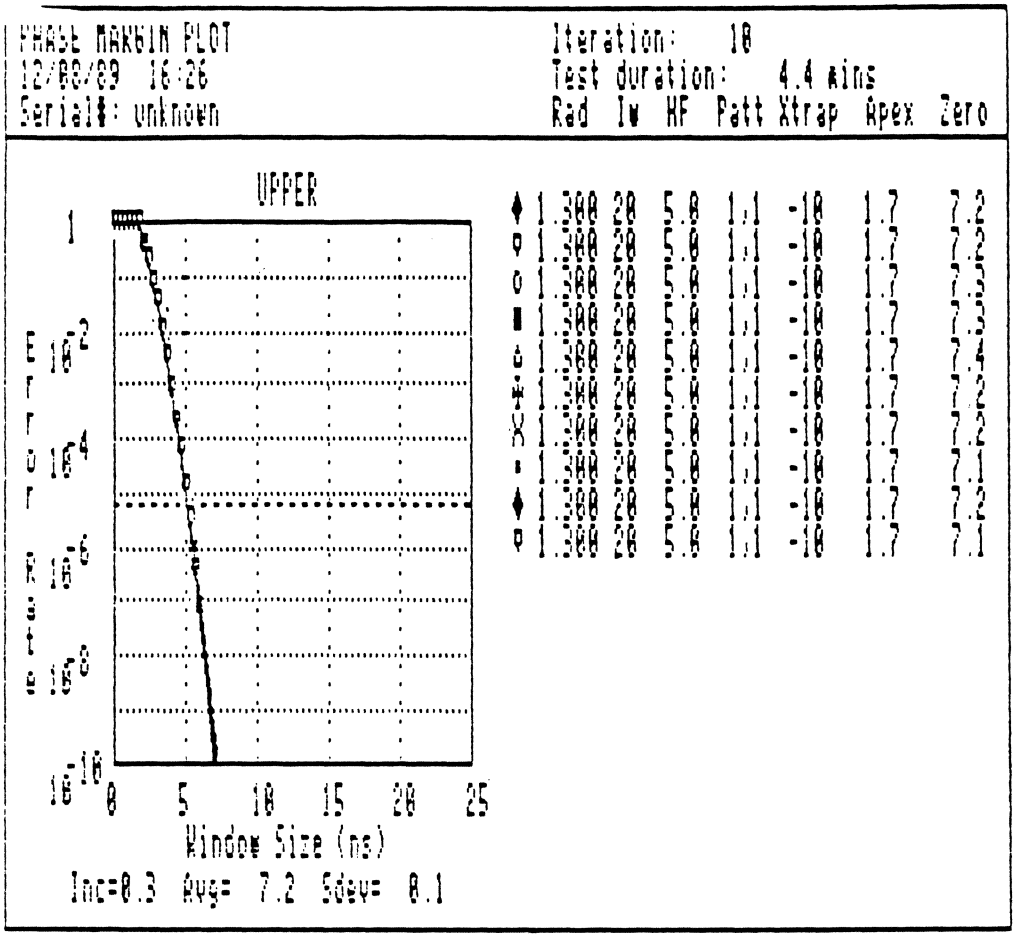

Fig 5: Phase margin plot for (1,1) pattern showing apex.

II. INTERSYMBOL INTERFERENCE

TFH PEAK SHIFT CALCULATIONS

$$V(K) = \frac{2\ V\ W\ Mr}{2} \cdot \frac{1 - e^{-Kt}}{Kt} \cdot \frac{e^{-K(d+a)}}{1} \cdot G(K) \quad \ldots (1)$$

$$K = \frac{2\ f}{V} \quad \ldots\ldots\ldots\ldots\ldots\ldots (2)$$

$$G(K) = \frac{\mathrm{SIN}\ (gK)}{gK} - \frac{1}{2(1+C)} \left\{ \frac{A}{A-jK(g+p1)} + \frac{BC}{B-jK(g+p1)} \right\} e^{jK(g+p1)}$$

$$- \frac{1}{2(1+C)} \left\{ \frac{A}{A-jK(g+p2)} + \frac{BC}{B-jK(g+p2)} \right\} e^{jK(g+p2)} \quad \ldots\ldots (3)$$

$$a = \left(\frac{a1}{2r} - \frac{t}{4}\right) + \left[\left(\frac{a1}{2r} - \frac{t}{4}\right)^{2} + \left(\frac{t}{2} + 2t\ \frac{Mr}{4Hc}\right) \frac{a1}{r} \right]^{1/2}$$

$$\ldots\ldots\ldots\ldots\ldots\ldots (4)$$

$$V(X) = \frac{1}{T} \sum_{n=1}^{\infty} V(nK) \cdot \left\{ \mathrm{SIN}\left(n.\frac{2\pi}{T}.x\right) - \mathrm{SIN}\left(n.\ \frac{2\pi}{T}(x+T1)\right) \right.$$

$$\left. - \mathrm{SIN}\left(n.\ \frac{2\pi}{T}(x+T2)\right) \right\} \cdot \left\{ (1 - \mathrm{COS}(n\pi)).(i)^{n-1} \right\} \quad \ldots\ldots (5)$$

Where T = time period for isolated pulse

T1 = time period between positive peaks.

T2 = time period between positive and negative peak.

A.Singh & P.G.Bischoff," Optimization of thin film heads for Resolution, Peak shift and overwrite", IEEE Trans Mag, Vol. MAG-21, No.5 pp 1572.

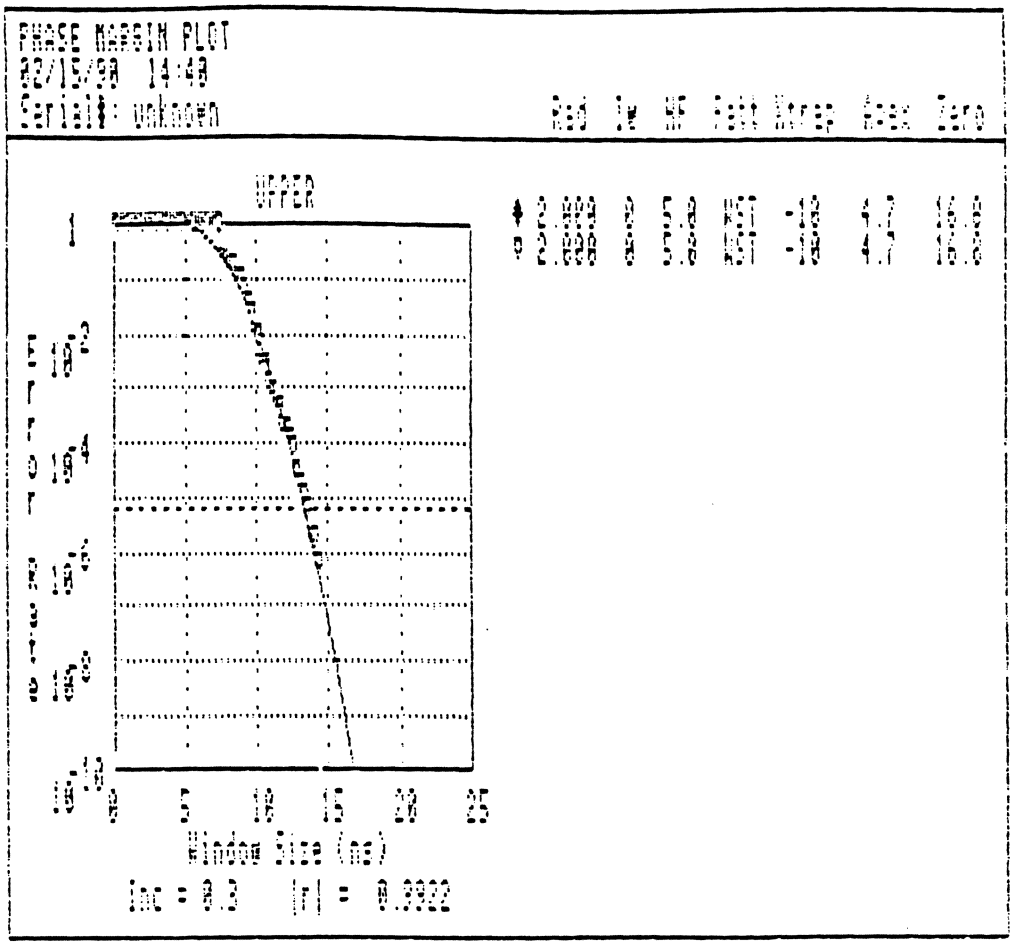

Fig 6: Phase margin plot for (1,3) MFM pattern.

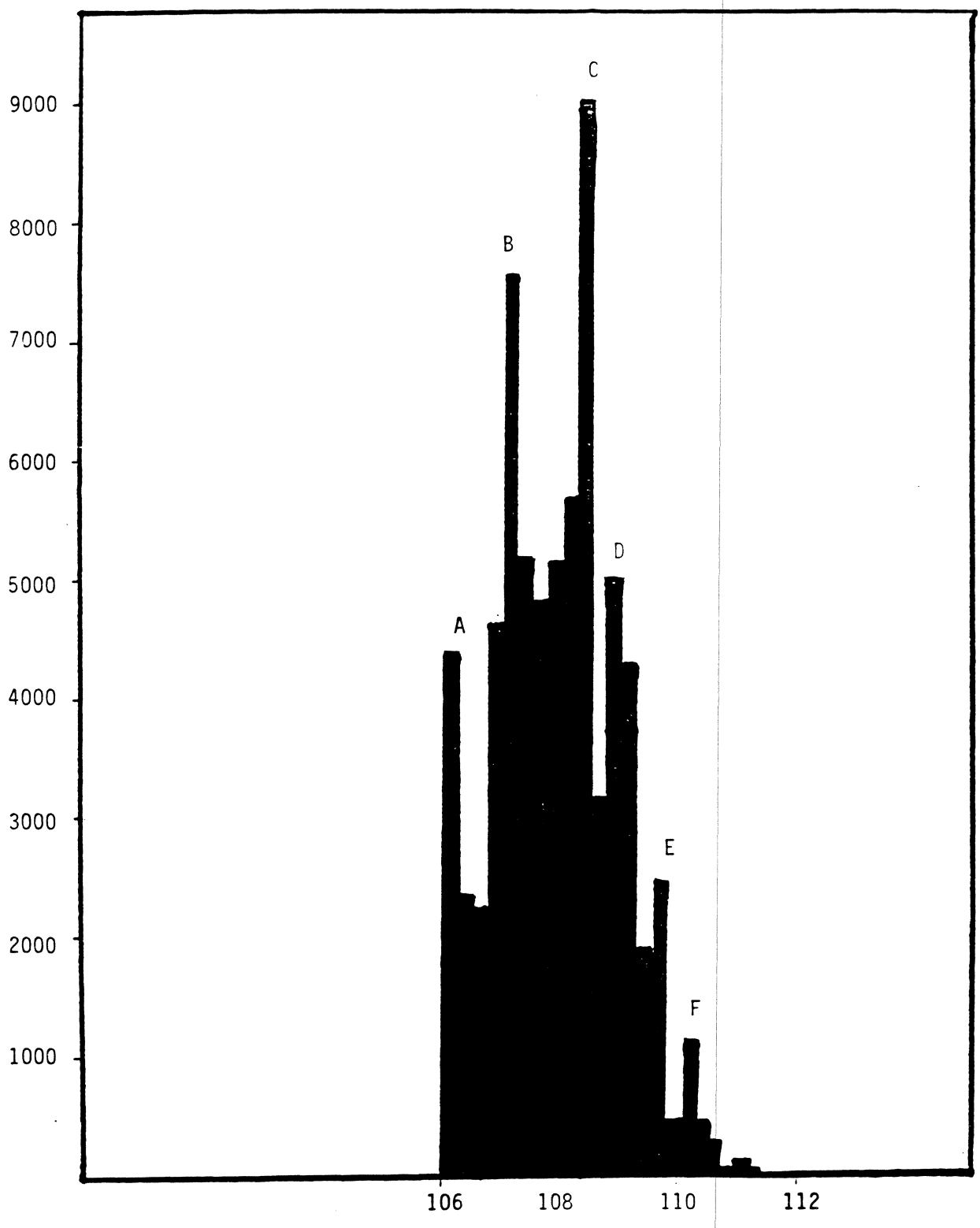

Fig 7: Peak shift distribution for (1,3) MFM pattern.

III - PEAK SHIFT DUE TO HARD TRANSITION EFFECT

$$\frac{P[2\cdot f_D - f_B]}{P[f_D]} = 2\cdot[2\cdot f_D - f_B]\cdot\left|\frac{E[2\cdot f_D - f_B]}{E[f_D]}\right| t$$

Where P(f) denotes the intensity of a spectral peak at frequency f .
E(f) denotes the amplitude of the Fourier Transform of the the easy transition waveform at frequency f and t is the hard transition peak shift in time.

$$t = \text{OVW}\left[\frac{500}{2f_0 - f_B}\right]$$

OVERWRITE

C. Tsang, Y. Tang, "An experimental study of hard transition peakshifts through the overwrite spectra.", IEEE Trans. Magn., MAG-24, 6 (1988).

PEAK SHIFT DUE TO HARD TRANSITION EFFECT

Algorithm:

1. Write low frequency Cw fb.

2. Then write high frequency fd.

3. Measure spectral peaks

Overwrite parameter OWP =

$$OWP := \frac{P\left[2 \cdot f_D - f_B\right]}{P\left[f_D\right]}$$

4. Measure spectral ratio RO

$$RO := \frac{E\left[2 \cdot f_D - f_B\right]}{E\left[f_D\right]}$$

$$= \frac{f_D}{\left[2 \cdot f_D - f_B\right]} \cdot \frac{V\left[2 \cdot f_D - f_B\right]}{V\left[f_D\right]}$$

5. Normalize OWP to remove effect of head disk resolution

$$OWQ := \frac{OWP}{RO}$$

6. Hard transition peak shift t

$$t := OWQ \cdot \left[\frac{500}{\left[2 \cdot f_D - f_B\right]}\right]$$

where t is in nanoseconds & fD and fB are in MHz.

C. Tsang, Y. Tang, "An experimental study of hard transition peakshifts through the overwrite spectra.", IEEE Trans. Magn., MAG-24, 6 (1988).

IV INTERTRACK INTERFERENCE

- ITI IS ONE OF THE MAIN CAUSES OF TIMING ERROR.

- ITI CONTRIBUTION TO TIMING ERROR IS EMBEDDED IN THE PHASE MARGIN PLOT.

- DSP TECHNIQUE CAN BE USED TO MEASURE TRACK MISREGISTRATION.

- TECHNIQUE CAN BE FURTHER MODIFIED TO PROVIDE TIMING ERROR DUE TO INTERTRACK INTERFERENCE.

T.J.Chainer et al," A technique for the measurement of track misregistration in disk file," paper presented at MMM- Intermag Conf. Pittsburg, Pennsylvania,1991.

4. PHASE MARGIN CIRCUIT DESIGN & ANALYSIS

(A) FILTER DESIGN

- NOISE MINIMIZATION
- PRESERVE WAVE SHAPE
- CONSTANT GROUP DELAY
- LINEAR PHASE
- CORRECT ERRORS INTRODUCED BY THE NON-IDEAL PHASE CHARACTERISTICS OF INPUT READ HEAD
- PROGRAMMABLE TRACKING FILTER
  (ONLY IF SNR BETTER THAN 60 DB)

DSP TO ANALYZE NON-IDEAL PHASE CHARACTERISTICS

- HIGH SPEED ADC
- DIGITAL SIGNAL PROCESSING
  -FFT, CONVOLUTION etc
- DIGITAL FILTER DESIGN FOR ANALYSIS

(B) DIFFERENTIATOR DESIGN

THE DIFFERENTIATOR OUTPUT CHANGES STATE WHEN THE INPUT PULSE CHANGES DIRECTION. NORMALLY THIS WILL BE AT THE PEAKS. BUT THE DIFFERENTIATOR CAN ALSO RESPOND TO NOISE NEAR THE BASELINE UNLESS THRESHOLD OR GATING CIRCUIT IS IMPLEMENTED.

(AMPLITUDE COMPARATOR CIRCUIT, ENABLING THE DIGITIZING COMPARATOR CAN BE USED AS GATING CIRCUIT.)

TYPES OF DIFFERENTIATOR

1. **RC DIFFERENTIATOR**
   - SIMPLE
   - PHASE DISTORTION
   - SNR DEGRADATION
2. **GL DIFFERENTIATOR**
   - SNR DEGRADATION
3. **DELAY LINE DEFFERENTIATOR**

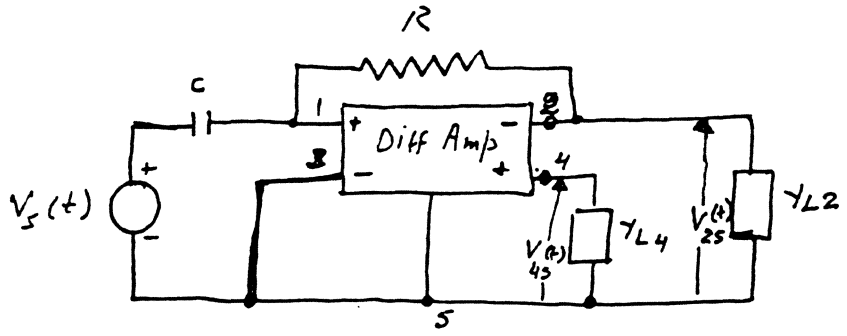

$$V_{25}(t) = -V_{45}(t) = -RC\frac{dV_s(t)}{dt}$$

Fig B-1 RC Differentiator.

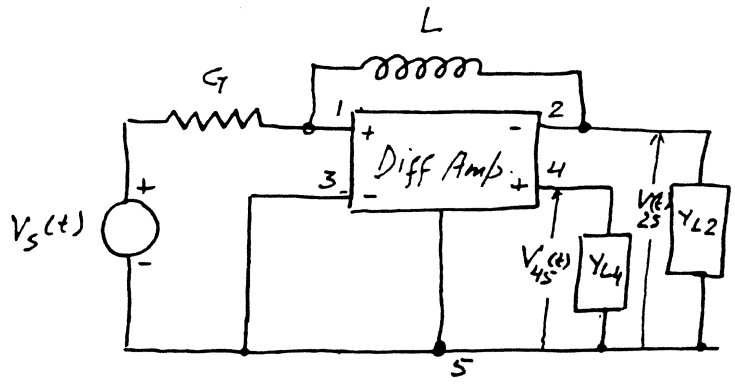

$$V_{25}(t) = -V_{45}(t) = -LG\frac{dV_s(t)}{dt}$$

Fig 13-2 GL Differentiator.

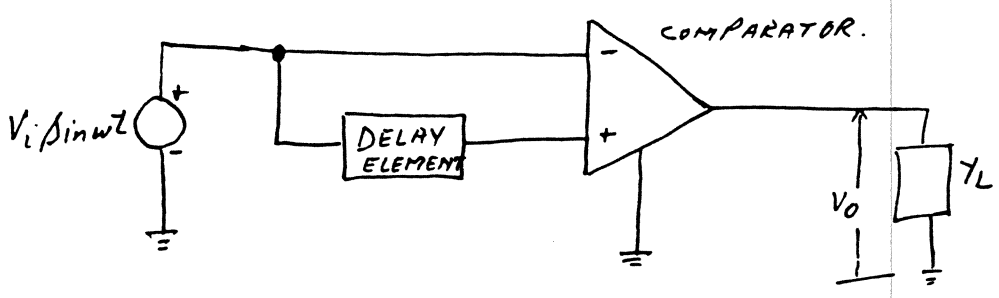

$$V_o = K \cos \omega\left(t - \frac{t_d}{2}\right)$$

Fig 13-3 DELAY LINE Differentiator.

DELAY LINE DIFFERENTIATOR

$$Vo = A \cdot Vi \cdot \sin(w \cdot (t + td)) - A \cdot Vi \cdot \sin(w \cdot t)$$

$$VO = 2 \cdot A \cdot Vi \cdot \sin\left[w \cdot \frac{td}{2}\right] \cdot \cos\left[w \cdot \left[t - \frac{td}{2}\right]\right]$$

$$VO = K \cdot \cos\left[w \cdot \left[t - \frac{td}{2}\right]\right]$$

Where $K = 2 \cdot A \cdot Vi \cdot \sin\left[w \cdot \frac{td}{2}\right]$

K will have the peak value when

$$w = \frac{p}{td}$$

or

$$f = \frac{0.5}{td}$$

Where Vi = input voltage
Vo = output voltage
A = Gain
td = delay
f = cut off frequency of the differentiator

Code = (2, 7) HF = 5Mhz				
Ptrn = FF	Delay Line = 60nS			
Tap	**#1**	**#2**	**#3**	**#4**
Run #1	6.8	6.9	5.8	5.8
Run #2	6.6	7.0	5.8	5.8
Run #3	6.8	7.0	6.0	5.8
Run #4	6.6	6.9	6.0	5.9
Delay (nS)	18.0	30.0	48.0	60.0
Average	**6.7**	**7.0**	**5.9**	**5.8**
Stdev	**0.1**	**0.1**	**0.1**	**0.1**

Code = (2, 7) HF = 5Mhz				
Ptrn = FF	Delay Line = 100nS			
Tap	**#1**	**#2**	**#3**	**#4**
Run #1	7.1	6.6	5.2	5.5
Run #2	7.3	6.7	5.3	5.3
Run #3	7.3	6.8	5.3	5.5
Run #4	7.3	6.6	5.4	5.3
Delay (nS)	30.0	50.0	80.0	100.0
Average	**7.3**	**6.7**	**5.3**	**5.4**
Stdev	**0.1**	**0.1**	**0.1**	**0.1**

Ptrn = (2,7)	Delay Line = 60nS			
Tap	**#1**	**#2**	**#3**	**#4**
Run #1	11.6	11.6	13.1	14.8
Run #2	11.8	11.9	13.1	14.9
Run #3	12.0	11.7	13.2	15.0
Run #4	11.9	11.6	13.3	14.8
Delay (nS)	18.0	30.0	48.0	60.0
Average	**11.8**	**11.7**	**13.2**	**14.9**
Stdev	**0.2**	**0.1**	**0.1**	**0.1**

Ptrn = (2,7)	Delay Line = 100nS			
Tap	**#1**	**#2**	**#3**	**#4**
Run #1	11.9	13.8		
Run #2	11.9	13.9		
Run #3	12.2	14.2		
Run #4	12.4	14.1		
Delay (nS)	30.0	50.0	80.0	100.0
Average	**12.1**	**14.0**	**####**	**####**
Stdev	**0.2**	**0.2**	**####**	**####**

Ptrn = FF		Δ p.s
Delay (nS)		
18	8.7	3.1
30	7.1	4.8
48	5.9	7.3
50	6.7	7.3
60	5.8	9.1
80	5.3	
100	5.4	

Ptrn = (2,7)	
Delay (nS)	
18	11.8
30	11.9
48	13.2
50	14.0
60	14.9
80	
100	

PHASE MARGIN PLOT
11/30/89 15:28
Serial#: unknown

Iteration: 4

	Rad	Iw	HF	Patt	Xtrap	Apex	Zero
▪	2.100	20	5.0	HST	-10	6.3	14.8

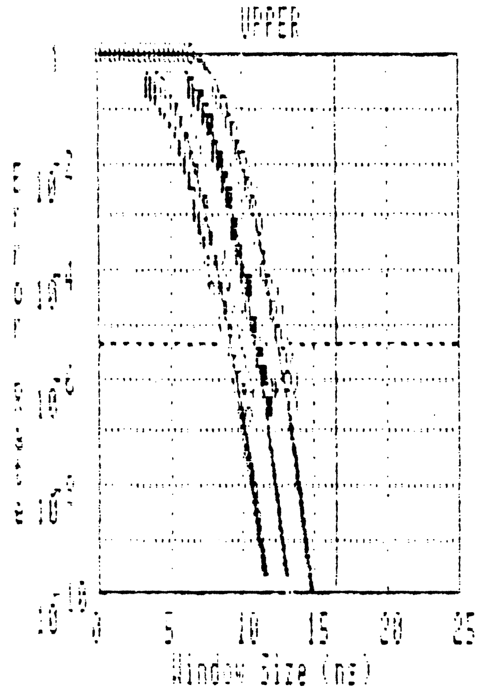

Inc = 0.3 |r| = 0.9957

	Rad	Iw	HF	Patt	Xtrap	Apex	Zero
♦	2.100	20	5.0	HST	-10	1.5	11.6
n	2.100	20	5.0	HST	-10	1.4	11.8
o	2.100	20	5.0	HST	-10	1.3	12.0
■	2.100	20	5.0	HST	-10	1.5	11.9
o	2.100	20	5.0	HST	-10	2.6	11.6
+	2.100	20	5.0	HST	-10	2.4	11.9
X	2.100	20	5.0	HST	-10	2.6	11.7
•	2.100	20	5.0	HST	-10	2.6	11.6
♦	2.100	20	5.0	HST	-10	4.8	13.1
n	2.100	20	5.0	HST	-10	4.8	13.1
o	2.100	20	5.0	HST	-10	4.7	13.2
■	2.100	20	5.0	HST	-10	4.6	13.3
o	2.100	20	5.0	HST	-10	6.2	14.0
+	2.100	20	5.0	HST	-10	6.1	14.9
X	2.100	20	5.0	HST	-10	6.0	15.0
•	2.100	20	5.0	HST	-10	6.3	14.0
o	2.100	20	5.0	HST	-10	6.2	14.8

DELAY LINE = 60ns
PM. FILTER = 15MHz

TAP #1
TAP #2
TAP #3
TAP #4

(C) PHASE LOCK LOOP DESIGN

DESIGN PARAMETERS

1. VCO Gain (Ko)

For MC1648 at VCO center frequency 128 MHz

$Ko = 16 \text{ MHz / Volt}$

$= 2\pi * 16E6 \text{ Rad / Sec / V}$

2. Phase Detector Gain (Kd)

For MC12040 Phase Detector

$Kd = 1/2\pi * A * (Voh - Vol) \text{ Volts / Rad}$

where A = Signal attenuation

Voh = -1.8 V

Vol = -0.9 V

PROGRAMMABLE GAIN CONTROL IS MOST SUITABLE FOR TEST EQUIPMENT.

3. Loop Gain (K)

$K = Ko * Kd / N \text{ / Sec}$

where N is frequency division ratio.

4. PLL Bandwidth (BW) & Damping Factor (ξ)

For linear continuous second order system

Bandwidth $BW = fo = 2\xi f$

$= 2\xi Wn / 2$

where

fo = Open loop unity gain cross over frequency.

fn = Close loop Natural frequency

ξ = Closed loop Damping Factor

Notes: 1. Normally high frequency operation is more critical and difficult to optimize. Optimize the system for high and verify at low frequency.

2. For Test equipment design low PLL jitter or noise is more important rather than quick response. Hence Damping Factor should be fairly large approx equal to 3.

3. Good approximation for BW = 50 KHz

5. PLL Transfer Function

$$G(S) = K * F(S) / S$$

where F(S) = Transfer function of loop filter.
1 / S = VCO act as integrator

Normally pole frequency should be much higher than BW or fo. Loop filter can be active or passive, but **IT IS BETTER TO HAVE SELECTABLE LOOP FILTERS.**

6. FREQUENCY CONTROL LOOP

Contribution of VCO jitter to PLL noise is more than any other components. A pretune DAC is used to tune the VCO to the required frequency with enough resolution for PLL to acquire lock easily. To reduce the VCO phase noise one or more frequency control loops can be placed around the VCO.

5. SAMPLE VS PHASE MARGIN TESTING

- Sample Margin Test Technique (SMTT) is logical extention to DSP technique.

- High speed ADC with DSP processor will supplement SMTT.

- SMTT with DSP can produce
  - Bar Graph
  - Gaussian curve

- SMTT more suitable for higher frequency and easier to implement.

INSTRUMENTATION BASED TEST SYSTEM

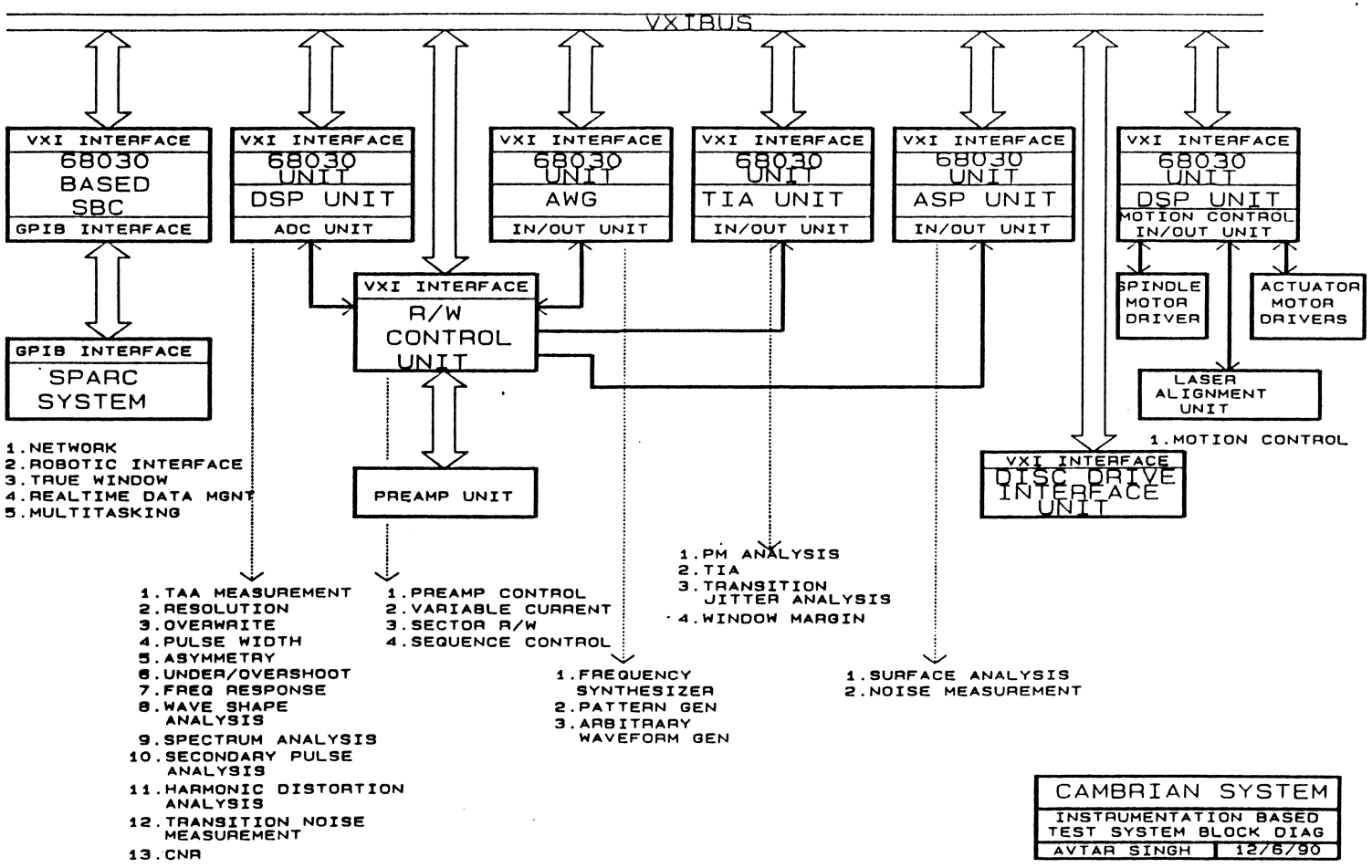

CAMBRIAN SYSTEM	
INSTRUMENTATION BASED TEST SYSTEM BLOCK DIAG	
AVTAR SINGH	12/6/90

ELECTRONIC FUNCTION INTEGRATION

Steve Dines

Cirrus Logic

AGENDA

- Integration environment
- Why does DSP impact integration
- Packaging & Test Issues
- Integration Scenarios

INTEGRATION ENVIRONMENT

- ***Everybody*** **claims to be able to integrate** ***everything***

EUROPE 100 B.C.

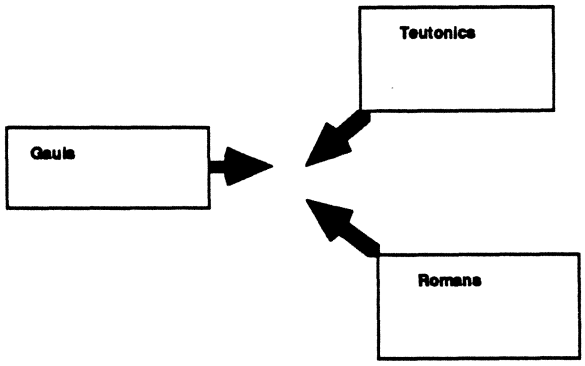

DISK ELECTRONICS SUPPLIERS TODAY

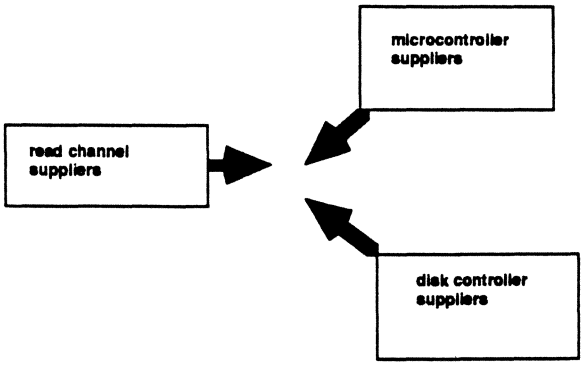

- Buyer beware!

WHY DOES DSP IMPACT INTEGRATION?

- Channel
- Servo
- Flexibility
- Power management
- Pin-out

SYNCHRONOUS CHANNELS AND INTEGRATION

- highly tuned analog --> analog front end + digital algorithms => CMOS
- Force to CMOS paves the way for integration with other logic elements
- Scalability of digital vs analog
- Flexibility gains ensure customer value added

BIPOLAR to CMOS 50% to 100% reduction of power

DSP to

SYNCHRONOUS CHANNEL INTEGRATION BENEFITS

- Space reduction
- Power deduction
- Pin-out reduction

DIGITAL SERVO AND INTEGRATION

- Servo becomes logic element plus analog periphery (A to D and D to A)
- Easier to integrate

DIGITAL SERVO INTEGRATION BENEFITS

- Integrated servo is an areal capacity argument

  Integrated header - avoid repeating track info in data fields and servo fields
  5% benefit (linear only)

- Eases pseudo-sector mark generation
- More integrated power management
- Servo is becoming more hardware path - fits better with data channel
- Totally concurrent servo processing
  - no interdependence between micro and servo engine
- Preserves commodity micro benefits
- Removes major complexity from ASIC

OPTIMIZED SERVO PROCESSING

- Servo engine targeted at magnetic disk head control
- Key hardware modules added
- Reduces code
  - space
  - time
  - engineering effort
- Overkill avoidance - eg sub 100ns multiplies not needed for typical sample rates

FLEXIBILITY

- How do electronics suppliers ensure customer flexibility in the face of ever increasing integration
- Synchronous channels provide digital flexibility
- Digitally based servo allows user to implement his servo approach

DSP IMPROVES FLEXIBILITY

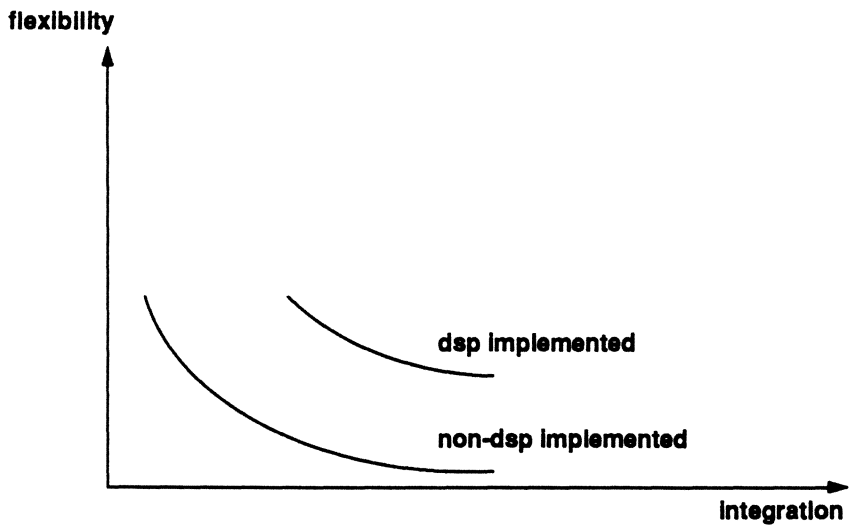

CIRRUS LOGIC

DSP IMPROVES POWER MANAGEMENT

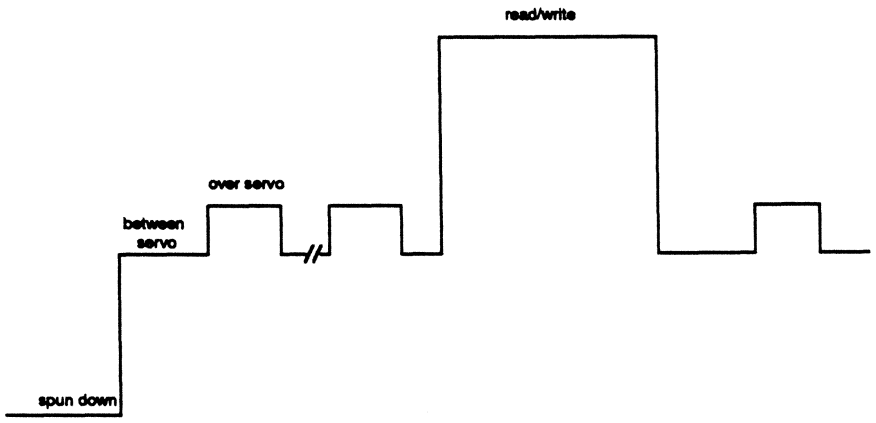

CIRRUS LOGIC

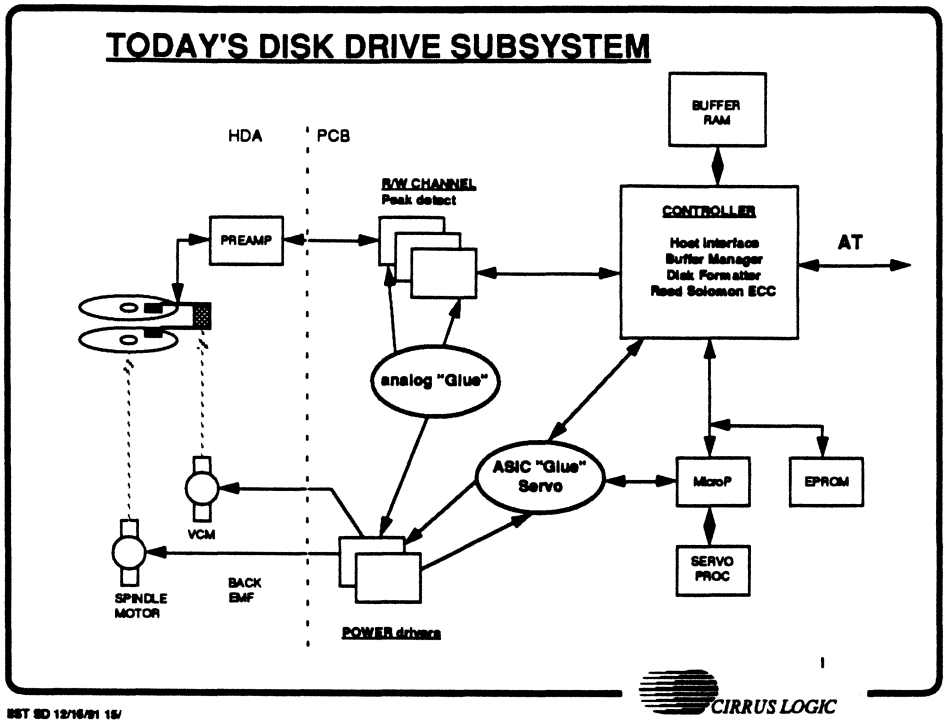
TODAY'S DISK DRIVE SUBSYSTEM
HDA
PCB
BUFFER RAM
R/W CHANNEL
Peak detect
PREAMP
CONTROLLER
Host Interface
Buffer Manager
Disk Formatter
Read Solomon ECC
AT
analog "Glue"
ASIC "Glue"
Servo
MicroP
EPROM
SERVO PROC
VCM
SPINDLE MOTOR
BACK EMF
POWER drivers
CIRRUS LOGIC

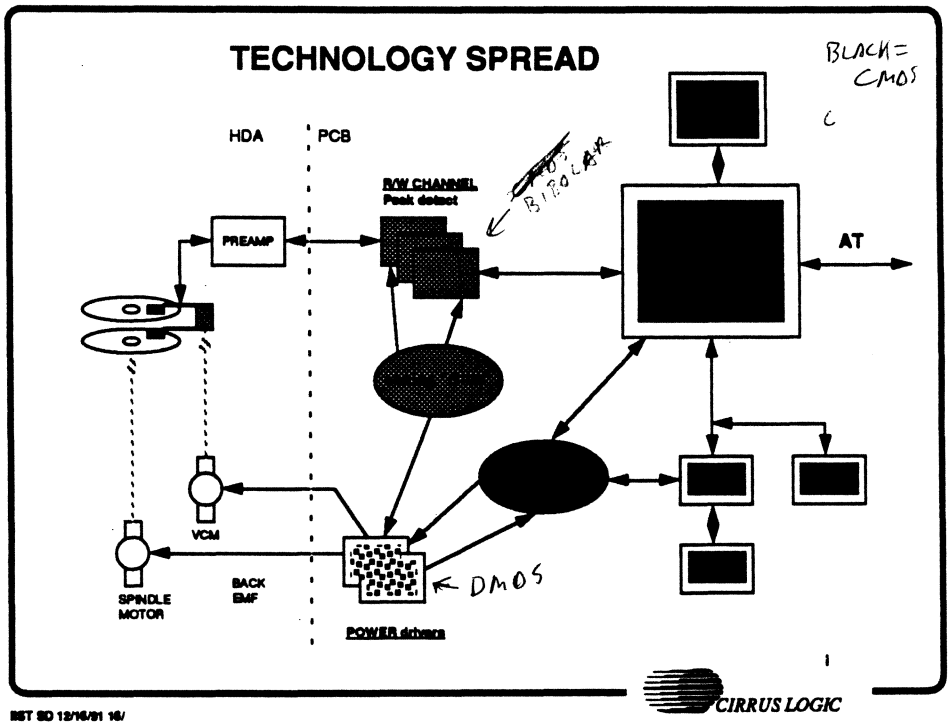
TECHNOLOGY SPREAD
BLACK = CMOS
HDA
PCB
R/W CHANNEL
Peak detect
PREAMP
AT
VCM
SPINDLE MOTOR
BACK EMF
DMOS
POWER drivers
CIRRUS LOGIC

PACKAGING & TEST ISSUES

- Integration should match packaging
- Relationship to form factor
- Die considerations

CIRRUS LOGIC

1.8 " AND QFP

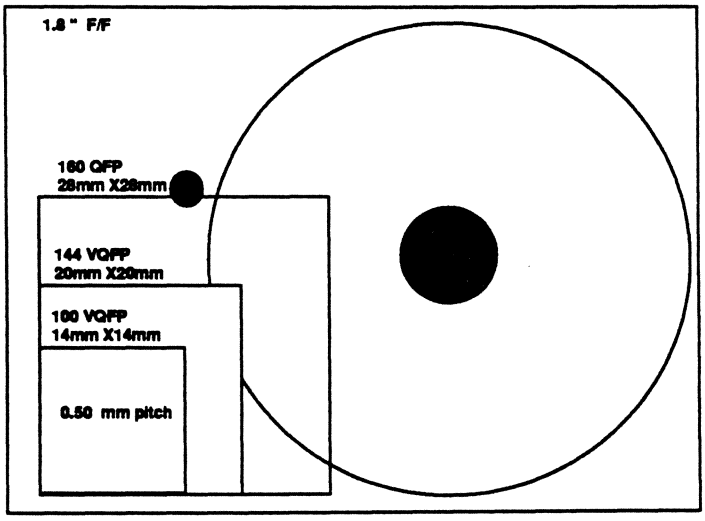

CIRRUS LOGIC

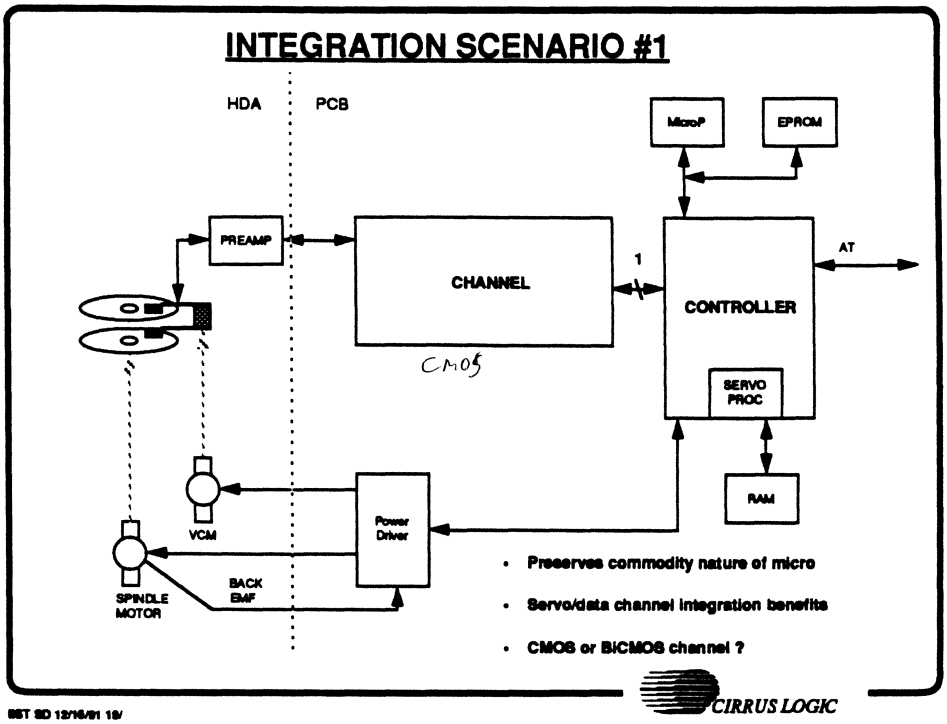
INTEGRATION SCENARIO #1
HDA
PCB
MicroP
EPROM
PREAMP
CHANNEL
1
CONTROLLER
AT
CMOS
SERVO PROC
RAM
VCM
Power Driver
SPINDLE MOTOR
BACK EMF
• Preserves commodity nature of micro
• Servo/data channel integration benefits
• CMOS or BiCMOS channel ?
CIRRUS LOGIC

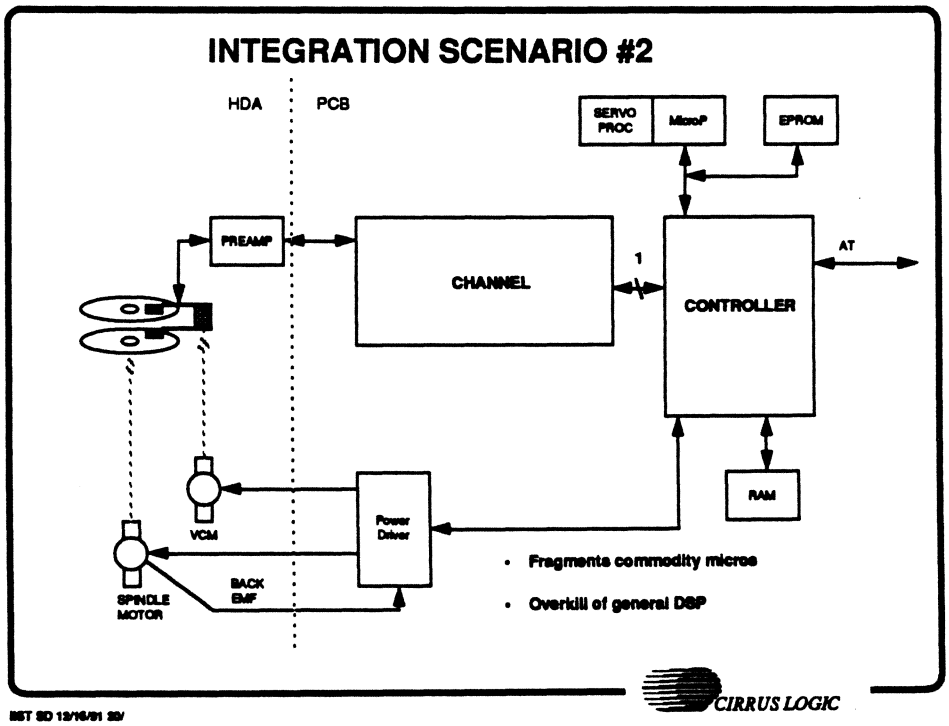
INTEGRATION SCENARIO #2
HDA
PCB
SERVO PROC
MicroP
EPROM
PREAMP
CHANNEL
1
CONTROLLER
AT
RAM
VCM
Power Driver
SPINDLE MOTOR
BACK EMF
• Fragments commodity micros
• Overkill of general DSP
CIRRUS LOGIC

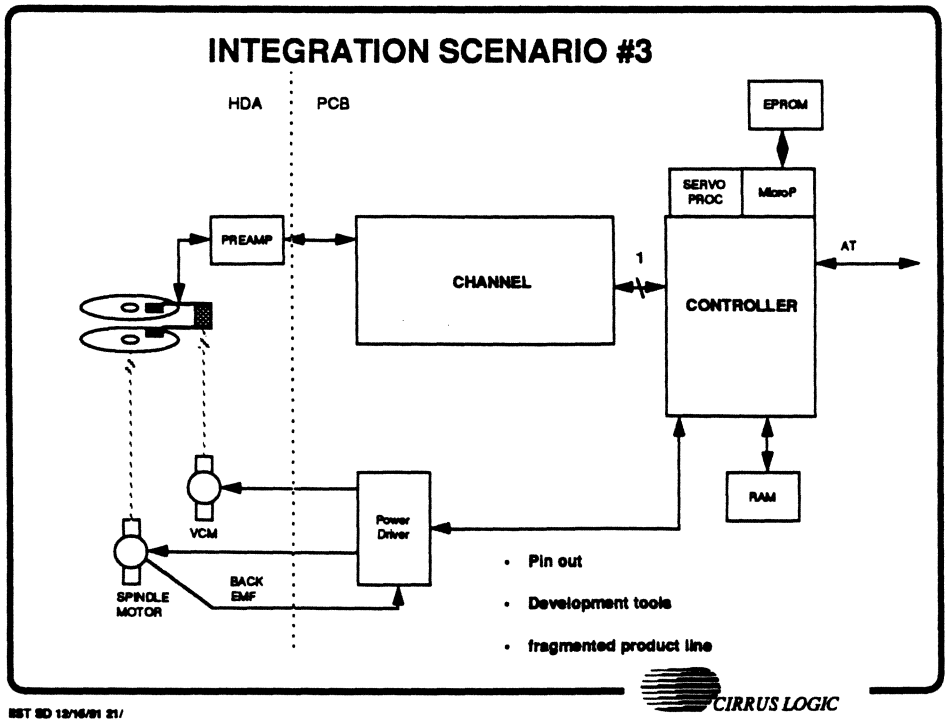
INTEGRATION SCENARIO #3
HDA
PCB
EPROM
SERVO PROC
MicroP
PREAMP
CHANNEL
1
CONTROLLER
AT
VCM
Power Driver
RAM
SPINDLE MOTOR
BACK EMF
• Pin out
• Development tools
• fragmented product line
CIRRUS LOGIC

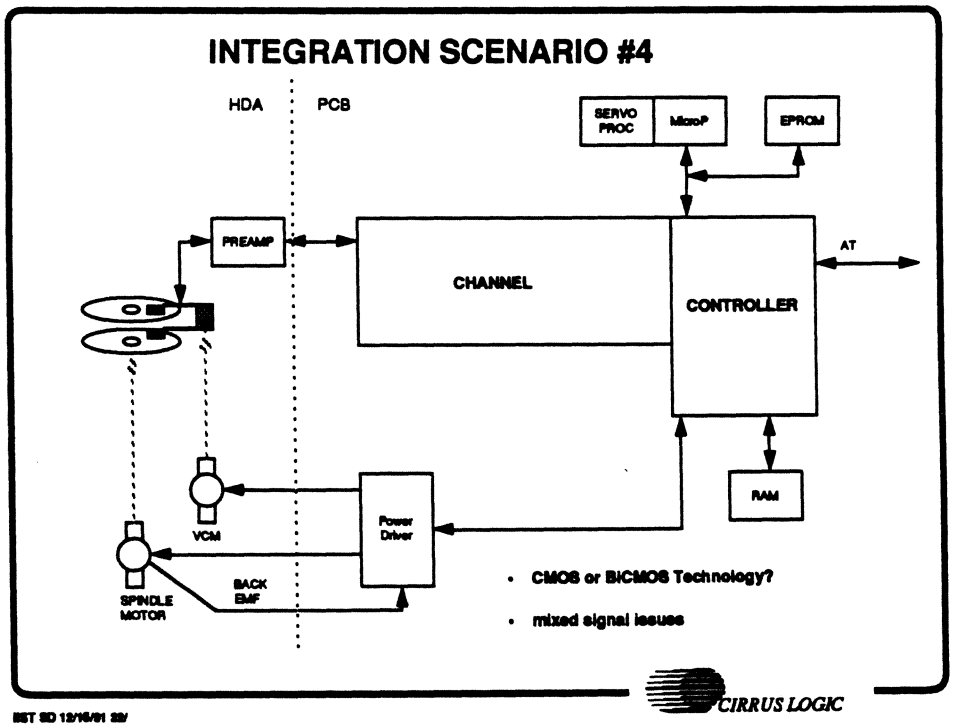
INTEGRATION SCENARIO #4
HDA
PCB
SERVO PROC
MicroP
EPROM
PREAMP
CHANNEL
CONTROLLER
AT
VCM
Power Driver
RAM
SPINDLE MOTOR
BACK EMF
• CMOS or BiCMOS Technology?
• mixed signal issues
CIRRUS LOGIC

INTEGRATION SCENARIO #5

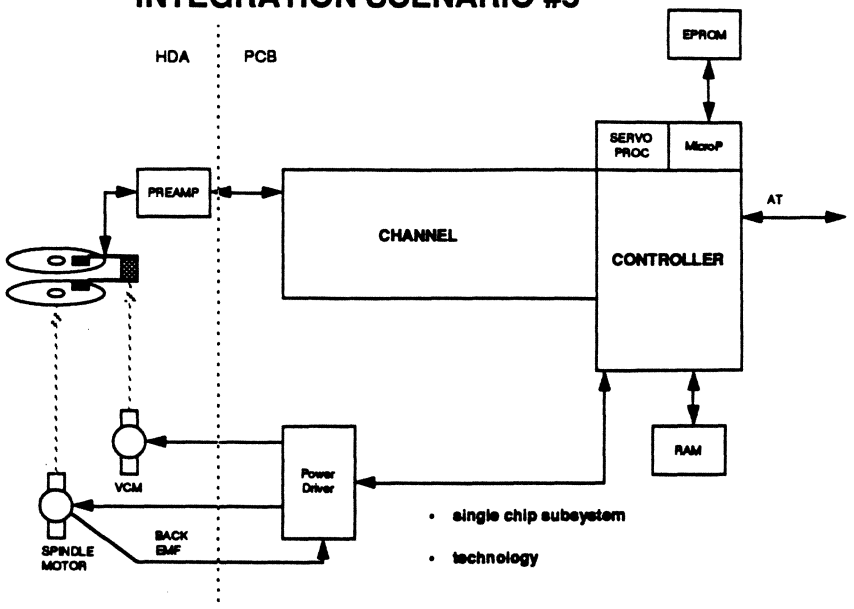

CIRRUS LOGIC

SUMMARY

- **Buyer must beware**
- **Most cost efficient vehicle for transistor delivery**
- **Understand your commodity benefits**
- **Exploit the digital drive!**

CIRRUS LOGIC

DRIVE SELF TESTING AND DIAGNOSTICS

Jonathan D. Coker

For IIST's "The Impact of DSP on Future Generation HDDs"
December 17-19, 1991

IBM Storage Systems Products Division, Rochester, MN

Redwing 5.25" DSP Drive

3.50" DSP Drive - Just announced

Overview

- PRML channel primer
- Error rate performance estimation
- Flying height change detection
- Disk surface analysis

Signal Flow in a PRML Channel

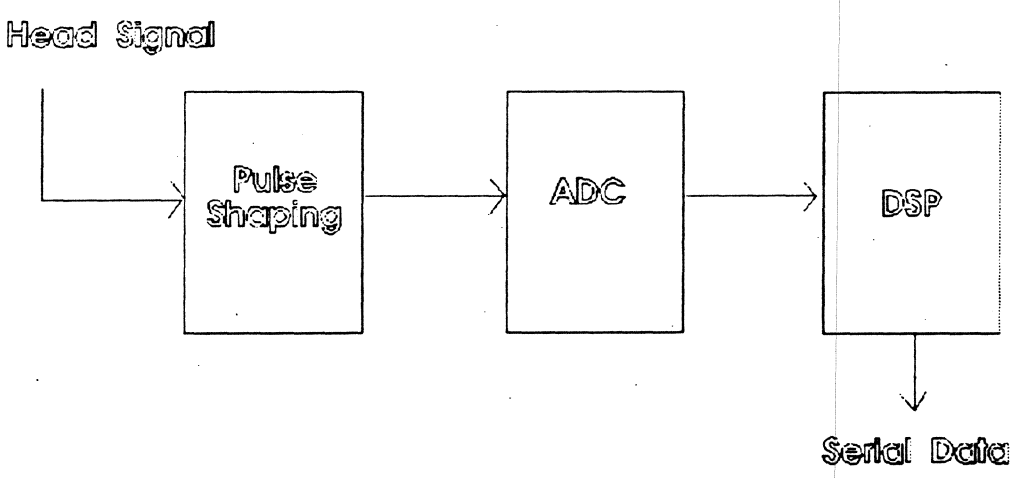

Partial Response IV Conventions

$$y_k \equiv a_k - a_{k-2}$$ - output node

$$a_k \in \{\pm 1\}$$ - input node

$$\Rightarrow \quad y_k \in \{0, \pm 2\}$$

Partial Response IV Tidbits

- Interleaves are independent
- Output "2"s must alternate polarity within an interleave

Output Sequence Examples

NOT LEGAL

-2 -2 0 0 2 2 0 0 **-1** 0 2

-2 2 0 -2 0 0 2 0 -2 2 0 0 2

-2 2 0 -2 0 0 **2** 0 **2** -2 0 0 2

NOT LEGAL

Precoding

Peak Detection:

Input

... 01001000101 ...

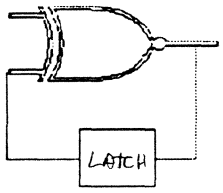

Output

... 10001111001 ...

OR

... 01110000110 ...

Partial Response IV:

Input

... 01001000101 ...

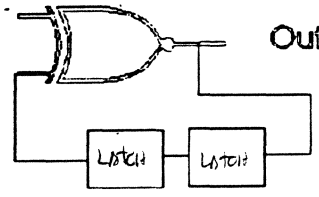

Output

... 01011111011 ...

Precoding guarantees a non-zero output iff the input is 1.

Noisy Readback Sequence

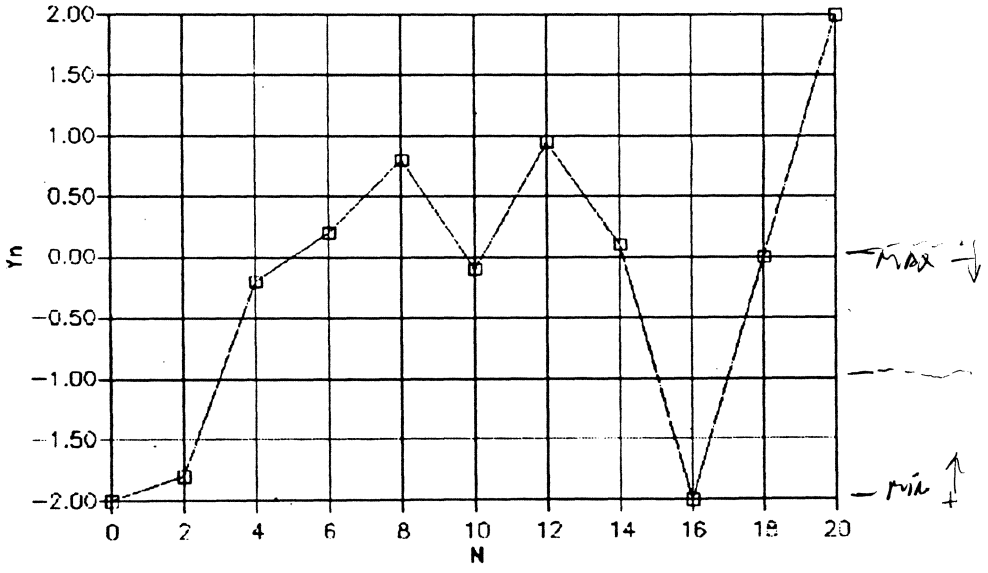

With PR-IV, Viterbi detection consists of a minimum/maximum finder with a polarity latch.

PRML Error - Example 1

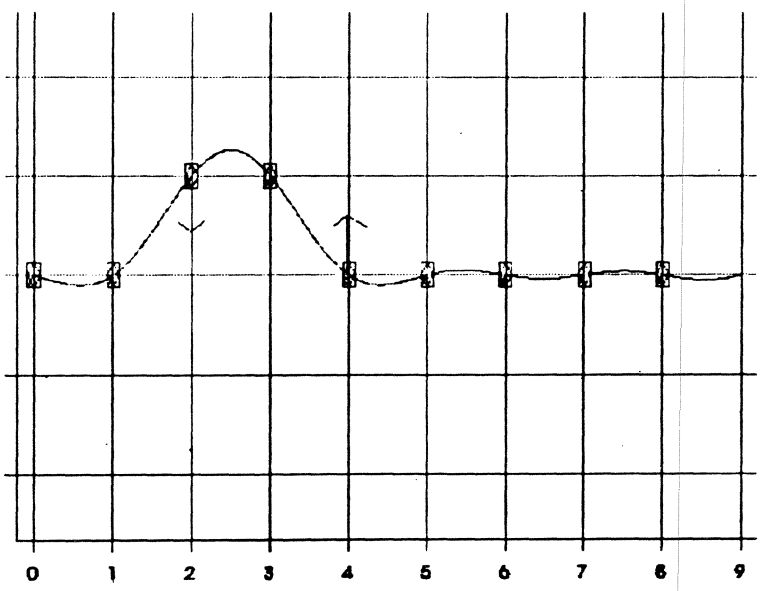

0 0 +1 +1 -1 -1 -1

Condition for error: EX 1

$$n1 + n2 > 2$$

PRML Error - Example 2

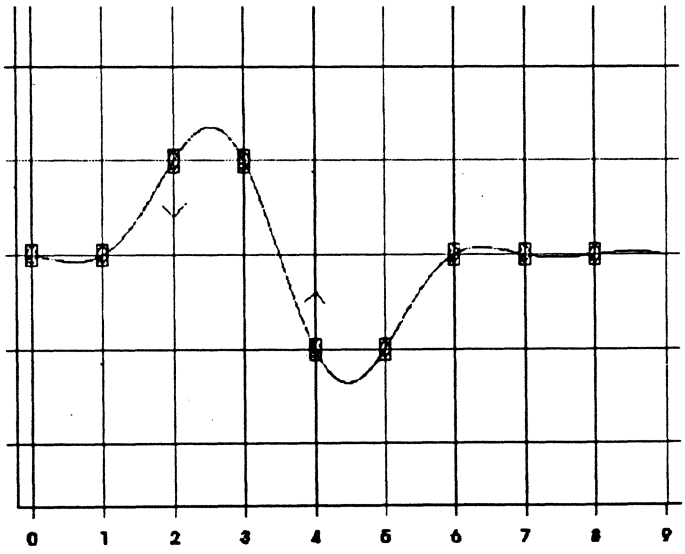

Condition for error:

$$n1 + n2 > 2$$

Error Rate Performance Estimation

- Error rate performance may be estimated by measurement of noise statistics in fraction of time necessary for a true error rate test
- Simplest case assumption of white Gaussian noise allows compact implementation

Possible Uses

- quick performance indicators during the manufacture of the drive
- early detection of error rate changes in the field
- field diagnostics

Mean-Square-Error Circuit

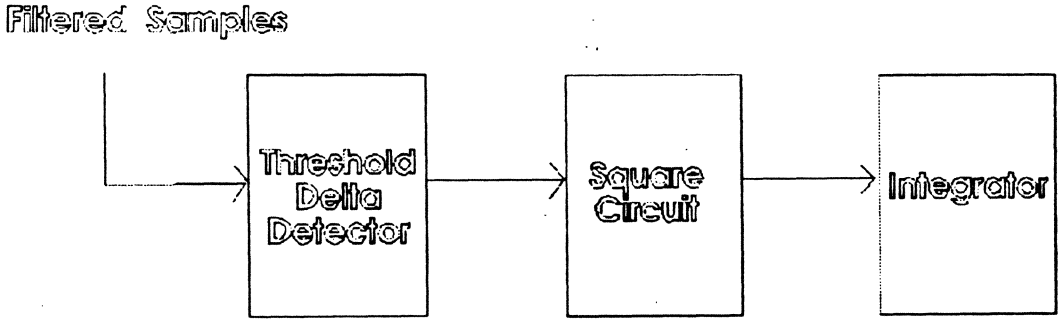

Error Probability with WGN

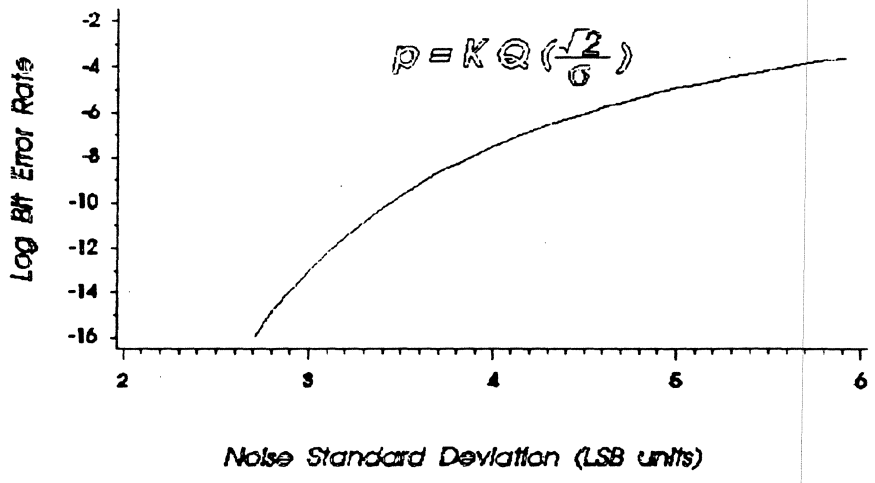

WGN is typically a bad presumption.

Equalization typically introduces significant noise correlation effects.

Correlation Effects in a Digital Tap Delay Line

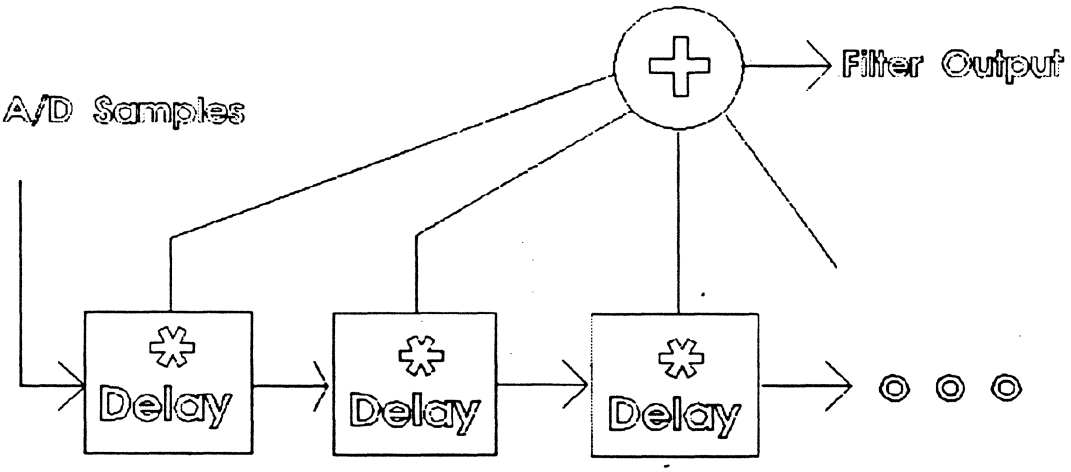

PRML "cares" about the following quantities:

$$Y(n) - Y(n+2)$$
$$Y(n) - Y(n+4)$$
$$Y(n) - Y(n+6)$$

o o o

Noise Multipliers

These quantities are zero-mean Gaussian variables whose standard deviations are related to the input by the following factors:

$$M^2(n) = \left(\sum t^2(i) - \sum t(i)t(i+n) \right)$$

Noise multipliers are functions of time spacing.

Noise Multipliers - Example

$$\sum t^2(i) = 1.2^2$$

M(2) = 1.3

M(4) = 1.5

M(6) = 1.3

M(8) = 1.2

M(10) = 1.2

...

When noise correlation is significant, the overall error rate can be dominated by a single most-likely error length.

Flying Height Change Measurement

- Technique uses frequency response changes to detect flying height differences
- Frequency response changes described by the Wallace equation

Test Pattern

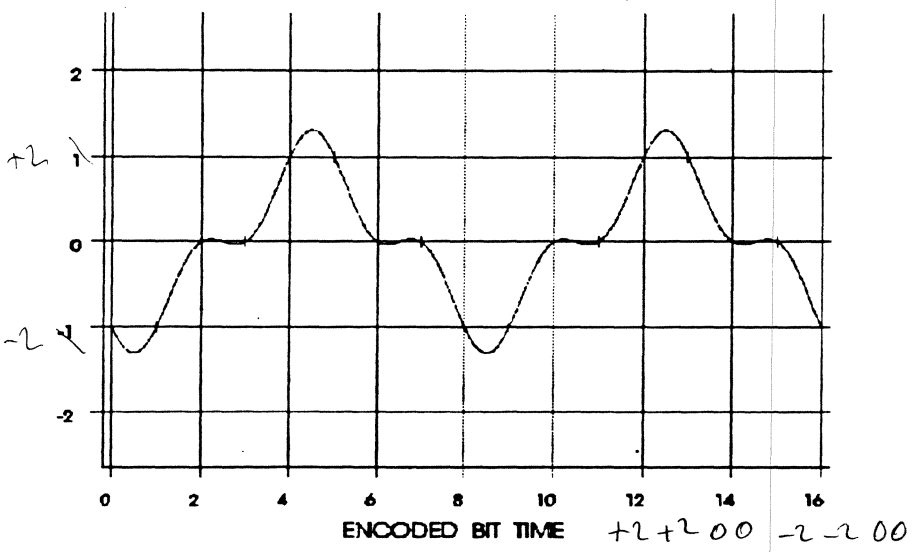

Description of Test Pattern

$$f(t) = (1 + \sqrt{2}) \cos\left(\frac{\pi}{4} t\right) + \cos\left(\frac{3\pi}{4} t\right)$$

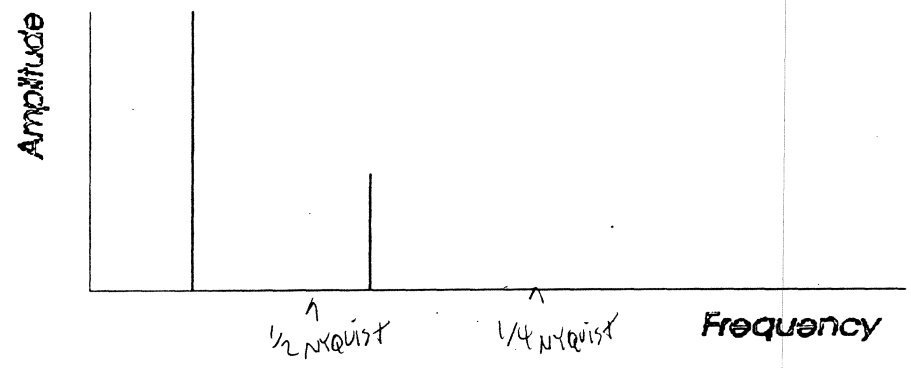

Effect of Lower Separation Loss

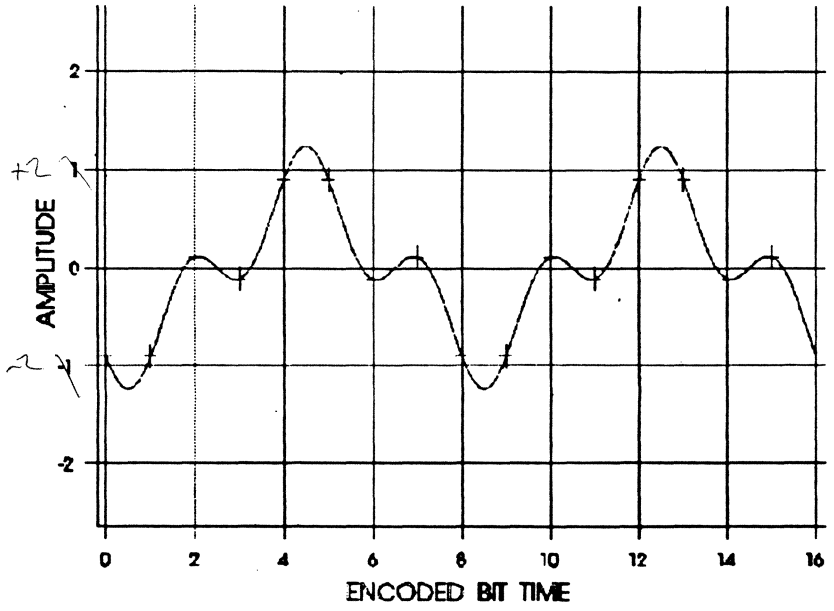

Effect of Higher Separation Loss

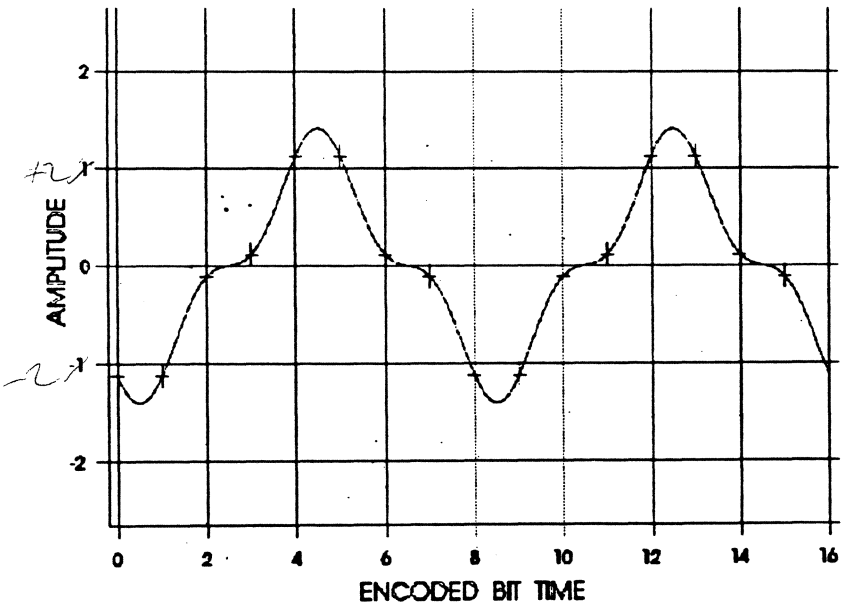

Wallace Equation Application

$$f(t) = (1 + \sqrt{2})\, e^{-k\frac{\pi}{4}} \cos\left(\frac{\pi}{4} t\right) + e^{-3k\frac{\pi}{4}} \cos\left(\frac{3\pi}{4} t\right)$$

$$f(-0.5) + f(0.5) = 4$$

$$\Longrightarrow \delta(k) = \frac{2\left(1 - e^{-k\frac{\pi}{2}}\right)}{\cot\left(\frac{\pi}{8}\right) + \tan\left(\frac{\pi}{8}\right) e^{-k\frac{\pi}{2}}}$$

Delta versus Separation for Various Linear Densities

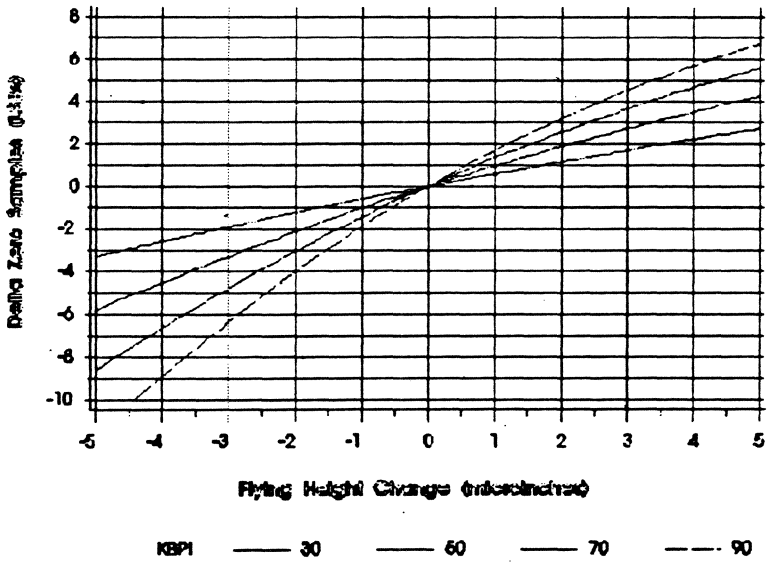

Fly Height Change Detector Circuit

A/D Samples

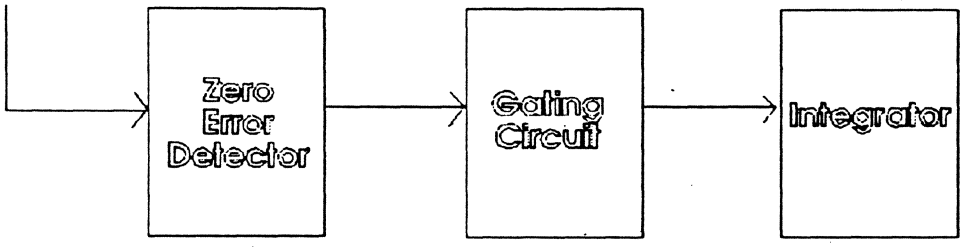

Measurement Error Analysis

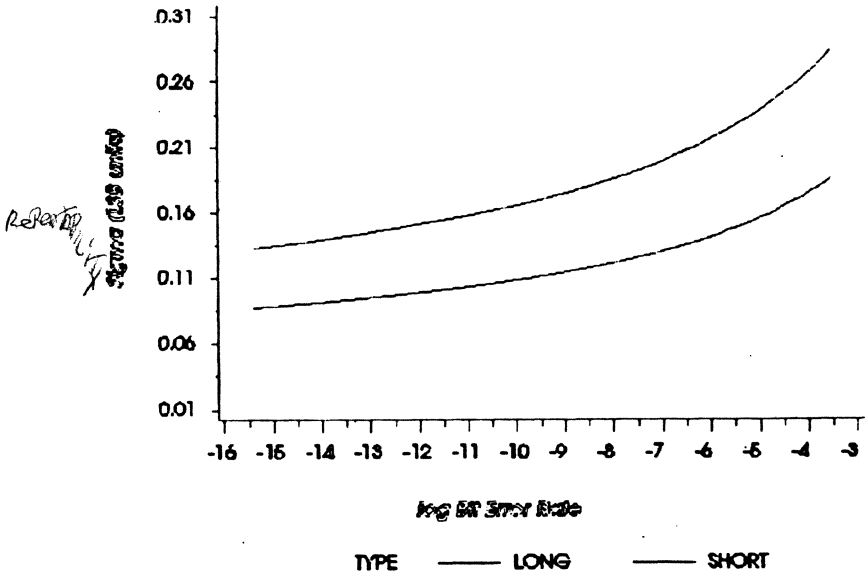

Disk Surface Analysis

==> Purpose: to mark and deallocate magnetic imperfections on the disk surface

==> typically performed during the manufacture of the drive

Surface Analysis Test Pattern

a_k : -1, -1, +1, +1, ...

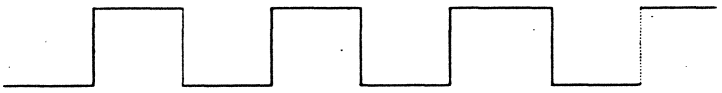

y_k : -2, -2, +2, +2, ...

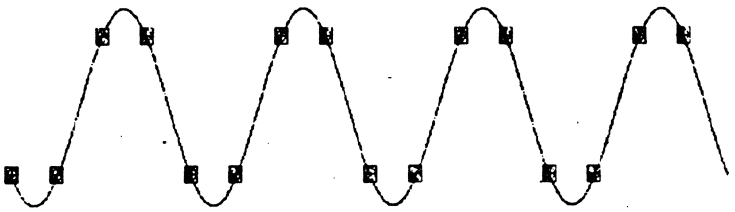

Missing Bit Defect Example

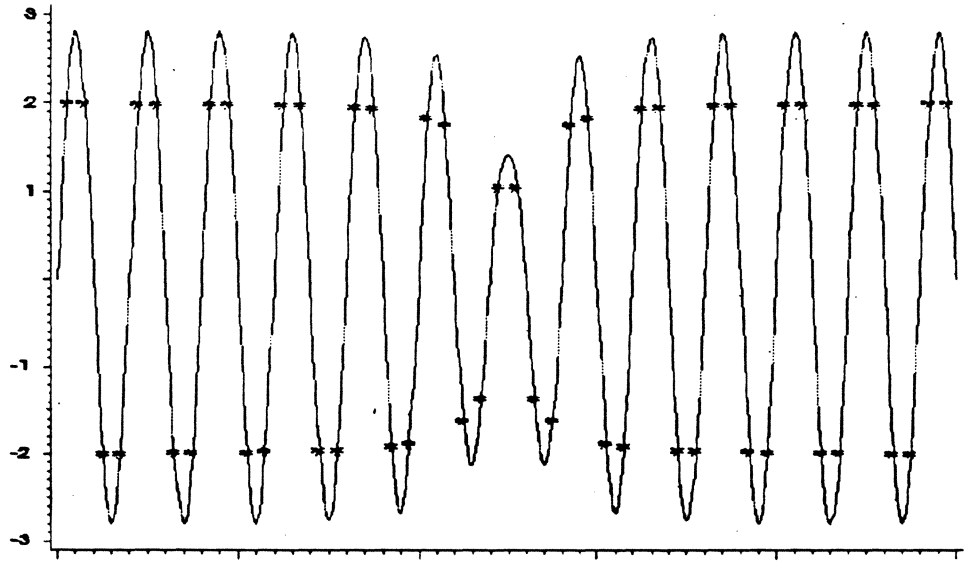

Defect Detection Circuit

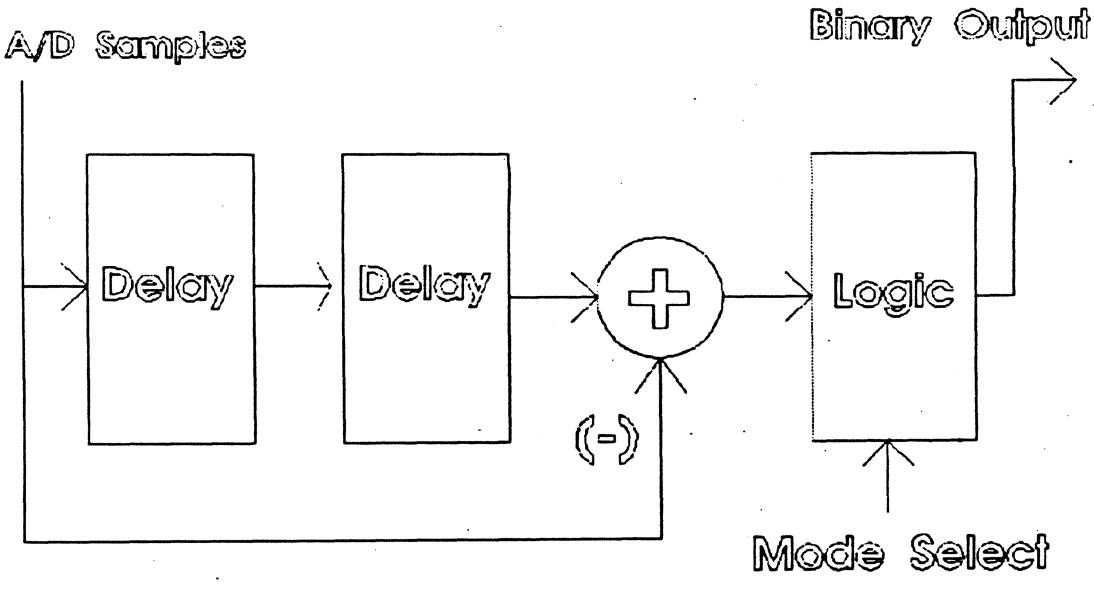

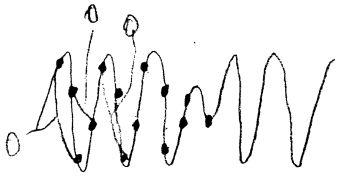

WILL REPORT A LONG ERROR AS A SHORT ERROR SEPARATED BY SPACE EQUAL TO ERROR LENGTH.

Test Distribution Function

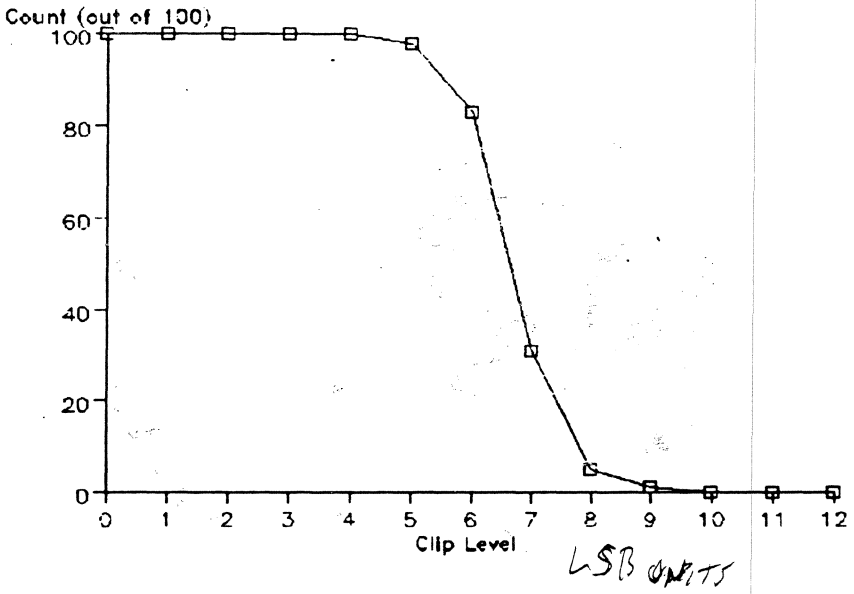

Void Defect Contour

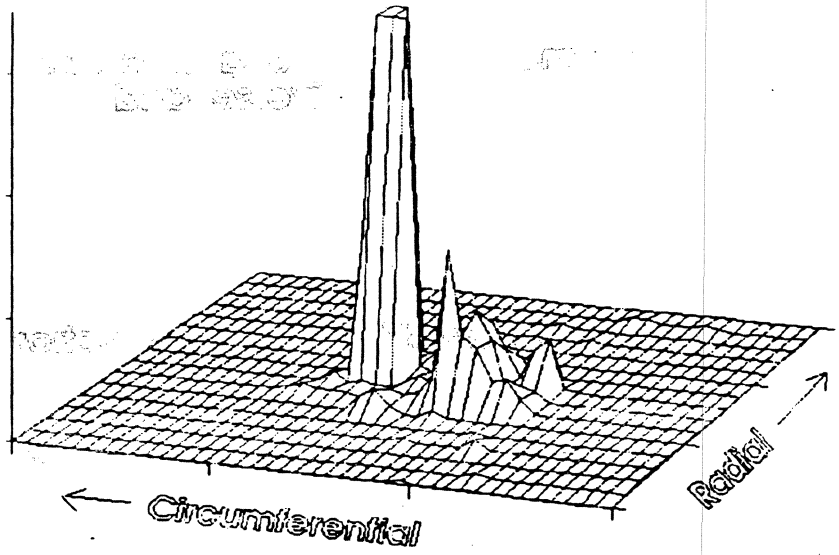

Scratch Defect Contour

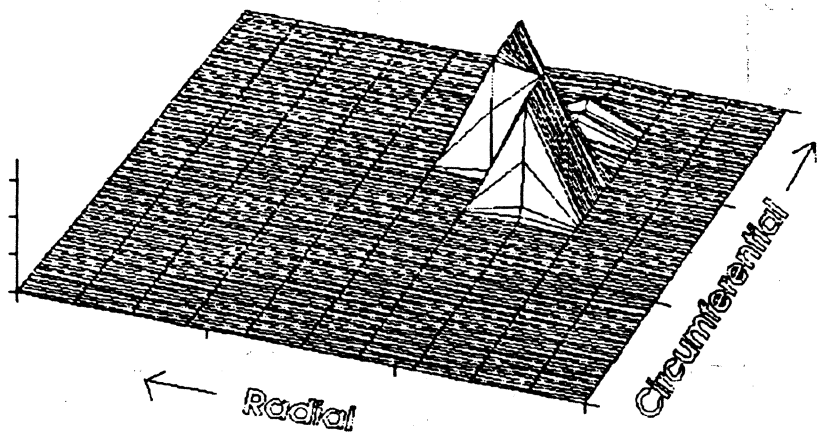

Summary

Incremental modifications to a standard PRML channel provide diverse and powerful applications:

- Disk surface analysis
- Flying height change detection
- Error rate performance estimation

CHARACTERIZATION AND STRUCTURE/PROPERTY RELATIONSHIP OF AMORPHOUS CARBON FILMS

Bruno Marchon
Seagate Technology
Recording Media Group

Seagate
INFORMATION, THE WAY YOU WANT IT

Carbon Overcoat for Rigid Media

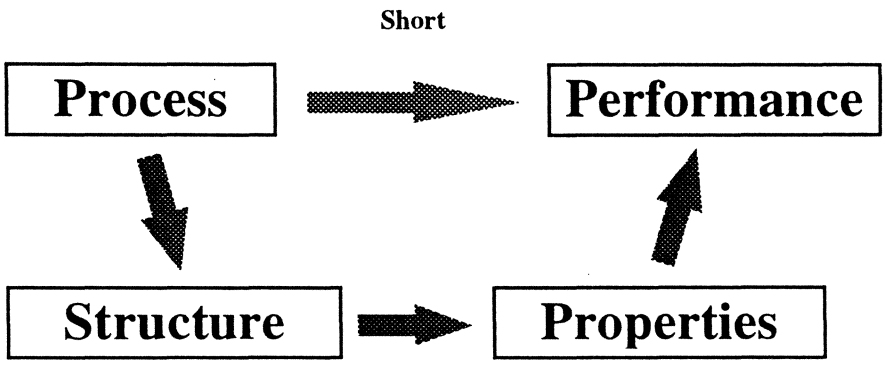

Bruno Marchon
IIST Dec 16, 1997

Seagate
INFORMATION, THE WAY YOU WANT IT

Carbon Overcoat for Rigid Media

PROCESS	STRUCTURE	PROPERTY	PERFORMANCE
Dopant (H, N, O)	H, N, O Content	Stress	
		Hardness	
Pressure	sp2/sp3	Modulus	
		Adhesion	TRIBOLOGY
Temperature	Disorder	Toughness	
Bias	Dopant Bonding	Band gap	
		Optical	
	Dangling Bonds	Density	
			CORROSION
	Surface Groups	Tribochemistry	
Deposition Rate	Coverage	Lubricant Bonding	
Time			
	Thickness		
		Lube Diffusion	
		Electrical	

Seagate
INFORMATION, THE WAY YOU WANT IT

Carbon Overcoat for Rigid Media

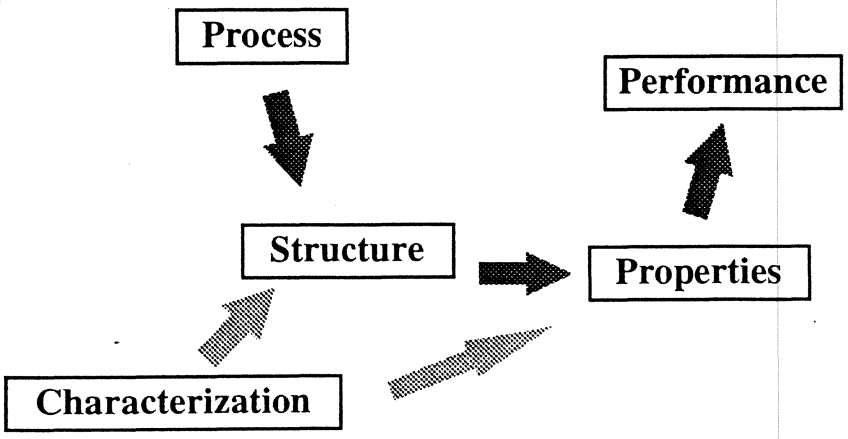

Seagate
INFORMATION, THE WAY YOU WANT IT

Carbon Overcoat Characterization

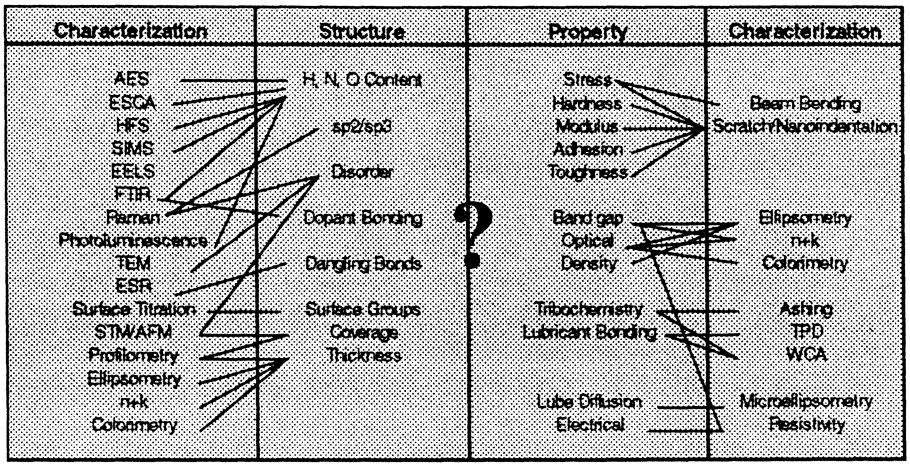

Bruno Marchon
IIST Dec 16, 1997

Seagate
INFORMATION, THE WAY YOU WANT IT

Carbon Overcoat for Rigid Media

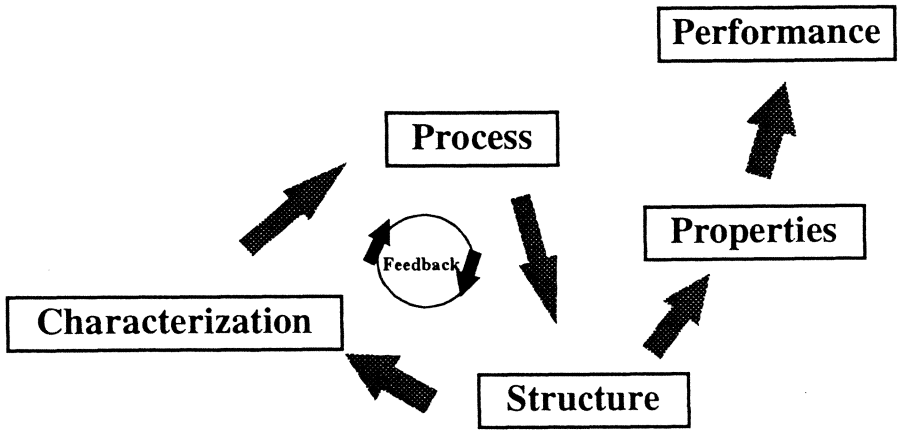

Bruno Marchon
IIST Dec 16, 1997

Seagate
INFORMATION, THE WAY YOU WANT IT

Bonding in the a-C:H System

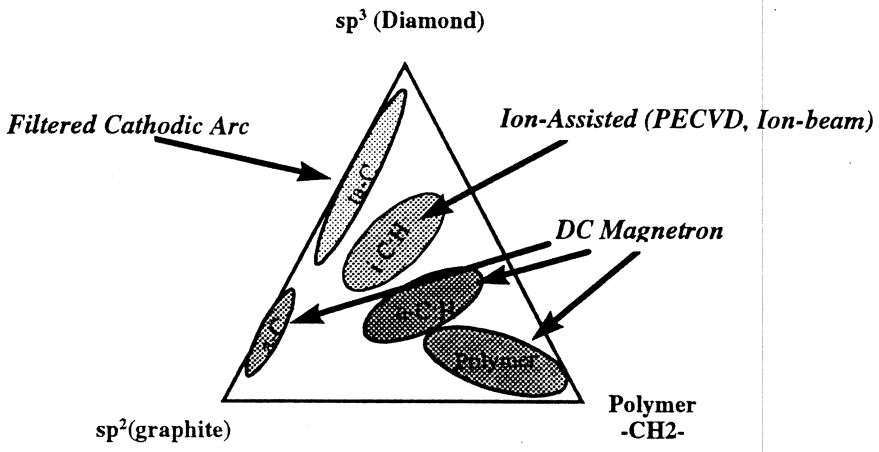

Seagate
INFORMATION, THE WAY YOU WANT IT

STM: Structure of Amorphous Carbon

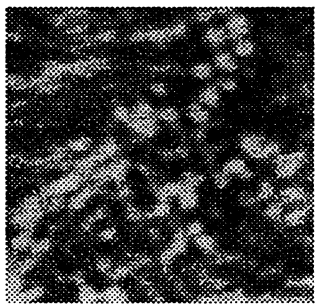

40x40A STM Image a-C
B. Marchon et al. Phys. Rev. 1989

Bruno Marchon
IIST Dec 16, 1997

Seagate
INFORMATION, THE WAY YOU WANT IT

a-CH: G Peak Position and Temperature

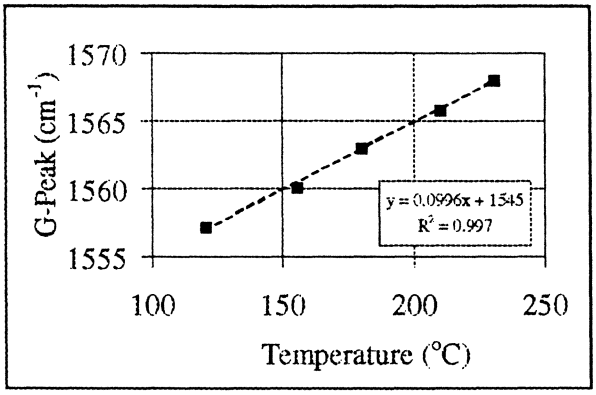

B. Marchon et al., IEEE Trans. Magn. (1997)

Seagate
INFORMATION, THE WAY YOU WANT IT

sp^2 and sp^3 Bonding: EELS

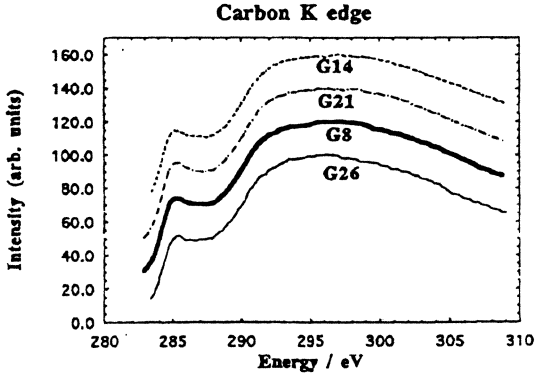

From P.R. Silva and J. Robertson, U. Cambridge

Seagate
INFORMATION, THE WAY YOU WANT IT

a-CH: G Peak Position and EELS %sp^3

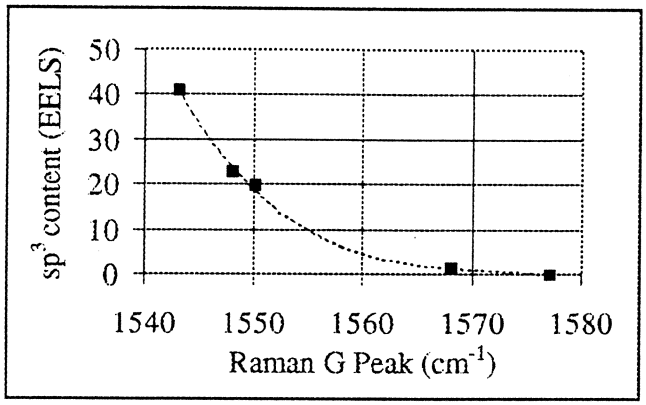

B. Marchon et al., IEEE Trans. Magn. (1997)

Seagate
INFORMATION, THE WAY YOU WANT IT

a-CH: Abrasion Resistance vs. G Position

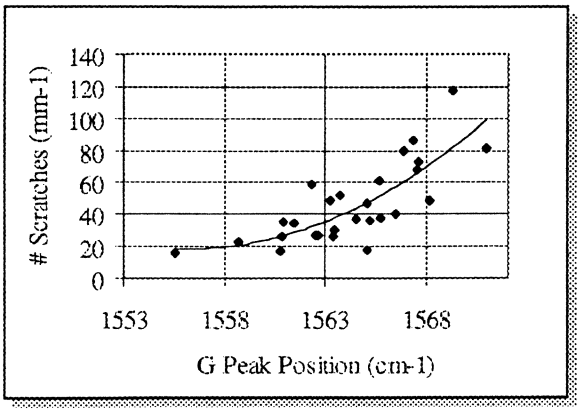

B. Marchon et al., IEEE Trans. Magn. (1997)

Seagate
INFORMATION, THE WAY YOU WANT IT

Raman on a-CH

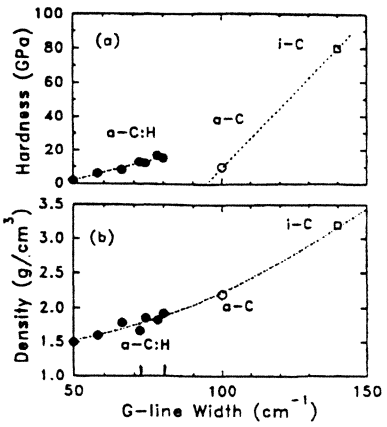

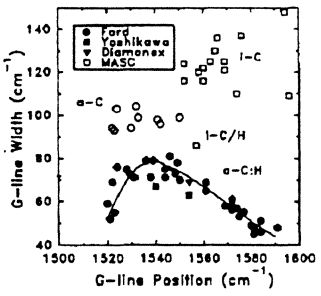

Tamor et al., J. Appl. Phys. (1994)

Seagate
INFORMATION, THE WAY YOU WANT IT

a-CH: Photoluminescence

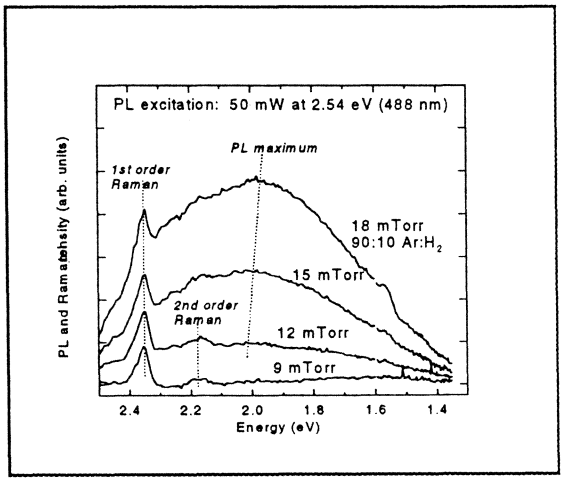

B. Marchon et al., IEEE Trans. Magn. (1997)

Seagate
INFORMATION, THE WAY YOU WANT IT

a-CH: Raman PL and Hydrogen Content

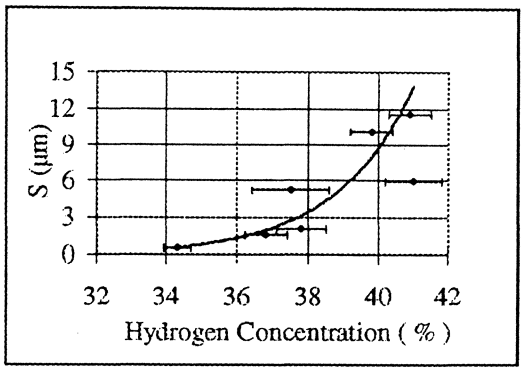

B. Marchon et al., IEEE Trans. Magn. (1997)

Seagate
INFORMATION, THE WAY YOU WANT IT

Raman Slope and Sputter Process

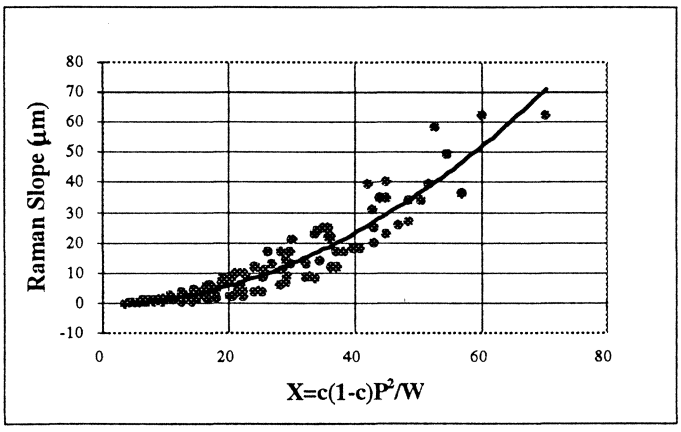

c: %H in Ar P: Sputter Pressure W: Sputter Power

Seagate
INFORMATION, THE WAY YOU WANT IT

a-CH: Mechanical Properties and %H

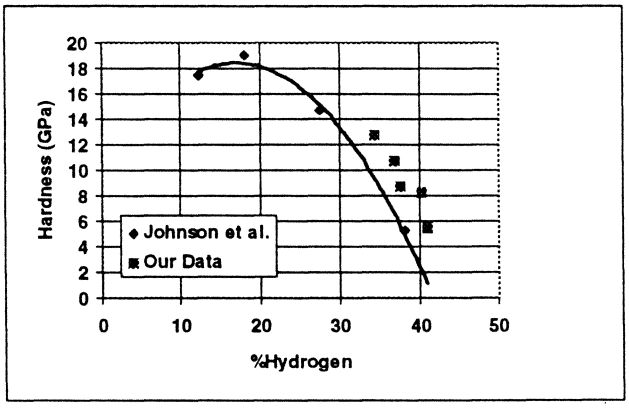

Johnson et al., IBM J. Res. Develop. (1996)

B. Marchon et al., IEEE Trans. Magn. (1997)

Seagate
INFORMATION, THE WAY YOU WANT IT

Ion-beam Carbon: Raman and Stress

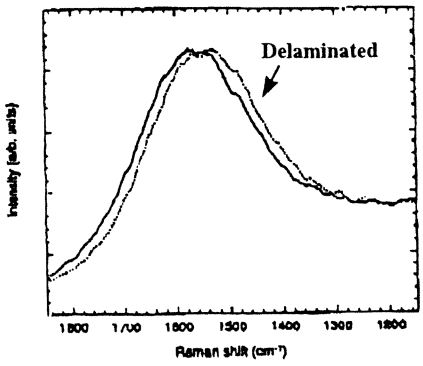

Ager et al. , Appl. Phys. Lett. (1995)

Seagate
INFORMATION, THE WAY YOU WANT IT

Filtered Cathodic Arc: ta-C, a-D

C+ Ions Selected in a Narrow Energy Window

Filters out bigger Clusters

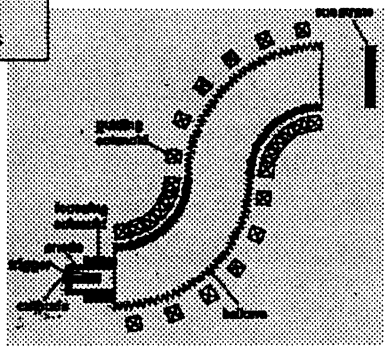

Anders et al., J. Appl. Phys. (1993)

Seagate
INFORMATION, THE WAY YOU WANT IT

UV Raman and sp^3 Content

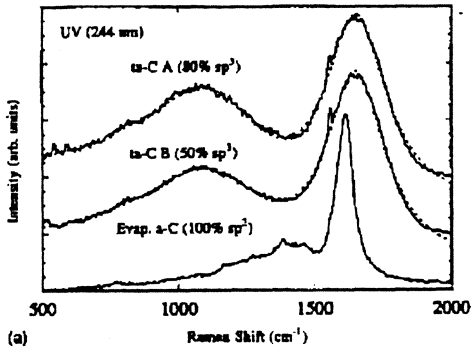

Gilkes et al., Appl. Phys. Lett. (1997)

Bruno Marchon
IIST Dec 16, 1997

Seagate
INFORMATION, THE WAY YOU WANT IT

Raman for Thin Carbon

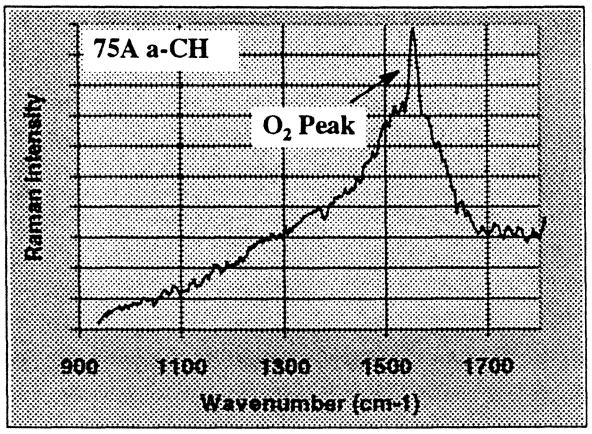

Nitrogen-Doped Carbon: Why does it work ?

- Higher sp^3 Content ?
- Harder (Carbon Nitride ?)
- Lower Stress ?
- Better Affinity for Lubricant ?
- All of the Above ?

Bruno Marchon
IIST Dec 16, 1997

a-CN Characterization (ESCA)

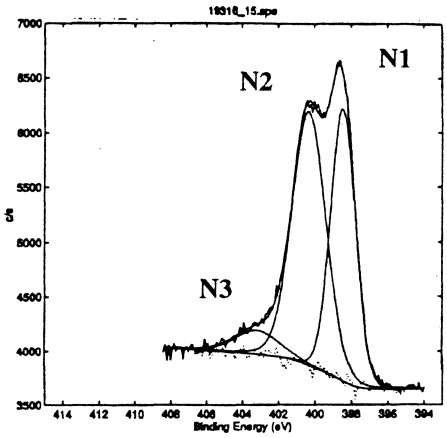

N1: Nitrile (sp)
N2: Amine (sp3)
N3: Aromatic (sp2)

Seagate
INFORMATION, THE WAY YOU WANT IT

a-CN Characterization (ESCA)

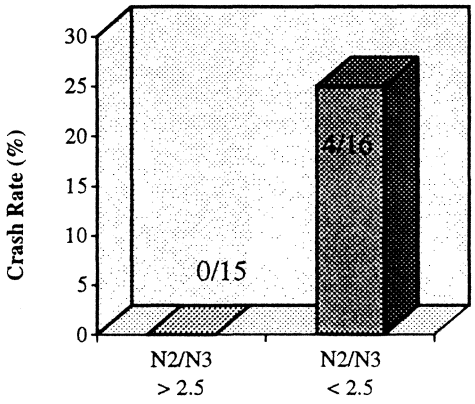

Seagate
INFORMATION, THE WAY YOU WANT IT

Carbon Surface Chemistry

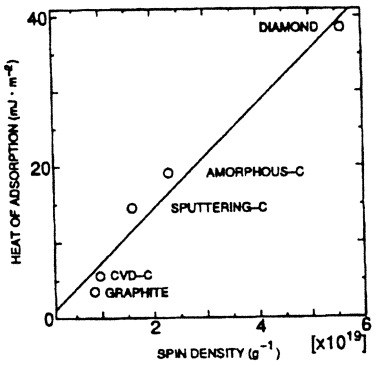

Fig. 4—Relation between heat of adsorption for PFPE diol and dangling bond density of carbon.

Yanagisawa
J. Tribol. (1994)

Carbon Surface Chemistry

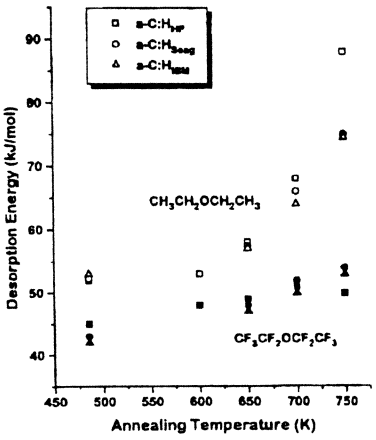

Cornaglia et al.,
J. Vac. Sci. Technol
(1997)

Bruno Marchon
IIST Dec 16, 1997

Zdol Diffusion on a-C

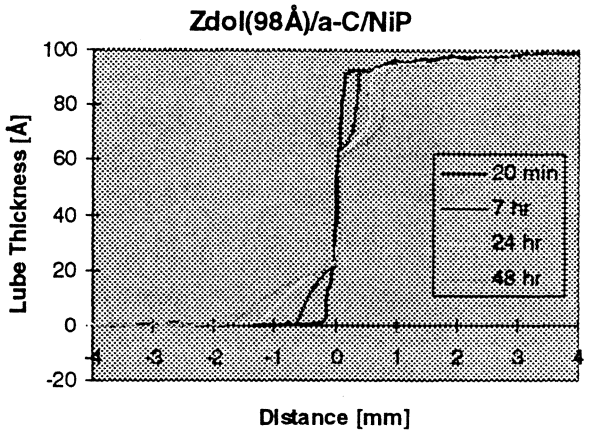

Bruno Marchon
IIST Dec 16, 1997

Seagate
INFORMATION, THE WAY YOU WANT IT

Zdol Diffusion on a-C

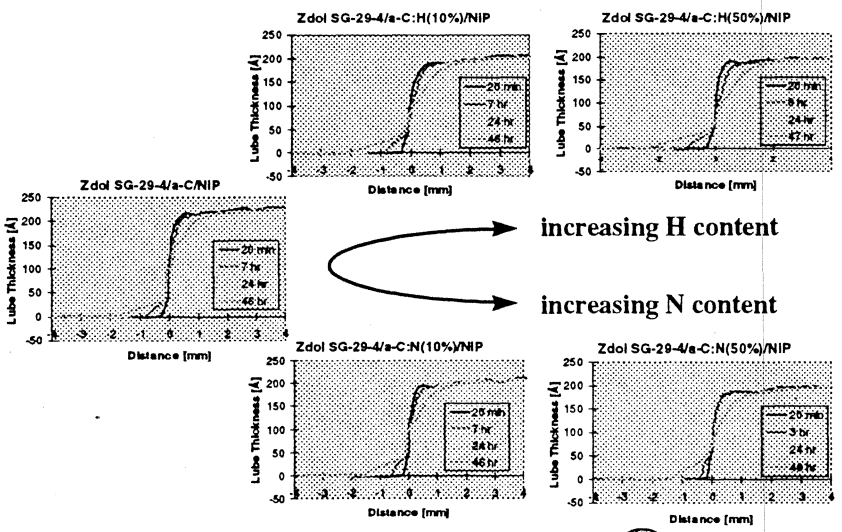

Bruno Marchon
IIST Dec 16, 1997

Seagate
INFORMATION, THE WAY YOU WANT IT

Zdol Diffusion on a-C

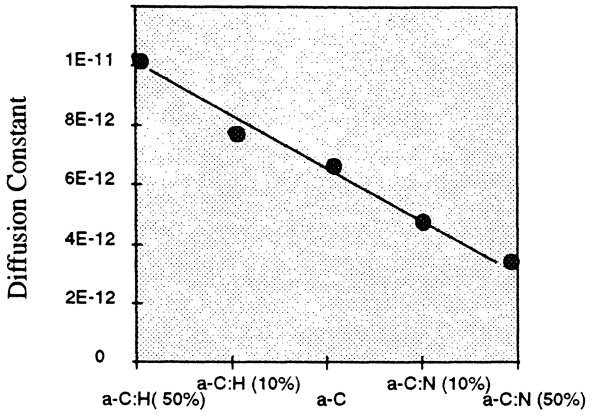

Seagate
INFORMATION, THE WAY YOU WANT IT

Zdol Diffusion on a-C: OSA

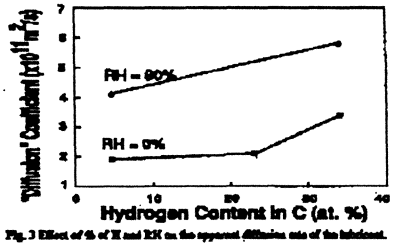

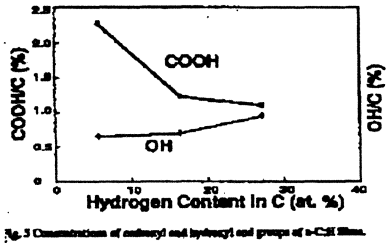

Wang et al., IEEE Trans. Magn., (1996)

Seagate
INFORMATION, THE WAY YOU WANT IT

Conclusion

			Understanding
Process	→	Structure	Fair
Characterization	→	Structure	Fair
Characterization	→	Properties	Good
Properties	→	Performance	Poor
Structure	→	Properties	Very Poor

Acknowledgments

Jing Gui
Kevin Grannen
Laura Smoliar
Gunther Barth
Gary Rauch

Joel Ager (LBL)
Simone Anders (LBL)
Miquel Salmeron (LBL)
John Robertson (Cambridge)
David Brown (Diamonex)
Andy Gellman (CMU)
Xiaoding Ma (CMU)

Bruno Marchon
IIST Dec 16, 1997

A Practitioner's Guide to Media Noise and Signal-to-Noise Analysis

Giora J. Tarnopolsky
Recording Technology Department
Seagate San Jose Design Center

IIST - Santa Clara University
December 15-16 1997

Outline

Outline

- **Overview of media noise phenomena**
  - **Origin**
  - **Localization**
  - **Parametric dependencies**
  - **Models**
- **Noise power & signal power**
  - **Estimate**
  - **Noise budget**
  - **Experimental verification**
- **SNR at high recording densities. Jitter limits.**

Seagate Recording Technology - San Jose

Medium Noise Partial Bibliography

- **There is a vast literature of media noise research. A limited sample of references follows:**
- Introduction to the Theory of Random Signals and Noise, W. B. Davenport & W. L. Root, IEEE Press (1987)
- Noise in Digital Magnetic Recording, T. C. Arnoldussen & L. L. Nunnelley, Editors (1992)
- Theory of Magnetic Recording, H. Neal Bertram (1994)
- Spatial Structure of Media Noise in Film Disks, E. J. Yarmchuck, IEEE Trans. Mag. vol. 22, 877 (1986)
- Noise Autocorrelation in High Density Recording on Metal Disks, Yaw-Shing Tang, IEEE Trans. Mag. vol. 22, 883 (1986)
- Recording and Transition Noise Simulations in Thin-Film Media, J.-G. Zhu & H. Neal Bertram, IEEE Trans. Mag. vol. 24, 2706 (1988)
- Magnetization Fluctuations in Uniformly Magnetized Thin-Film Recording Media, T. J. Silva & H. Neal Bertram, IEEE Trans. Mag. vol. 26, 3129 (1990)
- Magnetization Fluctuations and Characteristic Lengths for Sputtered CoP/Cr Thin Film Media, Giora J. Tarnopolsky, N. Neal Bertram and L. Tran, J. Appl. Phys. vol. 69, 4730 (1991)
- Magnetization Correlations and Noise in Thin Film Recording Media , H. N. Bertram & R. Arias, J. Appl. Phys. vol. 71, 3449 (1992)
- Fundamental Magnetization Processes in Thin-Film.Recording Media, H. Neal Bertram & J.-G. Zhu, in Solid State Physics Review, vol. 46,Academic Press (19992)

Seagate Recording Technology - San Jose

Medium Noise Partial Bibliography (cont')

- Noise of Interacting Transitions in Thin-Film Recording Media, J.-G. Zhu, IEEE Trans. Mag. vol. 27, 5040 (1992)
- Experimental Studies of Noise Autocorrelation in Thin Film Media, G. Herbert Lin & H. Neal Bertram, IEEE Trans. Mag. vol. 29, 3697 (1993)
- General Analysis of Noise in Recorded Transitions, H. Neal Bertram & Xiaodong Che, IEEE Trans. Mag vol. 29, 201 (1993)
- Transition Noise Analysis of Thin-Film Magnetic Recording Media , B. Slutsky & H. Neal Bertram, IEEE Trans. Mag. vol. 30, 2808 (1994)
- Transition Noise Spectral Measurements in Thin Film Media, G. Herbert Lin & H. Neal Bertram, IEEE Trans. Mag. vol. 30, 3987 (1994)
- Microtrack Model of Recorded Transitions, J. Carroselli & J. K. Wolf, IEEE Trans. Mag. vol. 32, 3917 (1996)
- Media Noise and Signal-to-Noise Ratio Estimates for High Areal Density Recording, Giora J. Tarnopolsky & P. R. Pitts, J. Appl. Phys. vol. 81, 4837 (1997)

Seagate Recording Technology - San Jose

What is Medium Noise?

- The reproduce voltage results from the read head sensing the "magnetic charge" of the media: $-\nabla \cdot M(x)$, the divergence of the magnetization
- The medium is an array of columnar magnetic grains having: irregular boundaries, dispersion in the direction of the uniaxial anisotropy axis, intergranular exchange and magnetostatic coupling, and coercivity and remanence that vary from grain to grain.
- Superimposed onto the intended magnetization magnetization reversals (user data) there appear the magnetization spatial fluctuations. They result in unwanted and unpredictable deviations of the reproduce voltage from ideal response.
- Bit position need not match grain boundaries.

Seagate Recording Technology - San Jose

Idealized View of Transitions & Noise

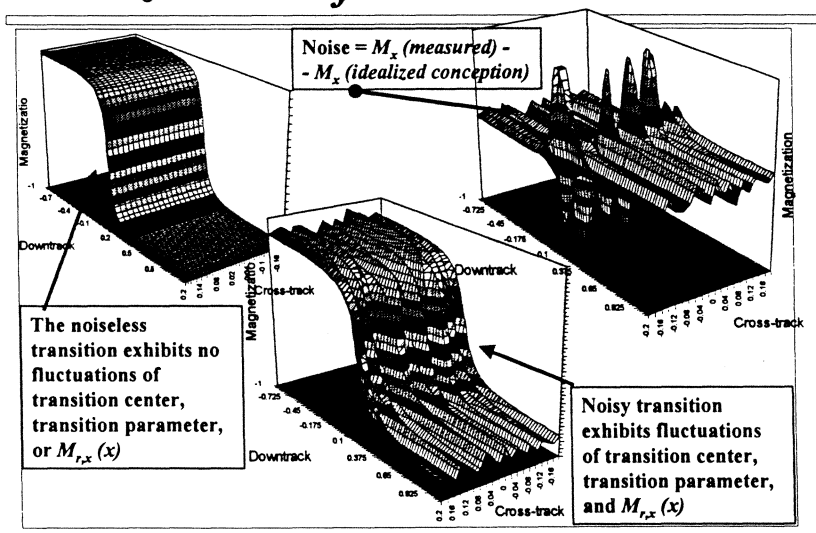

Seagate Recording Technology - San Jose

Signal & Noise Power vs. Read Width

- **The recorded "noiseless" signal is in phase across the track. Its power is proportional to the square of the track width.**

$$\text{Signal Power} = \left[\sum_{i=1}^{N} V_i(x)\right]^2 = N^2 V^2_{(\mu\text{track})}(x) = \left(\frac{\text{Read width}}{\Delta z}\right)^2 \cdot V^2_{(\mu\text{track})}(x)$$

- **The noise components are incoherent. The noise power is proportional to the track width.**

$$\text{Noise Power} = \left[\sum_{i=1}^{N} \delta V_i(x)\right] \cdot \left[\sum_{j=1}^{N} \delta V_j(x)\right] = \sum_{i=j}^{N} \delta V_i(x)\delta V_j(x) + \sum_{i \neq j}^{N} \delta V_i(x)\delta V_j(x) =$$

$$= N < \delta V^2(x) > = \left(\frac{\text{Read width}}{\Delta z}\right) \cdot < \delta V^2(x) >$$

- **Signal-to-noise power ratio ∝ Read width**

Seagate Recording Technology - San Jose

Medium Noise Characteristics

- **Medium noise appears most prominently in regions where $M(x) \approx 0$**
  - **at the magnetic transition - hence "transition noise"**
  - **at the track edge**
  - **in the servo fields**
- **Once recorded, the noisy magnetization pattern does not change with time. It is read out by the magnetic channel just as the data is. Thus, the noise spectrum shows, in a spectrum analyzer, a shape proportional to the envelope of the fundamental and its harmonics**
- **Equalization enhances high-frequency components (generally, to slim the isolated pulse.) It thus enhances the high frequency component of the medium noise.**

Seagate Recording Technology - San Jose

How is Media Noise Modeled?

- Media strips, microtracks (Arnoldussen, Carroselli & Wolf)
  - Media divided into stripes along the downtrack co-ordinate, each stripe exhibiting fluctuations in transition position and sharpness
  - Micromagnetic models (Bertram and collaborators, Zhu and collaborators)
  - Media volume subdivided into regular hexagonal tiles
  - Anisotropy axis orientation, magnetostatic interactions, inter- and intra-granular exchange interactions
  - Proved that exchange-coupled grains are noisier
- Analytical models of the readback voltage (Bertram and collaborators.) Example will follow.

Seagate Recording Technology - San Jose

Media Noise Higher Where M(x)=0

- Ensemble mean and variance of the transition profiles for planar isotropic longitudinal films for different intergranular exchange coupling, and both 2D and 3D random easy axis orientation. A large variance occurs at the transition center. The exchange-coupled film shows much higher magnetization noise in all cases. Bertram & Zhu, IEEE Trans. Mag. vol. 27, 5043 (© IEEE 1991)
- The transition noise power P_n increases with the number of transitions per unit length, or density.
- The measurement of P_n*(density)* affords a determination of media intrinsic noise parameters.

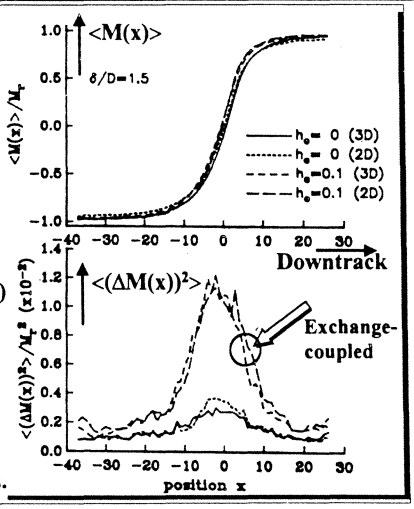

Seagate Recording Technology - San Jose

Media Noise Reduction

How to reduce media noise?

- **Achieve grains of uniform size. The reduction of the variance of columnar sizes will improve media performance, and is of more immediate concern than media thermal decay.**
  - **Underlayers: Epitaxial growth**
  - **Clean sputtering systems**
- **Reduce exchange coupling between grains**
  - **Non-magnetic material segregation to boundary**
- **Reduce the volume where noise originates**
  - **Shorter transition length**
  - **Lower $M_r\delta$**
  - **Higher H_c**

Seagate Recording Technology - San Jose

Media Noise & High-Density Recording

- **"Transition jitter", σ_{jitter} = 3 to 10 nm**
- **For linear recording densities ≤ 1,000 kfci:**
  - **σ_{jitter} for given signal-to-noise ratio *SNR*?**
  - **(σ_{jitter} /bit length *B*) vs. *PW50*, *SNR*, and density?**
  - **Grain sizes and uniformity for n × 10 Gbit/in^2?**
- **Recorded bit boundary: shifted from ideal position**
- **Pulse width (*PW50*): fluctuates around track**
- **Peak amplitude V_0: varies bit-to-bit due to head**

Seagate Recording Technology - San Jose

Transition Jitter: Magnetization Noise

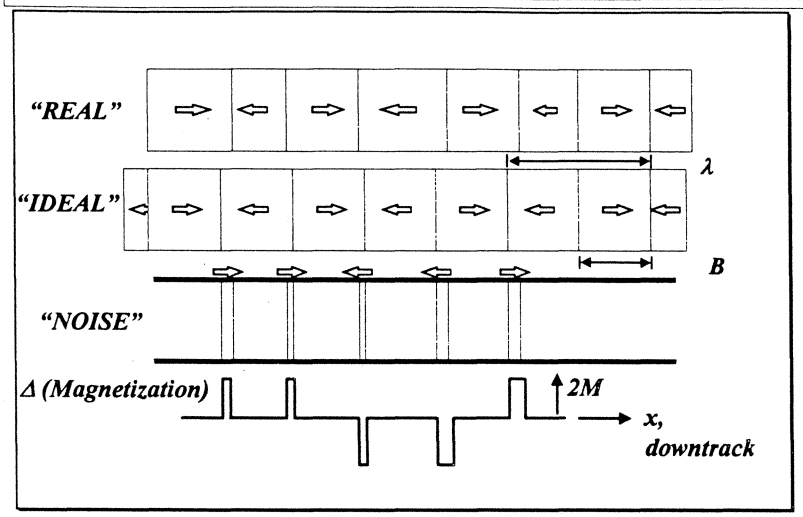

Seagate Recording Technology - San Jose

"Real" & Ideal Waveforms & Noise

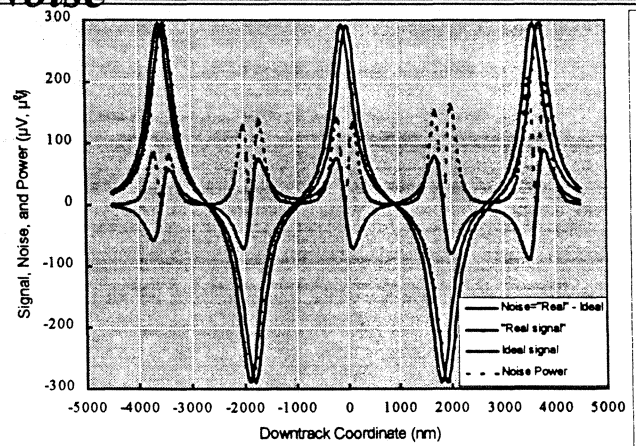

Chart shows i) an ideal noiseless trace, ii) a trace affected by transition jitter (shifted from nominal), iii) the difference between real and ideal voltages - and iv) the

Seagate Recording Technology - San Jose

"Real" & Ideal Waveforms & Noise

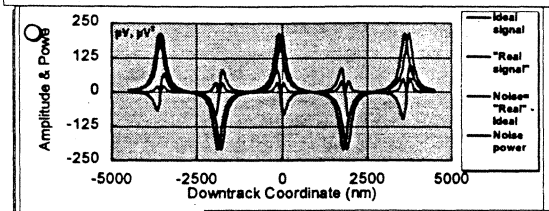

"Jitter:" pulse center shifted from ideal position

"PW50:" pulse width broadening or slimming from ideal (a_x fluctuations)

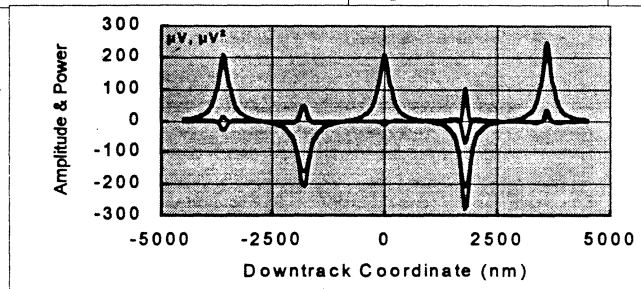

Seagate Recording Technology - San Jose

Replay Voltage

- **Replay noiseless voltage**

$$\tilde{V}(x) = \sum_{n=-\infty}^{n=\infty} (-1)^n V_{iso}(x - nB)$$

•Bertram & collaborators, 1987 - 1996, Noise formalism

•See: Bertram: Theory of Magnetic Recording

- **Add, say, transition jitter δx_n**

$$V(x) = \Sigma_{n=-\infty}^{n=\infty} (-1)^n V_{iso}(x - nB - \delta x_n),$$

$$\therefore V(x) = \tilde{V}(x) + \Sigma(-1)^n \delta x_n \frac{\partial V_{iso}(x - nB)}{\partial x}$$

- **Signal = noiseless voltage + *one term per fluctuating property***
- **Assume Lorentzian pulses, compute noise power**

Seagate Recording Technology - San Jose

Noise Power Density

$$V_{iso}(x) = \frac{2A}{\pi PW50}\left(1\Big/1+\left(\frac{2x}{PW50}\right)^2\right) = V_0\left(1\Big/1+\left(\frac{2x}{PW50}\right)^2\right)$$

Lorentzian
A = area, V_0 amplitude

- **Consider position fluctuations, pulse-width fluctuations, and MR head amplitude fluctuations:**

  σ_{jitter} σ_{PW50} σ_{V_0}

- **Noise power density at head's terminals:**

$$PSD(k) = \frac{|V_{iso}(k)|^2}{B} \times \left[k^2\sigma_{jitter}^2 + \frac{k^2\sigma_{PW50}^2}{4} + \frac{\sigma_{V_0}^2}{V_0^2}\right]$$

k=2π/λ , FT variable
$V_{iso}(k)$ = FT isolated pulse

Seagate Recording Technology - San Jose

Noise Power

- **Noise power *density* equalized by channel transfer function *G(k)*:**

$$PSD(k) = \frac{|G(k)V_{iso}(k)|^2}{B} \times \left[k^2\sigma_{jitter}^2 + \frac{k^2\sigma_{PW50}^2}{4} + \frac{\sigma_{V_0}^2}{V_0^2}\right]$$

k=2π/λ , FT variable
$V_{iso}(k)$ = FT isolated pulse

- **The broad-band media noise power = integral of *PSD(k)* over all frequencies:**

P_n = broad – band noise power =

$$= \frac{\pi}{2}V_0^2\frac{\sigma_{jitter}^2}{B \cdot PW50} \times \left(1 + \frac{1}{4}\frac{\sigma_{PW50}^2}{\sigma_{jitter}^2}\right) + \frac{\pi\sigma_{V_0}^2 PW50}{4B}$$

Media jitter scaled by bit length and PW50

Seagate Recording Technology - San Jose

Transition Noise vs. Density: Many Alloys

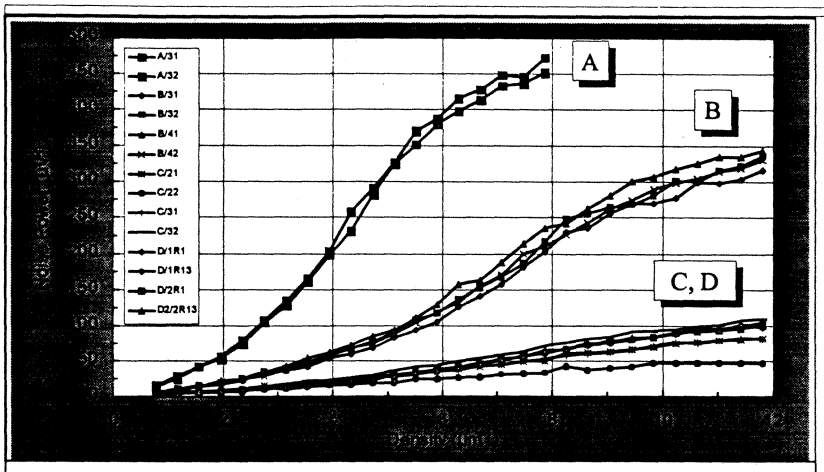

- Get σ_{jitter} from initial slopes.

Slope gives jitter value ⇒ noise budget of system

Slope cuts above & below break point

Seagate Recording Technology - San Jose

Transition Noise vs. Density: Many Alloys

Table I. Experimental Results

Disk	H_c	$M_r\delta$	V_o	PW50	OW	Iw	σ	σ_{low}	σ_{high}	#
	kOe	$\frac{memu}{cm^2}$	μV	nm	dB	mA	nm	nm	nm	
A/31	2.2	1.00	383	378	39	34		8.0	12.5	
A/32	2.2	1.00	382	372	39	34		7.9	12.3	
<A>	**2.2**	**1.00**	**383**	**375**	**39**	**34**		**8.0**	**12.4**	**2**
B/31	2.5	0.70	311	295	41.6	35		5.8	9.3	
B/32	2.5	0.70	309	298		35		6.2	9.6	
B/41	2.5	0.70	305	303		35		6.2	9.9	
B/42	2.5	0.70	300	300		35		6.1	9.7	
<B>	**2.5**	**0.70**	**306**	**299**	**41.6**	**35**		**6.1**	**9.6**	**4**
C/21	2.77	0.68	226	296	36.5	45	5.4			
C/22	2.77	0.68	206	295		45	4.2			
C/31	2.77	0.68	221	294		45	5.7			
C/32	2.77	0.68	239	299		45	6.1			
<C>	**2.77**	**0.68**	**223**	**296**	**36.5**	**45**	**5.4**			**4**
<D>	**3**	**0.55**	**222**	**290**	**39**	**45**		**3.7**	**6.4**	**4**

Seagate Recording Technology - San Jose

SNR Budget: What σ_{eff} For 6 Gbit/in^2?

- 16:1 BPI/TPI Ratio: 310 kbpi x 19.4 ktpi
- Density, HF 329 kfci
- Density, MF 165 kfci
- $V_{0\text{-}p}$ (Iso) 500 μV
- $V_{0\text{-}p}$ (MF) 251 μV
- Radius (ID) 0.627 in
- Bandwidth 49 MHz
- Input noise voltage 0.5 nV/rt Hz
- Input noise current 20 pA/rt Hz
- Resistance 55 Ω
- B = bit length 82 nm
- PW50 ~8.4 μin

- Preamp noise 12.3 μV²
- Current source 59.3 μV²
- Johnson noise, $4k_BT\Delta fR$ 46.6 μV²
- Electronics + Johnson 118.2 μV2
- SNR(E) 27.3 dB
- If 70% of the total noise is due to the media and 30% is due to electronics then σ_{eff} = 3.5 nm and the total SNR = 22 dB.
- The SNR required to achieve an on-track error rate of 10^{-7} is about 21 dB. For this case the media noise component is 382 μV². This leads to an effective jitter of σ_{eff} = 4.1 nm.

Seagate Recording Technology - San Jose

Transition Jitter vs. Read Track Width

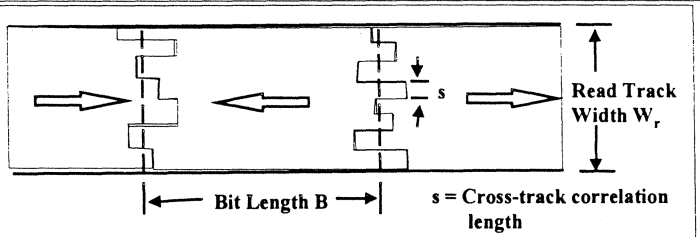

The number of sub-transitions is given by W_r/s. The relation between the net transition position variance and the sub-transition variance is:

$$\sigma^2_{jitter} = \frac{s}{W_r}\sigma^2_s$$ (H.N. Bertram, Theory of Magnetic Recording, p. 317.)

Analytic modeling of the transition noise with a tanh transition shape yields:

$$\sigma_{jitter} \frac{\pi^2 a}{4}\sqrt{\frac{s}{3W_r}}$$ (B. Slutsky and H.N. Bertram, *IEEE Trans. Magn.*, vol. 30, (no. 5), pp. 2808-2817, 1994.)

Eric Champion

S = cross-track correlation length

PRML
w/ HF equalized
out (?)

Seagate Recording Technology - San Jose

SNR Estimate

- **Peak amplitude of linear superposition of Lorentzian pulses**

$$V_{peak}(1/B) = V_0 \times \frac{\pi \cdot \frac{PW50}{2B}}{\sinh\left(\pi \cdot \frac{PW50}{2B}\right)} = V_0 \times \frac{(\pi U/2)}{\sinh(\pi U/2)}$$

U=channel density

Comstock & Williams (1973)

- **SNR = (Peak mid-frequency signal power)/(broad band noise power of high-frequency fundamental)**

$$SNR = \frac{V_{peak}^2(1/2B)}{P_n(1/B)} = \frac{\left(\frac{2B \cdot PW50}{\pi \sigma_{jitter}^2}\right)}{\left[1 + \frac{1}{4}\frac{\sigma_{PW50}^2}{\sigma_{jitter}^2} + \frac{1}{2}\frac{\sigma_{V_n}^2}{V_0^2}\left(\frac{PW50}{\sigma_{jitter}}\right)^2\right]} \times \frac{(\pi U/4)^2}{\sinh^2(\pi U/4)}$$

1T, 1/(2T) hi-freq, "1/(4T)" mid-freq

Could lump all noise sources into σ_n [Spectrum analyzer]

Seagate Recording Technology - San Jose

Resolution of Lorentzian Waveform

- **A rainy afternoon in the complex plane**

$$\frac{1}{2\pi j}\oint_C \frac{\pi}{B}\frac{V_{iso}(x-z;PW50)}{\sin\left(\frac{\pi z}{B}\right)}dz =$$

R. L. Comstock & M. Williams, IEEE Trans. Magn., MAG-9(3), 342 (1973)

Morse & Feshbach, Vol. I, Ch. 4, PP. 378 - 414

$$= \sum_{n=-\infty}^{\infty}(-1)^n V_{iso}(x-nB;PW50) + \left\{\begin{array}{l}\text{residues of} \\ V_{iso}(x-z;PW50) \\ \text{at } z = x \mp j\left(\frac{PW50}{2}\right)\end{array}\right\} = 0$$

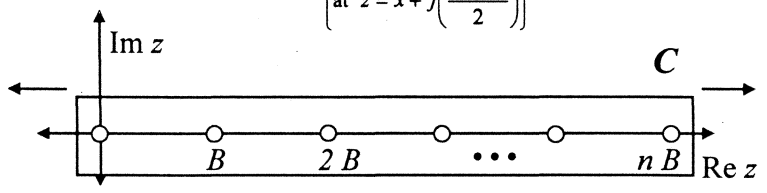

Seagate Recording Technology - San Jose

TAA Formula vs. Experiment

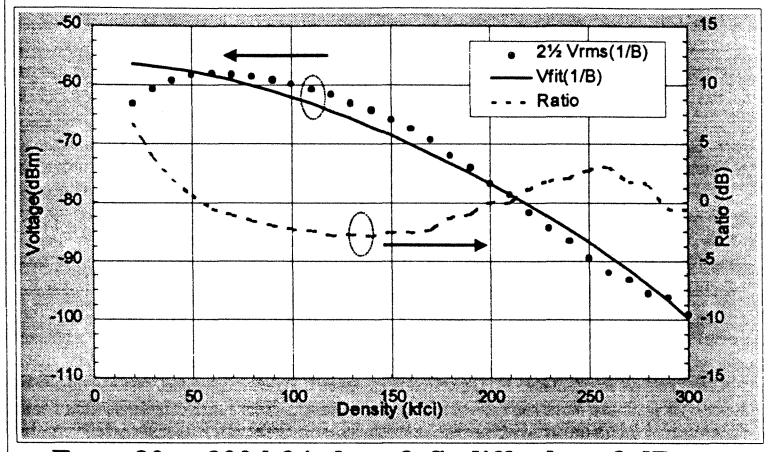

- From 30 to 300 kfci, data & fit differ by < 3 dB

Seagate Recording Technology - San Jose

SNR Estimate

- *SNR* = (Peak *mid-frequency* signal power)/(broad band noise power of *high-frequency* fundamental)

1T, 1/(2T) hi-freq, "1/(4T)" mid-freq

$$SNR = \frac{V_{peak}^2(1/2B)}{P_n(1/B)} = \frac{\left(\frac{2B \cdot PW50}{\pi\sigma_{jitter}^2}\right)}{\left[1 + \frac{1}{4}\frac{\sigma_{PW50}^2}{\sigma_{jitter}^2} + \frac{1}{2}\frac{\sigma_{V_0}^2}{V_0^2}\left(\frac{PW50}{\sigma_{jitter}}\right)^2\right]} \times \frac{(\pi U/4)^2}{\sinh^2(\pi U/4)}$$

Could lump all noise sources into σ_n [Spectrum analyzer]

Seagate Recording Technology - San Jose

SNR Estimate (cont...)

- **SNR definition and formula:**

$$SNR = \frac{2B \cdot PW50}{\pi\sigma_n^2} \times \frac{(\pi U/4)^2}{\sinh^2(\pi U/4)}$$

- **Media & head noise < total system noise**
- **Use P_n = fraction α of total noise P_{system} , $\alpha = 3/4 < 1$**

$$SNR_{sys} = \alpha \frac{2B \cdot PW50}{\pi\sigma_n^2} \times \frac{(\pi U/4)^2}{\sinh^2(\pi U/4)}$$

- **For U = 2.5, $\sigma_{PW50} = \sigma_{jitter}/4$, $\sigma_{V0} = 0$,**

$$SNR_{sys}(U = 2.5) \cong 0.5\alpha\left(B/\sigma_{jitter}\right)^2$$

At constant channel density, ratio (σ_{jitter}/bit length) is function of *SNR* alone

Seagate Recording Technology - San Jose

Ratio Transition Jitter/Bit Length vs. SNR_{sys}

- **If the head gap scales with density, U = constant**
- **Jitter/Bit = *f(SNR)* only**
- **To maintain any given SNR, σ_{jitter} must scale with B**

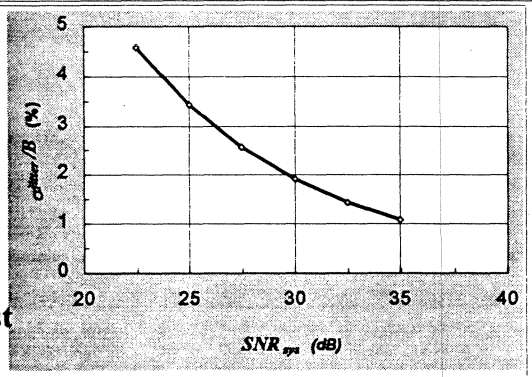

- **Example: 500 kfci, B = 50 nm, PW50 = 125 nm, σ_{jitter} = 1.5 nm @ 26 dB**

Giora J Tarnopolsky © 1997 IIST - Santa Clara University 1997 Magnetic Media Symposium II Seagate THE DATA TECHNOLOGY COMPANY

Seagate Recording Technology - San Jose

Jitter vs. Density, Various System SNR's

- Media jitter must decrease for SNR = constant

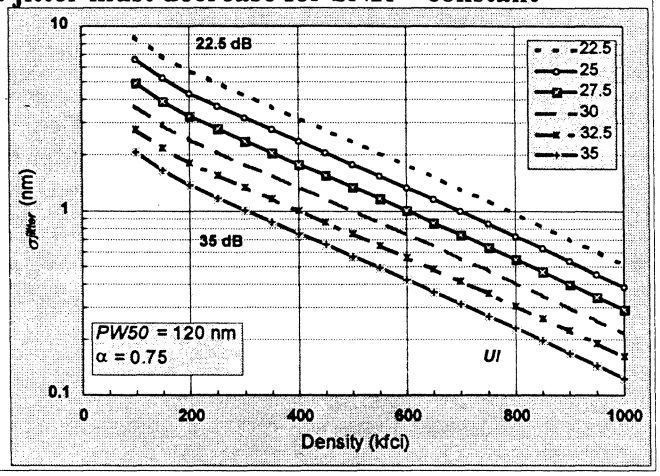

Seagate Recording Technology - San Jose

System SNR, Various Media Jitter Values

- At constant media jitter, SNR decreases

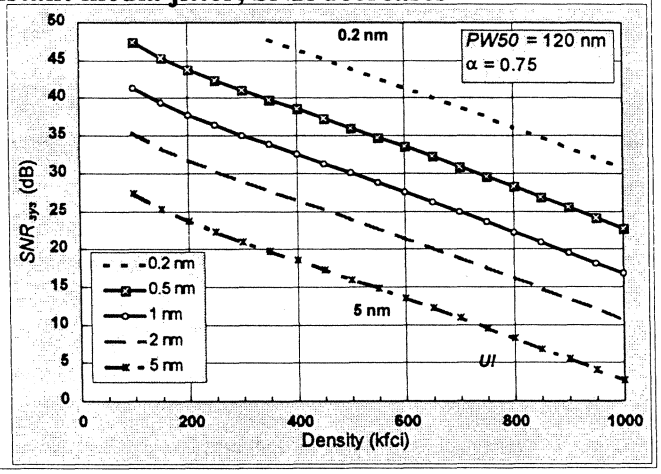

Seagate Recording Technology - San Jose

Areal Density Estimators

- H. Neal Bertram has postulated an expression for media jitter,

$$\sigma^2_{jitter} = \left(\frac{\pi}{2}\right)^4 a_x^2 \frac{s}{3(RW)}$$

Cross track correlation length

B. Slutsky & H. N. Bertram, IEEE Trans. Mag. vol. 30, 2808 (1994)

which allows to link the SNR values derived here to properties of the media (a_x) and of the recording system (RW).

a_x = transition parameter
s = cross-track correlation length
RW = head's read width

Seagate Recording Technology - San Jose

Outline

Outline

- Overview of media noise phenomena
  - Origin
  - Localization
  - Parametric dependencies
  - Models
- Noise power & signal power
  - Estimate
  - Noise budget
  - Experimental verification
- SNR at high recording densities. Jitter limits.

Media Noise & SNR for High Density Recording

- Expressions for:
  - Noise Power Spectral Density
  - Total Noise Power
  - SNR(mid-freq/broad band HF noise)
- For constant channel density, ratio (jitter/bit length) depends only on SNR, not on density

$$SNR_{sys}(U = 2.5) \cong 0.5\alpha\left(B/\sigma_{jitter}\right)^2$$

  - $\sigma_{jitter} / B = 3\%$ @ 26 dB SNR, 1.5 nm for 500 kfci
- At 1000 kfci, transition jitter < 1 nm. Difficult to accomplish. Thermal & coercivity issues.

S. Charap et al., TMRC '96

Conclusions

- Media noise power unambiguous index of media performance. As a function of commonly measured properties,

$$P_n = \text{broad-band media noise power} = \frac{\pi}{2} V_0^2 \frac{\sigma^2_{effective}}{B \cdot PW50} \propto$$

$$\propto [M_r\delta \;\&\; \text{head effiency}]^2 \frac{(\text{effective jitter})^2}{\text{magnetic bit length } x\; PW50}$$

- Signal-to-noise ratio

$$SNR_{sys} = \alpha \frac{2B \cdot PW50}{\pi\sigma^2_{effective}} \times \frac{(\pi U/4)^2}{\sinh^2(\pi U/4)}$$

- Uniform grain size films, grain segregation now more urgent than thermal decay limit mitigation.

Scanning Probe Microscopy of Thin Film Media: Instrumentation and Applications

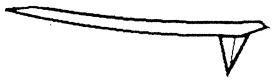

Ken Babcock
Digital Instruments

- SPM basics: AFM and MFM
- Media Applications
- Metrology: Automated Measurement of LZT
- Advanced Topics

di

SPMs for Data Storage

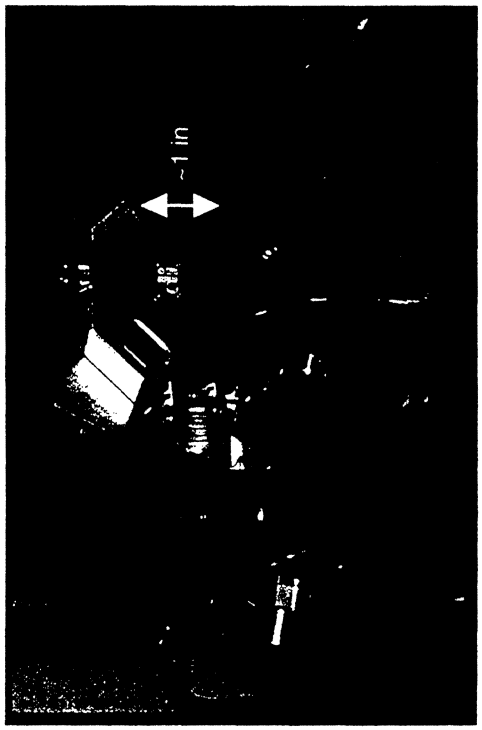

- stage accomodates large samples
- performs AFM and MFM
- integrated optics for easy feature location
- acoustic and vibration isolation
- scan range: 100 µm lateral, 5-10 µm vertical
- optional automation capabilities

TappingMode AFM

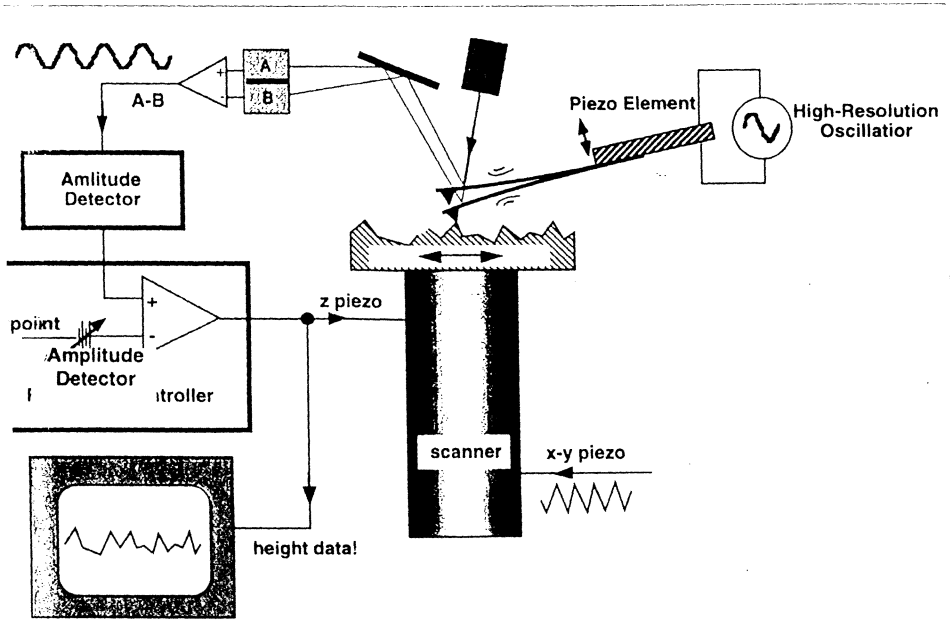

- oscillate cantilever at its resonant frequency with a miniature piezo element

- the tip lightly taps the sample surface, reducing the oscillation amplitude relative to "free air"

- feedback maintains a fixed oscillation amplitude

- typical tip amplitudes 20-100 nm.

SPM Probes

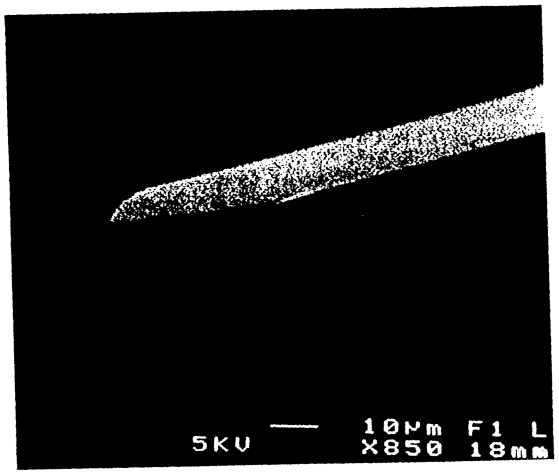

- single-Xtal Si
- end radii ~ 5 nm
- can be magnetically coated for MFM
- used for TappingMode AFM or rapid contact mode AFM
- AC modes: resonant frequencies ~ 100 kHz

Laser Textured Disks

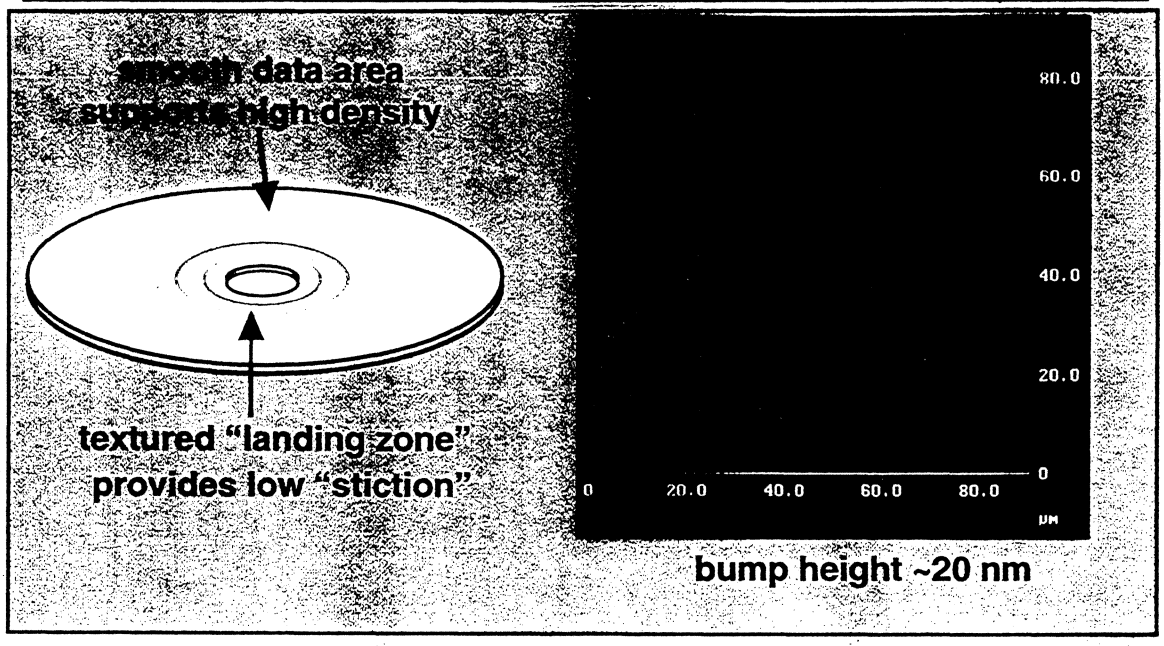

di

Conventional Measurements of LZT: interference microscopes

advantages:

- fast
- repeatable
- automated

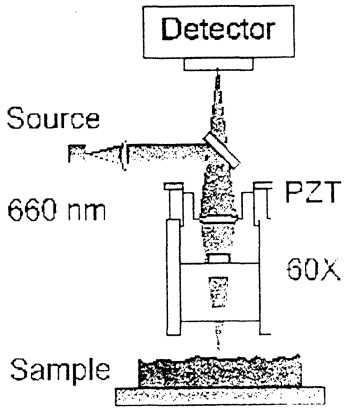

disadvantages:

- insufficient resolution for small features and future small bumps
- cannot measure through overcoats

di

Compare Scanning Probe Microscopes

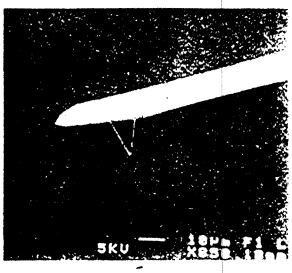

- SPM has ample resolution for measurement of laser texture

- Additional requirements:
  - fast scanning
  - automation
  - dedicated analysis of bump parameters

di

Rapid Scanning with Atomic force Microscopy

using Contact Mode, images of bumps can be acquired
in seconds, with excellent repeatability

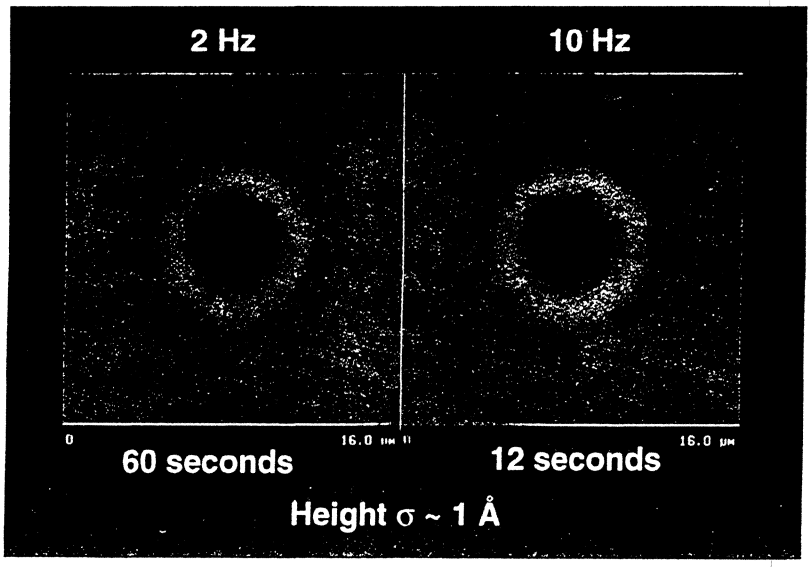

Dedicated Bump Analysis

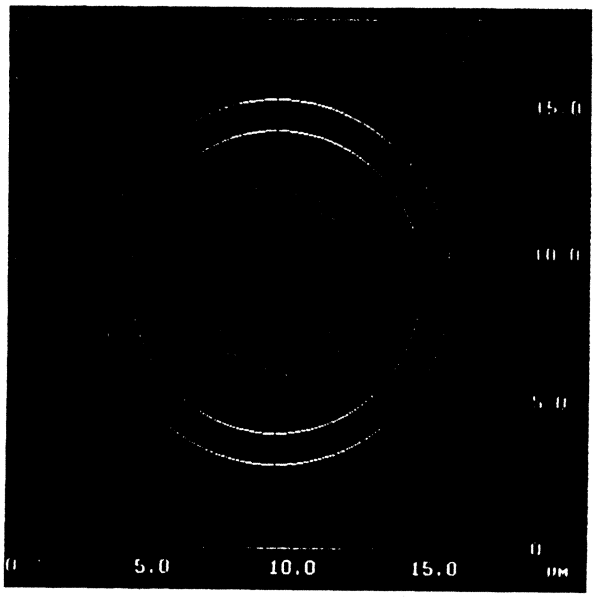

- one-click or automated measurement
- measures bump parameters and "wear" characteristics

Bump Statistics	
Type	Crater
Height	15.125 nm
Height sigma	1.914 nm
Peak height	19.196 nm
Diameter	6.067 µm
Depth	-47.471 nm
Wear height	7.000 nm
Wear area	13.228 µm
Ctr. Mass X Off	13.075 nm
Ctr. Mass Y Off	-306.96 nm

Repeatability: ~1 Å

Automated LZT Measurements I

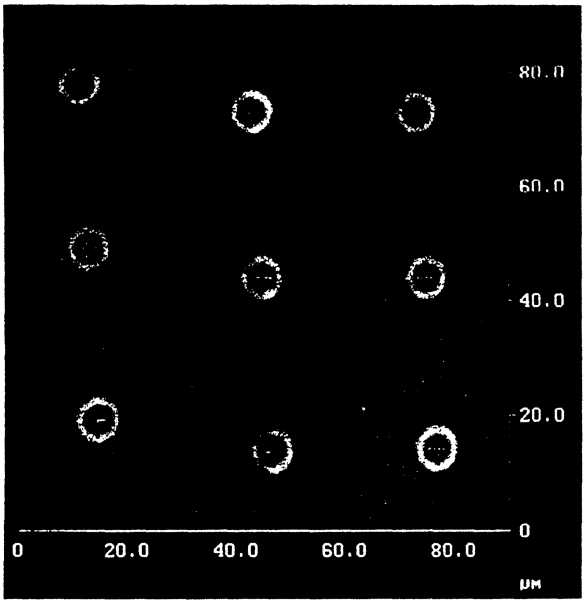

- "push-button" operation
- rapid scanning of bump groups at desired sites
- pattern recognition locates bumps within image
- each bump automatically analyzed

Automated LZT Measurements II

- One click loads disk, scans desired sites, analyzes images, and displays results
- Sites can be input using polar coordinates
- Output is spreadsheet compatible
- Repeatability: <2 Å (group); <1 Å (single bump)
- Accuracy: < 4 Å
- Throughput: ~ 6 seconds/bump (disks with 20 μm bump spacing)
- AFM resolution "sees" sub-100 nm details; can analyze bumps < 1 μm: *resolution for the future*
- AFM not affected by overcoats or rouhgness variations
- Available as Dimension LZT3100 and Dimension LZT5000

MFM Probes

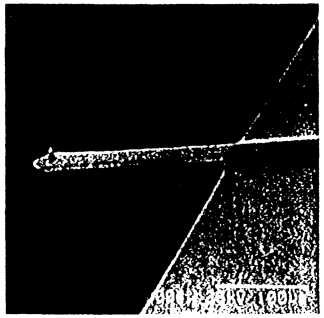

batch-fabricated silicon
(NanoProbe)

$f_0 = 80$ kHz

$Q = 203 \pm 33$ (air)

Magnetic Thin-Films Sputter Coated
Advanced Research Corporation
CoCr: "Hard" or NiFe: "Soft"
Magnetize in $\hat{z}$ or $\hat{x}$.
(this work)

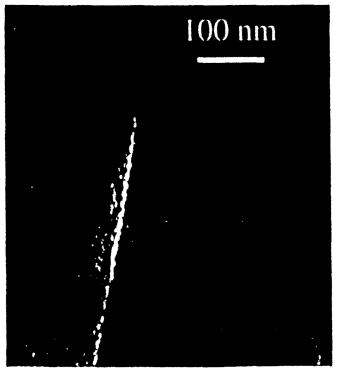

F.I.B. Milled

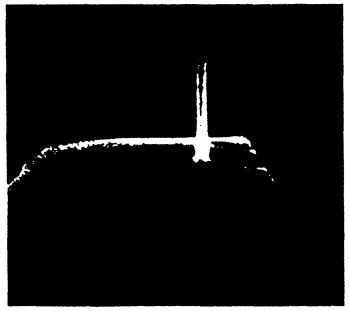

MFM = Scanning Probe Microscopy with a Magnetized Tip

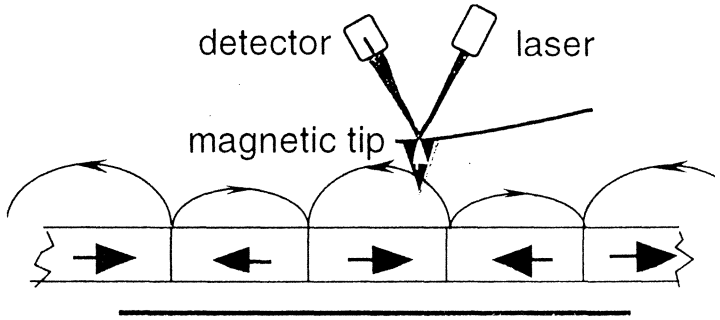

$$\vec{F}_{tip} = \int_{tip} \vec{\nabla}\left(\vec{m}\cdot\vec{H}\right) d^3r$$

simplify:

$$F_z \cong m_x \frac{\partial H_x}{\partial z} + m_y \frac{\partial H_y}{\partial z} + m_z \frac{\partial H_z}{\partial z}$$

ex) Hard Disk

1 m features, M_r=500 emu/cc $\Rightarrow$ $\frac{\partial H_z}{\partial z} \approx 10^7\ Oe/cm$

k = 1 N/m, $m_{tip}=10^{-11}$ emu $\Rightarrow$ $\Delta z \approx 1$ nm

MFM Image Interpretation I: Hard Disk Model

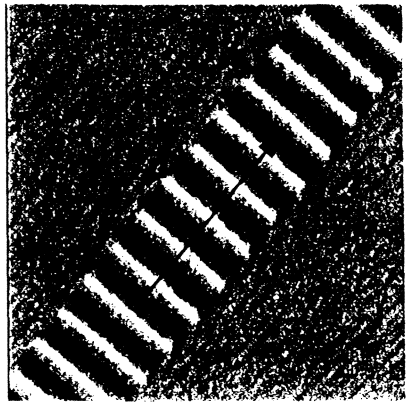

25 μm

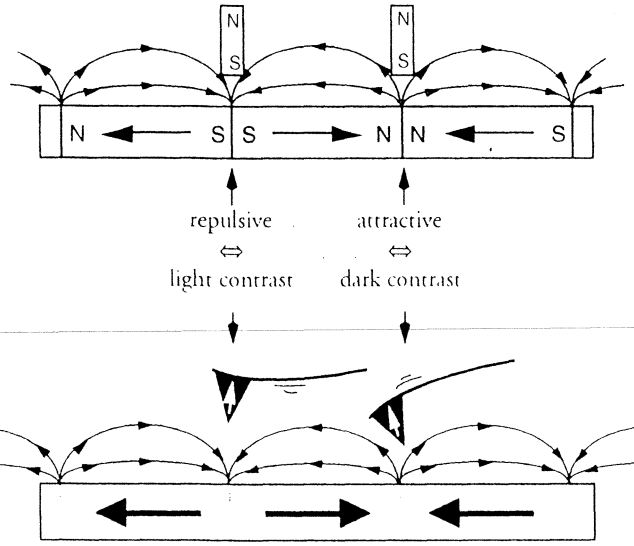

MFM Techniques

LiftMode: scanline-by-scanline:

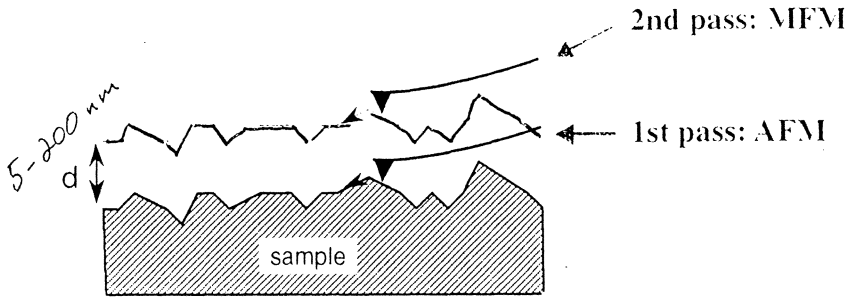

Topography

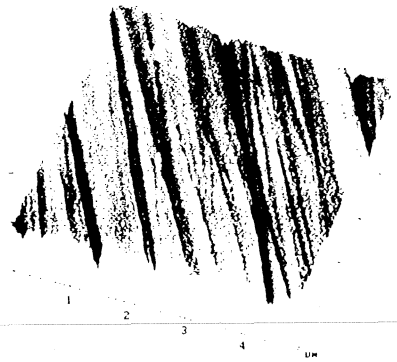

Magnetic Force Gradient

resolution < 50 nm

- actually sees flux gradient rather than force

- **separate AFM/MFM data**
- **fast, flexible**
- **d→0: resolution is probe-limited**

Track Characteristics

This MFM image shows the results of an overwrite test: two "data tracks" were written side-by-side, then a lower-frequency "all-1's" track was overwritten, down the center. Such images allow immediate meaurements of track characteristics such as track width, skew, erase-band width, and transition fringing and other irregularities caused by head defects,

- Demagnetized -

Topography (Tapping Mode)

Hard Disk Magnetic Force Gradient

XYDMAFM Images

clusters

Hard Disk: Texture and Domain Structure

Defects and Failure Analysis

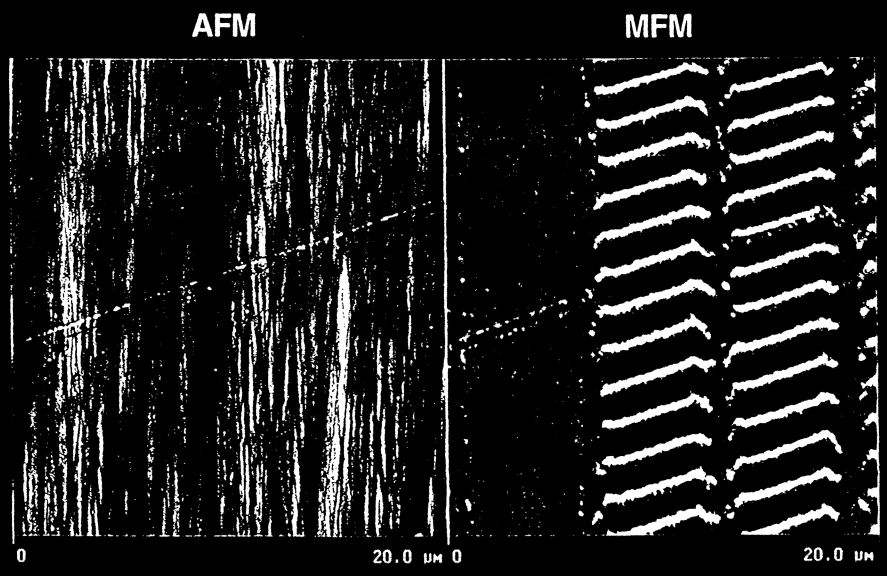

Servo Patterns

MFM gives direct visualization of servo performance by showing transition and track alignment in servo "All-1's" and "burst" patterns.

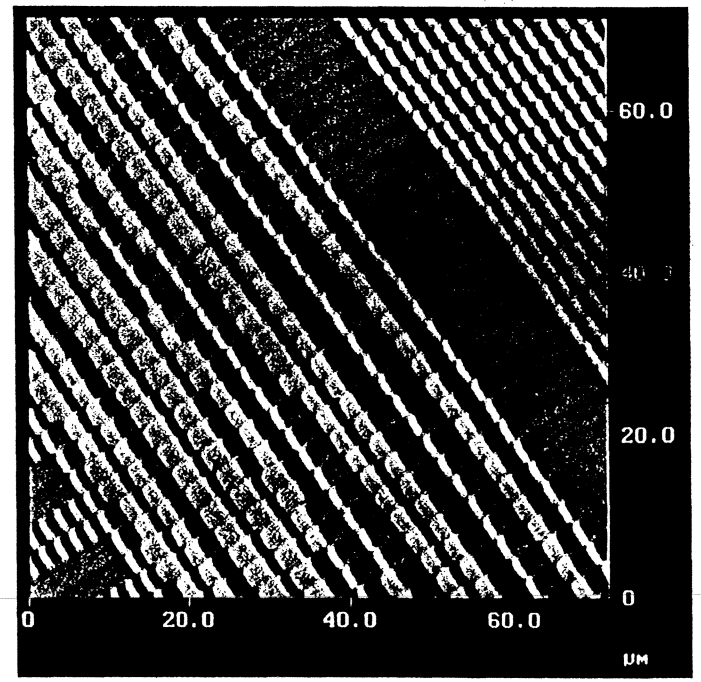

Media Development

NTT : Y. Maeda, T. Ichihara

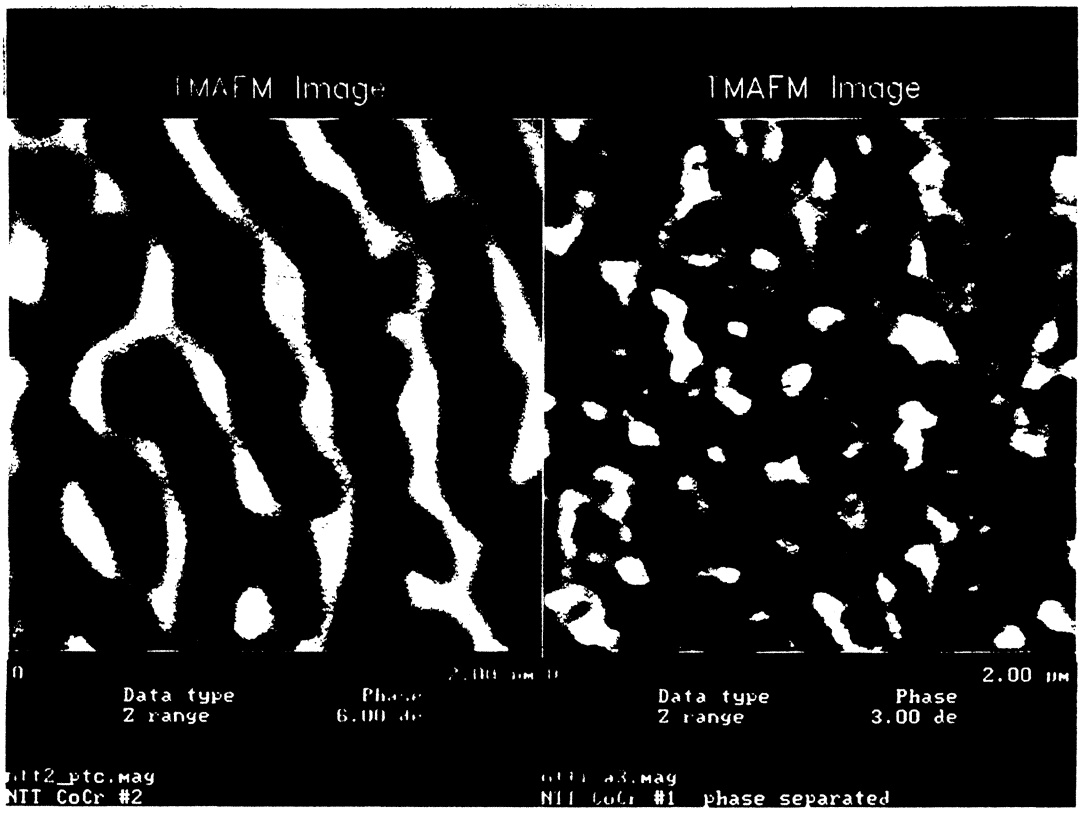

Co-Cr media

Perpendicular Media (MO)

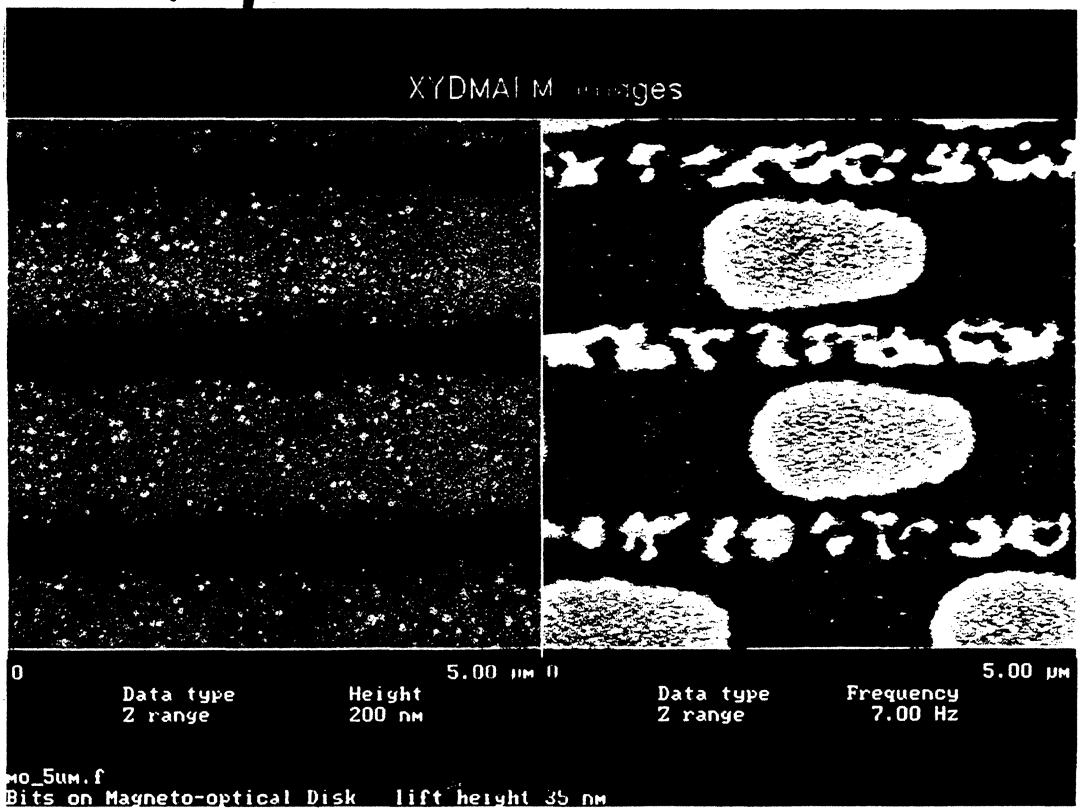

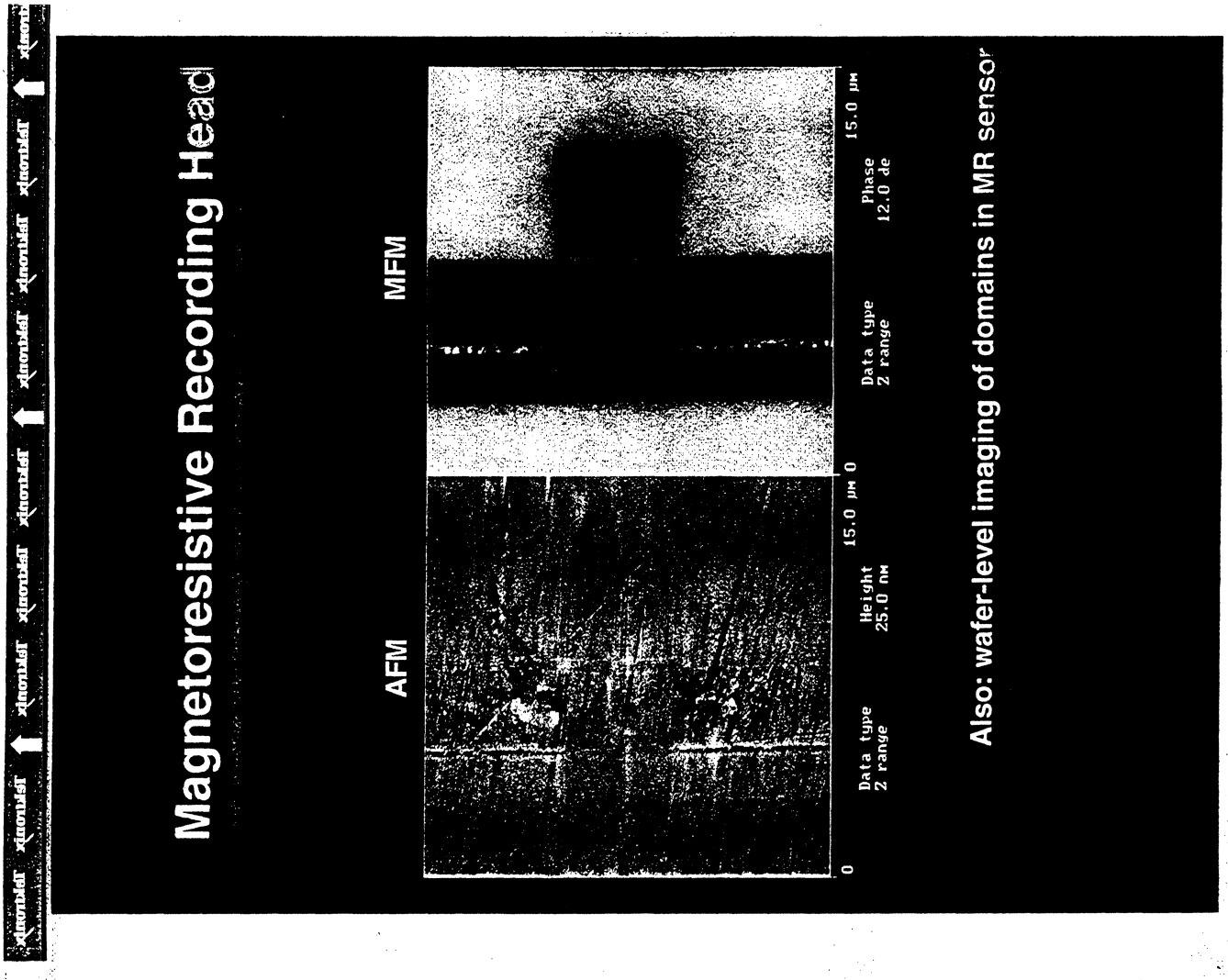

MR Sensor + Bias Elements

Topography

Magnetic Force Gradient

RSTMAFM Images

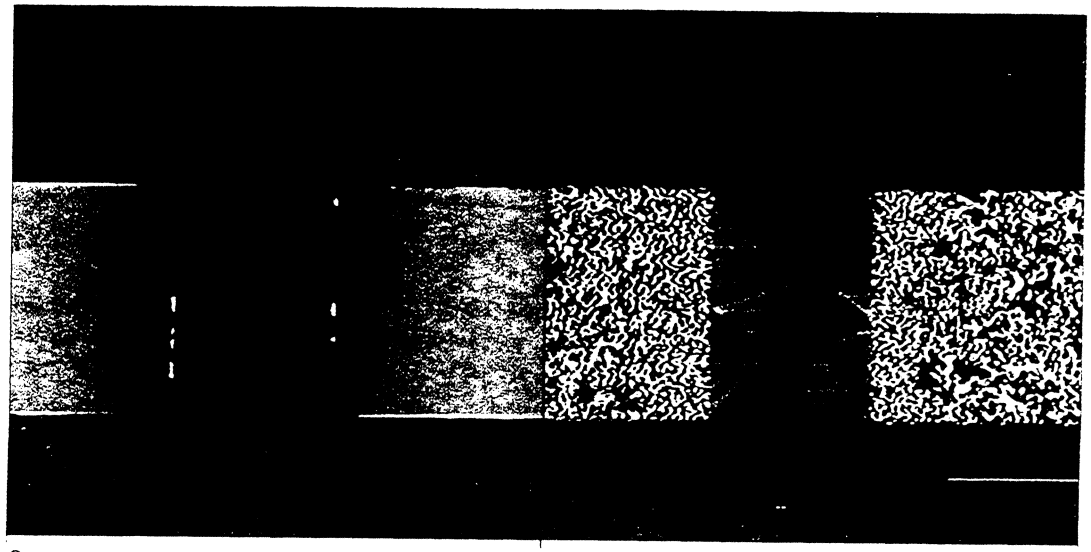

rdbqka38.qd1
Domain Structure by Frequency Modulation

Dr. Allan Schultz, Seagate Tech.

Use: write fringing fields

Mel Gomez and Ed Burke
University of Maryland
– MFM in Applied Fields –

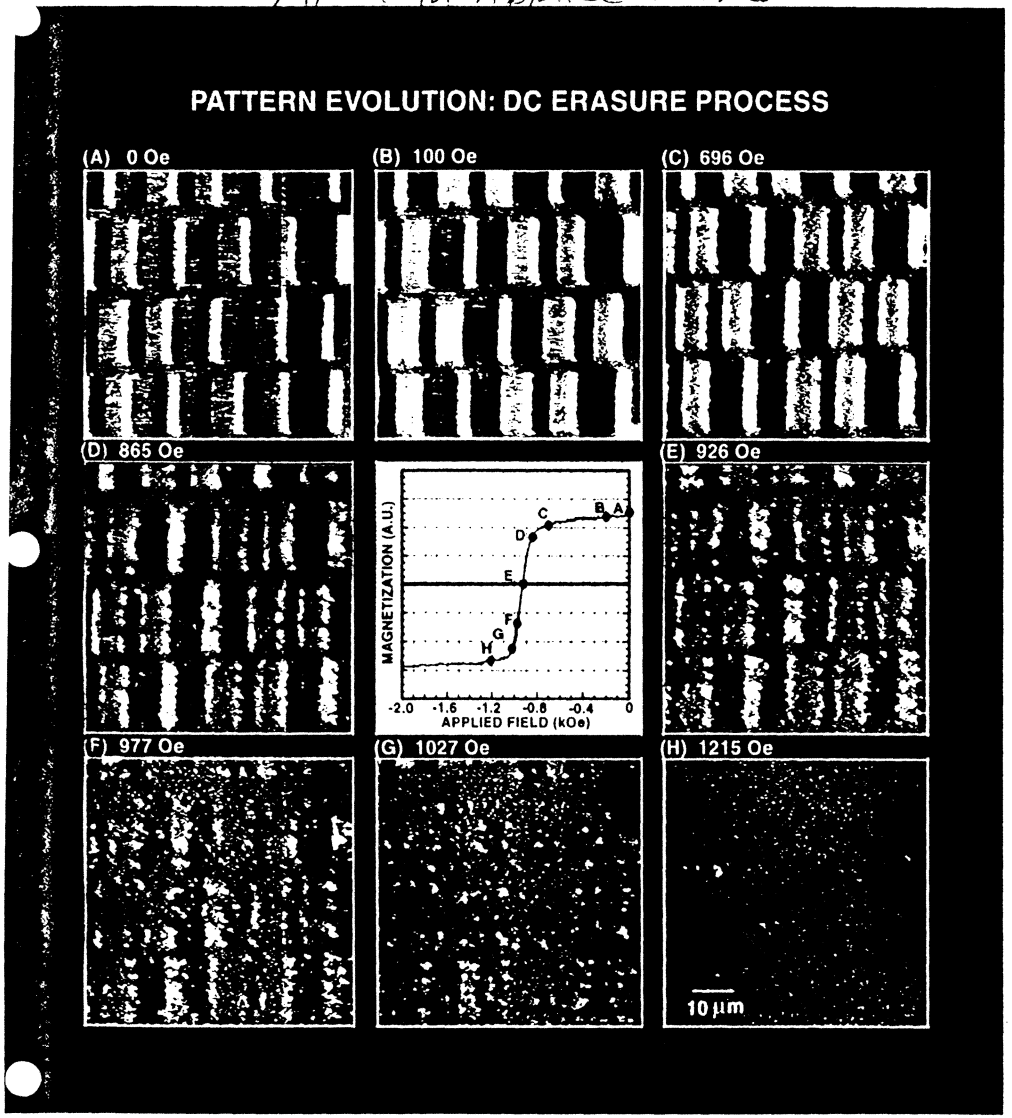

MFM of write gap

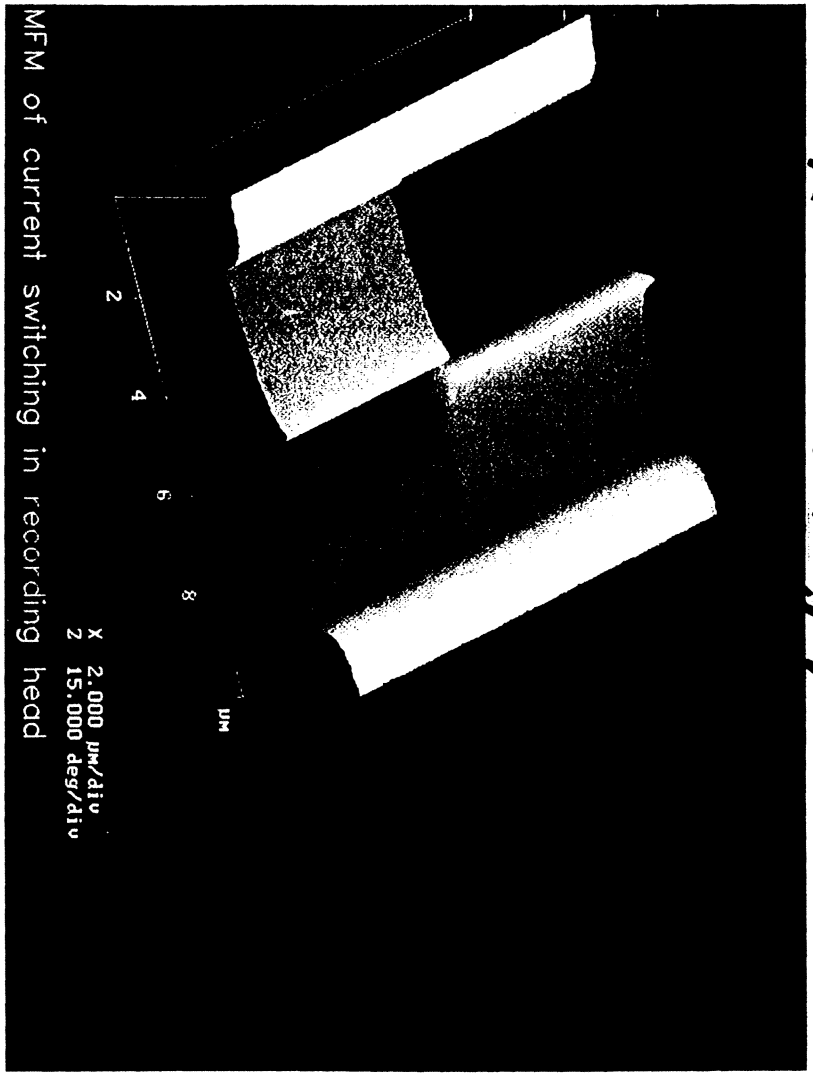

Other MFM Applications

- **dc Track Interactions at Close Spacing**, *E. Glavinas et al, IEEE Trans. Magn., 1996*
- **Spatial Correlation Between MFM Images and Recording Head Output**, *P. Rice and J.R. Hoinville, IEE Trans. Magn. 1996.*
- **MFM Studies of Recording Phenomena in High Density Longitudinal Recordings**, *P. Glijer etal, IEEE Trans. Magn. 1996*
- **MFM Observation of Track-Edge Over-write Pattern in a CoCrTa/Cr AnisotropicMedium**, *X.B. Yang et al, J. Phys. D., 1995*
- **MFM Study of Submicron Track Width Recording in Thin-Film Media**, *Y. Luo et al, J. Appl. Phys., 1996*
- **MFM Images of Ultra-high Density Bit Patterns Recorded on High-Coercivity Longitudinal and Perpendicular Thin-Film Media**, *X. Song et al, J. Appl. Phys., 1996*
- **Recording Study of Isotropic vs. Anisotropic Media with MR Head,** *E.M.T. Velu et al, IEEE Trans. Magn., 1997.*
- **Quantitative MFM Study on Percolation Mechanisms of Longitudinal Magnetic Recording**, *E. T. Yen et al, IEEE Trans. Magn., 1997.*
- **Effect of Track edge Erasure and On-Track Percolation on Mdeia Noise at HighR ecording Density in Longitudinal Thin Film Media**, *S.S. Malhotra et al, IEEE Trans. Magn., 1997.*

di

Pole Tip Recession

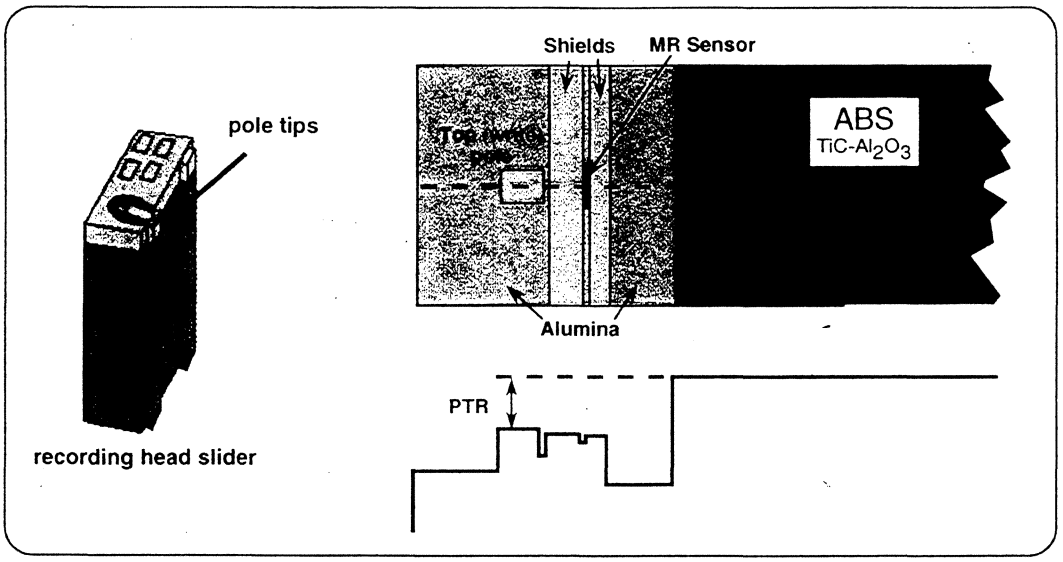

Pole tips located on trailing edge of slider

Pole tip recession = height of pole tips relative to plane defined by air bearing surface (ABS)

- PTR prevents contact damage, allows for thermal expansion
- As flying heights shrink, PTR becoming a large portion of spacing loss:

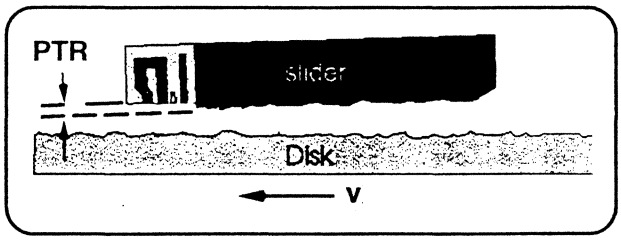

Spacing Loss ~ $\exp(-2\pi D/\lambda)$
D= flying height + overcoats + PTR

- Maintaining small PTR requires stringent process control
- Ideal PTR ~ 1-5 nm
- Shrinking features, need for ~ 1 nm *accuracy* ⇒
  conventional measurements insufficient

Conventional measurements:
Interference Microscopes also used for PTR

advantages

- fast
- repeatable
- automated

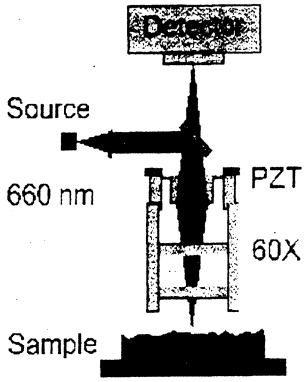

disadvantages:

- material-dependence introduces errors (~5-15 nm)
- difficulty imaging with overc
- limited lateral resolution

PTR Measurement Geometry

consider effects of out-of-plane scanning error:
(i.e., if a flat surface such as the ABS is not measured as flat)

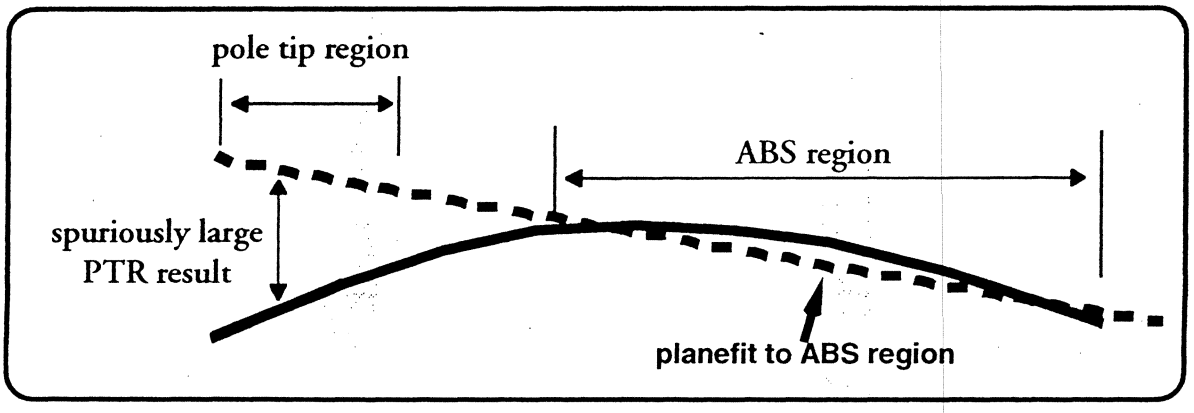

Virtually *any* scanning error prevents direct measurements with 1 nm accuracy

AFM Measurement of PTR Part II

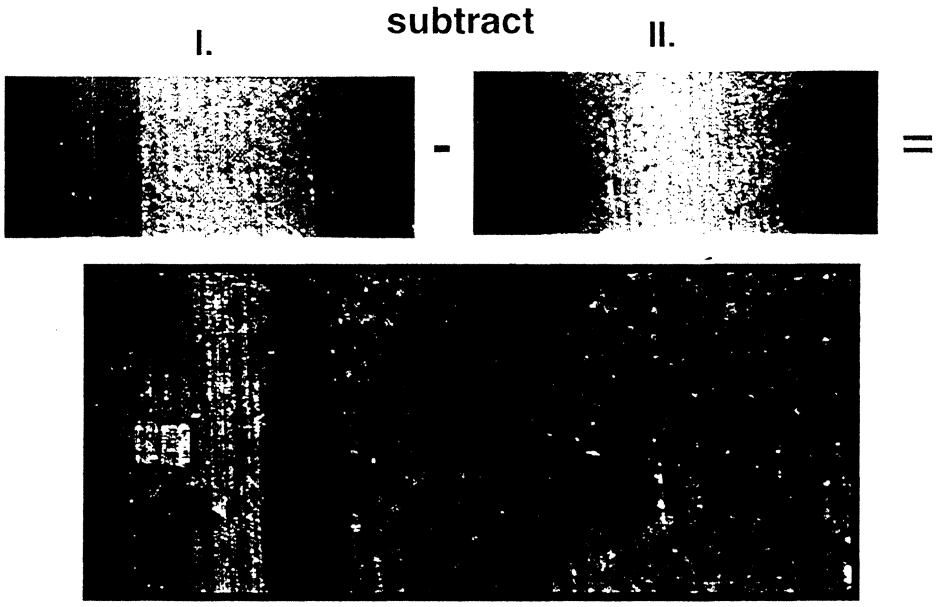

Scanner curvature removed!

AFM Measurement of PTR Part II

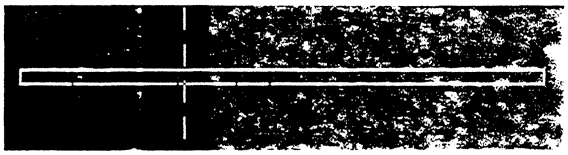

- ABS flat and level
- accurate PTR!

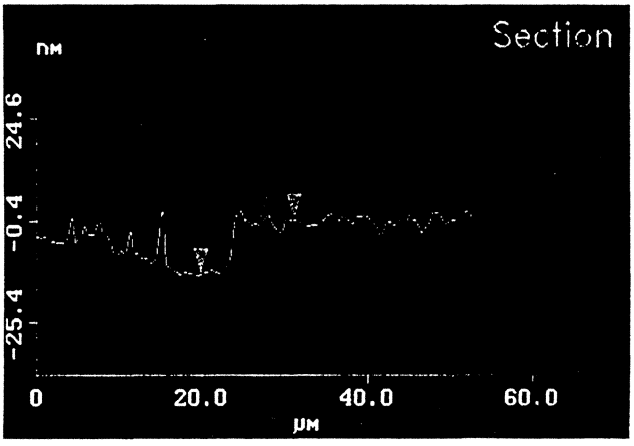

alternatives (curve fitting or "standard" reference subtraction of a fixed reference)
do not work!!

PTR Measurement Accuracy

- capture pole tip and reference images in trace; repeat using retrace
- scanner effects different in trace and retrace
- subtraction should give same results for PTR

Write Pole (nm)

	Subtraction Trace	Subtraction Retrace	No Sub Trace	No Sub Retrace
Head A1	2.7	3.1	9.9	-32.0
Head A2	-7.1	-7.2	-8.3	-18.5
Head B1	-2.6	-2.5	-4.7	-24.7
Head B2	-1.3	-2.0	-8.8	-22.2

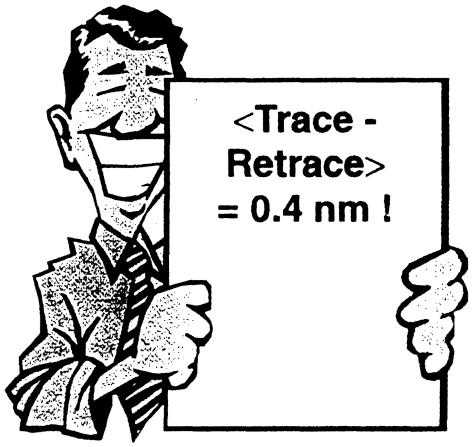

These results indicate measurement accuracy < 0.5 nm!

di

Automated Measurement of PTR

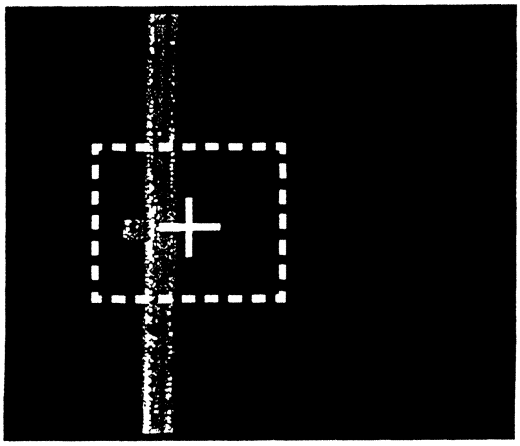

push-button operation

fast scanning

pattern recognition allows automatic sample positioning, data acquisition, and analysis

accuracy: < 1 nm
repeatability: 0.4 nm
time: 2 minutes/slider

di

PTR Automation using Slider Trays

Graphically select sliders to be measured

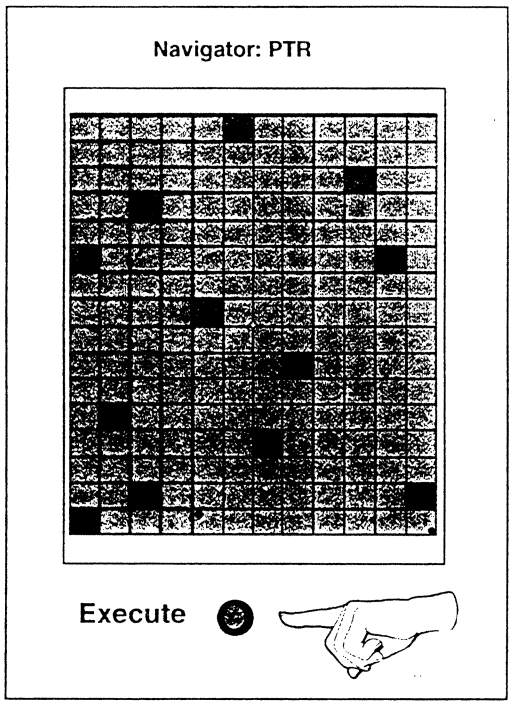

All measurement and analysis done automatically, giving spreadsheet-compatible output

bmpret.res

Page 1

NanoScope Automated Data Analysis, Version 4.32a

This Result File: auto\result\bmpret.res
Date: 10-31-97 Time: 17:21:46
Auto Program File: auto\program\bmp.prg

Data file	AIO	P1	P2
rep.000	17.102 nm	19.126 nm	6.408 um
rep.002	17.048 nm	20.354 nm	6.377 um
rep.004	17.037 nm	19.686 nm	6.394 um
rep.006	17.122 nm	20.866 nm	6.407 um
rep.008	17.067 nm	19.067 nm	6.405 um
Average	17.075 nm	19.820 nm	6.398 um
Std dev	0.032 nm	0.699 nm	11.660 nm

Number of files: 50

- Available as Dimension PTR3100 and Dimension PTR5000

Compare "High-Resolution Profilometers"

AFM after H.R.P.

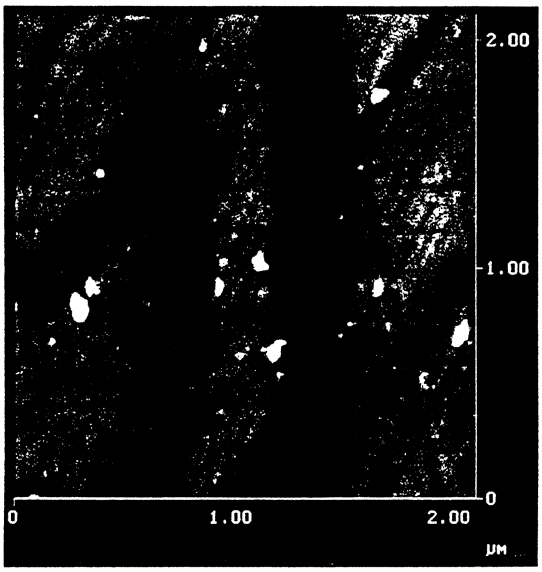

grooves 7 nm deep, vary with material

"H.R.P." uses relatively large force
: ⇒ must choose between resolution and nondestructive imaging

typ. baseline curvature > 1 nm

slower than AFM

Other SPM Measurements: Read/Write Alignment

AFM/MFM of pole tip region:

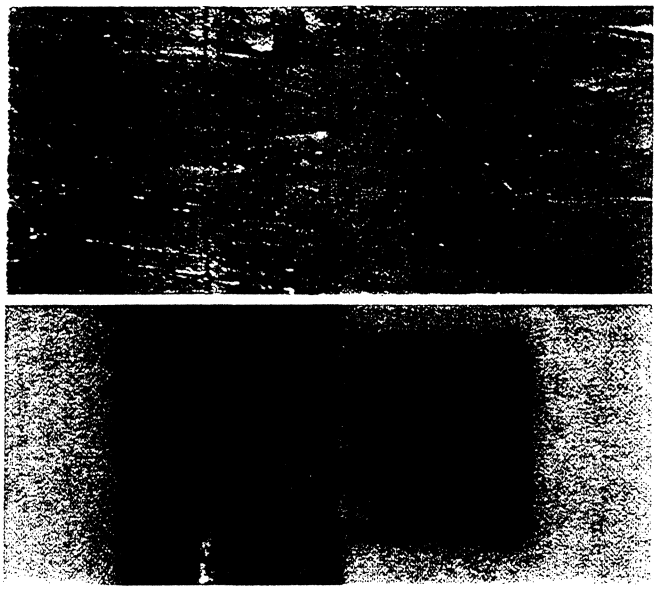

AFM

MFM

8 μm

Other SPM Measurements:MR Sensitivity Profile

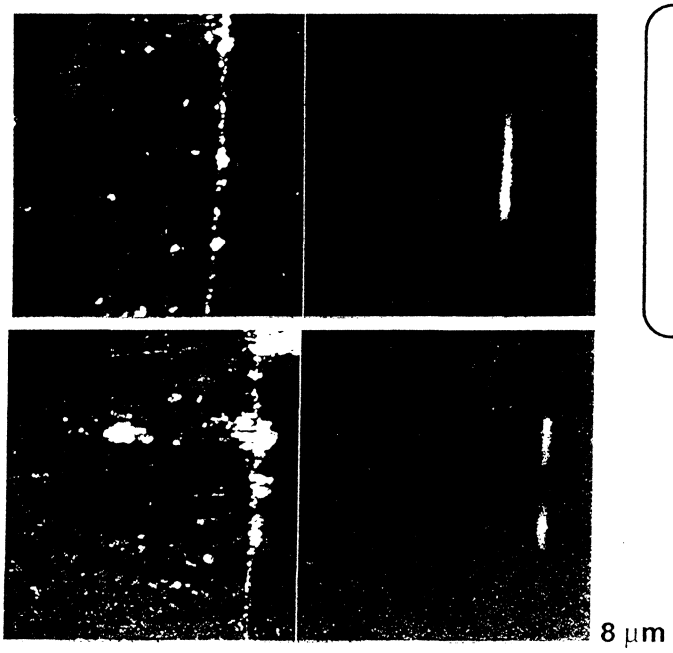

- scan MFM tip
- map response of MR sensor (head output) to tip field

c/o Darryl Louder, Seagate Technology

Thermal Imaging

- Contact AFM with modified SiN cantilevers
- Thermoresistive element at tip
- Lateral resolution ~ 100 nm
- Applications:
  - heating and thermal conduction of biased MR sensors
  - failure analysis

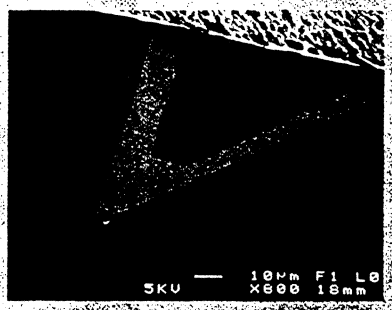

Biased MR Head

contact AFM

thermal

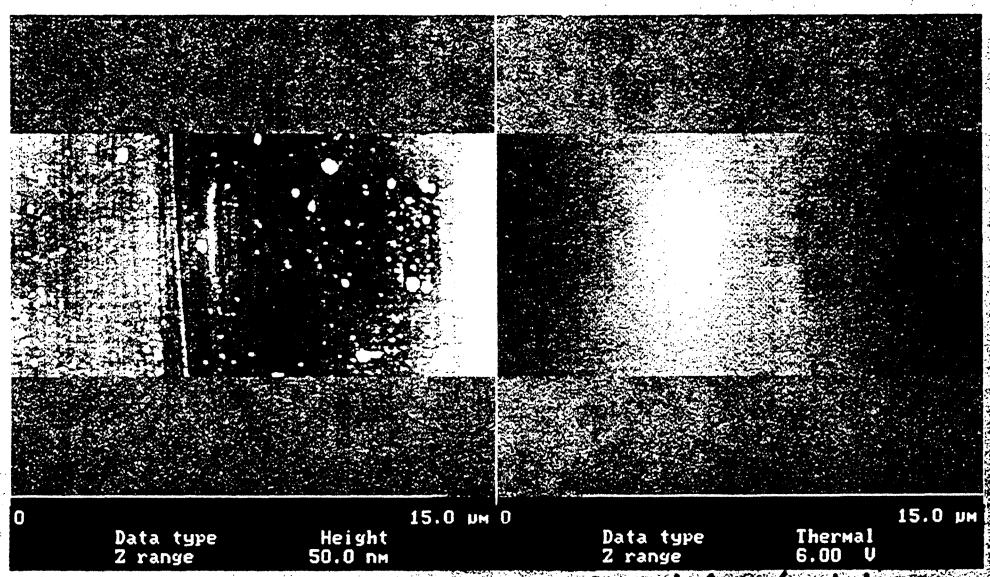

uncalibrated!

Thin Film Characterization: Nano-modification and Scratch-Testing

- diamond tips: radii <30 nm
- foil cantilevers: k~100-300 N/m
- surface modification with forces down to ~ 0.1 μN
- image results *nondestructively* with same tip using TappingMode
- meaningful *in-situ* characterization of thin (nm-scale) films

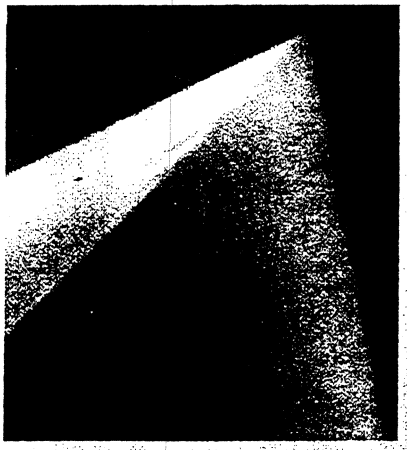

di

Sub-nm dents on 5 nm DLC

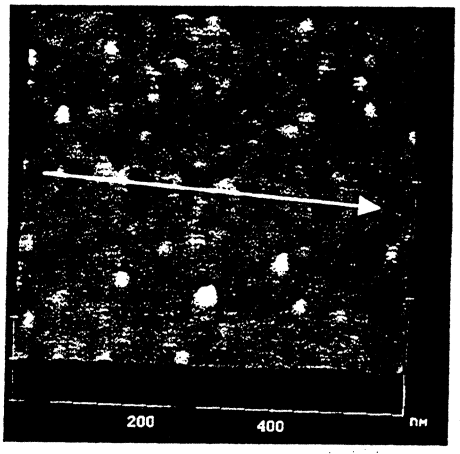

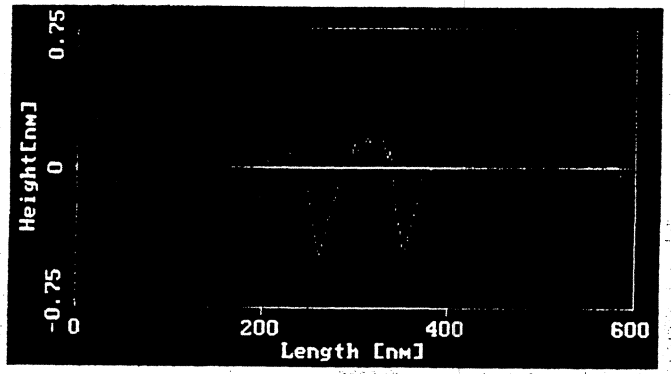

di

Probe Forces

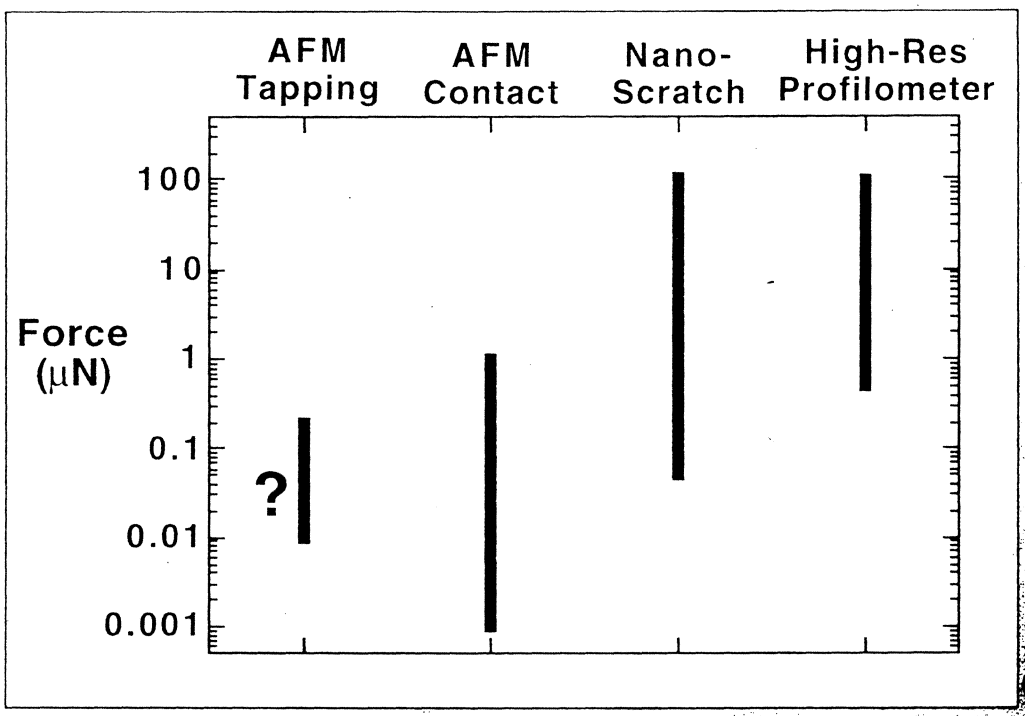

Carbon overcoat comparison

Disk A (same two forces) Disk B

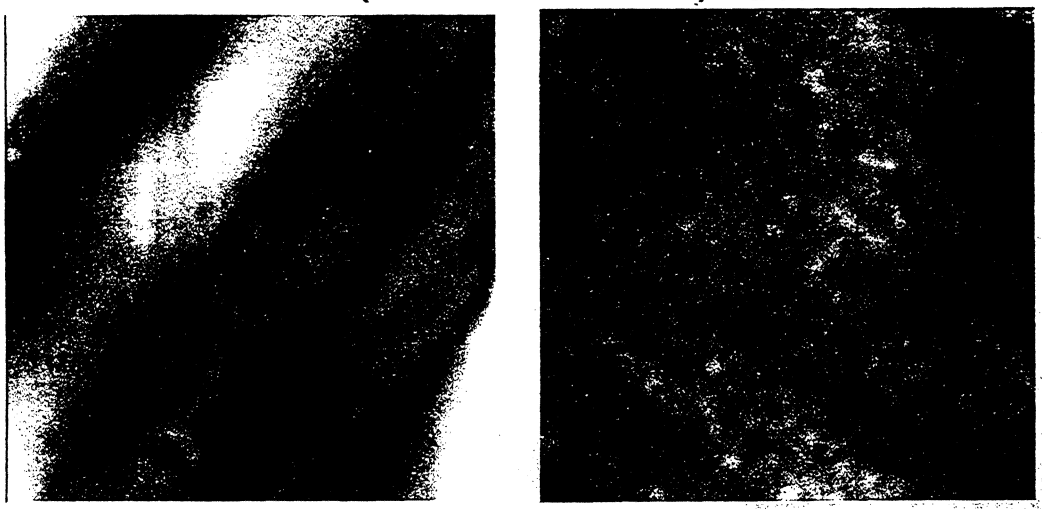

600 nm

Scratch Testing

1) indent and translate with desired normal force

2) image with TappingMode

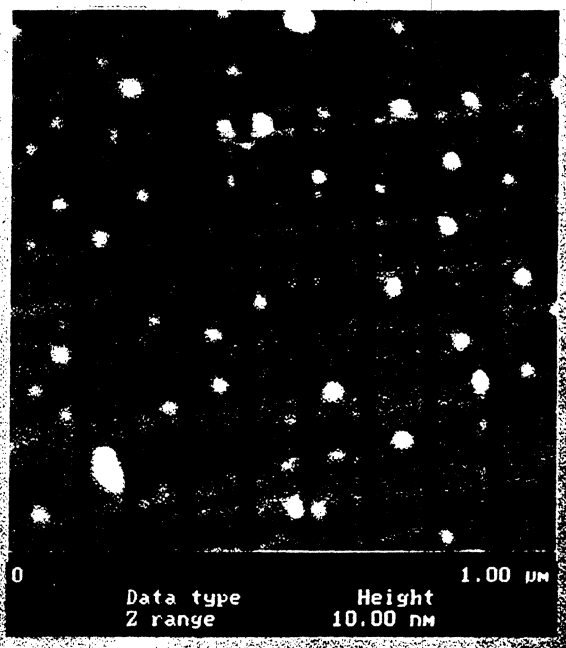

Conclusions

- Applications of AFM and MFM in data storage are extensive and growing
- New measurement capabilities such as nanoindentation and thermal imaging are further increasing SPM's versatility
- SPMs have resolution and accuracy superior to optical instruments, with no dependency on materials or overcoats
- Advances in SPM automation have produced faster, fully-automated metrology tools suitable for development *and* production environments
- Automated LZT measurement: 2 Å repeatability,
  ~ 6 seconds/bump
- Automated PTR measurement: ~ 0.5 nm repeatability
  ~ two minutes/slider, true PTR!

Methodologies in Media Analysis

Brent D. Hermsmeier

MaxMedia,
2001 Fortune Dr., San Jose, CA
95131

HYUNDAI

Overview

- Views on Root Cause Analysis
- Under-Utilized Techniques
- Disk Manufacturing Defect Failure Analysis
- Drive Defect Failure Analysis
- The Bigger Picture
- Fundamental Process Development Studies
- Future Directions

HYUNDAI

Brent D. Hermsmeier MaxMedia Thin Film Symposium II 12-3507-1

Introduction: Analysis Charter

• Expert Analysis	Working Cause Root Cause
• Customer Support	Drive FA
• Quality Support	Source FA
• Manufacturing Support	Process FA
• R&D	Material Analysis
• Fundamental Studies	Experiments

HYUNDAI

Introduction: Root Cause

Incident - Many

↓

Working Cause - Expert conclusion based on analysis gathered at any given moment.
- Free to change as new data becomes available.

↓

Process Origin - Source of problem is linked to a process tool or procedure.
- Often considered closed.

↓

Root Cause
- Origin of the problem is fully understood.
- Rarely achieved, Always desired.
- Often requires experiments not just analysis.

HYUNDAI

Introduction: Alphabet Soup of Analysis

EDX	Elemental analysis, Particles.
Raman	Diamond, Al_2O_3 particles, Organics.
FTIR	Organic functional group identification.
HPLC	Organic analysis, Quantitative, Non Volatiles.
GCMS	Organics, Quantitative, Volatile species.
HPIC	Inorganic, Quantitative.
ICP	Ultra sensitive elemental analysis.
AES	Particles, composition of films.
SIMS	Organic surface analysis, Thin films.
XPS	Surface chemistry, Lube characterization.
OSA	Lube characteristics, Carbon wear.

HYUNDAI

Under-Utilized Techniques

Depth Profile Energy Dispersive Spectroscopy

Focused Ion Beam Aided Analysis

Zalar Depth Profiles

HYUNDAI

Under-Utilized Techniques: EDSDP

Energy Dispersive Spectroscopy Depth Profiles

Scanning Electron Microscope with

Field Emission Gun

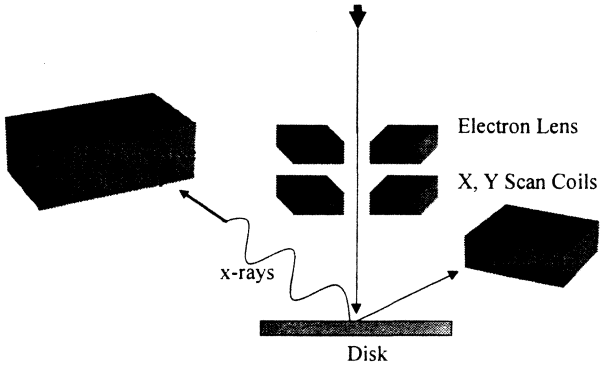

HYUNDAI

MaxMedia

Under-Utilized Techniques: EDSDP

Electron Beam Depth Penetration vs. Acceleration Voltage

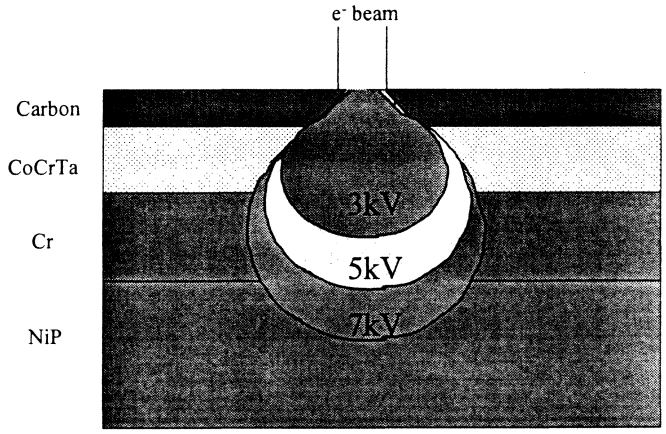

HYUNDAI

MaxMedia

Under-Utilized Techniques: EDSDP

Energy Dispersive Spectroscopy (EDS) "Depth Profiles"

Monte Carlo Simulation

2kV 5kV 20kV

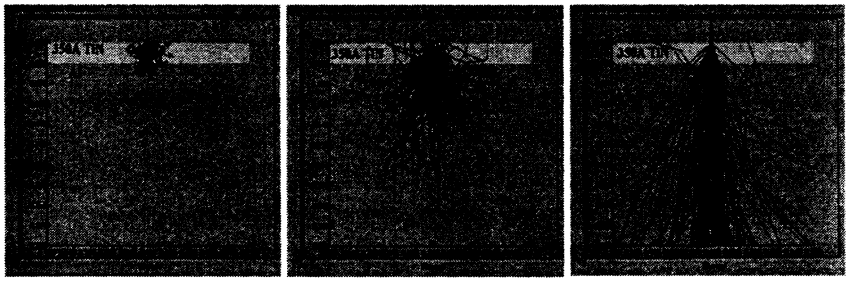

Primary beam interaction with 350Å TiN film on Al substrate

HYUNDAI MaxMedia

Under-Utilized Techniques: EDSDP

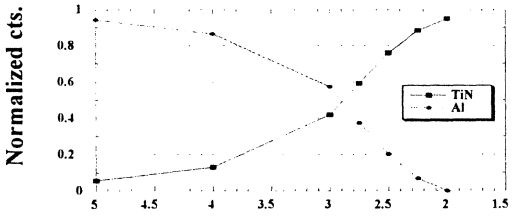

- Fast: thin film depth information for typical media film thicknesses
- Element specific analysis: (Not chemical specific however)
- Small spatial area analysis:
  - Surface defects, particles, scratches ...

HYUNDAI MaxMedia

Under-Utilized Techniques: EDSDP

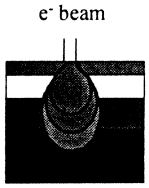

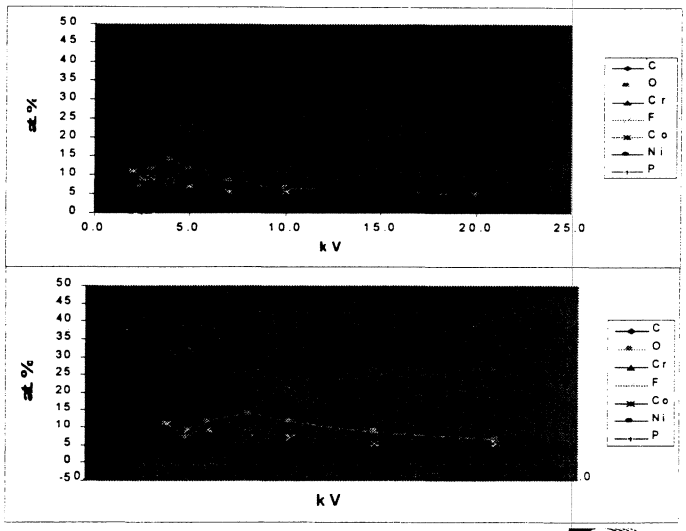

Under-Utilized Techniques: FIB

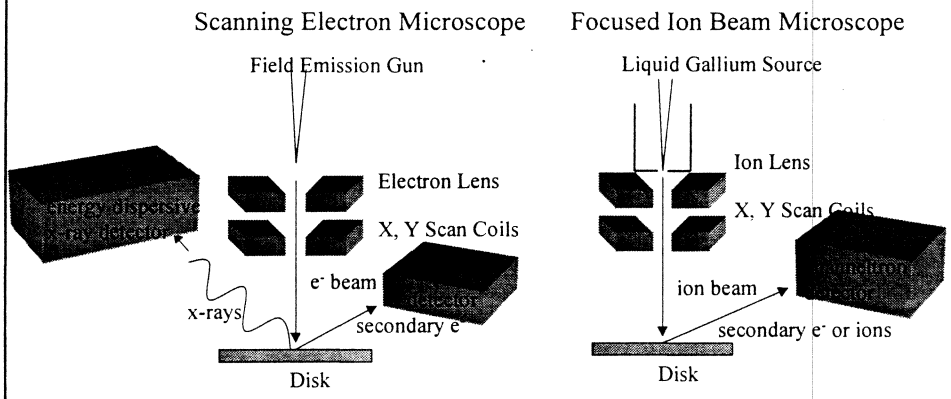

Under-Utilized Techniques: FIB

Image Comparison Between FIB and SEM

FIB cross-section of defect

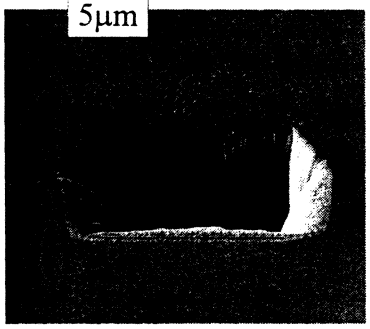

FIB Micrograph: contrast dependent upon sputter yield, in this micrograph Al and NiP have similar contrast

SEM Micrograph: contrast dependent upon secondary electron yield, in this micrograph Al and NiP have different contrast

HYUNDAI

MaxMedia

Zalar

HYUNDAI

MaxMedia

Under-Utilized Techniques: Zalar Depth Profiles

Scanning Auger Microscopy Characterization of Hard Disks

Jingyu Huang
David Harris
David Neiman*
Jeffrey Kingsley

CHARLES EVANS & ASSOCIATES
Sunnyvale, CA 94086

* Hewlett Packard
Corvallis, OR 97330

HYUNDAI MaxMedia

Under-Utilized Techniques: Zalar™ Depth Profiles

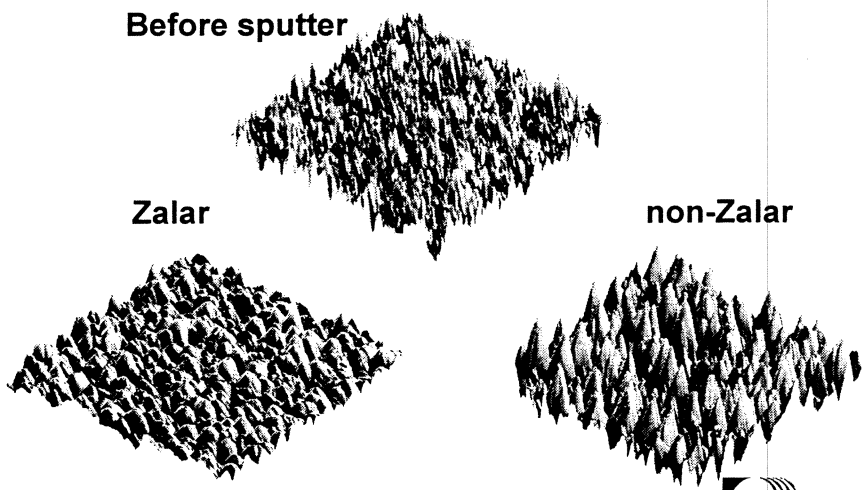

HYUNDAI MaxMedia

Under-Utilized Techniques: Zalar™ Depth Profiles

Zalar™ Enhanced Auger Depth profiles

- Reduce sputtering induced surface roughness
- Improvement of depth resolution, Sharper interface
- Detect contamination at deep interfaces

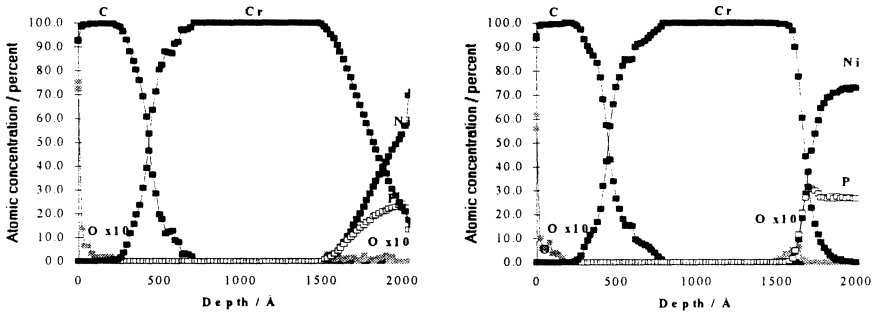

HYUNDAI

MaxMedia

Media Manufacturing Failure Analysis

HYUNDAI

Media Manufacturing FA: Glide

Defects are found at Glide and at Certification test

Glide: A physical protrusion is detected

- Loose Asperities
  - Liquid droplets, Debris, Particles, …
- Fixed Asperities
  - Embedded particles, Delaminations, Texture ridges, Substrates bumps, …

Drive Failure: Hard for the drive to handle

- Amplitude loss, TA, Head crash, ...

HYUNDAI

Brent D. Hermsmeier MaxMedia Thin Film Symposium II 12-3507-1

Media Manufacturing FA: Certification

Defects are found at Glide and at Certification test

Certification: Absence of magnetic signal is detected

- Large "continuous" string of missing pulses
  - Scratches
- Isolated missing pulses
  - Voids, Substrate pits, Texture defects…

Drive Failure: Easy for the drive to handle

- Space allocation errors, ECC errors, ...

HYUNDAI

Media Manufacturing FA: Pareto

Category	*Defect Type*
Substrate	Embedded Polish Particle
	Stress Bump
	Polish Scratch
	Substrate Pit
	Ni Pockets
	Substrate Damage
	Ni Plating Defect
	NiP Nodules
Texture	Embedded Grit
	Texture Ridge
	Texture Start Mark
	Texture Table
Pre-Sputter.	Micro Defect
	Inorganic Blisters
	Organic Blisters
	Covered Debris
Sputter	Sputter Arcing
	Underlayer Surface Mark
	Spitting

Category	*Defect Type*
Sputter Con.	Pre Underlayer Film Flakes
	Lint
	Conversion
Post-Sputter	Surface Debris/Contam.
	Smear
Tape Burnish	Tape Burnish Scratch
	Start Mark
Test	Soft Head Disk Ding
	Hard Disk Ding
	Head Load / Unload Damage
	OD Stress
Mech. Dam.	Tool Damage
	Disk Lifter
Handling Dam	Pre-Texture
	Pre-Sputter
	Post-Sputter
Other	Not Found
	Glove Prints
	Rough Surface

HYUNDAI

Media Manufacturing FA: Example

Blister

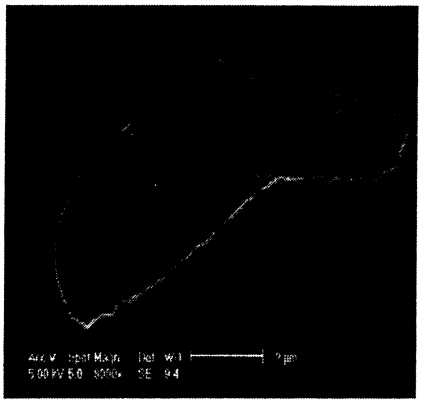

Substrate Plating Porosity

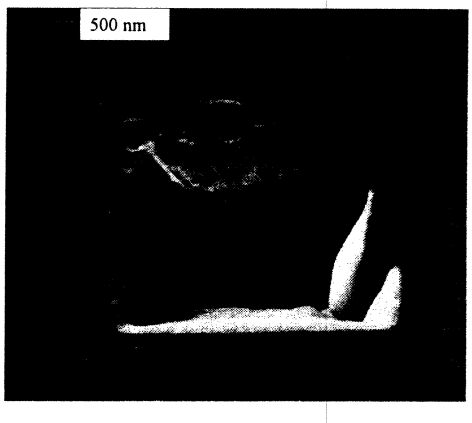

HYUNDAI

MaxMedia

Media Manufacturing FA: Example

Blister?

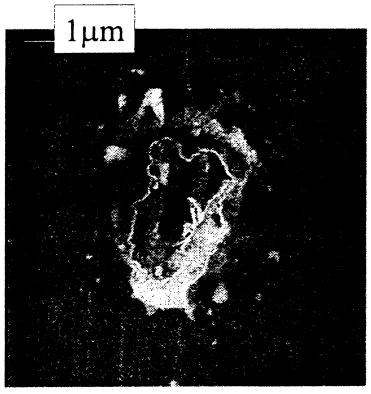

No, Substrate Carbon Particle Inclusion

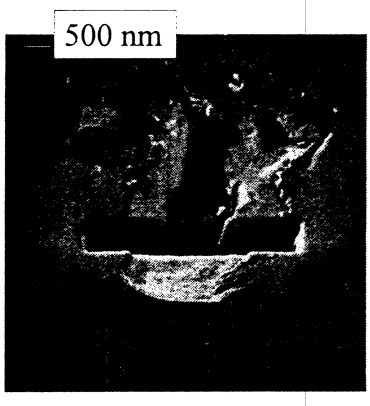

HYUNDAI

MaxMedia

Failure Analysis on Drive Media Defects

HYUNDAI

MaxMedia

Drive Media Defects: Test Process

Drive Test Sequence

Line Process Test

- Write / Read Primary Defect Log
- TA Count → Guard Banding Needed
- Timing Evaluation

Line Audit Test

- Write / Read Performance Comparison

Reliability Test

- Grown Defect Log → TA's, Non ECC Correctables
- Reallocation Record
- Error Rate Degradation Test

HYUNDAI

MaxMedia

Brent D. Hermsmeier MaxMedia Thin Film Symposium II 12-3507-1

Drive Media Defects: FA Flow

Drive FA

Electrical Diagnostics	Dropout Width
Head location	Outer Surfaces
Polar Plots	Defect Symmetry and Geometry
TA Specific Scans	TA Locations vs. Initial Defect List
Physical Inspection	Defect Symmetry and Geometry
Optical Image	Neighboring Effects
Height Determination	Above the Glide Height
SEM Image	High Spatial Resolution Identification
EDS	Elemental Analysis

Typical Defects: Embedded Particles, Voids, Contamination, Blisters,...

HYUNDAI

MaxMedia

Drive Media Defect: Example

Transient TA

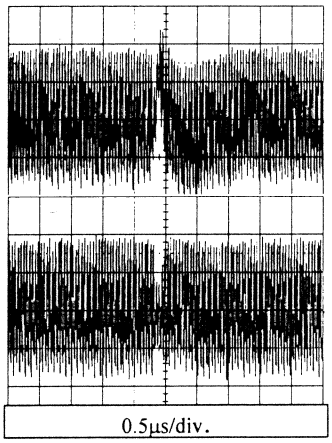

Reliability Test

Error Found during a Read Operation

Error Location scoped → TA

TA disappeared after sitting on Track for a short time

r = 27.2mm
5400 rpm
— ≈3μm size defect

HYUNDAI

MaxMedia

Drive Media Defects: Example

Substrate Pit with Redeposited Material 2.5μm in Diameter

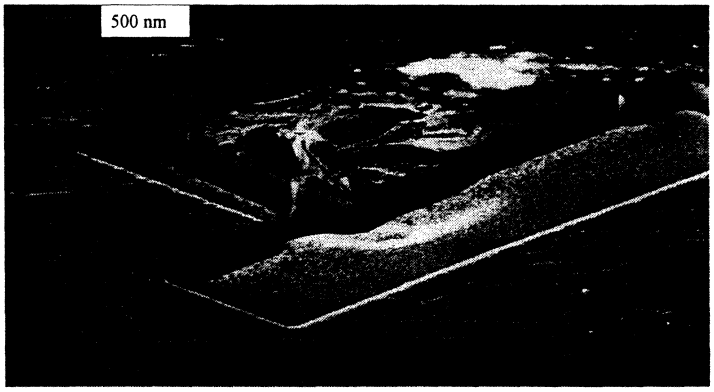

HYUNDAI

MaxMedia

Drive Media Defects: Example

Embedded Al_2O_3 particle found as a grown defect

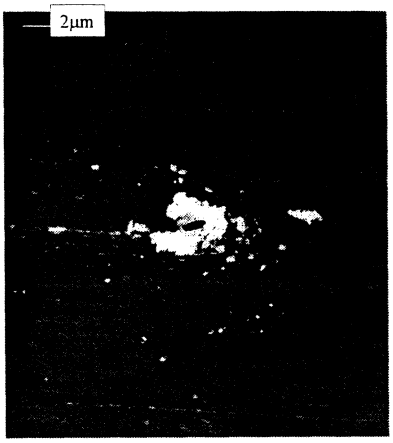

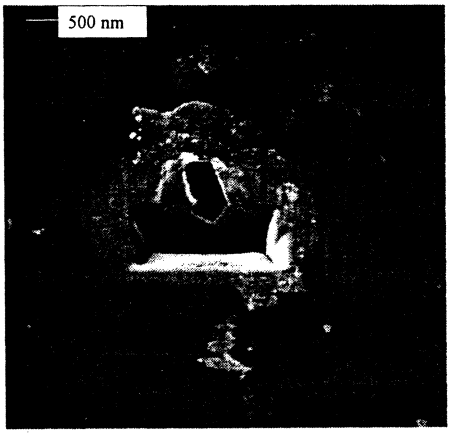

HYUNDAI

MaxMedia

Drive Media Defects: Example

Post Sputter Embedded Si(O) Particle

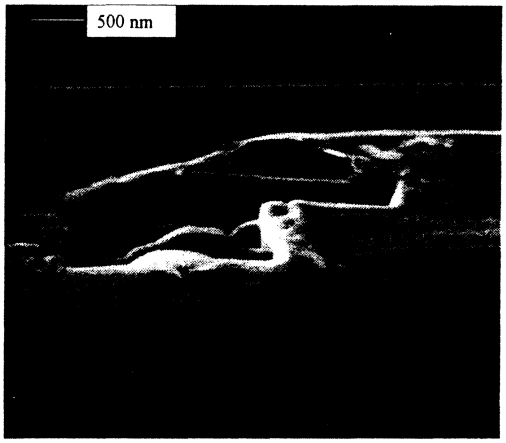

HYUNDAI

MaxMedia

The Bigger Picture

Taking the Study Beyond the Analysis

HYUNDAI

MaxMedia

The Bigger Picture: From Defect to Local Heating

Drive ORT Failure	Glass Media
	Nominal Fly Height = 1.2μ"
Grown Defect	Servo Field (no ECC)
	r = 21mm
	Lateral Size = 30μm
	Height = 500Å

Signal degraded over several hours

3/4 of the magnetic layer missing as seen by EDS

Cause: Substrate Plateau originating from incomplete polish

HYUNDAI MaxMedia

The Bigger Picture: From Defect to Local Heating

SEM cross section of a glass disk

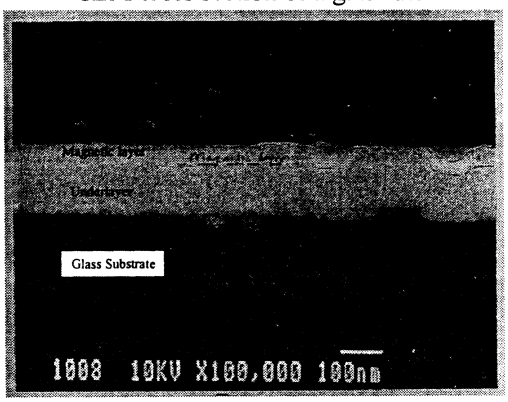

Magnetic layer is CoCrPtTa

T_c = 550°C

Assume a Bias Field of 200Oe

Effective T_c = 400°C

Temperature induced by the head wear which removed the C overcoat and the 3/4 of the Magnetic layer stayed below 400°C.

HYUNDAI MaxMedia

Fundamental Process Development Studies

Nucleation and Growth of Ultra Thin Carbon overcoats

HYUNDAI

MaxMedia

Nucleation and Growth: Ultra Thin C

Principles of Angle Resolved X-ray Photoelectron Spectroscopy

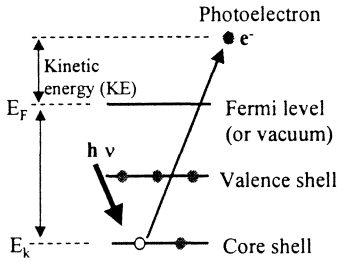

$$KE = h\nu - BE$$

Depth Profile With Angle-resolved XPS

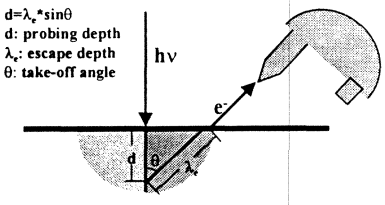

$$\lambda_e \propto e^{-1/KE}$$

HYUNDAI

MaxMedia

Nucleation and Growth: Ultra Thin C

Sample: 5, 10, 20, 40 Å a-C overcoat on supersmooth substrate.
Experiment: Angle-resolved XPS on C1s, Co2p, Cr2p, Ta4f, and O1s.
Information Obtained: Chemistry at the carbon/mag interface

Conclusions:
1) ~40 Å is minimum thickness for stopping the oxygen diffusion and surface passivation. - This is the physical limit of the carbon thickness

2) The carbon goes through layer-by-layer growth

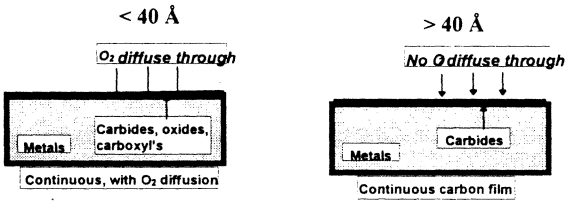

HYUNDAI MaxMedia

Nucleation and Growth: Ultra Thin C

C 1s signal change between 20Å and 40Å of C overcoat

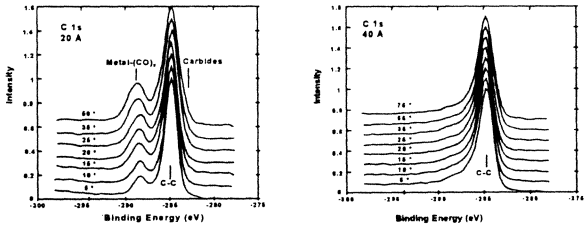

Co 2p signal change between 20Å and 40Å of C overcoat

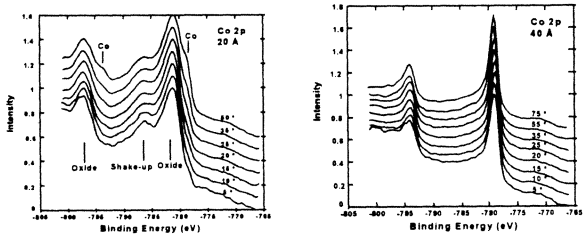

HYUNDAI MaxMedia

Nucleation and Growth: Ultra Thin C

Cr 2p signal between 5Å and 40Å of C

Cr (O) signal disappears after 10Å of C overcoat

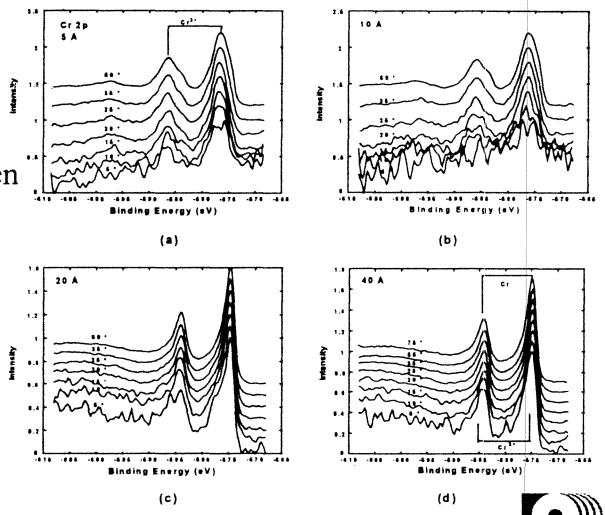

HYUNDAI

Sudden Change at 20A

MaxMedia

Nucleation and Growth: Ultra Thin C

(A) Island Growth, No O_2 diffuse through	(B) Island Growth, O_2 diffuse through	(C) Layer-by-layer Growth, O_2 diffuse through

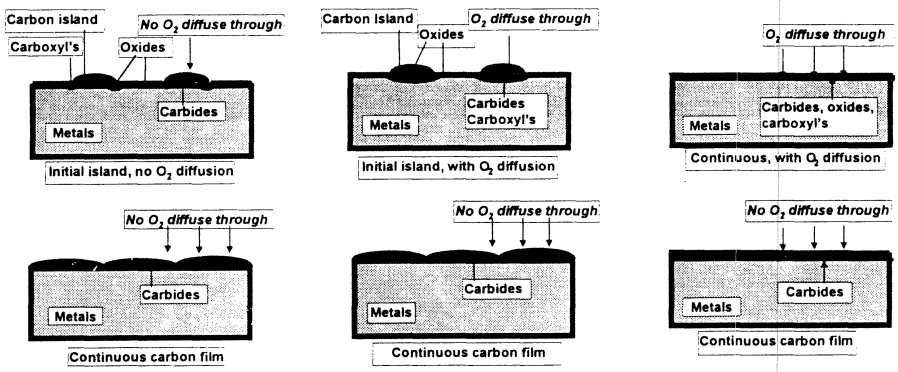

HYUNDAI

MaxMedia

On The Horizon

More Focus Ion Beam (FIB)

Inductively Coupled Plasma-Mass Spectroscopy (ICP-MS)

Optical Surface Analyzer (OSA)

Time of Flight-Secondary Ion Mass Spectroscopy (TOF-SIMS)

Synchrotron Radiation

- High Resolution X-ray Microscopy
- Grazing Angle X-ray Reflection
- Near Edge X-ray Absorption Fine Structure (NEXAFS)

HYUNDAI

Acknowledgements

• Cecilia Martner	MaxMedia
• Peter Sobol	MaxMedia
• David Chan	MaxMedia
• JiFeng Ying	MaxMedia
• Sabina Misquitta	MaxMedia
• Siew Peng Mong	MaxMedia
• Charlotte Fenno	Integral Peripherals
• Jingyu Huang	Charles Evens & Associates.
• Paul King	Advanced Micro Devices
• David Joy	Univ. Of Tennessee

HYUNDAI